

**ADVANCES IN PHYSICAL SYSTEMS MODELING USING
EXPLICITLY CORRELATED GAUSSIAN FUNCTIONS**

by

Nikita Kirnosov

A Dissertation Submitted to the Faculty of the

DEPARTMENT OF PHYSICS

In Partial Fulfillment of the Requirements
For the Degree of

DOCTOR OF PHILOSOPHY

In the Graduate College

THE UNIVERSITY OF ARIZONA

2015

THE UNIVERSITY OF ARIZONA
GRADUATE COLLEGE

As members of the Dissertation Committee, we certify that we have read the dissertation prepared by Nikita Kirnosov
entitled Advances In Physical Systems Modeling Using Explicitly Correlated Gaussian Functions
and recommend that it be accepted as fulfilling the dissertation requirement for the Degree of Doctor of Philosophy.

Date: 2 December 2015

Dr. Ludwik Adamowicz

Date: 2 December 2015

Dr. Brian Anderson

Date: 2 December 2015

Dr. Andrei Lebed

Date: 2 December 2015

Dr. Srinivas Manne

Date: 2 December 2015

Dr. Oliver Monti

Final approval and acceptance of this dissertation is contingent upon the candidate's submission of the final copies of the dissertation to the Graduate College.
I hereby certify that I have read this dissertation prepared under my direction and recommend that it be accepted as fulfilling the dissertation requirement.

Date: 2 December 2015

Dissertation Director: Dr. Ludwik Adamowicz

STATEMENT BY AUTHOR

This dissertation has been submitted in partial fulfillment of requirements for an advanced degree at the University of Arizona and is deposited in the University Library to be made available to borrowers under rules of the Library.

Brief quotations from this dissertation are allowable without special permission, provided that accurate acknowledgment of source is made. Requests for permission for extended quotation from or reproduction of this manuscript in whole or in part may be granted by the head of the major department or the Dean of the Graduate College when in his or her judgment the proposed use of the material is in the interests of scholarship. In all other instances, however, permission must be obtained from the author.

SIGNED: Nikita Kirnosov

ACKNOWLEDGEMENTS

My acknowledgement goes to my adviser, Dr. Ludwik Adamowicz, and the group:

- Dr. Keeper Sharkey
- Dr. Wei-Cheng Tung
- Keith Jones
- Martin Formanek

TABLE OF CONTENTS

LIST OF FIGURES	7
LIST OF TABLES	8
ABSTRACT	9
CHAPTER 1 INTRODUCTION	10
1.1 Dissertation Structure	10
1.2 Coordinate Frame and Hamiltonian	11
1.3 Explicitly Correlated Gaussian Functions	13
1.4 General Method Description	15
CHAPTER 2 NON-BORN-OPPENHEIMER CALCULATIONS	17
2.1 Coordinate Frame	17
2.2	17
2.3	17
CHAPTER 3 PROGRAMMATIC IMPLEMENTATION	18
3.1	18
3.2	18
3.3	18
CHAPTER 4 FUTURE DIRECTIONS	19
4.1 Muonic Systems	19
4.2 Ultra Cold Atoms	19
APPENDIX A Analytical energy gradient used in variational Born- Oppenheimer calculations with all-electron explicitly correlated Gaussian functions for molecules containing one π electron	20
APPENDIX B Einstein coefficients for rovibrational transitions of the LiH molecule in the ground $X^1\Sigma^+$ electronic state	32
APPENDIX C An algorithm for quantum mechanical finite-nuclear-mass varia- tional calculations of atoms with $L = 3$ using all-electron explicitly correlated Gaussian basis functions	59

TABLE OF CONTENTS – *Continued*

APPENDIX D An algorithm for non-Born-Oppenheimer quantum mechanical variational calculations of N = 1 rotationally excited states of diatomic molecules using all-particle explicitly correlated Gaussian functions	76
APPENDIX E Charge asymmetry in rovibrationally excited HD ⁺ determined using explicitly correlated all-particle Gaussian functions	97
APPENDIX F Lifetimes of rovibrational levels of HD ⁺	106
APPENDIX G Charge asymmetry in the rovibrationally excited HD molecule	112
APPENDIX H Charge asymmetry and rovibrational excitations of HD ⁺ . . .	121
APPENDIX I Nuclear-nuclear correlation function from non-Born-Oppenheimer calculations of diatomic rovibrational states with total angular momentum equal to two (N=2). Charge asymmetry in HD.	154
APPENDIX J Paraortho isomerization of H ₂ ⁺ . Non-BornOppenheimer direct variational calculations with explicitly correlated all-particle Gaussian functions	170
APPENDIX K Non-Born-Oppenheimer method for direct variational calculations of diatomic first excited rotational states using explicitly correlated all-particle Gaussian functions	178
APPENDIX L Direct non-Born-Oppenheimer variational calculations of all bound vibrational states corresponding to the first rotational excitation of D ₂ performed with explicitly correlated all-particle Gaussian functions . .	183
APPENDIX M Orthopara nuclear-spin isomerization energies for all bound vibrational states of ditritium (T ₂) from non-BornOppenheimer variational calculations performed with explicitly correlated all-particle Gaussian functions	191
APPENDIX N Non-BornOppenheimer variational method for calculation of rotationally excited binuclear systems	199
APPENDIX O A comparison of two types of explicitly correlated Gaussian functions for non-Born-Oppenheimer molecular calculations using a model potential	215

LIST OF FIGURES

1.1 Coordinate frame transformation	12
---	----

LIST OF TABLES

ABSTRACT

This is where the body of your abstract goes, limited to 150 words for a thesis, and 350 words for a dissertation or document. The word count limits apply to the regular Abstract in the thesis and to the separate Special Abstract. Use the same text for both; just adjust the margins and heading. The abstract should summarize your work. The UMI booklet listed in the resources section of the U of A manual provides some writing tips. The abstract for a dissertation or document may be longer than one page; word count is more important than page length in this section.

If you are doing a paper submission, submit one copy of the special abstract, and two extra copies of your title page, in the box with the final copies of your thesis. If you are doing an electronic submission, you can ignore the special abstract.

CHAPTER 1

INTRODUCTION

1.1 Dissertation Structure

This dissertation has an article-based format. All the manuscripts produced during the candidacy are included as appendices. While each manuscript is self-contained and self-explanatory, in the context of this dissertation they would be addressed as sources of the detailed description and more specific analysis. The goal of this dissertation is to provide a reader with good understanding of the method applicability and its' advantages and disadvantages in comparison to the other methods used for certain classes of problems.

In this chapter we will consider general approach to the accurate modeling of the system wave function with a linear combination of explicitly correlated Gaussian functions (ECG). In order to relief the following chapters from the technical details, most of the mathematical concepts are be introduced here. The simplest form of the ECG function is considered and its properties are discussed.

In chapter 2 some applications of this method to various systems with Coulomb interactions (atoms, molecules, *etc.*) considered with no Born-Oppenheimer approximation made. Modifications needed to be made to the basis function for each class of systems are discussed.

Chapter 3 contains the description of the code used for calculations and discusses the nuances of the particular system implementation. Moreover, some ways of increasing code performance and decreasing space requirements are considered.

Finally, chapter 4 gives an overview of the avenues of research opened as a result of the work constituting this dissertation.

1.2 Coordinate Frame and Hamiltonian

A system of $n + 1$ particles with masses M_i and charges Q_i can be described at any moment of time with $n + 1$ coordinate vectors

$$R_i = \begin{pmatrix} x_i \\ y_i \\ z_i \end{pmatrix} \quad (1.1)$$

and $n + 1$ momenta vectors

$$P_i = \begin{pmatrix} p_{x,i} \\ p_{y,i} \\ p_{z,i} \end{pmatrix}. \quad (1.2)$$

The Hamiltonian operator for this system can be written as

$$H = \sum_i^{n+1} \frac{P_i^2}{2M_i} + \sum_{i,j>i}^{n+1} \frac{Q_i Q_j}{R_{ij}}, \quad (1.3)$$

where

$$R_{ij} = \|R_i - R_j\|. \quad (1.4)$$

It is easy to see that this laboratory frame Hamiltonian includes the center of mass motion. In order to rigorously separate it out, a transformation of the coordinate system should be performed. Instead of considering a system as $n + 1$ particles with charges Q_{i+1} and masses M_{i+1} , we will consider n pseudo-particles with charges $q_i = Q_{i+1}$ and reduced masses $\mu_i = \frac{M_1 M_{i+1}}{M_1 + M_{i+1}}$ moving in the central field of the reference particle charge q_0 .

Figure 1.1 illustrates the transition to the internal coordinate frame which has its center places on one of the particles. Normally for the reference particle the most distinguishable (a nucleus in the atom) or the heaviest (deuteron in HD^+) particle

is chosen. The position of that particle with respect to the laboratory Cartesian coordinate frame is described by a vector $r_0 = R_1$, and other particles' coordinates are defined with respect to the reference particle: $r_i = R_1 - R_{i+1}$.

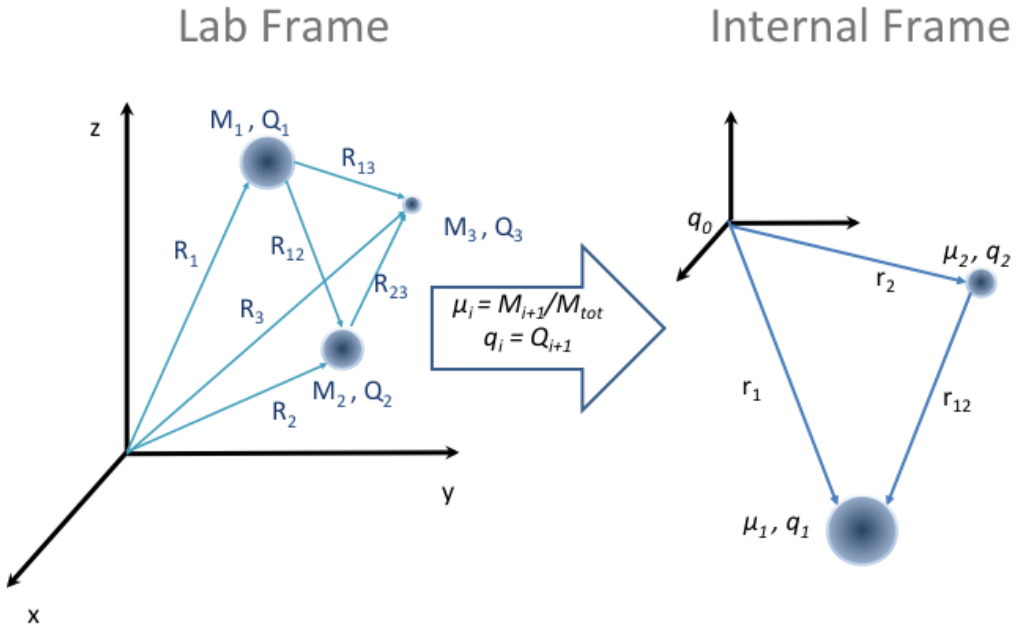


Figure 1.1: Coordinate frame transformation.

The internal Hamiltonian of the considered system now becomes

$$H_{int} = \sum_{i=1}^n \frac{P_i^2}{2\mu_i} + \sum_{i \neq j}^n \frac{P_i P_j}{2m_0} + \sum_i^n \frac{q_i q_0}{\|r_i\|} + \sum_{i,j > i}^n \frac{q_i q_j}{\|r_i - r_j\|}. \quad (1.5)$$

Substituting

$$P_i = \frac{\nabla_{r_i}}{i} \quad (1.6)$$

$$r_{ij} = r_i - r_j, \quad (1.7)$$

we obtain the final form of the internal Hamiltonian operator:

$$H_{int} = -\frac{1}{2} \left(\sum_{i=1}^n \frac{\nabla_{r_i}^2}{\mu_i} + \sum_{i \neq j}^n \frac{\nabla_{r_i} \nabla_{r_j}}{m_0} \right) + \sum_i^n \frac{q_i q_0}{\|r_i\|} + \sum_{i,j > i}^n \frac{q_i q_j}{\|r_{ij}\|}. \quad (1.8)$$

It can be seen that the first term of the internal Hamiltonian describes individual kinetic energies of the particles, while the third and the fourth terms are used to take into account the Coulomb interactions between all charges in the system. Second term is called a mass-polarization term and originates from the choice of the internal coordinate system, which is a non-inertial coordinate frame.

This Hamiltonian possesses a number of important properties. It

1. describes all particles as quantum particles,
2. accounts for all interactions,
3. provides one-step variational approach,
4. reduces problem dimensionality,
5. is isotropic.

It has to be mentioned that this Hamiltonian does not include the description of relativistic effects and thus should be more accurately called non-relativistic internal Hamiltonian. The direct inclusion of additional terms to describe relativistic as well as other interactions is possible in principle.

1.3 Explicitly Correlated Gaussian Functions

Since the Schrodinger equation

$$H\Psi = E\Psi \quad (1.9)$$

is insoluble by current standards, we have to find a way around this problem.

One possibility is to expand a wave function in a complete set of functions that obey the same boundary conditions:

$$\Psi(r) = \sum_k^\infty c_k \phi_k(r), \quad (1.10)$$

where c_k are the linear expansion coefficients.

Note that in the equation above infinity symbol is used to communicate the completeness; the actual number of basis functions does not have to be infinite. Nevertheless, the complete basis set is not achievable for many cases and has to be truncated:

$$\Phi(r) = \sum_k^K c_k \phi_k(r). \quad (1.11)$$

The wave function representation (1.11) can be adequate for an accurate description of a relatively simple and confined wave functions with a number of basis functions K being relatively small. The degree of completeness of such basis set may be evaluated by variational principle, which states that the expectation value of the Hamiltonian computed with the trial function is higher or equal to the true energy value:

$$E = \frac{\langle \Psi | H | \Psi \rangle}{\langle \Psi | \Psi \rangle} \leq \frac{\langle \Phi | H | \Phi \rangle}{\langle \Phi | \Phi \rangle} \quad (1.12)$$

In our work we have chosen to use functions of the following type as basis functions:

$$\phi_k = \exp [-r'(A_k \otimes I_3)r], \quad (1.13)$$

where r' is a row vector of length $3n$ containing pseudo-particles' coordinates in an internal coordinate frame ($r' = [x_1, y_1, z_1, \dots, x_n, y_n, z_n]$) and A_k is $n \times n$ symmetric matrix. Since the function (1.13) must be square-integrable in order to be used for description of the bound states, the matrix A_k has to be positive definite. That can be achieved through the use of Cholesky factorization $A_k = L_k L'_k$, where L_k is a lower triangular matrix. In simplest case, all off-diagonal elements of A_k matrix can be set to zero; however, in order to describe the correlation effects between the particles, they should also be optimized. The resulting function would contain the correlation explicitly and thus be called Explicitly Correlated Gaussian function.

It has to be noticed that according to the Pauli principle, the total wave function which includes the spin degrees of freedom of a quantum system must either be symmetric or antisymmetric with respect to permutations of identical particles. Thus,

our basis set expansion should take this requirement into account. In variational calculations this puts a constraint on the symmetry of the basis functions that can be used.

In general, in order to build properly (anti)symmetric wave functions, we have to deal with both the spatial and spin coordinates. Due to the fact that the Hamiltonian of a nonrelativistic Coulomb system does not depend on the spin of particles, it is possible to completely eliminate the spin variables from consideration. The projection operators Y for irreducible representations of the symmetric group (called Young operators) are obtained from their corresponding Young tableaux. Thus, our properly symmetrized trial wafe function would have the following form:

$$\Phi(r) = \sum_k^K c_k Y \phi_k(r). \quad (1.14)$$

1.4 General Method Description

All the calculations were performed within the framework of the Ritz variational method. The main idea of the variational method in nonrelativistic quantum mechanics is based on the fact that the expectation value of the Hamiltonian of the system computed with a trial wave function is always an upper bound to the exact ground state energy. This general property of the energy functional facilitates a way to obtain very accurate approximations to the exact wave function by the optimization of the parameters, both linear and nonlinear, which the function comprises. This optimization is accomplished by the energy minimization.

Therefore, in order to find the minimum of the Hamiltonian operator expectation value, a secular equation

$$Hc = ESc \quad (1.15)$$

solution needs to be minimized

$$E = \min \frac{c' H c}{c' S c} \quad (1.16)$$

with respect to both linear and nonlinear parameters constituting basis functions.

In order to perform such minimization, Hamiltonian and overlap matrices need to be calculated. The individual matrix elements will be referred to as H_{kl} and S_{kl} , respectively. The following p -dimensional Gaussian integral is used most often for this purpose:

$$\int_{-\infty}^{+\infty} \exp[-r'Br + v'r] = \frac{\pi^{p/2}}{|B|^{1/2}} \exp[-v'B^{-1}v]. \quad (1.17)$$

Therefore, and overlap of simple ECG functions (1.13) would be

$$\langle \phi_k | \phi_l \rangle = \frac{\pi^{p/2}}{|A_k + A_l|^{3/2}}. \quad (1.18)$$

Later on, when we will be considering functions containing a prefactor, a generator function approach will be used. This approach consists in coming up with a generator function which, when differentiated by a parameter, will produce a basis set function. Since a parameter is independent from coordinate variables, it is possible to integrate the generator functions using equation (1.17) and later take a derivative. This approach is described in great detail in appendices C, D, and N.

A very important aspect of the calculations with ECG functions is that achieving high accuracy is possible only when the nonlinear exponential parameters of basis functions are extensively optimized. This process usually takes large amounts of computer time. To accelerate the basis set optimization in the ECG calculations, analytic energy gradient with respect to the nonlinear parameters can be employed. Evaluating the components of the gradient analytically as opposed to using finite differences of the energy allows to reduce the total number of operations and avoid numerical precision issues to a certain extent. This procedure is described for different cases in appendices A, D, and N.

CHAPTER 2

NON-BORN-OPPENHEIMER CALCULATIONS

2.1 Coordinate Frame

2.2

2.3

CHAPTER 3

PROGRAMMATIC IMPLEMENTATION

3.1

3.2

3.3

CHAPTER 4

FUTURE DIRECTIONS

4.1 Muonic Systems

4.2 Ultra Cold Atoms

APPENDIX A

Analytical energy gradient used in variational Born-Oppenheimer calculations with all-electron explicitly correlated Gaussian functions for molecules containing one π electron

Analytical energy gradient used in variational Born-Oppenheimer calculations with all-electron explicitly correlated Gaussian functions for molecules containing one π electron

Wei-Cheng Tung,¹ Michele Pavanello,² Keeper L. Sharkey,¹ Nikita Kirnosov,³ and Ludwik Adamowicz^{1,3}

¹Department of Chemistry and Biochemistry, University of Arizona, Tucson, Arizona 85721, USA

²Department of Chemistry, Rutgers, The State University of New Jersey, Newark, New Jersey 07102, USA

³Department of Physics, University of Arizona, Tucson, Arizona 85721, USA

(Received 26 November 2012; accepted 27 February 2013; published online 22 March 2013)

An algorithm for variational calculations of molecules with one π electron performed with all-electron explicitly correlated Gaussian (ECG) functions with floating centers is derived and implemented. The algorithm includes the analytic gradient of the Born-Oppenheimer electronic energy determined with respect to the ECG exponential parameters and the coordinates of the Gaussian centers. The availability of the gradient greatly accelerates the variational energy minimization. The algorithm is tested in calculations of four electronic excited states, $c^3\Pi_u$, $C^1\Pi_u$, $i^3\Pi_g$, and $I^1\Pi_g$, of the hydrogen molecule at a single internuclear distance specific to each state. With the use of the analytical energy gradient, the present calculations yield new, lowest-to-date, variational energy upper bounds for all four states. © 2013 American Institute of Physics. [<http://dx.doi.org/10.1063/1.4795094>]

I. INTRODUCTION

It is understood that to obtain a very accurate solution of an atomic or molecular electronic Schrödinger equation, the wave function needs to be expanded in terms of basis functions explicitly dependent on the interelectronic distances. Only such functions are capable in describing the correlated motion of the electrons in the system. The explicitly correlated Gaussian functions (ECGs) introduced by Boys¹ and Singer² in 1960 are examples of such functions. Due to the simplicity of the calculation of the Hamiltonian matrix elements with such functions for an arbitrary number of electrons, ECGs have become increasingly popular in very accurate quantum mechanical calculations of small atoms and molecules in the last 20 years. They have been successfully applied in very accurate atomic and molecular calculations performed with and without the assumption of the Born-Oppenheimer (BO) approximation for systems with various numbers of particles.³ The calculations include very accurate determination of BO potential energy surfaces (PESs) of two-electron,^{4,5} three-electron,^{6,7} and four-electron^{8,9} systems.

In recent years, we have developed and implemented several methods for more efficient generation of potential energy curves (PECs) of two-, three-, and four-electron diatomic molecular systems with σ electrons employing ECGs without angular premultipliers. Though these calculations have reproduced the experimental rovibrational transitions very accurately, small differences have still been shown between the theoretical and the experimental data. It has been clear that these differences are not caused by inaccuracies of the BO PECs but due to the exclusion of the nonadiabatic, relativistic, and quantum electrodynamic (QED) effects in the calculations. Thus it became apparent that to improve the accuracy of the molecular calculation, one should first calculate the adi-

abatic and nonadiabatic corrections to the BO energies to correct the deficiency arising from assuming the BO approximation. Second, as the nonrelativistic Schrödinger equation does not account for the magnetic interactions between particles, they need to be accounted for by calculating the relativistic corrections. Finally, one should also include the QED corrections which account for the interaction of the electrons with fluctuating electromagnetic field.

Implementation of the nonadiabatic corrections requires one to generate excited-state BO PECs.^{10,11} Also, in order to extend the BO ECG molecular calculations to larger systems and to widen the range of electronic states, ECGs which describe molecular systems with π electrons need to be implemented. In the present work we carry out the development of algorithms for such calculations.

Molecular BO calculation with ECGs require large amounts of computational resource. Building an adequate ECG basis set to achieve the desired high accuracy in the PEC/PES calculations and reoptimizing this basis set for each PEC point are the most time consuming steps in the PEC/PES calculations. We have demonstrated on several examples that the availability of the analytical energy gradient determined with respect to the Gaussian nonlinear parameters (the exponents and the coordinates of the shift vectors) greatly improves the effectiveness in the variational energy minimization with respect to those parameters. Also, with the gradient the rate of the energy convergence is faster and higher accuracy is achieved with fewer basis functions.

In the present work, algorithms for calculating energy gradient determined with respect to the nonlinear parameters of ECGs with floating centers used in calculating n -electron molecular systems with one π -electron are presented. The algorithms are tested in the calculations of some selected singlet and triplet Π states of the hydrogen molecule. With the use

of the gradient in the optimization we expect to obtain BO energies for the Π states as accurate as obtained before for Σ states. If this proves to be the case, PEC calculations for Π states of diatomic molecules with more than two electrons will be performed in future works. The future works will also include calculations of the PESs of Π states of some planar molecules such as, for example, the H_3^+ molecular ion.

II. BASIS FUNCTIONS

The spatial part of the electronic wave function representing the considered electronic state of the molecule is expanded as

$$\Psi(\mathbf{r}) = \sum_{k=1}^M c_k \phi_k(\mathbf{r}), \quad (1)$$

where M is the size of the basis set, c_k are the linear expansion coefficients, and for Π states of a linear or a planar molecule ϕ_k are the following all-electron ECGs with shifted centers (also called floating ECGs):

$$\phi_k(\mathbf{r}) = y_{m_k} \exp[-(\mathbf{r} - \mathbf{s}_k)'(A_k \otimes I_3)(\mathbf{r} - \mathbf{s}_k)]. \quad (2)$$

In Eq. (2), with n being the number of electrons, \mathbf{r} is the $3n$ -dimensional vector of the electron Cartesian coordinates, \mathbf{s}_k is a $3n$ -dimensional shift vector of the Gaussian centers, A_k is a $n \times n$ symmetric matrix, and y_{m_k} is one of the coordinates in the \mathbf{r} vector (m_k is an integer that depends on k with values from 1 to n). For a linear molecule the y_{m_k} coordinate has to be different than the coordinate along the molecular bonding axis (as the z coordinate is used here as the coordinate of the molecular bonding axis, y_{m_k} is either x or y coordinate of the m_k electron; without loss of generality we will assume that it is the y component).

To carry out matrix-vector multiplications related to the derivation of the Hamiltonian and overlap matrix elements, A_k is expanded to the size $3n \times 3n$ using the Kronecker product, \otimes , of A_k and the 3×3 identity matrix, I_3 . For $\phi_k(\mathbf{r})$ to be square integrable, A_k has to be a positive definite matrix³ which, in our approach, is achieved by representing A_k in the Cholesky-factorized form as: $A_k = L_k L_k'$, where L_k is a lower triangular matrix, and L_k' is its transpose. As A_k is positive definite for any values of the L_k matrix elements (i.e., these values can range from $-\infty$ to $+\infty$) it is convenient to use the L_k matrix elements as variational parameters in the calculation because their optimization can be carried out without any constraints. If A_k matrix elements were the variational parameters, constraints would need to be imposed on their values to keep A_k positive definite.

In the derivations we often use the following alternative representation of the basis function (2):

$$\begin{aligned} \phi_k &= \frac{\partial}{\partial \alpha_k} \exp[-(\mathbf{r} - \mathbf{s}_k)'(A_k \otimes I_3)(\mathbf{r} - \mathbf{s}_k) + \alpha_k y_{m_k}]|_{\alpha_k=0} \\ &= \frac{\partial}{\partial \alpha_k} \exp[-(\mathbf{r} - \mathbf{s}_k)'(A_k \otimes I_3)(\mathbf{r} - \mathbf{s}_k) + \alpha_k \mathbf{v}^k \mathbf{r}]|_{\alpha_k=0} \\ &= \frac{\partial}{\partial \alpha_k} \varphi_k|_{\alpha_k=0}, \end{aligned} \quad (3)$$

where ϕ_k is called generator function, α_k is a parameter, and \mathbf{v}^k is $3n$ vector whose all components are zero except the $3(m_k - 1) + 2$ component which is set to one. For example, if $n = 2$ and $m_k = 1$, the \mathbf{v}^k is

$$\mathbf{v}^k = \begin{pmatrix} 0 \\ 1 \\ 0 \\ 0 \\ 0 \\ 0 \end{pmatrix}. \quad (4)$$

III. PERMUTATIONAL SYMMETRY

The required antisymmetry of the wave function is implemented through appropriate symmetry projections applied to each basis function. As the so-called spin-free formalism is used in this work, the spatial symmetry projections need to be constructed. This is done using the Young projection operators, \hat{Y} , which are linear combinations of electron-pair permutational operators, \hat{P}_{ij} (for details of the formalism see, for example, Ref. 12). For the single states of the hydrogen molecule the Young operator is $\hat{Y} = (\hat{1} + \hat{P}_{12})$ and for the triplet state it is: $\hat{Y} = (\hat{1} - \hat{P}_{12})$, where \hat{P}_{ij} is the permutation operator of the spatial coordinates of the i th and j th electrons.

Under the BO approximation, the eigenfunctions of the Hamiltonian transform like irreducible representations of the point groups of the molecules. This is achieved by acting on each basis function with a projection operator for the particular irreducible representation of the point group to which the molecule belongs. In the present study of homonuclear diatomic molecule, such as H_2 , the electronic state that corresponds to ${}^1\Pi_g$ state has the *gerade* overall symmetry, the projection operator can be written as $\hat{P}_P = \hat{1} + \hat{i}$, where \hat{i} is the inversion operator. While for its ${}^1\Pi_u$ state, the corresponding projection operator is written as $\hat{P}_P = \hat{1} - \hat{i}$ to satisfy the *ungerade* overall symmetry. The projection operator is applied to each basis function, and action of the projection operator on the basis functions is similar to how the permutation operators do. Therefore, the permutation operator used in the present BO calculation is the product of operations belonging to the group of permutation of n electrons and elements of the point symmetry group the molecule belonging to¹³

$$\hat{P} = \hat{Y} \otimes \hat{P}_P. \quad (5)$$

As the Hamiltonian is invariant with respect to all permutations of the electronic labels, in the calculation of the Hamiltonian and overlap matrix elements \hat{P} is applied to the *ket* only. The operator can be represented as a permutation matrix, $\mathbf{P} = P \otimes I_3$, and the application of \hat{P} to the basis

functions gives

$$\begin{aligned}
 \hat{P}\phi_l &= \tilde{\phi}_l = \frac{\partial}{\partial \alpha_l} \tilde{\varphi}_l \Big|_{\alpha_l=0} \\
 &= \hat{P} \frac{\partial}{\partial \alpha_l} \exp[-(\mathbf{r} - \mathbf{s}_l)' \mathbf{A}_l (\mathbf{r} - \mathbf{s}_l) + \alpha_l (\mathbf{v}^l)' \mathbf{r}] \Big|_{\alpha_l=0} \\
 &= \frac{\partial}{\partial \alpha_l} \exp[-(\mathbf{Pr} - \mathbf{s}_l)' \mathbf{A}_l (\mathbf{Pr} - \mathbf{s}_l) + \alpha_l (\mathbf{v}^l)' (\mathbf{Pr})] \Big|_{\alpha_l=0} \\
 &= \frac{\partial}{\partial \alpha_l} \exp[-(\mathbf{Pr} - \mathbf{P}\mathbf{P}^{-1}\mathbf{s}_l)' \mathbf{A}_l (\mathbf{Pr} - \mathbf{P}\mathbf{P}^{-1}\mathbf{s}_l) \\
 &\quad + \alpha_l (\mathbf{P}'\mathbf{v}^l)' \mathbf{r}] \Big|_{\alpha_l=0} \\
 &= \frac{\partial}{\partial \alpha_l} \exp[-[\mathbf{P}(\mathbf{r} - \mathbf{P}^{-1}\mathbf{s}_l)]' \mathbf{A}_l [\mathbf{P}(\mathbf{r} - \mathbf{P}^{-1}\mathbf{s}_l)] \\
 &\quad + \alpha_l (\mathbf{P}'\mathbf{v}^l)' \mathbf{r}] \Big|_{\alpha_l=0} \\
 &= \frac{\partial}{\partial \alpha_l} \exp[-(\mathbf{r} - \mathbf{P}^{-1}\mathbf{s}_l)' \mathbf{P}' \mathbf{A}_l \mathbf{P} (\mathbf{r} - \mathbf{P}^{-1}\mathbf{s}_l) \\
 &\quad + \alpha_l (\mathbf{P}'\mathbf{v}^l)' \mathbf{r}] \Big|_{\alpha_l=0} \\
 &= \frac{\partial}{\partial \alpha_l} \exp[-(\mathbf{r} - \mathbf{Ps}_l)' \mathbf{P}' \mathbf{A}_l \mathbf{P} (\mathbf{r} - \mathbf{Ps}_l) + \alpha_l (\mathbf{P}'\mathbf{v}^l)' \mathbf{r}] \Big|_{\alpha_l=0}. \tag{6}
 \end{aligned}$$

IV. MATRIX ELEMENTS

The molecular integrals with Gaussians (2) have been published in different formats.¹⁴ The format used in this work is the most convenient for deriving the analytical energy gradient. Some definitions used in the integral formulae are

$$\begin{aligned}
 \tilde{\mathbf{v}}^l &= \mathbf{P}'\mathbf{v}^l, \\
 \tilde{\mathbf{A}}_l &= \mathbf{P}'\mathbf{A}_l\mathbf{P}, \\
 \tilde{\mathbf{A}}_{kl} &= \mathbf{A}_k + \tilde{\mathbf{A}}_l, \\
 \mathbf{A} &= \mathbf{A} \otimes \mathbf{I}_3, \\
 \mathbf{e}_k &= \mathbf{A}_k \mathbf{s}_k, \tilde{\mathbf{e}}_l = \tilde{\mathbf{A}}_l \tilde{\mathbf{s}}_l, \tilde{\mathbf{e}} = \mathbf{e}_k + \tilde{\mathbf{e}}_l, \\
 \tilde{\mathbf{s}} &= \tilde{\mathbf{A}}_{kl}^{-1} \tilde{\mathbf{e}}, \\
 \gamma &= -\mathbf{s}'_k \mathbf{A}_k \mathbf{s}_k - \tilde{\mathbf{s}}'_l \tilde{\mathbf{A}}_l \tilde{\mathbf{s}}_l + \tilde{\mathbf{e}}' \tilde{\mathbf{A}}_{kl}^{-1} \tilde{\mathbf{e}}. \tag{7}
 \end{aligned}$$

Terms used in the integrals and in the energy gradient with ECGs for molecular states with only σ electrons can be found in Ref. 3. The terms are used in the expressions for following integrals and the corresponding integral derivatives: \mathbf{S}_{kl}^Σ , \mathbf{T}_{kl}^Σ , $\mathbf{d}_{\mathbf{s}_k} \mathbf{S}_{kl}^\Sigma$, $\mathbf{d}_{\mathbf{s}_k} \mathbf{T}_{kl}^\Sigma$, $\mathbf{d}_k \mathbf{S}_{kl}^\Sigma$, and $\mathbf{d}_k \mathbf{T}_{kl}^\Sigma$.

The matrix elements with floating ECGs are evaluated using the following general p -dimensional integral:

$$\int_{-\infty}^{+\infty} \exp[-x'Ax + y'x] dx = \frac{\pi^{p/2}}{|A|^{1/2}} \exp\left[\frac{1}{4}y'A^{-1}y\right], \tag{8}$$

where x is a p -component vector of variable, A is a symmetric positive-definite $p \times p$ matrix, and y is a p -component constant vector. The matrix element of operator \hat{O} with the ECGs is evaluated as the following derivative of the corresponding matrix element expressed in terms of the generator functions:¹⁵

$$\langle \phi_k | \hat{O} | \tilde{\phi}_l \rangle = \frac{\partial}{\partial \alpha_k} \frac{\partial}{\partial \alpha_l} \langle \varphi_k | \hat{O} | \tilde{\varphi}_l \rangle \Big|_{\alpha_k, \alpha_l=0}, \tag{9}$$

where $\tilde{\phi}_l = \hat{P}\phi_l$ and $\tilde{\varphi}_l = \hat{P}\varphi_l$, and \hat{P} is the appropriate permutation operator.

A. Overlap integral

The derivation of the overlap integral is the simplest case for using Eq. (9). The first step in the derivation is the evaluation of the integral between two generator functions. This can be easily done by directly applying Eq. (8) to the product of the two generator functions involved in the overlap integral. We use the fact that $\tilde{\mathbf{A}}_{kl}^{-1} \equiv (\tilde{\mathbf{A}}_{kl} \otimes \mathbf{I}_3)^{-1} = \tilde{\mathbf{A}}_{kl}^{-1} \otimes \mathbf{I}_3$ and $|\tilde{\mathbf{A}}_{kl}| \equiv |\tilde{\mathbf{A}}_{kl} \otimes \mathbf{I}_3| = |\tilde{\mathbf{A}}_{kl}|^3$. The $\langle \phi_k | \tilde{\phi}_l \rangle$ integral can be obtained by differentiating $\langle \varphi_k | \tilde{\varphi}_l \rangle$ with respect to α_k and α_l , and setting both of these parameters to be zero at the end of the derivation.

$$\begin{aligned}
 \langle \phi_k | \tilde{\phi}_l \rangle &= \frac{\partial}{\partial \alpha_k} \frac{\partial}{\partial \alpha_l} \langle \varphi_k | \tilde{\varphi}_l \rangle \Big|_{\alpha_k, \alpha_l=0} \\
 &= \frac{\partial}{\partial \alpha_k} \frac{\partial}{\partial \alpha_l} \int_{-\infty}^{+\infty} \exp[-(\mathbf{r} - \mathbf{s}_k)' \mathbf{A}_k (\mathbf{r} - \mathbf{s}_k) \\
 &\quad + \alpha_k (\mathbf{v}^k)' \mathbf{r} - (\mathbf{r} - \tilde{\mathbf{s}}_l)' \tilde{\mathbf{A}}_l (\mathbf{r} - \tilde{\mathbf{s}}_l) + \alpha_l (\tilde{\mathbf{v}}^l)' \mathbf{r}] d\mathbf{r} \Big|_{\alpha_k, \alpha_l=0} \\
 &= \frac{\partial}{\partial \alpha_k} \frac{\partial}{\partial \alpha_l} \int_{-\infty}^{+\infty} \exp\left[-\mathbf{r}' \tilde{\mathbf{A}}_{kl} \mathbf{r} + 2\left(\mathbf{A}_k \mathbf{s}_k + \tilde{\mathbf{A}}_l \tilde{\mathbf{s}}_l \right. \right. \\
 &\quad \left. \left. + \frac{1}{2} \alpha_k \mathbf{v}^k + \frac{1}{2} \alpha_l \tilde{\mathbf{v}}^l \right)' \mathbf{r} \right] d\mathbf{r} \Big|_{\alpha_k, \alpha_l=0} \\
 &\quad \times \exp[-\mathbf{s}'_k \mathbf{A}_k \mathbf{s}_k - \tilde{\mathbf{s}}'_l \tilde{\mathbf{A}}_l \tilde{\mathbf{s}}_l] \\
 &= \left(\frac{\pi^n}{|\tilde{\mathbf{A}}_{kl}|} \right)^{3/2} \frac{\partial}{\partial \alpha_k} \frac{\partial}{\partial \alpha_l} \exp\left[\left(\tilde{\mathbf{e}} + \frac{1}{2} \alpha_k \mathbf{v}^k + \frac{1}{2} \alpha_l \tilde{\mathbf{v}}^l \right)' \right. \\
 &\quad \left. \times \tilde{\mathbf{A}}_{kl}^{-1} \left(\tilde{\mathbf{e}} + \frac{1}{2} \alpha_k \mathbf{v}^k + \frac{1}{2} \alpha_l \tilde{\mathbf{v}}^l \right) \right] \Big|_{\alpha_k, \alpha_l=0} \\
 &\quad \times \exp[-\mathbf{s}'_k \mathbf{A}_k \mathbf{s}_k - \tilde{\mathbf{s}}'_l \tilde{\mathbf{A}}_l \tilde{\mathbf{s}}_l] \\
 &= \left(\frac{\pi^n}{|\tilde{\mathbf{A}}_{kl}|} \right)^{3/2} \exp[\gamma] \left[\frac{1}{2} (\mathbf{v}^k)' \tilde{\mathbf{A}}_{kl}^{-1} \tilde{\mathbf{v}}^l + (\tilde{\mathbf{s}}' \mathbf{v}^k) (\tilde{\mathbf{s}}' \tilde{\mathbf{v}}^l) \right]. \tag{10}
 \end{aligned}$$

It is usually advantageous to use normalized ECGs in the derivation of the Hamiltonian and overlap matrix elements because with that the elements have similar magnitude which helps to make the calculation more numerically stable. The

overlap integral with the normalized ECGs is

$$\begin{aligned} S_{kl}^{\Pi} &= \frac{\langle \phi_k | \tilde{\phi}_l \rangle}{(\langle \phi_k | \phi_k \rangle \langle \tilde{\phi}_l | \tilde{\phi}_l \rangle)^{1/2}} \\ &= 2^{3n/2} \left(\frac{|A_k|^{1/2} |\tilde{A}_l|^{1/2}}{|\tilde{A}_{kl}|} \right)^{3/2} \exp[\gamma] \\ &\quad \times \left[\frac{1}{2} \mathbf{v}^k \tilde{\mathbf{A}}_{kl} \tilde{\mathbf{v}}^l + (\tilde{\mathbf{s}}' \mathbf{v}^k) (\tilde{\mathbf{s}}' \tilde{\mathbf{v}}^l) \right] \left[\frac{1}{4} \mathbf{v}^k \mathbf{A}_k \tilde{\mathbf{v}}^k + (\mathbf{s}'_k \mathbf{v}^k)^2 \right]^{-1/2} \\ &\quad \times \left[\frac{1}{4} \mathbf{v}^k \tilde{\mathbf{A}}_l \tilde{\mathbf{v}}^l + (\tilde{\mathbf{s}}'_l \tilde{\mathbf{v}}^l)^2 \right]^{-1/2} \\ &= S_{kl}^{\Sigma} \left[\frac{1}{2} \mathbf{v}^k \tilde{\mathbf{A}}_{kl} \tilde{\mathbf{v}}^l + (\tilde{\mathbf{s}}' \mathbf{v}^k) (\tilde{\mathbf{s}}' \tilde{\mathbf{v}}^l) \right] \left[\frac{1}{4} \mathbf{v}^k \mathbf{A}_k \tilde{\mathbf{v}}^k + (\mathbf{s}'_k \mathbf{v}^k)^2 \right]^{-1/2} \\ &\quad \times \left[\frac{1}{4} \mathbf{v}^k \tilde{\mathbf{A}}_l \tilde{\mathbf{v}}^l + (\tilde{\mathbf{s}}'_l \tilde{\mathbf{v}}^l)^2 \right]^{-1/2}. \end{aligned} \quad (11)$$

As shown in the above equation, the terms which are identical to those appearing in the integrals with σ ECGs are collecting together and denoted by superscript Σ . We use the notation throughout this work. For example, the overlap with σ ECGs is denoted as S_{kl}^{Σ} , the kinetic energy integral as \mathbf{T}_{kl}^{Σ} , the derivative of S_{kl}^{Σ} with respect to \mathbf{s}_k as $d_{\mathbf{s}_k} S_{kl}^{\Sigma}$, the derivative of \mathbf{T}_{kl}^{Σ} with respect to \mathbf{s}_k as $d_{\mathbf{s}_k} \mathbf{T}_{kl}^{\Sigma}$, the derivative of S_{kl}^{Σ} with respect to \mathbf{A}_k as $d_k S_{kl}^{\Sigma}$, and the derivative of \mathbf{T}_{kl}^{Σ} with respect to \mathbf{A}_k as $d_k \mathbf{T}_{kl}^{\Sigma}$. These quantities can be found in Ref. 3.

B. Kinetic energy integral

The derivation of the kinetic energy integral follows the derivation of the overlap integral. The kinetic energy operator is

$$T = -\frac{1}{2} \nabla_{\mathbf{r}}' \nabla_{\mathbf{r}}, \quad (12)$$

where subscript \mathbf{r} denotes the gradient with respect to all $3n$ coordinates of n electrons. Thus the integral is

$$\begin{aligned} T_{kl}^{\Pi} &= -\frac{1}{2} \langle \phi_k | \nabla_{\mathbf{r}}' \nabla_{\mathbf{r}} | \tilde{\phi}_l \rangle = \frac{1}{2} \langle \nabla_{\mathbf{r}}' \phi_k | \nabla_{\mathbf{r}} \tilde{\phi}_l \rangle \\ &= \frac{1}{2} \frac{\partial}{\partial \alpha_k} \frac{\partial}{\partial \alpha_l} \langle \nabla_{\mathbf{r}}' \phi_k | \nabla_{\mathbf{r}} \tilde{\phi}_l \rangle \Big|_{\alpha_k, \alpha_l=0}. \end{aligned} \quad (13)$$

The gradient operator acting on the generator functions ϕ_k gives

$$\nabla_{\mathbf{r}} \phi_k = (-2 \mathbf{A}_k \mathbf{r} + 2 \mathbf{A}_k \mathbf{s}_k + \alpha_l \mathbf{v}^k) \phi_k. \quad (14)$$

Plugging Eq. (14) and the corresponding term for $\nabla_{\mathbf{r}} \tilde{\phi}_l$ into $\langle \nabla_{\mathbf{r}}' \phi_k | \nabla_{\mathbf{r}} \tilde{\phi}_l \rangle$ gives the following nine integrals:

$$\begin{aligned} \langle \nabla_{\mathbf{r}}' \phi_k | \nabla_{\mathbf{r}} \tilde{\phi}_l \rangle &= 4 \langle \phi_k | \mathbf{r}' \mathbf{A}_k \tilde{\mathbf{A}}_l \mathbf{r} | \tilde{\phi}_l \rangle \\ &\quad - 4 \langle \phi_k | \mathbf{r}' \mathbf{A}_k \tilde{\mathbf{A}}_l \tilde{\mathbf{s}}_l | \tilde{\phi}_l \rangle - 2 \langle \phi_k | \alpha_l \mathbf{r}' \mathbf{A}_k \tilde{\mathbf{v}}^l | \tilde{\phi}_l \rangle \\ &\quad - 4 \langle \phi_k | \mathbf{s}'_k \mathbf{A}_k \tilde{\mathbf{A}}_l \mathbf{r} | \tilde{\phi}_l \rangle + 4 \langle \phi_k | \mathbf{s}'_k \mathbf{A}_k \tilde{\mathbf{A}}_l \tilde{\mathbf{s}}_l | \tilde{\phi}_l \rangle \\ &\quad + 2 \langle \phi_k | \alpha_l \mathbf{s}'_k \mathbf{A}_k \tilde{\mathbf{v}}^l | \tilde{\phi}_l \rangle - 2 \langle \phi_k | \alpha_k \mathbf{v}^k \tilde{\mathbf{A}}_l \mathbf{r} | \tilde{\phi}_l \rangle \\ &\quad + 2 \langle \phi_k | \alpha_k \mathbf{v}^k \tilde{\mathbf{A}}_l \tilde{\mathbf{s}}_l | \tilde{\phi}_l \rangle + \langle \phi_k | \alpha_k \alpha_l \mathbf{v}^k \tilde{\mathbf{v}}^l | \tilde{\phi}_l \rangle. \end{aligned} \quad (15)$$

In order to use Eq. (8) for calculating the integrals in (15), one needs to make the term which appear in each integral between the vertical bars to be exponentiated. This can be done using the transformation described in Eq. (3). This leads to the following:

$$\langle \phi_k | C | \tilde{\phi}_l \rangle = -\frac{\partial}{\partial \beta} \langle \phi_k | \exp[-\beta C] | \tilde{\phi}_l \rangle \Big|_{\beta=0}, \quad (16)$$

where C can be a matrix, a vector, or a scalar. If it is a matrix, it must be symmetric. Therefore, in the first step one uses Eq. (16) to represent the integrals in Eq. (15). Then each integral is evaluated separately with a similar procedure as used in Eq. (10). In the first integral the product $\mathbf{A}_k \tilde{\mathbf{A}}_l$ is, in general, not symmetric and must be symmetrized before the integration is performed. To do that the following equality is used: $\mathbf{r}'(\mathbf{A}_k \tilde{\mathbf{A}}_l) \mathbf{r} = \frac{1}{2} \mathbf{r}'(\mathbf{A}_k \tilde{\mathbf{A}}_l + \mathbf{A}_l \tilde{\mathbf{A}}_k) \mathbf{r}$, which is true for any quadratic form. With that we have

$$\begin{aligned} &\frac{\partial}{\partial \alpha_k} \frac{\partial}{\partial \alpha_l} \left\langle \phi_k \left| \frac{\mathbf{r}'(\mathbf{A}_k \tilde{\mathbf{A}}_l + \tilde{\mathbf{A}}_l \mathbf{A}_k) \mathbf{r}}{2} \right| \tilde{\phi}_l \right\rangle \Big|_{\alpha_k, \alpha_l=0} \\ &= \pi^{3n/2} |\tilde{A}_{kl}|^{-3/2} \exp[\gamma] \\ &\quad \times \left\{ \left(\frac{3}{2} \text{tr} [\tilde{A}_{kl}^{-1} A_k \tilde{A}_l] + \tilde{\mathbf{s}}' \mathbf{A}_k \tilde{\mathbf{A}}_l \tilde{\mathbf{s}} \right) \right. \\ &\quad \times \left(\frac{1}{2} \mathbf{v}^k \tilde{\mathbf{A}}_{kl}^{-1} \tilde{\mathbf{v}}^l + (\tilde{\mathbf{s}}' \tilde{\mathbf{v}}^l) (\tilde{\mathbf{s}}' \mathbf{v}^k) \right) \\ &\quad + \frac{1}{4} \tilde{\mathbf{v}}'^l \tilde{\mathbf{A}}_{kl}^{-1} \mathbf{A}_k \tilde{\mathbf{A}}_l \tilde{\mathbf{A}}_{kl}^{-1} \mathbf{v}^k + \frac{1}{4} \mathbf{v}^k \tilde{\mathbf{A}}_{kl}^{-1} \mathbf{A}_k \tilde{\mathbf{A}}_l \tilde{\mathbf{A}}_{kl}^{-1} \tilde{\mathbf{v}}^l \\ &\quad + \left(\frac{1}{2} \mathbf{v}^k \tilde{\mathbf{A}}_{kl}^{-1} \mathbf{A}_k \tilde{\mathbf{A}}_l \tilde{\mathbf{s}} + \frac{1}{2} \tilde{\mathbf{s}}' \mathbf{A}_k \tilde{\mathbf{A}}_l \tilde{\mathbf{A}}_{kl}^{-1} \mathbf{v}^k \right) (\tilde{\mathbf{s}}' \tilde{\mathbf{v}}^l) \\ &\quad \left. + \left(\frac{1}{2} \tilde{\mathbf{v}}'^l \tilde{\mathbf{A}}_{kl}^{-1} \mathbf{A}_k \tilde{\mathbf{A}}_l \tilde{\mathbf{s}} + \frac{1}{2} \tilde{\mathbf{s}}' \mathbf{A}_k \tilde{\mathbf{A}}_l \tilde{\mathbf{A}}_{kl}^{-1} \tilde{\mathbf{v}}^l \right) (\tilde{\mathbf{s}}' \mathbf{v}^k) \right\}. \end{aligned} \quad (17)$$

The other integrals in (15) involve vectors so no additional complication arises. These integrals can be evaluated directly using (16). The integrals are

$$\begin{aligned} &\frac{\partial}{\partial \alpha_k} \frac{\partial}{\partial \alpha_l} \langle \phi_k | \mathbf{r}' \mathbf{A}_k \tilde{\mathbf{A}}_l \tilde{\mathbf{s}}_l | \tilde{\phi}_l \rangle \Big|_{\alpha_k, \alpha_l=0} \\ &= \pi^{3n/2} |\tilde{A}_{kl}|^{-3/2} \exp[\gamma] \left\{ \frac{1}{2} (\mathbf{v}^k \tilde{\mathbf{A}}_{kl}^{-1} \mathbf{A}_k \tilde{\mathbf{A}}_l \tilde{\mathbf{s}}_l) (\tilde{\mathbf{s}}' \tilde{\mathbf{v}}^k) \right. \\ &\quad + \frac{1}{2} (\tilde{\mathbf{v}}'^l \tilde{\mathbf{A}}_{kl}^{-1} \mathbf{A}_k \tilde{\mathbf{A}}_l \tilde{\mathbf{s}}_l) (\tilde{\mathbf{s}}' \mathbf{v}^k) \\ &\quad \left. + (\tilde{\mathbf{s}}' \mathbf{A}_k \tilde{\mathbf{A}}_l \tilde{\mathbf{s}}_l) \left[(\tilde{\mathbf{s}}' \tilde{\mathbf{v}}^l) (\tilde{\mathbf{s}}' \mathbf{v}^k) + \frac{1}{2} \mathbf{v}^k \tilde{\mathbf{A}}_{kl}^{-1} \tilde{\mathbf{v}}^l \right] \right\}, \end{aligned} \quad (18)$$

$$\begin{aligned} &\frac{\partial}{\partial \alpha_k} \frac{\partial}{\partial \alpha_l} \langle \phi_k | \alpha_l \mathbf{r}' \mathbf{A}_k \tilde{\mathbf{v}}^l | \tilde{\phi}_l \rangle \Big|_{\alpha_k, \alpha_l=0} \\ &= \pi^{3n/2} |\tilde{A}_{kl}|^{-3/2} \exp[\gamma] \left[\frac{1}{2} \mathbf{v}^k \tilde{\mathbf{A}}_{kl}^{-1} \mathbf{A}_k \tilde{\mathbf{v}}^l + (\tilde{\mathbf{s}}' \mathbf{A}_k \tilde{\mathbf{v}}^l) (\tilde{\mathbf{s}}' \mathbf{v}^k) \right], \end{aligned} \quad (19)$$

$$\begin{aligned} & \frac{\partial}{\partial \alpha_k} \frac{\partial}{\partial \alpha_l} \langle \varphi_k | \mathbf{s}'_k \mathbf{A}_k \tilde{\mathbf{A}}_l \mathbf{r} | \tilde{\varphi}_l \rangle \Big|_{\alpha_k, \alpha_l=0} \\ &= \pi^{3n/2} |\tilde{\mathbf{A}}_{kl}|^{-3/2} \exp[\gamma] \left\{ \frac{1}{2} (\mathbf{v}'^k \tilde{\mathbf{A}}_{kl}^{-1} \tilde{\mathbf{A}}_l \mathbf{A}_k \mathbf{s}_k) (\tilde{\mathbf{s}}' \tilde{\mathbf{v}}^k) \right. \\ & \quad \left. + \frac{1}{2} (\tilde{\mathbf{v}}'^l \tilde{\mathbf{A}}_{kl}^{-1} \tilde{\mathbf{A}}_l \mathbf{A}_k \mathbf{s}_k) (\tilde{\mathbf{s}}' \mathbf{v}^k) \right. \\ & \quad \left. + (\tilde{\mathbf{s}}' \tilde{\mathbf{A}}_l \mathbf{A}_k \mathbf{s}_k) \left[\frac{1}{2} \tilde{\mathbf{v}}'^l \tilde{\mathbf{A}}_{kl}^{-1} \mathbf{v}^k + (\tilde{\mathbf{s}}' \tilde{\mathbf{v}}^l) (\tilde{\mathbf{s}}' \mathbf{v}^k) \right] \right\}, \quad (20) \end{aligned}$$

$$\begin{aligned} & \frac{\partial}{\partial \alpha_k} \frac{\partial}{\partial \alpha_l} \langle \varphi_k | \mathbf{s}'_k \mathbf{A}_k \tilde{\mathbf{A}}_l \tilde{\mathbf{s}}_l | \tilde{\varphi}_l \rangle \Big|_{\alpha_k, \alpha_l=0} \\ &= \pi^{3n/2} |\tilde{\mathbf{A}}_{kl}|^{-3/2} \exp[\gamma] (\mathbf{s}'_k \mathbf{A}_k \tilde{\mathbf{A}}_l \tilde{\mathbf{s}}_l) \\ & \quad \times \left[\frac{1}{2} \tilde{\mathbf{v}}'^l \tilde{\mathbf{A}}_{kl}^{-1} \mathbf{v}^k + (\tilde{\mathbf{s}}' \tilde{\mathbf{v}}^l) (\tilde{\mathbf{s}}' \mathbf{v}^k) \right], \quad (21) \end{aligned}$$

$$\begin{aligned} & \frac{\partial}{\partial \alpha_k} \frac{\partial}{\partial \alpha_l} \langle \varphi_k | \alpha_l \mathbf{s}'_k \mathbf{A}_k \tilde{\mathbf{v}}^l | \tilde{\varphi}_l \rangle \Big|_{\alpha_k, \alpha_l=0} \\ &= \pi^{3n/2} |\tilde{\mathbf{A}}_{kl}|^{-3/2} \exp[\gamma] (\mathbf{s}'_k \mathbf{A}_k \tilde{\mathbf{v}}^l) (\tilde{\mathbf{s}}' \mathbf{v}^k), \quad (22) \end{aligned}$$

$$\begin{aligned} & \frac{\partial}{\partial \alpha_k} \frac{\partial}{\partial \alpha_l} \langle \varphi_k | \alpha_k \mathbf{v}^k \tilde{\mathbf{A}}_l \mathbf{r} | \tilde{\varphi}_l \rangle \Big|_{\alpha_k, \alpha_l=0} \\ &= \pi^{3n/2} |\tilde{\mathbf{A}}_{kl}|^{-3/2} \exp[\gamma] \left[\frac{1}{2} \mathbf{v}'^l \tilde{\mathbf{A}}_{kl}^{-1} \tilde{\mathbf{A}}_l \mathbf{v}^k + (\tilde{\mathbf{s}}' \tilde{\mathbf{A}}_l \mathbf{v}^k) (\tilde{\mathbf{s}}' \tilde{\mathbf{v}}^l) \right], \quad (23) \end{aligned}$$

$$\begin{aligned} & \frac{\partial}{\partial \alpha_k} \frac{\partial}{\partial \alpha_l} \langle \phi_k | \alpha_k \alpha_l \mathbf{v}^k \tilde{\mathbf{v}}^l | \tilde{\varphi}_l \rangle \Big|_{\alpha_k, \alpha_l=0} \\ &= \pi^{3n/2} |\tilde{\mathbf{A}}_{kl}|^{-3/2} \exp[\gamma] (\mathbf{v}^k \tilde{\mathbf{A}}_l \tilde{\mathbf{s}}_l) (\tilde{\mathbf{s}}' \tilde{\mathbf{v}}^l), \quad (24) \end{aligned}$$

$$\begin{aligned} & \frac{\partial}{\partial \alpha_k} \frac{\partial}{\partial \alpha_l} \langle \phi_k | \alpha_k \alpha_l \mathbf{v}^k \tilde{\mathbf{v}}^l | \tilde{\varphi}_l \rangle \Big|_{\alpha_k, \alpha_l=0} = \pi^{3n/2} |\tilde{\mathbf{A}}_{kl}|^{-3/2} \\ & \quad \times \exp[\gamma] (\mathbf{v}^k \tilde{\mathbf{v}}^l). \quad (25) \end{aligned}$$

By applying Eq. (9)–(15), plugging above integrals into it, and with some rearrangement of the terms, the kinetic energy integral for two normalized ECGs is

$$\begin{aligned} \mathbf{T}_{kl}^{\Pi} &= \frac{1}{2} \{ \mathbf{S}_{kl}^{\Sigma} [(\tilde{\mathbf{s}}' \mathbf{v}^k) (2\tilde{\mathbf{v}}'^l \tilde{\mathbf{A}}_{kl}^{-1} \mathbf{A}_k \tilde{\mathbf{A}}_l \tilde{\mathbf{s}} + 2\tilde{\mathbf{s}}' \mathbf{A}_k \tilde{\mathbf{A}}_l \tilde{\mathbf{A}}_{kl}^{-1} \mathbf{v}^l \\ & \quad - 2\tilde{\mathbf{v}}'^l \tilde{\mathbf{A}}_{kl}^{-1} \mathbf{A}_k \tilde{\mathbf{e}}_l - 2\tilde{\mathbf{v}}'^l \tilde{\mathbf{A}}_{kl}^{-1} \tilde{\mathbf{A}}_l \mathbf{e}_k \\ & \quad - 2\tilde{\mathbf{s}}' \mathbf{A}_k \tilde{\mathbf{v}}^l + 2\mathbf{e}'_k \tilde{\mathbf{v}}^l) + (\tilde{\mathbf{s}}' \mathbf{v}^l) (2\mathbf{v}^k \tilde{\mathbf{A}}_{kl}^{-1} \mathbf{A}_k \tilde{\mathbf{A}}_l \tilde{\mathbf{e}}_l \\ & \quad + 2\tilde{\mathbf{s}}' \mathbf{A}_k \tilde{\mathbf{A}}_l \tilde{\mathbf{A}}_{kl}^{-1} \tilde{\mathbf{v}}^k - 2\mathbf{v}^k \tilde{\mathbf{A}}_{kl}^{-1} \mathbf{A}_k \tilde{\mathbf{e}}_l \\ & \quad - 2\mathbf{v}^k \tilde{\mathbf{A}}_{kl}^{-1} \tilde{\mathbf{A}}_l \mathbf{e}_k - 2\tilde{\mathbf{s}}' \tilde{\mathbf{A}}_l \mathbf{v}^k \\ & \quad + 2\mathbf{v}^k \tilde{\mathbf{e}}_l) + \tilde{\mathbf{v}}'^l \tilde{\mathbf{A}}_{kl}^{-1} \mathbf{A}_k \tilde{\mathbf{A}}_l \tilde{\mathbf{A}}_{kl}^{-1} \mathbf{v}^k + \mathbf{v}^k \tilde{\mathbf{A}}_{kl}^{-1} \mathbf{A}_k \tilde{\mathbf{A}}_l \tilde{\mathbf{A}}_{kl}^{-1} \tilde{\mathbf{v}}^l \\ & \quad - \mathbf{v}^k \tilde{\mathbf{A}}_{kl}^{-1} \mathbf{A}_k \tilde{\mathbf{v}}^l - \tilde{\mathbf{v}}'^l \tilde{\mathbf{A}}_{kl}^{-1} \tilde{\mathbf{A}}_l \mathbf{v}^k + \mathbf{v}^k \tilde{\mathbf{v}}^l] \\ & \quad + \mathbf{T}_{kl}^{\Sigma} [\mathbf{v}^k \tilde{\mathbf{A}}_{kl}^{-1} \tilde{\mathbf{v}}^l + 2(\tilde{\mathbf{s}}' \mathbf{v}^k) (\tilde{\mathbf{s}}' \tilde{\mathbf{v}}^l)] \} \\ & \quad \times \left[\frac{1}{4} \mathbf{v}^k \tilde{\mathbf{A}}_{kl}^{-1} \mathbf{v}^k + (\mathbf{v}^k \mathbf{s}_k)^2 \right]^{-1/2} \\ & \quad \times \left[\frac{1}{4} \tilde{\mathbf{v}}'^l \tilde{\mathbf{A}}_l^{-1} \tilde{\mathbf{v}}^l + (\tilde{\mathbf{v}}'^l \tilde{\mathbf{s}}_l)^2 \right]^{-1/2}. \quad (26) \end{aligned}$$

C. Potential energy integral

Two potential energy integral, the electron repulsion integral and the nuclear attraction integral, are derived in a similar way as

$$\mathbf{V}_{kl,ij}^{\Pi} = \left\langle \phi_k \left| \frac{1}{r_{ij}} \right| \tilde{\varphi}_l \right\rangle = \frac{\partial}{\partial \alpha_k} \frac{\partial}{\partial \alpha_l} \left\langle \varphi_k \left| \frac{1}{r_{ij}} \right| \tilde{\varphi}_l \right\rangle \Big|_{\alpha_k=\alpha_l=0}, \quad (27)$$

where the $1/r_{ij}$ can be represented by the following Gaussian transformation:

$$\begin{aligned} \frac{1}{r_{ij}} &= \frac{2}{\pi^{1/2}} \int_{-\infty}^{\infty} \exp[-u^2 r_{ij}^2] du \\ &= \frac{1}{\pi^{1/2}} \int_{-\infty}^{\infty} \exp[-u^2 \mathbf{r}' \mathbf{J}_{ij} \mathbf{r}] du. \quad (28) \end{aligned}$$

The matrix $\mathbf{J}_{ij} = J_{ij} \otimes \mathbf{I}_3$ has the matrix elements, J_{ij} , defined as

$$J_{ij} = \begin{cases} E_{ii} & \text{if } i = j \\ E_{ii} + E_{jj} - E_{ij} - E_{ji} & \text{if } i \neq j \end{cases}. \quad (29)$$

In order to apply a similar procedure as used to derive the potential energy integral with σ ECGs, we define the following two vectors and a scalar:

$$\begin{aligned} \mathbf{e}^p &= \mathbf{A}_k \mathbf{s}_k + \tilde{\mathbf{A}}_l \tilde{\mathbf{s}}_l + \frac{1}{2} \alpha_k \mathbf{v}^k + \frac{1}{2} \alpha_l \tilde{\mathbf{v}}^l, \\ \mathbf{s}^p &= \tilde{\mathbf{A}}_{kl}^{-1} \tilde{\mathbf{e}}^p, \\ \gamma^p &= -\mathbf{s}'_k \mathbf{A}_k \mathbf{s}_k - \tilde{\mathbf{s}}'_l \tilde{\mathbf{A}}_l \tilde{\mathbf{s}}_l + \tilde{\mathbf{e}}^p \tilde{\mathbf{A}}_{kl}^{-1} \tilde{\mathbf{e}}^p, \end{aligned} \quad (30)$$

and rearrange $\varphi_k \tilde{\varphi}_l$ to the following form:

$$\varphi_k \tilde{\varphi}_l = \exp[(\mathbf{r} - \tilde{\mathbf{s}}^p)' \tilde{\mathbf{A}}_{kl} (\mathbf{r} - \tilde{\mathbf{s}}^p) + \gamma^p]. \quad (31)$$

Now, by plugging Eqs. (28) and (31) into Eq. (27), the expression obtained in Eq. (32) is the same as the starting point of the derivation of $\mathbf{V}_{kl,ij}^{\Sigma}$. $\alpha_k \mathbf{v}^k$ and $\alpha_l \mathbf{v}^l$ are absorbed in $\tilde{\mathbf{s}}^p$. Therefore, one can apply the same procedure to derive the $\mathbf{V}_{kl,ij}^{\Pi}$ integral as used before to derive the $\mathbf{V}_{kl,ij}^{\Sigma}$ integral³ and we get

$$\begin{aligned} \left\langle \varphi_k \left| \frac{1}{r_{ij}} \right| \varphi_l \right\rangle &= \frac{2}{\pi^{1/2}} \exp[\gamma^p] \int_0^{+\infty} \int_{-\infty}^{+\infty} \\ & \quad \times \exp[-(\mathbf{r} - \tilde{\mathbf{s}}^p)' \tilde{\mathbf{A}}_{kl} (\mathbf{r} - \tilde{\mathbf{s}}^p) - u^2 \mathbf{r}' \mathbf{J}_{ij} \mathbf{r}] d\mathbf{r} du \\ &= \frac{2}{\pi^{1/2}} \exp[\gamma^p] \exp[-\tilde{\mathbf{s}}^p \tilde{\mathbf{A}}_{kl}^{-1} \tilde{\mathbf{s}}^p] \\ & \quad \times \int_0^{+\infty} \int_{-\infty}^{+\infty} \exp[-\mathbf{r}' (\tilde{\mathbf{A}}_{kl} + u^2 \mathbf{J}_{ij}) \mathbf{r}] \\ & \quad - 2(\tilde{\mathbf{A}}_{kl} \tilde{\mathbf{s}}^p)' \mathbf{r}] d\mathbf{r} du \\ &= 2\pi^{(3n-1)/2} \exp[\gamma^p] \exp[-\tilde{\mathbf{s}}^p \tilde{\mathbf{A}}_{kl}^{-1} \tilde{\mathbf{s}}^p] \\ & \quad \times \int_0^{+\infty} |\tilde{\mathbf{A}}_{kl} + u^2 \mathbf{J}_{ij}|^{-3/2} \\ & \quad \times \exp[\tilde{\mathbf{s}}^p \tilde{\mathbf{A}}_{kl} (\tilde{\mathbf{A}}_{kl} + u^2 \mathbf{J}_{ij})^{-1} \tilde{\mathbf{A}}_{kl} \tilde{\mathbf{s}}^p] du. \quad (32) \end{aligned}$$

The determinant in the above formula can be written as

$$\begin{aligned} |\tilde{A}_{kl} + u^2 J_{ij}| &= |\tilde{A}_{kl}| |I + u^2 \tilde{A}_{kl}^{-1} J_{ij}| \\ &= |\tilde{A}_{kl}| (1 + u^2 \text{tr}[J_{ij} \tilde{A}_{kl}^{-1}]), \end{aligned} \quad (33)$$

where I is the $n \times n$ identity matrix. We use the fact that $(\mathbf{A} + \mathbf{B})^{-1} = (A + B)^{-1} \otimes I_3$. The inverse term in Eq. (32) is evaluated by using the Sherman-Morrison formula, which states that for an arbitrary invertible matrix X and vectors y and z , such that $1 + z'X^{-1}y \neq 0$, the following applies:

$$(X + yz')^{-1} = X^{-1} - \frac{X^{-1}yz'X^{-1}}{1 + z'X^{-1}y}. \quad (34)$$

The matrices J_{ii} and J_{ij} can be represented as¹⁵

$$j^i(j^i)' = J_{ii}, (j^j - j^i)(j^j - j^i)' = J_{ij}, \quad (35)$$

where j^i is an n -component vector whose i th component is one, while all others are zero. With that, we can rewrite the inverse term in Eq. (32) as

$$\begin{aligned} (\tilde{A}_{kl} + u^2 J_{ij})^{-1} &= \tilde{A}_{kl}^{-1} - \frac{u^2 \tilde{A}_{kl}^{-1}(j^j - j^i)(j^j - j^i)' \tilde{A}_{kl}^{-1}}{1 + u^2 (j^j - j^i)' \tilde{A}_{kl}^{-1} (j^j - j^i)} \\ &= \tilde{A}_{kl}^{-1} - \frac{u^2 \tilde{A}_{kl}^{-1} J_{ij} \tilde{A}_{kl}^{-1}}{1 + u^2 \text{tr}[J_{ij} \tilde{A}_{kl}^{-1}]} \end{aligned} \quad (36)$$

Hence,

$$\begin{aligned} \left\langle \varphi_k \left| \frac{1}{r_{ij}} \right| \varphi_l \right\rangle &= 2\pi |\tilde{A}_{kl}|^{-3/2} \exp[\gamma] \\ &\times \int_0^{+\infty} (1 + u^2 \text{tr}[J_{ij} \tilde{A}_{kl}^{-1}])^{-3/2} \\ &\times \exp \left[-\frac{u^2 \tilde{s}' \mathbf{J}_{ij} \tilde{s}^p}{1 + u^2 \text{tr}[J_{ij} \tilde{A}_{kl}^{-1}]} \right] du. \end{aligned} \quad (37)$$

The integral in the above equation can be converted to the error function using the following identity:

$$\begin{aligned} \int_0^{+\infty} (1 + \alpha u^2)^{-3/2} \exp \left[-\frac{\beta u^2}{1 + \alpha u^2} \right] du \\ = \frac{\pi^{1/2}}{2\beta^{1/2}} \text{erf} \left[\left(\frac{\beta}{\alpha} \right)^{1/2} \right]. \end{aligned} \quad (38)$$

With this, we get

$$\begin{aligned} \left\langle \varphi_k \left| \frac{1}{r_{ij}} \right| \varphi_l \right\rangle &= \pi^{3n/2} |\tilde{A}_{kl}|^{-3/2} \exp[\gamma] \frac{1}{(\tilde{s}' \mathbf{J}_{ij} \tilde{s}^p)^{1/2}} \\ &\times \text{erf} \left[\left(\frac{\tilde{s}' \mathbf{J}_{ij} \tilde{s}^p}{\text{tr}[J_{ij} \tilde{A}_{kl}^{-1}]} \right)^{1/2} \right]. \end{aligned} \quad (39)$$

Now, we use the following identity to convert the error function to the F_0 function

$$F_0[t] = \frac{1}{2} \left(\frac{\pi}{t} \right)^{1/2} \text{erf}[t^{1/2}]. \quad (40)$$

Hence,

$$\begin{aligned} \left\langle \varphi_k \left| \frac{1}{r_{ij}} \right| \varphi_l \right\rangle &= 2\pi^{(3n-1)/2} |\tilde{A}_{kl}|^{-3/2} \exp[\gamma] (\text{tr}[J_{ij} \tilde{A}_{kl}^{-1}])^{-1/2} \\ &\times F_0 \left[\frac{\tilde{s}' \mathbf{J}_{ij} \tilde{s}^p}{\text{tr}[J_{ij} \tilde{A}_{kl}^{-1}]} \right]. \end{aligned} \quad (41)$$

We now differentiate the above equation with respect to the parameters α_k and α_l and set both parameters to be zero. With some rearrangement, the electron repulsion integral over normalized ECGs is

$$\begin{aligned} ER_{kl,ij}^{\Pi} &= \frac{2}{(\pi\alpha)^{1/2}} S_{kl}^{\Sigma} \left\{ \left[\frac{1}{2} \mathbf{v}' \tilde{\mathbf{A}}_{kl}^{-1} \mathbf{v}^l + (\tilde{\mathbf{s}}' \mathbf{v}^k)(\tilde{\mathbf{s}}' \mathbf{v}^l) \right] F_0 \left[\frac{\rho}{\alpha} \right] \right. \\ &+ \left[(\tilde{\mathbf{s}}' \mathbf{v}^k) \left(\frac{\tilde{\mathbf{s}}' \mathbf{J}_{ij} \tilde{\mathbf{A}}_{kl}^{-1} \tilde{\mathbf{v}}^l}{\alpha} \right) + (\tilde{\mathbf{s}}' \tilde{\mathbf{v}}^l) \left(\frac{\tilde{\mathbf{s}}' \mathbf{J}_{ij} \tilde{\mathbf{A}}_{kl}^{-1} \mathbf{v}^k}{\alpha} \right) \right. \\ &+ \left. \left. + \frac{\mathbf{v}' \tilde{\mathbf{A}}_{kl}^{-1} \mathbf{J}_{ij} \tilde{\mathbf{A}}_{kl}^{-1} \mathbf{v}^l}{2\alpha} \right] F_1 \left[\frac{\rho}{\alpha} \right] \right. \\ &+ \left. \left. + \left(\frac{\tilde{\mathbf{s}}' \mathbf{J}_{ij} \tilde{\mathbf{A}}_{kl}^{-1} \tilde{\mathbf{v}}^l}{\alpha} \right) \left(\frac{\tilde{\mathbf{s}}' \mathbf{J}_{ij} \tilde{\mathbf{A}}_{kl}^{-1} \mathbf{v}^k}{\alpha} \right) F_2 \left[\frac{\rho}{\alpha} \right] \right\} \right. \\ &\times \left[\frac{1}{4} \mathbf{v}' \tilde{\mathbf{A}}_{kl}^{-1} \mathbf{v}^k + (\mathbf{v}' \mathbf{s}_k)(\mathbf{v}' \mathbf{s}_k) \right]^{-1/2} \\ &\times \left[\frac{1}{4} \tilde{\mathbf{v}}'^l \tilde{\mathbf{A}}_{kl}^{-1} \tilde{\mathbf{v}}^l + (\tilde{\mathbf{v}}'^l \tilde{\mathbf{s}}_l)(\tilde{\mathbf{v}}'^l \tilde{\mathbf{s}}_l) \right]^{-1/2}, \end{aligned} \quad (42)$$

where α and ρ in this case (i.e., for the electron repulsion integral) are $\alpha = \text{tr}[J_{ij} \tilde{A}_{kl}^{-1}]$ and $\rho = \tilde{\mathbf{s}}' \mathbf{J}_{ij} \tilde{\mathbf{s}}$.

In deriving the nuclear attraction integral we use the following $3n$ vector \mathbf{t} which contains three coordinates of the t th nucleus repeated n times:

$$\mathbf{t} = \begin{pmatrix} r_{tx} \\ r_{ty} \\ r_{tz} \\ \vdots \\ r_{tx} \\ r_{ty} \\ r_{tz} \end{pmatrix}, \quad (43)$$

and the following quadratic form representing the square of the distance between the t th nucleus and i th electron:

$$r_{it}^2 = (\mathbf{r} - \mathbf{t})' \mathbf{J}_{ii} (\mathbf{r} - \mathbf{t}). \quad (44)$$

Following the same approach as used in deriving the electron repulsion integral, the nuclear attraction integral is now found

to be

$$\begin{aligned}
 \text{NA}_{kl,it}^{\Pi} = & \frac{2}{(\pi\alpha')^{1/2}} \mathbf{S}_{kl}^{\Sigma} \left\{ \left[\frac{1}{2} \mathbf{v}' \tilde{\mathbf{A}}_{kl}^{-1} \mathbf{v}^k + (\tilde{\mathbf{s}}' \mathbf{v}^k)(\tilde{\mathbf{s}}' \tilde{\mathbf{v}}^l) \right] \mathbf{F}_0 \left[\frac{\rho'}{\alpha'} \right] \right. \\
 & + \left[(\tilde{\mathbf{s}}' \mathbf{v}^k) \left(\frac{(\tilde{\mathbf{s}} - \mathbf{t})' \mathbf{J}_{ii} \tilde{\mathbf{A}}_{kl}^{-1} \tilde{\mathbf{v}}^l}{\alpha'} \right) \right. \\
 & + (\tilde{\mathbf{s}}' \tilde{\mathbf{v}}^l) \left(\frac{(\tilde{\mathbf{s}} - \mathbf{t})' \mathbf{J}_{ii} \tilde{\mathbf{A}}_{kl}^{-1} \mathbf{v}^k}{\alpha'} \right) + \frac{\mathbf{v}' \tilde{\mathbf{A}}_{kl}^{-1} \mathbf{J}_{ii} \tilde{\mathbf{A}}_{kl}^{-1} \tilde{\mathbf{v}}^l}{2\alpha'} \left. \right] \\
 & \times \mathbf{F}_1 \left[\frac{\rho'}{\alpha'} \right] \\
 & + \left(\frac{(\tilde{\mathbf{s}} - \mathbf{t})' \mathbf{J}_{ii} \tilde{\mathbf{A}}_{kl}^{-1} \tilde{\mathbf{v}}^l}{\alpha'} \right) \left(\frac{(\tilde{\mathbf{s}} - \mathbf{t})' \mathbf{J}_{ii} \tilde{\mathbf{A}}_{kl}^{-1} \mathbf{v}^k}{\alpha'} \right) \\
 & \times \mathbf{F}_2 \left[\frac{\rho'}{\alpha'} \right] \left. \right\} \\
 & \times \left[\frac{1}{4} \mathbf{v}' \mathbf{A}_k^{-1} \mathbf{v}^k + (\mathbf{v}' \tilde{\mathbf{s}}_k)(\mathbf{v}' \mathbf{s}_k) \right]^{-1/2} \\
 & \times \left[\frac{1}{4} \tilde{\mathbf{v}}' \tilde{\mathbf{A}}_l^{-1} \tilde{\mathbf{v}}^l + (\tilde{\mathbf{v}}' \tilde{\mathbf{s}}_l)(\tilde{\mathbf{v}}' \mathbf{s}_l) \right]^{-1/2}, \quad (45)
 \end{aligned}$$

where α' and ρ' in this case (i.e., for the nuclear attraction integral) are $\alpha' = \text{tr}[J_{ii} \tilde{\mathbf{A}}_{kl}^{-1}]$ and $\rho' = (\tilde{\mathbf{s}} - \mathbf{t})' \mathbf{J}_{ii} (\tilde{\mathbf{s}} - \mathbf{t})$.

V. ENERGY GRADIENT

If the non-zero component of the $3n$ \mathbf{v} vector is not on the same axes as the Gaussian shift centers, the terms that simultaneously involve the Gaussian shift vector and the \mathbf{v} vector vanish. This is because $\mathbf{v}' \mathbf{s}_k = 0$ and $\mathbf{v}' (W \otimes I_3) \mathbf{s}_k = 0$, where W is a $n \times n$ matrix. Therefore, the above-derived normalized integrals reduce to

$$\mathbf{S}_{kl}^{\Pi} = \mathbf{S}_{kl}^{\Sigma} \eta_1^{\text{S}} \eta_2^{\text{S}}, \quad (46)$$

$$\mathbf{T}_{kl}^{\Pi} = \frac{1}{2} [\mathbf{S}_{kl}^{\Sigma} (\eta_1^{\text{T}} + \eta_2^{\text{T}} - \eta_3^{\text{T}} - \eta_4^{\text{T}} + \eta_5^{\text{T}}) + \mathbf{T}_{kl}^{\Sigma} \eta_6^{\text{T}}] \eta_2^{\text{S}}, \quad (47)$$

$$\mathbf{ER}_{kl}^{\Pi} = 2(\pi\alpha)^{-1/2} \mathbf{S}_{kl}^{\Sigma} \left(\eta_1^{\text{S}} \mathbf{F}_0 \left[\frac{\rho}{\alpha'} \right] + \alpha^{-1} \eta_1^{\text{ER}} \mathbf{F}_1 \left[\frac{\rho}{\alpha'} \right] \right) \eta_2^{\text{S}}, \quad (48)$$

$$\text{NA}_{kl}^{\Pi} = 2(\pi\alpha')^{-1/2} \mathbf{S}_{kl}^{\Sigma} \left(\eta_1^{\text{S}} \mathbf{F}_0 \left[\frac{\rho'}{\alpha'} \right] + \alpha^{-1} \eta_1^{\text{NA}} \mathbf{F}_1 \left[\frac{\rho'}{\alpha'} \right] \right) \eta_2^{\text{S}}, \quad (49)$$

where the following abbreviations are used:

$$\begin{aligned}
 \eta_1^{\text{S}} &= \frac{1}{2} \mathbf{v}' \tilde{\mathbf{A}}_{kl}^{-1} \tilde{\mathbf{v}}^l, \\
 \eta_2^{\text{S}} &= 4 (\mathbf{v}' \mathbf{A}_k^{-1} \mathbf{v}^k)^{-1/2} (\tilde{\mathbf{v}}' \tilde{\mathbf{A}}_l^{-1} \tilde{\mathbf{v}}^l)^{-1/2}, \\
 \eta_1^{\text{T}} &= \tilde{\mathbf{v}}' \tilde{\mathbf{A}}_{kl}^{-1} \mathbf{A}_k \tilde{\mathbf{A}}_l \tilde{\mathbf{A}}_{kl}^{-1} \mathbf{v}^k, \\
 \eta_2^{\text{T}} &= \mathbf{v}' \tilde{\mathbf{A}}_{kl}^{-1} \mathbf{A}_k \tilde{\mathbf{A}}_l \tilde{\mathbf{A}}_{kl}^{-1} \tilde{\mathbf{v}}^l, \\
 \eta_3^{\text{T}} &= \mathbf{v}' \tilde{\mathbf{A}}_{kl}^{-1} \mathbf{A}_k \tilde{\mathbf{v}}^l, \\
 \eta_4^{\text{T}} &= \tilde{\mathbf{v}}' \tilde{\mathbf{A}}_{kl}^{-1} \tilde{\mathbf{A}}_l \mathbf{v}^k, \\
 \eta_5^{\text{T}} &= \mathbf{v}' \tilde{\mathbf{v}}^l, \\
 \eta_6^{\text{T}} &= 2 \eta_1^{\text{S}}, \\
 \eta_1^{\text{ER}} &= \frac{1}{2} \mathbf{v}' \tilde{\mathbf{A}}_{kl}^{-1} \mathbf{J}_{ij} \tilde{\mathbf{A}}_{kl}^{-1} \tilde{\mathbf{v}}^l, \\
 \eta_1^{\text{NA}} &= \frac{1}{2} \mathbf{v}' \tilde{\mathbf{A}}_{kl}^{-1} \mathbf{J}_{ii} \tilde{\mathbf{A}}_{kl}^{-1} \tilde{\mathbf{v}}^l. \quad (50)
 \end{aligned}$$

Following Kinghorn,¹⁶ the gradient of a molecular integral over k th and l th ECGs with respect to the nonlinear parameters of the k th ECG (i.e., the exponential parameters L_k and the Gaussian centers \mathbf{s}_k) is derived using the methods of the matrix differential calculus. The calculation of the gradient of the BO energy with respect to $\text{vech } L_k$ and \mathbf{s}_k involves the following derivatives of the Hamiltonian and overlap matrices elements:

$$\frac{\partial \mathbf{H}_{kl}}{\partial (\text{vech } L_k)}, \frac{\partial \mathbf{S}_{kl}}{\partial (\text{vech } L_k)}, \frac{\partial \mathbf{H}_{kl}}{\partial \mathbf{s}_k}, \frac{\partial \mathbf{S}_{kl}}{\partial \mathbf{s}_k}, \quad (51)$$

where vech transforms an $n \times n$ matrix into a $n(n+1)/2$ -component vector.¹⁵ For example, if X is a 3×3 matrix with elements X_{ij} , then

$$\text{vech } X = \begin{pmatrix} X_{11} \\ X_{12} \\ X_{13} \\ X_{22} \\ X_{23} \\ X_{33} \end{pmatrix}. \quad (52)$$

We will now derive the derivative for each individual integral.

A. Overlap derivative

The derivative of the overlap integral with respect to \mathbf{s}_k is simply:

$$d_{\mathbf{s}_k} \mathbf{S}_{kl}^{\Pi} = d_{\mathbf{s}_k} (\mathbf{S}_{kl}^{\Sigma}) \eta_1^{\text{S}} \eta_2^{\text{S}}, \quad (53)$$

and the derivative of the overlap integral with respect to L_k is

$$d_k S_{kl}^{\Pi} = d_k (\mathbf{S}_{kl}^{\Sigma}) \eta_1^S \eta_2^S + \mathbf{S}_{kl}^{\Sigma} d_k(\eta_1^S) \eta_2^S + \mathbf{S}_{kl}^{\Sigma} \eta_1^S d_k(\eta_2^S). \quad (54)$$

In order to determine $\frac{\partial S_{kl}}{\partial(\text{vech } L_k)}$, we use the following relation to remove the Kronecker products:^{3,16}

$$\mathbf{v}' \mathbf{A} \mathbf{v} = \text{tr}[(\mathbf{v} \cdot \mathbf{v}) A]. \quad (55)$$

With that, the differentials of $d_k(\eta_1^S)$ and $d_k(\eta_2^S)$ are

$$\begin{aligned} d_k \eta_1^S &= -\frac{1}{2} \mathbf{v}' \tilde{\mathbf{A}}_{kl}^{-1} d(\mathbf{A}_k) \tilde{\mathbf{A}}_{kl}^{-1} \tilde{\mathbf{v}} \\ &= -\frac{1}{2} \text{tr} [\tilde{\mathbf{A}}_{kl}^{-1} (\tilde{\mathbf{v}}' \cdot \mathbf{v}') \tilde{\mathbf{A}}_{kl}^{-1} d(\mathbf{A}_k)] \\ &= -\frac{1}{2} \{ \text{vech} [\tilde{\mathbf{A}}_{kl}^{-1} (\tilde{\mathbf{v}}' \cdot \mathbf{v}') \tilde{\mathbf{A}}_{kl}^{-1} L_k] \\ &\quad + \text{vech} [(\tilde{\mathbf{A}}_{kl}^{-1} (\tilde{\mathbf{v}}' \cdot \mathbf{v}') \tilde{\mathbf{A}}_{kl}^{-1})' L_k] \}' \text{vech}[dL_k], \\ d_k \eta_2^S &= 2 [\tilde{\mathbf{v}}' \tilde{\mathbf{A}}_l^{-1} \tilde{\mathbf{v}}']^{-1/2} [\mathbf{v}' \mathbf{A}_k^{-1} \mathbf{v}]^{-3/2} [\mathbf{v}' \mathbf{A}_k^{-1} d(\mathbf{A}_k) \mathbf{A}_k^{-1} \mathbf{v}] \\ &= 2 [\tilde{\mathbf{v}}' \tilde{\mathbf{A}}_l^{-1} \tilde{\mathbf{v}}']^{-1/2} [\mathbf{v}' \mathbf{A}_k^{-1} \mathbf{v}]^{-3/2} \\ &\quad \times \text{tr} [A_k^{-1} (\mathbf{v}' \cdot \mathbf{v}) A_k^{-1} d(\mathbf{A}_k)] \\ &= 4 [\tilde{\mathbf{v}}' \tilde{\mathbf{A}}_l^{-1} \tilde{\mathbf{v}}']^{-1/2} [\mathbf{v}' \mathbf{A}_k^{-1} \mathbf{v}]^{-3/2} \\ &\quad \times \text{vech} [A_k^{-1} (\mathbf{v}' \cdot \mathbf{v}) A_k^{-1} L_k]' \text{vech}[dL_k]. \end{aligned} \quad (56)$$

B. Kinetic energy derivative

The differential of kinetic energy integral with respect to s_k is

$$\begin{aligned} d_{s_k} (\mathbf{T}_{kl}^{\Pi}) &= \frac{1}{2} [d_{s_k} (\mathbf{S}_{kl}^{\Sigma}) (\eta_1^T + \eta_2^T - \eta_3^T - \eta_4^T + \eta_5^T) \\ &\quad + d_{s_k} (\mathbf{T}_{kl}^{\Sigma}) \eta_6^T] \eta_2^S \end{aligned} \quad (57)$$

and the differential of the kinetic energy integral with respect to L_k is

$$\begin{aligned} d_k (\mathbf{T}_{kl}^{\Pi}) &= \frac{1}{2} [d_k (\mathbf{S}_{kl}^{\Sigma}) (\eta_1^T + \eta_2^T - \eta_3^T - \eta_4^T + \eta_5^T) \\ &\quad + \mathbf{S}_{kl}^{\Sigma} d_k (\eta_1^T + \eta_2^T - \eta_3^T - \eta_4^T + \eta_5^T) \\ &\quad + d_k (\mathbf{T}_{kl}^{\Sigma}) \eta_6^T + \mathbf{T}_{kl}^{\Sigma} d_k(\eta_6^T)] \eta_2^S \\ &\quad + \frac{\mathbf{T}_{kl}^{\Pi}}{\eta_2^S} d_k(\eta_2^S). \end{aligned} \quad (58)$$

The differential of the η -dependent terms in the above expression are derived as

$$\begin{aligned} d_k \eta_1^T &= -\tilde{\mathbf{v}}' \tilde{\mathbf{A}}_{kl}^{-1} d(\mathbf{A}_k) \tilde{\mathbf{A}}_{kl}^{-1} \mathbf{A}_k \tilde{\mathbf{A}}_l \tilde{\mathbf{A}}_{kl}^{-1} \mathbf{v}' + \tilde{\mathbf{v}}' \tilde{\mathbf{A}}_{kl}^{-1} d(\mathbf{A}_k) \tilde{\mathbf{A}}_l \tilde{\mathbf{A}}_{kl}^{-1} \mathbf{v}' \\ &\quad - \tilde{\mathbf{v}}' \tilde{\mathbf{A}}_{kl}^{-1} \mathbf{A}_k \tilde{\mathbf{A}}_l \tilde{\mathbf{A}}_{kl}^{-1} d(\mathbf{A}_k) \tilde{\mathbf{A}}_{kl}^{-1} \mathbf{v}' \\ &= -\text{tr} [\tilde{\mathbf{A}}_{kl}^{-1} \mathbf{A}_k \tilde{\mathbf{A}}_l \tilde{\mathbf{A}}_{kl}^{-1} (\mathbf{v}' \cdot \tilde{\mathbf{v}}') \tilde{\mathbf{A}}_{kl}^{-1} d(\mathbf{A}_k)] \\ &\quad + \text{tr} [\tilde{\mathbf{A}}_l \tilde{\mathbf{A}}_{kl}^{-1} (\mathbf{v}' \cdot \tilde{\mathbf{v}}') \tilde{\mathbf{A}}_{kl}^{-1} d(\mathbf{A}_k)] \\ &\quad - \text{tr} [\tilde{\mathbf{A}}_{kl}^{-1} (\mathbf{v}' \cdot \tilde{\mathbf{v}}') \tilde{\mathbf{A}}_{kl}^{-1} \mathbf{A}_k \tilde{\mathbf{A}}_l \tilde{\mathbf{A}}_{kl}^{-1} d(\mathbf{A}_k)] \\ &= \{ -\text{vech} [\tilde{\mathbf{A}}_{kl}^{-1} \mathbf{A}_k \tilde{\mathbf{A}}_l \tilde{\mathbf{A}}_{kl}^{-1} (\mathbf{v}' \cdot \tilde{\mathbf{v}}') \tilde{\mathbf{A}}_{kl}^{-1} L_k] \\ &\quad - \text{vech} [(\tilde{\mathbf{A}}_{kl}^{-1} \mathbf{A}_k \tilde{\mathbf{A}}_l \tilde{\mathbf{A}}_{kl}^{-1} (\mathbf{v}' \cdot \tilde{\mathbf{v}}') \tilde{\mathbf{A}}_{kl}^{-1})' L_k] \\ &\quad + \text{vech} [A_l \tilde{\mathbf{A}}_{kl}^{-1} (\mathbf{v}' \cdot \tilde{\mathbf{v}}') \tilde{\mathbf{A}}_{kl}^{-1} L_k] \\ &\quad + \text{vech} [(A_l \tilde{\mathbf{A}}_{kl}^{-1} (\mathbf{v}' \cdot \tilde{\mathbf{v}}') \tilde{\mathbf{A}}_{kl}^{-1})' L_k] \\ &\quad - \text{vech} [\tilde{\mathbf{A}}_{kl}^{-1} (\mathbf{v}' \cdot \tilde{\mathbf{v}}') \tilde{\mathbf{A}}_{kl}^{-1} A_k \tilde{\mathbf{A}}_l \tilde{\mathbf{A}}_{kl}^{-1} L_k] \\ &\quad - \text{vech} [(\tilde{\mathbf{A}}_{kl}^{-1} (\mathbf{v}' \cdot \tilde{\mathbf{v}}') \tilde{\mathbf{A}}_{kl}^{-1} A_k \tilde{\mathbf{A}}_l \tilde{\mathbf{A}}_{kl}^{-1})' L_k] \}' \\ &\quad \times \text{vech}[dL_k], \end{aligned} \quad (59)$$

$$\begin{aligned} d_k \eta_2^T &= -\mathbf{v}' \tilde{\mathbf{A}}_{kl}^{-1} d(\mathbf{A}_k) \tilde{\mathbf{A}}_{kl}^{-1} \mathbf{A}_k \tilde{\mathbf{A}}_l \tilde{\mathbf{A}}_{kl}^{-1} \tilde{\mathbf{v}}' + \mathbf{v}' \tilde{\mathbf{A}}_{kl}^{-1} d(\mathbf{A}_k) \tilde{\mathbf{A}}_l \tilde{\mathbf{A}}_{kl}^{-1} \tilde{\mathbf{v}}' \\ &\quad - \mathbf{v}' \tilde{\mathbf{A}}_{kl}^{-1} \mathbf{A}_k \tilde{\mathbf{A}}_l \tilde{\mathbf{A}}_{kl}^{-1} d(\mathbf{A}_k) \tilde{\mathbf{A}}_{kl}^{-1} \tilde{\mathbf{v}}' \\ &= -\text{tr} [\tilde{\mathbf{A}}_{kl}^{-1} \mathbf{A}_k \tilde{\mathbf{A}}_l \tilde{\mathbf{A}}_{kl}^{-1} (\tilde{\mathbf{v}}' \cdot \mathbf{v}') \tilde{\mathbf{A}}_{kl}^{-1} d(\mathbf{A}_k)] \\ &\quad + \text{tr} [\tilde{\mathbf{A}}_l \tilde{\mathbf{A}}_{kl}^{-1} (\tilde{\mathbf{v}}' \cdot \mathbf{v}') \tilde{\mathbf{A}}_{kl}^{-1} d(\mathbf{A}_k)] \\ &\quad - \text{tr} [\tilde{\mathbf{A}}_{kl}^{-1} (\tilde{\mathbf{v}}' \cdot \mathbf{v}') \tilde{\mathbf{A}}_{kl}^{-1} A_k \tilde{\mathbf{A}}_l \tilde{\mathbf{A}}_{kl}^{-1} d(\mathbf{A}_k)] \\ &= \{ -\text{vech} [\tilde{\mathbf{A}}_{kl}^{-1} \mathbf{A}_k \tilde{\mathbf{A}}_l \tilde{\mathbf{A}}_{kl}^{-1} (\tilde{\mathbf{v}}' \cdot \mathbf{v}') \tilde{\mathbf{A}}_{kl}^{-1} L_k] \\ &\quad - \text{vech} [(\tilde{\mathbf{A}}_{kl}^{-1} \mathbf{A}_k \tilde{\mathbf{A}}_l \tilde{\mathbf{A}}_{kl}^{-1} (\tilde{\mathbf{v}}' \cdot \mathbf{v}') \tilde{\mathbf{A}}_{kl}^{-1})' L_k] \\ &\quad + \text{vech} [A_l \tilde{\mathbf{A}}_{kl}^{-1} (\tilde{\mathbf{v}}' \cdot \mathbf{v}') \tilde{\mathbf{A}}_{kl}^{-1} L_k] \\ &\quad + \text{vech} [(A_l \tilde{\mathbf{A}}_{kl}^{-1} (\tilde{\mathbf{v}}' \cdot \mathbf{v}') \tilde{\mathbf{A}}_{kl}^{-1})' L_k] \\ &\quad - \text{vech} [\tilde{\mathbf{A}}_{kl}^{-1} (\tilde{\mathbf{v}}' \cdot \mathbf{v}') \tilde{\mathbf{A}}_{kl}^{-1} A_k \tilde{\mathbf{A}}_l \tilde{\mathbf{A}}_{kl}^{-1} L_k] \\ &\quad - \text{vech} [(\tilde{\mathbf{A}}_{kl}^{-1} (\tilde{\mathbf{v}}' \cdot \mathbf{v}') \tilde{\mathbf{A}}_{kl}^{-1} A_k \tilde{\mathbf{A}}_l \tilde{\mathbf{A}}_{kl}^{-1})' L_k] \}' \\ &\quad \times \text{vech}[dL_k], \end{aligned} \quad (60)$$

$$\begin{aligned} d_k \eta_3^T &= -\mathbf{v}' \tilde{\mathbf{A}}_{kl}^{-1} d(\mathbf{A}_k) \tilde{\mathbf{A}}_{kl}^{-1} \mathbf{A}_k \tilde{\mathbf{v}}' + \mathbf{v}' \tilde{\mathbf{A}}_{kl}^{-1} d(\mathbf{A}_k) \tilde{\mathbf{v}}' \\ &= -\text{tr} [\tilde{\mathbf{A}}_{kl}^{-1} \mathbf{A}_k (\tilde{\mathbf{v}}' \cdot \mathbf{v}') \tilde{\mathbf{A}}_{kl}^{-1} d(\mathbf{A}_k)] \\ &\quad + \text{tr} [(\tilde{\mathbf{v}}' \cdot \mathbf{v}') \tilde{\mathbf{A}}_{kl}^{-1} d(\mathbf{A}_k)] \\ &= \{ -\text{vech} [\tilde{\mathbf{A}}_{kl}^{-1} \mathbf{A}_k (\tilde{\mathbf{v}}' \cdot \mathbf{v}') \tilde{\mathbf{A}}_{kl}^{-1} L_k] \\ &\quad - \text{vech} [(\tilde{\mathbf{A}}_{kl}^{-1} \mathbf{A}_k (\tilde{\mathbf{v}}' \cdot \mathbf{v}') \tilde{\mathbf{A}}_{kl}^{-1})' L_k] \\ &\quad + \text{vech} [(\tilde{\mathbf{v}}' \cdot \mathbf{v}') \tilde{\mathbf{A}}_{kl}^{-1} L_k] + \text{vech} [((\tilde{\mathbf{v}}' \cdot \mathbf{v}') \tilde{\mathbf{A}}_{kl}^{-1})' L_k] \}' \\ &\quad \times \text{vech}[dL_k], \end{aligned} \quad (61)$$

$$\begin{aligned}
d_k \eta_4^T &= -\tilde{\mathbf{v}}'^l \tilde{\mathbf{A}}_{kl}^{-1} d(\mathbf{A}_k) \tilde{\mathbf{A}}_{kl}^{-1} \tilde{\mathbf{A}}_l \tilde{\mathbf{v}}^k \\
&= -\text{tr} [\tilde{\mathbf{A}}_{kl}^{-1} \tilde{\mathbf{A}}_l (\mathbf{v}^k \cdot \tilde{\mathbf{v}}') \tilde{\mathbf{A}}_{kl}^{-1} d(A_k)] \\
&= -\{ \text{vech} [\tilde{\mathbf{A}}_{kl}^{-1} \tilde{\mathbf{A}}_l (\mathbf{v}^k \cdot \tilde{\mathbf{v}}') \tilde{\mathbf{A}}_{kl}^{-1} L_k] \\
&\quad + \text{vech} [(\tilde{\mathbf{A}}_{kl}^{-1} \tilde{\mathbf{A}}_l (\mathbf{v}^k \cdot \tilde{\mathbf{v}}') \tilde{\mathbf{A}}_{kl}^{-1})' L_k] \}' \text{vech}[dL_k], \tag{62}
\end{aligned}$$

$$\begin{aligned}
d_k \eta_6^T &= -\tilde{\mathbf{v}}'^l \tilde{\mathbf{A}}_{kl}^{-1} d(\mathbf{A}_k) \tilde{\mathbf{A}}_{kl}^{-1} \mathbf{v}^k \\
&= -\text{tr} [\tilde{\mathbf{A}}_{kl}^{-1} \tilde{\mathbf{A}}_l (\mathbf{v}^k \cdot \tilde{\mathbf{v}}') \tilde{\mathbf{A}}_{kl}^{-1} d(A_k)] \\
&= \{ -\text{vech} [\tilde{\mathbf{A}}_{kl}^{-1} (\mathbf{v}^k \cdot \tilde{\mathbf{v}}') \tilde{\mathbf{A}}_{kl}^{-1} L_k] \\
&\quad - \text{vech} [(\tilde{\mathbf{A}}_{kl}^{-1} (\mathbf{v}^k \cdot \tilde{\mathbf{v}}') \tilde{\mathbf{A}}_{kl}^{-1})' L_k] \}' \text{vech}[d(L_k)]. \tag{63}
\end{aligned}$$

C. Potential energy derivative

The differential of the electron repulsion integral with respect to \mathbf{s}_k is

$$\begin{aligned}
d_{s_k} (\mathbf{ER}_{kl}^\Pi) &= 2(\pi\alpha)^{-1/2} \left[d_{s_k} (\mathbf{S}_{kl}^\Sigma) \left(\eta_1^S F_0 \left[\frac{\rho}{\alpha} \right] + \alpha^{-1} \eta_1^{\text{ER}} F_1 \left[\frac{\rho}{\alpha} \right] \right) \right. \\
&\quad \left. + \mathbf{S}_{kl}^\Sigma \left(\eta_1^S \alpha^{-1} F_1 \left[\frac{\rho}{\alpha} \right] + \eta_1^{\text{ER}} \alpha^{-2} F_2 \left[\frac{\rho}{\alpha} \right] \right) d_{s_k}(\rho) \right] \eta_2^S, \tag{64}
\end{aligned}$$

where $d_{s_k}(\rho) = 2\tilde{\mathbf{s}}' \mathbf{J}_{ij} \tilde{\mathbf{A}}_{kl}^{-1} \mathbf{A}_k d(\mathbf{s}_k)$. The differential of electron repulsion integral with respect to L_k is

$$\begin{aligned}
d_k (\mathbf{ER}_{kl}^\Pi) &= 2\pi^{-1/2} d_k \left[\alpha^{-1/2} \mathbf{S}_{kl}^\Sigma \left(\eta_1^S F_0 \left[\frac{\rho}{\alpha} \right] + \alpha^{-1} \eta_1^{\text{ER}} F_1 \left[\frac{\rho}{\alpha} \right] \right) \right] \eta_2^S \\
&\quad + \frac{\mathbf{ER}_{kl}^\Pi}{\eta_2^S} d_k (\eta_2^S) \\
&= 2\pi^{-1/2} \left\{ \alpha^{-1/2} d_k (\mathbf{S}_{kl}^\Sigma) \left(\eta_1^S F_0 \left[\frac{\rho}{\alpha} \right] + \alpha^{-1} \eta_1^{\text{ER}} F_1 \left[\frac{\rho}{\alpha} \right] \right) \right. \\
&\quad - \frac{1}{2} \alpha^{-3/2} d_k(\alpha) \mathbf{S}_{kl}^\Sigma \left(\eta_1^S F_0 \left[\frac{\rho}{\alpha} \right] + \alpha^{-1} \eta_1^{\text{ER}} F_1 \left[\frac{\rho}{\alpha} \right] \right) \\
&\quad + \alpha^{-1/2} \mathbf{S}_{kl}^\Sigma \left[d_k (\eta_1^S) F_0 \left[\frac{\rho}{\alpha} \right] + \eta_1^S \frac{\alpha d_k(\rho) + \rho d_k(\alpha)}{\alpha^2} \right. \\
&\quad \times F_1 \left[\frac{\rho}{\alpha} \right] \\
&\quad - \alpha^{-2} d_k(\alpha) \eta_1^{\text{ER}} F_1 \left[\frac{\rho}{\alpha} \right] + \alpha^{-1} d_k (\eta_1^{\text{ER}}) F_1 \left[\frac{\rho}{\alpha} \right] \\
&\quad \left. + \eta_1^{\text{ER}} \frac{\alpha d_k(\rho) + \rho d_k(\alpha)}{\alpha^3} F_2 \left[\frac{\rho}{\alpha} \right] \right] \eta_2^S \\
&\quad + \frac{\mathbf{ER}_{kl}^\Pi}{\eta_2^S} d_k (\eta_2^S). \tag{65}
\end{aligned}$$

The $d_k(\alpha)$, $d_k(\rho)$, and $d_k(\eta_1^{\text{ER}})$ are derived as follows:

$$\begin{aligned}
d_k(\alpha) &= -\text{tr} [\mathbf{J}_{ij} \tilde{\mathbf{A}}_{kl}^{-1} d_k(\mathbf{A}_k) \tilde{\mathbf{A}}_{kl}^{-1}] \\
&= -\text{vech} [\tilde{\mathbf{A}}_{kl}^{-1} \mathbf{J}_{ij} \tilde{\mathbf{A}}_{kl}^{-1}]' \text{vech}[dL_k], \tag{66}
\end{aligned}$$

$$\begin{aligned}
d_k(\rho) &= d_k (\tilde{\mathbf{s}}' \mathbf{J}_{ij} \tilde{\mathbf{s}}) \\
&= d_k \left[(\mathbf{s}'_k \mathbf{A}_k + \tilde{\mathbf{s}}' \tilde{\mathbf{A}}_l) \tilde{\mathbf{A}}_{kl}^{-1} \mathbf{J}_{ij} \tilde{\mathbf{A}}_{kl}^{-1} (\mathbf{A}_k \mathbf{s}_k + \tilde{\mathbf{A}}_l \tilde{\mathbf{s}}_l) \right] \\
&= 2 \text{tr} [\tilde{\mathbf{A}}_{kl}^{-1} \mathbf{J}_{ij} (\tilde{\mathbf{s}} \cdot \mathbf{s}_k) d(A_k)] - 2 \text{tr} [\tilde{\mathbf{A}}_{kl}^{-1} \mathbf{J}_{ij} (\tilde{\mathbf{s}} \cdot \tilde{\mathbf{s}}) d(A_k)] \\
&= \{ 2 \text{vech} [(\mathbf{s}_k \cdot \tilde{\mathbf{s}}) \mathbf{J}_{ij} \tilde{\mathbf{A}}_{kl}^{-1} L_k] \\
&\quad + 2 \text{vech} [((\mathbf{s}_k \cdot \tilde{\mathbf{s}}) \mathbf{J}_{ij} \tilde{\mathbf{A}}_{kl}^{-1})' L_k] \\
&\quad - 4 \text{vech} [(\tilde{\mathbf{s}} \cdot \tilde{\mathbf{s}}) \mathbf{J}_{ij} \tilde{\mathbf{A}}_{kl}^{-1} L_k] \}' \text{vech}[dL_k], \tag{67}
\end{aligned}$$

$$\begin{aligned}
d_k(\eta_1^{\text{ER}}) &= -\frac{1}{2} (\mathbf{v}'^k \tilde{\mathbf{A}}_{kl}^{-1} d(\mathbf{A}_k) \tilde{\mathbf{A}}_{kl}^{-1} \mathbf{J}_{ij} \tilde{\mathbf{A}}_{kl}^{-1} \tilde{\mathbf{v}}') \\
&\quad - \frac{1}{2} (\mathbf{v}'^k \tilde{\mathbf{A}}_{kl}^{-1} \mathbf{J}_{ij} \tilde{\mathbf{A}}_{kl}^{-1} d(\mathbf{A}_k) \tilde{\mathbf{A}}_{kl}^{-1} \tilde{\mathbf{v}}') \\
&= -\frac{1}{2} \text{tr} [\tilde{\mathbf{A}}_{kl}^{-1} \mathbf{J}_{ij} (\tilde{\mathbf{v}}' \cdot \mathbf{v}^k) \tilde{\mathbf{A}}_{kl}^{-1} d(A_k)] \\
&\quad - \frac{1}{2} \text{tr} [\tilde{\mathbf{A}}_{kl}^{-1} (\tilde{\mathbf{v}}' \cdot \mathbf{v}^k) \tilde{\mathbf{A}}_{kl}^{-1} \mathbf{J}_{ij} \tilde{\mathbf{A}}_{kl}^{-1} d(A_k)] \\
&= \left\{ -\frac{1}{2} \text{vech} [\tilde{\mathbf{A}}_{kl}^{-1} \mathbf{J}_{ij} \tilde{\mathbf{A}}_{kl}^{-1} (\tilde{\mathbf{v}}' \cdot \mathbf{v}^k) \tilde{\mathbf{A}}_{kl}^{-1} L_k] \right. \\
&\quad - \frac{1}{2} \text{vech} [(\tilde{\mathbf{A}}_{kl}^{-1} \mathbf{J}_{ij} \tilde{\mathbf{A}}_{kl}^{-1} (\tilde{\mathbf{v}}' \cdot \mathbf{v}^k) \tilde{\mathbf{A}}_{kl}^{-1})' L_k] \\
&\quad - \frac{1}{2} \text{vech} [\tilde{\mathbf{A}}_{kl}^{-1} (\tilde{\mathbf{v}}' \cdot \mathbf{v}^k) \tilde{\mathbf{A}}_{kl}^{-1} \mathbf{J}_{ij} \tilde{\mathbf{A}}_{kl}^{-1} L_k] \\
&\quad \left. - \frac{1}{2} \text{vech} [(\tilde{\mathbf{A}}_{kl}^{-1} (\tilde{\mathbf{v}}' \cdot \mathbf{v}^k) \tilde{\mathbf{A}}_{kl}^{-1} \mathbf{J}_{ij} \tilde{\mathbf{A}}_{kl}^{-1} L_k)' L_k] \right\}' \\
&\quad \times \text{vech}[dL_k]. \tag{68}
\end{aligned}$$

The formula of the differential of the nuclear attraction integral is very similar to the formula for the electron repulsion integral. One simply replaces ρ by ρ' , α by α' , \mathbf{J}_{ij} by \mathbf{J}_{ii} , J_{ij} by J_{ii} , and $\tilde{\mathbf{s}}$ by $(\tilde{\mathbf{s}} - \mathbf{t})$ in the expression for the electron repulsion integral.

D. Numerical test

The formulas for calculating the Hamiltonian, overlap matrix elements, and their derivatives have been implemented in a computer program. The variational optimization of the wave function is carried out by the minimization of the Rayleigh quotient:

$$E = \frac{\langle \Psi | \hat{H} | \Psi \rangle}{\langle \Psi | \Psi \rangle} \tag{69}$$

with respect to the linear expansion coefficients (c_k) in Eq. (1) and the nonlinear L_k and \mathbf{s}_k parameters in Eq. (2). The nonlinear parameters are optimized using a quasi-Newton procedure and the optimal linear parameters are obtained by solving the secular equation in each optimization step. To expedite the quasi-Newton optimization, the analytical energy gradient determined with respect to the L_k and \mathbf{s}_k parameters is supplied to the procedure in the calculation. The availability of the gradient considerably accelerates the optimization process. The norm of the gradient is also calculated to determine how well

TABLE I. Comparison of the BO energy convergence between this work and the best previous calculations for the considered Π states of the H_2 molecule at selected internuclear distances (R). Energies are in E_h .

M	$t^3\Pi_g$	$I^1\Pi_g$	This work	$c^3\Pi_u$	Cencek <i>et al.</i>
				$C^1\Pi_u$	
75	-0.659 561 213 8	-0.659 511 343 8	-0.737 477 353 5	-0.718 366 590 4	-0.718 366 558
150	-0.659 565 353 2	-0.659 515 029 3	-0.737 478 804 7	-0.718 367 943 3	-0.718 367 912
300	-0.659 565 533 7	-0.659 515 330 8	-0.737 478 902 6	-0.718 368 021 4	-0.718 368 012
600	-0.659 565 537 4	-0.659 515 336 0	-0.737 478 909 9	-0.718 368 028 9	-0.718 368 027
Best previous	-0.659 565 253	-0.659 515 056	-0.737 478 627		
Ref.	17 ^a	18 ^b	17 ^c		19 ^d
$R(a_0)$	2.0	2.0	2.0		1.952

^aCalculated with 177 generalized James-Coolidge functions.

^bCalculated with 193 generalized James-Coolidge functions.

^cCalculated with 142 generalized James-Coolidge functions.

^dCalculated with ECGs.

converged is the energy. If the gradient in our calculation falls below 10^{-12} a.u. the optimization is terminated and considered finished.

In order to test the correctness of the derived formulas and their implementation and to illustrate the performance of the method, four Π electronic states of the hydrogen molecule are calculated at a single selected internuclear distance specific to each state. The considered states and the corresponding symmetry operators are

$$i^3\Pi_g : (1 - \hat{P}_{12})(1 + \hat{i}),$$

$$I^1\Pi_g : (1 + \hat{P}_{12})(1 + \hat{i}),$$

$$c^3\Pi_u : (1 - \hat{P}_{12})(1 - \hat{i}),$$

$$C^1\Pi_u : (1 + \hat{P}_{12})(1 - \hat{i}).$$

The following can be noted about the computational time needed for a Π -state calculation. Due to the more complicated nature of the algorithms for the Π states shown in the present work in comparison with the corresponding algorithms for the Σ states, the time required to evaluate the integrals and their derivatives with respect to the ECG nonlinear parameters is four times longer. We have also observed that the time needed to optimize the ECG nonlinear parameters for a Π state is on average four times longer than to perform a similar optimization for a Σ state, if one aims to achieve a similar convergence level for the energy.

The convergence of the BO energy of the hydrogen molecule in the $C^1\Pi_u$ state obtained at $R = 1.952 a_0$ is compared with that of the best previous ECG calculations of Cencek *et al.*¹⁹ in Table I. As it can be seen in the table our BO energy converges noticeably faster than theirs for $M \leq 300$. We attribute this higher efficiency to the use of the analytical gradient in optimizing the ECG nonlinear parameters.^{7,9} The convergence pattern is very similar as in our previous calculations of the ground state HeH^+ molecule.⁵ In the work on the HeH^+ calculations, we concluded the basis set of 600 ECGs is virtually complete for describing a two-electron molecular system. This seems also to be the case with the $C^1\Pi_u$ state of H_2 . Therefore, as expected, Cencek *et al.* and our BO energies are almost identical at $M = 600$.

In Table I we also compare our BO energies for the other three Π states of the hydrogen molecule with the best literature results calculated with generalized James-Coolidge (JC) functions. The effectiveness of both basis functions are shown to be similar when describing the H_2 molecule in its ground states.^{13,20} In the present work, we observe a small improvement over the previous calculations of about $10^{-7} E_h$ when the similar number of JC and ECG basis functions are adopted in the calculation of the Π states of the H_2 molecule. The accuracy of our BO energies are estimated to be about $10^{-8} E_h$ when 600 ECGs are used to expand the electronic wave function. Though the improvement is minor, our experience shows that the advantage of using the analytical gradient in the variational optimization of the nonlinear parameters of the ECGs will be more pronounced for molecular systems with more than two electrons.⁹ For such systems one needs to use many more ECGs reaching into thousands to describe the BO wave functions with a similar accuracy as for H_2 . In such cases, if the optimization can be made more effective, one can use fewer ECGs to achieve the desired level of the energy convergence. PES/PEC calculations of Π states of some three- and four-electron systems, which are forthcoming, will allow for further testing this feature.

VI. SUMMARY

In this work, we derived formulas to calculate the overlap, kinetic energy, and potential energy integrals with ECGs capable of describing molecules with an arbitrary number of electrons including a single π electron. To accelerate the variational optimization of the ECG nonlinear parameters (the Gaussian exponents and the coordinates of the Gaussian centers), we also derived formulas for the analytical derivatives of the BO electronic energy with respect to these parameters. In the calculation the gradient is determined and provided to the quasi-Newton procedure which does the optimization in each iteration, and this expedites the search for the energy minimum. The formulas for the gradient are implemented in a computer codes which utilizes the parallel computer architecture and the message passing interface (MPI). The efficiency and the correctness of the implementation is tested in calculations of four Π excited states of the hydrogen molecule. It

is found that the efficiency as well as the accuracy of the final results are similar as achieved in our previous calculations of Σ states. For all four Π states considered in the calculations we obtained new improved energy upper bounds.

As mentioned, the next step to improve the accuracy of the PEC/PES after the BO calculations are completed is to include the adiabatic and nonadiabatic corrections. In our previous work we have included both corrections, but the inclusion of the nonadiabatic correction was done in an effective way through the modification of the vibrational and rotational masses used in the calculations of the rovibrational energy levels. These masses were invariant on the geometry of the system. A more correct and accurate accounting for the nonadiabatic effects can be done with a perturbation-theory approach.^{10,11} It involves a sum-over-state procedure. Thus excited-state BO PECs/PESs need to be calculated. The present work facilitates a procedure for such calculations. Besides, the procedure can be also used to probe molecular properties in excited states, as well as to describe ground states of molecules, which have the Π symmetry, such as the CH radical.

ACKNOWLEDGMENTS

This work has been supported in part by the National Science Foundation through the graduate research fellowship

program (GRFP) awarded to Keeper L. Sharkey, Grant No. DGE1-1143953.

- ¹S. F. Boys, *Proc. R. Soc. London, Ser. A* **258**, 402 (1960).
- ²K. Singer, *Proc. R. Soc. London, Ser. A* **258**, 412 (1960).
- ³S. Bubin, M. Cafiero, and L. Adamowicz, *Adv. Chem. Phys.* **131**, 377 (2005).
- ⁴M. Pavanello, W.-C. Tung, F. Leonarski, and L. Adamowicz, *J. Chem. Phys.* **130**, 074105 (2009).
- ⁵W.-C. Tung, M. Pavanello, and L. Adamowicz, *J. Chem. Phys.* **137**, 164305 (2012).
- ⁶M. Pavanello, W.-C. Tung, and L. Adamowicz, *J. Chem. Phys.* **131**, 184106 (2009).
- ⁷W.-C. Tung, M. Pavanello, and L. Adamowicz, *J. Chem. Phys.* **136**, 104309 (2012).
- ⁸W.-C. Tung, M. Pavanello, and L. Adamowicz, *J. Chem. Phys.* **133**, 124106 (2010).
- ⁹W.-C. Tung, M. Pavanello, and L. Adamowicz, *J. Chem. Phys.* **134**, 064117 (2011).
- ¹⁰T. Orlikowski and L. Wolniewicz, *Chem. Phys. Lett.* **24**, 461 (1974).
- ¹¹C. Schwartz and R. J. Le Roy, *J. Mol. Spectrosc.* **121**, 420 (1987).
- ¹²M. Hamermesh, *Group Theory and Its Application to Physical Problems* (Addison-Wesley, Reading, MA, 1962).
- ¹³S. Bubin, M. Pavanello, W.-C. Tung, K. L. Sharkey, and L. Adamowicz, *Chem. Rev.* **113**, 36 (2013).
- ¹⁴J. Komasa and J. Rychlewski, *Chem. Phys. Lett.* **342**, 185 (2001).
- ¹⁵S. Bubin and L. Adamowicz, *J. Chem. Phys.* **128**, 114107 (2008).
- ¹⁶D. B. Kinghorn, *Int. J. Quantum Chem.* **57**, 141 (1996).
- ¹⁷W. Kłos and J. Rychlewski, *Comput. Methods Sci. Technol.* **5**, 39 (1999).
- ¹⁸L. Wolniewicz, *J. Mol. Spectrosc.* **169**, 329 (1995).
- ¹⁹W. Cencek, J. Komasa, and J. Rychlewski, *Chem. Phys. Lett.* **246**, 417 (1995).
- ²⁰W. Cencek and K. Szalewicz, *Int. J. Quantum Chem.* **108**, 2191 (2008).

APPENDIX B

Einstein coefficients for rovibrational transitions of the LiH molecule in the ground
 $X^1\Sigma^+$ electronic state

Einstein coefficients for rovibrational transitions of the LiH molecule in the ground $X^1\Sigma^+$ electronic state

Leonardo G. Diniz

*Coordenação de Ciências, Centro Federal de Educação Tecnológica de Minas Gerais,
30.421-169, Belo Horizonte, MG, Brasil.**

Nikita Kirnosov

Department of Physics, the University of Arizona, Tucson, Arizona 85721, USA.†

Alexander Alijah

*Groupe de Spectrométrie Moléculaire et Atmosphérique, GSMA,
UMR CNRS 7331, University of Reims Champagne-Ardenne,
U.F.R. Sciences Exactes et Naturelles, 51687 Reims Cedex 2, France.‡*

José R. Mohallem

*Laboratório de Átomos e Moléculas Especiais,
Departamento de Física, ICEx, Universidade Federal de Minas Gerais,
PO Box 702, 31270-901, Belo Horizonte, MG, Brasil.§*

Ludwik Adamowicz

*Department of Chemistry and Biochemistry,
the University of Arizona, Tucson, Arizona 85721, USA.¶*

(Dated: September 15, 2015)

Abstract

A very accurate dipole moment curve (DMC) for the ground $X^1\Sigma^+$ electronic state of the ${}^7\text{LiH}$ molecule is reported. It is calculated with the use of all-particle explicitly correlated Gaussian functions with shifted centers. This DMC, the most accurate to our knowledge, and the corresponding highly accurate potential energy curve are used to evaluate the transition energies, the transition dipole moments, and the Einstein coefficients for the rovibrational transitions with $\Delta J = -1$ and $\Delta v \leq 5$. Using the model of a vibrational R -dependent effective reduced mass in the rovibrational calculations introduced earlier (Diniz et al., Chem. Phys. Lett. **633**, 89 (2015)) the importance of the non-adiabatic effects for these properties is evaluated. The results are used to assess the quality of the two complete linelists of ${}^7\text{LiH}$ available in the literature.

Keywords: dipole moment, Einstein coefficients, coordinate-dependent reduced mass

*Electronic address: leogabriel@deii.cefetmg.br

†Electronic address: kirnosov@email.arizona.edu

‡Electronic address: alexander.alijah@univ-reims.fr

§Electronic address: rachid@fisica.ufmg.br

¶Electronic address: ludwik@u.arizona.edu

I. INTRODUCTION

The LiH molecule has been the focus of several theoretical and experimental works in the last decades (see, for example, Stwalley and Zemke [1]). This smallest neutral heteronuclear molecule with just only four electrons has been a model system for testing state-of-the-art *ab initio* electronic structure calculations (see, for example, Tung et al. [2] and Holka et al. [3]). Besides, its small mass and the existence of four stable isotopic species, ^7LiH , ^6LiH , ^7LiD , and ^6LiD , makes it a good model to study non-adiabatic (or non-Born-Oppenheimer) effects. An avoided crossing between the low-lying potential energy curves (PECs) corresponding to the ground $X^1\Sigma^+$ state and the first excited $A^1\Sigma^+$ state around $5.7 a_0$ makes this study particularly interesting.

LiH is an important system in astrophysics, as it plays a fundamental role in the cooling process of primordial gas clouds in the early universe [4, 5]. Due to the high temperature of these clouds, the raise of the first objects via gravitational collapse would not be possible in the absence of the molecular cooling. The cooling process occurs via ro-vibrational transitions of such primordial molecules as H_2 , H_2^+ , HeH^+ , LiH , LiH^+ , H_3^+ and their respective isotopologues. With the largest permanent dipole moment among the primordial molecules, LiH is particularly important for the cooling process [4]. The chemistry of Li compounds in the primordial universe was described by Bougleux and Galli [6] and by Lepp et al. [7].

The spectroscopy of LiH was studied in detail by Dulick et al. [8]. The PECs of the $X^1\Sigma^+$ and $A^1\Sigma^+$ states of LiH were empirically derived by Coxon and Dickson [9] from a large set of spectral lines of the four isotopologues of this system. An empirical PEC for the LiH ground state was also derived by Chan et al. [10]. One of the goals of those two works was to investigate the post-Born-Oppenheimer effects in the LiH rovibrational transitions.

In a recent work, where a review of the previous studies of the LiH rovibrational spectrum can be found, Holka et al. [3] obtained a highly accurate PEC from MR-CISD (multi-reference configuration-interaction single-double) electronic calculations including size-extensivity, relativistic, and diagonal adiabatic corrections. The non-adiabatic effects in the energies of the vibrational levels were included using the *ab initio* formalism of Bunker and Moss [11]. The calculated rovibrational transitions obtained at this level of calculations differed from the experimental values by 1 to 2 cm^{-1} . In another work, Tung et al. [2] employed all-electron explicitly correlated Gaussian functions with shifted centers to evaluate

the non-relativistic PEC for LiH. Non-adiabatic corrections in that work were included in an approximate way with the use of the atomic masses instead of the nuclear masses in the calculation of the vibrational frequencies (though this was not explicitly mentioned in their paper). Even with this high accuracy level of the PEC, the differences between the calculated and the experimental vibrational transition energies were of the order of $1\text{-}2 \text{ cm}^{-1}$, which undoubtedly resulted from an inadequate account of the non-adiabatic effects. Recently, a new approach for accounting for the non-adiabatic effects was proposed by Diniz et al. [12]. In the approach the reduced vibrational mass of the system was made dependent on the internuclear distance, R , of the molecule. The application of the approach in the calculations of the vibrational transition energies of LiH allowed for increasing the accuracy of the results to the level of about 0.2 cm^{-1} .

With the increased accuracy of the vibrational transitions achieved with the R -dependent effective reduced-mass approach a question appeared whether the use of the approach would also lead to higher accuracy in predicting other spectroscopic quantities such as the transition dipole moments and the transition probabilities, also called Einstein coefficients. Elucidation of this point is one of the goals of the present work. The Einstein coefficients have fundamental importance in the study of the cooling of primordial clouds. The accuracy of the evaluation of this property demands not only on the accuracy of the PEC but also on the accuracy of the dipole moment curve (DMC). As far as we know, the only available DMC for LiH was obtained in 1981 in the CI calculations by Partridge and Langhoff [13]. More recently (1998) Tunega et al. [14] studied electrical properties of LiH using the MBPT-R12 approach but the dipole moment in that study was only calculated at the equilibrium distance. In the present work an all-electron explicitly correlated Gaussians with shifted centers are employed in the calculation of the LiH DMC. With that the resulting DMC is likely the most accurate to date for this molecule. Details of the calculations are presented in section II.

As far as we know, there are only two recent reports on the complete ro-vibrational linelist of LiH in the literature. In the first one, published in 2011, Coppola et al. [4] used their own PEC and DMC obtained with the internally contracted multi-reference averaged-pair functional (IC-ACPF) calculations. The calculations were performed with the basis set consisting of the aug-cc-pVnZ ($n=T,Q,5$) Dunning basis set for the hydrogen atom [15] and the aug-cc-pwCnZ(-DK) ($n=T,Q,5$) basis set of Prascher et al. for the lithium atom [16]. In

the calculations of the second linelist published in 2013 by Shi et al. [5], the empirical Coxon and Dickinson PEC [9] and the theoretical Partridge and Langhoff DMC [13] were used. Although the latter authors used a very accurate PEC generated from fitting experimental spectral lines, the DMC they used was less accurate. Due to these inaccuracies it is difficult to determine which of the two linelists is more accurate. However, as the present calculations are performed with very accurate PEC and DMC, the relative quality of the two previous linelists can be evaluated. The present calculations are performed for the rovibrational transitions corresponding to $\Delta J = -1$ and $\Delta v \leq 5$.

Another interesting point which the present calculations enable to elucidate is how the nonadiabatic effects affect the values of the Einstein coefficients. Both Shi et al. [5] and Coppola et al. [4] included these effects in the calculations of the rovibrational frequencies by using the atomic reduced mass instead of the nuclear reduced mass. In the present calculations we also use these masses and we compare the results with the results obtained with the approach of Diniz et al. [12] that employs an R -dependent effective reduced mass. That approach, as mentioned, produced the most accurate rovibrational transition energies as compared to the experimental values.

In section II the method used in the present calculations of the DMC is described and some computational details are discussed. In section III the approach used to solve the rovibrational problem and to calculate the transition probabilities is presented. Section IV is dedicated to the results and discussion. Finally, in section V the main conclusions of this work are presented.

II. COMPUTATION OF THE DIPOLE MOMENT

In the present calculations the spatial component of the electronic wave function of the LiH molecule, $\Phi_M(\mathbf{r})$, where \mathbf{r} is a 12-dimensional vector of the spatial coordinates of the four electrons, is expanded in terms of a set of M explicitly correlated all-electron Gaussians (ECGs), $\{g_k\}_{k=1,\dots,M}$, with shifted centers as:

$$\Phi_m(\mathbf{r}) = \sum_{k=1}^M c_k \mathcal{P} g_k(\mathbf{r}), \quad (1)$$

where \mathcal{P} is the operator that imposes the right permutational symmetry of the wave function, c_k are the linear expansion coefficients, and g_k are ECGs. They are the following

12-dimensional functions:

$$g_k(\mathbf{r}) = \exp [-(\mathbf{r} - \mathbf{s}_k)' \mathbf{A}_k (\mathbf{r} - \mathbf{s}_k)], \quad (2)$$

where \mathbf{s}_k is a 12-dimensional vector of the Cartesian coordinates of the Gaussian shifts, prime denotes vector transposition, and \mathbf{A}_k is a 12×12 dimensional symmetric matrix of the Gaussian exponential parameters defined as:

$$\mathbf{A}_k = A_k \otimes \mathbf{I}_3, \quad (3)$$

with \mathbf{I}_3 being a 3×3 identity matrix, \otimes denoting the Kronecker product, and A_k being a 4×4 symmetric matrix. As in the present calculations, the LiH molecule is placed along the z axis, the Gaussian shifts are also restricted to this axis (the x and y components of the \mathbf{S}_k vectors are set to zero).

For Gaussian (2) to be square integrable, as a basis function used for expanding the wave function of a bound electronic state should be, A_k has to be positive definite. This automatically happens if A_k is represented in the Cholesky-factored form as $L_k L'_k$ with L_k being a lower triangular matrix whose elements are real numbers ranging from $-\infty$ to $+\infty$.

The so-called spin-free formalism [17, 18] is used to construct the permutation symmetry operator, \mathcal{P} . In this formalism, an appropriate symmetry projector is applied to the spatial parts of the wave function to impose the desired symmetry properties. The symmetry projector can be constructed using the standard procedure involving Young operators as described, for example, in ref. [19]. In the case of the singlet ground electronic state of the LiH molecule the permutation operator, \mathcal{P} , used in the present calculations has the following form: $(1 - P_{13})(1 - P_{24})(1 + P_{12})(1 + P_{34})$, where \hat{P}_{ij} denotes the permutation of the spatial coordinates of the i -th and j -th electrons. As the electronic Hamiltonian is invariant upon any permutation of the electron labels, in the calculation of a Hamiltonian or overlap matrix element, the permutation operators can be moved to either the basis function in the *bra* or the *ket*. The combined symmetry operator, $\mathcal{P}^\dagger \mathcal{P}$ consists of $4! = 24$ terms. Thus, each matrix elements is a sum of 24 contributions corresponding to the different components of the permutation operator.

The linear coefficients, c_k , in the expansion of the wave function in terms of the basis functions and the nonlinear parameters of the basis functions, *i.e.*, the exponent matrices, L_k and the shifts, \mathbf{s}_k , are obtained using the variational method by the minimization of the

total energy:

$$E(\{L_k\}, \{\mathbf{s}_k\}, \{c_k\}) = \min_{\{L_k\}, \{\mathbf{s}_k\}, \{c_k\}} \frac{c' H(\{L_k\}, \{\mathbf{s}_k\}) c}{c' S(\{L_k\}, \{\mathbf{s}_k\}) c}, \quad (4)$$

where $H(\{L_k\}, \{\mathbf{s}_k\})$ and $S(\{L_k\}, \{\mathbf{s}_k\})$ are the Hamiltonian and overlap matrices, respectively. Both matrices depend on the nonlinear parameters of the basis functions. c is a column vector of the c_k coefficients.

To achieve high accuracy in the calculation of each PEC point, the linear and non-linear parameters of the Gaussians have to be extensively optimized. As each Gaussian contains 14 non-linear parameters, there are $14M$ non-linear parameters to optimize in the basis set of M ECGs. To expedite this optimization the analytic gradient of the energy determined in terms of the Gaussian nonlinear parameters was used [2]. The use of the analytical gradient was key in achieving high accuracy and in lowering the computational cost of the PEC calculation. More information about the approach used in growing the basis set to the size of 2000 ECGs for the PEC point corresponding to the equilibrium internuclear distance and about optimizing the basis set for each PEC point can be found in Ref. [2].

The ECG wave functions generated before in the LiH PEC calculations [2] are used in this work to calculate a dipole-moment curve (DMC). The dipole moment vector, μ , for each PEC point is determined as the expectation value of the dipole operator as:

$$\mu = \sum_{k,l}^M c_k c_l \langle \mathcal{P} g_k(\mathbf{r}) | \left(-\sum_{i=1}^4 \mathbf{r}_i \right) | \mathcal{P} g_l(\mathbf{r}) \rangle + \sum_{\alpha=1}^2 Q_\alpha \mathbf{R}_\alpha \quad (5)$$

$$= \sum_{k,l}^M c_k c_l \langle g_k(\mathbf{r}) | \left(-\sum_{i=1}^4 \mathbf{r}_i \right) | \mathcal{P}^\dagger \mathcal{P} g_l(\mathbf{r}) \rangle + \sum_{\alpha=1}^2 Q_\alpha \mathbf{R}_\alpha, \quad (6)$$

where \mathbf{r}_i is the coordinate vector of electron i and Q_α and \mathbf{R}_α are the charges and the coordinates of the nuclei, respectively. In Eq. (6), we use the fact that the electronic dipole-moment operator, $-\sum_{i=1}^4 \mathbf{r}_i$, is symmetric with respect to the permutation of the electrons. Also, the spatial wave function is assumed to be normalized. The dipole moment matrix element involving two ECGs, $g_k(\mathbf{r})$ and $g_l(\mathbf{r})$, is given as:

$$\langle g_k(\mathbf{r}) | \mathbf{r}_i | g_l(\mathbf{r}) \rangle = S_{kl} \{ [\mathbf{A}_k + \mathbf{A}_l]^{-1} [\mathbf{A}_k \mathbf{s}_k + \mathbf{A}_l \mathbf{s}_l] \}_i, \quad (7)$$

where \mathbf{v}_i denotes the i -th component of vector \mathbf{v} and $S_{kl} = \langle g_k | g_l \rangle$ is the overlap integral.

III. ROVIBRATIONAL EIGENVALUES AND TRANSITION PROBABILITIES

The radial (vibrational) Schrödinger within the adiabatic approximation equation for a diatomic molecule is:

$$[-\frac{1}{2\mu_v} \frac{d^2}{dR^2} + E_e(R) + \frac{J(J+1)}{2\mu_r R^2} - E_{vJ}] \chi_{vJ}(R) = 0, \quad (8)$$

where R is the internuclear distance, μ_v is the vibrational reduced mass, μ_r is the rotational reduced mass, $E_e(R)$ is the PEC obtained in the electronic calculations, and χ_{vJ} is the vibrational wave function corresponding to the vibrational quantum numbers v and the rotational quantum number J . In the adiabatic approximation μ_v and μ_r are equal to the nuclear reduced mass. For the LiH molecule the PEC used in the present work is taken from the work of Tung et al. [2]. It includes the Born-Oppenheimer energy curve calculated on a grid of points with 2000 fully optimized explicitly correlated Gaussians with shifted centers, the diagonal adiabatic correction (DBOC) curve, and the leading relativistic correction curve taken from the work of Holka et al. [3]. In order to improve the numerical stability of the calculations of the higher vibrational states the PEC is extended to distances smaller than the smallest distance of $1.8 a_0$ reported by Tung et al. [2]. The extension is done through extrapolation involving fitting the PEC in the interval between $1.8a_0$ and $2.5a_0$ with function $f(R) = a + b \exp(cR)$ and using the function to determine the PEC points for distances smaller than $1.8 a_0$. The fitting results in the following values of the adjustable parameters involved in the fitting function: $a = (-8.0852 \pm 0.0009) E_h$, $b = (7.8 \pm 0.4) E_h$, and $c = (-2.26 \pm 0.03) a_0^{-1}$. The PEC is extrapolated up to $R=1.2 a_0$.

The Einstein probabilities are determined using the DMC according to the following expression:

$$A_{\nu' J' \rightarrow \nu'' J''} = \left(\frac{16\pi^3}{3\epsilon_0 h} \right) \frac{S(J', J'')}{2J' + 1} \nu^3 |\langle \chi_{v' J'} | D(R) | \chi_{v'' J''} \rangle|^2, \quad (9)$$

where

$$S(J', J'') = \begin{cases} J'' & \text{if } J'' - J' = -1 \quad (P - \text{branch}) \\ J'' + 1 & \text{if } J'' - J' = 1 \quad (R - \text{branch}) \end{cases} \quad (10)$$

is the Hönl-London rotational intensity factor, ν is the transition frequency, and $D(R)$ is the DMC. With ν given in cm^{-1} and $D(R)$ in debye, the constant in the parenthesis in eq. 9 is equal to $3.1361891 \times 10^{-7} \text{cm}^3 \text{D}^{-2} \text{s}^{-1}$.

The radial vibrational equation 8 is solved with the renormalized Numerov code [20]

adapted to allow for a R -dependent reduced mass [21]. The numerical integration is performed in the range $1.2a_0 \leq R \leq 30.0a_0$. The convergence criterion for the eigenvalues is $10^{-14}E_h$. The nonadiabatic effects in the calculation of rovibrational levels away from avoided crossings can be accounted for in an approximate way by replacing the nuclear vibrational reduced mass, μ_v in eq. 8, with an effective R -dependent reduced mass $\mu_v(R)$. Recently, Diniz et al. [12] proposed a model for determining the R -dependent vibrational reduced mass that significantly improves the accuracy of the calculated vibrational levels of LiH in comparison with the results obtained using the conventional approach where the vibrational mass is taken as the atomic reduced mass and rotational mass is taken as the nuclear reduced mass [22]. The conventional model and the Diniz et al. model are used in the present calculations.

IV. RESULTS AND DISCUSSION

The Einstein A coefficients obtained in the present calculations are presented in Table I. The transition frequencies and the transition dipole moments for rovibrational transitions $\Delta J = -1$ and $\Delta v \leq 5$ are also shown in the table. The present values of the Einstein coefficients are compared in the table with the values from the two recently published linelists by Coppola et al. [4] and by Shi et al. [5]. As mentioned, the Coppola et al. linelist calculations involved their own potential energy and dipole moment curves, and in the linelist calculations by Shi et al. [5] the empirical potential energy curve derived from experimental data by Coxon and Dickinson [9] and the dipole moment curve of Partridge and Langhoff [13] were used. While the two linelists were obtained with the use of the atomic reduced mass in the rovibrational calculation, our results are obtained with three different reduced masses, i.e., the nuclear mass, the atomic mass, and the effective R -dependent mass taken from the work of Diniz et al. [12].

Comparing the present results obtained with the three reduced masses, one can see some interesting features. As expected, the use of different reduced masses has an noticeable effect of the order of 1 cm^{-1} on the transition energies. As shown in [12], the use of the effective mass considerably improves the agreement between the theoretical and experimental vibrational transitions. However, the effect of the different masses has rather negligible effect on the transition dipole moments. As it can be seen in the table, the values obtained with the

nuclear reduced mass differ very little from the the values obtained with the atomic reduced mass. The values of the Einstein coefficients are also insensitive to the mass model used. The difference between the values obtained with the atomic mass and with the effective mass are the order of only $0.01 s^{-1}$. Thus, we conclude that, while the use the effective mass in calculating the transition energies is important, the simpler model involving the use of the atomic reduced mass in the calculations of the transition dipole moments and the transition probabilities is quite adequate.

The present calculations allow for assessing the accuracy of the two previously published LiH linelists [4, 5]. The different PECs and DMCs used in those two calculations do not allow for an easy evaluation of which calculation is more accurate. While Coppola et al. [4] did not compare their results with any previous calculations, Shi et al. [5] compared their Einstein coefficients with those previously calculated by Coppola et al. and by Partridge and Langhoff [13]. In Table II we compare all previously calculated linelists with ours. The comparison shows that there is an approximately 3% difference between the values of the Einstein coefficient obtained in the different calculations. As the results of Shi et al. are obtained using an empirical PEC, their transition energies agree best with the experiment. However, as the DMC used by them is not empirical, it is unclear whether their transition probabilities are as accurate as their transition energies. Some clue concerning this point can be obtained by comparing the transition probabilities of Shi et al. with our values, as the DMC used in the present calculations is definitely the most accurate ever calculated (the DMC is provided as supplemental material [23]). In Figures 1 and 2 we compare our DMC with the DMCs used in the two previous calculations, while in Figure 3 the difference between those two curves and our curve is shown. This difference indicates that the DMC used by Coppola et al. agrees better with ours. This explains the better agreement of our Einstein coefficients with their values, as can be seen in Table II.

However, a question remains whether, despite the poorer quality of the DMC used by Shi et al., their use of a more accurate empirical PEC leads to more accurate results concerning the transition probabilities? To elucidate this point, we calculate the Einstein coefficients using our PEC and the DMC of Shi et al. As the results of this calculation reproduce the values of Shi et al. (see the fifth column in the table II), it is the quality of the DMC that determines the accuracy of the Einstein coefficients. Thus, while the linelist by Shi et al. is more accurate in terms of the transition energies, the linelist from Coppola et al. is more

accurate in terms of the transition probabilities.

The dipole moment for the LiH was measured [24] for the three lowest vibrational states and the $J = 1$ rotational state. By averaging our DMC over the wave functions of these vibrational states, a direct comparison between the calculated values and the experimental results can be made. A similar comparison can be made for the dipole moments obtained using the DMC of Partridge and Langhoff [13]. The comparison is shown in Table III. While Partridge and Langhoff dipoles are outside the range of the experimental error, our results lie within this range. In Table IV the vibrational averages of the dipole moment for the five lowest vibrational states and the $J = 0$ rotational state are presented. For the lowest state, the result is very close to dipole moment value obtained by Cafiero et al. [25] in the calculations where the Born-Oppenheimer approximation was not assumed.

V. CONCLUSIONS

Summarizing, a very accurate dipole moment and potential energy curves together with an effective model to simulate the nonadiabatic effects are used in the calculations of the rovibrational spectrum of the ^7LiH molecule. The results show that, while the nonadiabatic effects are important for the transition energies, their effect on the transition dipole moments and the transition probabilities is negligible. The computed vibrationally averaged dipole moments are found to be in very good agreement with the experiment. The present very accurate results are used to assess the quality of the two complete rovibrational linelists available in the literature for ^7LiH . The results suggest that, despite the higher accuracy of the transition energies in the linelist of Shi et al. [5] as compared to those of Coppola et al. [4], the Einstein coefficients in the latter linelist are more accurate.

Acknowledgments

We acknowledge CNPq and Capes for a financial support (PEV grant 401846/2013-0), the ROMEO HPC Center at the University of Reims Champagne-Ardenne and COST action CM 1405 Molecules in Motion (MOLIM). This work has been supported in part by the National Science Foundation with grant #1444127. We thank J. Tennyson for providing their DMC (private communication).

TABLE I: Einstein coefficients (A), transition frequencies (ν) and Dipole moments (D) for the $\Delta J = -1$ and $\Delta v \leq 5$ rovibrational transitions of ^7LiH . The present data are obtained using the nuclear, atomic, and effective (i.e. $\mu_v(R)$) vibrational reduced masses. Einstein coefficients are compared with those obtained by Coppola et al. [4] and by Shi et al. [5].

upper	lower	nuclear mass			atomic mass			effective mass			Coppola	Shi		
		v'	J'	v''	J''	A/s^{-1}	ν/cm^{-1}	$D/e a_0$	A/s^{-1}	ν/cm^{-1}	$D/e a_0$	A/s^{-1}		
1	0	0	1	46.87511	1345.352	-0.24775	46.82827	1345.027	-0.24772	46.83441	1344.861	-0.24778	46.61900	45.39155
2	0	0	1	2.07712	2660.625	-0.01875	2.07444	2659.990	-0.01875	2.07828	2659.674	-0.01877	2.10130	1.98851
3	0	0	1	0.00944	3931.937	-0.00070	0.00942	3931.014	-0.00070	0.00951	3930.570	-0.00071	0.01035	0.00170
4	0	0	1	0.00226	5160.121	0.00023	0.00226	5158.931	0.00023	0.00234	5158.361	0.00023	0.00205	0.00358
5	0	0	1	0.00216	6344.928	0.00016	0.00216	6344.491	0.00016	0.00215	6343.804	0.00016	0.00195	0.00093
2	0	1	1	85.78738	1300.876	-0.35250	85.70384	1300.573	-0.35245	85.70914	1300.416	-0.35252	85.26200	82.76289
3	0	1	1	6.49990	2572.188	-0.03490	6.49145	2571.597	-0.03489	6.49753	2571.312	-0.03491	6.56780	6.43546
4	0	1	1	0.05458	3800.373	-0.00178	0.05448	3799.514	-0.00178	0.05570	3799.103	-0.00180	0.05925	0.05226
5	0	1	1	0.00678	4986.179	0.00042	0.00677	4985.075	0.00042	0.00667	4984.546	0.00041	0.00549	0.00699
6	0	1	1	0.00813	6130.242	0.00034	0.00812	6128.910	0.00034	0.00879	6128.283	0.00035	0.00829	0.00539
3	0	2	1	116.72422	1257.333	-0.43272	116.61407	1257.051	-0.43266	116.63104	1256.916	-0.43276	115.93000	112.53576
4	0	2	1	13.49541	2485.517	-0.05294	13.47781	2484.969	-0.05292	13.48309	2484.707	-0.05294	13.62900	13.39541

Continued on next page

TABLE I: Einstein coefficients, transition frequencies and Dipole moments for ${}^7\text{LiH}$; continued

v'	upper	lower	nuclear mass	atomic mass			effective mass	Coppola	Shi			
	J'	v''	J''	A/s^{-1}	ν/cm^{-1}	$D/e a_0$	A/s^{-1}	ν/cm^{-1}	$D/e a_0$	A/s^{-1}	A/s^{-1}	
5	0	2	1	0.18975	3671.324	-0.00350	0.18941	3670.529	-0.00349	0.18952	3670.150	-0.00350
6	0	2	1	0.00900	4815.386	0.00051	0.00899	4814.365	0.00051	0.00882	4813.887	0.00050
7	0	2	1	0.02060	5918.249	0.00056	0.02057	5917.021	0.00056	0.02029	5916.454	0.00056
												0.01998
												0.02212
4	0	3	1	139.81264	1214.616	-0.49879	139.68579	1214.355	-0.49872	139.69523	1214.222	-0.49882
5	0	3	1	23.24930	2400.422	-0.07321	23.21891	2399.915	-0.07319	23.22919	2399.665	-0.07321
6	0	3	1	0.48229	35 44 .484	-0.00588	0.48141	3543.751	-0.00587	0.48320	3543.402	-0.00588
7	0	3	1	0.00743	4647.347	0.00049	0.00744	4646.407	0.00049	0.00735	4645.968	0.00048
8	0	3	1	0.04021	5709.400	0.00083	0.04015	5708.274	0.00083	0.03944	5707.751	0.00082
												0.03562
												0.04056
5	0	4	1	155.17906	1172.642	-0.55395	155.04512	1172.402	-0.55388	155.06016	1172.278	-0.55399
6	0	4	1	35.89941	2316.704	-0.09595	35.85233	2316.238	-0.09591	35.86042	2316.015	-0.09594
7	0	4	1	1.01649	3419.567	-0.00900	1.01467	3418.894	-0.00900	1.02027	3418.581	-0.00902
8	0	4	1	0.00112	4481.620	0.00020	0.00113	4480.761	0.00020	0.00105	4480.364	0.00019
9	0	4	1	0.05393	5503.051	0.00102	0.05387	5502.026	0.00102	0.05398	5501.556	0.00102
												0.05128
												0.05762

Continued on next page

TABLE I: Einstein coefficients, transition frequencies and Dipole moments for ${}^7\text{LiH}$; continued

v'	upper	lower	nuclear mass	atomic mass	effective mass	Coppola	Shi					
	J'	v''	J''	A/s^{-1}	ν/cm^{-1}	$D/e a_0$	A/s^{-1}	ν/cm^{-1}	$D/e a_0$	A/s^{-1}	A/s^{-1}	
6	0	5	1	163.04673	1131.296	-0.59923	162.91496	1131.076	-0.59916	162.94399	1130.970	-0.59930
7	0	5	1	51.69897	2234.159	-0.12158	51.63106	2233.732	-0.12154	51.63113	2233.536	-0.12155
8	0	5	1	1.90261	3296.212	-0.01302	1.89917	3295.599	-0.01301	1.90537	3295.319	-0.01303
9	0	5	1	0.00141	4317.642	-0.00024	0.00140	4316.864	-0.00024	0.00161	4316.511	-0.00025
10	0	5	1	0.06553	5298.446	0.00119	0.06546	5297.522	0.00118	0.06542	5297.108	0.00118
												0.06131
												0.07238
7	0	6	1	163.73055	10 2 1.490	-0.63450	163.60935	1090.289	-0.63444	163.64622	1090.193	-0.63460
8	0	6	1	70.60605	2152.543	-0.15024	70.51324	2152.156	-0.15018	70.51163	2151.975	-0.15020
9	0	6	1	3.27771	3173.974	-0.01808	3.27185	3173.421	-0.01807	3.27569	3173.168	-0.01808
10	0	6	1	0.02580	4154.777	-0.00107	0.02568	4154.080	-0.00107	0.02679	4153.765	-0.00109
11	0	6	1	0.06508	5094.639	0.00125	0.06505	5093.819	0.00125	0.06382	5093.453	0.00124
												0.06050
												0.07673
8	0	7	1	157.71084	1050.070	-0.65903	157.60797	1049.889	-0.65898	157.64772	1049.798	-0.65915
9	0	7	1	92.83907	2071.501	-0.18249	92.71701	2071.154	-0.18241	92.72231	2070.990	-0.18244
10	0	7	1	5.28720	3052.304	-0.02435	5.27770	3051.812	-0.02433	5.28089	3051.587	-0.02434
11	0	7	1	0.10288	3992.166	-0.00227	0.10251	3991.552	-0.00227	0.10416	3991.276	-0.00229

Continued on next page

TABLE I: Einstein coefficients, transition frequencies and Dipole moments for ${}^7\text{LiH}$; continued

upper	lower	nuclear mass			atomic mass			effective mass			Coppola	Shi
v'	J'	v''	J''	A/s^{-1}	ν/cm^{-1}	$D/e a_0$	A/s^{-1}	ν/cm^{-1}	$D/e a_0$	A/s^{-1}	A/s^{-1}	
12	0	7	1	0.05184	4890.451	0.00119	0.05186	4889.737	0.00119	0.05024	4889.422	0.00117
											0.04639	0.06101
9	0	8	1	145.53309	1009.834	-0.67128	145.45493	1009.673	-0.67126	145.49879	1009.595	-0.67144
10	0	8	1	118.31572	1990.638	-0.21869	118.16049	1990.332	-0.21860	118.16760	1990.192	-0.21863
11	0	8	1	8.13515	2930.500	-0.03210	8.12043	2930.071	-0.03208	8.12527	2929.880	-0.03210
12	0	8	1	0.27526	3828.785	-0.00395	0.27441	3828.257	-0.00395	0.27602	3828.026	-0.00396
13	0	8	1	0.02649	4684.431	0.00091	0.02655	4683.829	0.00091	0.02546	4683.572	0.00089
											0.02251	0.03256
10	0	9	1	128.00713	969.593	-0.66916	127.95840	969.453	-0.66918	128.00728	969.385	-0.66938
11	0	9	1	146.87921	1909.455	-0.25937	146.68766	1909.192	-0.25925	146.68651	1909.074	-0.25927
12	0	9	1	12.12280	2807.740	-0.04179	12.10058	2807.377	-0.04176	12.10864	2807.219	-0.04178
13	0	9	1	0.60511	3663.386	-0.00626	0.60342	3662.950	-0.00626	0.60498	3662.765	-0.00627
14	0	9	1	0.00235	4474.684	0.00029	0.00240	4474.204	0.00029	0.00218	4474.008	0.00028
											0.00198	0.00569
11	0	10	1	106.19760	929.038	-0.64984	106.18072	928.920	-0.64991	106.23630	928.863	-0.65014
12	0	10	1	178.08803	1827.323	-0.30507	177.85908	1827.105	-0.30492	177.84214	1827.009	-0.30493

Continued on next page

TABLE I: Einstein coefficients, transition frequencies and Dipole moments for ${}^7\text{LiH}$; continued

v'	upper	lower	nuclear mass	atomic mass			effective mass			Coppola	Shi	
	J'	v''	J''	A/s^{-1}	ν/cm^{-1}	$D/e a_0$	A/s^{-1}	ν/cm^{-1}	$D/e a_0$	A/s^{-1}	A/s^{-1}	
13	0	10	1	17.71451	2682.969	-0.05408	17.68070	2682.677	-0.05404	17.69066	2682.555	-0.05406
14	0	10	1	1.11417	3494.268	-0.00913	1.11130	3493.932	-0.00911	1.11365	3493.798	-0.00912
15	0	10	1	0.01325	4258.785	-0.00074	0.01311	4258.439	-0.00074	0.01343	4258.310	-0.00074
12	0	11	1	81.56031	887.851	-0.60958	81.57391	887.756	-0.60973	81.63510	887.710	-0.61000
13	0	11	1	210.36381	1743.497	-0.35576	210.10234	1743.328	-0.35559	210.06901	1743.256	-0.35558
14	0	11	1	25.81635	25 54 4.796	-0.07026	25.76501	2554.582	-0.07020	25.77330	2554.499	-0.07021
15	0	11	1	1.93782	3319.313	-0.01300	1.93275	3319.090	-0.01298	1.93672	3319.012	-0.01300
16	0	11	1	0.09103	4033.628	-0.00210	0.09049	4033.436	-0.00210	0.09108	4033.382	-0.00210
13	0	12	1	56.12168	845.609	-0.54401	56.16022	845.539	-0.54427	56.22328	845.507	-0.54460
14	0	12	1	241.26848	1656.908	-0.41125	240.98594	1656.793	-0.41105	240.94120	1656.750	-0.41103
15	0	12	1	37.49739	2421.425	-0.09177	37.41918	2421.301	-0.09168	37.41852	2421.263	-0.09168
16	0	12	1	3.27766	3135.740	-0.01841	3.26892	3135.647	-0.01839	3.27490	3135.633	-0.01840
17	0	12	1	0.29530	3795.037	-0.00415	0.29393	3795.027	-0.00414	0.29507	3795.061	-0.00415

Continued on next page

TABLE I: Einstein coefficients, transition frequencies and Dipole moments for ${}^7\text{LiH}$; continued

v'	upper	lower	nuclear mass	atomic mass	effective mass	Coppola	Shi					
	J'	v''	J''	A/s^{-1}	ν/cm^{-1}	$D/e a_0$	A/s^{-1}	ν/cm^{-1}	$D/e a_0$	A/s^{-1}	A/s^{-1}	
14	0	13	1	32.30180	801.670	-0.44711	32.35422	801.629	-0.44751	32.41206	801.612	-0.44793
15	0	13	1	266.49218	1566.187	-0.47030	266.21568	1566.137	-0.47008	266.17422	1566.125	-0.47005
16	0	13	1	54.69454	2280.502	-0.12126	54.57417	2280.483	-0.12113	54.55373	2280.495	-0.12111
17	0	13	1	5.50161	2939.799	-0.02628	5.48604	2939.862	-0.02624	5.49236	2939.923	-0.02625
18	0	13	1	0.71107	3537.510	-0.00716	0.70844	3537.720	-0.00714	0.71090	3537.858	-0.00715
												0.67354
												0.57593
15	0	14	1	13.14106	755 .314	-0.31183	13.19006	755.307	-0.31242	13.23319	755.307	-0.31293
16	0	14	1	278.63223	1469.629	-0.52906	278.41242	1469.653	-0.52884	278.39984	1469.677	-0.52881
17	0	14	1	80.11157	2128.926	-0.16271	79.92938	2129.033	-0.16251	79.87753	2129.106	-0.16245
18	0	14	1	9.74351	2726.636	-0.03915	9.71087	2726.890	-0.03908	9.71125	2727.040	-0.03908
19	0	14	1	1.39163	3254.160	-0.01135	1.38649	3254.642	-0.01132	1.39006	3254.904	-0.01134
												1.34950
												1.17000
16	0	15	1	1.87776	705.562	-0.13056	1.90189	705.596	-0.13139	1.92024	705.615	-0.13202
17	0	15	1	267.36200	1364.859	-0.57905	267.27035	1364.976	-0.57888	267.31816	1365.043	-0.57889
18	0	15	1	114.78017	1962.569	-0.22004	114.52891	1962.833	-0.21975	114.44308	1962.977	-0.21964
19	0	15	1	18.95537	2490.092	-0.06257	18.88205	2490.584	-0.06243	18.86308	2490.842	-0.06239

Continued on next page

TABLE I: Einstein coefficients, transition frequencies and Dipole moments for 7LiH; continued

	upper	lower	nuclear mass	atomic mass			effective mass	Coppola	Shi			
v'	J'	v''	J''	A/s^{-1}	ν/cm^{-1}	$D/e a_0$	A/s^{-1}	ν/cm^{-1}	$D/e a_0$	A/s^{-1}	A/s^{-1}	
20	0	15	1	2.95836	2936.200	-0.01930	2.94453	2937.025	-0.01925	2.94562	2937.440	-0.01925
												2.92010
												2.69759
17	0	16	1	0.95113	651.031	0.10484	0.93116	651.115	0.10371	0.91768	651.158	0.10295
18	0	16	1	222.81399	1248.741	-0.60403	222.92481	1248.972	-0.60402	223.05944	1249.093	-0.60411
19	0	16	1	153.05778	1776.264	-0.29510	152.79029	1776.724	-0.29472	152.69843	1776.957	-0.29458
20	0	16	1	38.66619	2222.371	-0.10598	38.51377	2223.164	-0.10572	38.45505	2223.555	-0.10561
21	0	16	1	7.96812	2572.367	-0.03863	7.92188	2573.624	-0.03849	7.90741	2574.224	-0.03845
												8.11530
												8.14158
18	0	17	1	10.27594	589.981	0.39944	10.20858	590.129	0.39798	10.16562	590.201	0.39707
19	0	17	1	144.02741	1117.504	-0.57365	144.34528	1117.881	-0.57399	144.55528	1118.066	-0.57427
20	0	17	1	170.72360	1563.611	-0.37736	170.63547	1564.321	-0.37700	170.62843	1564.664	-0.37687
21	0	17	1	69.79844	1913.607	-0.17821	69.60365	1914.781	-0.17780	69.52134	1915.333	-0.17762
22	0	17	1	20.77196	2150.847	-0.08159	20.68829	2152.638	-0.08132	20.65101	2153.454	-0.08120
												21.97100
												23.20804
19	0	18	1	24.64734	520.403	0.74675	24.56497	520.631	0.74501	24.51253	520.739	0.74398
20	0	18	1	54.11338	966.510	-0.43716	54.46522	967.072	-0.43820	54.65942	967.338	-0.43880
												50.32000
												45.80926

Continued on next page

TABLE I: Einstein coefficients, transition frequencies and Dipole moments for ${}^7\text{LiH}$; continued

upper	lower	nuclear mass		atomic mass		effective mass		Coppola	Shi					
v'	J'	v''	J''	A/s^{-1}	ν/cm^{-1}	$D/e a_0$	A/s^{-1}	ν/cm^{-1}	$D/e a_0$	A/s^{-1}	A/s^{-1}			
21	0	18	1	125.21867	1316.506	-0.41831	125.56395	1317.532	-0.41840	125.74623	1318.006	-0.41848		
22	0	18	1	74.67857	1553.745	-0.25196	74.82777	1555.389	-0.25181	74.89279	1556.127	-0.25174		
23	0	18	1	15.63281	1661.678	-0.10423	15.84695	1664.072	-0.10472	15.92709	1665.112	-0.10488		
												-		
20	0	19	1	32.90817	439.693	1.11103	32.87882	440.026	1.10928	32.85258	440.179	1.10826	33.58600	35.15559
21	0	19	1	2.98008	789.689	-0.13891	3.07583	790.486	-0.14091	3.12535	790.847	-0.14194	2.35070	1.49705
22	0	19	1	29.99677	10 26 .928	-0.29718	30.39551	1028.342	-0.29854	30.58159	1028.968	-0.29918	28.51600	27.29492
23	0	19	1	11.13717	1134.861	-0.15587	11.42923	1137.026	-0.15745	11.55010	1137.953	-0.15809	10.90100	-
21	0	20	1	25.28232	344.427	1.40463	25.34571	344.889	1.40356	25.36561	345.093	1.40287	25.34400	25.64423
22	0	20	1	5.55963	581.667	0.30013	5.50240	582.746	0.29775	5.47188	583.214	0.29657	5.93090	6.79759
23	0	20	1	0.11999	689.600	0.03416	0.11064	691.429	0.03267	0.10628	692.199	0.03197	0.15849	-
22	0	21	1	8.00073	232.709	1.42280	8.07892	233.322	1.42410	8.10961	233.581	1.42443	7.96060	8.22570
23	0	21	1	2.86561	340.642	0.48079	2.92636	342.005	0.48296	2.94907	342.566	0.48364	2.90310	-
23	0	22	1	0.21219	104.718	0.76759	0.22079	105.461	0.77473	0.22419	105.57	0.77739	0.21410	-

TABLE II: Einstein coefficients, A (s^{-1}), for some transitions of ${}^7\text{LiH}$ in the ground $X^1\Sigma^+$ electronic state.

$v'J'v''J''$	nuclear	atomic	effective	Shi [5]	Coppola [4]	Partridge [13]
1 0 0 1	46.9	46.8	46.8	45.4	46.6	43.1
2 0 0 1	2.1	2.1	2.1	2.0	2.1	1.9
2 0 1 1	85.8	85.7	85.7	82.8	85.3	78.5
3 0 1 1	6.5	6.5	6.5	6.4	6.6	6.3
3 0 2 1	116.7	116.6	116.6	112.5	115.9	106.7
4 0 2 1	13.5	13.5	13.5	13.4	13.6	13.3
4 0 3 1	139.8	139.7	139.7	134.5	138.7	127.3
5 0 3 1	23.2	23.2	23.2	23.1	23.5	22.7
5 0 4 1	155.2	155.0	155.1	148.7	153.7	140.3
6 0 4 1	35.9	35.9	35.9	35.9	36.3	34.5
6 0 5 1	163.0	162.9	162.9	155.6	161.3	145.7
7 0 5 1	51.7	51.6	51.6	51.8	52.3	49.3

TABLE III: Vibrationally averaged dipole moments (Debye) of ${}^7\text{LiH}$ in the ground $X^1\Sigma^+$ electronic state and in the $J = 1$ rotational state.

v	Partridge [13]	nuclear	atomic	effective	experiment [24]
0	5.889	5.884	5.884	5.884	5.882 ± 0.003
1	5.996	5.992	5.993	5.992	5.990 ± 0.003
2	6.104	6.101	6.101	6.101	6.098 ± 0.003

TABLE IV: Vibrationally averaged dipole moments (Debye) of ${}^7\text{LiH}$ in the ground $X^1\Sigma^+$ electronic state and in the $J = 0$ rotational state.

v	Partridge [13]	nuclear atomica	effective	Cafiero [25]	
0	5.888	5.883	5.883	5.883	5.882
1	5.995	5.992	5.992	5.992	-
2	6.103	6.100	6.100	6.100	-
3	6.210	6.208	6.208	6.208	-
4	6.312	6.313	6.313	6.313	-
5	6.408	6.416	6.416	6.416	-

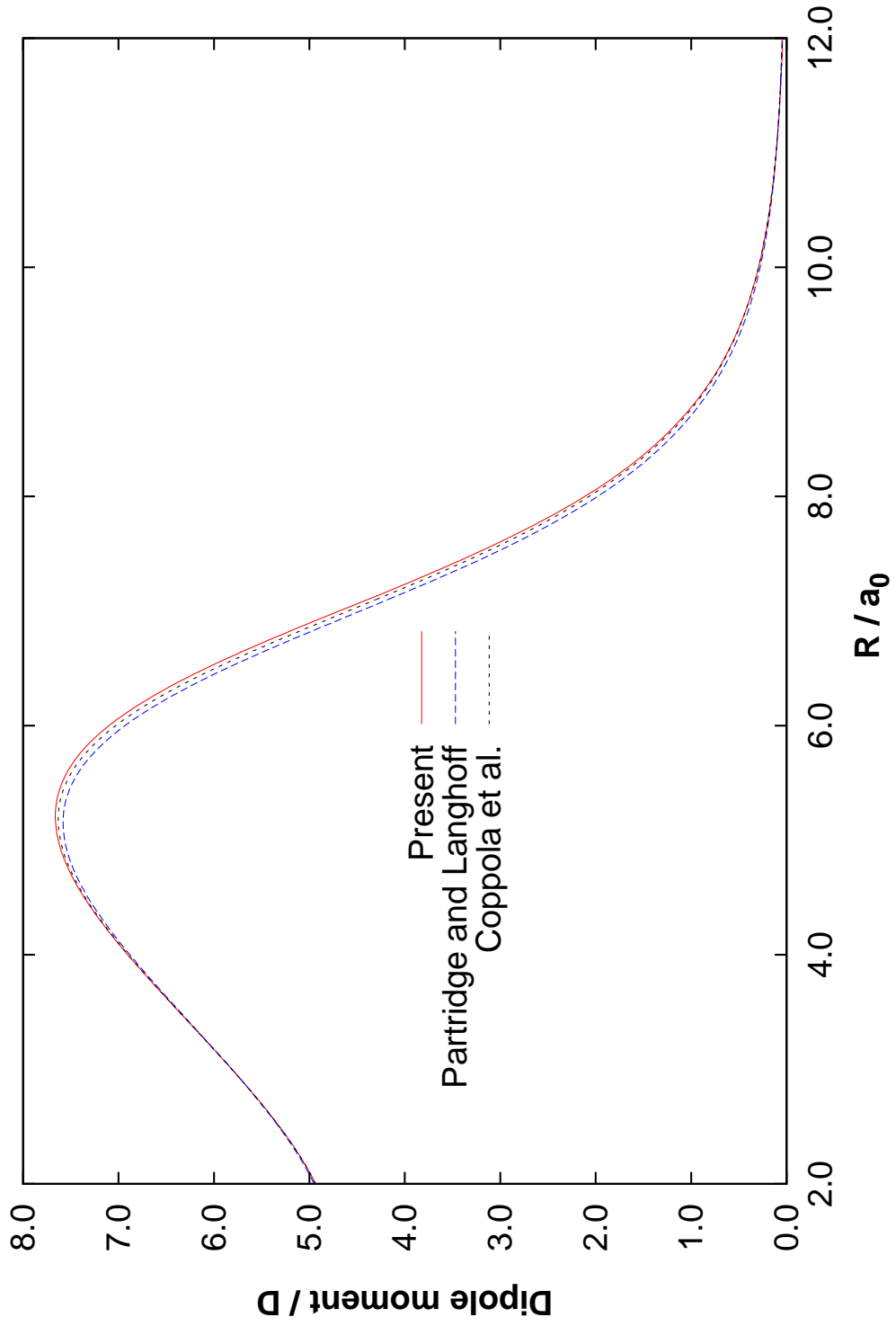


FIG. 1: Comparison of the DMC of the LiH molecule in the ground $\mathbf{X}^1\Sigma^+$ electronic state obtained in this work with the previous theoretical curves of Partridge and Langhoff [13] and Coppola et al. [4].

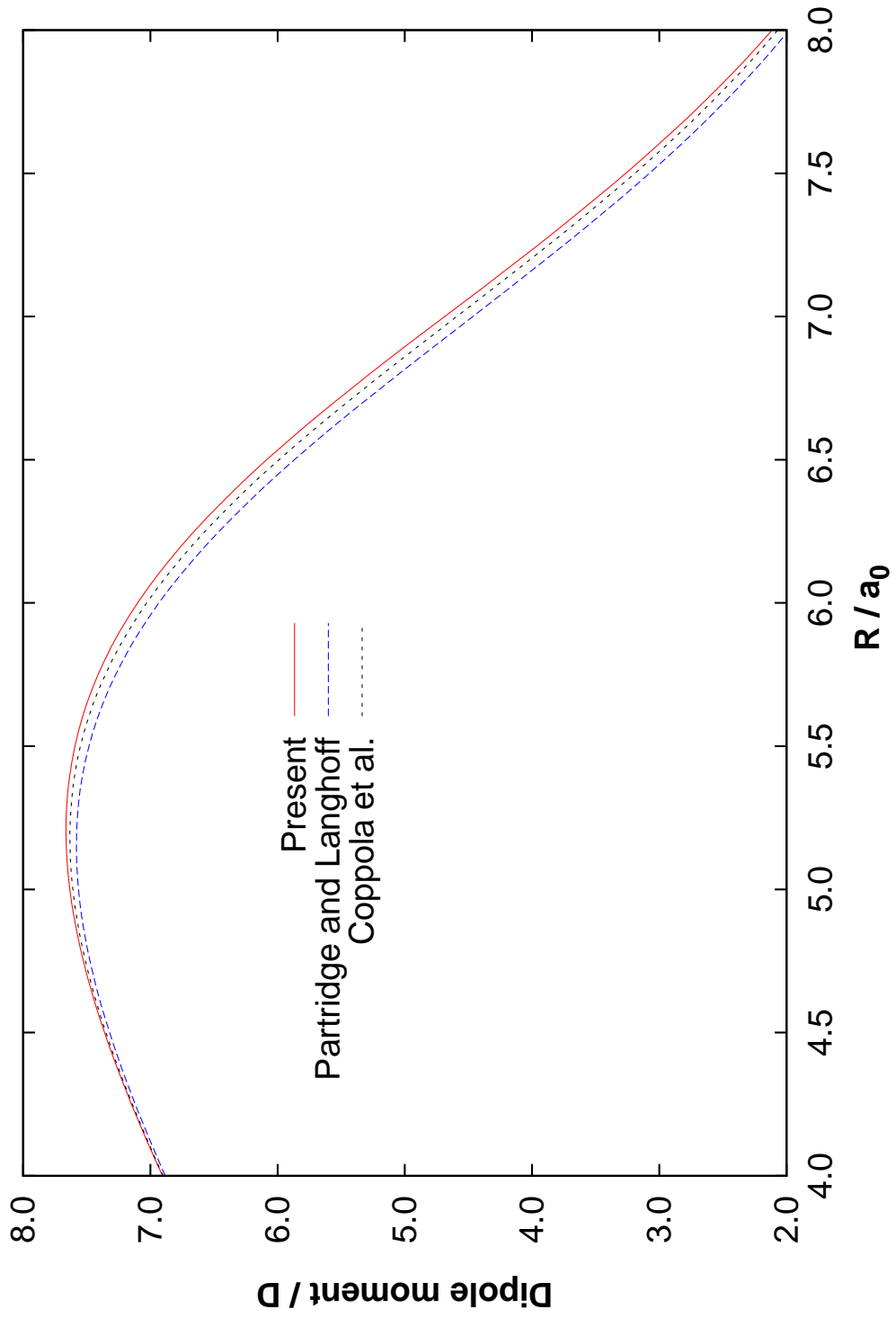


FIG. 2: Comparison of the DMC of LiH in the ground $\mathbf{X}^1\Sigma^+$ electronic state obtained in this work with the previous theoretical curves of Partridge and Langhoff [13] and Coppola et al. [4]

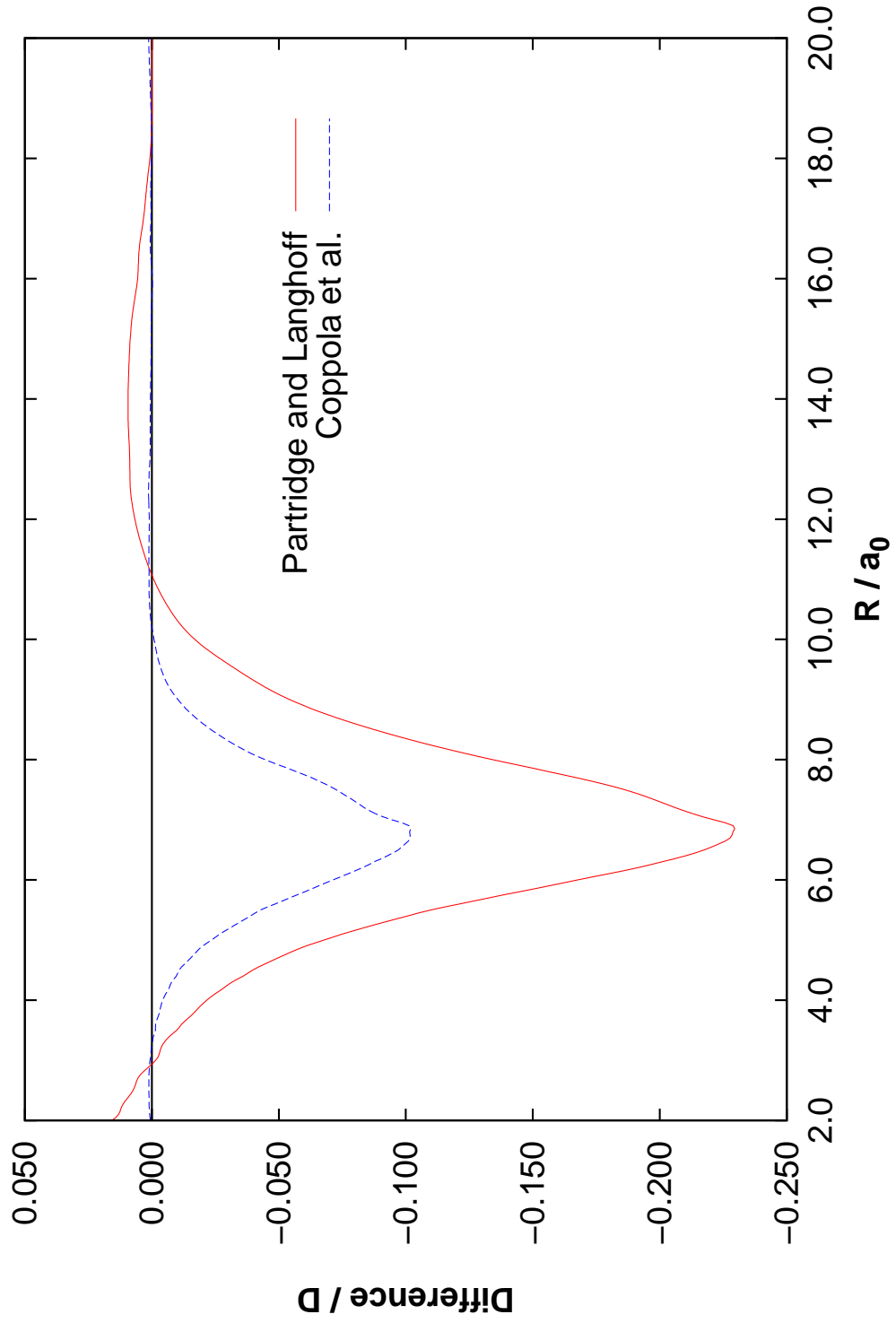


FIG. 3: Differences between the DMCs of Partridge and Langhoff [13] and of Coppola et al. [4] and the DMC obtained in this work.

-
- [1] W. C. Stwalley and W. Zemke, J. Chem. Phys. **22**, 87 (1993).
 - [2] Wei-Cheng Tung, Michele Pavanello and Ludwik Adamowicz, J. Chem. Phys. **134**, 064117-1 (2011).
 - [3] Filip Holka, Péter G. Szalay, Julien Fremont, Michael Rey, Kirk A. Peterson and Vladimir G. Tyuterev, J. Chem. Phys. **134**, 94306-1 (2011).
 - [4] C. M. Coppola, L. Lodi and J. Tennyson, Mon. Not. R. Astron. Soc. **415**, 487 (2011).
 - [5] Y. B. Shi, P. C. Stancil and J. G. Wang, Astronomy & Astrophysics **551**, A140 (2013).
 - [6] E. Bougleux and D. Galli, MNRAS **288**, 638 (1997).
 - [7] S. Lepp, P. C. Stancil and A. Dalgarno, J. Phys. B. **35**, R57 (2002).
 - [8] M. Dulick, K. Q. Zhang, B. Guo and P. F. Bernath, J. Mol. Spectrosc. **188**, 14 (1998).
 - [9] J. A. Coxon and C. S. Dickinson, J. Chem. Phys. **121**, 9378 (2004).
 - [10] Y. C. Chan, D. R. Harding and W. C. Stwalley, J. Chem. Phys. **85**, 2436 (1986).
 - [11] P. R. Bunker and R. E. Moss, Mol. Phys. **33**, 417 (1977).
 - [12] L. G. Diniz, A. Alijah, L. Adamowicz and J. R. Mohallem, Chem. Phys. Lett. **633**, 89 (2015).
 - [13] H. Partridge and S. R. Langhoff, J. Chem. Phys. **74**, 2361 (1981).
 - [14] D. Tunega and J. Noga, Teor. Chem. Acc. **100**, 78 (1998).
 - [15] Jr. T. H. Dunning. J. Chem. Phys. **90**, 1007 (1989).
 - [16] B. P. Prascher, D. E. Woon, K. A. Peterson, T. H. Dunning Jr. and A. K. Wilson, Theor. Chem. Acc. **128**, 69 (2011).
 - [17] F. A. Matsen and R. Pauncz, *The Unitary Group in Quantum Chemistry*, (Elsevier, Amsterdam, 1986).
 - [18] R. Pauncz, *The Symmetry Group in Quantum Chemistry*, (CRC Press, Boca Raton, 1995).
 - [19] M. Hamermesh, *Group Theory and Its Application to Physical Problems*, (Addison-Wesley, Reading, MA, 1962).
 - [20] B. R. Johnson, J. Chem. Phys. **67**, 4086 (1977).
 - [21] A. Alijah and G. Duxbury, Mol. Phys. **70**, 605 (1990).
 - [22] A. Alijah, D. Andrae and J. Hinze, Theor. Chem. Acc. **127**, 149 (2010).
 - [23] See supplemental material at [URL will be inserted by AIP] for the dipole moment curve data used in the present calculations.

- [24] L. Wharton, L. P. Gold and W. Klemperer, J. Chem. Phys. **37**, 2149 (1962).
- [25] M. Duran M. Cafiero, L. Adamowicz and J. M . Luis, J. Mol. Struc. **633**, 113 (2003).

APPENDIX C

An algorithm for quantum mechanical finite-nuclear-mass variational calculations
of atoms with $L = 3$ using all-electron explicitly correlated Gaussian basis
functions

An algorithm for quantum mechanical finite-nuclear-mass variational calculations of atoms with $L = 3$ using all-electron explicitly correlated Gaussian basis functions

Keeper L. Sharkey,¹ Nikita Kirnosov,² and Ludwik Adamowicz^{1,2}

¹Department of Chemistry, University of Arizona, Tucson, Arizona 85721, USA

²Department of Physics, University of Arizona, Tucson, Arizona 85721, USA

(Received 18 January 2013; accepted 20 February 2013; published online 12 March 2013)

A new algorithm for quantum-mechanical nonrelativistic calculation of the Hamiltonian matrix elements with all-electron explicitly correlated Gaussian functions for atoms with an arbitrary number of s electrons and with three p electrons, or one p electron and one d electron, or one f electron is developed and implemented. In particular the implementation concerns atomic states with $L = 3$ and $M = 0$. The Hamiltonian used in the approach is obtained by rigorously separating the center-of-mass motion from the laboratory-frame all particle Hamiltonian, and thus it explicitly depends on the finite mass of the nucleus. The approach is employed to perform test calculations on the lowest 2F state of the two main isotopes of the lithium atom, ^7Li and ^6Li . © 2013 American Institute of Physics. [http://dx.doi.org/10.1063/1.4794192]

I. INTRODUCTION

In recent years there has been a renewed interest in very accurate quantum mechanical calculations of the electronic structures of small atoms.^{1–13} The interest has been motivated by both new, more accurate spectral measurements performed on these systems and by the development of new computational methods that allow the spectral levels of these systems to be calculated with much higher accuracy than before. Most of the work in the field has been centered on two- and three-electron atomic systems because they can be very accurately calculated using Hylleraas type functions. As the extension of the Hylleraas function approach to atoms with more than three electrons has not yet been achieved due to difficulties in determining the Hamiltonian matrix elements,¹² alternative approaches had to be found. One of them is based on employing explicitly correlated all-electron Gaussian (ECG) functions. This research group has been actively contributing to the development of ECG methods for very accurate atomic calculations^{14–19} for several years now. There have been two important features in these methods that set that development apart from the works carried by others. The first has been the explicit inclusion of the nuclear motion in the nonrelativistic Hamiltonian used in the variational calculations of the energies and the wave functions of the atomic system under consideration. The second has been the use of the analytical energy gradient determined with respect to the Gaussian exponential parameters in the variational optimization of the Gaussians. For example, in the recent work on the beryllium atom,¹⁹ where the gradient was used in the ECG optimization, it was demonstrated that calculations utilizing large basis sets of Gaussians that also include lowest order relativistic and QED corrections can reproduce the lowest excitation transition energy of this system with the accuracy matching that of the most accurate experiments.

In order to extend the use of ECGs to larger atomic systems and to widen the range of electronic states in the calculations procedures need to be developed to describe states where some electrons have non-zero angular momenta. Thus this research group carried out the development and implementation of algorithms for calculating energy and energy gradient for atomic states with an arbitrary number of s electrons and one p electron,¹⁷ and states with s electrons and two p electrons or one d electron.^{20,21} These algorithms have enabled calculations of the ground state for the boron and carbon atoms. The next step, which is carried out in the present work, is extending the ECG approach to atomic states where, besides some number of s electrons, there are either three p electrons, or one p and one d electron, or one f electron. States of these kinds include, for example, the ground $1s^2 2s^2 2p^3$ state of the nitrogen atom. The development presented in this work includes the derivation of the overlap and Hamiltonian matrix elements for ECGs used to calculate of energies of such states. Derivations of the Hamiltonian matrix elements is carried out using the matrix-calculus approach. The derived algorithms are implemented and tested for correctness in calculations of the lowest 2F state of two isotops of the lithium atom, ^7Li and ^6Li . The results of these tests are shown in Sec. VII.

It is worth mentioning that the formulas for the atomic systems with the angular momentum of $L = 3$ have broader applicability than just the calculations of atomic F states. Some elements and formulas obtained in the present derivations can be useful in deriving the overlap and Hamiltonian matrix elements for atoms with higher orbital angular momenta, as well as for diatomic systems in higher rotational states. For instance, the general form of the potential energy matrix elements for an atom with $L = 3$ can be used to calculate overlap matrix elements for rotationally excited $J = 3$ states of diatomic molecules when the Born-Oppenheimer approximation is not assumed. Also, one part of the formula for

the kinetic energy matrix elements can be used to calculate the overlap matrix elements for atoms with $L = 4$ granted that certain matrices are redefined. This is a unique aspect of the calculations preformed using ECGs.

F states of small atoms have not been as accurately measured as S, P, and D states. For example, there are only two ^2F states reported in the NIST Atomic Spectra Database²² for ^7Li . These are the lowest $1s^24f$ state and the first excited $1s^25f$ state. For both of them the reported transition energies in wavenumbers determined with respect to the ^2S ground state are given with only one significant figure after the decimal point. The theoretical calculations not only deliver higher accuracy in predicting the energies of these states but the calculations can also provide data on more of them. This has been the motivation for the development carried out in this work.

The prototype computer code which has been written is not yet in a form that can be used to perform large-scale production calculations involving thousands of ECGs. To run such calculations an algorithm for calculating the analytical energy gradient has to be developed and implemented. This task will be pursued in the near future. The implementation will involve efficient message passing interface (MPI) parallelization of the calculation which takes advantage of multi-processor computer environment. Procedures for calculating the lowest order relativistic corrections will also need to be implemented. Only then can calculations of transition energies for such systems as the nitrogen atom can be expected to provide high-accuracy results.

II. NOTATION

In the beginning, it is necessary to briefly explain the notation scheme used throughout this work. The scheme is the same as the one used in our previous work.¹⁷ To start, small greek letters are used to denote scalar quantities, bold small greek letters represent three-component vectors, while capital greek letters are used for 3×3 matrices. Small latin letters denote n -component vectors (n is the number of electrons in the atom; see the beginning of Sec. III) and bold small latin letters denote $3n$ -component vectors. If such a letter has an index (subscript) this means it is a 3-component vector. For example, \mathbf{r} is a $3n$ -component vector, while \mathbf{r}_i is a 3-component vector. Capital latin letters are used for $n \times n$ matrices and bold capital latin letters are used for $3n \times 3n$ matrices.

All matrix-matrix and matrix-vector products that appear in formulas are calculated using the conventional matrix algebra. For example, a product of a $p \times q$ matrix and a $q \times k$ matrices yields a $p \times k$ matrix. Vector or matrix transposition is denoted by a prime (\prime) symbol and, at last, vertical bars around a matrix denote its determinant, while vertical bars around a vector or a scalar stand for the absolute value or the length, respectively.

III. THE HAMILTONIAN

We consider a nonrelativistic atomic system consisting of N particles, i.e., $N - 1$ electrons and a nucleus. The i th particle has mass M_i , charge Q_i , and the position vector in the laboratory Cartesian coordinate frame (LCCF), \mathbf{R}_i . The

nonrelativistic LCCF Hamiltonian for the system is

$$\hat{H}_{\text{lab}} = - \sum_{i=1}^N \frac{1}{2M_i} \nabla_{\mathbf{R}_i}^2 + \sum_{i>j=1}^N \frac{Q_i Q_j}{R_{ij}}, \quad (1)$$

where $\nabla_{\mathbf{R}_i}$ is the gradient with respect to \mathbf{R}_i , and R_{ij} is the distance between the i th and j th particles, $R_{ij} = |\mathbf{R}_j - \mathbf{R}_i|$.

The center-of-mass motion of the system can be separated out in the LCCF Hamiltonian (1) to yield a Hamiltonian describing the center-of-mass motion and another Hamiltonian describing the internal motion of the electrons relative to the nucleus. The separation can be accomplished by representing the LCCF Hamiltonian in a new coordinate system whose first three coordinates are the LCCF coordinates of the center of mass and the remaining $3N-3$ coordinates are the relative internal coordinates describing the positions of the electrons with respect to the nucleus. By placing the nucleus at the origin of the new, internal Cartesian coordinate system it becomes the reference particle for all other particles (electrons) in the atom. The internal coordinates are defined as: $\mathbf{r}_i = \mathbf{R}_{i+1} - \mathbf{R}_1$. The three coordinates describing the center of mass are denoted as \mathbf{r}_0 and the total mass of the system is $M_{\text{tot}} = \sum_{i=1}^N M_i$.

The internal Hamiltonian obtained using the above coordinate transformation depends only on the internal coordinates. For an atom, it describes the motion of $n = N - 1$ pseudoelectrons in the central field of the nucleus. We use the term “pseudoelectron” because, even though the charges of the particles described by the internal Hamiltonian are electron charges, their masses are not electron masses but reduced masses. Denoting the mass of the nucleus as m_0 and the charge as q_0 , setting the pseudoelectron reduced masses to be $\mu_i = m_0 m_i / (m_0 + m_i)$ with $m_i = M_{i+1}$, and with the pseudoelectron charges equal to $q_i = Q_{i+1}$, the internal Hamiltonian is

$$\begin{aligned} \hat{H} = & -\frac{1}{2} \left(\sum_{i=1}^n \frac{1}{\mu_i} \nabla_{\mathbf{r}_i}^2 + \sum_{i=1, j=1, i \neq j}^n \frac{1}{m_0} \nabla'_{\mathbf{r}_i} \nabla_{\mathbf{r}_j} \right) \\ & + \sum_{i=1}^n \frac{q_0 q_i}{r_i} + \sum_{i>j=1}^n \frac{q_i q_j}{r_{ij}}. \end{aligned} \quad (2)$$

The motions of the pseudoelectrons are described by their kinetic energy term, $-\frac{1}{2} \sum_{i=1}^n \frac{1}{\mu_i} \nabla_{\mathbf{r}_i}^2$, the kinetic-energy coupling term also known as the mass polarization term, $-\frac{1}{2} \sum_{i=1, j=1, i \neq j}^n (1/m_0) \nabla'_{\mathbf{r}_i} \nabla_{\mathbf{r}_j}$, and the Coulombic interactions of each pseudoelectron with the nucleus and all other pseudoelectrons. The Coulombic interactions are dependent on the distances between the pseudoparticles and the origin of the internal coordinate system, r_i , and on the relative distances between the pseudoparticles, r_{ij} , where $r_{ij} = |\mathbf{r}_j - \mathbf{r}_i|$. This Hamiltonian is used in the present calculations.

IV. THE BASIS FUNCTIONS

To obtain the energy eigenvalues of Hamiltonian (2) the Rayleigh-Ritz variational scheme is used. Since the total

internal atomic wave function, Ψ , is dependent on the spatial coordinates, \mathbf{r} , and the spin coordinates, \mathbf{m} , of the pseudoelectrons: $\Psi = \Psi(\mathbf{r}, \mathbf{m})$, and because internal Hamiltonian (2) is spin independent, the calculation of the Hamiltonian and overlap matrix elements can be carried out by first integrating over spin variables, which leaves behind only spatially dependent integrals. The spatial wave functions, $\Psi(\mathbf{r})$, in those integrals are approximated by linear combinations of K basis functions, $\psi_k(\mathbf{r})$:

$$\Psi(\mathbf{r}) = \sum_{k=1}^K c_k \hat{Y} \psi_k(\mathbf{r}), \quad (3)$$

where c_k is the linear variational parameter, and \hat{Y} is some permutational symmetry projection operator discussed in Sec. V.

The basis function $\psi_k(\mathbf{r})$ for an *n*electron atomic system with only *s* electrons have only a radial part and it is spherically symmetric (or rotationally invariant). In our calculations $\psi_k(\mathbf{r})$ has the form of an ECG function,

$$\psi_k = \exp[-\mathbf{r}'(A_k \otimes I_3)\mathbf{r}], \quad (4)$$

where A_k is an $n \times n$ symmetric matrix, \otimes is the Kronecker product symbol, and I_3 is a 3×3 identity matrix. In ECGs all one-pseudoelectron exponential variables and all two-pseudoelectron coupling exponential variables are included by the use of a quadratic form involving a vector-matrix-vector product, $\mathbf{r}'(A_k \otimes I_3)\mathbf{r}$ (this form is used frequently in this work as it allows for some ease in the evaluation of Hamiltonian and overlap matrix elements).

It is required that the basis functions used in a bound-state calculation are square integrable which effectively imposes restrictions on the A_k matrix. The A_k matrix must be positive definite. Rather than restricting the A_k matrix elements, A_k is represented in a Cholesky factored form as: $A_k = L_k L'_k$, where L_k is a lower triangular matrix. With this representation, A_k is automatically positive definite. It should also be mentioned that this form of A_k matrix does not limit the flexibility of the basis functions since any allowable choice of the A_k matrix can be represented by some L_k matrix. This is because any symmetric positive matrix can be represented in a Cholesky factored form.

For an atomic system, where some electrons have non-zero angular momenta, the ECG functions (4) need additional multiplicative components to be placed in front of the exponent. As mentioned, in the recent works this group has developed methods for calculating atomic systems with one electron in a *p* state,^{14,17} and either two electrons in *p* states,²⁰ or one electron is in a *d* state²³ (all other electrons are in *s* states). The focus in this work is on states with total orbital angular momentum of $L = 3$ and its projection on the z axis of $M = 0$. Such states correspond to atoms with either one *f* electron, or one *p* electron and one *d* electron, or three *p* electrons (again, all other electrons are in *s* states).

For a state with one *f* electron the basis functions can be obtained by using the following non-normalized form of spherical harmonic function Y_3^0 expressed in the Cartesian coordinates:

$$(3x_i^2 + 3y_i^2 - 2z_i^2) z_i, \quad (5)$$

where the common constant factor and the $1/r_i^{l_i}$ factor were dropped; l_i is the angular momentum quantum number of the *i*th electron. To be all inclusive, this particular state ($L = 3$ and $M = 0$) can also be formed by one *p* and one *d* electron, or three *p* electrons and explicit angular functions can be obtained with a standard procedure of coupling angular momenta with the use of Clebsch-Gordan coefficients. Our previous work²⁰ describes a method for coupling two electrons, *i* and *j*. A similar procedure is applied here and for the angular component of the basis function corresponding a $L = 3$ and $M = 0$ configuration with one *p* and one *d* electron is

$$(x_i^2 + y_i^2 - 2z_i^2) z_j + 2(x_i x_j + y_i y_j) z_i \quad (6)$$

and again, the constant factor and the $1/r_i^{l_i} r_j^{l_j}$ factor were dropped.

For the three *p* electron case the procedure is analogical. Let us suppose that the orbital quantum numbers of electrons *i*, *j*, and *k* (*k* in this case is not the index for the basis function expansion) are l_i, m_i, l_j, m_j, l_k , and m_k . Using the bra-ket notation, the angular part of the a basis function corresponding to particular *L* and *M* can be represented as the following linear combination:

$$\begin{aligned} |L M\rangle = & \sum_{\substack{m_i, m_j, m_k \\ m_i + m_j + m_k = M}} (L M | l_i m_i l_j m_j l_k m_k) \\ & \times (l_j m_j | l_j m_j l_k m_k) | l_i m_i \rangle | l_j m_j \rangle | l_k m_k \rangle, \end{aligned} \quad (7)$$

where the $(L M | l_i m_i l_j m_j l_k m_k)$ and $(l_j m_j | l_j m_j l_k m_k)$ factors are the Clebsch-Gordan coefficients.²⁴ With that, the angular part of the basis function becomes

$$(x_i x_j + y_i y_j - 2z_i z_j) z_k + (x_i x_k + y_i y_k) z_j + (x_j x_k + y_j y_k) z_i \quad (8)$$

after the common constant factors and the $1/(r_i^{l_i} r_j^{l_j} r_k^{l_k})$ factor were dropped.

The three angular functions shown in (5), (6) and (8) can be represented using a single expression

$$(x_i x_j + y_i y_j - 2z_i z_j) z_k + (x_i x_k + y_i y_k) z_j + (x_j x_k + y_j y_k) z_i, \quad (9)$$

which is the same as (8). By setting $j = i$ and $k = i$ (9) becomes (5) and by setting $j = i$ and $k = j$ it becomes (6). Therefore, (9) is the suitable general form of the angular factor for an ECG basis function for the $L = 3$ and $M = 0$ states. The three-electron lithium atom is the smallest system for testing the correctness of the Hamiltonian integrals over ECGs with the general angular factor (9). However, in this work testing has been also performed using one electron functions (the hydrogen atom) and two-electron ECGs (the helium atom). The testing concerned the correctness of the integral formulas, as well as the correctness of the computer code written using FORTRAN 90.

As an aside, (7) is the formula to use to determine the angular factor for the main configurations that need to be used to describe the ground state of the nitrogen atom. For nitrogen atom, with $L = 0$ and $M = 0$, the ECGs need to have the

following angular factors:

$$(x_j y_i - x_i y_j) z_k + (x_i y_k - x_k y_i) z_j + (x_k y_j - x_j y_k) z_i. \quad (10)$$

The nitrogen ground state will be calculated in a future project after the pilot FORTRAN 90 code developed in this project is made more efficient and after the analytical energy gradient is evaluated. This will be discussed further in Sec. VII.

It should be mentioned that for the lithium atom in an excited $L = 3$ and $M = 0$ state, ECGs with angular factor (5) are expected to be the most contributing functions in the wave function expansion. Only a small percentage of the basis functions needed to describe such a state are expected to have the (6) and (8) angular factors. Therefore, it is not the focus of this work to include these small contributions in the basis set. The primary focus of this work is to show, based on the lithium 2F state calculations, the correctness of the derived Hamiltonian and overlap matrix elements (see Sec. VI). Thus, as in generating the numerical results presented in Sec. VII only ECGs with angular factor type (5) are utilized, the ECG basis set is not strictly complete.

To construct the full form of the basis function, $\Psi_k(\mathbf{r})$, for $L = 3$ and $L = 0$ states, the rotationally invariant ECG (4) and the angular portion in the general form, (9), are multiplied together

$$\begin{aligned} \psi_k &= \{(x_{i_k} x_{j_k} + y_{i_k} y_{j_k} - 2z_{i_k} z_{j_k}) z_{k_k} + (x_{i_k} x_{k_k} + y_{i_k} y_{k_k}) z_{j_k} \\ &\quad + (x_{j_k} x_{k_k} + y_{j_k} y_{k_k}) z_{i_k}\} \exp[-\mathbf{r}'(\mathbf{A}_k)\mathbf{r}] \\ &= \{(\mathbf{r}' \mathbf{W}_k^1 \mathbf{r}) (\mathbf{v}_k^{1'} \mathbf{r}) + (\mathbf{r}' \mathbf{W}_k^2 \mathbf{r}) (\mathbf{v}_k^{2'} \mathbf{r}) + (\mathbf{r}' \mathbf{W}_k^3 \mathbf{r}) (\mathbf{v}_k^{3'} \mathbf{r})\} \\ &\quad \times \exp[-\mathbf{r}'(\mathbf{A}_k)\mathbf{r}], \end{aligned} \quad (11)$$

where general quadratic forms replaced $(x_{i_k} x_{j_k} + y_{i_k} y_{j_k} - 2z_{i_k} z_{j_k})$, $(x_{i_k} x_{k_k} + y_{i_k} y_{k_k})$, and $(x_{j_k} x_{k_k} + y_{j_k} y_{k_k})$, and vector-vector products replaced z_i , z_j , z_k . These replacements allow for a more generalized approach in deriving the expressions for the Hamiltonian matrix elements. $\mathbf{W}_k^{(1,2,3)}$ used in (11) are sparse $3n \times 3n$ symmetric matrices comprising mostly zeros. Note that $\mathbf{W}_k^{(1,2,3)}$ cannot be represented as a Kronecker product of $\mathbf{W}_k^{(1,2,3)}$ and I_3 : $\mathbf{W}_k^{(1,2,3)} \neq \mathbf{W}_k^{(1,2,3)} \otimes I_3$. Vectors $\mathbf{v}_k^{(1,2,3)}$ used in (11) are $3n$ row vectors. Each has a single non-zero element equal to one placed in the $3(k_k - 1) + 3$ position in $\mathbf{v}_k^{1'}$, in the $3(j_k - 1) + 3$ position $\mathbf{v}_k^{2'}$, and in the $3(i_k - 1) + 3$ position in $\mathbf{v}_k^{3'}$. Finally, $\mathbf{A}_k = A_k \otimes I_3$.

In general, the $\mathbf{W}_k^{(1,2,3)}$ matrices have only non-zero elements corresponding to the coefficient of the polynomial term divided by 2 and placed symmetrically in the matrix in positions to obtain the correct quadratic form. In other words

$$\mathbf{W}_k^{(1,2,3)} = (1/2)(\mathbf{V}_k^{(1,2,3)} + \mathbf{V}_k^{(1,2,3)\prime}), \quad (12)$$

where $\mathbf{V}_k^{(1,2,3)}$ is as an asymmetric matrix. This is called matrix symmetrization. For instance, the sum of quadratic coordinate products, $(x_{i_k} x_{j_k} + y_{i_k} y_{j_k} - 2z_{i_k} z_{j_k})$, corresponds to \mathbf{W}_k^1 , where the first term is represented by the non-zero element both equal to 1/2 placed as the following two elements in the matrix: $\mathbf{W}_k^1(3(i_k - 1) + 1, 3(j_k - 1) + 1)$ and $\mathbf{W}_k^1(3(j_k - 1) + 1, 3(i_k - 1) + 1)$, and likewise for the second term, 1/2 is placed as the following matrix elements: $\mathbf{W}_k^1(3(i_k - 1) + 2, 3(j_k - 1) + 2)$ and $\mathbf{W}_k^1(3(j_k - 1) + 2, 3(i_k - 1) + 2)$, and for the third term, $-2/2 = -1$ is placed as

the following matrix elements: $\mathbf{W}_k^1(3(i_k - 1) + 3, 3(j_k - 1) + 3)$ and $\mathbf{W}_k^1(3(j_k - 1) + 3, 3(i_k - 1) + 3)$. Alternatively, the representation with asymmetric matrix \mathbf{V}_k^1 can be used. In this case \mathbf{V}_k^1 has 1 in the $\mathbf{V}_k^1(3(i_k - 1) + 1, 3(j_k - 1) + 1)$ and $\mathbf{V}_k^1(3(i_k - 1) + 2, 3(j_k - 1) + 2)$ positions, and -2 in the $\mathbf{V}_k^1(3(i_k - 1) + 3, 3(j_k - 1) + 3)$ position. The matrix-symmetrization formula is used in this work in deriving the integrals contributing to the Hamiltonian matrix elements. The derivation is described in VI.

Finally, due to linearity of (10) and (11), we can rewrite them as

$$\psi_k(\mathbf{r}) = \sum_{q=1}^3 (\mathbf{r}' \mathbf{W}_k^q \mathbf{r}) (\mathbf{v}_k^{q'} \mathbf{r}) \exp[-\mathbf{r}'(\mathbf{A}_k)\mathbf{r}]. \quad (13)$$

With that the total spatial wave function becomes

$$\Psi(\mathbf{r}) = \sum_{k=1}^K c_k \hat{Y} \sum_{q=1}^3 (\mathbf{r}' \mathbf{W}_k^q \mathbf{r}) (\mathbf{v}_k^{q'} \mathbf{r}) \exp[-\mathbf{r}'(\mathbf{A}_k)\mathbf{r}]. \quad (14)$$

Thus, for simplicity, in the derivation of the Hamiltonian and overlap matrix elements, we will be considering the following general ECG with a cubic pre-exponential factor:

$$\phi_k = (\mathbf{r}' \mathbf{W}_k \mathbf{r}) (\mathbf{v}_k' \mathbf{r}) \exp[-\mathbf{r}'(\mathbf{A}_k)\mathbf{r}], \quad (15)$$

where we have dropped the notation that indicates that ϕ_k is a function of \mathbf{r} and the summation over index q . The derivation of the Hamiltonian and overlap matrix elements will be carried out with functions (15). The summation over q is implemented at the stage of writing the FORTRAN 90 computer code. As q changes from one to three for each basis function $\psi_k(\mathbf{r})$, the overlap and Hamiltonian matrix elements determined for $\psi_k(\mathbf{r})$ and $\psi_l(\mathbf{r})$ will be a sum of nine elements determined with functions (15). Each of these nine elements includes a sum over permutation-symmetry operators which is described next.

V. PERMUTATIONAL SYMMETRY

For atoms, the basis functions used in the wave function expansion should possess the proper symmetry with respect to the permutations of identical particles (electrons) involved in the system. Since the Hamiltonian is spin independent, the spin can be completely eliminated from the consideration leading to a nontrivial symmetry projection operator, \hat{Y} , that needs to be applied to the spatial wave function and, thus, to each basis function. This operator is a linear combination of some permutation operators and its construction is described below.

In calculating the overlap and Hamiltonian matrix elements all the permutations, in general, can be applied to the ket as $\hat{P} = \hat{Y}^\dagger \hat{Y}$ (the dagger stands for conjugate). This results in each matrix element being a sum of elemental matrix elements in which the ket basis function is transformed by different permutation operators \hat{P} . Thus for (15) we have

$$\langle \phi_k | \hat{P} | \phi_l \rangle = \langle \phi_k | \tilde{\phi}_l \rangle \text{ and } \langle \phi_k | \hat{H} \hat{P} | \phi_l \rangle = \langle \phi_k | \hat{H} | \tilde{\phi}_l \rangle, \quad (16)$$

where $\tilde{\phi}_l$ stands for permuted ϕ_l . As the calculation of matrix elements with permuted kets can be done using the same procedure as for nonpermuted ones, \hat{P} will be dropped from the

notation for simplicity. The permutation operation transformation \mathbf{r} to $\hat{P}\mathbf{r}$. But this in effect is equivalent to transforming matrices \mathbf{A}_l and \mathbf{W}_l , and vector \mathbf{v}_l according to

$$\begin{aligned} \hat{P}(\mathbf{r}'\mathbf{W}_l\mathbf{r})(\mathbf{v}'_l\mathbf{r})\exp[-\mathbf{r}'\mathbf{A}_l\mathbf{r}] \\ = (\mathbf{r}'\mathbf{P}'\mathbf{W}_l\mathbf{P}\mathbf{r})(\mathbf{v}'_l\mathbf{P}\mathbf{r})\exp[-\mathbf{r}'\mathbf{P}'\mathbf{A}_l\mathbf{P}\mathbf{r}] \\ = [\mathbf{r}'(\mathbf{P}'\mathbf{W}_l\mathbf{P})\mathbf{r}][(\mathbf{v}'_l\mathbf{P})\mathbf{r}]\exp[-\mathbf{r}'(\mathbf{P}'\mathbf{A}_l\mathbf{P})\mathbf{r}], \end{aligned} \quad (17)$$

where $\mathbf{P} = P \otimes I_3$ is the permutation matrix corresponding to permutation operator \hat{P} .

To build the permutation symmetry projector for fermions, a Young tableaux is constructed. For n fermions and for the total spin of the system being s , the so-called symmetry quantum number, p , is calculated as $p = \frac{n}{2} - s$. Then a partition is defined as $\mu = [2^p 1^{n-2p}]$. The partition describes the structure of the Young tableaux for the state of the system under consideration. The tableaux consists of two boxes in the first p rows and one box in the remaining $n - 2p$ rows. The lithium atom with three electrons and the total spin of one half has a partition of $\mu = [2^1 1^1]$ and the following Young tableaux:

	3	4
2		

where, as the nucleus is labeled as “1”, the labels for the electrons are “2”, “3”, and “4”.

With this, the permutation symmetry projector can now be constructed using the Young tableaux in the following way:

$$\hat{Y} = \hat{S}\hat{A}, \quad (18)$$

where \hat{S} and \hat{A} are idempotent symmetrization and antisymmetrization operators. \hat{S} is constructed as a product of symmetrizers over particles in each row of the Young tableaux and \hat{A} is constructed as a product of antisymmetrizers over particles in each column.

Thus, in the case of the lithium atom in a 2F state (with $L = 3$ and $M = 0$), the symmetrization operator is $\hat{S} = (\hat{1} + \hat{P}_{34})$ and the antisymmetrizer is $\hat{A} = (\hat{1} - \hat{P}_{23})$ with $\hat{1}$ being the identity operator. Hence the total permutation operator, \hat{P} , has $n! = 3! = 6$ terms and this is the number of elemental terms that need to be calculated for each Hamiltonian or overlap matrix element. Each of these six terms comprises nine terms due to the use of (14), as alluded at the end of Sec. IV. Therefore, for lithium, each Hamiltonian or overlap matrix element involves using the formula for calculating the corresponding elemental matrix element 54 times.

VI. MATRIX ELEMENTS

The following general p -dimensional Gaussian integral is used to evaluate the Hamiltonian and overlap matrix elements:

$$\int_{-\infty}^{+\infty} \exp[-x'Ax + y'x] dx = \frac{\pi^{p/2}}{|A|^{1/2}} \exp\left[\frac{1}{4}y'A^{-1}y\right], \quad (19)$$

where x is a p -component vector of the integration variables, A is a symmetric $p \times p$ positive-definite matrix to ensure

square integrability of the integrand, y is a p -component constant vector, and A^{-1} is the inverse of A . The use of (19) requires that A_k and \mathbf{W}_k have to be symmetric and positive definite (as eluded in Sec. IV).

A. Overlap matrix elements

The overlap integral between two Gaussian basis functions with cubic polynomial pre-exponential multipliers, (15), is the most important integral to consider because it aids in building a mathematical framework for the derivation of the kinetic and potential matrix elements. All necessary mathematical manipulations used in the overlap derivation are also used in deriving the kinetic and potential matrix elements. There are very few additional tools needed in these other derivations. Should we need any additional operation, it will be explained in the section where the particular integral is derived.

The overlap integral between two cubic ECGs (15) is

$$\langle \phi_k | \phi_l \rangle = \int_{-\infty}^{+\infty} (\mathbf{r}'\mathbf{W}_k\mathbf{r})(\mathbf{v}'_k\mathbf{r})(\mathbf{r}'\mathbf{W}_l\mathbf{r})(\mathbf{v}'_l\mathbf{r}) \times \exp[-\mathbf{r}'(\mathbf{A}_{kl})\mathbf{r}] d\mathbf{r}, \quad (20)$$

where $\mathbf{A}_{kl} \equiv \mathbf{A}_k + \mathbf{A}_l$. To apply (19) to (20) one needs to express the pre-exponential multipliers in the form of a Gaussian exponent. There are two different methods one can use to accomplish this. Both methods in the end lead to the same final result, but each method has its unique advantage and involves different difficulties that need to be overcome. It should be mentioned that in the derivation of the kinetic-energy matrix elements both methods are needed and in the derivation of the potential-energy matrix elements only one method can be used.

The first method (indicated by superscript “I” in front of the matrix element) involves rewriting basis function (15) as a derivative with respect to parameters ω_k and v_k :

$$\begin{aligned} \phi_k &= (\mathbf{v}'_k\mathbf{r})(\mathbf{r}'\mathbf{W}_k\mathbf{r})\exp[-\mathbf{r}'\mathbf{A}_k\mathbf{r}] \\ &= -\frac{\partial}{\partial v_k} \frac{\partial}{\partial \omega_k} \exp[-\mathbf{r}'(\mathbf{A}_k + \omega_k \mathbf{W}_k)\mathbf{r} + v_k \mathbf{v}'_k \mathbf{r}]|_{v_k=\omega_k=0}. \end{aligned} \quad (21)$$

The following Gaussian function is now the function to integrate:

$${}^I\varphi_k = \exp[-\mathbf{r}'(\mathbf{A}_k + \omega_k \mathbf{W}_k)\mathbf{r} + v_k \mathbf{v}'_k \mathbf{r}]. \quad (22)$$

The overlap integral has the following form:

$$\begin{aligned} {}^I\langle \phi_k | \phi_l \rangle &= \frac{\partial}{\partial \omega_k} \frac{\partial}{\partial \omega_l} \frac{\partial}{\partial v_k} \frac{\partial}{\partial v_l} \langle {}^I\varphi_k | {}^I\varphi_l \rangle \Big|_{\omega_k=\omega_l=v_k=v_l=0} \\ &= \frac{\partial}{\partial \omega_k} \frac{\partial}{\partial \omega_l} \frac{\partial}{\partial v_k} \frac{\partial}{\partial v_l} \int_{-\infty}^{+\infty} \exp[-\mathbf{r}'(\mathbf{A}_{kl} + \omega_k \mathbf{W}_k \\ &\quad + \omega_l \mathbf{W}_l)\mathbf{r} + (v_k \mathbf{v}'_k + v_l \mathbf{v}'_l)\mathbf{r}] d\mathbf{r} \Big|_{\omega_k=\omega_l=v_k=v_l=0}. \end{aligned} \quad (23)$$

By directly applying equality (19), the above becomes

$$\begin{aligned} {}^I \langle \phi_k | \phi_l \rangle &= \pi^{3n/2} \frac{\partial}{\partial \omega_k} \frac{\partial}{\partial \omega_l} \frac{\partial}{\partial v_k} \frac{\partial}{\partial v_l} |\mathbf{A}_{kl} + \omega_k \mathbf{W}_k + \omega_l \mathbf{W}_l|^{-1/2} \\ &\times \exp \left[\frac{1}{4} (v_k \mathbf{v}_k + v_l \mathbf{v}_l)' (\mathbf{A}_{kl} + \omega_k \mathbf{W}_k + \omega_l \mathbf{W}_l)^{-1} \right. \\ &\quad \left. \times (v_k \mathbf{v}_k + v_l \mathbf{v}_l) \right] \Big|_{\omega_k = \omega_l = v_k = v_l = 0}, \end{aligned} \quad (24)$$

which now needs to be differentiated. The order of the differentiation does not matter in this case because the differentiation is a linear operation.

Let us first take the derivative with respect to v_k and v_l and then set these parameters to zero. As the exponent is the only term dependent on the v_k and v_l parameters, the result is

$$\begin{aligned} \frac{1}{4} \mathbf{v}'_k (\mathbf{A}_{kl} + \omega_k \mathbf{W}_k + \omega_l \mathbf{W}_l)^{-1} \mathbf{v}_l + \frac{1}{4} \mathbf{v}'_l (\mathbf{A}_{kl} + \omega_k \mathbf{W}_k + \omega_l \mathbf{W}_l)^{-1} \mathbf{v}_k \\ = \frac{1}{2} \mathbf{v}'_k (\mathbf{A}_{kl} + \omega_k \mathbf{W}_k + \omega_l \mathbf{W}_l)^{-1} \mathbf{v}_l \end{aligned}$$

$$= \frac{1}{2} \mathbf{v}'_l (\mathbf{A}_{kl} + \omega_k \mathbf{W}_k + \omega_l \mathbf{W}_l)^{-1} \mathbf{v}_k, \quad (25)$$

where we used the fact that the inverse of $\mathbf{A}_{kl} + \omega_k \mathbf{W}_k + \omega_l \mathbf{W}_l$ is a symmetric matrix. Conveniently we can choose which one of the right-hand-side terms we wish to use and for the overlap formula shown below we use the second of the two.

Now we can take the derivative with respect to ω_k and ω_l . In general, the differential of a determinant of an arbitrary matrix X raised to power p and the differential of its inverse are

$$d|X|^p = p|X|^p \text{tr}[X^{-1} dX], \quad (26)$$

where $\text{tr}[\dots]$ denotes the trace of the matrix and,

$$dX^{-1} = -X^{-1} (dX) X^{-1}. \quad (27)$$

Applying (26) and (27), taking the derivatives with respect to ω_k and ω_l of the remaining terms, and setting these parameters equal to zero, the final expression for the overlap matrix element is

$$\begin{aligned} {}^I \langle \phi_k | \phi_l \rangle &= \pi^{3n/2} |\mathbf{A}_{kl}|^{-1/2} \\ &\times \left\{ \frac{1}{8} \text{tr} [\mathbf{A}_{kl}^{-1} \mathbf{W}_k] \text{tr} [\mathbf{A}_{kl}^{-1} \mathbf{W}_l] \mathbf{v}'_l \mathbf{A}_{kl}^{-1} \mathbf{v}_k \right. \\ &+ \frac{1}{4} (\text{tr} [\mathbf{A}_{kl}^{-1} \mathbf{W}_k \mathbf{A}_{kl}^{-1} \mathbf{W}_l] \mathbf{v}'_l \mathbf{A}_{kl}^{-1} \mathbf{v}_k + \text{tr} [\mathbf{A}_{kl}^{-1} \mathbf{W}_k] \mathbf{v}'_l \mathbf{A}_{kl}^{-1} \mathbf{W}_l \mathbf{A}_{kl}^{-1} \mathbf{v}_k + \text{tr} [\mathbf{A}_{kl}^{-1} \mathbf{W}_l] \mathbf{v}'_l \mathbf{A}_{kl}^{-1} \mathbf{W}_k \mathbf{A}_{kl}^{-1} \mathbf{v}_k) \\ &+ \frac{1}{2} (\mathbf{v}'_l \mathbf{A}_{kl}^{-1} \mathbf{W}_k \mathbf{A}_{kl}^{-1} \mathbf{W}_l \mathbf{A}_{kl}^{-1} \mathbf{v}_k + \mathbf{v}'_l \mathbf{A}_{kl}^{-1} \mathbf{W}_l \mathbf{A}_{kl}^{-1} \mathbf{W}_k \mathbf{A}_{kl}^{-1} \mathbf{v}_k) \Big\} \\ &= \pi^{3n/2} |\mathbf{A}_{kl}|^{-3/2} \\ &\times \left\{ \frac{1}{8} \eta_k \eta_l \text{tr} [\mathbf{A}_{kl}^{-1} \mathbf{v}_k \mathbf{v}'_l] \right. \\ &+ \frac{1}{4} (\eta_{kl} \text{tr} [\mathbf{A}_{kl}^{-1} \mathbf{v}_k \mathbf{v}'_l] + \eta_k \text{tr} [\mathbf{A}_{kl}^{-1} \mathbf{W}_l \mathbf{A}_{kl}^{-1} \mathbf{v}_k \mathbf{v}'_l] + \eta_l \text{tr} [\mathbf{A}_{kl}^{-1} \mathbf{W}_k \mathbf{A}_{kl}^{-1} \mathbf{v}_k \mathbf{v}'_l]) \\ &+ \frac{1}{2} (\text{tr} [\mathbf{A}_{kl}^{-1} \mathbf{W}_k \mathbf{A}_{kl}^{-1} \mathbf{W}_l \mathbf{A}_{kl}^{-1} \mathbf{v}_k \mathbf{v}'_l] + \text{tr} [\mathbf{A}_{kl}^{-1} \mathbf{W}_l \mathbf{A}_{kl}^{-1} \mathbf{W}_k \mathbf{A}_{kl}^{-1} \mathbf{v}_k \mathbf{v}'_l]) \Big\} \\ &= \pi^{3n/2} |\mathbf{A}_{kl}|^{-3/2} \left\{ \frac{1}{8} \eta_k \eta_l \eta_v + \frac{1}{4} (\eta_{kl} \eta_v + \eta_k \eta_{lv} + \eta_l \eta_{kv}) + \frac{1}{2} (\eta_{klv} + \eta_{lkv}) \right\}. \end{aligned} \quad (28)$$

There are a few manipulations that can be done to simplify the overlap formula. First, the determinant of \mathbf{A}_{kl} , can be reduced to an expression involving the determinant of the A_{kl} matrix. In general, if \mathbf{X} is an $3n \times 3n$ matrix is in the form $\mathbf{X} = X \otimes I_3$, its determinant can be calculated as

$$|\mathbf{X}| = |X \otimes I_3| = |X|^3. \quad (29)$$

Second, to obtain the last expression in (28) we replaced each quadratic form appearing on the left-hand side of Eq. (28) by the corresponding trace. For example, the quadratic form

$\mathbf{v}'_l \mathbf{A}_{kl}^{-1} \mathbf{v}_k$ was replaced by $\text{tr} [\mathbf{A}_{kl}^{-1} \mathbf{v}_k \mathbf{v}'_l]$. This transformation needs to be remembered when the first method for deriving the overlap integral is compared with the second method. Also we have introduced a new abbreviated notation for the trace (i.e., $\text{tr}[\dots] = \eta$), where the subscript of η denotes the matrix/matrices involved in the trace. Due to the fact that every trace is dependent on at least one angular component matrix, \mathbf{W}_k , \mathbf{W}_l , or $\mathbf{v}_k \mathbf{v}'_l$ multiplied by the \mathbf{A}_{kl}^{-1} matrix, the presence of \mathbf{A}_{kl}^{-1} under the trace is not explicitly shown. Also, we represented the matrix product $\mathbf{A}_{kl}^{-1} \mathbf{W}_k$ by a subscript k in η ,

the matrix product $\mathbf{A}_{kl}^{-1}\mathbf{W}_l$ by subscript l , and the product $\mathbf{A}_{kl}^{-1}\mathbf{v}_k\mathbf{v}'_l$ by subscript v . As the terms involved in the overlap integral also show up in the kinetic and potential energy matrix elements, this notation also simplifies the lengthy formulas obtained for those elements.

The second method for evaluating the overlap integral (indicated with a superscript “II” on the matrix element) involves replacing the product $(\mathbf{v}'_k\mathbf{r})(\mathbf{v}'_l\mathbf{r})$ in (20) with the following quadratic form: $(\mathbf{r}'\mathbf{v}'_k\mathbf{v}'_l\mathbf{r})$. Since $\mathbf{v}'_k\mathbf{v}'_l$ is an asymmetric matrix, but (19) requires that the matrices are symmetric, (12) is used:

$$\mathbf{W}_{v_{kl}} = \frac{1}{2}(\mathbf{v}'_k\mathbf{v}'_l + \mathbf{v}'_l\mathbf{v}'_k). \quad (30)$$

In (20) we factor out the $1/2$ from the matrix $\mathbf{W}_{v_{kl}}$:

$$\begin{aligned} {}^{II}\langle\phi_k|\phi_l\rangle &= \frac{1}{2} \int_{-\infty}^{+\infty} (\mathbf{r}'\mathbf{W}_k\mathbf{r})(\mathbf{r}'\mathbf{W}_l\mathbf{r})(\mathbf{r}'\mathbf{W}_{v_{kl}}\mathbf{r}) \\ &\times \exp[-\mathbf{r}'(\mathbf{A}_{kl}\mathbf{r})] d\mathbf{r}. \end{aligned} \quad (31)$$

Here, the major difference from method “I” is the absence of the exponential term. Now, all left to be done is to deal with the determinant. This by itself is much less complicated than dealing with both the determinant and the exponent. We use the same trick as in method “I” and represent the prefactors in the integrand as derivatives of a Gaussian function:

$$\begin{aligned} {}^{II}\langle\phi_k|\phi_l\rangle &= -\frac{1}{2} \frac{\partial}{\partial\omega_k} \frac{\partial}{\partial\omega_l} \frac{\partial}{\partial\omega_v} \langle{}^{II}\phi_k| \exp[-\mathbf{r}'\omega_v\mathbf{W}_{v_{kl}}\mathbf{r}] |{}^{II}\phi_l\rangle \Big|_{\omega_k=\omega_l=\omega_v=0} \\ &= -\frac{1}{2} \frac{\partial}{\partial\omega_k} \frac{\partial}{\partial\omega_l} \frac{\partial}{\partial\omega_v} \int_{-\infty}^{+\infty} \exp[-\mathbf{r}'(\mathbf{A}_{kl} + \omega_k\mathbf{W}_k + \omega_l\mathbf{W}_l + \omega_v\mathbf{W}_{v_{kl}})\mathbf{r}] d\mathbf{r} \Big|_{\omega_k=\omega_l=\omega_v=0}, \end{aligned} \quad (32)$$

where ${}^{II}\phi_k = \exp[-\mathbf{r}'(\mathbf{A}_k + \omega_k\mathbf{W}_k)\mathbf{r}]$. Now, (19) can be directly applied to the above yielding the following derivative:

$${}^{II}\langle\phi_k|\phi_l\rangle = -\pi^{3n/2} \frac{1}{2} \frac{\partial}{\partial\omega_k} \frac{\partial}{\partial\omega_l} \frac{\partial}{\partial\omega_v} |\mathbf{A}_{kl} + \omega_k\mathbf{W}_k + \omega_l\mathbf{W}_l + \omega_v\mathbf{W}_{v_{kl}}|^{-1/2} \Big|_{\omega_k=\omega_l=\omega_v=0}. \quad (33)$$

Differentiating the above with respect to ω_v , ω_l , and ω_k using only (26) and (27), and setting these parameters equal to zero results in

$$\begin{aligned} {}^{II}\langle\phi_k|\phi_l\rangle &= \frac{1}{2}\pi^{3n/2}|\mathbf{A}_{kl}|^{-3/2} \\ &\times \left\{ \frac{1}{8}\eta_k\eta_l\text{tr}[\mathbf{A}_{kl}\mathbf{W}_{v_{kl}}] \right. \\ &+ \frac{1}{4}(\eta_{kl}\text{tr}[\mathbf{A}_{kl}\mathbf{W}_{v_{kl}}] + \eta_l\text{tr}[\mathbf{A}_{kl}\mathbf{W}_k\mathbf{A}_{kl}\mathbf{W}_{v_{kl}}] + \eta_k\text{tr}[\mathbf{A}_{kl}\mathbf{W}_l\mathbf{A}_{kl}\mathbf{W}_{v_{kl}}]) \\ &+ \frac{1}{2}(\text{tr}[\mathbf{A}_{kl}\mathbf{W}_k\mathbf{A}_{kl}\mathbf{W}_l\mathbf{A}_{kl}\mathbf{W}_{v_{kl}}] + \text{tr}[\mathbf{A}_{kl}\mathbf{W}_l\mathbf{A}_{kl}\mathbf{W}_k\mathbf{A}_{kl}\mathbf{W}_k\mathbf{A}_{kl}\mathbf{W}_{v_{kl}}]) \Big\} \\ &= \frac{1}{2}\pi^{3n/2}|\mathbf{A}_{kl}|^{-3/2} \\ &\times \left\{ \frac{1}{8}\eta_k\eta_l\text{tr}[\mathbf{A}_{kl}^{-1}(\mathbf{v}_l\mathbf{v}'_k + \mathbf{v}_k\mathbf{v}'_l)] \right. \\ &+ \frac{1}{4}(\eta_{kl}\text{tr}[\mathbf{A}_{kl}^{-1}(\mathbf{v}_l\mathbf{v}'_k + \mathbf{v}_k\mathbf{v}'_l)] + \eta_k\text{tr}[\mathbf{A}_{kl}^{-1}\mathbf{W}_l\mathbf{A}_{kl}^{-1}(\mathbf{v}_l\mathbf{v}'_k + \mathbf{v}_k\mathbf{v}'_l)] + \eta_l\text{tr}[\mathbf{A}_{kl}^{-1}\mathbf{W}_k\mathbf{A}_{kl}^{-1}(\mathbf{v}_l\mathbf{v}'_k + \mathbf{v}_k\mathbf{v}'_l)]) \\ &+ \frac{1}{2}(\text{tr}[\mathbf{A}_{kl}^{-1}\mathbf{W}_k\mathbf{A}_{kl}^{-1}\mathbf{W}_l\mathbf{A}_{kl}^{-1}(\mathbf{v}_l\mathbf{v}'_k + \mathbf{v}_k\mathbf{v}'_l)] + \text{tr}[\mathbf{A}_{kl}^{-1}\mathbf{W}_l\mathbf{A}_{kl}^{-1}\mathbf{W}_k\mathbf{A}_{kl}^{-1}(\mathbf{v}_l\mathbf{v}'_k + \mathbf{v}_k\mathbf{v}'_l)]) \Big\} \\ &= {}^I\langle\phi_k|\phi_l\rangle. \end{aligned} \quad (34)$$

It is usually advantageous to reduce the number of operations performed in calculating a matrix element by, for example, reducing the number of traces that need to be calculated. This can be done in the last two terms in (34). Using the following matrix identities for A, B, C, \dots , being $p \times p$ matrices: $(AB)' = B'A'$ and $(ABC)' = (C'B'A')$, and the identity concerning cyclic permutation of matrices in a trace, $\text{tr}[ABC\dots] = \text{tr}[BC\dots A] = \text{tr}[C\dots AB]$, (28) can be transformed to the overlap formula, (28), obtained with method “I”. This involves the following:

$$\begin{aligned} \text{tr}[\mathbf{A}_{kl}^{-1}\mathbf{W}_{v_{kl}}] &= \text{tr}[\mathbf{A}_{kl}^{-1}(\mathbf{v}_k\mathbf{v}'_l + \mathbf{v}_l\mathbf{v}'_k)] = \text{tr}[\mathbf{A}_{kl}^{-1}\mathbf{v}_k\mathbf{v}'_l] + \text{tr}[\mathbf{v}_k\mathbf{v}'_l\mathbf{A}_{kl}^{-1}] \\ &= 2\text{tr}[\mathbf{A}_{kl}^{-1}\mathbf{v}_k\mathbf{v}'_l] = \eta_v, \end{aligned} \quad (35)$$

$$\begin{aligned} \text{tr}[\mathbf{A}_{kl}^{-1}\mathbf{W}_k\mathbf{A}_{kl}^{-1}\mathbf{W}_{v_{kl}}] &= \text{tr}[\mathbf{A}_{kl}^{-1}\mathbf{W}_k\mathbf{A}_{kl}^{-1}(\mathbf{v}_k\mathbf{v}'_l + \mathbf{v}_l\mathbf{v}'_k)] = \text{tr}[\mathbf{A}_{kl}^{-1}\mathbf{W}_k\mathbf{A}_{kl}^{-1}\mathbf{v}_k\mathbf{v}'_l] + \text{tr}[\mathbf{v}_k\mathbf{v}'_l\mathbf{A}_{kl}^{-1}\mathbf{W}_k\mathbf{A}_{kl}^{-1}] \\ &= 2\text{tr}[\mathbf{A}_{kl}^{-1}\mathbf{W}_k\mathbf{A}_{kl}^{-1}\mathbf{v}_k\mathbf{v}'_l] = \eta_{kv}, \end{aligned} \quad (36)$$

$$\begin{aligned} \text{tr}[\mathbf{A}_{kl}^{-1}\mathbf{W}_l\mathbf{A}_{kl}^{-1}\mathbf{W}_{v_{kl}}] &= \text{tr}[\mathbf{A}_{kl}^{-1}\mathbf{W}_l\mathbf{A}_{kl}^{-1}(\mathbf{v}_k\mathbf{v}'_l + \mathbf{v}_l\mathbf{v}'_k)] = \text{tr}[\mathbf{A}_{kl}^{-1}\mathbf{W}_l\mathbf{A}_{kl}^{-1}\mathbf{v}_k\mathbf{v}'_l] + \text{tr}[\mathbf{v}_k\mathbf{v}'_l\mathbf{A}_{kl}^{-1}\mathbf{W}_l\mathbf{A}_{kl}^{-1}] \\ &= 2\text{tr}[\mathbf{A}_{kl}^{-1}\mathbf{W}_l\mathbf{A}_{kl}^{-1}\mathbf{v}_k\mathbf{v}'_l] = \eta_{lv}, \end{aligned} \quad (37)$$

and

$$\frac{1}{2}(\text{tr}[\mathbf{A}_{kl}^{-1}\mathbf{W}_k\mathbf{A}_{kl}^{-1}\mathbf{W}_l\mathbf{A}_{kl}^{-1}(\mathbf{v}_k\mathbf{v}'_l + \mathbf{v}_l\mathbf{v}'_k)] + \text{tr}[\mathbf{A}_{kl}^{-1}\mathbf{W}_l\mathbf{A}_{kl}^{-1}\mathbf{W}_k\mathbf{A}_{kl}^{-1}(\mathbf{v}_k\mathbf{v}'_l + \mathbf{v}_l\mathbf{v}'_k)]) = \eta_{klv} + \eta_{lkv}. \quad (38)$$

It is worth mentioning that I_3 cannot be factored out from the traces using $\text{tr}[\mathbf{A}] = \text{tr}[A \otimes I_3] = 3\text{tr}[A]$ to simplify the overlap formulas because $\mathbf{W}_{(k,l,v_{kl})} \neq W_{(k,l,v_{kl})} \otimes I_3$. If $\mathbf{W}_{(k,l,v_{kl})}$ did equal $W_{(k,l,v_{kl})} \otimes I_3$ then applying the following general property of the matrix product:

$$(A \otimes B)(C \otimes D) = (AC \otimes BD), \quad (39)$$

to the traces in (28) would be necessary. Here, \mathbf{A} and \mathbf{C} are arbitrary $3n \times 3n$ matrices in the following form $\mathbf{A} = A \otimes I_3$, and B and D are equal to I_3 (not to be confused with $\mathbf{A}_k = A_k \otimes I_3$).

It should also be stated that the sparsity of the $\mathbf{W}_{(k,l,v_{kl})}$ matrices and the $\mathbf{v}_{(k,l)}$ vectors cannot be explicitly exploited at the level the formula derivation. It has to be handled when the formulas are coded in the FORTRAN 90 computer program and it involves eliminating multiplications by zeros. This elimination should significantly reduce the calculation time of the matrix elements and needs to be implemented before the computer program developed in the present work is applied to calculate larger atomic systems.

B. Kinetic energy matrix elements

The kinetic-energy operator in (2) is expressed as a sum which can be written in the following form:

$$-\frac{1}{2} \left(\sum_{i=1}^n \frac{1}{\mu_i} \nabla_{\mathbf{r}_i}^2 + \sum_{i=1, j=1, i \neq j}^n \frac{1}{m_0} \nabla'_{\mathbf{r}_i} \nabla_{\mathbf{r}_j} \right) = -\nabla'_{\mathbf{r}} \mathbf{M} \nabla_{\mathbf{r}}. \quad (40)$$

Here the mass matrix \mathbf{M} is $\mathbf{M} = M \otimes I_3$, where in the M matrix the diagonal elements are set to $1/(2m_1)$, $1/(2m_2)$, ..., $1/(2m_n)$, while the off-diagonal elements are set to $1/(2m_0)$. Again, for an atom m_0 is the mass of the nucleus and m_1, \dots , and m_n are the electron masses.

In the derivations of the formulas for the kinetic-energy matrix elements, we are going to use the “asymmetric” form of the basis functions (15) and the integral to calculate is

$$\langle \phi_k | -\nabla'_{\mathbf{r}} \mathbf{M} \nabla_{\mathbf{r}} | \phi_l \rangle = \langle \nabla_{\mathbf{r}} \phi_k | \mathbf{M} | \nabla_{\mathbf{r}} \phi_l \rangle. \quad (41)$$

The gradient operator acting ϕ_k produces:

$$\begin{aligned} \nabla_{\mathbf{r}} \phi_k &= \{\mathbf{v}'_k(\mathbf{r}'\mathbf{W}_k\mathbf{r}) + 2(\mathbf{W}_k\mathbf{r})(\mathbf{v}'_k\mathbf{r}) - (\mathbf{A}_k\mathbf{r})(\mathbf{v}'_k\mathbf{r})(\mathbf{r}'\mathbf{W}_k\mathbf{r})\} \\ &\quad \times \exp[-\mathbf{r}'(\mathbf{A}_k)\mathbf{r}], \end{aligned} \quad (42)$$

where we have included the necessary symmetry required by (19). Thus, the following nine integrals need to be calculated:

$$\langle \phi_k | -\nabla'_{\mathbf{r}} \mathbf{M} \nabla_{\mathbf{r}} | \phi_l \rangle$$

$$= \mathbf{v}'_k \mathbf{M} \mathbf{v}_l \langle (\mathbf{r}'\mathbf{W}_k\mathbf{r})(\mathbf{r}'\mathbf{W}_l\mathbf{r}) \exp[-\mathbf{r}'(\mathbf{A}_{kl})\mathbf{r}] \rangle \quad (43)$$

$$+ 2 \langle (\mathbf{r}'\mathbf{W}_k\mathbf{r})(\mathbf{v}'_k \mathbf{M} \mathbf{W}_l \mathbf{r})(\mathbf{v}'_l \mathbf{r}) \exp[-\mathbf{r}'(\mathbf{A}_{kl})\mathbf{r}] \rangle \quad (44)$$

$$+ 2 \langle (\mathbf{v}'_k \mathbf{r})(\mathbf{r}'\mathbf{W}_k\mathbf{M}\mathbf{v}_l)(\mathbf{r}'\mathbf{W}_l\mathbf{r}) \exp[-\mathbf{r}'(\mathbf{A}_{kl})\mathbf{r}] \rangle \quad (45)$$

$$+ 4 \langle (\mathbf{v}'_k \mathbf{r})(\mathbf{r}'\mathbf{W}_k\mathbf{M}\mathbf{W}_l\mathbf{r})(\mathbf{v}'_l \mathbf{r}) \exp[-\mathbf{r}'(\mathbf{A}_{kl})\mathbf{r}] \rangle \quad (46)$$

$$- 2 \langle (\mathbf{v}'_k \mathbf{r})(\mathbf{r}'\mathbf{W}_k\mathbf{r})(\mathbf{r}'\mathbf{W}_l\mathbf{r})(\mathbf{r}'\mathbf{A}_k\mathbf{M}\mathbf{v}_l) \exp[-\mathbf{r}'(\mathbf{A}_{kl})\mathbf{r}] \rangle \quad (47)$$

$$- 4 \langle (\mathbf{v}'_k \mathbf{r})(\mathbf{r}'\mathbf{W}_k\mathbf{r})(\mathbf{r}'\mathbf{A}_k\mathbf{M}\mathbf{W}_l\mathbf{r})(\mathbf{v}'_l \mathbf{r}) \exp[-\mathbf{r}'(\mathbf{A}_{kl})\mathbf{r}] \rangle \quad (48)$$

$$- 4 \langle (\mathbf{v}'_k \mathbf{r})(\mathbf{r}'\mathbf{W}_k\mathbf{M}\mathbf{A}_l\mathbf{r})(\mathbf{r}'\mathbf{W}_l\mathbf{r})(\mathbf{v}'_l \mathbf{r}) \exp[-\mathbf{r}'(\mathbf{A}_{kl})\mathbf{r}] \rangle \quad (49)$$

$$- 4 \langle (\mathbf{v}'_k \mathbf{r})(\mathbf{r}'\mathbf{W}_k\mathbf{r})(\mathbf{r}'\mathbf{A}_k\mathbf{M}\mathbf{A}_l\mathbf{r})(\mathbf{v}'_l \mathbf{r}) \exp[-\mathbf{r}'(\mathbf{A}_{kl})\mathbf{r}] \rangle \quad (50)$$

$$+ 4 \langle (\mathbf{v}'_k \mathbf{r})(\mathbf{r}'\mathbf{W}_k\mathbf{r})(\mathbf{r}'\mathbf{A}_k\mathbf{M}\mathbf{A}_l\mathbf{r})(\mathbf{v}'_l \mathbf{r})(\mathbf{r}'\mathbf{W}_l\mathbf{r}) \exp[-\mathbf{r}'(\mathbf{A}_{kl})\mathbf{r}] \rangle. \quad (51)$$

Note that not all necessary matrix symmetrizations have been applied, but they will be included as each integral is discussed. Due to the fact that each of the nine integrals are different, the evaluation of each may or may not require

the use of all transformations and manipulations described in Sec. V. Each evaluation is discussed in the following passages.

The first of the nine intergals in (43) has a similar form as one of the integrals derived in Ref. 20, i.e., the overlap between two ECGs with quadratic pre-exponential multipliers, and, therefore, the result is straightforward to write

$$\begin{aligned} & \mathbf{v}'_k \mathbf{M} \mathbf{v}_l \langle (\mathbf{r}' \mathbf{W}_k \mathbf{r}) (\mathbf{r}' \mathbf{W}_l \mathbf{r}) \exp[-\mathbf{r}' (\mathbf{A}_{kl}) \mathbf{r}] \rangle \\ &= \text{tr} [\mathbf{M} \mathbf{v}_l \mathbf{v}'_k] \pi^{3n/2} |A_{kl}|^{-3/2} \left\{ \frac{1}{4} \text{tr} [\mathbf{A}_{kl}^{-1} \mathbf{W}_k] \text{tr} [\mathbf{A}_{kl}^{-1} \mathbf{W}_l] \right. \\ & \quad \left. + \frac{1}{2} \text{tr} [\mathbf{A}_{kl}^{-1} \mathbf{W}_k \mathbf{A}_{kl}^{-1} \mathbf{W}_l] \right\} \\ (43) = & \text{tr} [\mathbf{M} \mathbf{v}_k \mathbf{v}'_l] \pi^{3n/2} |A_{kl}|^{-3/2} \left\{ \frac{1}{4} \eta_k \eta_l + \frac{1}{2} \eta_{kl} \right\}, \end{aligned} \quad (52)$$

where $\text{tr} [\mathbf{M} \mathbf{v}_k \mathbf{v}'_l] = \text{tr} [\mathbf{M} \mathbf{v}_l \mathbf{v}'_k]$ is obtained by using the above-mentioned matrix transpositions and cyclic permutation of matrices in the trace, and η_k , η_l , and η_{kl} are the overlap-integral trace components. The only other integral of the nine that has the same form as (43) is (46). If method “II” from the overlap-integral derivation is used and 1/2 is factored out from the $\mathbf{W}_{v_{kl}}$ matrix and if the product of $\mathbf{r}' \mathbf{W}_k \mathbf{M} \mathbf{W}_l \mathbf{r}$ is symmetrized and substituted with:

$$\mathbf{r}' \mathbf{W}_k \mathbf{M} \mathbf{W}_l \mathbf{r} = \frac{1}{2} \mathbf{r}' (\mathbf{W}_k \mathbf{M} \mathbf{W}_l + \mathbf{W}_l \mathbf{M} \mathbf{W}_k) \mathbf{r}, \quad (53)$$

and denoted as $\frac{1}{2} \mathbf{r}' \mathbf{M} \mathbf{A}_{46} \mathbf{r}$, (46) becomes:

$$\begin{aligned} & 4 \langle (\mathbf{v}'_k \mathbf{r}) (\mathbf{r}' \mathbf{W}_k \mathbf{M} \mathbf{W}_l \mathbf{r}) (\mathbf{v}'_l \mathbf{r}) \exp[-\mathbf{r}' (\mathbf{A}_{kl}) \mathbf{r}] \rangle \\ &= 4 \frac{1}{2} \frac{1}{2} \langle (\mathbf{r}' \mathbf{W}_{v_{kl}} \mathbf{r}) (\mathbf{r}' \mathbf{M} \mathbf{A}_{46} \mathbf{r}) \exp[-\mathbf{r}' (\mathbf{A}_{kl}) \mathbf{r}] \rangle \\ (46) = & \pi^{3n/2} |A_{kl}|^{-3/2} \left\{ \frac{1}{4} \text{tr} [\mathbf{A}_{kl}^{-1} \mathbf{W}_{v_{kl}}] \text{tr} [\mathbf{A}_{kl}^{-1} \mathbf{M} \mathbf{A}_{46}] \right. \\ & \quad \left. + \frac{1}{2} \text{tr} [\mathbf{A}_{kl}^{-1} \mathbf{W}_{v_{kl}} \mathbf{A}_{kl}^{-1} \mathbf{M} \mathbf{A}_{46}] \right\} \\ (46) = & \pi^{3n/2} |A_{kl}|^{-3/2} \left\{ \eta_v \text{tr} [\mathbf{A}_{kl}^{-1} \mathbf{W}_k \mathbf{M} \mathbf{W}_l] \right. \\ & \quad \left. + \text{tr} [\mathbf{A}_{kl}^{-1} \mathbf{W}_k \mathbf{M} \mathbf{W}_l \mathbf{A}_{kl}^{-1} \mathbf{W}_{v_{kl}}] \right\}. \end{aligned} \quad (54)$$

Here, it is more advantageous from a programming standpoint, to have $\text{tr} [\mathbf{A}_{kl}^{-1} \mathbf{W}_k \mathbf{M} \mathbf{W}_l \mathbf{A}_{kl}^{-1} \mathbf{W}_{v_{kl}}]$ instead of $\text{tr} [\mathbf{A}_{kl}^{-1} \mathbf{W}_k \mathbf{M} \mathbf{W}_l \mathbf{A}_{kl}^{-1} \mathbf{v}_k \mathbf{v}'_l] + \text{tr} [\mathbf{A}_{kl}^{-1} \mathbf{W}_l \mathbf{M} \mathbf{W}_k \mathbf{A}_{kl}^{-1} \mathbf{v}_k \mathbf{v}'_l]$.

Next, after realizing that integrals (44) and (45) are similar in structure, they can be derived using method “I” described in Sec. VI A. As the only difference is one less derivative to take, the end result is similar in form as the previous two described integrals, (43) and (46). There are no new manipulation nor new formulas that need to be used in the derivation. Therefore, the derivation of these integrals, which follows, will not be explained in detail,

$$\begin{aligned} 2 \langle (\mathbf{r}' \mathbf{W}_k \mathbf{r}) (\mathbf{v}'_k \mathbf{M} \mathbf{W}_l \mathbf{r}) (\mathbf{v}'_l \mathbf{r}) \exp[-\mathbf{r}' (\mathbf{A}_{kl}) \mathbf{r}] \rangle &= -2 \frac{\partial}{\partial \omega_k} \frac{\partial}{\partial v_m} \frac{\partial}{\partial v_l} \\ & \times \langle \exp[-\mathbf{r}' (\mathbf{A}_{kl} + \omega_k \mathbf{W}_k) \mathbf{r} + (v_m \mathbf{W}_l \mathbf{M} \mathbf{v}_k + v_l \mathbf{v}_l)' \mathbf{r}] \rangle \Big|_{\omega_k=v_m=v_l=0} \\ (44) = & \pi^{3n/2} |A_{kl}|^{-3/2} \left\{ \frac{1}{2} \eta_k \text{tr} [\mathbf{A}_{kl}^{-1} \mathbf{W}_l \mathbf{M} \mathbf{v}_k \mathbf{v}'_l] \right. \\ & \quad \left. + \text{tr} [\mathbf{A}_{kl}^{-1} \mathbf{W}_k \mathbf{A}_{kl}^{-1} \mathbf{W}_l \mathbf{M} \mathbf{A}_{kl}^{-1} \mathbf{v}_k \mathbf{v}'_l] \right\}, \\ 2 \langle (\mathbf{v}'_k \mathbf{r}) (\mathbf{r}' \mathbf{W}_k \mathbf{M} \mathbf{v}_l) (\mathbf{r}' \mathbf{W}_l \mathbf{r}) \exp[-\mathbf{r}' (\mathbf{A}_{kl}) \mathbf{r}] \rangle &= -2 \frac{\partial}{\partial \omega_l} \frac{\partial}{\partial v_m} \frac{\partial}{\partial v_k} \\ & \times \langle \exp[-\mathbf{r}' (\mathbf{A}_{kl} + \omega_l \mathbf{W}_l) \mathbf{r} + (v_m \mathbf{W}_k \mathbf{M} \mathbf{v}_l + v_k \mathbf{v}_k)' \mathbf{r}] \rangle \Big|_{\omega_l=v_m=v_k=0} \\ (45) = & \pi^{3n/2} |A_{kl}|^{-3/2} \left\{ \frac{1}{2} \eta_l \text{tr} [\mathbf{A}_{kl}^{-1} \mathbf{W}_k \mathbf{M} \mathbf{v}_l \mathbf{v}'_k] \right. \\ & \quad \left. + \text{tr} [\mathbf{A}_{kl}^{-1} \mathbf{W}_l \mathbf{A}_{kl}^{-1} \mathbf{W}_k \mathbf{M} \mathbf{v}_l \mathbf{v}'_k] \right\}. \end{aligned} \quad (55)$$

Note that in integral (45) $\mathbf{v}_l \mathbf{v}'_k$ is used and not $\mathbf{v}_k \mathbf{v}'_l$ like all other previous integrals.

Integrals (47) and (48) have the same form as those which appeared when method “I” was applied to evaluate the overlap matrix element. These two integrals are

$$\begin{aligned} -2 \langle (\mathbf{r}' \mathbf{W}_k \mathbf{r}) (\mathbf{v}'_k \mathbf{M} \mathbf{A}_l \mathbf{r}) (\mathbf{r}' \mathbf{v}_l) (\mathbf{r}' \mathbf{W}_l \mathbf{r}) \exp[-\mathbf{r}' (\mathbf{A}_{kl}) \mathbf{r}] \rangle &= -2 \frac{\partial}{\partial \omega_k} \frac{\partial}{\partial \omega_l} \frac{\partial}{\partial v_m} \frac{\partial}{\partial v_l} \\ & \times \langle \exp[-\mathbf{r}' (\mathbf{A}_{kl} + \omega_k \mathbf{W}_k + \omega_l \mathbf{W}_l) \mathbf{r} \\ & \quad + (v_m \mathbf{A}_l \mathbf{M} \mathbf{v}_k + v_l \mathbf{v}_l)' \mathbf{r}] \rangle \Big|_{\omega_k=\omega_l=v_m=v_l=0} \\ (47) = & -\pi^{3n/2} |A_{kl}|^{-3/2} \left\{ \frac{1}{4} \eta_k \eta_l \text{tr} [\mathbf{A}_{kl}^{-1} \mathbf{A}_l \mathbf{M} \mathbf{v}_k \mathbf{v}'_l] \right. \\ & \quad \left. + \frac{1}{2} (\eta_k \text{tr} [\mathbf{A}_{kl}^{-1} \mathbf{W}_l \mathbf{A}_{kl}^{-1} \mathbf{A}_l \mathbf{M} \mathbf{v}_k \mathbf{v}'_l] \right. \\ & \quad \left. + \eta_l \text{tr} [\mathbf{A}_{kl}^{-1} \mathbf{W}_k \mathbf{A}_{kl}^{-1} \mathbf{A}_l \mathbf{M} \mathbf{v}_l \mathbf{v}'_k]) \right\} \end{aligned}$$

$$\begin{aligned}
& + \eta_l \text{tr} [\mathbf{A}_{kl}^{-1} \mathbf{W}_k \mathbf{A}_{kl}^{-1} \mathbf{A}_l \mathbf{M} \mathbf{v}_k \mathbf{v}'_l] + \eta_{kl} \text{tr} [\mathbf{A}_{kl}^{-1} \mathbf{A}_l \mathbf{M} \mathbf{v}_k \mathbf{v}'_l] \\
& + \text{tr} [\mathbf{A}_{kl}^{-1} \mathbf{W}_k \mathbf{A}_{kl}^{-1} \mathbf{W}_l \mathbf{A}_{kl}^{-1} \mathbf{A}_l \mathbf{M} \mathbf{v}_k \mathbf{v}'_l] \\
& + \text{tr} [\mathbf{A}_{kl}^{-1} \mathbf{W}_l \mathbf{A}_{kl}^{-1} \mathbf{W}_k \mathbf{A}_{kl}^{-1} \mathbf{A}_l \mathbf{M} \mathbf{v}_k \mathbf{v}'_l] \}, \tag{56}
\end{aligned}$$

$$\begin{aligned}
-2 \langle (\mathbf{v}'_k \mathbf{r}) (\mathbf{r}' \mathbf{W}_k \mathbf{r}) (\mathbf{r}' \mathbf{W}_l \mathbf{r}) (\mathbf{r}' \mathbf{A}_k \mathbf{M} \mathbf{v}_l) \exp[-\mathbf{r}' (\mathbf{A}_{kl}) \mathbf{r}] \rangle = -2 \frac{\partial}{\partial \omega_k} \frac{\partial}{\partial \omega_l} \frac{\partial}{\partial v_m} \frac{\partial}{\partial v_k} \\
\times \langle \exp[-\mathbf{r}' (\mathbf{A}_{kl} + \omega_k \mathbf{W}_k + \omega_l \mathbf{W}_l) \mathbf{r} \\
+ (v_m \mathbf{A}_k \mathbf{M} \mathbf{v}_l + v_k \mathbf{v}_k)' \mathbf{r}] \rangle \Big|_{\omega_k=\omega_l=v_m=v_k=0} \\
(48) = -\pi^{3n/2} |A_{kl}|^{-3/2} \left\{ \frac{1}{4} \eta_k \eta_l \text{tr} [\mathbf{A}_{kl}^{-1} \mathbf{A}_k \mathbf{M} \mathbf{v}_l \mathbf{v}'_k] \right. \\
+ \frac{1}{2} (\eta_k \text{tr} [\mathbf{A}_{kl}^{-1} \mathbf{W}_l \mathbf{A}_{kl}^{-1} \mathbf{A}_k \mathbf{M} \mathbf{v}_l \mathbf{v}'_k] \\
+ \eta_l \text{tr} [\mathbf{A}_{kl}^{-1} \mathbf{W}_k \mathbf{A}_{kl}^{-1} \mathbf{A}_k \mathbf{M} \mathbf{v}_l \mathbf{v}'_k] + \eta_{kl} \text{tr} [\mathbf{A}_{kl}^{-1} \mathbf{A}_k \mathbf{M} \mathbf{v}_l \mathbf{v}'_k]) \\
+ \text{tr} [\mathbf{A}_{kl}^{-1} \mathbf{W}_k \mathbf{A}_{kl}^{-1} \mathbf{W}_l \mathbf{A}_{kl}^{-1} \mathbf{A}_k \mathbf{M} \mathbf{v}_l \mathbf{v}'_k] \\
\left. + \text{tr} [\mathbf{A}_{kl}^{-1} \mathbf{W}_l \mathbf{A}_{kl}^{-1} \mathbf{W}_k \mathbf{A}_{kl}^{-1} \mathbf{A}_k \mathbf{M} \mathbf{v}_l \mathbf{v}'_k] \right\}. \tag{57}
\end{aligned}$$

Integrals (49) and (50) are similar to those which appeared when the overlap matrix element was derived with method “II”. Symmetrization needs to be applied to the ECG prefactors in both integrals

$$\mathbf{r}' \mathbf{A}_k \mathbf{M} \mathbf{W}_l \mathbf{r} = \frac{1}{2} \mathbf{r}' (\mathbf{A}_k \mathbf{M} \mathbf{W}_l + \mathbf{W}_l \mathbf{M} \mathbf{A}_k) \mathbf{r} \tag{58}$$

and

$$\mathbf{r}' \mathbf{W}_k \mathbf{M} \mathbf{A}_l \mathbf{r} = \frac{1}{2} \mathbf{r}' (\mathbf{W}_k \mathbf{M} \mathbf{A}_l + \mathbf{A}_l \mathbf{M} \mathbf{W}_k) \mathbf{r}. \tag{59}$$

These prefactors are denoted as $\frac{1}{2} \mathbf{r}' \mathbf{M}_{49} \mathbf{r}$ and $\frac{1}{2} \mathbf{r}' \mathbf{M}_{50} \mathbf{r}$, respectively. Thus

$$-4 \langle (\mathbf{v}'_k \mathbf{r}) (\mathbf{r}' \mathbf{W}_k \mathbf{r}) (\mathbf{r}' \mathbf{A}_k \mathbf{M} \mathbf{W}_l \mathbf{r}) (\mathbf{v}'_l \mathbf{r}) \exp[-\mathbf{r}' (\mathbf{A}_{kl}) \mathbf{r}] \rangle = -4 \frac{1}{2} \frac{1}{2} \langle (\mathbf{r}' \mathbf{W}_k \mathbf{r}) (\mathbf{r}' \mathbf{M}_{49} \mathbf{r}) (\mathbf{r}' \mathbf{W}_{v_{kl}} \mathbf{r}) \exp[-\mathbf{r}' (\mathbf{A}_{kl}) \mathbf{r}] \rangle$$

$$\begin{aligned}
(49) = -\pi^{3n/2} |A_{kl}|^{-3/2} \left\{ \frac{1}{8} \eta_k \text{tr} [\mathbf{A}_{kl}^{-1} \mathbf{W}_{v_{kl}}] \text{tr} [\mathbf{A}_{kl}^{-1} \mathbf{M}_{49}] \right. \\
+ \frac{1}{4} (\text{tr} [\mathbf{A}_{kl}^{-1} \mathbf{W}_k \mathbf{A}_{kl}^{-1} \mathbf{W}_{v_{kl}}] \text{tr} [\mathbf{A}_{kl}^{-1} \mathbf{M}_{49}] \\
+ \eta_k \text{tr} [\mathbf{A}_{kl}^{-1} \mathbf{M}_{49} \mathbf{A}_{kl}^{-1} \mathbf{W}_{v_{kl}}] \\
+ \text{tr} [\mathbf{A}_{kl}^{-1} \mathbf{W}_{v_{kl}}] \text{tr} [\mathbf{A}_{kl}^{-1} \mathbf{W}_k \mathbf{A}_{kl}^{-1} \mathbf{M}_{49}]) \\
+ \frac{1}{2} (\text{tr} [\mathbf{A}_{kl}^{-1} \mathbf{W}_k \mathbf{A}_{kl}^{-1} \mathbf{M}_{49} \mathbf{A}_{kl}^{-1} \mathbf{W}_{v_{kl}}] \\
\left. + \text{tr} [\mathbf{A}_{kl}^{-1} \mathbf{M}_{49} \mathbf{A}_{kl}^{-1} \mathbf{W}_k \mathbf{A}_{kl}^{-1} \mathbf{W}_{v_{kl}}]) \right\}
\end{aligned}$$

$$(49) = -\pi^{3n/2} |A_{kl}|^{-3/2} \left\{ \frac{1}{2} \eta_k \eta_v \text{tr} [\mathbf{A}_{kl}^{-1} \mathbf{A}_k \mathbf{M} \mathbf{W}_l] \right.$$

$$\begin{aligned}
& + \eta_{kv} \text{tr} [\mathbf{A}_{kl}^{-1} \mathbf{A}_k \mathbf{M} \mathbf{W}_l] + \eta_{vv} \text{tr} [\mathbf{A}_{kl}^{-1} \mathbf{W}_k \mathbf{A}_{kl}^{-1} \mathbf{A}_k \mathbf{M} \mathbf{W}_l] \\
& + \frac{1}{2} \eta_k \text{tr} [\mathbf{A}_{kl}^{-1} \mathbf{A}_k \mathbf{M} \mathbf{W}_l \mathbf{A}_{kl}^{-1} \mathbf{W}_{v_{kl}}]
\end{aligned}$$

$$\begin{aligned}
& + \text{tr} [\mathbf{A}_{kl}^{-1} \mathbf{W}_k \mathbf{A}_{kl}^{-1} \mathbf{A}_k \mathbf{M} \mathbf{W}_l \mathbf{A}_{kl}^{-1} \mathbf{W}_{v_{kl}}] \\
& + \text{tr} [\mathbf{A}_{kl}^{-1} \mathbf{A}_k \mathbf{M} \mathbf{W}_l \mathbf{A}_{kl}^{-1} \mathbf{W}_k \mathbf{A}_{kl}^{-1} \mathbf{W}_{v_{kl}}] \Big\} \\
-4\langle (\mathbf{v}'_k \mathbf{r}) (\mathbf{r}' \mathbf{W}_k \mathbf{M} \mathbf{A}_l \mathbf{r}) (\mathbf{r}' \mathbf{W}_l \mathbf{r}) (\mathbf{v}'_l \mathbf{r}) \exp[-\mathbf{r}'(\mathbf{A}_{kl}) \mathbf{r}] \rangle & = -4 \frac{1}{2} \frac{1}{2} \langle (\mathbf{r}' \mathbf{M}_{50} \mathbf{r}) (\mathbf{r}' \mathbf{W}_l \mathbf{r}) (\mathbf{r}' \mathbf{W}_{v_{kl}} \mathbf{r}) \exp[-\mathbf{r}'(\mathbf{A}_{kl}) \mathbf{r}] \rangle \\
(50) & = -\pi^{3n/2} |A_{kl}|^{-3/2} \left\{ \frac{1}{8} \eta_l \text{tr} [\mathbf{A}_{kl}^{-1} \mathbf{W}_{v_{kl}}] \text{tr} [\mathbf{A}_{kl}^{-1} \mathbf{M}_{50}] \right. \\
& + \frac{1}{4} (\text{tr} [\mathbf{A}_{kl}^{-1} \mathbf{W}_l \mathbf{A}_{kl}^{-1} \mathbf{W}_{v_{kl}}] \text{tr} [\mathbf{A}_{kl}^{-1} \mathbf{M}_{50}] \\
& + \eta_l \text{tr} [\mathbf{A}_{kl}^{-1} \mathbf{M}_{50} \mathbf{A}_{kl}^{-1} \mathbf{W}_{v_{kl}}] \\
& + \text{tr} [\mathbf{A}_{kl}^{-1} \mathbf{W}_{v_{kl}}] \text{tr} [\mathbf{A}_{kl}^{-1} \mathbf{W}_l \mathbf{A}_{kl}^{-1} \mathbf{M}_{50}]) \\
& + \frac{1}{2} (\text{tr} [\mathbf{A}_{kl}^{-1} \mathbf{W}_l \mathbf{A}_{kl}^{-1} \mathbf{M}_{50} \mathbf{A}_{kl}^{-1} \mathbf{W}_{v_{kl}}] \\
& \left. + \text{tr} [\mathbf{A}_{kl}^{-1} \mathbf{M}_{50} \mathbf{A}_{kl}^{-1} \mathbf{W}_l \mathbf{A}_{kl}^{-1} \mathbf{W}_{v_{kl}}]) \right\} \\
(50) & = -\pi^{3n/2} |A_{kl}|^{-3/2} \left\{ \frac{1}{2} \eta_l \eta_v \text{tr} [\mathbf{A}_{kl}^{-1} \mathbf{W}_k \mathbf{M} \mathbf{A}_l] \right. \\
& + \eta_{lv} \text{tr} [\mathbf{A}_{kl}^{-1} \mathbf{W}_k \mathbf{M} \mathbf{A}_l] + \eta_{vv} \text{tr} [\mathbf{A}_{kl}^{-1} \mathbf{W}_l \mathbf{A}_{kl}^{-1} \mathbf{W}_k \mathbf{M} \mathbf{A}_l] \\
& + \frac{1}{2} \eta_k \text{tr} [\mathbf{A}_{kl}^{-1} \mathbf{W}_k \mathbf{M} \mathbf{A}_l \mathbf{A}_{kl}^{-1} \mathbf{W}_{v_{kl}}] \\
& + \text{tr} [\mathbf{A}_{kl}^{-1} \mathbf{W}_l \mathbf{A}_{kl}^{-1} \mathbf{W}_k \mathbf{M} \mathbf{A}_l \mathbf{A}_{kl}^{-1} \mathbf{W}_{v_{kl}}] \\
& \left. + \text{tr} [\mathbf{A}_{kl}^{-1} \mathbf{W}_k \mathbf{M} \mathbf{A}_l \mathbf{A}_{kl}^{-1} \mathbf{W}_l \mathbf{A}_{kl}^{-1} \mathbf{W}_{v_{kl}}] \right\}. \quad (61)
\end{aligned}$$

The last integral has not appeared in any of our prior works. However its derivation does not require any new manipulations. It is evaluated in the same way as the overlap integral was using method “II”. Using the following symmetrized term:

$$\mathbf{r}' \mathbf{A}_k \mathbf{M} \mathbf{A}_l \mathbf{r} = \frac{1}{2} \mathbf{r}' (\mathbf{A}_k \mathbf{M} \mathbf{A}_l + \mathbf{A}_l \mathbf{M} \mathbf{A}_k) \mathbf{r}, \quad (62)$$

denoted as $\frac{1}{2} \mathbf{r}' \mathbf{M}_{51} \mathbf{r}$ we obtain

$$\begin{aligned}
4\langle (\mathbf{v}'_k \mathbf{r}) (\mathbf{r}' \mathbf{W}_k \mathbf{r}) (\mathbf{r}' \mathbf{A}_k \mathbf{M} \mathbf{A}_l \mathbf{r}) (\mathbf{v}'_l \mathbf{r}) (\mathbf{r}' \mathbf{W}_l \mathbf{r}) \exp[-\mathbf{r}'(\mathbf{A}_{kl}) \mathbf{r}] \rangle \\
= 4 \frac{1}{2} \frac{1}{2} \langle (\mathbf{r}' \mathbf{W}_k \mathbf{r}) (\mathbf{r}' \mathbf{M}_{51} \mathbf{r}) (\mathbf{r}' \mathbf{W}_l \mathbf{r}) (\mathbf{r}' \mathbf{W}_{v_{kl}} \mathbf{r}) \exp[-\mathbf{r}'(\mathbf{A}_{kl}) \mathbf{r}] \rangle \\
= \frac{\partial}{\partial \omega_k} \frac{\partial}{\partial \omega_l} \frac{\partial}{\partial \omega_v} \frac{\partial}{\partial \omega_m} \langle \exp[-\mathbf{r}'(\mathbf{A}_{kl} + \omega_k \mathbf{W}_k + \omega_l \mathbf{W}_l + \omega_v \mathbf{W}_{v_{kl}} + \omega_m \mathbf{M}_{51}) \mathbf{r}] \rangle \Big|_{\omega_k=\omega_l=\omega_v=\omega_m=0} \\
= \pi^{3n/2} \frac{\partial}{\partial \omega_k} \frac{\partial}{\partial \omega_l} \frac{\partial}{\partial \omega_v} \frac{\partial}{\partial \omega_m} |(\mathbf{A}_{kl} + \omega_k \mathbf{W}_k + \omega_l \mathbf{W}_l + \omega_v \mathbf{W}_{v_{kl}} + \omega_m \mathbf{M}_{51})|^{-1/2} \Big|_{\omega_k=\omega_l=\omega_v=\omega_m=0} \\
= \pi^{3n/2} |A_{kl}|^{-3/2} \left\{ \frac{1}{16} \eta_k \eta_l \text{tr} [\mathbf{A}_{kl}^{-1} \mathbf{W}_{v_{kl}}] \text{tr} [\mathbf{A}_{kl}^{-1} \mathbf{M}_{51}] + \frac{1}{8} (\eta_{kl} \text{tr} [\mathbf{A}_{kl}^{-1} \mathbf{W}_{v_{kl}}] \text{tr} [\mathbf{A}_{kl}^{-1} \mathbf{M}_{51}] \right. \\
& + \eta_k \text{tr} [\mathbf{A}_{kl}^{-1} \mathbf{W}_l \mathbf{A}_{kl}^{-1} \mathbf{W}_{v_{kl}}] \text{tr} [\mathbf{A}_{kl}^{-1} \mathbf{M}_{51}] + \eta_l \text{tr} [\mathbf{A}_{kl}^{-1} \mathbf{W}_k \mathbf{A}_{kl}^{-1} \mathbf{M}_{51}] \text{tr} [\mathbf{A}_{kl}^{-1} \mathbf{W}_{v_{kl}}] \\
& + \eta_l \text{tr} [\mathbf{A}_{kl}^{-1} \mathbf{W}_k \mathbf{A}_{kl}^{-1} \mathbf{W}_{v_{kl}}] \text{tr} [\mathbf{A}_{kl}^{-1} \mathbf{M}_{51}] + \eta_l \text{tr} [\mathbf{A}_{kl}^{-1} \mathbf{W}_k \mathbf{A}_{kl}^{-1} \mathbf{M}_{51}] \text{tr} [\mathbf{A}_{kl}^{-1} \mathbf{W}_{v_{kl}}]) \\
& + \frac{1}{4} (\eta_l \text{tr} [\mathbf{A}_{kl}^{-1} \mathbf{W}_l \mathbf{A}_{kl}^{-1} \mathbf{M}_{51} \mathbf{A}_{kl}^{-1} \mathbf{W}_{v_{kl}}] + \eta_k \text{tr} [\mathbf{A}_{kl}^{-1} \mathbf{M}_{51} \mathbf{A}_{kl}^{-1} \mathbf{W}_l \mathbf{A}_{kl}^{-1} \mathbf{W}_{v_{kl}}] + \eta_l \text{tr} [\mathbf{A}_{kl}^{-1} \mathbf{W}_k \mathbf{A}_{kl}^{-1} \mathbf{M}_{51} \mathbf{A}_{kl}^{-1} \mathbf{W}_{v_{kl}}] \\
& + \eta_l \text{tr} [\mathbf{A}_{kl}^{-1} \mathbf{M}_{51} \mathbf{A}_{kl}^{-1} \mathbf{W}_k \mathbf{A}_{kl}^{-1} \mathbf{W}_{v_{kl}}] + \text{tr} [\mathbf{A}_{kl}^{-1} \mathbf{W}_k \mathbf{A}_{kl}^{-1} \mathbf{W}_l \mathbf{A}_{kl}^{-1} \mathbf{W}_{v_{kl}}] \text{tr} [\mathbf{A}_{kl}^{-1} \mathbf{M}_{51}] \\
& \left. + \text{tr} [\mathbf{A}_{kl}^{-1} \mathbf{W}_l \mathbf{A}_{kl}^{-1} \mathbf{W}_k \mathbf{A}_{kl}^{-1} \mathbf{W}_{v_{kl}}] \text{tr} [\mathbf{A}_{kl}^{-1} \mathbf{M}_{51}] + \text{tr} [\mathbf{A}_{kl}^{-1} \mathbf{W}_k \mathbf{A}_{kl}^{-1} \mathbf{W}_l \mathbf{A}_{kl}^{-1} \mathbf{M}_{51}] \text{tr} [\mathbf{A}_{kl}^{-1} \mathbf{W}_{v_{kl}}] \right\}
\end{aligned}$$

$$\begin{aligned}
& + \text{tr} [\mathbf{A}_{kl}^{-1} \mathbf{W}_l \mathbf{A}_{kl}^{-1} \mathbf{W}_k \mathbf{A}_{kl}^{-1} \mathbf{M}_{51}] \text{tr} [\mathbf{A}_{kl}^{-1} \mathbf{W}_{v_{kl}}] + \eta_{kl} \text{tr} [\mathbf{A}_{kl}^{-1} \mathbf{M}_{51} \mathbf{A}_{kl}^{-1} \mathbf{W}_{v_{kl}}] \\
& + \text{tr} [\mathbf{A}_{kl}^{-1} \mathbf{W}_k \mathbf{A}_{kl}^{-1} \mathbf{W}_{v_{kl}}] \text{tr} [\mathbf{A}_{kl}^{-1} \mathbf{W}_l \mathbf{A}_{kl}^{-1} \mathbf{M}_{51}] + \text{tr} [\mathbf{A}_{kl}^{-1} \mathbf{W}_k \mathbf{A}_{kl}^{-1} \mathbf{M}_{51}] \text{tr} [\mathbf{A}_{kl}^{-1} \mathbf{W}_l \mathbf{A}_{kl}^{-1} \mathbf{W}_{v_{kl}}] \\
& + \frac{1}{2} (\text{tr} [\mathbf{A}_{kl}^{-1} \mathbf{M}_{51} \mathbf{A}_{kl}^{-1} \mathbf{W}_k \mathbf{A}_{kl}^{-1} \mathbf{W}_l \mathbf{A}_{kl}^{-1} \mathbf{W}_{v_{kl}}] + \text{tr} [\mathbf{A}_{kl}^{-1} \mathbf{W}_k \mathbf{A}_{kl}^{-1} \mathbf{W}_l \mathbf{A}_{kl}^{-1} \mathbf{M}_{51} \mathbf{A}_{kl}^{-1} \mathbf{W}_{v_{kl}}]) \\
& + \text{tr} [\mathbf{A}_{kl}^{-1} \mathbf{M}_{51} \mathbf{A}_{kl}^{-1} \mathbf{W}_l \mathbf{A}_{kl}^{-1} \mathbf{W}_k \mathbf{A}_{kl}^{-1} \mathbf{W}_{v_{kl}}] + \text{tr} [\mathbf{A}_{kl}^{-1} \mathbf{W}_l \mathbf{A}_{kl}^{-1} \mathbf{M}_{51} \mathbf{A}_{kl}^{-1} \mathbf{W}_k \mathbf{A}_{kl}^{-1} \mathbf{W}_{v_{kl}}] \\
& + \text{tr} [\mathbf{A}_{kl}^{-1} \mathbf{W}_l \mathbf{A}_{kl}^{-1} \mathbf{W}_k \mathbf{A}_{kl}^{-1} \mathbf{M}_{51} \mathbf{A}_{kl}^{-1} \mathbf{W}_{v_{kl}}] + \text{tr} [\mathbf{A}_{kl}^{-1} \mathbf{W}_k \mathbf{A}_{kl}^{-1} \mathbf{M}_{51} \mathbf{A}_{kl}^{-1} \mathbf{W}_l \mathbf{A}_{kl}^{-1} \mathbf{W}_{v_{kl}}) \Big\}. \quad (63)
\end{aligned}$$

The above expression needs to be simplified to reduce the number of terms. The simplification is achieved by using the same procedure as shown in the overlap derivation preformed with method "II". As an aside, it is worth mentioning that at this stage of the derivation the above formula has the same form as the overlap integral for ECGs with quartic-polynomial angular factors which are needed to calculate atomic $L = 4$ and $M = 0$ states with one g electron, if appropriate matrix replacement is done. Now, the simplification gives the following:

$$\begin{aligned}
(51) = & \pi^{3n/2} |A_{kl}|^{-3/2} \left\{ \frac{1}{4} \eta_k \eta_l \eta_v \text{tr} [\mathbf{A}_{kl}^{-1} \mathbf{A}_k \mathbf{M} \mathbf{A}_l] + \frac{1}{2} (\eta_{kl} \eta_v \text{tr} [\mathbf{A}_{kl}^{-1} \mathbf{A}_k \mathbf{M} \mathbf{A}_l] \right. \\
& + \eta_k \eta_l \eta_v \text{tr} [\mathbf{A}_{kl}^{-1} \mathbf{A}_k \mathbf{M} \mathbf{A}_l] + \eta_k \eta_v \text{tr} [\mathbf{A}_{kl}^{-1} \mathbf{W}_l \mathbf{A}_{kl}^{-1} \mathbf{A}_k \mathbf{M} \mathbf{A}_l] + \frac{1}{2} \eta_k \eta_l \text{tr} [\mathbf{A}_{kl}^{-1} \mathbf{A}_k \mathbf{M} \mathbf{A}_l \mathbf{A}_{kl}^{-1} \mathbf{W}_{v_{kl}}] \\
& + \eta_l \eta_{kv} \text{tr} [\mathbf{A}_{kl}^{-1} \mathbf{A}_k \mathbf{M} \mathbf{A}_l] + \eta_l \eta_v \text{tr} [\mathbf{A}_{kl}^{-1} \mathbf{W}_k \mathbf{A}_{kl}^{-1} \mathbf{A}_k \mathbf{M} \mathbf{A}_l] \\
& + \eta_k (\text{tr} [\mathbf{A}_{kl}^{-1} \mathbf{W}_l \mathbf{A}_{kl}^{-1} \mathbf{A}_k \mathbf{M} \mathbf{A}_l \mathbf{A}_{kl}^{-1} \mathbf{W}_{v_{kl}}] + \text{tr} [\mathbf{A}_{kl}^{-1} \mathbf{A}_k \mathbf{M} \mathbf{A}_l \mathbf{A}_{kl}^{-1} \mathbf{W}_l \mathbf{A}_{kl}^{-1} \mathbf{W}_{v_{kl}}]) \\
& + \eta_l (\text{tr} [\mathbf{A}_{kl}^{-1} \mathbf{W}_k \mathbf{A}_{kl}^{-1} \mathbf{A}_k \mathbf{M} \mathbf{A}_l \mathbf{A}_{kl}^{-1} \mathbf{W}_{v_{kl}}] + \text{tr} [\mathbf{A}_{kl}^{-1} \mathbf{A}_k \mathbf{M} \mathbf{A}_l \mathbf{A}_{kl}^{-1} \mathbf{W}_k \mathbf{A}_{kl}^{-1} \mathbf{W}_{v_{kl}}]) \\
& + (\eta_{klv} + \eta_{lkv}) \text{tr} [\mathbf{A}_{kl}^{-1} \mathbf{A}_k \mathbf{M} \mathbf{A}_l] + \eta_v (\text{tr} [\mathbf{A}_{kl}^{-1} \mathbf{W}_k \mathbf{A}_{kl}^{-1} \mathbf{W}_l \mathbf{A}_{kl}^{-1} \mathbf{A}_k \mathbf{M} \mathbf{A}_l] + \text{tr} [\mathbf{A}_{kl}^{-1} \mathbf{W}_l \mathbf{A}_{kl}^{-1} \mathbf{W}_k \mathbf{A}_{kl}^{-1} \mathbf{A}_k \mathbf{M} \mathbf{A}_l]) \\
& + \frac{1}{2} \eta_{kl} \text{tr} [\mathbf{A}_{kl}^{-1} \mathbf{A}_k \mathbf{M} \mathbf{A}_l \mathbf{A}_{kl}^{-1} \mathbf{W}_{v_{kl}}] + \eta_{kv} \text{tr} [\mathbf{A}_{kl}^{-1} \mathbf{W}_l \mathbf{A}_{kl}^{-1} \mathbf{A}_k \mathbf{M} \mathbf{A}_l] + \eta_{lv} \text{tr} [\mathbf{A}_{kl}^{-1} \mathbf{W}_k \mathbf{A}_{kl}^{-1} \mathbf{A}_k \mathbf{M} \mathbf{A}_l] \\
& + \text{tr} [\mathbf{A}_{kl}^{-1} \mathbf{A}_k \mathbf{M} \mathbf{A}_l \mathbf{A}_{kl}^{-1} \mathbf{W}_k \mathbf{A}_{kl}^{-1} \mathbf{W}_l \mathbf{A}_{kl}^{-1} \mathbf{W}_{v_{kl}}] + \text{tr} [\mathbf{A}_{kl}^{-1} \mathbf{W}_k \mathbf{A}_{kl}^{-1} \mathbf{W}_l \mathbf{A}_{kl}^{-1} \mathbf{A}_k \mathbf{M} \mathbf{A}_l \mathbf{A}_{kl}^{-1} \mathbf{W}_{v_{kl}}] \\
& + \text{tr} [\mathbf{A}_{kl}^{-1} \mathbf{A}_k \mathbf{M} \mathbf{A}_l \mathbf{A}_{kl}^{-1} \mathbf{W}_l \mathbf{A}_{kl}^{-1} \mathbf{W}_k \mathbf{A}_{kl}^{-1} \mathbf{W}_{v_{kl}}] + \text{tr} [\mathbf{A}_{kl}^{-1} \mathbf{W}_l \mathbf{A}_{kl}^{-1} \mathbf{A}_k \mathbf{M} \mathbf{A}_l \mathbf{A}_{kl}^{-1} \mathbf{W}_k \mathbf{A}_{kl}^{-1} \mathbf{W}_{v_{kl}}] \\
& + \text{tr} [\mathbf{A}_{kl}^{-1} \mathbf{W}_l \mathbf{A}_{kl}^{-1} \mathbf{W}_k \mathbf{A}_{kl}^{-1} \mathbf{A}_k \mathbf{M} \mathbf{A}_l \mathbf{A}_{kl}^{-1} \mathbf{W}_{v_{kl}}] + \text{tr} [\mathbf{A}_{kl}^{-1} \mathbf{W}_k \mathbf{A}_{kl}^{-1} \mathbf{A}_k \mathbf{M} \mathbf{A}_l \mathbf{A}_{kl}^{-1} \mathbf{W}_l \mathbf{A}_{kl}^{-1} \mathbf{W}_{v_{kl}}] \Big\} \\
= & 6^I \langle \phi_k | \phi_l \rangle \text{tr} [\mathbf{A}_{kl}^{-1} \mathbf{A}_k \mathbf{M} \mathbf{A}_l] + \pi^{3n/2} |A_{kl}|^{-3/2} \\
& \times \left\{ \frac{1}{2} \left(\eta_k \eta_v \text{tr} [\mathbf{A}_{kl}^{-1} \mathbf{W}_l \mathbf{A}_{kl}^{-1} \mathbf{A}_k \mathbf{M} \mathbf{A}_l] + \frac{1}{2} \eta_k \eta_l \text{tr} [\mathbf{A}_{kl}^{-1} \mathbf{A}_k \mathbf{M} \mathbf{A}_l \mathbf{A}_{kl}^{-1} \mathbf{W}_{v_{kl}}] + \eta_l \eta_v \text{tr} [\mathbf{A}_{kl}^{-1} \mathbf{W}_k \mathbf{A}_{kl}^{-1} \mathbf{A}_k \mathbf{M} \mathbf{A}_l] \right. \right. \\
& + \eta_k (\text{tr} [\mathbf{A}_{kl}^{-1} \mathbf{W}_l \mathbf{A}_{kl}^{-1} \mathbf{A}_k \mathbf{M} \mathbf{A}_l \mathbf{A}_{kl}^{-1} \mathbf{W}_{v_{kl}}] + \text{tr} [\mathbf{A}_{kl}^{-1} \mathbf{A}_k \mathbf{M} \mathbf{A}_l \mathbf{A}_{kl}^{-1} \mathbf{W}_l \mathbf{A}_{kl}^{-1} \mathbf{W}_{v_{kl}}]) \\
& + \eta_l (\text{tr} [\mathbf{A}_{kl}^{-1} \mathbf{W}_k \mathbf{A}_{kl}^{-1} \mathbf{A}_k \mathbf{M} \mathbf{A}_l \mathbf{A}_{kl}^{-1} \mathbf{W}_{v_{kl}}] + \text{tr} [\mathbf{A}_{kl}^{-1} \mathbf{A}_k \mathbf{M} \mathbf{A}_l \mathbf{A}_{kl}^{-1} \mathbf{W}_k \mathbf{A}_{kl}^{-1} \mathbf{W}_{v_{kl}}]) \\
& + \eta_v (\text{tr} [\mathbf{A}_{kl}^{-1} \mathbf{W}_k \mathbf{A}_{kl}^{-1} \mathbf{W}_l \mathbf{A}_{kl}^{-1} \mathbf{A}_k \mathbf{M} \mathbf{A}_l] + \text{tr} [\mathbf{A}_{kl}^{-1} \mathbf{W}_l \mathbf{A}_{kl}^{-1} \mathbf{W}_k \mathbf{A}_{kl}^{-1} \mathbf{A}_k \mathbf{M} \mathbf{A}_l]) \\
& + \frac{1}{2} \eta_{kl} \text{tr} [\mathbf{A}_{kl}^{-1} \mathbf{A}_k \mathbf{M} \mathbf{A}_l \mathbf{A}_{kl}^{-1} \mathbf{W}_{v_{kl}}] + \eta_{kv} \text{tr} [\mathbf{A}_{kl}^{-1} \mathbf{W}_l \mathbf{A}_{kl}^{-1} \mathbf{A}_k \mathbf{M} \mathbf{A}_l] + \eta_{lv} \text{tr} [\mathbf{A}_{kl}^{-1} \mathbf{W}_k \mathbf{A}_{kl}^{-1} \mathbf{A}_k \mathbf{M} \mathbf{A}_l] \\
& + \text{tr} [\mathbf{A}_{kl}^{-1} \mathbf{A}_k \mathbf{M} \mathbf{A}_l \mathbf{A}_{kl}^{-1} \mathbf{W}_k \mathbf{A}_{kl}^{-1} \mathbf{W}_l \mathbf{A}_{kl}^{-1} \mathbf{W}_{v_{kl}}] + \text{tr} [\mathbf{A}_{kl}^{-1} \mathbf{W}_k \mathbf{A}_{kl}^{-1} \mathbf{W}_l \mathbf{A}_{kl}^{-1} \mathbf{A}_k \mathbf{M} \mathbf{A}_l \mathbf{A}_{kl}^{-1} \mathbf{W}_{v_{kl}}] \\
& + \text{tr} [\mathbf{A}_{kl}^{-1} \mathbf{A}_k \mathbf{M} \mathbf{A}_l \mathbf{A}_{kl}^{-1} \mathbf{W}_l \mathbf{A}_{kl}^{-1} \mathbf{W}_k \mathbf{A}_{kl}^{-1} \mathbf{W}_{v_{kl}}] + \text{tr} [\mathbf{A}_{kl}^{-1} \mathbf{W}_l \mathbf{A}_{kl}^{-1} \mathbf{A}_k \mathbf{M} \mathbf{A}_l \mathbf{A}_{kl}^{-1} \mathbf{W}_k \mathbf{A}_{kl}^{-1} \mathbf{W}_{v_{kl}}] \\
& + \text{tr} [\mathbf{A}_{kl}^{-1} \mathbf{W}_l \mathbf{A}_{kl}^{-1} \mathbf{W}_k \mathbf{A}_{kl}^{-1} \mathbf{A}_k \mathbf{M} \mathbf{A}_l \mathbf{A}_{kl}^{-1} \mathbf{W}_{v_{kl}}] + \text{tr} [\mathbf{A}_{kl}^{-1} \mathbf{W}_k \mathbf{A}_{kl}^{-1} \mathbf{A}_k \mathbf{M} \mathbf{A}_l \mathbf{A}_{kl}^{-1} \mathbf{W}_l \mathbf{A}_{kl}^{-1} \mathbf{W}_{v_{kl}}] \Big\}. \quad (64)
\end{aligned}$$

This concludes the derivation of all elementary integrals needed to calculate the kinetic-energy matrix element.

C. The Dirac delta function and potential energy integral

The potential-energy operator in the internal Hamiltonian (2) depends on inverses of the interparticle distances between the electrons and between the electrons and the nucleus, r_{ij} and r_i . Therefore, the following general elemental integral needs to be considered:

$$\langle \phi_k | r_{ij}^\nu | \phi_l \rangle, \quad \nu > -3. \quad (65)$$

This integral allows for calculating all required integrals contributing to the potential energy matrix element by setting $\nu = -1$. The criteria that $\nu > -3$ will be clarified in the derivation. To integrate (65) we first need to evaluate the following auxiliary integral that involves a three-dimensional Dirac delta function:

$$\begin{aligned} \delta(a_1 \mathbf{r}_1 + a_2 \mathbf{r}_2 + \dots + a_n \mathbf{r}_n - \boldsymbol{\xi}) \\ \equiv \delta((a \otimes I_3)' \mathbf{r} - \boldsymbol{\xi}) \\ = \lim_{\beta \rightarrow \infty} \left(\frac{\beta}{\pi} \right)^{3/2} \exp[-\beta((a \otimes I_3)' \mathbf{r} - \boldsymbol{\xi})^2], \end{aligned} \quad (66)$$

where a is a real n -component vector, $\boldsymbol{\xi}$ is a real three-dimensional parameter, and β is a parameter. When we set $a = e^i - e^j$, where e^m is an n -component vector whose m th component is 1 and all others are zeros, then (65) can be expressed as

$$\begin{aligned} \langle \phi_k | r_{ij}^\nu | \phi_l \rangle \\ = \int_{-\infty}^{+\infty} |\boldsymbol{\xi}|^\nu \langle \phi_k | \delta((a \otimes I_3)' \mathbf{r} - \boldsymbol{\xi}) | \phi_l \rangle d\boldsymbol{\xi} \\ = \frac{1}{2} \int_{-\infty}^{+\infty} \frac{\partial}{\partial \omega_v} \frac{\partial}{\partial \omega_k} \frac{\partial}{\partial \omega_l} |\boldsymbol{\xi}|^\nu \langle^{II} \varphi_k | \\ \times \exp[-\mathbf{r}' \omega_v \mathbf{W}_{v_{kl}} \mathbf{r}] \delta((a \otimes I_3)' \mathbf{r} - \boldsymbol{\xi}) |^{II} \varphi_l \rangle |_{\nu_k, \nu_l, \omega_k, \omega_l=0} d\boldsymbol{\xi}, \end{aligned} \quad (67)$$

where we used method “II” from the overlap-integral section, and where

$$\begin{aligned} \langle^{II} \varphi_k | \exp[-\mathbf{r}' \omega_v \mathbf{W}_{v_{kl}} \mathbf{r}] \delta((a \otimes I_3)' \mathbf{r} - \boldsymbol{\xi}) |^{II} \varphi_l \rangle \\ = \lim_{\beta \rightarrow \infty} \left(\frac{\beta}{\pi} \right)^{3/2} \langle^{II} \varphi_k | \exp[-\mathbf{r}' \omega_v \mathbf{W}_{v_{kl}} \mathbf{r}] \\ \times \exp[-\beta \mathbf{r}' (aa' \otimes I_3) \mathbf{r} + 2\beta((a \otimes I_3) \boldsymbol{\xi})' \mathbf{r} - \beta \boldsymbol{\xi}^2] |^{II} \varphi_l \rangle. \end{aligned} \quad (68)$$

It should be noted that integrals involving delta function (66) with different choices of vector a can be useful in evaluating matrix elements for many other important quantities. For this reason, even though we are only concerned here with the evaluation of potential-energy matrix elements, we will assume that the a vector has a general form when deriving integral (68).

Applying formula (19) in (68) we obtain

$$\begin{aligned} \langle^{II} \varphi_k | \exp[-\mathbf{r}' \omega_v \mathbf{W}_{v_{kl}} \mathbf{r}] \delta((a \otimes I_3)' \mathbf{r} - \boldsymbol{\xi}) |^{II} \varphi_l \rangle \\ = \pi^{3(n-1)/2} \lim_{\beta \rightarrow \infty} \beta^{3/2} | \mathbf{G}_{kl} + \beta(aa' \otimes I_3) |^{-1/2} \end{aligned}$$

$$\begin{aligned} \times \exp \left[\frac{1}{4} (2\beta((a \otimes I_3) \boldsymbol{\xi}))' (\mathbf{G}_{kl} + \beta(aa' \otimes I_3))^{-1} \right. \\ \left. \times (2\beta((a \otimes I_3) \boldsymbol{\xi})) \right] \exp[-\beta \boldsymbol{\xi}^2], \end{aligned} \quad (69)$$

where $\mathbf{G}_{kl} = \mathbf{A}_{kl} + \omega_k \mathbf{W}_k + \omega_l \mathbf{W}_l + \omega_v \mathbf{W}_v$. Taking the limit in (69) for β approaching infinity can be done by expanding both the determinant and the exponent into an inverse power series with respect to β . This approach is explained in detail in Ref. 20. Applying the approach to evaluate the limit of (69) with respect to infinite β gives:

$$\begin{aligned} \langle^{II} \varphi_k | \exp[-\mathbf{r}' \omega_v \mathbf{W}_{v_{kl}} \mathbf{r}] \delta((a \otimes I_3)' \mathbf{r} - \boldsymbol{\xi}) |^{II} \varphi_l \rangle \\ = \pi^{3(n-1)/2} | \mathbf{G}_{kl} |^{-1/2} | \Lambda_{kl} |^{-1} \exp[-\boldsymbol{\xi}' \Lambda_{kl}^{-1} \boldsymbol{\xi}]. \end{aligned} \quad (70)$$

The next step involves differentiating (70) with respect to ω_k , ω_l , and ω_v and setting $\omega_k = \omega_l = \omega_v = 0$. To perform the differentiation, let us recall another matrix identity for the differential of a matrix inverse in the form: $(Y'X^{-1}Y)^{-1}$, where X is some arbitrary square matrix and Y is a rectangular constant matrix (or a vector)

$$d(Y'X^{-1}Y)^{-1} = (Y'X^{-1}Y)^{-1} Y' X^{-1} (dX) X^{-1} Y (Y'X^{-1}Y)^{-1}. \quad (71)$$

In the differentiation it is important to notice that the following simplification can be done in the following product, which appears in the expression for the integral with the delta function:

$$(a' \otimes I_3) \Lambda_{kl}^{-1} (a \otimes I_3) = a' A_{kl}^{-1} a \otimes I_3 = \lambda I_3, \quad (72)$$

where $\lambda = \text{tr}[A_{kl}^{-1} aa']$. Using (71) and (72), and defining $J = aa'$ and $\mathbf{J} = J \otimes I_3$, we can make the final step in deriving the formula for the $\langle \phi_k | r_{ij}^\nu | \phi_l \rangle$ matrix element by integrating over $\boldsymbol{\xi} = \{\xi_x, \xi_y, \xi_z\}$. Here we need to specify a particular form of a . As mentioned above, in case of r_{ij} we simply set $a = e^i - e^j$. In case of the matrix element involving r_i we set $a = e^i$. With that matrix J has a very simple structure:

$$J = \begin{cases} E_{ii}, & i = j \text{ for } r_i \\ E_{ii} + E_{jj} - E_{ij} - E_{ji}, & i \neq j \text{ for } r_{ij} \end{cases}, \quad (73)$$

where E_{ij} is a matrix with 1 in the i, j th position and 0's elsewhere.

There are four types of integrals involved when integrating over $\boldsymbol{\xi}$. These integrals have the following general forms:

$$\int_{-\infty}^{+\infty} |\boldsymbol{\xi}|^\nu \exp[-\lambda^{-1} \boldsymbol{\xi}^2] d\boldsymbol{\xi}, \quad (74)$$

$$\int_{-\infty}^{+\infty} |\boldsymbol{\xi}|^\nu (\boldsymbol{\xi}' \Omega^{(1)} \boldsymbol{\xi}) \exp[-\lambda^{-1} \boldsymbol{\xi}^2] d\boldsymbol{\xi}, \quad (75)$$

$$\int_{-\infty}^{+\infty} |\boldsymbol{\xi}|^\nu (\boldsymbol{\xi}' \Omega^{(2)} \boldsymbol{\xi})(\boldsymbol{\xi}' \Omega^{(3)} \boldsymbol{\xi}) \exp[-\lambda^{-1} \boldsymbol{\xi}^2] d\boldsymbol{\xi}, \quad (76)$$

$$\int_{-\infty}^{+\infty} |\boldsymbol{\xi}|^\nu (\boldsymbol{\xi}' \Omega^{(4)} \boldsymbol{\xi})(\boldsymbol{\xi}' \Omega^{(5)} \boldsymbol{\xi})(\boldsymbol{\xi}' \Omega^{(6)} \boldsymbol{\xi}) \exp[-\lambda^{-1} \boldsymbol{\xi}^2] d\boldsymbol{\xi}, \quad (77)$$

where $\lambda = \text{tr}[A_{kl}^{-1} J]$, and $\Omega^{(1\dots 6)}$ are certain 3×3 matrices.

Integral (74) is the following standard integral:

$$\int_{-\infty}^{+\infty} |\xi|^\nu \exp[-\lambda^{-1}\xi^2] d\xi = 2\pi \Gamma\left(\frac{3+\nu}{2}\right) \lambda^{(3+\nu)/2}, \quad (78)$$

where ν must be greater than negative three to avoid the argument of the gamma function going zero or a negative value. Integrals (75) and (76) were evaluated in the previous work²⁰ and are

$$\begin{aligned} & \int_{-\infty}^{+\infty} |\xi|^\nu (\xi' \Omega^{(1)} \xi) \exp[-\lambda^{-1}\xi^2] d\xi \\ &= \frac{2\pi}{3} \Gamma\left(\frac{5+\nu}{2}\right) \lambda^{(5+\nu)/2} \text{tr}[\Omega^{(1)}], \end{aligned} \quad (79)$$

$$\begin{aligned} & \int_{-\infty}^{+\infty} |\xi|^\nu (\xi' \Omega^{(2)} \xi) (\xi' \Omega^{(3)} \xi) \exp[-\lambda^{-1}\xi^2] d\xi \\ &= \frac{2\pi}{15} \Gamma\left(\frac{7+\nu}{2}\right) \lambda^{(7+\nu)/2} \\ & \quad (2\text{tr}[\Omega^{(2)} \Omega^{(3)}] + \text{tr}[\Omega^{(2)}] \text{tr}[\Omega^{(3)}]). \end{aligned} \quad (80)$$

To evaluate integral (77) we have to explicitly write the following quadratic form: $(\xi' \Omega^{(4)} \xi) (\xi' \Omega^{(5)} \xi) (\xi' \Omega^{(6)} \xi)$. The lengthy resulting expression becomes much easier once we realize that odd functions yield zero value after integration. Integrating only the even terms we obtain the following formula for integral (77):

$$\begin{aligned} & \int_{-\infty}^{+\infty} |\xi|^\nu (\xi' \Omega^{(4)} \xi) (\xi' \Omega^{(5)} \xi) (\xi' \Omega^{(6)} \xi) \exp[-\lambda^{-1}\xi^2] d\xi \\ &= \frac{2\pi}{105} \Gamma\left(\frac{9+\nu}{2}\right) \lambda^{(9+\nu)/2} (4(\text{tr}[\Omega^{(4)} \Omega^{(5)} \Omega^{(6)}] \text{tr}[\Omega^{(5)} \Omega^{(4)} \Omega^{(6)}]) + 2\text{tr}[\Omega^{(4)} \Omega^{(5)}] \text{tr}[\Omega^{(6)}] + 2\text{tr}[\Omega^{(5)} \Omega^{(6)}] \text{tr}[\Omega^{(4)}] \\ & \quad + 2\text{tr}[\Omega^{(6)} \Omega^{(4)}] \text{tr}[\Omega^{(5)}] + \text{tr}[\Omega^{(4)}] \text{tr}[\Omega^{(5)}] \text{tr}[\Omega^{(6)}]). \end{aligned} \quad (81)$$

Using expressions (78)–(81) we can now perform integration and, after some rearrangement and simplification, we obtain the following final formula for the $\langle \phi_k | r_{ij}^\nu | \phi_l \rangle$ matrix element:

$$\begin{aligned} \langle \phi_k | r_{ij}^\nu | \phi_l \rangle &= \frac{\pi^{(3n-1)/2}}{|A_{kl}|^{3/2}} \Gamma\left(\frac{3+\nu}{2}\right) \lambda^{\nu/2} \left\{ 2|A_{kl}|^{3/2} \pi^{-3n/2} \langle \phi_k | \phi_l \rangle^1 \right. \\ & \quad + \lambda^{-1} \left(\frac{\nu}{3} \right) \left[\eta_{klJv} + \eta_{lkJv} + \eta_{Jklv} + \eta_{Jlkv} + \eta_{kJlv} + \eta_{lJkv} + \eta_{klJv} + \eta_{kvJl} + \eta_{lvJk} \right. \\ & \quad + \frac{1}{2} (\eta_k (\eta_{Jlv} + \eta_{Jv}) + \eta_l (\eta_{Jkv} + \eta_{Jv}) \eta_v (\eta_{klJ} + \eta_{lkJ})) + \frac{1}{4} (\eta_k \eta_l \eta_{Jv} + \eta_k \eta_{lJ} \eta_v + \eta_{kJ} \eta_l \eta_v) \Big] \\ & \quad + \lambda^{-2} \left(\frac{\nu(\nu-2)}{3 \times 5} \right) \left[\eta_{JklJv} + \eta_{JlkJv} + \eta_{JkJlv} + \eta_{JlJkv} + \eta_{kJlJv} + \eta_{lJkJv} \right. \\ & \quad + \frac{1}{2} (\eta_k \eta_{Jlv} + \eta_l \eta_{Jkv} + \eta_v \eta_{kJJ} + \eta_{kJ} (\eta_{Jlv} + \eta_{Jv}) + \eta_{lJ} (\eta_{Jkv} + \eta_{Jv}) + \eta_{Jv} (\eta_{klJ} + \eta_{lkJ})) \\ & \quad + \frac{1}{4} (\eta_k \eta_{lJ} \eta_{Jv} + \eta_l \eta_{kJ} \eta_{Jv} + \eta_v \eta_{kJ} \eta_{lJ}) \Big] \\ & \quad + \lambda^{-3} \left(\frac{\nu(\nu-2)(\nu-4)}{3 \times 5 \times 7} \right) \left[\eta_{JkJlJv} + \eta_{JlJkJv} + \frac{1}{2} (\eta_{kJ} \eta_{JlJv} + \eta_{lJ} \eta_{kJv} + \eta_{Jv} \eta_{kJJ}) \right. \\ & \quad \left. \left. + \frac{1}{4} \eta_{kJ} \eta_{lJ} \eta_{Jv} \right] \right\}, \end{aligned} \quad (82)$$

where the traces appearing in the above expression were defined in the overlap-integral section. The subscript **J** in η indicates the matrix product of $A_{kl}^{-1} \mathbf{J}$.

The case when $\nu = -1$ represents the integrals that appear in the potential-energy matrix elements. In this case the matrix element becomes

$$\begin{aligned} \langle \phi_k | \frac{1}{r_{ij}} | \phi_l \rangle &= \frac{\pi^{(3n-1)/2}}{|A_{kl}|^{3/2}} \lambda^{-1/2} \left\{ 2|A_{kl}|^{3/2} \pi^{-3n/2} \langle \phi_k | \phi_l \rangle^1 \right. \\ & \quad - \lambda^{-1} \left(\frac{1}{3} \right) \left[\eta_{klJv} + \eta_{lkJv} + \eta_{Jklv} + \eta_{Jlkv} + \eta_{kJlv} + \eta_{lJkv} + \eta_{klJv} + \eta_{kvJl} + \eta_{lvJk} \right. \\ & \quad + \frac{1}{2} (\eta_k (\eta_{Jlv} + \eta_{Jv}) + \eta_l (\eta_{Jkv} + \eta_{Jv}) \eta_v (\eta_{klJ} + \eta_{lkJ})) + \frac{1}{4} (\eta_k \eta_l \eta_{Jv} + \eta_k \eta_{lJ} \eta_v + \eta_{kJ} \eta_l \eta_v) \Big] \end{aligned}$$

$$\begin{aligned}
& + \lambda^{-2} \left(\frac{1}{5} \right) \left[\eta_{JklJv} + \eta_{JlkJv} + \eta_{Jk,lJv} + \eta_{Jl,Jkv} + \eta_{kJlJv} + \eta_{lJkJv} \right. \\
& + \frac{1}{2} (\eta_k \eta_{JlJv} + \eta_l \eta_{JkJv} + \eta_v \eta_{kJlJ} + \eta_{kJ} (\eta_{JlV} + \eta_{lJv}) + \eta_{lJ} (\eta_{Jkv} + \eta_{kJv}) + \eta_{Jv} (\eta_{klJ} + \eta_{lkJ})) \\
& \left. + \frac{1}{4} (\eta_k \eta_{lJ} \eta_{Jv} + \eta_l \eta_{kJ} \eta_{Jv} + \eta_v \eta_{kJ} \eta_{lJ}) \right] \\
& - \lambda^{-3} \left(\frac{1}{7} \right) \left[\eta_{JkJlJv} + \eta_{JlJkJv} + \frac{1}{2} (\eta_{kJ} \eta_{JlJv} + \eta_{lJ} \eta_{JkJv} + \eta_{Jv} \eta_{kJlJ}) + \frac{1}{4} \eta_{kJ} \eta_{lJ} \eta_{Jv} \right] \}. \quad (83)
\end{aligned}$$

It is worth noticing that, when v is zero, (82) should reproduce the formula for the overlap integral (28) and it does. This concludes the derivation of the potential-energy matrix element.

VII. NUMERICAL TESTS

The above-described formulas for the Hamiltonian and overlap matrix elements have been coded in FORTRAN 90 and implemented to run in a parallel environment using the MPI approach. The codes for individual integrals have been tested by comparing the results obtained by running the code with the results obtained using the MATHEMATICA program. The test concerned one-, two-, and three-particle cases. After the tests provided a consistent set of answers, the code for calculating the Hamiltonian and overlap matrix elements have been interfaced with a code for solving the secular equation problem and for the optimization of the Gaussian nonlinear parameters. The resulting computer problem has been used to perform calculations of the lowest 2F state of the lithium atom.

It should be noted that, due to the complexity of the expressions for the matrix elements, the code to calculate them, which has been written in this work, has the most simple and transparent structure possible. With that, this is not the most efficient code one can possibly generate in this case. Thus, even the lithium test calculations took a considerable amount of computer time. Also, as it was the case in the calculations of the lowest 2D states of lithium,²³ obtaining very well converged results requires generating several thousand of ECGs in the basis set. This had been accomplished for the 2D states by using the analytical energy gradient determined with respect to the Gaussian nonlinear parameters in growing and optimizing the ECG basis set. For the Li 2F states one needs to follow a similar approach and this will be pursued in our future work. At that stage the integral code will be rewritten to explicitly take advantage, among other things, of the sparsity of the matrices involved in calculating the matrix elements.

In the first step of the testing of the code for the lowest Li 2F state the basis set was grown from a small number of ECGs first to the size of 60 functions, then increased to 100, and finally increased to 140 functions. At each of these three basis-set sizes the basis set was thoroughly variationally optimized to get the lowest possible energy. As the total energy of the system in our approach explicitly depends on the nuclear mass, we chose to perform the optimization for the major lithium isotope, ^7Li . After the 60-, 100-, and 140-ECGs basis sets were generated for the lowest 2F state of ^7Li they were used to calculate the corresponding energies of ^6Li and $^{\infty}\text{Li}$. The results are shown in Table I. In the table we also in-

cluded the results obtained for the two lowest 2D states of ^7Li . This was done to compare the convergence rates, which for the lowest 2D and 2F states should be similar, and to compare the final energies, which for the 2F state and the second lowest 2D state should be close. The energies of all states considered in the calculations are compared with the estimated accurate energy values obtained by adding the experimental energies of the states determined with respect to the ground 2S state of ^7Li to our best nonrelativistic energy of ^7Li obtained in the previous calculations.²⁵ As one can see upon examining the results in Table I, the 2F state calculations show a similar convergence rate as the calculations for the two 2D states. Also the difference between the energy obtained for the higher of the two 2D states with 140 ECGs is higher than the estimated accurate energy value for that state by a similar amount as the corresponding difference for the 2F state. These features affirm that the results and the code used to generate them are correct.

The calculated energy values for the lowest 2F state of ^7Li and ^6Li allows for determining the isotopic shift in the energy corresponding to the transition between this state and the ground 2S state. The calculations of this shift are shown in Table II. Upon examining the values presented in the

TABLE I. The convergence of the total energies (in hartrees) of the lowest 2F ($1s^24f$) state of ^7Li , ^6Li , and $^{\infty}\text{Li}$.

Basis	$1s^23d$	$1s^24d$	$1s^24f$
^7Li			
60	-7.334 497 039	-7.309 958 039	-7.310 245 752
100	-7.334 840 132	-7.310 448 107	-7.310 503 729
140	-7.334 886 705	-7.310 507 219	-7.310 543 810
Estimated ^a	-7.334 915 639	-7.310 583 488	-7.310 552 459
^6Li			
60			-7.310 146 845
100			-7.310 404 819
140			-7.310 444 899
$^{\infty}\text{Li}$			
60			-7.310 840 062
100			-7.311 098 062
140			-7.311 138 147

^aCalculated by adding the experimental transition energy of ^7Li determined with respect to the ground state and reported in Ref. 22 to the ^7Li ground-state energy of -7.477 451 930 7 hartree taken from Ref. 25.

TABLE II. The convergence of the ${}^6\text{Li}$ - ${}^7\text{Li}$ isotopic shift of the transition between the ${}^2F(1s^24f)$ state and the ${}^2S(1s^22s)$ ground state^a with the number of ECG basis functions used in the expansion of the ${}^2F(1s^24f)$ state. All values are in cm^{-1} .

No. of basis functions	Transition energy for ${}^7\text{Li}$	Transition energy for ${}^6\text{Li}$	Difference
60	36697.51	36697.00	-0.51
100	36640.90	36640.38	-0.51
140	36632.10	36631.59	-0.51
Experiment	36630.2	36629.7	
	(measured ²²)	(predicted)	

^aGround-state energies of ${}^7\text{Li}$ and ${}^6\text{Li}$ of $-7.477\,451\,930\,7$ and $-7.477\,350\,681\,2$ hartree are from Ref. 25.

table one notices that the transition energy for ${}^7\text{Li}$, for which the experimental value is known,²² converges very well to the experimental energy. The transition energy obtained with 140 ECGs of $36\,632.10\,\text{cm}^{-1}$ is only by about $2\,\text{cm}^{-1}$ off from the value obtained in the experiment of $36\,630.2$.²² Interestingly, the calculation of the isotopic shift renders the same value of $-0.51\,\text{cm}^{-1}$ regardless of the size of the basis set indicating that this value is already well converged with 60 ECGs in the basis set. Adding this shift to the experimental transition energy for ${}^7\text{Li}$ gives an estimate for the corresponding transition for ${}^6\text{Li}$ of $36\,629.7\,\text{cm}^{-1}$. Perhaps, having this estimate, an experiment can be performed to measure this transition.

VIII. SUMMARY

In the present work we presented general formulas for calculating the Hamiltonian and overlap matrix elements with all-electron explicitly correlated Gaussian functions with cubic polynomial pre-exponential multipliers. Such ECGs can be used to calculate ground and excited states of atomic systems with either one f electron, or one p and one d electron, or three p electrons and an arbitrary number of s electrons. For example, such functions can be used to calculate the ground-state energy of the nitrogen atom. The formulas have been implemented and tested for correctness. Following the tests, variational calculations of the lowest 2F state of ${}^7\text{Li}$ have been performed with basis sets of three different lengths, 60, 100, 140 functions. They rendered values, which, when subtracted from the calculated ${}^7\text{Li}$ ground-state energy, gave values of the transition energy which shows good convergence to the experimental energy.

As the Hamiltonian used in the present approach is obtained by separating out the center of mass motion from the laboratory frame Hamiltonian, the calculated energy value is

directly dependent on the nuclear mass. Thus, repeating the calculations for the ${}^6\text{Li}$ isotope allowed for estimation of the isotopic shift the transition energy and for predicting the transition energy for ${}^6\text{Li}$. The availability of this prediction may help with the future measurement of this quantity.

ACKNOWLEDGMENTS

This work has been supported in part by the National Science Foundation through the graduate research fellowship program (GRFP) awarded to Keeper L. Sharkey (Grant No. DGE1-1143953). We are grateful to the University of Arizona Center of Computing and Information Technology for the use of their computer resources.

- ¹M. Smith, M. Brodeur, T. Brunner, S. Ettenauer, A. Lapierre, R. Ringle, V. L. Ryjkov, F. Ames, P. Bricault, G. W. F. Drake, P. Delheij, D. Lunney, F. Sarazin, and J. Dilling, *Phys. Rev. Lett.* **101**, 202501 (2008).
- ²Z. C. Yan, W. Nortershauer, and G. W. F. Drake, *Phys. Rev. Lett.* **100**, 243002 (2008).
- ³G. W. F. Drake and Z. C. Yan, *Adv. Quantum Chem.* **53**, 37 (2008).
- ⁴R. El-Wazni and G. W. F. Drake, *Phys. Rev. A* **80**, 064501 (2009).
- ⁵L. M. Wang, Z. C. Yan, H. X. Qiao, and G. W. F. Drake, *Phys. Rev. A* **83**, 034503 (2011).
- ⁶L. M. Wang, Z. C. Yan, H. X. Qiao, and G. W. F. Drake, *Phys. Rev. A* **85**, 052513 (2012).
- ⁷K. Pachucki, V. A. Yerokhin, and P. C. Pastor, *Phys. Rev. A* **85**, 042517 (2012).
- ⁸M. Puchalski, D. Kedziera, and K. Pachucki, *Phys. Rev. A* **82**, 062509 (2010).
- ⁹K. Pachucki and M. Krzysztof, *Opt. Commun.* **283**, 641 (2010).
- ¹⁰M. Puchalski and K. Pachucki, *Phys. Rev. A* **79**, 032510 (2009).
- ¹¹M. Puchalski and K. Pachucki, *Phys. Rev. A* **78**, 052511 (2008).
- ¹²M. Puchalski and K. Pachucki, *Phys. Rev. A* **73**, 022503 (2006).
- ¹³K. Pachucki and J. Komasa, *J. Chem. Phys.* **125**, 204304 (2006).
- ¹⁴S. Bubin and L. Adamowicz, *Phys. Rev. A* **79**, 022501 (2009).
- ¹⁵M. Stanke, J. Komasa, D. Kędziera, S. Bubin, and L. Adamowicz, *Phys. Rev. A* **78**, 052507 (2008).
- ¹⁶M. Stanke, J. Komasa, D. Kędziera, S. Bubin, and L. Adamowicz, *Phys. Rev. A* **77**, 062509 (2008).
- ¹⁷S. Bubin and L. Adamowicz, *J. Chem. Phys.* **128**, 114107 (2008).
- ¹⁸M. Stanke, D. Kędziera, S. Bubin, and L. Adamowicz, *J. Chem. Phys.* **127**, 134107 (2007).
- ¹⁹M. Stanke, D. Kędziera, S. Bubin, and L. Adamowicz, *Phys. Rev. Lett.* **99**, 043001 (2007).
- ²⁰K. L. Sharkey, M. Pavanello, S. Bubin, and L. Adamowicz, *Phys. Rev. A* **80**, 062510 (2009).
- ²¹K. L. Sharkey, S. Bubin, and L. Adamowicz, *J. Chem. Phys.* **134**, 044120 (2011).
- ²²Yu. Ralchenko, A. E. Kramida, J. Reader, and Nist ASD Team (2010), *NIST Atomic Spectra Database* (version 4.0.0), National Institute of Standards and Technology, Gaithersburg, MD. Available online at <http://physics.nist.gov/asd>.
- ²³K. L. Sharkey, S. Bubin, and L. Adamowicz, *J. Chem. Phys.* **134**, 194114 (2011).
- ²⁴R. N. Zare, *Angular Momentum* (Wiley, New York, 1988).
- ²⁵S. Bubin, J. Komasa, M. Stanke, and L. Adamowicz, *J. Chem. Phys.* **131**, 234112 (2009).

APPENDIX D

An algorithm for non-Born-Oppenheimer quantum mechanical variational calculations of $N = 1$ rotationally excited states of diatomic molecules using all-particle explicitly correlated Gaussian functions

An algorithm for non-Born-Oppenheimer quantum mechanical variational calculations of $N = 1$ rotationally excited states of diatomic molecules using all-particle explicitly correlated Gaussian functions

Keeper L. Sharkey,¹ N. Kirnosov,² and Ludwik Adamowicz^{1,2}

¹Department of Chemistry and Biochemistry, University of Arizona, Tucson, Arizona 85721, USA

²Department of Physics, University of Arizona, Tucson, Arizona 85721, USA

(Received 25 June 2013; accepted 8 October 2013; published online 30 October 2013)

An algorithm for quantum mechanical variational calculations of bound states of diatomic molecules corresponding to the total angular momentum quantum number equal to one ($N = 1$) is derived and implemented. The approach employs all-particle explicitly correlated Gaussian function for the wave-function expansion. The algorithm is tested in the calculations of the $N = 1$, $v = 0, \dots, 22$ states of the HD^+ ion. © 2013 AIP Publishing LLC. [<http://dx.doi.org/10.1063/1.4826450>]

I. INTRODUCTION

The development and implementation of a method for extending the very accurate non-BO calculations with all-particle explicitly correlated Gaussians (ECG) to states where the diatomic molecule is excited to the first rotational state and also vibrationally excited to an arbitrary level. The development includes the derivation and implementation of the Hamiltonian matrix elements and the matrix elements of the energy gradient determined with respect to the exponential parameters of the Gaussians. Details of the derivations of the matrix elements are described and the implementation procedure is discussed. By using the described approach, it is possible to calculate bound states of diatomic molecules with an arbitrary number of σ electrons whose rotational motion is excited to the first excited level ($N = 1$ states). This is done in direct all-particle variational calculations. An important feature of the approach is that the Born-Oppenheimer (BO) approximation is not assumed at this approach, i.e., the approach is non-BO.

Explicitly correlated Gaussians are becoming increasingly more popular in various types of molecular quantum mechanical calculations.^{1,2} The application of the ECGs in this work represents a direction where these functions are used to obtain very accurate energies of bound states of small molecular systems. As the goal of such calculation is to predict the energies of the ground and excited rovibrational states to the accuracy approaching 10^{-9} - 10^{-10} hartree, extensive optimization of the Gaussian nonlinear parameters needs to be performed. In this optimization, the availability of the analytic gradient is of key importance.

The variational minimization of the total energy is much faster and more effective with the use of the energy gradient. This is why in this work we also show the derivation of the derivatives of the Hamiltonian and overlap matrix elements, which are used to generate the gradient.

II. THE HAMILTONIAN

We consider a nonrelativistic molecular system in the laboratory coordinate frame with the total number of nuclei (*nuc*)

equal N_{nuc} and the total number of electrons (*elec*) equal N_{elec} . The total number of particles in the system is: $N_{\text{tot}} = N_{\text{nuc}} + N_{\text{elec}}$. The *i*th particle in the system has mass M_i , charge Q_i , and its position in the laboratory Cartesian coordinate frame is described by vector \mathbf{R}_i . The laboratory-frame nonrelativistic Hamiltonian for the system is

$$\hat{H}_{\text{lab}} = - \sum_{i=1}^{N_{\text{tot}}} \frac{1}{2M_i} \nabla_{\mathbf{R}_i}^2 + \sum_{i=1, j>i}^{N_{\text{tot}}} \frac{Q_i Q_j}{R_{ij}}, \quad (1)$$

where $\nabla_{\mathbf{R}_i}$ is the gradient with respect to the position coordinates of the particle, \mathbf{R}_i , and R_{ij} is the distance between the (*i,j*) pair of particles: $R_{ij} = ||\mathbf{R}_j - \mathbf{R}_i||$.

The center of mass motion (or translational motion of the system as a whole) can be rigorously separated out from the internal motion of the particles in the laboratory-frame Hamiltonian (1). This separation yields two Hamiltonians: one representing the kinetic energy of the motion of the center of mass described by the following vector in the laboratory coordinate frame:

$$\mathbf{r}_0 = \frac{M_1}{M_{\text{tot}}} \mathbf{R}_1 + \frac{M_2}{M_{\text{tot}}} \mathbf{R}_2 + \dots + \frac{M_{N_{\text{tot}}}}{M_{\text{tot}}} \mathbf{R}_{N_{\text{tot}}}, \quad (2)$$

where $M_{\text{tot}} = \sum_{i=1}^{N_{\text{tot}}} M_i$ is the total mass of the system, and the second representing the internal motion of the particles, which in this work is described by the following vectors referring particles $2, \dots, N_{\text{tot}}$ are referred to particle 1 (particle 1 is assumed to be the reference particle):

$$\begin{aligned} \mathbf{r}_1 &= -\mathbf{R}_1 + \mathbf{R}_2, \\ \mathbf{r}_2 &= -\mathbf{R}_1 + \mathbf{R}_3, \\ &\vdots \\ \mathbf{r}_{n_{\text{tot}}} &= -\mathbf{R}_1 + \mathbf{R}_{N_{\text{tot}}}. \end{aligned} \quad (3)$$

Thus, the internal coordinates are: $\mathbf{r}_i = \mathbf{R}_{i+1} - \mathbf{R}_1$, $i = 1, \dots, n_{\text{tot}}$, where $n_{\text{tot}} = N_{\text{tot}} - 1$. In this work, we are concerned with bound internal states of the system, and as a result, the center-of-mass Hamiltonian can be disregarded because the system's internal stationary states do not depend on the

position of the center of mass in free space. Therefore, only the internal Hamiltonian is considered. Thus, the separation of the laboratory-frame total Hamiltonian into the center-of-mass Hamiltonian and the internal Hamiltonian is accomplished by the coordinate transformation from the laboratory coordinates, \mathbf{R}_i , to the coordinate set consisting of the \mathbf{r}_0 vector and the \mathbf{r}_i , $i = 1, \dots, n_{tot}$, vectors obtained by placing one of the nuclei (usually the heaviest) at the origin of a new, internal Cartesian coordinate system such that it becomes the reference particle for all other particles in the molecule. As the transformation alters the masses of the particles (see below), the non-reference particles can be called pseudoparticles. The distance between pseudoparticles i and j is the same as the distance between the original particles: $r_{ij} = ||\mathbf{r}_{ij}|| = ||\mathbf{r}_j - \mathbf{r}_i|| = ||\mathbf{R}_{j+1} - \mathbf{R}_{i+1}||$.

In the new coordinate frame, the internal coordinates, \mathbf{r}_i , represent the motion of the n_{tot} pseudoparticles in the central field of the charge of the reference nucleus. The pseudoparticles described by the internal Hamiltonian have the same charges as before the transformation, but their masses are now reduced masses. Denoting the mass of the reference nucleus as m_0 and its charge as q_0 , setting the pseudoelectron reduced masses to be $\mu_i = m_0 m_i / (m_0 + m_i)$ with $m_i = M_{i+1}$, and with the pseudoparticle charges equaling $q_i = Q_{i+1}$, the internal Hamiltonian is³

$$\hat{H} = -\frac{1}{2} \left(\sum_{i=1}^{n_{tot}} \frac{1}{\mu_i} \nabla_{\mathbf{r}_i}^2 + \sum_{i \neq j}^{n_{tot}} \frac{1}{m_0} \nabla'_{\mathbf{r}_i} \nabla_{\mathbf{r}_j} \right) + \sum_{i=1}^{n_{tot}} \frac{q_0 q_i}{r_i} + \sum_{i=1, j>i}^{n_{tot}} \frac{q_i q_j}{r_{ij}}. \quad (4)$$

The motions of the pseudoparticles are coupled through the mass polarization term, $\sum_{i \neq j} (1/m_0) \nabla'_{\mathbf{r}_i} \nabla_{\mathbf{r}_j}$, and through the Coulombic interactions. The Coulombic interactions are dependent on the distances between the pseudoparticles and the origin of the internal coordinate system, r_i , and on the relative distances between a pair pseudoparticles, r_{ij} . In the calculations performed in this work for the HD⁺ ion, we use the following masses: the mass of proton $M_p = 1836.15267245 m_e$ and the mass of deuteron $M_d = 3670.4829652 m_e$, where m_e is the electron mass.

The problem represented by the internal Hamiltonian (4) is “atom-like” because it describes the motion of particles in a spherically symmetric (isotropic) potential. As a result, the Hamiltonian commutes with the square of the all-particle total angular-momentum operator, N^2 , which is a sum of the electronic, L , and nuclear, R , angular momenta (or, more precisely, the total angular momenta of the pseudoparticles), $N = L + R$. Thus, the commutation relation is $[\hat{H}, \hat{N}^2] = 0$.⁵ Therefore, by expanding the total internal wave function of the system in terms of basis functions which are eigenfunctions of the square of the total angular momentum operator, states corresponding to different eigenvalues of N^2 can be separated. While in the previous works we have considered states with $N = 0$, i.e., so-called pure vibrational states,⁴ in this work we consider states with $N = 1$, i.e., the first-rotationally excited states.

III. NOTATION

Let us start with briefly explaining the notation scheme used throughout this work. The scheme is the same as the one used in our recent atomic work,⁶ but it is somewhat different from the notation used in our previous diatomic work.⁷ Here is the notation convention used in this work:

- Lower-case Greek letters, e.g., $\alpha, \beta, \chi, \gamma, \nu, \eta, \tau, \lambda$, are used to denote scalar quantities, variables, and parameters;
- **Bold** lower-case Greek letters, e.g., ξ , represent vectors in 3D space; three-component vectors;
- CAPITAL Greek letters, e.g., Λ, Ω , are used for 3×3 matrices;
- Lower-case Roman font Latin letters, e.g., x, y, z , are used as variables;
- Lower-case Latin letters, e.g., a , denote n_{tot} -component vectors;
- Lower-case Sans – Serif font Latin letters, e.g., c , are used as k -component vectors (k is the number of basis functions used in a wave function expansion);
- **Bold** lower-case Latin letters, e.g., v , denote $3n_{tot}$ -component vector. One exception is if such a letter has an index/subscript corresponding to the particle index, then this means it is a 3-component vector. For example, \mathbf{r} is a $3n$ -component vector, while \mathbf{r}_i is a 3-component vector. An index/subscript on the basis functions k and l keeps the original definition;
- Capital Latin letters, e.g., A , are used for $n \times n$ matrices;
- **Bold** CAPITAL Latin letters, e.g., \mathbf{A} or \mathbf{W} , are used for $3n \times 3n$ matrices;
- CAPITAL Roman font Latin letters, e.g., S, T, V, R , are used for scalar quantities;
- Sans – Serif font Latin letters, e.g., \mathbf{S} and H , denote $k \times k$ matrices.

Vector or matrix transposition is denoted by a prime ($'$) symbol and, finally, vertical bars around a matrix denote that it is a determinant of a matrix, while vertical bars around a vector or a scalar stand for the absolute value or the length, respectively.

IV. THE BASIS FUNCTIONS

To obtain the energy eigenvalues of Hamiltonian (4), the standard Rayleigh-Ritz variational scheme is used

$$\frac{\langle \Psi | \hat{H} | \Psi \rangle}{\langle \Psi | \Psi \rangle} \geq E_0, \quad (5)$$

where E_0 is the exact non-relativistic energy of the system. The total molecular wave function, Ψ , depends on the spatial coordinates, \mathbf{r} , of the particles and their spins, \mathbf{s} . Due to the fact that (4) is spin independent, the calculation of the Hamiltonian and overlap matrix elements is first reduced by integrating over the spin variables, leaving behind only spatially dependent integrals, which can be calculated using the spatial wave function, $\Psi(\mathbf{r})$. This wave function is approximated by

a linear combination of K basis functions, $\phi_k(\mathbf{r})$

$$\Psi(\mathbf{r}) = \sum_{k=1}^K c_k \hat{Y} \phi_k(\mathbf{r}), \quad (6)$$

where c_k is the linear variational parameter, and \hat{Y} is a permutational symmetry projection operator specific to the considered state of the system. In the calculations of HD^+ described in this work, there are no indistinguishable particles, and therefore $\hat{Y} = \hat{1}$.

The basis functions describing the n_{tot} -pseudoparticle “atomic molecule” are constructed using, as one of their components, the following rotationally invariant ECG functions:

$$\phi_k(\mathbf{r}) \equiv \phi_k = \exp[-\mathbf{r}'(A_k \otimes I_3)\mathbf{r}], \quad (7)$$

where A_k is a $n_{tot} \times n_{tot}$ symmetric matrix, \otimes is the Kronecker product symbol, and I_3 is a 3×3 identity matrix. The basis functions used in a bound-state calculation must be square integrable and this effectively imposes restrictions on the A_k matrix. The A_k matrix must be positive definite. Rather than restricting the A_k matrix elements, A_k is represented in a Cholesky factorized form as $A_k = L_k L'_k$, where L_k is a lower triangular matrix. With this representation, A_k is automatically positive definite for any real values of the L_k matrix elements.

The ECG functions, unfortunately, have a maximum when the distance between two particles is zero. However, two particles with alike charges repel and the probability of them occupying the same point in space is very small (much smaller for a pair of nuclei than for a pair of electrons^{5,8}). Therefore, the ECG functions (7) must be modified to describe the virtually zero probability of two nuclei closely approaching each other. Also, as a purpose of the molecular non-BO calculations is to describe states where the molecule is excited to vibrationally excited states which are represented by wave functions with spatial nodes in terms of the coordinates describing the internuclear distances, additional flexibility needs to be introduced in the ECGs to describe these features. To achieve this, functions (7) are multiplied by non-negative even powers of the internuclear distances. In diatomic non-BO calculations, this factor is $r_1^{m_k}$ (r_1 is the deuteron-proton distance in the case of the HD^+ molecule)

$$\phi_k^{N=0} = r_1^{m_k} \phi_k, \quad (8)$$

such that $r_1 = (x_1^2 + y_1^2 + z_1^2)^{1/2} = (\mathbf{r}' \mathbf{J}_{11} \mathbf{r})^{1/2}$, where \mathbf{J}_{11} is a square diagonal $3n_{tot} \times 3n_{tot}$ matrix, whose (1,1), (2,2), and (3,3) elements are equal to one and the remaining elements are zero, and the m_k power in our calculations is optimized in the range from zero to 250. The above functions are used for expanding the wave functions of states with rotational quantum number equal to zero ($N = 0$). For the first excited rotational states of a diatomic molecule corresponding to the rotational quantum number $N = 1$ and $N_z = 0$ (i.e., the quantum number associated with the projection of the total angular momentum on the z axis), functions (8) are multiplied by an angular factors which in terms of the Cartesian coordinate are just z_i (for convenience in this work we replace z_i by x_i , as z_i and x_i are

completely equivalent)

$$\phi_k^{N=1} = x_i \phi_k^{N=0}. \quad (9)$$

However, as the electronic excitations are much higher in terms of energy than the rotational excitations, the contributions from basis functions (9) with x_i , where $i = 2, \dots, n_{tot}$, to the rovibrational states, where the molecule is in the ground electronic state, is rotationally excited to the first excited rotational state, and is vibrationally excited to an arbitrary level, are expected to be much smaller in comparison to the most contributing basis functions with $x_i = x_1$. The numerical results obtained for HD^+ presented later in this work support this conclusion. Also, it should be mentioned that the Gaussians used in the present calculations, even though they do not explicitly include x_i , $i = 2, \dots, n$ (for HD^+ , x_1 is the x coordinate of the vector pointing from the deuteron, which is the reference particle, to the proton and x_2 is the x coordinate of the vector pointing from the deuteron to the electron), preexponential multipliers effectively include contributions of the $x_i \phi_k^{N=0}$ functions because functions $x_1 \phi_k^{N=0}$ and functions $x_i \phi_k^{N=0}$, $i = 2, \dots, n$, have non-zero overlap if the A_k matrix has non-zero off-diagonal elements. Therefore, if the contributions of the $x_i \phi_k^{N=0}$, $i = 2, \dots, n$, basis functions are small, as they expect to be for the vibrational states of the HD^+ molecule excited to the first excited rotational state, these contributions should be well described by including only $x_1 \phi_k^{N=0}$ Gaussians in the basis set. If the contributions are larger (this, for example, is expected to happen for muonic molecules), one needs to explicitly include $x_i \phi_k^{N=0}$, $i = 2, \dots, n$, Gaussians in the calculation.

Thus, in this work the derivation of the integrals and their computational implementation only concerns basis functions

$$\phi_k^{N=1} = x_1 r_1^{m_k} \exp[-\mathbf{r}'(A_k \otimes I_3)\mathbf{r}]. \quad (10)$$

V. MATRIX ELEMENTS

In describing the derivation of the Hamiltonian and overlap matrix elements, we start with the overlap derivation because it is the simplest of the integrals involved. It is also convenient to start the explanation of the $N = 1$ overlap integral with the derivation of the overlap integral for the $N = 0$ case (basis functions (8)) because it was not described in detail in Ref. 7, where the integral was first used. Also, to better understand the derivation of the matrix elements of the internal Hamiltonian and the gradient operator for the $N = 1$ case, we will describe the derivation of the $N = 2$ overlap integral because the formula for this integral will be applied in the derivation of some integrals contributing to the kinetic-energy matrix element for the $N = 1$ case. The derivation of the kinetic-energy matrix element will be shown after the derivation of the overlap integral, and it will be followed by the derivation of the potential-energy matrix element. Before we start the explanation of the derivation of the overlap integral, we recall some commonly used integrals and matrix-calculus properties relevant to the derivations of integrals involving ECGs.

A. Useful transformation properties

The following general p -dimensional Gaussian integral is the primary integral used when evaluating the Hamiltonian and overlap matrix elements:

$$\int_{-\infty}^{+\infty} \exp[-x'Xx + y'x] dx = \frac{\pi^{p/2}}{|X|^{1/2}} \exp\left[\frac{1}{4}y'X^{-1}y\right], \quad (11)$$

where x is a p -component vector of variables, X is a symmetric $p \times p$ positive-definite matrix (this ensures square integrability of the integrand), y is a p -component constant vector, and X^{-1} is the inverse of X .

Some properties of the matrix algebra are useful in the present derivations, as well as in simplifying the final integral formulas for the computational implementation and for writing an optimal computer code. Therefore, the following few equations are given as useful tools, which are used throughout this work. For a $3p$ -dimension matrix obtained as $\mathbf{X} = X \otimes I_3$ such that X is a $p \times p$ matrix and I_3 is the 3×3 identity matrix, we have the following relation between the determinants of \mathbf{X} and X :

$$|\mathbf{X}| = |X|^3. \quad (12)$$

The determinant of the inverse of X is related to the determinant of the inverse of \mathbf{X} through the following:

$$|X^{-1}| = |X|^{-1}. \quad (13)$$

The inverse of $3p$ -dimensional matrix $\mathbf{X} = X \otimes I_3$ is

$$\mathbf{X}^{-1} = X^{-1} \otimes I_3. \quad (14)$$

When X is multiplied by a constant, e.g., αX , the determinant of the product is

$$|\alpha X| = \alpha^p |X|, \quad (15)$$

where p , again, is the dimension of X .

The following operations involving traces are used to simplify integral formulas and to determine the gradient of the integrals. For the trace of a product of two square symmetric matrices, X and Y , we have the following property:

$$\text{tr}[XY] = \text{tr}[YX]. \quad (16)$$

The trace of a product of three square matrices that are not symmetric is equal to the traces of the following transpositions of the matrices:

$$\text{tr}[XYZ] = \text{tr}[Y'X'Z'] = \text{tr}[Z'Y'X']. \quad (17)$$

If X , Y , and Z are symmetric, then $X' = X$, $Y' = Y$, and $Z' = Z$ can be substituted into the above.

The following “vec” and “vech” operations are used in the derivation of the energy gradient. The first operation allows us to represent the trace of a matrix product as a vector-vector product. Assuming that X and Y may not be symmetric, we have

$$(\text{vec } X)' \text{ vec } Y = \text{tr}[X'Y]. \quad (18)$$

Since the energy derivative is taken with respect to the matrix elements of lower triangular matrix L of a basis function, it is

useful to show how to get from the equation involving $(\text{vec } L)$ an equation involving $(\text{vech } L)$

$$(\text{vec } X)' \text{ vec } L = (\text{vech } X)' \text{ vech } L. \quad (19)$$

Two other useful matrix differential properties are: first, the derivative of a determinant is

$$d|X| = |X| \text{ tr}[X^1 dX], \quad (20)$$

and, second, the derivative of the trace of a matrix is

$$d \text{tr}[X] = \text{tr}[dX]. \quad (21)$$

Other useful transformations we refer to in the derivations are the following mixed-product property:

$$(W \otimes X)(Y \otimes Z) = WY \otimes XZ, \quad (22)$$

and the Woodbury matrix identity

$$(A + XYZ)^{-1} = A^{-1} - A^{-1}X(Y^{-1} + ZA^{-1}X)^{-1}ZA^{-1}. \quad (23)$$

The following is a usefully vector-matrix (x - A) rearrangement involving trace:

$$|xAx| = \text{tr}[Ax^2]. \quad (24)$$

And finally, the following separation property concerning the determinant of a sum of two matrices is also useful:

$$|X + Y| = |X||I_p + YX^{-1}| \quad (25)$$

and

$$|I_p + X| = 1 + \text{tr}[X]. \quad (26)$$

B. Overlap matrix elements and the 3D-Dirac delta function

1. Overlap integral and its gradient for $N=0$ states

The overlap between two basis functions (8) for the $N = 0$ states of a diatomic molecule with σ electrons is

$$\langle \phi_k^{N=0} | \phi_l^{N=0} \rangle = \langle \phi_k | r_1^{m_k+m_l} | \phi_l \rangle. \quad (27)$$

The presence of the $r_1^{m_k+m_l}$ prefactor of the multiplied basis functions, which depends on the distance between the central nucleus and the pseudonucleus, requires that the following general elemental integral is considered:

$$\langle \phi_k | r_1^\nu | \phi_l \rangle, \quad \nu > -3. \quad (28)$$

This integral allows for calculating the overlap matrix element by setting $\nu = (m_k + m_l)$. The condition that $\nu > -3$, which is related to the integration over the Gaussian variables, will be clarified in the derivation. To integrate (28), we first need to evaluate the following auxiliary integral that involves a three-dimensional Dirac delta function:

$$\begin{aligned} & \delta(a_1 \mathbf{r}_1 + a_2 \mathbf{r}_2 + \dots + a_n \mathbf{r}_n - \xi) \\ & \equiv \delta((a \otimes I_3)' \mathbf{r} - \xi) \\ & = \lim_{\beta \rightarrow \infty} \left(\frac{\beta}{\pi} \right)^{3/2} \exp[-\beta ((a \otimes I_3)' \mathbf{r} - \xi)^2], \end{aligned} \quad (29)$$

where a is a real n -component vector, ξ is a real three-dimensional parameter, and β is a parameter. When we set $a = e^1$, where e^1 is a n -component vector whose 1st element is 1 and all others are zero, then (28) can be expressed as

$$\langle \phi_k | r_1^\nu | \phi_l \rangle = \int_{-\infty}^{+\infty} |\xi|^\nu \langle \phi_k | \delta((a \otimes I_3)' \mathbf{r} - \xi) | \phi_l \rangle d\xi. \quad (30)$$

It should be noted that integrals involving delta function (29) with different choices of vector a are useful in evaluating matrix elements for many other important quantities. For this reason, even though we are only concerned here with the evaluation of the overlap matrix elements, we will assume that the a vector can have a general form when deriving integral (31). Now using (29) in (30) the following is obtained:

$$\begin{aligned} & \langle \phi_k | \delta((a \otimes I_3)' \mathbf{r} - \xi) | \phi_l \rangle \\ &= \lim_{\beta \rightarrow \infty} \left(\frac{\beta}{\pi} \right)^{3/2} \langle \phi_k | \exp[-\beta \mathbf{r}'(aa' \otimes I_3) \mathbf{r} \\ & \quad + 2\beta ((a \otimes I_3) \xi)' \mathbf{r} - \beta \xi' \xi] | \phi_l \rangle, \end{aligned} \quad (31)$$

of which integration over the \mathbf{r} variables is straightforward using (11). Substituting \mathbf{a} for $a \otimes I_3$ and $\mathbf{a}\mathbf{a}'$ for $aa' \otimes I_3$, (31)

becomes

$$\begin{aligned} & \langle \phi_k | \exp[-\beta \mathbf{r}' \mathbf{a} \mathbf{a}' \mathbf{r} + 2\beta (\mathbf{a} \xi)' \mathbf{r} - \beta \xi^2] | \phi_l \rangle \\ &= \pi^{3n/2} |\mathbf{A}_{kl} + \beta \mathbf{a} \mathbf{a}'|^{-1/2} \\ & \quad \times \exp \left[\frac{1}{4} (2\beta (\mathbf{a} \xi)' (\mathbf{A}_{kl} + \beta \mathbf{a} \mathbf{a}')^{-1} (2\beta (\mathbf{a} \xi))) \right] \exp[-\beta \xi' \xi]. \end{aligned} \quad (32)$$

In order to find the limit expression in terms of β of the above equation, let us suppose the limits of a function of x , $f(x)$, and another function, $g(x)$, at $x \rightarrow \infty$ exist. Then the limit of the product of $f(x)$ and $g(x)$ also exists

$$\lim_{x \rightarrow \infty} f(x) g(x) = \lim_{x \rightarrow \infty} f(x) \lim_{x \rightarrow \infty} g(x). \quad (33)$$

Therefore, taking the limits of the determinant and the exponent of (32) can be done independently. First, we will find the limit of the determinant function and then the limit of the exponential function.

When determining the limit (for either the determinant or the exponential term), the necessary transformations needed are (22) and (23) followed by a Maclaurin series expansion in terms of β . Remembering the $\beta^{3/2}$ factor of (31) and using (13), the steps of finding the limit of the determinant are as follows:

$$\begin{aligned} \lim_{\beta \rightarrow \infty} \beta^{3/2} |\mathbf{A}_{kl} + \beta \mathbf{a} \mathbf{a}'|^{-1/2} &= \lim_{\beta \rightarrow \infty} \beta^{3/2} \left| \mathbf{A}_{kl}^{-1} - \mathbf{A}_{kl}^{-1} \mathbf{a} \left[\frac{1}{\beta} I_{3n} + \mathbf{a}' \mathbf{A}_{kl}^{-1} \mathbf{a} \right] \mathbf{a}' \mathbf{A}_{kl}^{-1} \right|^{1/2} \\ &= \lim_{\beta \rightarrow \infty} \beta^{3/2} \left| \mathbf{A}_{kl}^{-1} - \mathbf{A}_{kl}^{-1} \mathbf{a} \left[(\mathbf{a}' \mathbf{A}_{kl}^{-1} \mathbf{a})^{-1} - \frac{1}{\beta} (\mathbf{a}' \mathbf{A}_{kl}^{-1} \mathbf{a})^{-2} \right] \mathbf{a}' \mathbf{A}_{kl}^{-1} \right|^{1/2}, \end{aligned} \quad (34)$$

where we only use the zero- and first-order terms of the Maclaurin expansion. Now using the (25) form of Sylvester's theorem, the above becomes

$$\begin{aligned} \lim_{\beta \rightarrow \infty} \beta^{3/2} |\mathbf{A}_{kl} + \beta \mathbf{a} \mathbf{a}'|^{-1/2} &= \lim_{\beta \rightarrow \infty} \beta^{3/2} \left| \mathbf{A}_{kl}^{-1} \right|^{1/2} \left| I_{3n_{tot}} - \mathbf{a} \left[(\mathbf{a}' \mathbf{A}_{kl}^{-1} \mathbf{a})^{-1} - \frac{1}{\beta} (\mathbf{a}' \mathbf{A}_{kl}^{-1} \mathbf{a})^{-2} \right] \mathbf{a}' \mathbf{A}_{kl}^{-1} \right|^{1/2} \\ &= \lim_{\beta \rightarrow \infty} \beta^{3/2} \left| \mathbf{A}_{kl}^{-1} \right|^{1/2} \left| I_{3n_{tot}} - \mathbf{a} (\mathbf{a}' \mathbf{A}_{kl}^{-1} \mathbf{a})^{-1} \mathbf{a}' \mathbf{A}_{kl}^{-1} + \frac{1}{\beta} \mathbf{a} (\mathbf{a}' \mathbf{A}_{kl}^{-1} \mathbf{a})^{-2} \mathbf{a}' \mathbf{A}_{kl}^{-1} \right|^{1/2}. \end{aligned} \quad (35)$$

In the second line of the above, the identity matrix, $I_{3n_{tot}}$, cancels out the series of matrices with the minus sign and the only surviving terms are

$$\lim_{\beta \rightarrow \infty} \beta^{3/2} |\mathbf{A}_{kl} + \beta (aa' \otimes I_3)|^{-1/2} = \lim_{\beta \rightarrow \infty} \beta^{3/2} \left| \mathbf{A}_{kl}^{-1} \right|^{1/2} \left| \frac{1}{\beta} (\mathbf{a}' \mathbf{A}_{kl}^{-1} \mathbf{a})^{-1} \right|^{1/2}, \quad (36)$$

where $1/\beta$ can be factored out of the determinant using (15). The final result is then

$$\begin{aligned} \lim_{\beta \rightarrow \infty} \beta^{3/2} |\mathbf{A}_{kl} + \beta (aa' \otimes I_3)|^{-1/2} &= \lim_{\beta \rightarrow \infty} \beta^{3/2} |\mathbf{A}_{kl}^{-1}|^{1/2} \left(\frac{1}{\beta} \right)^{3/2} \lambda^{-3/2} \\ &= |A_{kl}|^{-3/2} \lambda^{-3/2}, \end{aligned} \quad (37)$$

where (12) and (24) are used to simplify the final formula, and $\lambda = \text{tr}[A_{kl}^{-1} aa']$.

Next, the limit of the exponential term as β approaches infinity is obtained in a very similar fashion except we now use the second-order term in the expansion

$$\begin{aligned} \lim_{\beta \rightarrow \infty} \exp[\beta^2 (\mathbf{a}\xi)'(\mathbf{A}_{kl} + \beta\mathbf{a}\mathbf{a}')^{-1}(\mathbf{a}\xi) - \beta\xi'\xi] &= \lim_{\beta \rightarrow \infty} \exp[\beta^2 \xi' \mathbf{a}' \mathbf{A}_{kl}^{-1} \mathbf{a} \xi - \beta^2 \xi' \mathbf{a}' \mathbf{A}_{kl}^{-1} \mathbf{a} (\mathbf{a}' \mathbf{A}_{kl}^{-1} \mathbf{a})^{-1} \mathbf{a}' \mathbf{A}_{kl}^{-1} \mathbf{a} \xi - \beta \xi' \xi \\ &\quad + \beta^2 \xi' \mathbf{a}' \frac{1}{\beta} (\mathbf{a}' \mathbf{A}_{kl}^{-1} \mathbf{a})^{-2} \mathbf{a}' \mathbf{A}_{kl}^{-1} \mathbf{a} \xi - \beta^2 \xi' \mathbf{a}' \frac{1}{\beta^2} (\mathbf{a}' \mathbf{A}_{kl}^{-1} \mathbf{a})^{-3} \mathbf{a}' \mathbf{A}_{kl}^{-1} \mathbf{a} \xi] \\ &= \exp[-\xi' (\mathbf{a}' \mathbf{A}_{kl}^{-1} \mathbf{a})^{-1} \xi] = \exp[-\xi' \Lambda^{-1} \xi] = \exp[-\lambda^{-1} \xi' \xi], \end{aligned} \quad (38)$$

where $\Lambda = \mathbf{a}' \mathbf{A}_{kl}^{-1} \mathbf{a}$. This concludes finding the limit for β approaching infinity and (31) becomes

$$\begin{aligned} \langle \phi_k | \delta((a \otimes I_3)' \mathbf{r} - \xi) | \phi_l \rangle \\ = \pi^{3/2(n-1)} |A_{kl}|^{-3/2} \lambda^{-3/2} \exp[-\lambda^{-1} \xi' \xi]. \end{aligned} \quad (39)$$

By plugging the above back into Eq. (30), we are left with integration over ξ . The following 3D integral was determined in Ref. 6

$$\int_{-\infty}^{+\infty} |\xi|^\nu \exp[-\lambda^{-1} \xi^2] d\xi = 2\pi \Gamma\left(\frac{3+\nu}{2}\right) \lambda^{(3+\nu)/2}; \nu > -3, \quad (40)$$

and is applied to (39) after which we obtain

$$\begin{aligned} \langle \phi_k | r_1^\nu | \phi_l \rangle &= \pi^{3/2(n-1)} |A_{kl}|^{-3/2} \lambda^{-3/2} \int_{-\infty}^{+\infty} |\xi|^\nu \exp[-\lambda^{-1} \xi' \xi] d\xi \\ &= \frac{2}{\sqrt{\pi}} \pi^{3n/2} \Gamma\left(\frac{3+\nu}{2}\right) |A_{kl}|^{-3/2} \lambda^{\nu/2} \\ &= \frac{2}{\sqrt{\pi}} \Gamma\left(\frac{3+\nu}{2}\right) \langle \phi_k | \phi_l \rangle \lambda^{\nu/2}, \end{aligned} \quad (41)$$

where $\langle \phi_k | \phi_l \rangle$ is the overlap between two functions (7) which is

$$\langle \phi_k | \phi_l \rangle = \pi^{3n/2} |A_{kl}|^{-3/2}, \quad (42)$$

and $\lambda = \text{tr}[A_{kl}(aa')]$. To finalize the derivation of the $N = 0$ overlap formula, the following needs to be substituted in the above: $\nu = m_k + m_l$ and $a = e^1$ which leads to $\lambda = \text{tr}[A_{kl}^{-1} J_{11}] = (A_{kl}^{-1})_{11} = \alpha$. Thus, the final formula for the $N = 0$ overlap integral becomes

$$\begin{aligned} \langle \phi_k^{N=0} | \phi_l^{N=0} \rangle &= \langle \phi_k | r_1^{m_k+m_l} | \phi_l \rangle \\ &= \frac{2}{\sqrt{\pi}} \Gamma\left(\frac{3+m_k+m_l}{2}\right) \langle \phi_k | \phi_l \rangle \alpha^{(m_k+m_l)/2}, \end{aligned} \quad (43)$$

which was the equation presented in Ref. 7. As mentioned previously, the above-shown derivation was not explained in detail in that paper.

The method used to determine the $N = 0$ overlap integral will be now used for deriving the $N = 1$ and $N = 2$ overlap integrals. Again, we are also evaluating the overlap integral for the $N = 2$ states because the formula for this integral will be used in the derivation of the $N = 1$ kinetic-energy integral.

In the previous diatomic calculations, we found it helpful to use normalized ECGs in evaluating the integrals, be-

cause the range of values of the Hamiltonian and overlap matrix elements determined over normalized functions is much narrower than the range of values for unnormalized integrals. Thus, the normalization of the integrals significantly lowers the numerical noise in the calculations. So, to keep consistent with previous works, we also normalize the integrals in this work. To normalize the overlap integral, the following two integrals are needed:

$$\begin{aligned} \langle \phi_k^{N=0} | \phi_k^{N=0} \rangle &= \langle \phi_k | r_1^{2m_k} | \phi_k \rangle \\ &= \frac{2}{\sqrt{\pi}} \Gamma\left(\frac{3+2m_k}{2}\right) \langle \phi_k | \phi_k \rangle 2^{-m_k} (A_k^{-1})_{11}^{m_k}, \\ \langle \phi_l^{N=0} | \phi_l^{N=0} \rangle &= \langle \phi_l | r_1^{2m_l} | \phi_l \rangle \\ &= \frac{2}{\sqrt{\pi}} \Gamma\left(\frac{3+2m_l}{2}\right) \langle \phi_l | \phi_l \rangle 2^{-m_l} (A_l^{-1})_{11}^{m_l}. \end{aligned} \quad (44)$$

With this and some simplifications, the normalized overlap integral becomes

$$\begin{aligned} S_{kl}^{N=0} &= \frac{\langle \phi_k^{N=0} | \phi_l^{N=0} \rangle}{(\langle \phi_k^{N=0} | \phi_k^{N=0} \rangle \langle \phi_l^{N=0} | \phi_l^{N=0} \rangle)^{1/2}} \\ &= \gamma_1(m_k, m_l) S_{kl} \left[\left(\frac{\alpha}{(A_k^{-1})_{11}} \right)^{m_k} \left(\frac{\alpha}{(A_l^{-1})_{11}} \right)^{m_l} \right]^{1/2}, \end{aligned} \quad (45)$$

where γ_1 is a function of m_k and m_l equal to

$$\gamma_1(m_k, m_l) = \frac{2^{(m_k+m_l)/2} \Gamma\left(\frac{3+m_k+m_l}{2}\right)}{[\Gamma(m_k + \frac{3}{2}) \Gamma(m_l + \frac{3}{2})]^{1/2}}. \quad (46)$$

To effectively minimize the energy, the gradient with respect to the elements of $(\text{vech } L_k)'$ and $(\text{vech } L_l)'$ are needed. The calculation of the energy gradient involves evaluation of the derivatives of the Hamiltonian and overlap integrals with respect to the $(\text{vech } L_k)'$ and $(\text{vech } L_l)'$ elements. To determine the derivatives of the overlap integral, Eqs. (16)–(21) are used. The formulas for the overall derivatives are

$$\begin{aligned} \frac{\partial S_{kl}^{N=0}}{\partial (\text{vech } L_k)'} &= \frac{3}{2} S_{kl}^{N=0} \text{vech}[(L_k^{-1})' - 2A_{kl}^{-1}L_k]' \\ &\quad + m_k S_{kl}^{N=0} (A_k^{-1})_{11}^{-1} \text{vech}[A_k^{-1} J_{11} A_k^{-1} L_k]' \\ &\quad - (m_k + m_l) S_{kl}^{N=0} \alpha^{-1} \text{vech}[A_{kl}^{-1} J_{11} A_{kl}^{-1} L_k]', \end{aligned} \quad (47)$$

and

$$\begin{aligned} \frac{\partial S_{kl}^{N=0}}{\partial (\text{vech } L_l)'} &= \frac{3}{2} S_{kl}^{N=0} \text{vech} [(L_l^{-1})' - 2A_{kl}^{-1}L_l]' \\ &\quad + m_l S_{kl}^{N=0} (A_l^{-1})_{11}^{-1} \text{vech} [A_l^{-1} J_{11} A_l^{-1} L_l]' \\ &\quad - (m_k + m_l) S_{kl}^{N=0} \alpha^{-1} \text{vech} [A_{kl}^{-1} J_{11} A_{kl}^{-1} L_l]'. \end{aligned} \quad (48)$$

2. Overlap integral and its gradient for N=1 states

The overlap integral between two N = 1 basis functions (10) is determined using partial differentiation of a function where the prefactor x_1^2 is placed in the exponent of an exponential function

$$\begin{aligned} \langle \phi_k^{N=1} | \phi_l^{N=1} \rangle &= \langle \phi_k | x_1^2 r_1^{m_k+m_l} | \phi_l \rangle = \langle \phi_k | x_1^2 r_1^\nu | \phi_l \rangle \\ &= \frac{\partial}{\partial \nu_k} \frac{\partial}{\partial \nu_l} \langle \phi_k | r_1^{m_k+m_l} \exp [\mathbf{r} (\nu_k \mathbf{v}_k + \nu_l \mathbf{v}_l)'] | \phi_l \rangle \Big|_{\nu_k=\nu_l=0} \\ &= -\frac{\partial}{\partial \omega_{kl}} \langle \phi_k | r_1^{m_k+m_l} \exp [-\mathbf{r}' (\omega_{kl} \mathbf{W}_{kl}^{N=1}) \mathbf{r}] | \phi_l \rangle \Big|_{\omega_{kl}=0}, \end{aligned} \quad (49)$$

where \mathbf{v}_k and \mathbf{v}_l are n_{tot} -element vectors with one in the first element and zeros everywhere else, $\mathbf{W}_{kl}^{N=1}$ is a $3n_{tot} \times 3n_{tot}$ matrix with one as the (1,1) element and zeros everywhere else, and ν_k , ν_l , and ω_{kl} are parameters. This is the technique described in Ref. 9. Now using the Dirac delta function (29) to approximate $\nu_1^{m_k+m_l}$, as described in Sec. V B 1, it is an easy exercise to show that the integration over \mathbf{r} and taking the limit as β approaches infinity can be done in the same way as it was done there. Therefore, we will begin the derivation at (39) with the only modification being that $A_{kl} \rightarrow \mathbf{G}_{kl} = \mathbf{A}_{kl} + \omega_{kl} \mathbf{W}_{kl}^{N=1}$, which changes the definition of $\lambda^{-3/2}$ in the determinant to $\text{tr} [\mathbf{G}_{kl}^{-1} \mathbf{a} \mathbf{a}']^{-1/2} = |\mathbf{a}' \mathbf{G}_{kl}^{-1} \mathbf{a}|^{-1/2} = |\Lambda_{kl}|^{-1/2}$ and changes the definition of λ^{-1} in the exponent to $(\mathbf{a}' \mathbf{G}_{kl}^{-1} \mathbf{a})^{-1} = \Lambda_{kl}^{-1}$. Thus, we have

$$\begin{aligned} \langle \phi_k | x_1^2 r_1^\nu | \phi_l \rangle &= \langle \phi_k | x_1^2 \delta((a \otimes I_3)' \mathbf{r} - \xi) | \phi_l \rangle \\ &= -\frac{\partial}{\partial \omega_{kl}} \frac{\pi^{3n/2}}{\pi^{3/2}} |\mathbf{G}_{kl}|^{-1/2} |\Lambda|^{-1/2} \\ &\quad \times \int_{-\infty}^{+\infty} |\xi|^\nu \exp [-\xi' \Lambda_{kl}^{-1} \xi] \Big|_{\omega_{kl}=0} d\xi. \end{aligned} \quad (50)$$

Applying the derivative operator, the above becomes

$$\begin{aligned} \langle \phi_k | x_1^2 r_1^\nu | \phi_l \rangle &= \frac{\pi^{3n/2}}{\pi^{3/2}} |\Lambda_{kl}|^{-3/2} \lambda^{-3/2} \int_{-\infty}^{+\infty} |\xi|^\nu d\xi \exp[-\lambda^{-1} \xi' \xi] \\ &\quad \times \left(\frac{1}{2} \eta_{kl}^{N=1} - \frac{1}{2} \lambda^{-1} \text{tr} [\mathbf{A}_{kl}^{-1} \mathbf{W}_{kl}^{N=1} \mathbf{A}_{kl}^{-1} \mathbf{a} \mathbf{a}'] + \lambda^{-2} \xi' \mathbf{a}' \mathbf{A}_{kl}^{-1} \mathbf{W}_{kl}^{N=1} \mathbf{A}_{kl}^{-1} \mathbf{a} \xi \right), \end{aligned} \quad (51)$$

where $\eta_{kl}^{N=1} = \text{tr} [\mathbf{A}_{kl}^{-1} \mathbf{W}_{kl}^{N=1}]$ and λ recovers its original definition. Now both (40) and

$$\int_{-\infty}^{+\infty} |\xi|^\nu (\xi' \Omega^{(1)} \xi) \exp[-\lambda^{-1} \xi^2] d\xi = \frac{2\pi}{3} \Gamma \left(\frac{5+\nu}{2} \right) \lambda^{(5+\nu)/2} \text{tr} [\Omega^{(1)}]; \nu > -5, \quad (52)$$

which is a formula determined in Ref. 10 with $\Omega^{(1)}$ being a 3×3 symmetric matrix, can be applied to (51) yielding the following equation:

$$\begin{aligned} \langle \phi_k | x_1^2 r_1^\nu | \phi_l \rangle &= \frac{2}{\sqrt{\pi}} \Gamma \left(\frac{3+\nu}{2} \right) \langle \phi_k | \phi_l \rangle \lambda^{\nu/2} \\ &\quad \times \left(\frac{1}{2} \eta_{kl}^{N=1} - \frac{1}{2} \lambda^{-1} \text{tr} [\mathbf{A}_{kl}^{-1} \mathbf{W}_{kl}^{N=1} \mathbf{A}_{kl}^{-1} \mathbf{a} \mathbf{a}'] + \left(\frac{3+\nu}{2 \times 3} \right) \lambda \lambda^{-2} \text{tr} [\mathbf{A}_{kl}^{-1} \mathbf{W}_{kl}^{N=1} \mathbf{A}_{kl}^{-1} \mathbf{a} \mathbf{a}'] \right). \end{aligned} \quad (53)$$

Plugging in $\mathbf{a} = \mathbf{e}^1$ and $\nu = m_k + m_l$ allows for simplification of the terms in the above such that $\lambda \rightarrow \alpha$, $\eta_{kl} \rightarrow \alpha$, and $\text{tr} [\mathbf{A}_{kl}^{-1} \mathbf{W}_{kl}^{N=1} \mathbf{A}_{kl}^{-1} \mathbf{a} \mathbf{a}'] \rightarrow \alpha^2$, and the final formula for the overlap integral for $N = 1$ states is

$$\begin{aligned} \langle \phi_k^{N=1} | \phi_l^{N=1} \rangle &= \frac{2}{\sqrt{\pi}} \Gamma \left(\frac{3+m_k+m_l}{2} \right) \langle \phi_k | \phi_l \rangle \alpha^{(m_k+m_l)/2} \left(\frac{1}{2} \alpha - \frac{1}{2} \alpha^{-1} \alpha^2 + \left(\frac{3+m_k+m_l}{6} \right) \alpha \alpha^{-2} \alpha^2 \right) \\ &= \left(\frac{3+m_k+m_l}{6} \right) \langle \phi_k^{N=0} | \phi_l^{N=0} \rangle \alpha. \end{aligned} \quad (54)$$

To normalize this integral, the following two integrals are needed:

$$\langle \phi_k^{N=1} | \phi_k^{N=1} \rangle = \left(\frac{3 + 2 m_k}{6} \right) \langle \phi_k^{N=0} | \phi_k^{N=0} \rangle 2^{-1} \alpha, \quad (55)$$

and

$$\langle \phi_l^{N=1} | \phi_l^{N=1} \rangle = \left(\frac{3 + 2 m_l}{6} \right) \langle \phi_l^{N=0} | \phi_l^{N=0} \rangle 2^{-1} \alpha. \quad (56)$$

With that we have

$$\begin{aligned} S_{kl}^{N=1} &= \frac{\langle \phi_k^{N=1} | \phi_l^{N=1} \rangle}{(\langle \phi_k^{N=1} | \phi_k^{N=1} \rangle \langle \phi_l^{N=1} | \phi_l^{N=1} \rangle)^{1/2}} \\ &= 2 \gamma_{N=1}(m_k, m_l) \gamma_1(m_k, m_l) S_{kl} \\ &\times \left[\left(\frac{\alpha}{(A_k^{-1})_{11}} \right)^{m_k+1} \left(\frac{\alpha}{(A_l^{-1})_{11}} \right)^{m_l+1} \right]^{1/2}, \end{aligned} \quad (57)$$

where $\gamma_{N=1}$ is the following function of m_k and m_l :

$$\gamma_{N=1}(m_k, m_l) = \left(\frac{3 + m_k + m_l}{(9 + 6(m_k + m_l) + 4 m_k m_l)^{1/2}} \right). \quad (58)$$

The corresponding formulas for the gradient are

$$\begin{aligned} \frac{\partial S_{kl}^{N=1}}{\partial (\text{vech } L_k)'} &= S_{kl}^{N=1} \left\{ \frac{3}{2} \text{vech} [(L_k^{-1})' - 2A_{kl}^{-1} L_k]' \right. \\ &+ (m_k + 1) (A_k^{-1})_{11}^{-1} \text{vech} [A_k^{-1} J_{11} A_k^{-1} L_k]' \\ &\left. - (m_k + m_l + 2) \alpha^{-1} \text{vech} [A_{kl}^{-1} J_{11} A_{kl}^{-1} L_k]' \right\}, \end{aligned} \quad (59)$$

and

$$\begin{aligned} \frac{\partial S_{kl}^{N=1}}{\partial (\text{vech } L_l)'} &= S_{kl}^{N=1} \left\{ \frac{3}{2} \text{vech} [(L_l^{-1})' - 2A_{kl}^{-1} L_l]' \right. \\ &+ (m_l + 1) (A_l^{-1})_{11}^{-1} \text{vech} [A_l^{-1} J_{11} A_l^{-1} L_l]' \\ &\left. - (m_k + m_l + 2) \alpha^{-1} \text{vech} [A_{kl}^{-1} J_{11} A_{kl}^{-1} L_l]' \right\}. \end{aligned} \quad (60)$$

3. Overlap integral and its gradient for N=2 states

The particular ($N = 2$)-type basis function, which will be considered here has the preexponential factor equal to $(x_1^2 + y_1^2 - 2z_1^2)^2$. The overlap integral between two $N = 2$ functions of this type is determined using partial differentiation of a function where the prefactor $(x_1^2 + y_1^2 - 2z_1^2)^2$ is put into the exponent of an exponential function

$$\begin{aligned} \langle \phi_k^{N=2} | \phi_l^{N=2} \rangle &= \langle \phi_k | (x_1^2 + y_1^2 - 2z_1^2)^2 r_1^{m_k+m_l} | \phi_l \rangle = \langle \phi_k | (x_1^2 + y_1^2 - 2z_1^2)^2 r_1^v | \phi_l \rangle \\ &= \frac{\partial}{\partial \omega_k} \frac{\partial}{\partial \omega_l} \langle \phi_k | r_1^{m_k+m_l} \exp [-\mathbf{r}' (\omega_k \mathbf{W}_k^{N=2} + \omega_l \mathbf{W}_l^{N=2}) \mathbf{r}] | \phi_l \rangle \Big|_{\omega_k=\omega_l=0} \end{aligned} \quad (61)$$

using the method described in Ref. 10. Using again the Dirac delta function (29) to represent $r_1^{m_k+m_l}$, as it was done in Sec. V B 1, integrating over \mathbf{r} , and taking the limit as β approaches infinity is now done analogically as it was done before.

Thus, we again begin the derivation at (39) with the only modification being that $A_{kl} \rightarrow \mathbf{G}_{kl} = \mathbf{A}_{kl} + \omega_k \mathbf{W}_k^{N=2} + \omega_l \mathbf{W}_l^{N=2}$ which changes the definition of $\lambda^{-3/2}$ in the determinant to $\text{tr} [\mathbf{G}_{kl}^{-1} \mathbf{a} \mathbf{a}']^{-1/2} = |\mathbf{a}' \mathbf{G}_{kl}^{-1} \mathbf{a}|^{-1/2} = |\Lambda_{kl}|^{-1/2}$ and changes the definition of λ^{-1} in the exponent to $(\mathbf{a}' \mathbf{G}_{kl}^{-1} \mathbf{a})^{-1} = \Lambda_{kl}^{-1}$. What follows is

$$\begin{aligned} \langle \phi_k | (x_1^2 + y_1^2 - 2z_1^2)^2 r_1^v | \phi_l \rangle &= \langle \phi_k | (x_1^2 + y_1^2 - 2z_1^2)^2 \delta ((a \otimes I_3)' \mathbf{r} - \boldsymbol{\xi}) | \phi_l \rangle \\ &= \frac{\partial}{\partial \omega_k} \frac{\partial}{\partial \omega_l} \frac{\pi^{3n/2}}{\pi^{3/2}} |\mathbf{G}_{kl}|^{-1/2} |\Lambda_{kl}|^{-1/2} \int_{-\infty}^{+\infty} |\boldsymbol{\xi}|^v \exp [-\boldsymbol{\xi}' \Lambda_{kl}^{-1} \boldsymbol{\xi}] \Big|_{\omega_k=\omega_l=0} d\boldsymbol{\xi}. \end{aligned} \quad (62)$$

Now applying both derivatives, the above becomes

$$\begin{aligned}
\langle \phi_k | (x_1^2 + y_1^2 - 2z_1^2)^2 r_1^\nu | \phi_l \rangle &= \frac{\pi^{3n/2}}{\pi^{3/2}} |A_{kl}|^{-3/2} \lambda^{-3/2} \int_{-\infty}^{+\infty} |\xi|^\nu d\xi \exp[-\lambda^{-1}\xi'\xi] \\
&\times \left\{ \left(\frac{1}{2} \eta_k^{N=2} - \frac{1}{2} \lambda^{-1} \text{tr} [A_{kl}^{-1} W_k^{N=2} A_{kl}^{-1} \mathbf{a} \mathbf{a}'] + \lambda^{-2} \xi' \mathbf{a}' A_{kl}^{-1} W_k^{N=2} A_{kl}^{-1} \mathbf{a} \xi \right) \right. \\
&\times \left(\frac{1}{2} \eta_l^{N=2} - \frac{1}{2} \lambda^{-1} \text{tr} [A_{kl}^{-1} W_l^{N=2} A_{kl}^{-1} \mathbf{a} \mathbf{a}'] + \lambda^{-2} \xi' \mathbf{a}' A_{kl}^{-1} W_l^{N=2} A_{kl}^{-1} \mathbf{a} \xi \right) \\
&+ \frac{1}{2} \eta_{k,l}^{N=2} + \frac{1}{2} \lambda^{-2} \text{tr} [A_{kl}^{-1} W_k^{N=2} A_{kl}^{-1} \mathbf{a} \mathbf{a}' A_{kl}^{-1} W_l^{N=2} A_{kl}^{-1} \mathbf{a} \mathbf{a}'] \\
&- \frac{1}{2} \lambda^{-1} (\text{tr} [A_{kl}^{-1} W_k^{N=2} A_{kl}^{-1} W_l^{N=2} A_{kl}^{-1} \mathbf{a} \mathbf{a}'] + \text{tr} [A_{kl}^{-1} W_l^{N=2} A_{kl}^{-1} W_k^{N=2} A_{kl}^{-1} \mathbf{a} \mathbf{a}']) \\
&+ \lambda^{-2} (\xi' \mathbf{a}' A_{kl}^{-1} W_k^{N=2} A_{kl}^{-1} W_l^{N=2} A_{kl}^{-1} \mathbf{a} \xi + \xi' \mathbf{a}' A_{kl}^{-1} W_l^{N=2} A_{kl}^{-1} W_k^{N=2} A_{kl}^{-1} \mathbf{a} \xi) \\
&- \lambda^{-3} (\xi' \mathbf{a}' A_{kl}^{-1} W_k^{N=2} A_{kl}^{-1} \mathbf{a} \mathbf{a}' A_{kl}^{-1} W_l^{N=2} A_{kl}^{-1} \mathbf{a} \xi \\
&\left. + \xi' \mathbf{a}' A_{kl}^{-1} W_l^{N=2} A_{kl}^{-1} \mathbf{a} \mathbf{a}' A_{kl}^{-1} W_k^{N=2} A_{kl}^{-1} \mathbf{a} \xi \right\}, \quad (63)
\end{aligned}$$

where $\eta_k^{N=2} = \text{tr}[A_{kl}^{-1} W_k^{N=2}]$, $\eta_l^{N=2} = \text{tr}[A_{kl}^{-1} W_l^{N=2}]$, $\eta_{k,l}^{N=2} = \text{tr}[A_{kl}^{-1} W_k^{N=2} A_{kl}^{-1} W_l^{N=2}]$, and λ reverses to its original definition. Now (40), (52), and

$$\begin{aligned}
&\int_{-\infty}^{+\infty} |\xi|^\nu (\xi' \Omega^{(2)} \xi) (\xi' \Omega^{(3)} \xi) \exp[-\lambda^{-1}\xi^2] d\xi \\
&= \frac{2\pi}{3 \times 5} \Gamma\left(\frac{7+\nu}{2}\right) \lambda^{(7+\nu)/2} \{2 \text{tr}[\Omega^{(2)} \Omega^{(3)}] + \text{tr}[\Omega^{(2)}] \text{tr}[\Omega^{(3)}]\}; \nu > -7, \quad (64)
\end{aligned}$$

which is a formula determined in Ref. 11, where $\Omega^{(2)}$ and $\Omega^{(3)}$ are 3×3 symmetric matrices, are applied to (63) yielding

$$\begin{aligned}
\langle \phi_k | (x_1^2 + y_1^2 - 2z_1^2)^2 r_1^\nu | \phi_l \rangle &= \frac{2}{\sqrt{\pi}} \Gamma\left(\frac{3+\nu}{2}\right) \langle \phi_k | \phi_l \rangle \lambda^{\nu/2} \left\{ \frac{1}{4} \eta_k^{N=2} \eta_l^{N=2} + \frac{1}{2} \eta_{k,l}^{N=2} \right. \\
&- \lambda^{-1} \left(\frac{1}{4} \eta_k^{N=2} \text{tr} [A_{kl}^{-1} W_l^{N=2} A_{kl}^{-1} \mathbf{a} \mathbf{a}'] + \frac{1}{4} \eta_l^{N=2} \text{tr} [A_{kl}^{-1} W_k^{N=2} A_{kl}^{-1} \mathbf{a} \mathbf{a}'] \right. \\
&+ \frac{1}{2} \text{tr} [A_{kl}^{-1} W_k^{N=2} A_{kl}^{-1} W_l^{N=2} A_{kl}^{-1} \mathbf{a} \mathbf{a}'] + \frac{1}{2} \text{tr} [A_{kl}^{-1} W_l^{N=2} A_{kl}^{-1} W_k^{N=2} A_{kl}^{-1} \mathbf{a} \mathbf{a}'] \Big) \\
&+ \lambda^{-2} \left(\frac{1}{2} \text{tr} [A_{kl}^{-1} W_k^{N=2} A_{kl}^{-1} \mathbf{a} \mathbf{a}' A_{kl}^{-1} W_l^{N=2} A_{kl}^{-1} \mathbf{a} \mathbf{a}'] \right. \\
&+ \frac{1}{4} \text{tr} [A_{kl}^{-1} W_k^{N=2} A_{kl}^{-1} \mathbf{a} \mathbf{a}'] \text{tr} [A_{kl}^{-1} W_l^{N=2} A_{kl}^{-1} \mathbf{a} \mathbf{a}'] \Big) \\
&+ \left(\frac{3+\nu}{3} \right) \left[\lambda^{-1} \left(\frac{1}{4} \eta_k^{N=2} \text{tr} [A_{kl}^{-1} W_l^{N=2} A_{kl}^{-1} \mathbf{a} \mathbf{a}'] + \frac{1}{4} \eta_l^{N=2} \text{tr} [A_{kl}^{-1} W_k^{N=2} A_{kl}^{-1} \mathbf{a} \mathbf{a}'] \right) \right. \quad (65)
\end{aligned}$$

$$\begin{aligned}
& + \frac{1}{2} \text{tr} [\mathbf{A}_{kl}^{-1} \mathbf{W}_k^{\text{N}=2} \mathbf{A}_{kl}^{-1} \mathbf{W}_l^{\text{N}=2} \mathbf{A}_{kl}^{-1} \mathbf{aa}'] + \frac{1}{2} \text{tr} [\mathbf{A}_{kl}^{-1} \mathbf{W}_l^{\text{N}=2} \mathbf{A}_{kl}^{-1} \mathbf{W}_k^{\text{N}=2} \mathbf{A}_{kl}^{-1} \mathbf{aa}'] \\
& - \lambda^{-2} (\text{tr} [\mathbf{A}_{kl}^{-1} \mathbf{W}_l^{\text{N}=2} \mathbf{A}_{kl}^{-1} \mathbf{aa}'] \text{tr} [\mathbf{A}_{kl}^{-1} \mathbf{W}_k^{\text{N}=2} \mathbf{A}_{kl}^{-1} \mathbf{aa}']) \\
& + 2 \text{tr} [\mathbf{A}_{kl}^{-1} \mathbf{W}_l^{\text{N}=2} \mathbf{A}_{kl}^{-1} \mathbf{aa}' \mathbf{A}_{kl}^{-1} \mathbf{W}_k^{\text{N}=2} \mathbf{A}_{kl}^{-1} \mathbf{aa}']) \\
& + \frac{1}{15} \left(\frac{3+\nu}{2} \right) \left(\frac{5+\nu}{2} \right) \lambda^{-2} (2 \text{tr} [\mathbf{A}_{kl}^{-1} \mathbf{W}_k^{\text{N}=1} \mathbf{A}_{kl}^{-1} \mathbf{aa}' \mathbf{A}_{kl}^{-1} \mathbf{W}_l^{\text{N}=1} \mathbf{A}_{kl}^{-1} \mathbf{aa}'] \\
& + \text{tr} [\mathbf{A}_{kl}^{-1} \mathbf{W}_k^{\text{N}=1} \mathbf{A}_{kl}^{-1} \mathbf{aa}'] \text{tr} [\mathbf{A}_{kl}^{-1} \mathbf{W}_l^{\text{N}=1} \mathbf{A}_{kl}^{-1} \mathbf{aa}']) \Big\}. \tag{65}
\end{aligned}$$

Plugging in $\mathbf{a} = \mathbf{e}^1$ and $\nu = m_k + m_l$, the terms in the above simplify such that $\lambda \rightarrow \alpha$, $\eta_k^{\text{N}=2} = 0$, $\eta_l^{\text{N}=2} = 0$, and $\eta_{k,l}^{\text{N}=2} = 6\alpha$, the above becomes

$$\langle \phi_k^{\text{N}=2} | \phi_l^{\text{N}=2} \rangle = \frac{2}{\sqrt{\pi} \Gamma \left(\frac{3+m_k+m_l}{2} \right)} \langle \phi_k | \phi_l \rangle \alpha^{(m_k+m_l)/2} \left(\frac{15 + m_k^2 + m_l^2 + 2 m_k m_l + 8(m_k + m_l)}{5} \right) \alpha^2, \tag{66}$$

$$\langle \phi_k^{\text{N}=2} | \phi_l^{\text{N}=2} \rangle = \left(\frac{15 + m_k^2 + m_l^2 + 2 m_k m_l + 8(m_k + m_l)}{5} \right) \langle \phi_k^{\text{N}=0} | \phi_l^{\text{N}=0} \rangle \alpha^2. \tag{67}$$

To normalize the above integral, the following two integrals are needed:

$$\langle \phi_k^{\text{N}=2} | \phi_k^{\text{N}=2} \rangle = \left(\frac{15 + 4 m_k^2 + 16 m_k}{5} \right) \langle \phi_k^{\text{N}=0} | \phi_k^{\text{N}=0} \rangle 2^{-2} (A_k^{-1})_{11}^2, \tag{68}$$

and

$$\langle \phi_l^{\text{N}=2} | \phi_l^{\text{N}=2} \rangle = \left(\frac{15 + 4 m_l^2 + 16 m_l}{5} \right) \langle \phi_l^{\text{N}=0} | \phi_l^{\text{N}=0} \rangle 2^{-2} (A_l^{-1})_{11}^2. \tag{69}$$

The final formula for the overlap $N=2$ integral is

$$\begin{aligned}
S_{kl}^{\text{N}=2} &= \frac{\langle \phi_k^{\text{N}=2} | \phi_l^{\text{N}=2} \rangle}{(\langle \phi_k^{\text{N}=2} | \phi_k^{\text{N}=2} \rangle \langle \phi_l^{\text{N}=2} | \phi_l^{\text{N}=2} \rangle)^{1/2}} \\
&= 2^2 \gamma_{\text{N}=2}(m_k, m_l) \gamma_1(m_k, m_l) S_{kl} \left[\left(\frac{\alpha}{(A_k^{-1})_{11}} \right)^{m_k+2} \left(\frac{\alpha}{(A_l^{-1})_{11}} \right)^{m_l+2} \right]^{1/2}, \tag{70}
\end{aligned}$$

where $\gamma_{\text{N}=2}$ is a function of m_k and m_l defined by

$$\gamma_{\text{N}=2}(m_k, m_l) = \left(\frac{15 + m_k^2 + m_l^2 + 2 m_k m_l + 8(m_k + m_l)}{(225 + 256 m_k m_l + 240(m_k + m_l) + 64(m_k^2 m_l + m_l^2 m_k) + 60(m_k^2 + m_l^2) + 16 m_k^2 m_l^2)^{1/2}} \right). \tag{71}$$

The gradient of the above overlap integral is

$$\begin{aligned}
\frac{\partial S_{kl}^{\text{N}=2}}{\partial (\text{vech } L_k)'} &= S_{kl}^{\text{N}=2} \left\{ \frac{3}{2} \text{vech} [(L_k^{-1})' - 2 A_{kl}^{-1} L_k]' \right. \\
&+ (m_k + 2) (A_k^{-1})_{11}^{-1} \text{vech} [A_k^{-1} J_{11} A_k^{-1} L_k]' \\
&\left. - (m_k + m_l + 4) \alpha^{-1} \text{vech} [A_{kl}^{-1} J_{11} A_{kl}^{-1} L_k]' \right\}, \tag{72}
\end{aligned}$$

and

$$\begin{aligned}
\frac{\partial S_{kl}^{\text{N}=2}}{\partial (\text{vech } L_l)'} &= S_{kl}^{\text{N}=2} \left\{ \frac{3}{2} \text{vech} [(L_l^{-1})' - 2 A_{kl}^{-1} L_l]' \right. \\
&+ (m_k + 2) (A_l^{-1})_{11}^{-1} \text{vech} [A_l^{-1} J_{11} A_l^{-1} L_l]' \\
&\left. - (m_k + m_l + 4) \alpha^{-1} \text{vech} [A_{kl}^{-1} J_{11} A_{kl}^{-1} L_l]' \right\}. \tag{73}
\end{aligned}$$

C. Kinetic energy integral

The kinetic energy operator in (4) can be written in the following quadratic form:

$$-\frac{1}{2} \left(\sum_{i=1}^n \frac{1}{\mu_i} \nabla_{\mathbf{r}_i}^2 + \sum_{i \neq j}^n \frac{1}{m_0} \nabla'_{\mathbf{r}_i} \nabla_{\mathbf{r}_j} \right) = -\nabla'_{\mathbf{r}} \mathbf{M} \nabla_{\mathbf{r}}. \quad (74)$$

In (74), the mass matrix \mathbf{M} is $\mathbf{M} = M \otimes I_3$, where in the M matrix the diagonal elements are set to $1/(2\mu_1)$, $1/(2\mu_2)$, ..., $1/(2\mu_{n_{tot}})$ while the off-diagonal elements are set to $1/(2m_0)$. Again, m_0 is the mass of the reference nucleus and $\mu_1, \dots, \mu_{n_{tot}}$ are the reduced masses of the pseudoparticles.

The kinetic energy matrix element is

$$\langle \phi_k^{N=1} | -\nabla'_{\mathbf{r}} \mathbf{M} \nabla_{\mathbf{r}} | \phi_l^{N=1} \rangle = \langle \nabla_{\mathbf{r}} \phi_k^{N=1} | \mathbf{M} | \nabla'_{\mathbf{r}} \phi_l^{N=1} \rangle. \quad (75)$$

First, we determine the derivative of the basis function (10)

$$\begin{aligned} \langle \nabla_{\mathbf{r}} \phi_k^{N=1} | &= \langle \mathbf{v}_k^{N=1} (\mathbf{r}' \mathbf{J}_{11} \mathbf{r})^{m_k/2} \exp[-\mathbf{r}' \mathbf{A}_k \mathbf{r}] | \\ &+ \langle m_k (\mathbf{v}_k^{N=1'} \mathbf{r}) (\mathbf{r}' \mathbf{J}_{11} \mathbf{r})^{m_k/2-1} (\mathbf{J}_{11} \mathbf{r}) \exp[-\mathbf{r}' \mathbf{A}_k \mathbf{r}] | \\ &- \langle 2(\mathbf{A}_k \mathbf{r}) (\mathbf{v}_k^{N=1'} \mathbf{r}) (\mathbf{r}' \mathbf{J}_{11} \mathbf{r})^{m_k/2} \exp[-\mathbf{r}' \mathbf{A}_k \mathbf{r}] | \\ &= \langle \mathbf{v}_k^{N=1} \phi_k^{N=0} | + \langle \frac{m_k}{r_1^2} (\mathbf{J}_{11} \mathbf{r}) \phi_k^{N=1} | - \langle 2(\mathbf{A}_k \mathbf{r}) \phi_k^{N=1} |. \end{aligned} \quad (76)$$

Multiplying the above by the mass matrix and then by the corresponding *ket* containing the l -basis function, the following nine integrals are obtained:

$$\langle \nabla_{\mathbf{r}} \phi_k^{N=1} | \mathbf{M} | \nabla_{\mathbf{r}} \phi_l^{N=1} \rangle = \langle \phi_k^{N=0} | \mathbf{v}_k^{N=1'} \mathbf{M} \mathbf{v}_l^{N=1} | \phi_l^{N=0} \rangle, \quad (77)$$

$$+ m_l \langle \phi_k^{N=0} | \frac{\mathbf{v}_k^{N=1'} \mathbf{M} \mathbf{J}_{11} \mathbf{r}}{r_1^2} | \phi_l^{N=1} \rangle, \quad (78)$$

$$- 2 \langle \phi_k^{N=0} | \mathbf{v}_k^{N=1'} \mathbf{M} \mathbf{A}_l \mathbf{r} | \phi_l^{N=1} \rangle, \quad (79)$$

$$+ m_k \langle \phi_k^{N=1} | \frac{\mathbf{r}' \mathbf{J}_{11} \mathbf{M} \mathbf{v}_l^{N=1}}{r_1^2} | \phi_l^{N=0} \rangle, \quad (80)$$

$$+ m_k m_l \langle \phi_k^{N=1} | \frac{\mathbf{r}' \mathbf{J}_{11} \mathbf{M} \mathbf{J}_{11} \mathbf{r}}{r_1^4} | \phi_l^{N=1} \rangle, \quad (81)$$

$$\begin{aligned} \langle \phi_k^{N=0} | \frac{\mathbf{v}_k^{N=1'} \mathbf{M} \mathbf{J}_{11} \mathbf{r}}{r_1^2} | \phi_l^{N=1} \rangle &= m_k M_{11} \left(\frac{3+m_k+m_l-2}{6} \right) \frac{2}{\sqrt{\pi}} \Gamma \left(\frac{3+m_k+m_l-2}{2} \right) \langle \phi_k | \phi_l \rangle \alpha^{(m_k+m_l-2)/2} \alpha \\ &= \alpha^{-1} m_k M_{11} \left(\frac{2}{3+m_k+m_l} \right) \langle \phi_k^{N=1} | \phi_l^{N=1} \rangle, \end{aligned} \quad (90)$$

where we used the same method as in the first of nine integrals to normalize the integral. Thus, the normalized formula is

$$\frac{\langle \phi_k^{N=0} | \frac{\mathbf{v}_k^{N=1'} \mathbf{M} \mathbf{J}_{11} \mathbf{r}}{r_1^2} | \phi_l^{N=1} \rangle}{(\langle \phi_k^{N=1} | \phi_k^{N=1} \rangle \langle \phi_l^{N=1} | \phi_l^{N=1} \rangle)^{1/2}} = \alpha^{-1} m_k M_{11} S_{kl}^{N=1} \left(\frac{2}{3+m_k+m_l} \right). \quad (91)$$

The fourth integral (80) is analogical integral to the above. The quadratic form in this integral, $\mathbf{r}' \mathbf{J}_{11} \mathbf{M} \mathbf{v}_l^{N=1} = x_1 M_{11} = \mathbf{v}_k^{N=1'} \mathbf{M} \mathbf{J}_{11} \mathbf{r}$, is the same as in the above integral and, therefore, the result can be immediately

$$- 2 m_k \langle \phi_k^{N=1} | \frac{\mathbf{r}' \mathbf{J}_{11} \mathbf{M} \mathbf{A}_l \mathbf{r}}{r_1^2} | \phi_l^{N=1} \rangle, \quad (82)$$

$$- 2 \langle \phi_k^{N=1} | \mathbf{r}' \mathbf{A}_k \mathbf{M} \mathbf{v}_l^{N=1} | \phi_l^{N=0} \rangle, \quad (83)$$

$$- 2 m_l \langle \phi_k^{N=1} | \frac{\mathbf{r}' \mathbf{A}_k \mathbf{M} \mathbf{J}_{11} \mathbf{r}}{r_1^2} | \phi_l^{N=1} \rangle, \quad (84)$$

$$+ 4 \langle \phi_k^{N=1} | \mathbf{r}' \mathbf{A}_k \mathbf{M} \mathbf{A}_l \mathbf{r} | \phi_l^{N=1} \rangle. \quad (85)$$

Each of the above nine integrals are evaluated separately.

The first of the nine integrals, (77), contains the vector-matrix-vector product $\mathbf{v}_k^{N=1'} \mathbf{M} \mathbf{v}_l^{N=1} = M_{11}$ which can be pulled out of the *bra-ket* because it is not a quantity dependent on the integration variables \mathbf{r} . This results in the following formula:

$$\langle \phi_k^{N=0} | \mathbf{v}_k^{N=1'} \mathbf{M} \mathbf{v}_l^{N=1} | \phi_l^{N=0} \rangle = M_{11} \langle \phi_k^{N=0} | \phi_l^{N=0} \rangle. \quad (86)$$

To normalize this term, we rewrite the above in terms of the overlap integral for the k and l $N = 1$ basis functions. To do this, we divide it by the ratio of (45) and (57)

$$\begin{aligned} \langle \phi_k^{N=0} | \mathbf{v}_k^{N=1'} \mathbf{M} \mathbf{v}_l^{N=1} | \phi_l^{N=0} \rangle & \\ = \alpha^{-1} M_{11} \frac{6}{(3+m_k+m_l)} \langle \phi_k^{N=1} | \phi_l^{N=1} \rangle. \end{aligned} \quad (87)$$

After that the final normalized form of the integral is

$$\begin{aligned} \frac{\langle \phi_k^{N=0} | \mathbf{v}_k^{N=1'} \mathbf{M} \mathbf{v}_l^{N=1} | \phi_l^{N=0} \rangle}{(\langle \phi_k^{N=1} | \phi_k^{N=1} \rangle \langle \phi_l^{N=1} | \phi_l^{N=1} \rangle)^{1/2}} & \\ = \alpha^{-1} M_{11} \frac{6}{(3+m_k+m_l)} S_{kl}^{N=1}. \end{aligned} \quad (88)$$

The second of the nine integrals (78) contains a vector-matrix-vector product $\mathbf{v}_k^{N=1'} \mathbf{M} \mathbf{J}_{11} \mathbf{r}$ that is dependent on the integration variables \mathbf{r} , but can be simplified to $x_1 M_{11}$ which changes the integral in the following way:

$$\langle \phi_k^{N=0} | \frac{\mathbf{v}_k^{N=1'} \mathbf{M} \mathbf{J}_{11} \mathbf{r}}{r_1^2} | \phi_l^{N=1} \rangle = M_{11} \langle \phi_k^{N=1} | \frac{1}{r_1^2} | \phi_l^{N=1} \rangle. \quad (89)$$

This integral is not new because $\frac{1}{r_1^2}$ multiplied by $r_1^{m_k+m_l}$ equals $r_1^{m_k+m_l-2}$ and we can use the overlap formula (53) with v (the general power of r_1) equal to $m_k + m_l - 2$ instead of $m_k + m_l$. With this we obtain the following formula:

written as

$$\frac{\langle \phi_k^{N=1} | \frac{\mathbf{r}' \mathbf{J}_{11} \mathbf{M} \mathbf{v}_l^{N=1}}{r_1^2} | \phi_l^{N=0} \rangle}{(\langle \phi_k^{N=1} | \phi_k^{N=1} \rangle \langle \phi_l^{N=1} | \phi_l^{N=1} \rangle)^{1/2}} = \alpha^{-1} m_l M_{11} S_{kl}^{N=1} \left(\frac{2}{3 + m_k + m_l} \right). \quad (92)$$

The next integral to evaluate is the fifth integral (81). This integral contains the vector-matrix-vector product $\mathbf{r}' \mathbf{J}_{11} \mathbf{M} \mathbf{J}_{11} \mathbf{r}$ that equals to $M_{11} r_1^2$. This results in a very similar integral as the previous two integrals

$$\begin{aligned} \langle \phi_k^{N=1} | \frac{\mathbf{r}' \mathbf{J}_{11} \mathbf{M} \mathbf{J}_{11} \mathbf{r}}{r_1^4} | \phi_l^{N=1} \rangle &= m_k m_l M_{11} \langle \phi_k^{N=1} | \frac{1}{r_1^2} | \phi_l^{N=1} \rangle \\ &= m_k m_l M_{11} \left(\frac{3 + m_k + m_l - 2}{6} \right) \frac{2}{\sqrt{\pi}} \Gamma \left(\frac{3 + m_k + m_l - 2}{2} \right) \langle \phi_k | \phi_l \rangle \alpha^{(m_k + m_l - 2)/2} \alpha \\ &= \alpha^{-1} m_k m_l M_{11} \left(\frac{2}{3 + m_k + m_l} \right) \langle \phi_k^{N=1} | \phi_l^{N=1} \rangle, \end{aligned} \quad (93)$$

and after the normalization we obtain

$$\frac{\langle \phi_k^{N=1} | \frac{\mathbf{r}' \mathbf{J}_{11} \mathbf{M} \mathbf{J}_{11}}{r_1^2} | \phi_l^{N=1} \rangle}{(\langle \phi_k^{N=1} | \phi_k^{N=1} \rangle \langle \phi_l^{N=1} | \phi_l^{N=1} \rangle)^{1/2}} = \alpha^{-1} m_k m_l M_{11} S_{kl}^{N=1} \left(\frac{2}{3 + m_k + m_l} \right). \quad (94)$$

Now we evaluate the third (79) and seventh (83) integrals together by first combining the x_1 prefactor of $\phi_k^{N=1}$ and $\phi_l^{N=1}$ with their respective vector-matrix-vector products. Next, we add the two together and by combining like terms we get

$$\begin{aligned} -2 \langle \phi_k^{N=0} | \mathbf{v}_k^{N=1} \mathbf{M} \mathbf{A}_l \mathbf{r} | \phi_l^{N=1} \rangle - 2 \langle \phi_k^{N=1} | \mathbf{r}' \mathbf{A}_k \mathbf{M} \mathbf{v}_l^{N=1} | \phi_l^{N=0} \rangle &= -2 \langle \phi_k^{N=0} | \mathbf{W}_{kl}^{N=1} \mathbf{M} \mathbf{A}_l \mathbf{r} | \phi_l^{N=0} \rangle \\ &\quad - 2 \langle \phi_k^{N=0} | \mathbf{r}' \mathbf{A}_k \mathbf{M} \mathbf{W}_{kl}^{N=1} | \phi_l^{N=0} \rangle \\ &= -2 \langle \phi_k^{N=0} | \mathbf{r}' \mathbf{A}_{kl} \mathbf{M} \mathbf{W}_{kl}^{N=1} \mathbf{r} | \phi_l^{N=0} \rangle \\ &= -2 M_{11} \left(\frac{3 + m_k + m_l}{6} \right) \frac{2}{\sqrt{\pi}} \Gamma \left(\frac{3 + m_k + m_l}{2} \right) \\ &\quad \times \langle \phi_k | \phi_l \rangle \alpha^{(m_k + m_l)} \\ &= -2 \alpha^1 M_{11} \langle \phi_k^{N=1} | \phi_l^{N=1} \rangle. \end{aligned} \quad (95)$$

After normalization, the formula is

$$-2 \frac{\langle \phi_k^{N=0} | \mathbf{r}' \mathbf{A}_{kl} \mathbf{M} \mathbf{W}_{kl}^{N=1} \mathbf{r} | \phi_l^{N=0} \rangle}{(\langle \phi_k^{N=1} | \phi_k^{N=1} \rangle \langle \phi_l^{N=1} | \phi_l^{N=1} \rangle)^{1/2}} = -2 \alpha^{-1} M_{11} S_{kl}^{N=1}. \quad (96)$$

To evaluate integrals sixth (82) and eighth (84), we add their vector-matrix-vector products together. Notice that the resulting integral resembles the $N = 2$ overlap integral (65). To obtain an expression for the two integrals, we replace $W_k^{N=2}$ with $W_{kl}^{N=1}$, $W_l^{N=2}$ with $(m_l \mathbf{A}_k + m_k \mathbf{A}_l) \mathbf{M} \mathbf{J}_{11}$, and v with $m_k + m_l - 2$. After some simplifications, we obtain the following:

$$\begin{aligned}
& -2 \langle \phi_k^{N=1} | \frac{\mathbf{r}'(m_l \mathbf{A}_k + m_k \mathbf{A}_l) \mathbf{M} \mathbf{J}_{11} \mathbf{r}}{r_1^2} | \phi_l^{N=1} \rangle \\
& = -2 \frac{2}{\sqrt{\pi}} \Gamma\left(\frac{3+m_k+m_l-2}{2}\right) \langle \phi_k | \phi_l \rangle \alpha^{(m_k+m_l-2)/2} \\
& \times \left\{ \frac{3}{4} \eta_{kl}^{N=1} \text{tr} [A_{kl}^{-1} (m_l A_k + m_k A_l) M J_{11}] + \frac{1}{2} \text{tr} [\mathbf{A}_{kl}^{-1} \mathbf{W}_{kl}^{N=1} \mathbf{A}_{kl}^{-1} (m_l \mathbf{A}_k + m_k \mathbf{A}_l) \mathbf{M} \mathbf{J}_{11}] \right. \\
& \left(\frac{m_k+m_l-2}{3} \right) \alpha^{-1} \left(\frac{3}{4} \eta_{kl}^{N=1} \text{tr} [A_{kl}^{-1} (m_l A_k + m_k A_l) M J_{11} A_{kl}^{-1} J_{11}] \right. \\
& + \frac{3}{4} \text{tr} [A_{kl}^{-1} (m_l A_k + m_k A_l) M J_{11}] \text{tr} [\mathbf{A}_{kl}^{-1} \mathbf{W}_{kl}^{N=1} \mathbf{A}_{kl}^{-1} \mathbf{J}_{11}] \\
& + \frac{1}{2} \text{tr} [\mathbf{A}_{kl}^{-1} \mathbf{W}_{kl}^{N=1} \mathbf{A}_{kl}^{-1} (m_l \mathbf{A}_k + m_k \mathbf{A}_l) \mathbf{M} \mathbf{J}_{11} A_{kl}^{-1} \mathbf{J}_{11}] + \frac{1}{2} \text{tr} [\mathbf{A}_{kl}^{-1} (m_l \mathbf{A}_k + m_k \mathbf{A}_l) \mathbf{M} \mathbf{J}_{11} \mathbf{A}_{kl}^{-1} \mathbf{W}_{kl}^{N=1} \mathbf{A}_{kl}^{-1} \mathbf{J}_{11}] \Big) \\
& \left(\frac{3+m_k^2+m_l^2+2m_km_l-4(m_k+m_l)}{15} \right) \left(\frac{1}{2} \text{tr} [\mathbf{A}_{kl}^{-1} \mathbf{W}_{kl}^{N=1} \mathbf{A}_{kl}^{-1} \mathbf{J}_{11} \mathbf{A}_{kl}^{-1} (m_l \mathbf{A}_k + m_k \mathbf{A}_l) \mathbf{M} \mathbf{J}_{11} \mathbf{A}_{kl}^{-1} \mathbf{J}_{11}] \right. \\
& \left. \left. + \frac{1}{4} \text{tr} [\mathbf{A}_{kl}^{-1} \mathbf{W}_{kl}^{N=1} \mathbf{A}_{kl}^{-1} \mathbf{J}_{11}] \text{tr} [A_{kl}^{-1} (m_l A_k + m_k A_l) M J_{11} A_{kl}^{-1} J_{11}] \right) \right\} \\
& = -2 \left(\frac{1+m_k+m_l}{2} \right) \left(\frac{3+m_k+m_l}{6} \right) \frac{2}{\sqrt{\pi}} \Gamma\left(\frac{1+m_k+m_l}{2}\right) \langle \phi_k | \phi_l \rangle \alpha^{(m_k+m_l-2)/2} \alpha (A_{kl}^{-1} (m_l A_k + m_k A_l) M)_{11} \\
& = -2 \alpha^{-1} \langle \phi_k^{N=1} | \phi_l^{N=1} \rangle (A_{kl}^{-1} (m_l A_k + m_k A_l) M)_{11}. \tag{97}
\end{aligned}$$

After normalization, the formula becomes

$$\frac{-2 \langle \phi_k^{N=1} | \frac{\mathbf{r}'(m_l \mathbf{A}_k + m_k \mathbf{A}_l) \mathbf{M} \mathbf{J}_{11} \mathbf{r}}{r_1^2} | \phi_l^{N=1} \rangle}{(\langle \phi_k^{N=1} | \phi_k^{N=1} \rangle \langle \phi_l^{N=1} | \phi_l^{N=1} \rangle)^{1/2}} = -2 \alpha^{-1} S_{kl}^{N=1} (A_{kl}^{-1} (m_l A_k + m_k A_l) M)_{11}. \tag{98}$$

The ninth integral (85) also requires the use of (65), where $W_k^{N=2}$ becomes $W_{kl}^{N=1}$, $W_l^{N=1}$ becomes $1/2 (\mathbf{A}_k \mathbf{M} \mathbf{A}_l + \mathbf{A}_l \mathbf{M} \mathbf{A}_k)$ (to satisfy required symmetry), and ν remains as $m_k + m_l$

$$\begin{aligned}
4 \langle \phi_k^{N=1} | \mathbf{r}' \mathbf{A}_k \mathbf{M} \mathbf{A}_l \mathbf{r} | \phi_l^{N=01} \rangle & = 4 \frac{2}{\sqrt{\pi}} \Gamma\left(\frac{3+m_k+m_l}{2}\right) \langle \phi_k | \phi_l \rangle \alpha^{(m_k+m_l)/2} \left\{ \left(\frac{3+m_k+m_l}{4} \right) \alpha \text{tr} [A_{kl}^{-1} A_k M A_l] \right. \\
& \left. + \left(\frac{2+m_k+m_l}{2} \right) \left(\frac{3+m_k+m_l}{3} \right) (A_{kl}^{-1} A_k M A_l A_{kl}^{-1})_{11} \right\} \\
& = \langle \phi_k^{N=1} | \phi_l^{N=1} \rangle \{6 \text{tr} [A_{kl}^{-1} A_k M A_l] + \alpha^{-1} 2 (m_k + m_l + 2) (A_{kl}^{-1} A_k M A_l A_{kl}^{-1})_{11}\}. \tag{99}
\end{aligned}$$

After normalization, the formula becomes

$$\frac{4 \langle \phi_k^{N=1} | \mathbf{r}' \mathbf{A}_k \mathbf{M} \mathbf{A}_l \mathbf{r} | \phi_l^{N=1} \rangle}{(\langle \phi_k^{N=1} | \phi_k^{N=1} \rangle \langle \phi_l^{N=1} | \phi_l^{N=1} \rangle)^{1/2}} = S_{kl}^{N=1} \{6 \text{tr} [A_{kl}^{-1} A_k M A_l] + 2 (m_k + m_l + 2) \alpha^{-1} (A_{kl}^{-1} A_k M A_l A_{kl}^{-1})_{11}\}. \tag{100}$$

To finalize the kinetic-energy part of the Hamiltonian matrix element, we now combine all nine normalized integrals

$$\begin{aligned}
T_{kl}^{N=1} & = \frac{S_{kl}^{N=1}}{\alpha} \left\{ M_{11} \left(\left(\frac{6}{3+m_k+m_l} \right) + (m_k + m_l + m_k m_l) \frac{2}{3+m_k+m_l} - 2 \right) \right. \\
& \left. + 6 \tau_1 \alpha + 2 (2 + m_k + m_l) \tau_2 - 2 \tau_3 \right\} \\
& = \frac{S_{kl}^{N=1}}{\alpha} \left\{ M_{11} \left(\frac{2 m_k m_l}{3+m_k+m_l} \right) + 6 \tau_1 \alpha + 2 (2 + m_k + m_l) \tau_2 - 2 \tau_3 \right\}, \tag{101}
\end{aligned}$$

such that $\tau_1 = \text{tr} [A_{kl}^{-1} A_k M A_l]$, $\tau_2 = (A_{kl}^{-1} A_k M A_l A_{kl}^{-1})_{11}$, and $\tau_3 = (A_{kl}^{-1} (m_l A_k + m_k A_l) M)_{11}$.

The gradient of the kinetic-energy matrix element is

$$\begin{aligned} \frac{\partial T_{kl}^{N=1}}{\partial (\text{vech } L_k)'} &= \frac{\partial S_{kl}^{N=1}}{\partial (\text{vech } L_k)'} \frac{T_{kl}^{N=1}}{S_{kl}^{N=1}} - \alpha^{-1} T_{kl}^{N=1} \frac{\partial \alpha}{\partial (\text{vech } L_k)'} \\ &\quad + \frac{S_{kl}^{N=1}}{\alpha} \left\{ 6\alpha \frac{\partial \tau_1}{\partial (\text{vech } L_k)'} + 6\tau_1 \frac{\partial \alpha}{\partial (\text{vech } L_k)'} + 2(2+m_k+m_l) \frac{\partial \tau_2}{\partial (\text{vech } L_k)'} - 2 \frac{\partial \tau_3}{\partial (\text{vech } L_k)'} \right\}, \end{aligned} \quad (102)$$

and

$$\begin{aligned} \frac{\partial T_{kl}^{N=1}}{\partial (\text{vech } L_l)'} &= \frac{\partial S_{kl}^{N=1}}{\partial (\text{vech } L_l)'} \frac{T_{kl}^{N=1}}{S_{kl}^{N=1}} - \alpha^{-1} T_{kl}^{N=1} \frac{\partial \alpha}{\partial (\text{vech } L_l)'} \\ &\quad + \frac{S_{kl}^{N=1}}{\alpha} \left\{ 6\alpha \frac{\partial \tau_1}{\partial (\text{vech } L_l)'} + 6\tau_1 \frac{\partial \alpha}{\partial (\text{vech } L_l)'} 2(2+m_k+m_l) \frac{\partial \tau_2}{\partial (\text{vech } L_l)'} - 2 \frac{\partial \tau_3}{\partial (\text{vech } L_l)'} \right\}. \end{aligned} \quad (103)$$

For the τ_1 derivatives, we obtain

$$\begin{aligned} \frac{\partial \tau_1}{\partial (\text{vech } L_k)'} &= -(\text{vech } A_{kl}^{-1} A_k M A_l A_{kl}^{-1} L_k)' - (\text{vech } A_{kl}^{-1} A_l M A_k A_{kl}^{-1} L_k)' \\ &\quad + (\text{vech } M A_l A_{kl}^{-1} L_k)' + (\text{vech } A_{kl}^{-1} A_l M L_k)', \end{aligned} \quad (104)$$

and

$$\begin{aligned} \frac{\partial \tau_1}{\partial (\text{vech } L_l)'} &= -(\text{vech } A_{kl}^{-1} A_k M A_l A_{kl}^{-1} L_l)' - (\text{vech } A_{kl}^{-1} A_l M A_k A_{kl}^{-1} L_l)' \\ &\quad + (\text{vech } A_{kl}^{-1} A_k M L_l)' + (\text{vech } M A_k A_{kl}^{-1} L_l)'. \end{aligned} \quad (105)$$

For τ_2 , we have

$$\begin{aligned} \frac{\partial \tau_2}{\partial (\text{vech } L_k)'} &= -(\text{vech } A_{kl}^{-1} A_k M A_l A_{kl}^{-1} W_{kl}^{N=1} A_{kl}^{-1} L_k)' \mathcal{T} - (\text{vech } A_{kl}^{-1} W_{kl}^{N=1} A_{kl}^{-1} A_l M A_k A_{kl}^{-1} L_k)' \mathcal{T} \\ &\quad - (\text{vech } A_{kl}^{-1} A_l M A_k A_{kl}^{-1} W_{kl}^{N=1} A_{kl}^{-1} L_k)' \mathcal{T} - (\text{vech } A_{kl}^{-1} W_{kl}^{N=1} A_{kl}^{-1} A_k M A_l A_{kl}^{-1} L_k)' \mathcal{T} \\ &\quad + (\text{vech } M A_l A_{kl}^{-1} W_{kl}^{N=1} A_{kl}^{-1} L_k)' \mathcal{T} + (\text{vech } A_{kl}^{-1} W_{kl}^{N=1} A_{kl}^{-1} A_l M L_k)' \mathcal{T}, \end{aligned} \quad (106)$$

and

$$\begin{aligned} \frac{\partial \tau_2}{\partial (\text{vech } L_l)'} &= -(\text{vech } A_{kl}^{-1} A_k M A_l A_{kl}^{-1} W_{kl}^{N=1} A_{kl}^{-1} L_l)' \mathcal{T} - (\text{vech } A_{kl}^{-1} W_{kl}^{N=1} A_{kl}^{-1} A_l M A_k A_{kl}^{-1} L_l)' \mathcal{T} \\ &\quad - (\text{vech } A_{kl}^{-1} A_l M A_k A_{kl}^{-1} W_{kl}^{N=1} A_{kl}^{-1} L_l)' \mathcal{T} - (\text{vech } A_{kl}^{-1} W_{kl}^{N=1} A_{kl}^{-1} A_k M A_l A_{kl}^{-1} L_l)' \mathcal{T} \\ &\quad + (\text{vech } A_{kl}^{-1} W_{kl}^{N=1} A_{kl}^{-1} A_k M L_l)' \mathcal{T} + (\text{vech } M A_k A_{kl}^{-1} W_{kl}^{N=1} A_{kl}^{-1} L_l)' \mathcal{T}. \end{aligned} \quad (107)$$

To transform the expression to the correct form, a transformation matrix, \mathcal{T} , must be applied to the appropriate terms. This transformation matrix has the dimensions $\frac{3n(3n+1)}{2} \times \frac{n(n+1)}{2}$ and is defined as

$$\mathcal{T} = \frac{d \text{vech } L_k (\text{vech } L_k)'}{d (\text{vech } L_k)'} \quad (108)$$

The notation $\text{vech } \mathbf{L}_k$ ($\text{vech } L_k$) indicates that the $3n(3n+1)/2$ -dimension vector $\text{vech } \mathbf{L}_k$ is a function of the $n(n+1)/2$ -dimension vector $\text{vech } L_k$. The derivative of $\text{vech } \mathbf{L}_k$ with respect to $\text{vech } L_k$ is defined as the $3n(3n+1)/2 \times n(n+1)/2$ matrix of partial derivatives whose ij th element is the partial derivative of the i th component of $\text{vech } \mathbf{L}_k$ (a column vector) with respect to the j th element of $(\text{vech } L_k)'$ (a row vector). It should be noted that \mathcal{T} is independent of index k and is a matrix consisting of 0's and 1's. (108) can be now rearranged to the following form:

$$d \text{vech } \mathbf{L}_k = \mathcal{T} \text{vech } L_k, \quad (109)$$

and a similar form for $d \text{vech } \mathbf{L}_l$. The approach was first used in Ref. 12. Next, we substitute $(d \text{vech } \mathbf{L}_k)$ and $(d \text{vech } \mathbf{L}_l)$ with (109).

For τ_3 , we have

$$\begin{aligned} \frac{\partial \tau_3}{\partial (\text{vech } L_k)'} &= -(\text{vech } A_{kl}^{-1} (m_l A_k + m_k A_l) M J_{11} A_{kl}^{-1} L_k)' - (\text{vech } A_{kl}^{-1} J_{11} M (m_l A_k + m_k A_l) A_{kl}^{-1} L_k)' \\ &\quad + m_l (\text{vech } M J_{11} A_{kl}^{-1} L_k)' + m_l (\text{vech } A_{kl}^{-1} J_{11} M L_k)', \end{aligned} \quad (110)$$

and

$$\begin{aligned} \frac{\partial \tau_3}{\partial (\text{vech } L_l)'} &= -(\text{vech } A_{kl}^{-1} (m_l A_k + m_k A_l) M J_{11} A_{kl}^{-1} L_l)' - (\text{vech } A_{kl}^{-1} J_{11} M (m_l A_k + m_k A_l) A_{kl}^{-1} L_l)' \\ &\quad + m_k (\text{vech } M J_{11} A_{kl}^{-1} L_l)' + m_k (\text{vech } A_{kl}^{-1} J_{11} M L_l)'. \end{aligned} \quad (111)$$

This concludes the derivation of the kinetic-energy part of the Hamiltonian matrix elements.

D. Potential energy integral

In the derivation of the diatomic potential-energy part of the Hamiltonian, there are four types of integrals that need to be considered. They involve four different types of the electrostatic interactions which are present in the internal Hamiltonian. The interactions are: first, the Coulombic interaction of the reference nucleus with the pseudonucleus, second, the Coulombic interactions of the reference nucleus with each pseudoelectron, third, the Coulombic interaction of the pseudonucleus with each pseudoelectron, and fourth, the Coulombic interaction of each pseudoelectron with another pseudoelectrons. The first integral type is the simplest because the operator involved contains r_1 which also appears in the $r_1^{m_k}$ and $r_1^{m_l}$ factors of the basis function for which the matrix element is calculated. Thus, the derivation of this integral can be carried out using the same method as used to evaluate the overlap integral (and the same as used in the derivations of the kinetic-energy integral). The other three integral types will be derived using a different approach and the derivation will be carried out for all of them together.

We start the derivation of the potential-energy matrix element with the derivation of the integral containing the $1/r_1$ operator

$$\begin{aligned} \langle \phi_k^{\text{N}=1} | \frac{1}{r_1} | \phi_l^{\text{N}=1} \rangle &= \left\langle (x_1^2) \frac{r_1^{(m_k+m_l)}}{r_1} \exp[-\mathbf{r}' \mathbf{A}_{kl} \mathbf{r}] \right\rangle \\ &= \langle (x_1^2) r_1^{(m_k+m_l)-1} \exp[-\mathbf{r}' \mathbf{A}_{kl} \mathbf{r}] \rangle. \end{aligned} \quad (112)$$

One can easily recognize that (41) can be applied to the above with $\nu = m_k + m_l - 1$. With this, the potential energy formula

$$\begin{aligned} \langle \phi_k^{\text{N}=1} | \frac{1}{r_{ij}} | \phi_l^{\text{N}=1} \rangle &= \left\langle (x_1^2) r_1^{(m_k+m_l)} \frac{1}{r_{ij}} \exp[-\mathbf{r}' \mathbf{A}_{kl} \mathbf{r}] \right\rangle \\ &= -\frac{\partial}{\partial \omega_{kl}} (-1)^m \frac{\partial^m}{\partial u^m} \frac{2}{\sqrt{\pi}} \int_0^{+\infty} \langle \exp[-\mathbf{r}' (\mathbf{A}_{kl} + \omega_{kl} \mathbf{W}_{kl}^{\text{N}=1} + u \mathbf{J}_{11} + t^2 \mathbf{J}_{ij}) \mathbf{r}] \rangle dt|_{\omega_{kl}=u=0}, \end{aligned} \quad (118)$$

where $m_k + m_l = 2m$, $m = 0, 1, 2, \dots$, and $\mathbf{W}_{kl}^{\text{N}=1}$ has only one non-zero element with a value of 1 in the (1, 1) position. Continuing, we have

$$\begin{aligned} \langle \exp[-\mathbf{r}' (\mathbf{A}_{kl} + \omega_{kl} \mathbf{W}_{kl}^{\text{N}=1} + u \mathbf{J}_{11} + t^2 \mathbf{J}_{ij}) \mathbf{r}] \rangle &= \pi^{3n/2} |\mathbf{A}_{kl} + \omega_{kl} \mathbf{W}_{kl}^{\text{N}=1} + u \mathbf{J}_{11} + t^2 \mathbf{J}_{ij}|^{-1/2} \\ &= \pi^{3n/2} |A_{kl}|^{-3/2} \\ &\quad \times |I_{3n} + \omega_{kl} \mathbf{W}_{kl}^{\text{N}=1} \mathbf{A}_{kl}^{-1} + u \mathbf{J}_{11} \mathbf{A}_{kl}^{-1} + t^2 \mathbf{J}_{ij} \mathbf{A}_{kl}^{-1}|^{-1/2}, \end{aligned} \quad (119)$$

for the integral-type one is

$$\begin{aligned} \langle \phi_k^{\text{N}=1} | \frac{1}{r_1} | \phi_l^{\text{N}=1} \rangle &= \frac{2}{\sqrt{\pi}} \left(\frac{3+m_k+m_l-1}{6} \right) \\ &\quad \times \Gamma \left(\frac{3+m_k+m_l-1}{2} \right) \langle \phi_k | \phi_l \rangle \alpha^{(m_k+m_l-1)/2} \alpha. \end{aligned} \quad (113)$$

Now we normalize this integral. Rewriting the above in terms of $\langle \phi_k^{\text{N}=1} | \phi_l^{\text{N}=1} \rangle$ allows us to express the above in terms of $S_{kl}^{\text{N}=1}$. This enables us to perform the normalization. To do this, we multiply the above by

$$\left(\frac{6}{3+m_k+m_l} \right) \frac{1}{\Gamma \left(\frac{3+m_k+m_l}{2} \right)} \frac{1}{\alpha}, \quad (114)$$

which results in the following final formula for the integral involving the $1/r_1$ potential-energy operator:

$$R_{kl}^{\text{N}=1(1,1)} = S_{kl}^{\text{N}=1} \gamma_2(m_k, m_l) \left(\frac{2+m_k+m_l}{3+m_k+m_l} \right) \frac{1}{\sqrt{\alpha}}, \quad (115)$$

where

$$\gamma_2(m_k, m_l) = \frac{\Gamma(2+m_k+m_l)}{\Gamma(3+m_k+m_l)}. \quad (116)$$

Apart from its contribution to the complete potential-energy Hamiltonian matrix element, the above formula is also used to verify the correctness of the integral involving the potential-energy operator $1/r_{ij}$, which is derived next.

Now we consider the potential-energy integral involving the $1/r_{ij}$ operator. For this operator, we use the following integral transform:

$$\frac{1}{r_{ij}} = \frac{2}{\sqrt{\pi}} \int_0^\infty \exp[-u^2 r_{ij}^2] du, \quad (117)$$

along with partial differentiation

where (25) was used. Applying $-\frac{\partial}{\partial \omega_{kl}}$ to the above, setting ω to zero, and using (26) the above becomes

$$\frac{1}{2}\pi^{3n/2}|A_{kl}|^{-3/2}[I_n + uJ_{11}A_{kl}^{-1} + t^2J_{ij}A_{kl}^{-1}]^{-3/2}\eta_{kl}^{N=1} \quad (120)$$

with

$$\eta_{kl}^{N=1} = \text{tr}[\mathbf{DW}_{kl}^{N=1}\mathbf{A}_{kl}^{-1}] = \frac{(\alpha + t^2(\alpha\beta - \chi))}{(1 + u\alpha + t^2\beta + ut^2(\alpha\beta - \chi))}, \quad (121)$$

where $\mathbf{D} = (I_{3n} + u\mathbf{J}_{11}\mathbf{A}_{kl}^{-1} + t^2\mathbf{J}_{ij}\mathbf{A}_{kl}^{-1})^{-1}$, $\alpha = \text{tr}[A_{kl}^{-1}J_{11}] = (A_{kl}^{-1})_{11}$, $\beta = \text{tr}[A_{kl}^{-1}J_{ij}]$, and $\chi = \text{tr}[A_{kl}^{-1}J_{11}A_{kl}^{-1}J_{ij}]$. Now applying (26) to the determinant simplifies the integration over \mathbf{r} to

$$\begin{aligned} \frac{\partial}{\partial \omega_{kl}} \langle \exp[-\mathbf{r}'(\mathbf{A}_{kl} + \omega_{kl}\mathbf{W}_{kl}^{N=1} + u\mathbf{J}_{11} + t^2\mathbf{J}_{ij})\mathbf{r}] \rangle &= \frac{1}{2}\pi^{3n/2}|A_{kl}|^{-3/2}(1 + u\alpha + t^2\beta + ut^2(\alpha\beta - \chi))^{-3/2} \\ &\times \frac{\alpha + t^2(\alpha\beta - \chi)}{(1 + u\alpha + t^2\beta + ut^2(\alpha\beta - \chi))} \\ &= \frac{1}{2}\pi^{3n/2}|A_{kl}|^{-3/2} \frac{\alpha + t^2(\alpha\beta - \chi)}{(1 + u\alpha + t^2\beta + ut^2(\alpha\beta - \chi))^{5/2}}. \end{aligned} \quad (122)$$

The next step is to integrate over t by plugging the above back into (118) and applying the following integrals that are obtained from MATHEMATICA:

$$\int_0^{+\infty} 1/(s + rt^2)^{5/2} dt = \frac{2}{3} \left(\frac{r}{s}\right)^{-1/2} s^{-5/2} = \frac{2}{3} r^{-1/2} s^{-2}, \quad (123)$$

and

$$\int_0^{+\infty} t^2/(s + rt^2)^{5/2} dt = \frac{1}{3} \left(\frac{r}{s}\right)^{-3/2} s^{-5/2} = \frac{1}{3} r^{-3/2} s^{-1}. \quad (124)$$

With that we have

$$\begin{aligned} \langle \phi_k^{N=1} | \frac{1}{r_{ij}} | \phi_l^{N=1} \rangle &= \frac{1}{2} \frac{2}{\sqrt{\pi}} \pi^{3n/2} |A_{kl}|^{-3/2} (-1)^m \frac{\partial^m}{\partial u^m} \int_0^{+\infty} \frac{\alpha + t^2(\alpha\beta - \chi)}{(1 + u\alpha + t^2\beta + ut^2(\alpha\beta - \chi))^{-5/2}} dt \Big|_{u=0} \\ &= \frac{a}{2} \frac{2}{\sqrt{\pi}} \pi^{3n/2} |A_{kl}|^{-3/2} (-1)^m \frac{\partial^m}{\partial u^m} \\ &\times \left\{ \frac{2}{3} (\beta + u(\alpha\beta - \chi))^{-1/2} (1 + u\alpha)^{-2} + \frac{(\alpha\beta - \chi)/\alpha}{3} (\beta + u(\alpha\beta - \chi))^{-3/2} (1 + u\alpha)^{-1} \right\} \Big|_{u=0}. \end{aligned} \quad (125)$$

Finally, the partial differentiation operator can be applied. Using the well-known Leibniz formula for differentiating the n th derivative of a product of functions, Faa' di Bruno method for the n th derivative of the composite function, and setting $r = (\beta + u(\alpha\beta - \chi))$ and $s = (1 + u\alpha)$ we obtain

$$\frac{d^q r^{-1/2}}{du^q} = (-1)^q \frac{\Gamma(1/2 + q)}{\Gamma(1/2)} b^{-1/2-q} (ab - c)^q, \quad (126)$$

$$\frac{d^q r^{-3/2}}{du^q} = (-1)^q \frac{\Gamma(3/2 + q)}{\Gamma(3/2)} b^{-3/2-q} (ab - c)^q, \quad (127)$$

$$\frac{d^{q-m} s^{-1}}{du^{m-q}} = (-1)^{m-q} \frac{\Gamma(-q + m + 1)}{\Gamma(1)} a^{m-q}, \quad (128)$$

and

$$\frac{d^{q-m} s^{-2}}{du^{m-q}} = (-1)^{m-q} \frac{\Gamma(-q + m + 2)}{\Gamma(2)} a^{m-q}. \quad (129)$$

With that the final formula is

$$\begin{aligned} \langle \phi_k^{N=1} | \frac{1}{r_{ij}} | \phi_l^{N=1} \rangle &= \alpha \frac{1}{2} \frac{2}{\sqrt{\pi}} \pi^{3n/2} |A_{kl}|^{-3/2} \frac{1}{3} \frac{\alpha^m}{\sqrt{\beta}} \Gamma(m + 1) \\ &\times \left\{ \sum_{q=0}^m \gamma_3(q) \left(1 - \frac{\chi}{\alpha\beta}\right)^q \left[2(-q + m + 1) + \frac{1/2 + q}{1/2} \left(1 - \frac{\chi}{\alpha\beta}\right) \right] \right\}. \end{aligned} \quad (130)$$

To normalize the above, we need to write it in terms of $\langle \phi_k^{N=1} | \phi_l^{N=1} \rangle$. By multiplying the above by

$$\frac{6}{(3+2m) \Gamma\left(\frac{3+2m}{2}\right)}, \quad (131)$$

and replacing $\langle \phi_k^{N=1} | \phi_l^{N=1} \rangle$ with $S_{kl}^{N=1}$, the following normalized formula is obtained:

$$R_{kl}^{N=1,ij} = \frac{S_{kl}^{N=1}}{(3+2m)} \frac{\gamma_2(m)}{\sqrt{\beta}} \times \left\{ (3+2m) - \frac{\chi}{\alpha\beta} + 2 \sum_{q=1}^m \gamma_3(q) \left(1 - \frac{\chi}{\alpha\beta}\right)^q \left[(-q+m+1) + (1/2+q) \left(1 - \frac{\chi}{\alpha\beta}\right) \right] \right\}, \quad (132)$$

where

$$\gamma_2(m) = \frac{\Gamma(m+1)}{\Gamma(m+3/2)}, \quad (133)$$

and

$$\gamma_3(q) = \frac{\Gamma(1/2+q)}{\Gamma(q+1)\Gamma(1/2)}. \quad (134)$$

It is easily shown that for the $1/r_1$ potential-energy operator the above reduces to (116) with $m_k + m_l = 2m$, $\beta = \alpha$, and $\chi = \alpha^2$.

Now we consider the gradient of the potential-energy matrix element determined with respect to $(\text{vech } L_k)'$

and $(\text{vech } L_l)'$

$$\frac{\partial \alpha}{\partial (\text{vech } L_k)'} = -2 \text{vech} [A_{kl}^{-1} J_{11} A_{kl}^{-1} L_k], \quad (135)$$

$$\frac{\partial \beta}{\partial (\text{vech } L_k)'} = -2 \text{vech} [A_{kl}^{-1} J_{ij} A_{kl}^{-1} L_k], \quad (136)$$

$$\begin{aligned} \frac{\partial \chi}{\partial (\text{vech } L_k)'} &= -2 \text{vech} [A_{kl}^{-1} J_{11} A_{kl}^{-1} J_{ij} A_{kl}^{-1} L_k] \\ &- 2 \text{vech} [A_{kl}^{-1} J_{ij} A_{kl}^{-1} J_{11} A_{kl}^{-1} L_k], \end{aligned} \quad (137)$$

$$\begin{aligned} \frac{\partial R_{kl}^{N=1,ij}}{\partial (\text{vech } L_k)'} &= \frac{\partial S_{kl}^{N=1}}{\partial (\text{vech } L_k)'} \frac{R_{kl}^{N=1,ij}}{S_{kl}^{N=1}} - \frac{1}{2\beta} R_{kl}^{N=1} \frac{\partial \beta}{\partial (\text{vech } L_k)'} \\ &+ \frac{S_{kl}^{N=1}}{(3+2m)} \frac{\gamma_2(m)}{\sqrt{\beta}} \frac{\chi}{(\alpha\beta)^2} \left(\frac{\partial \alpha}{\partial (\text{vech } L_k)'} \beta + \frac{\partial \beta}{\partial (\text{vech } L_k)'} \alpha - \frac{\alpha\beta}{\chi} \frac{\partial \chi}{\partial (\text{vech } L_k)'} \right) \\ &\times \left\{ 1 + 2 \sum_{q=1}^m \gamma_3(q) \left(1 - \frac{\chi}{\alpha\beta}\right)^q \left[q(-q+m+1) \left(1 - \frac{\chi}{\alpha\beta}\right)^{-1} + q(1/2+q) + (1/2+q) \right] \right\}. \end{aligned} \quad (138)$$

This concludes the derivation of the gradient for the potential-energy matrix element.

VI. NUMERICAL ILLUSTRATION

The algorithms for the Hamiltonian matrix elements and the corresponding matrix elements of the energy gradient have been implemented in a computer program written using Fortran90 and MPI (message passing interface) parallel protocol. After checking the code for correctness using various tests, such as direct numerical integration and differentiation performed with MATHEMATICA, a production version was generated and used in the present calculations.

A diatomic model system for which very accurate calculations for an extended range of rovibrational states have been published in the literature^{13–16} is the HD⁺ ion. This system is particularly interesting to be calculated with a non-Born-Oppenheimer approach because in the highest bound vibrational states the electronic charge distribution becomes asymmetric as a result of the electron becoming more stable when its density shifts towards the deuteron and away from the proton. This effect is purely nonadiabatic in nature and

can only be described if either direct non-BO method is used in the calculation or if nonadiabatic corrections are calculated to the BO electronic wave function using the perturbation theory scheme.

In the present calculation, we considered all bound rovibrational states corresponding to the total angular momentum quantum number equal to one ($N = 1$), i.e., the $(v,1)$ states, where $v = 0, \dots, 22$. The purpose of the calculations has been to first calculate the total non-BO energies of these states and determine the corresponding $(v,0) \rightarrow (v,1)$ transition energies and the dissociation energies, and then to compare them with the literature values. This comparison is done to validate the correctness of the method implemented in this work.

The first step of the calculations has involved generating the ECG basis set for each of the 23 $(v,1)$ vibrational states. This task has been carried out independently for each state and has involved the following procedure. The starting point in the procedure involved taking the ECG basis sets generated before for the $(v,0)$ states and, by multiplying all the basis functions by x_1 , producing the initial basis sets for the $(v,1)$ state calculations. In the next step, the ECGs in these basis sets have been variationally optimized using the gradient-based procedure. Only exponential L_k parameters have been adjusted with the m_k powers in the preexponential factor $r_1^{m_k}$ kept the same as they were in the $(v,0)$ basis functions. In the optimization procedure, the ECGs have been optimized one-by-one by cycling over the whole basis set several times. As such optimization occasionally makes functions linearly dependent, a procedure has been implemented to monitor the ECGs for linear dependency and remove/modify the functions when a linear dependency appears.

After the first optimization step has been completed for all $(v,1)$ states, the basis set for each state has been increased by a thousand ECGs, with the m_k and L_k for each added function optimized. After each basis set has been grown by a thousand functions, several cyclic optimizations have been performed for each set to increase the accuracy of the energy. The results of the basis set optimization are shown in Table I. For each state, we show the energy calculated before the addition of the thousand functions and after the addition. We also show the number of ECGs used in the calculations. One can see that the final number of functions varies from state to state and it is smaller for lower states than for the top ones. This is typical for calculating states corresponding to different excitation levels, which differ in terms of the number of nodes in their wave functions. As the higher states have more nodes than the lower states, more ECGs are needed to represent their wave functions with an accuracy which is more-less uniform throughout the whole set of states. As one notices, the addition of a thousand ECGs to each basis set, leads to very small improvement of the total energy (the largest one is of the order of 1.0×10^{-9} hartree) indicating that the energies of all states are very well converged.

In the next step, the $(v,0) \rightarrow (v,1)$ transition energies are calculated. This is done by subtracting from our best energies of the $(v,1)$ states calculated in this work the energies of the $(v,0)$ states obtained with the same number of ECGs

TABLE I. Convergence of the total energy for the $(v,1)$ rovibrational states of HD^+ with the number of ECGs (# ECGs). Energy is given in hartrees.

v	# ECGs	Energy	v	# ECGs	Energy
0	1000	-0.597698117270	1	1000	-0.588991101048
	2000	-0.597698117430		2000	-0.588991101393
2	2000	-0.580721817887	3	2000	-0.572877266933
	3000	-0.580721817949		3000	-0.572877267102
4	2000	-0.565446156398	5	2000	-0.558418853179
	3000	-0.565446156586		3000	-0.558418853772
6	3000	-0.551787358384	7	3000	-0.545545294252
	4000	-0.551787358546		4000	-0.545545294365
8	3000	-0.539687917327	9	3000	-0.534212153253
	4000	-0.539687917664		4000	-0.534212153571
10	3000	-0.529116643823	11	3000	-0.524401837382
	4000	-0.529116644298		4000	-0.524401837887
12	3000	-0.520070088900	13	3000	-0.516125824708
	4000	-0.520070089352		4000	-0.516125825569
14	4000	-0.512575697349	15	4000	-0.509428840269
	5000	-0.512575697721		5000	-0.509428841143
16	5000	-0.506697146745	17	5000	-0.504395560512
	6000	-0.506697147635		6000	-0.504395562033
18	5000	-0.502542374245	19	6000	-0.501159138174
	6000	-0.502542376164		7000	-0.501159139178
20	6000	-0.500269319648	21	6000	-0.499902780157
	7000	-0.500269319879		7000	-0.499902780540
22	6000	-0.499864341698			
	7000	-0.499864342032			

as used for the $(v,1)$ states. The results are shown in Table II and compared with the transition energies taken from other works, where the calculations were performed using the standard approach based on the zeroth-order on the BO approximation. As one can see, the present results differ by less than 0.001 cm^{-1} from the results obtained by Blaist-Kurti *et al.*¹³ except for the next to the last state where the difference increases to 0.0011 cm^{-1} . The last $v = 22$ state was not calculated by Blaist-Kurti *et al.*,¹³ but for this state, as well as for two lower states, there are very accurate results obtained by Wolniewicz and Orlikowski.¹⁶ As one can see in the table, our results agree with these latter results to 0.001 cm^{-1} , as well as with the experimental results.^{17,18}

Finally, in Table III we show dissociation energies calculated for the $(v,0)$ and $(v,1)$ states obtained using our non-BO energies. Our results are compared with the results of Moss,¹⁴ Wolniewicz and Orlikowski,¹⁶ and Blaist-Kurti.¹³ As one can see, our results are very close to the results obtained by those authors. However, as one can also notice, the dissociation energies for the $(v,0)$ states obtained in the present calculations are somewhat closer to the literature results than the energies for the $(v,1)$ states. However, the overall agreement is still very good. For example, for the top three states our results for both $(v,0)$ and $(v,1)$ states agree with very accurate results of Wolniewicz and Orlikowski¹⁶ to 0.001 cm^{-1} .

VII. SUMMARY

In conclusion, a new very accurate method for direct variational non-BO calculations of first-rotationally excited states

TABLE II. The total energy of the ($v,0$) rovibrational states of HD^+ in hartrees, energy difference between the ($v,0$) and ($v,1$) states, Δ in cm^{-1} , difference between Δ obtained in this work and Δ taken from calculations performed by others in cm^{-1} , and difference between the Δ obtained in this work and the experimental Δ .

v	Energy($v,0$)	Δ	Present ^a	Present ^b	Present ^c	Present ^d	Exp ^e -present
0	-0.597897968559	43.8623	-0.0010	-0.0024			
1	-0.589181829407	41.8600	-0.0010	-0.0024			
2	-0.580903700198	39.9185	-0.0008	-0.0021			
3	-0.573050546421	38.0304	-0.0009	-0.0021			
4	-0.565611041956	36.1882	-0.0009	-0.0021			
5	-0.558575520587	34.3844	-0.0008	-0.0020			
6	-0.551935948624	32.6118	-0.0008	-0.0020			
7	-0.545685914996	30.8627	-0.0007	-0.0019			
8	-0.539820640551	29.1293	-0.0007	-0.0018			
9	-0.534337013108	27.4035	-0.0006	-0.0018			
10	-0.529233634746	25.6764	-0.0005	-0.0017			
11	-0.524510909642	23.9385	-0.0004	-0.0017			
12	-0.520171143833	22.1789	-0.0003	-0.0015			
13	-0.516218708875	20.3855	-0.0003	-0.0014			
14	-0.512660191254	18.5442	-0.0005	-0.0015			
15	-0.509504647351	16.6375	-0.0002	-0.0013			
16	-0.506763873460	14.6446	-0.0002	-0.0011	-0.004		
17	-0.504452691198	12.5384	0.0004	-0.0009	-0.003		-0.001 ^e
18	-0.502589226577	10.2825	0.0001	-0.0006	-0.003		
19	-0.501194793353	7.8252	0.0000	-0.0007	-0.004		
20	-0.500292453455	5.0772	0.0000	-0.0005	0.016	0.000	
21	-0.499910359334	1.6634	0.0011	-0.0002	-0.064	-0.001	-0.0006 ^e
22	-0.499865778314	0.3152		0.0000	-0.049	0.000	-0.0002 ^e

^aReference 13.^bReference 14.^cReference 15.^dReference 16.

^eThe experimental values for the (21,0)→(21,1) and (22,0)→(22,1) transitions are taken from Ref. 18; the experimental value for the (17,0)→(17,1) transition is determined using the (17,0)→(22,0) and (17,1)→(22,1) transitions taken from Ref. 17, and the (22,0)→(22,1) transition s taken from Ref. 18.

of diatomic molecules with σ electrons utilizing explicitly correlated all-particle Gaussian functions have been developed and implemented in this work. The above-shown comparison with the literature results validates the correctness of the algorithms and of the corresponding computer code which have been generated in this work. As the method is not limited

to any particular number of electrons, several interesting applications concerning rovibrational states of diatomics can be performed. Particularly interesting would be the application of the new method to systems with more than two electrons which are more scarce than those for one- and two-electron systems. Such applications will be forthcoming.

TABLE III. Comparison of the dissociation energies obtained in this work for the ($v,0$) and ($v,1$) states of HD^+ with the literature values. All results are in cm^{-1} .

v/N	Present study		Present ^a		Present ^b		Present ^c	
	0	1	0	1	0	1	0	1
0	21 516.0097	21 472.1474	-0.0001	0.0023			-0.0001	0.0009
1	19 603.0382	19 561.1783	0.0000	0.0023			0.0000	0.0009
2	17 786.1989	17 746.2803	0.0000	0.0022			0.0000	0.0009
3	16 062.6308	16 024.6004	0.0001	0.0022			0.0001	0.0010
4	14 429.8483	14 393.6602	0.0001	0.0021			0.0001	0.0009
5	12 885.7299	12 851.3455	0.0001	0.0021			0.0001	0.0009
6	11 428.5123	11 395.9005	0.0001	0.0021			0.0001	0.0009
7	10 056.7885	10 025.9258	0.0001	0.0020			0.0001	0.0008
8	8769.5095	8740.3802	0.0003	0.0021			0.0003	0.0010
9	7565.9924	7538.5889	0.0001	0.0019			0.0002	0.0008
10	6445.9303	6420.2539	0.0002	0.0019			0.0003	0.0008
11	5409.4120	5385.4735	0.0001	0.0018			0.0004	0.0008

TABLE III. (*Continued.*)

v/N	Present study		Present ^a		Present ^b		Present ^c	
	0	1	0	1	0	1	0	1
12	4456.9435	4434.7646	0.0009	0.0024			0.0011	0.0014
13	3589.4843	3569.0987	0.0003	0.0018			0.0004	0.0008
14	2808.4799	2789.9357	0.0003	0.0018			0.0003	0.0008
15	2115.9181	2099.2805	0.0009	0.0023			0.0010	0.0013
16	1514.3877	1499.7431	0.0010	0.0021			0.0009	0.0011
17	1007.1419	994.6035	0.0017	0.0026			0.0017	0.0013
18	598.1586	587.8762	0.0017	0.0022			0.0001	-0.0001
19	292.1159	284.2907	0.0013	0.0020			0.0014	0.0014
20	94.0752	88.9980	0.0002	0.0007	0.001	0.001	0.0002	0.0002
21	10.2152	8.5519	0.0005	0.0006	0.000	0.001	-0.0012	-0.0024
22	0.4308	0.1156	0.0001	0.0001	-0.001	-0.001		

^aReference 14.^bReference 16.^cReference 13.

ACKNOWLEDGMENTS

This work has been supported in part by the National Science Foundation (NSF) through the graduate research fellowship program (GRFP) awarded to Keeper L. Sharkey; Grant No. DGE1-1143953. We are grateful to the University of Arizona Center of Computing and Information Technology for the use of their computer resources.

- ¹J. Mitroy, S. Bubin, W. Horiuchi, Y. Suzuki, L. Adamowicz, W. Cencek, K. Szalewicz, J. Komasa, D. Blume, and K. Varga, *Rev. Mod. Phys.* **85**, 693 (2013).
- ²S. Bubin, M. Pavanello, W. C. Tung, K. L. Sharkey, and L. Adamowicz, *Chem. Rev.* **113**, 36 (2013).
- ³D. B. Kinghorn and R. D. Poshusta, *Int. J. Quantum Chem.* **62**, 223 (1997).
- ⁴D. B. Kinghorn and L. Adamowicz, *Phys. Rev. Lett.* **83**, 2541 (1999).
- ⁵M. Cafiero and L. Adamowicz, *Int. J. Quantum Chem.* **107**, 2679 (2007).

⁶S. Bubin and L. Adamowicz, *J. Chem. Phys.* **128**, 114107 (2008).⁷D. B. Kinghorn and L. Adamowicz, *J. Chem. Phys.* **110**, 7166 (1999).⁸K. L. Sharkey and L. Adamowicz, *J. Chem. Phys.* **134**, 194114 (2011).⁹K. L. Sharkey, N. Kirnosov, and L. Adamowicz, *J. Chem. Phys.* **138**, 104107 (2013).¹⁰K. L. Sharkey, M. Pavanello, S. Bubin, and L. Adamowicz, *Phys. Rev. A* **80**, 062510 (2009).¹¹K. L. Sharkey, S. Bubin, and L. Adamowicz, *J. Chem. Phys.* **134**, 044120 (2011).¹²K. L. Sharkey, S. Bubin, and L. Adamowicz, *Phys. Rev. A* **83**, 012506 (2011).¹³G. G. Balint-Kurti, R. E. Moss, I. A. Sadler, and M. Shapiro, *Phys. Rev. A* **41**, 4913 (1990).¹⁴R. E. Moss, *Mol. Phys.* **78**, 371 (1993).¹⁵R. A. Kennedy, R. E. Moss, and I. A. Sadler, *Mol. Phys.* **64**, 177 (1988).¹⁶L. Wolniewicz and T. Orlowski, *Mol. Phys.* **74**, 103 (1991).¹⁷A. Carrington, I. R. McNab, and C. A. Montgomerie, *Mol. Phys.* **65**, 751 (1988).¹⁸A. Carrington, I. R. McNab, C. A. Montgomerie, and J. M. Brown, *Mol. Phys.* **66**, 1279 (1989).

APPENDIX E

Charge asymmetry in rovibrationally excited HD+ determined using explicitly correlated all-particle Gaussian functions

Charge asymmetry in rovibrationally excited HD⁺ determined using explicitly correlated all-particle Gaussian functions

Nikita Kirnosov,¹ Keeper L. Sharkey,² and Ludwik Adamowicz^{1,2,a)}

¹Department of Physics, University of Arizona, Tucson, Arizona 85721, USA

²Department of Chemistry and Biochemistry, University of Arizona, Tucson, Arizona 85721, USA

(Received 23 September 2013; accepted 13 November 2013; published online 27 November 2013)

Very accurate non-Born-Oppenheimer quantum-mechanical calculations are performed to determine the average values of the interparticle distances and the proton-deuteron density function for the rovibrationally excited HD⁺ ion. The states corresponding to excitations to all bound vibrational states ($v = 0, \dots, 22$) and simultaneously excited to the first excited rotational state ($N = 1$) are considered. To describe each state up to 8000 explicitly correlated all-particle Gaussian functions are used. The nonlinear parameters of the Gaussians are variationally optimized using a procedure that employs the analytical energy gradient determined with respect to these parameters. The results show an increasing asymmetry in the electron distribution with the vibrational excitation as the electron density shifts towards deuteron and away from the proton. © 2013 AIP Publishing LLC.
[\[http://dx.doi.org/10.1063/1.4834596\]](http://dx.doi.org/10.1063/1.4834596)

I. INTRODUCTION

Due to asymmetric mass distribution the HD⁺ molecular ion has been an interesting model system for studies of the nonadiabatic coupling between the electronic and nuclear motions. The charge asymmetry of the HD⁺ has been investigated both theoretically^{1–6} and experimentally.^{7–9} Ben-Itzhak *et al.*⁸ studied the dissociation of HD⁺ in the electronic ground state following ionization of HD by fast proton impact and discovered that the H⁺ + D(1s) dissociation channel is more likely than the H(1s) + D⁺ channel by about 7%. This symmetry breakdown can only be explained if the finite nuclear mass correction to the Born-Oppenheimer (BO) approximation is taken into account. In the non-BO calculations performed with explicitly correlated Gaussian functions,^{1,2} it was shown that, while in the first 21 vibrational states ($v = 0, 1, \dots, 20$) only minor charge asymmetry is present in the wave functions, in the highest two states ($v = 21$ and $v = 22$) HD⁺ is strongly polarized and the system can be described as a complex of D atom interacting with a distant proton (D + H⁺ is also the lowest energy dissociation product of the HD⁺ ion). In this work we investigate the effects of the rotational excitation on the charge asymmetry in the HD⁺ system.

II. THE HAMILTONIAN

Let us begin with placing a molecule consisting of N_{nuc} nuclei and N_{elec} electrons in a laboratory (*lab*) frame of Cartesian coordinates. Let in this system the position of i th particle with mass M_i and charge Q_i be described by vector \mathbf{R}_i . The nonrelativistic total Hamiltonian for the system is

$$\hat{H}_{lab} = -\sum_{i=1}^{N_{tot}} \frac{1}{2M_i} \nabla_{\mathbf{R}_i}^2 + \sum_{i=1, j>i}^{N_{tot}} \frac{Q_i Q_j}{R_{ij}}, \quad (1)$$

^{a)}Author to whom correspondence should be addressed. Electronic mail: ludwik@u.arizona.edu

where $\nabla_{\mathbf{R}_i}$ is the gradient with respect to the particle coordinates, $R_{ij} = |\mathbf{R}_j - \mathbf{R}_i|$, and $N_{tot} = N_{elec} + N_{nuc}$. We can rigorously separate the center-of-mass motion from the internal motion of the particles using a transformation to a new coordinate system whose first three coordinates are the Cartesian coordinates of the center of mass in the laboratory coordinate system (\mathbf{r}_0) and the remaining $3(N_{tot} - 1)$ coordinates (\mathbf{r}_i) are the relative coordinates describing the positions of particles 2, ..., N_{tot} with respect to particle 1 called the reference particle (usually the reference particle is chosen to be the heaviest particle in the system):

$$\begin{aligned} \mathbf{r}_0 &= \sum_{j=1}^{N_{tot}} \frac{M_j}{M_{tot}} \mathbf{R}_j, \\ \mathbf{r}_i &= \mathbf{R}_{i+1} - \mathbf{R}_1, \end{aligned} \quad (2)$$

where index i varies from 1 to $n_{tot} = N_{tot} - 1$. The internal motion is represented by the following internal Hamiltonian:

$$\begin{aligned} \hat{H} &= -\frac{1}{2} \left(\sum_{i=1}^{n_{tot}} \frac{1}{\mu_i} \nabla_{\mathbf{r}_i}^2 + \sum_{i \neq j}^{n_{tot}} \frac{1}{m_0} \nabla'_{\mathbf{r}_i} \nabla_{\mathbf{r}_j} \right) \\ &\quad + \sum_{i=1}^{n_{tot}} \frac{q_0 q_i}{r_i} + \sum_{i=1, j>i}^{n_{tot}} \frac{q_i q_j}{r_{ij}}, \end{aligned} \quad (3)$$

where $\mu_i = m_0 m_i / (m_0 + m_i)$ is the i th reduced mass, $m_i = M_{i+1}$, $q_i = Q_{i+1}$, and $r_{ij} = |\mathbf{r}_j - \mathbf{r}_i|$. One notices that \hat{H} describes the motion of n_{tot} “pseudoparticles” with masses μ_i and charges q_i in the central field of the charge of the reference particle placed in the center of the coordinate system. As \hat{H} describes a system which is atom-like, its eigenfunctions, which are also eigenfunctions of the square of the total angular momentum and its projection on a selected axis, transform as irreducible representations of the group of rotations.¹⁰

It was shown in Refs. 11 and 12 that the basis set consisting of explicitly correlated Gaussian functions with preexponential multipliers x_1 and $r_1^{m_k}$

$$\phi_k^{N=1} = x_1 r_1^{m_k} \exp[-\mathbf{r}'(A_k \otimes I_3) \mathbf{r}] \quad (4)$$

is suitable for accurately describing nonadiabatic states of a diatomic system with the total angular momentum equal to one ($N = 1$). In function (4), the positive-definite symmetric matrix A_k contains the nonlinear parameters of the Gaussian, \mathbf{r} is a $3n \times 1$ vector of the internal Cartesian coordinates of the n pseudoparticles, and I_3 is a 3×3 identity matrix. The prime ("') denotes the vector/matrix transposition. The $r_1^{m_k}$ term (r_1 is the distance between the two nuclei) uniformly shifts the Gaussian peak some distance away from the origin, allows the basis to go to zero when the r_1 distance becomes zero, and describes the nodal properties of the wave function in excited vibrational states. In our calculations the m_k power is an even-number variational parameter which can vary from 1 to 250. x_1 in (4) ensures the correct angular behavior of the wave function consistent with the $N = 1$ total angular momentum.

It should be noted that (in general) the basis function (4) should contain the premultiplier x_i instead of x_1 in the prefactor, but since electrons are much lighter than nuclei, we can safely assume that the excitation to the $N = 1$ state almost exclusively involves exciting the nuclear motion and not the motion of the electrons. For HD^+ such an electron excitation, which can mix with the corresponding excitation of the nuclear motion, would involve promoting the electron to a π state, which is high on the energy scale. It should be also noted that, as the overlap integral between Gaussian (4) and a Gaussian where x_1 is replaced by x_2 is not zero if the off-diagonal elements of matrix A_k are not zero, some contributions of the x_2 -type Gaussians are included in the calculations even if the basis set only includes x_1 -type Gaussians. This is certainly not the most effective way to include these contributions (the most effective way would be to include them directly), but if they are very small it should suffice.

The algorithms for calculating the Hamiltonian and overlap matrix elements, as well as for calculating the matrix elements of the analytic energy gradient determined with respect to the nonlinear parameters of the Gaussians, for $N = 1$ rovibrational states of diatomic molecules, including the HD^+ ion, were derived in our previous work.¹¹ The calculations of the energies of all 23 bound vibrational states of HD^+ shown in that work provided an illustration of the procedure. In the present work the wave functions generated in Ref. 11 are used to calculate the average interparticle distances and the internuclear density function (also called the nuclear correlation function) for the considered states. The main focus of the work is the analysis of how the rovibrational excitation affects the charge asymmetry in HD^+ .

III. FORMULA DERIVATION

The following general p -dimensional Gaussian integral is the primary integral form used when evaluating matrix elements (whether those elements are Hamiltonian, overlap, or

any particular expectation value):

$$\int_{-\infty}^{+\infty} \exp[-x'Xx + y'x] dx = \frac{\pi^{p/2}}{|X|^{1/2}} \exp\left[\frac{1}{4}y'X^{-1}y\right]. \quad (5)$$

In the above formula, x is a p -component vector of variables, A is a symmetric $p \times p$ positive-definite matrix, y is a p -component constant vector, and X^{-1} is the inverse of X . To apply this formula, it is advantageous to represent all terms in the integrand (the Gaussian basis functions and all multiplicative factors) as Gaussian functions. To determine the nuclear correlation function the delta function involved in the formula is also written in the form of a Gaussian function.

A. Nuclear correlation function

The Gaussian representation of the 3D Dirac delta function is used to evaluate the matrix elements for the nucleus-nucleus correlation function for a diatomic molecule in an $N = 1$ excited state:

$$\begin{aligned} & \langle \phi_k^{N=1} | \delta(\mathbf{r} - \boldsymbol{\xi}) | \phi_l^{N=1} \rangle \\ &= \langle (x_1) \phi_k^{N=0} | \delta(\mathbf{r} - \boldsymbol{\xi}) | (x_1) \phi_l^{N=0} \rangle \\ &= \lim_{\beta \rightarrow \infty} \left(\frac{\beta}{\pi} \right)^{3/2} \langle (x_1^2) r_1^{m_k+m_l} \exp[-\mathbf{r}'(\mathbf{A}_{kl} + \beta \mathbf{J}_{11}) \mathbf{r} \\ & \quad + 2\beta \boldsymbol{\xi}'(a'_1 \otimes I_3) \mathbf{r} - \beta \boldsymbol{\xi}' \boldsymbol{\xi}] \rangle, \end{aligned} \quad (6)$$

where $\boldsymbol{\xi}$ is a vector of coordinates of a point at which the nuclear correlation function is determined. The plotting of the correlation function is done by first calculating this function on a grid of points and then plotting the results. β is the limit variable in the Gaussian representation of the 3D Dirac delta function. \mathbf{J}_{11} is a $3n \times 3n$ symmetric matrix defined as: $\mathbf{J}_{11} = J_{11} \otimes I_3$, where J_{11} is an $n \times n$ matrix with only one element equal to one in the (1,1) position built from $J_{11} = a_1 a'_1$, where a_1 is a n -component vector with zeros everywhere except in the first position.

In the next step of the derivation a Gaussian transformation is used to represent the pre-exponential multipliers of the two Gaussians involved in the matrix element. The product of the pre-exponential multipliers $x_1 \times x_1 = x_1^2$ is represented in the Gaussian form as

$$x_1^2 = -\frac{\partial}{\partial \omega} \exp[-\omega \mathbf{r}' \mathbf{W} \mathbf{r}] \Big|_{\omega=0}, \quad (7)$$

where ω is the differentiation variable and \mathbf{W} is a $3n \times 3n$ matrix with only one element of value one in the (1, 1) position and zeros everywhere else. It should be mentioned that I_3 cannot be factored from \mathbf{W} , i.e., $\mathbf{W} \neq W \otimes I_3$. The product of pre-exponential multipliers $r_1^{m_k} r_1^{m_l} = r_1^{m_k+m_l}$ is also represented in the Gaussian form as

$$r_1^{m_k+m_l} = (-1)^{\frac{m_k+m_l}{2}} \frac{\partial^{\frac{m_k+m_l}{2}}}{\partial u^{\frac{m_k+m_l}{2}}} \exp[-u \mathbf{r}' \mathbf{J}_{11} \mathbf{r}] \Big|_{u=0}, \quad (8)$$

where the u is the differentiation variable. Let $m = (m_k + m_l)/2$. With this the integral becomes

$$\begin{aligned} & \langle \phi_k^{N=1} | \delta(\mathbf{r} - \boldsymbol{\xi}) | \phi_l^{N=1} \rangle \\ &= (-1)^{m+1} \frac{\partial}{\partial \omega} \frac{\partial^m}{\partial u^m} \lim_{\beta \rightarrow \infty} \left(\frac{\beta}{\pi} \right)^{3/2} \\ & \quad \times \langle \exp[-\mathbf{r}'(\mathbf{A}_{kl} + (\beta + u)\mathbf{J}_{11} + \omega\mathbf{W})\mathbf{r}] \\ & \quad + 2\beta\boldsymbol{\xi}'(a'_1 \otimes I_3)\mathbf{r} - \beta\boldsymbol{\xi}'\boldsymbol{\xi}] \rangle \Big|_{u=\omega=0}. \end{aligned} \quad (9)$$

Applying (5) to the above and taking the limit as β approaches infinity involve a Taylor series expansion and some matrix transformations. The outcome of this exercise has been shown as an intermediate result in Refs. 13 and 14. In fact, in the latter paper, one derivative was determined after taking the limit. The corresponding derivative operation in this work is $-\partial/\partial\omega$ and, therefore, using the result from Refs. 13 and 14, the following is immediately obtained:

$$\langle \phi_k^{N=1} | \delta(\mathbf{r}_1 - \boldsymbol{\xi}) | \phi_l^{N=1} \rangle = \xi_x^2 \langle \phi_k^{N=0} | \delta(\mathbf{r}_1 - \boldsymbol{\xi}) | \phi_l^{N=0} \rangle. \quad (10)$$

By rewriting the formula in terms of the overlap integral¹¹ the following is obtained:

$$\begin{aligned} & \langle \phi_k^{N=1} | \phi_l^{N=1} \rangle \\ &= \frac{2}{3} \pi^{(3n-1)/2} |A_{kl}|^{-3/2} \alpha^{m+1} \left(m + \frac{3}{2} \right) \Gamma \left(m + \frac{3}{2} \right), \end{aligned} \quad (11)$$

where $\alpha = (A_{kl}^{-1})_{11}$. Finally the following is obtained:

$$\begin{aligned} & \langle \phi_k^{N=1} | \delta(\mathbf{r}_1 - \boldsymbol{\xi}) | \phi_l^{N=1} \rangle \\ &= \langle \phi_k^{N=1} | \phi_l^{N=1} \rangle \left(\frac{6}{3+2m} \right) \frac{1}{2\pi \Gamma(m + \frac{3}{2})} \alpha^{-5/2} \xi_x^2 \left(\frac{\xi_x^2}{\alpha} \right)^m \\ & \quad \times \exp \left[-\frac{\xi_x^2}{\alpha} \right]. \end{aligned} \quad (12)$$

This concludes the derivation of the nuclear correlation function.

B. Average interparticle distances

To evaluate the expectation values of interparticle distances ($\langle r_{ij} \rangle$) with the non-BO $N = 1$ wave function the following relation is used:

$$r_{ij}^{-1} = \frac{2}{\sqrt{\pi}} \int_0^\infty \exp[-t^2 r_{ij}^2] dt. \quad (13)$$

Since $r_{ij} = r_{ij}^2/r_{ij}$, we can represent r_{ij} as

$$\begin{aligned} r_{ij} &= \frac{2}{\sqrt{\pi}} \int_0^\infty r_{ij}^2 \exp[-t^2 r_{ij}^2] dt \\ &= -\frac{\partial}{\partial \gamma} \frac{2}{\sqrt{\pi}} \int_0^\infty \exp[-(t^2 + \gamma)\mathbf{r}'\mathbf{J}_{ij}\mathbf{r}] dt|_{\gamma=0}, \end{aligned} \quad (14)$$

and then the matrix element of the expectation value with the basis functions $\phi_k^{N=1}$ and $\phi_l^{N=1}$ can be written as

$$\begin{aligned} & \langle \phi_k^{N=1} | r_{ij} | \phi_l^{N=1} \rangle \\ &= (-1)^m \frac{2}{\sqrt{\pi}} \frac{\partial}{\partial \gamma} \frac{\partial}{\partial \omega} \frac{\partial^m}{\partial u^m} \int_0^\infty \langle \exp[-\mathbf{r}'(\mathbf{A}_{kl} + \omega\mathbf{W} + \mathbf{u}\mathbf{J}_{11} \\ & \quad + (t^2 + \gamma)\mathbf{J}_{ij})\mathbf{r}] \rangle dt \Big|_{\gamma=\omega=u=o}. \end{aligned} \quad (15)$$

Equation (122) from the potential energy derivation shown in Ref. 11 immediately yields integration over \mathbf{r} :

$$\begin{aligned} & -\frac{\partial}{\partial \omega} \langle \exp[-\mathbf{r}'(\mathbf{A}_{kl} + \omega\mathbf{W} + \mathbf{u}\mathbf{J}_{11} + (t^2 + \gamma)\mathbf{J}_{ij})\mathbf{r}] \rangle|_{\omega=0} \\ &= \frac{1}{2} \pi^{3n/2} |A_{kl}|^{-3/2} \\ & \quad \times \frac{\alpha + (t^2 + \gamma)(\alpha\beta - \chi)}{(1 + u\alpha + (t^2 + \gamma)\beta + u(t^2 + \gamma)(\alpha\beta - \chi))^{5/2}}, \end{aligned} \quad (16)$$

where $\beta = \text{tr}[A_{kl}^{-1} J_{ij}]$ and $\chi = \text{tr}[A_{kl}^{-1} J_{11} A_{kl}^{-1} J_{ij}]$. Next we apply $-\partial/\partial\gamma$ to the above and obtain the following:

$$\begin{aligned} & -\frac{\partial}{\partial \gamma} \int_0^\infty \frac{\alpha + (t^2 + \gamma)(\alpha\beta - \chi)}{(1 + u\alpha + (t^2 + \gamma)\beta + u(t^2 + \gamma)(\alpha\beta - \chi))^{5/2}} dt \Big|_{\gamma=0} \\ &= \frac{1}{3} \frac{\chi + 3\alpha(\beta + u(\alpha\beta - \chi))}{(1 + \alpha u)^3 (\beta + u(\alpha\beta - \chi))^{1/2}}. \end{aligned} \quad (17)$$

Finally we take the $(-1)^n \partial^n / \partial u^n$ derivative. After applying the Leibniz and Faa Di Bruno formulas the following is obtained:

$$\frac{\partial^n}{\partial u^n} \frac{1}{(1 + \alpha u)^3} \Big|_{u=0} = (-1)^n \alpha^n \frac{\Gamma(n+3)}{\Gamma(3)}, \quad (18)$$

$$\begin{aligned} & \frac{\partial^n}{\partial u^n} \frac{1}{(\beta + u(\alpha\beta - \chi))^{1/2}} \Big|_{u=0} \\ &= (-1)^n (\alpha\beta - \chi)^n \beta^{-n-1/2} \frac{\Gamma(n+1/2)}{\Gamma(1/2)}, \end{aligned} \quad (19)$$

and

$$\begin{aligned} & \frac{\partial^n}{\partial u^n} (\beta + u(\alpha\beta - \chi))^{1/2} \Big|_{u=0} \\ &= (-1)^n (\alpha\beta - \chi)^n \beta^{1/2-n} (-1/2)_n, \end{aligned} \quad (20)$$

where $(x)_n$ is a Pochhammer symbol. Now one can apply the Leibniz formula and after some rearrangement the following

TABLE I. The convergence of the total energy and some expectation values involving interparticle distances for the $v = 22$ state with the number of the basis functions (K). All quantities are expressed in atomic units.

K	E	$\langle r_{dp} \rangle$	$\langle r_{de} \rangle$	$\langle r_{pe} \rangle$	$\langle r_{dp}^2 \rangle$	$\langle r_{de}^2 \rangle$	$\langle r_{pe}^2 \rangle$
1000	-0.4998518601	20.81309798	1.819888001	20.53105321	458.7510388	7.085406975	457.1731248
2000	-0.4998643218	35.08555795	1.551042561	35.06196102	1414.711596	3.639133601	1416.77289
3000	-0.4998643389	35.34866671	1.551914622	35.32414937	1452.088547	3.651517233	1454.13787
4000	-0.4998643413	35.47303704	1.551978876	35.44842811	1470.831535	3.652596283	1472.88009
5000	-0.4998643417	35.46903403	1.552034539	35.44437200	1470.601019	3.653445646	1472.64868
6000	-0.4998643419	35.47070779	1.552058351	35.44602242	1471.135261	3.653785862	1473.182576
7000	-0.4998643421	35.46808699	1.552099031	35.44336231	1470.907782	3.654366541	1472.954496
8000	-0.4998643421	35.46784927	1.552103730	35.44312008	1470.903784	3.654435028	1472.950427

is obtained:

$$\begin{aligned} & \langle \phi_k^{N=1} | r_{ij} | \phi_l^{N=1} \rangle \\ &= \frac{S_{kl}^{N=1} \gamma_2(m)}{4(m+3/2)\alpha\sqrt{\beta}} \left((m+1)(m+2)(3\alpha\beta + \chi) \right. \\ &+ \sum_{k=1}^m (m-k+1)(m-k+2)\gamma_3(k) \\ &\times \left. \left(1 - \frac{\chi}{\alpha\beta} \right)^k \left(\chi - \frac{3\alpha\beta}{2k-1} \right) \right), \end{aligned} \quad (21)$$

where

$$\begin{aligned} \gamma_2(m) &= \frac{\Gamma(m+1)}{\Gamma(m+3/2)}, \\ \gamma_3(k) &= \frac{\Gamma(k+1/2)}{\Gamma(k+1)\Gamma(1/2)}. \end{aligned}$$

To evaluate the matrix elements for the average values of the squared interparticle distances, $\langle r_{ij}^2 \rangle$, we can write the expectation value in the following form:

$$\begin{aligned} \langle \phi_k^{N=1} | r_{ij}^2 | \phi_l^{N=1} \rangle &= (-1)^m \frac{\partial}{\partial \gamma} \frac{\partial}{\partial \omega} \frac{\partial^m}{\partial u^m} \langle \exp[-\mathbf{r}'(\mathbf{A}_{kl} + \omega \mathbf{W} \\ &+ u \mathbf{J}_{11} + \gamma \mathbf{J}_{ij}) \mathbf{r}] \rangle \Big|_{\gamma=\omega=u=0}. \end{aligned} \quad (22)$$

Applying Eq. (16) and taking the m th derivative with respect to u , we obtain

$$\begin{aligned} & (-1)^{m+1} \frac{\partial}{\partial \omega} \frac{\partial^m}{\partial u^m} \langle \exp[-\mathbf{r}'(\mathbf{A}_{kl} + \omega \mathbf{W} + u \mathbf{J}_{11} + \gamma \mathbf{J}_{ij}) \mathbf{r}] \rangle \Big|_{\omega=u=0} \\ &= \frac{1}{4} \pi^{3n/2} |A_{kl}|^{-3/2} (\alpha + \gamma(\alpha\beta - \chi))^{m+1} \\ &\times (1 + \gamma\beta)^{-m-5/2} \frac{\Gamma(m+5/2)}{\Gamma(5/2)}. \end{aligned} \quad (23)$$

Taking the derivative with respect to γ and rearranging the expression the result can be expressed in terms of the overlap as

$$\langle \phi_k^{N=0} | r_{ij}^2 | \phi_l^{N=1} \rangle = \frac{1}{2\alpha} S_{kl}^{N=1} (3\alpha\beta + 2(1+m)\chi). \quad (24)$$

IV. RESULTS

In recent years there has been an ongoing discussion concerning the concepts of the molecular geometry and the molecular structure in the context of the non-BO approach (for example, see Refs. 15–21). Since the nuclei are treated on equal footing with the electrons in this approach, i.e., as quantum particles, the concept of the molecular geometry becomes elusive. The information about the molecular structure available from the non-BO wave function is provided as expectation values of the structural parameters such as the interparticle distances.

As it is usually the case, well converged values of the interparticle distance is much harder to obtain than well converge values of the total energies. The results shown in Table I, where some expectation values calculated for the $v = 22$, $N = 1$ rovibrational state of HD^+ , provide examples of this behavior. As this state is located very close to the dissociation limit and has many radial oscillations it is the hardest to describe. Thus the convergence pattern of its expectation values provides a good test of how converged our results for the expectation values and the total energy are. Very likely the convergence for the lower states is better than for the $v = 22$ state. Upon examining the convergence of the expectation values shown in Table I we conclude that at least four significant figures for each expectation value are converged. The energy is converged much better than that. All figures shown in the table are converged.

The calculated average interparticle distances and the averages of the squares of the internuclear distances for all 23 vibrational states of HD^+ corresponding to the $N = 1$ total rotational quantum number are presented in Table II. As expected, the expectation value of the internuclear distance, $\langle r_{dp} \rangle$, increases with the vibrational excitation, and this increase accelerates for top states. In the table we also show the differences between the expectation values calculated for the $N = 0$ and $N = 1$ states. Due to the rotational excitation the $\langle r_{dp} \rangle$ values are, as expected, consistently larger for the $N = 1$ states than for the $N = 0$ states. For the top $v = 22$, $N = 1$ state $\langle r_{dp} \rangle$ increases by as much as 6.849 a.u. Similarly as for the $N = 0$ vibrational states also for the $N = 1$ states the electron charge asymmetry is increasing with the vibrational excitation. In the top $v = 22$ state the electron is completely shifted from the proton to the deuteron and the bond, which is covalent in low vibrational levels, becomes purely

TABLE II. Dissociation energies (in millihartrees) and expectation values (in a.u.) of the deuteron-proton distance, r_{dp} , the deuteron-electron distance, r_{de} , and the proton-electron distance, r_{pe} , and their squares for the $v = 0, \dots, 22, N = 1$ rovibrational levels of HD^+ . Δ is the difference between the corresponding quantities of the $N = 1$ and $N = 0$ states. For example, $\Delta\langle r_{dp} \rangle = \langle r_{dp}^{N=1} \rangle - \langle r_{dp}^{N=0} \rangle$. All quantities are expressed in atomic units.

v	E_{dis}	$\langle r_{dp} \rangle$	$\langle r_{de} \rangle$	$\langle r_{pe} \rangle$	$\langle r_{dp}^2 \rangle$	$\langle r_{de}^2 \rangle$	$\langle r_{pe}^2 \rangle$	ΔE_{dis}	$\Delta\langle r_{dp} \rangle$	$\Delta\langle r_{de} \rangle$	$\Delta\langle r_{pe} \rangle$	$\Delta\langle r_{dp}^2 \rangle$	$\Delta\langle r_{de}^2 \rangle$	$\Delta\langle r_{pe}^2 \rangle$
0	97.83430222	2.057	1.689	1.690	4.277	3.538	3.541	-0.1998511395	0.0018	0.0008	0.0015	0.0087	0.0044	0.0041
1	89.12728619	2.173	1.751	1.752	4.864	3.844	3.848	-0.1907280143	0.0024	0.0007	0.0015	0.0091	0.0053	0.0046
2	80.85800275	2.294	1.815	1.816	5.502	4.175	4.179	-0.1818822487	0.0020	0.0016	0.0015	0.0101	0.0056	0.0055
3	73.0134519	2.419	1.881	1.882	6.197	4.532	4.537	-0.1732793185	0.0020	0.0008	0.0009	0.0116	0.0064	0.0061
4	65.58234139	2.549	1.950	1.951	6.955	4.921	4.927	-0.1648853694	0.0021	0.0017	0.0009	0.0126	0.0064	0.0061
5	58.55503857	2.685	2.026	2.023	7.785	5.346	5.353	-0.1566668155	0.0020	0.0015	0.0010	0.0137	0.0071	0.0072
6	51.92354335	2.828	2.097	2.099	8.697	5.812	5.821	-0.1485900780	0.0027	0.0019	0.0016	0.0154	0.0083	0.0080
7	45.68147917	2.978	2.176	2.178	9.706	6.327	6.338	-0.1406206304	0.0032	0.0013	0.0013	0.0172	0.0089	0.0088
8	39.82410246	3.138	2.260	2.263	10.83	6.899	6.913	-0.1327228892	0.0029	0.0014	0.0019	0.0178	0.0108	0.0105
9	34.34833837	3.309	2.350	2.353	12.08	7.539	7.557	-0.1248595366	0.0036	0.0021	0.0022	0.0239	0.0122	0.0118
10	29.2528291	3.493	2.447	2.450	13.50	8.263	8.286	-0.1169904485	0.0036	0.0015	0.0024	0.0231	0.0131	0.0140
11	24.53802269	3.693	2.551	2.556	15.12	9.090	9.121	-0.1090717542	0.0038	0.0021	0.0020	0.0337	0.0161	0.0156
12	20.20627415	3.913	2.666	2.672	17.00	10.05	10.09	-0.1010544812	0.0040	0.0018	0.0022	0.0380	0.0171	0.0185
13	16.26201037	4.159	2.793	2.802	19.20	11.17	11.23	-0.0928833064	0.0048	0.0022	0.0028	0.0405	0.0215	0.0196
14	12.71188252	4.438	2.937	2.949	21.84	12.52	12.60	-0.0844935329	0.0058	0.0030	0.0028	0.0502	0.0276	0.0324
15	9.565025943	4.761	3.102	3.120	25.08	14.17	14.30	-0.0758062081	0.0071	0.0032	0.0035	0.0741	0.0372	0.0373
16	6.833332435	5.146	3.297	3.324	29.20	16.25	16.46	-0.0667258250	0.0082	0.0047	0.0046	0.0942	0.0494	0.0535
17	4.531746833	5.622	3.532	3.578	34.68	18.98	19.37	-0.0571291649	0.0112	0.0054	0.0062	0.1281	0.0615	0.0706
18	2.678560964	6.243	3.828	3.918	42.45	22.75	23.58	-0.0468504123	0.0157	0.0070	0.0083	0.1952	0.0939	0.1107
19	1.295323978	7.123	4.207	4.436	54.70	28.29	30.59	-0.0356541750	0.0242	0.0091	0.0149	0.3536	0.1554	0.2138
20	0.405504679	8.601	4.572	5.565	78.64	35.82	47.39	-0.0231335763	0.0508	0.0031	0.0487	0.8966	0.1617	0.7466
21	0.038965340	13.27	2.189	12.63	184.9	11.49	178.6	-0.0075787947	0.3225	-0.1169	0.4405	8.895	-1.4541	10.44
22	0.000526832	35.47	1.552	35.44	1471.	3.654	1473.	-0.0014362818	6.849	-0.0479	6.894	561.0	-0.6118	561.7

ionic. In this state the average deuteron-electron distance of 1.552 a.u. is very close to $\langle r_{de} \rangle = 1.500$ in the deuterium atom. Strong asymmetry of the electron density is significant only in the two top vibrational levels. To explain this phenomenon one needs to compare the stability of the hydrogen and deuterium atoms. Due to the slightly larger reduced mass of the pseudoelectron in D than in H, D is a slightly more stable system. Thus, near the dissociation limit the electron is increasingly more “attracted” to the deuteron resulting in the charge asymmetry which eventually leads to the $\text{D} + \text{H}^+$ dissociation channel being lower in energy than the $\text{H} + \text{D}^+$ channel.

Another property allowing to elucidate the non-BO $N = 1, v = 0, \dots, 22$, rovibrational states is the nuclear correlation functions. In Fig. 1 we compare the correlation functions for the 1st, 4th, 10th, and 18th, $N = 1$ vibrational states with the corresponding $N = 0$ states. One can see that, while rotationless ($N = 0$) states are spherically symmetric, the $N = 1$ states are not. In Fig. 1 the nuclear correlation functions for $N = 1$ states are shown at the cross section along the xy plane. The cross section along the xz plane is identical to the xy cross section, but along the yz plane the $N = 1$ nuclear correlation function is zero.

Similar to the $N = 0$ case, the $N = 1$ nuclear correlation function shows an oscillatory behavior with number of oscillations equal to v . Also, the spatial extent of the correlation function increases with the increasing vibrational quantum number. In all states the highest density maximum is the one closest to the origin of the coordinate system and the last

maximum is the broadest. In the top two states, $v = 21$ and 22, there is a dramatic increase of the extend of the correlation function. The last maximum for the $v = 22$ state is shifted beyond 20 a.u.

We found it interesting to compare some details of the nuclear correlations functions for the $v = 20, 21$, and $22, N = 0$ and $N = 1$ states. This comparison is shown in 2D plots of the correlation function along the x axis in Fig. 2. Upon a careful inspection of the tails of these functions we notice that the last minimum in the $v = 21$ and 22 functions for both $N = 0$ and $N = 1$ shows a gap between the axis and the curve representing the function. The last minimum in the curves does not touch the x axis indicating that there is no node of the function at this point. There is a simple explanation of this behavior. In non-BO calculations the electronic and nuclear motions are coupled. In a lower state the corresponding non-BO wave function is to a very good approximation a product of a single electronic, a single vibrational, and a single rotational wave function. In the top states, state mixing is more significant due to degeneracy. In the non-BO wave functions for these states, besides the contribution from the single component that dominates the wave functions for the lower states, other components may appear, where an excited electronic state is combined with vibrational wave functions with lower v values. Such a contribution would not have nodes in the same points as the main component. This leads to the behavior one sees in Fig. 2. It is easy to see which electronic wave functions become degenerate especially at larger internuclear separation. A

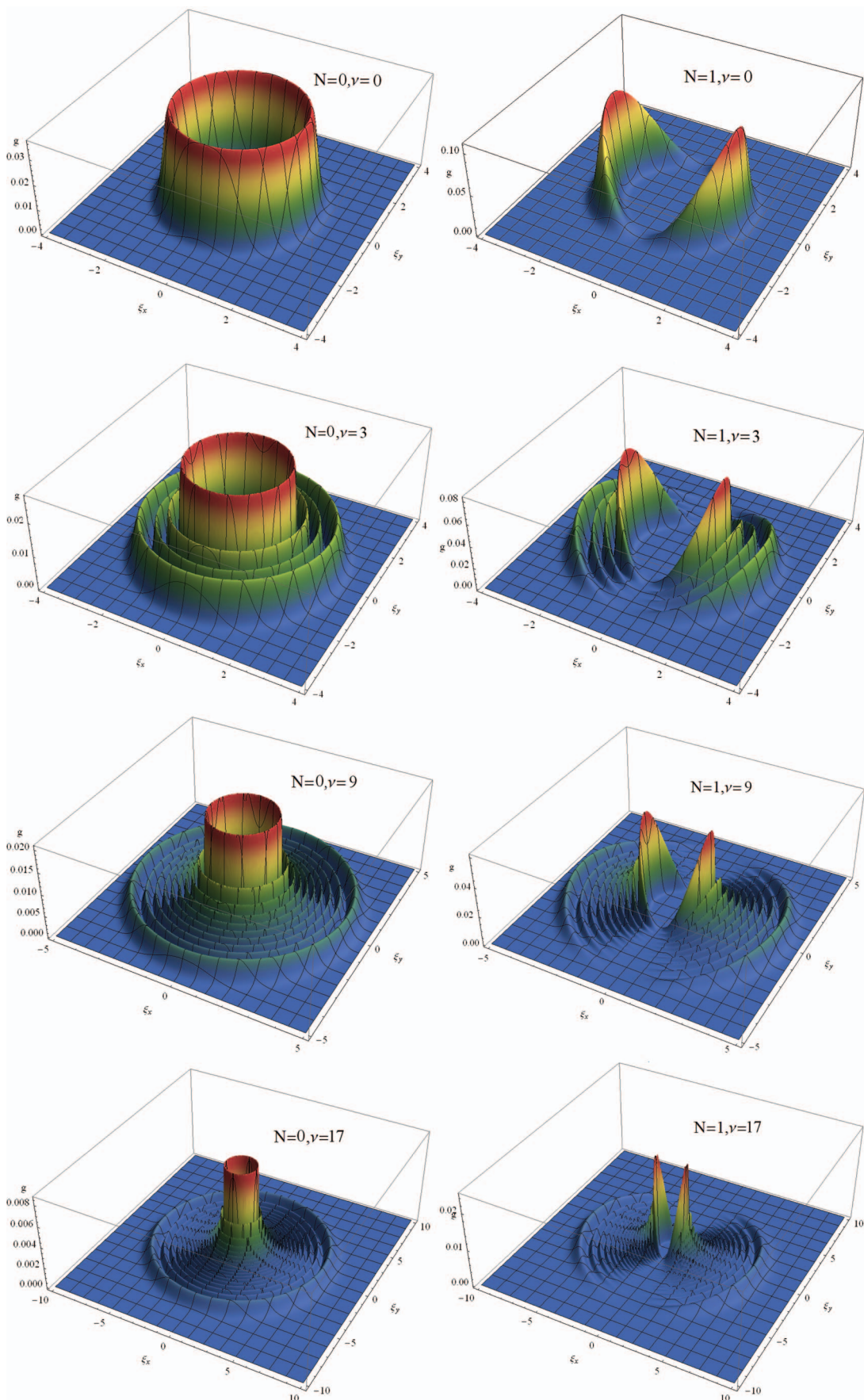


FIG. 1. Comparison of the nuclear correlation functions for the $v = 0, 3, 9$, and $17, N = 0$ states (on the left) and the $v = 0, 3, 9$, and $17, N = 1$ states (on the right) of HD^+ .

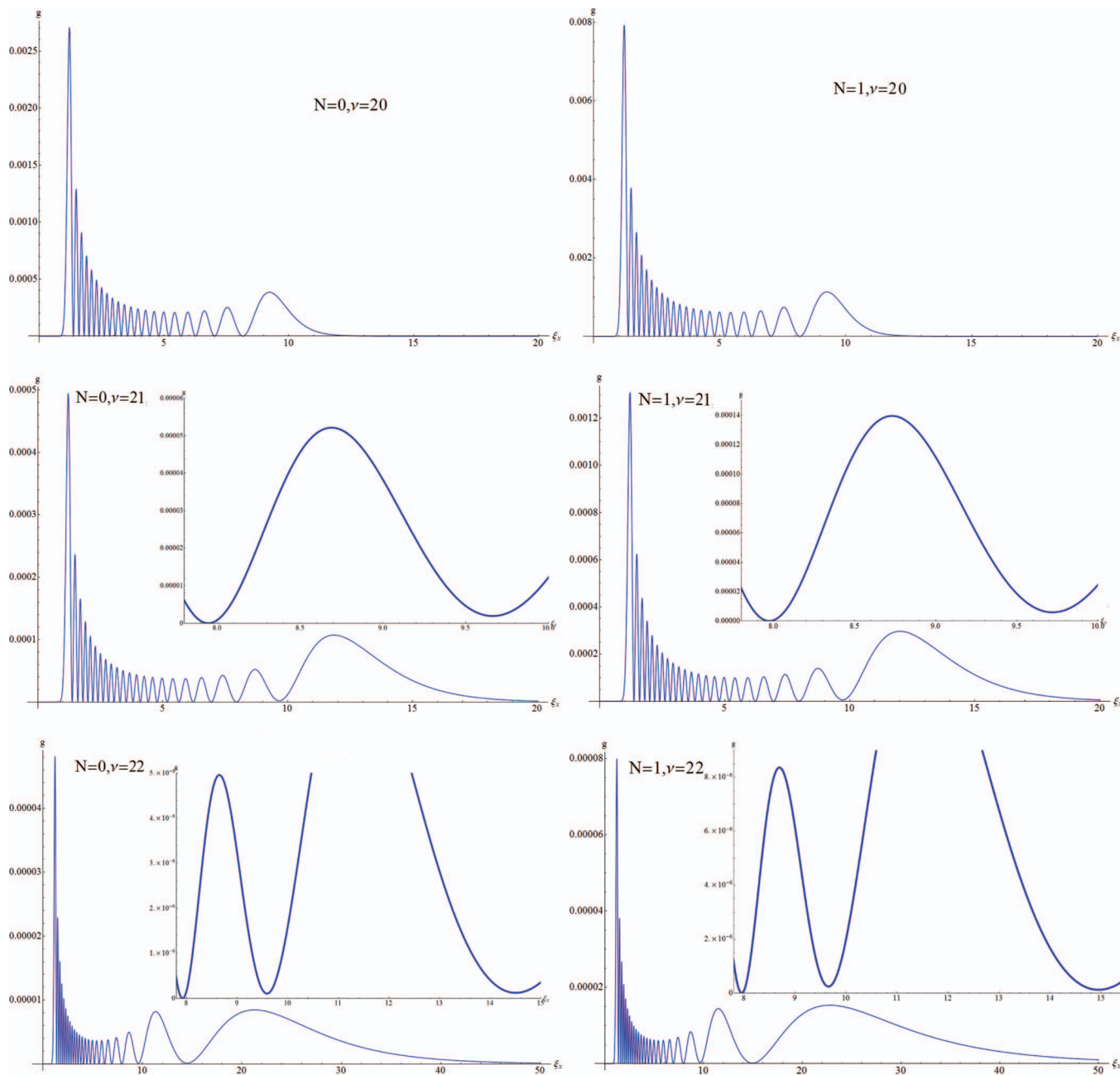


FIG. 2. The nuclear correlation functions for the $v = 20, 21$, and 22 , $N = 0$ states (on the left) and the $v = 20, 21$, and 22 , $N = 1$ states (on the right) of HD^+ .

pair of such functions includes the function which describes the electron localization at the deuteron and a function which describes its localization at the proton. Perhaps, due to the contribution of the latter function to the total non-BO wave function of the $v = 22$ state, there is non-zero probability of HD^+ dissociating not only to $\text{D} + \text{H}^+$ but also to $\text{H} + \text{D}^+$.

V. CONCLUSION

To summarize, explicitly correlated Gaussian functions are used in highly accurate description of the HD^+ system in rovibrational states corresponding to $v = 0, \dots, 22$ and $N = 1$. Calculations are performed without the Born-Oppenheimer approximation and all three particles forming

HD^+ are treated on equal footing. The non-BO wave functions are used to calculate the nuclear correlation function and some expectation values involving interparticle distances. As previously observed for the $N = 0$ states of HD^+ , charge asymmetry appears in the electronic density. It increases with the vibrational excitation. In effect, the bond in the HD^+ ion, which is covalent in the lower vibrational states, becomes ionic in the top two states. This transformation of the nature of the bond is a purely nonadiabatic effect.

ACKNOWLEDGMENTS

We are grateful to the University of Arizona Research Computing Center for the use of their computer resources. This work has been supported in part by the National Science

Foundation through the graduate research fellowship awarded to Keeper L. Sharkey, Grant No. DGE1-1143953.

- ¹S. Bubin and L. Adamowicz, *Chem. Phys. Lett.* **403**, 185 (2005).
- ²S. Bubin, E. Bednarz, and L. Adamowicz, *J. Chem. Phys.* **122**, 041102 (2005).
- ³R. E. Moss and I. A. Sadler, *Mol. Phys.* **61**, 905 (1987).
- ⁴B. D. Esry and H. R. Sadeghpour, *Phys. Rev. A* **60**, 3604 (1999).
- ⁵R. E. Moss and L. Valenzano, *Mol. Phys.* **100**, 649 (2002).
- ⁶K. Strasburger, *J. Chem. Phys.* **131**, 134103 (2009).
- ⁷A. Carrington, I. R. McNab, and C. A. Montgomerie, *J. Phys. B* **22**, 3551 (1989).
- ⁸I. Ben-Itzhak, E. Wells, K. D. Carnes, V. Krishnamurthi, O. L. Weaver, and B. D. Esry, *Phys. Rev. Lett.* **85**, 58 (2000).
- ⁹A. Carrington, I. R. McNab, C. A. Montgomerie-Leach, and R. A. Kennedy, *Mol. Phys.* **72**, 735 (1991).
- ¹⁰M. Cafiero, S. Bubin, and L. Adamowicz, *Phys. Chem. Chem. Phys.* **5**, 1491 (2003).
- ¹¹K. L. Sharkey, N. Kirnosov, and L. Adamowicz, *J. Chem. Phys.* **139**, 164119 (2013).
- ¹²K. L. Sharkey, N. Kirnosov, and L. Adamowicz, *Phys. Rev. A* **88**, 032513 (2013).
- ¹³K. L. Sharkey, M. Pavanello, S. Bubin, and L. Adamowicz, *Phys. Rev. A* **80**, 062510 (2009).
- ¹⁴K. L. Sharkey and L. Adamowicz, *J. Chem. Phys.* **134**, 194114 (2011).
- ¹⁵M. Tachikawa and Y. Osamura, *Theor. Chem. Acc.* **104**, 29 (2000).
- ¹⁶J. R. Mohalleb, *J. Mol. Struct., Theochem.* **709**, 11 (2004).
- ¹⁷A. M. Kuznetsov and I. G. Medvedev, *Chem. Phys.* **324**, 148 (2006).
- ¹⁸E. Mátyus, J. Hutter, U. Müller-Herold, and M. Reiher, *J. Chem. Phys.* **135**, 204302 (2011).
- ¹⁹E. Mátyus, J. Hutter, U. Müller-Herold, and M. Reiher, *Phys. Rev. A* **83**, 052512 (2011).
- ²⁰M. Goli and Sh. Shahbazian, *Theor. Chem. Acc.* **131**, 1208 (2012).
- ²¹M. Goli and Sh. Shahbazian, *Theor. Chem. Acc.* **132**, 1365 (2013).

APPENDIX F

Lifetimes of rovibrational levels of HD⁺

Lifetimes of rovibrational levels of HD⁺

Nikita Kirnosov,¹ Keeper L. Sharkey,² and Ludwik Adamowicz^{1,2,*}

¹Department of Physics, University of Arizona, Tucson, Arizona 85721, USA

²Department of Chemistry and Biochemistry, University of Arizona, Tucson, Arizona 85721, USA

(Received 6 December 2013; published 27 January 2014; corrected 30 January 2014)

A method for calculating the oscillator strengths for rovibrational transitions of a diatomic system within an approach that is not based on the Born-Oppenheimer (BO) approximation is presented. The non-BO wave functions representing the bound states of the system are expanded in terms of explicitly correlated Gaussian functions. The method is applied to calculate oscillator strengths for the HD⁺ ion for transitions between rotationless vibrational states and vibrational states which are rotationally singly excited. The effect of the asymmetry of the HD⁺ charge distribution on the oscillator strengths and on the lifetimes of the states is elucidated.

DOI: 10.1103/PhysRevA.89.012513

PACS number(s): 33.15.Mt, 33.70.Ca

I. INTRODUCTION

The simplest heteronuclear diatomic molecule, HD⁺, is a popular model for highly accurate quantum-mechanical calculations. The HD⁺ dissociation energies corresponding to bound rovibrational states of the system were extensively studied in calculations performed with various methods [1–11]. The lifetimes of the states and the oscillator strengths corresponding to interstate transitions were also investigated by methods based on the Born-Oppenheimer (BO) approximation [12,13] and methods where the BO approximation was not assumed [9,10]. Due to the HD⁺ uneven charge distribution which is caused by the mass difference between the proton and the deuteron and which increases with vibrational and rotational excitation [14,15], this ion is an interesting system to study. In the current article we calculate the oscillator strengths between vibrational levels in the $N(0 \rightarrow 1)$ rotational band and investigate the charge asymmetry effect on the lifetimes of the rotationless levels. Here these quantities are calculated without the Born-Oppenheimer approximation for the whole vibrational spectrum of HD⁺.

II. THE METHOD

We consider the oscillator strengths of the transitions between rovibrational states with the rotational quantum numbers $N = 0$ and $N = 1$. In general, the oscillator strength of the $N \leftarrow N + 1$ rotational transition is given by the following formula:

$$f_{i \rightarrow f} = \frac{2}{3(2N_f + 1)} (E_i - E_f) |\langle \psi_i | \hat{T} | \psi_f \rangle|^2. \quad (1)$$

In the present calculations, $N_f = 0$, $|\psi_i\rangle = |\psi_v^{N=0}\rangle = \sum_k c_k r_1^{m_k} \exp[-\mathbf{r}' \mathbf{A}_k \mathbf{r}]$, and $|\psi_f\rangle = |\psi_v^{N=1}\rangle = \sum_l c_l x_1 r_1^{m_l} \exp[-\mathbf{r}' \mathbf{A}_l \mathbf{r}]$, and E_i and E_f are the corresponding state energies. For HD⁺ the \mathbf{r} vector consists of six Cartesian coordinates. The first three of them, x_1 , y_1 , and z_1 , are the coordinates of the vector which describes the position of the proton with respect to the deuteron, and the last three, x_2 , y_2 , and z_2 , are the coordinates of the vector which describes the

position of the electron with respect to the deuteron. The prime denotes the vector transposition. \mathbf{A}_k and \mathbf{A}_l are symmetric $3n \times 3n$ matrices of exponential parameters and c_k and c_l are linear expansion coefficients of the wave functions in terms of the Gaussian basis functions. The internal coordinate system used in the calculations, the form of the wave functions, and the major mathematical relations to calculate the needed Hamiltonian and overlap matrix elements are presented in detail in Ref. [11]. Operator \hat{T} in (1) is defined in the following way:

$$\hat{T} = \sum_{j=1}^n \left[\sum_{i=0}^n q_i \left(\delta_{ij} - \frac{m_j}{M} \right) \right] x_j, \quad (2)$$

where n is a number of particles in the system minus one (i.e., the number of pseudoparticles), q_i and m_j are charges and masses of the particles, respectively (index 0 corresponds to the reference particle located in the center of the internal coordinate system), and M is total mass of the system. In the present calculations the deuteron is the reference particle, and the two pseudoparticles are the pseudoproton and pseudoelectron. We use the term pseudoparticle, because, while the particles described by the internal Hamiltonian have the same charges as the original particles, their masses are not the original masses, but the reduced masses. For HD⁺ the \hat{T} operator in atomic units is

$$\hat{T}(\text{HD}^+) = \left(1 - \frac{m_p}{M} \right) x_1 - \left(1 + \frac{1}{M} \right) x_2. \quad (3)$$

In (3), $M = m_p + m_d + 1$ is the sum of the mass of the proton, m_p , the mass of the deuteron, m_d , and the mass of the electron, 1.

To calculate $f_{i \rightarrow f}$ the following two integrals need to be evaluated: $\langle \phi_k^{N=0} | x_j | \phi_l^{N=1} \rangle$, $j = 1$ and 2. The first integral with x_1 corresponds to the proton and the second integral with x_2 corresponds to the electron. Using the overlap integral derived for two $N = 1$ wave functions in Ref. [11] the following is obtained:

$$\begin{aligned} \langle \phi_k^{N=0} | x_j | \phi_l^{N=1} \rangle &= \frac{\pi^{\frac{3n-1}{2}}}{|A_{kl}|^{3/2}} \Gamma \left[\frac{3 + m_k + m_l}{2} \right] \frac{m_k + m_l + 3}{3} \\ &\times (A_{kl}^{-1})_{11}^{\frac{m_k+m_l}{2}} (A_{kl}^{-1})_{j1}. \end{aligned} \quad (4)$$

*Corresponding author: ludwik@u.arizona.edu

After including the proper normalization factor, $1/\sqrt{\langle\phi_k^{N=0}|\phi_k^{N=0}\rangle\langle\phi_l^{N=1}|\phi_l^{N=1}\rangle}$, the normalized expression for the integral is

$$\begin{aligned} & \frac{\langle\phi_k^{N=0}|x_j|\phi_l^{N=1}\rangle}{\sqrt{\langle\phi_k^{N=0}|\phi_k^{N=0}\rangle\langle\phi_l^{N=1}|\phi_l^{N=1}\rangle}} \\ &= \gamma_1(m_k, m_l) \frac{3 + m_k + m_l}{\sqrt{3(3 + 2m_l)}} S_{kl} \\ & \times \left(\frac{(A_{kl}^{-1})_{11}}{(A_k^{-1})_{11}} \right)^{\frac{m_k}{2}} \left(\frac{(A_{kl}^{-1})_{11}}{(A_l^{-1})_{11}} \right)^{\frac{m_l}{2}} \frac{(A_{kl}^{-1})_{1j}}{(A_l^{-1})_{11}^{1/2}}, \quad (5) \end{aligned}$$

where

$$\gamma_1 = \frac{2^{\frac{m_k+m_l}{2}} \Gamma\left[\frac{3+m_k+m_l}{2}\right]}{\sqrt{\Gamma[m_k+3/2] \Gamma[m_l+3/2]}}, \quad (6)$$

$$S_{kl} = 2^{\frac{3n}{2}} \frac{\|L_k\|^{3/2} \|L_l\|^{3/2}}{|A_{kl}|^{3/2}}. \quad (7)$$

III. RESULTS

The total non-BO wave functions for the rovibrational states of HD^+ corresponding to the $N = 0$ and $N = 1$ total rotational quantum numbers and to all 23 bound vibrational states are expanded in terms of 1000–9000 explicitly correlated Gaussian (ECG) functions which allowed to converge energy up to the ninth decimal place. As the oscillatory nature of the vibrational states increases with the level of excitation [15], more Gaussians are needed for the higher states than for the lower ones. These ECGs for $N = 0$ rovibrational states were obtained in Ref. [14] and for $N = 1$ in Ref. [11]. The ECG basis for each state was generated and optimized in a separate calculation. The oscillator strengths and transition probabilities per unit time for all possible 23^2 transitions corresponding to the $N(0 \rightarrow 1)$ excitations and all possible vibrational excitations and deexcitations (including the pure rotational excitations, i.e., where the system is rotationally excited, but remains in the same vibrational state) are calculated.

TABLE I. Oscillator strengths for $N(1 \rightarrow 0)$ transitions. Vibrational numbers v correspond to $N = 0$ states, and v' to $N = 1$. Notation $a[b]$ means $a \times 10^b$. Every second line is a rounded value obtained by Tian *et al.*

v	0	1	2	3	4	5
0	1.567[-05]	6.838[-06]	2.179[-07]	1.598[-08]	1.879[-09]	3.046[-10]
	1.566[-05]	6.839[-06]	2.180[-07]	1.599[-08]	1.881[-09]	3.049[-10]
1	-7.857[-06]	1.670[-05]	1.322[-05]	6.190[-07]	5.901[-08]	8.459[-09]
	-7.858[-06]	1.669[-05]	1.322[-05]	6.192[-07]	5.904[-08]	8.464[-09]
2	-2.227[-07]	-1.527[-05]	1.774[-05]	1.916[-05]	1.175[-06]	1.368[-07]
	-2.227[-07]	-1.527[-05]	1.773[-05]	1.917[-05]	1.175[-06]	1.369[-07]
3	-1.548[-08]	-6.356[-07]	-2.224[-05]	1.880[-05]	2.468[-05]	1.862[-06]
	-1.549[-08]	-6.358[-07]	-2.225[-05]	1.879[-05]	2.469[-05]	1.862[-06]
4	-1.763[-09]	-5.747[-08]	-1.212[-06]	-2.880[-05]	1.987[-05]	2.978[-05]
	1.764[-09]	-5.749[-08]	-1.213[-06]	-2.880[-05]	1.986[-05]	2.978[-05]
5	-2.792[-10]	-7.973[-09]	-1.339[-07]	-1.931[-06]	-3.493[-05]	2.096[-05]
	-2.794[-10]	-7.977[-09]	-1.339[-07]	-1.932[-06]	-3.494[-05]	2.095[-05]

TABLE II. Oscillator strengths for $N(1 \rightarrow 0)$ transitions. Vibrational numbers v correspond to $N = 0$ states, and v' to $N = 1$.

v	v'											
	0	1	2	3	4	5	6	7	8	9	10	11
0	1.567[-05]	6.838[-06]	2.179[-07]	1.598[-08]	1.879[-09]	3.046[-10]	6.259[-11]	1.550[-11]	4.468[-12]	1.467[-12]	5.351[-13]	2.162[-13]
1	-7.857[-06]	1.670[-05]	1.322[-05]	6.190[-07]	5.901[-08]	8.459[-09]	1.605[-09]	3.759[-10]	1.040[-10]	3.306[-11]	1.182[-11]	4.599[-12]
2	-2.227[-07]	-1.527[-05]	1.774[-05]	1.916[-05]	1.175[-06]	1.368[-07]	2.298[-08]	4.971[-09]	1.301[-09]	3.970[-10]	1.372[-10]	5.286[-11]
3	-1.548[-08]	-6.356[-07]	-2.224[-05]	1.880[-05]	2.468[-05]	1.862[-06]	2.547[-07]	4.883[-08]	1.182[-08]	3.410[-09]	1.134[-09]	4.223[-10]
4	-1.763[-09]	-5.747[-08]	-1.212[-06]	-2.880[-05]	1.987[-05]	2.978[-05]	2.661[-06]	4.168[-07]	8.947[-08]	2.388[-08]	7.515[-09]	2.698[-09]
5	-2.792[-10]	-7.973[-09]	-1.339[-07]	-1.931[-06]	-3.493[-05]	2.096[-05]	3.445[-05]	3.555[-06]	6.260[-07]	1.484[-07]	4.323[-08]	1.471[-08]
6	-5.636[-11]	-1.478[-09]	-2.176[-08]	-2.506[-07]	-2.775[-06]	-4.064[-05]	2.206[-05]	3.870[-05]	4.529[-06]	8.848[-07]	2.293[-07]	7.227[-08]
7	-1.378[-11]	-3.402[-10]	-4.601[-09]	-4.649[-08]	-4.122[-07]	-3.728[-06]	-4.592[-05]	2.317[-05]	4.249[-05]	5.570[-06]	1.196[-06]	3.360[-07]
8	-3.918[-12]	-9.284[-11]	-1.184[-09]	-1.100[-08]	-8.564[-08]	-6.224[-07]	-4.777[-06]	-5.074[-05]	2.429[-05]	4.581[-05]	6.664[-06]	1.561[-06]
9	-1.265[-12]	-2.916[-11]	-3.561[-10]	-3.119[-09]	-2.234[-08]	-1.428[-07]	-8.849[-07]	-5.911[-06]	-5.507[-05]	2.543[-05]	4.862[-05]	7.792[-06]
10	-4.766[-13]	-1.029[-11]	-1.216[-10]	-1.022[-09]	-6.908[-09]	-4.066[-08]	-2.220[-07]	-1.203[-06]	-7.118[-06]	-5.888[-05]	2.658[-05]	5.088[-05]
11	-1.798[-13]	-4.059[-12]	-4.671[-11]	-3.775[-10]	-2.449[-09]	-1.361[-08]	-6.838[-08]	-3.272[-07]	-1.581[-06]	-8.383[-06]	-6.211[-05]	2.775[-05]
12	-7.756[-14]	-1.711[-12]	-1.935[-11]	-1.545[-10]	-9.662[-10]	-5.151[-09]	-2.455[-08]	-1.084[-07]	-4.634[-07]	-2.021[-06]	-9.687[-06]	-6.469[-05]
13	-3.786[-14]	-7.990[-13]	-8.912[-12]	-6.925[-11]	-4.249[-10]	-2.195[-09]	-9.953[-09]	-4.155[-08]	-1.641[-07]	-6.355[-07]	-2.527[-06]	-1.100[-05]
14	-1.984[-14]	-4.026[-13]	-4.387[-12]	-3.309[-11]	-2.005[-10]	-1.007[-09]	-4.460[-09]	-1.788[-08]	-6.684[-08]	-2.396[-07]	-8.493[-07]	-3.100[-06]
15	-1.078[-14]	-2.133[-13]	-2.270[-12]	-1.710[-11]	-1.001[-10]	-4.999[-10]	-2.171[-09]	-8.454[-09]	-3.039[-08]	-1.032[-07]	-3.396[-07]	-1.110[-06]
16	-5.937[-15]	-1.158[-13]	-1.242[-12]	-9.474[-12]	-5.454[-11]	-2.657[-10]	-1.132[-09]	-4.303[-09]	-1.505[-08]	-4.923[-08]	-1.539[-07]	-4.687[-07]
17	-3.304[-15]	-6.591[-14]	-7.128[-13]	-5.378[-12]	-3.128[-11]	-1.501[-10]	-6.213[-10]	-2.320[-09]	-7.947[-09]	-2.536[-08]	-7.644[-08]	-2.215[-07]
18	-1.857[-15]	-3.846[-14]	-4.191[-13]	-3.098[-12]	-1.803[-11]	-8.524[-11]	-3.512[-10]	-1.299[-09]	-4.354[-09]	-1.365[-08]	-4.016[-08]	-1.129[-07]
19	-1.029[-15]	-2.201[-14]	-2.399[-13]	-1.744[-12]	-1.010[-11]	-4.731[-11]	-1.952[-10]	-7.171[-10]	-2.385[-09]	-7.356[-09]	-2.125[-08]	-5.850[-08]
20	-4.962[-16]	-1.082[-14]	-1.181[-13]	-8.496[-13]	-4.890[-12]	-2.288[-11]	-9.435[-11]	-3.452[-10]	-1.142[-09]	-3.484[-09]	-9.968[-09]	-2.705[-08]
21	-8.522[-17]	-1.856[-15]	-2.043[-14]	-1.457[-13]	-8.366[-13]	-3.924[-12]	-1.615[-11]	-5.894[-11]	-1.946[-10]	-5.910[-10]	-1.685[-09]	-4.543[-09]
22	-8.242[-18]	-1.806[-16]	-1.967[-15]	-1.409[-14]	-8.080[-14]	-3.784[-13]	-1.558[-12]	-5.688[-12]	-1.878[-11]	-5.698[-11]	-1.624[-10]	-4.375[-10]
	12	13	14	15	16	17	18	19	20	21	22	
0	9.420[-14]	4.459[-14]	2.256[-14]	1.215[-14]	6.822[-15]	3.989[-15]	2.258[-15]	1.324[-15]	6.438[-16]	1.018[-16]	6.138[-18]	
1	2.026[-12]	9.598[-13]	4.598[-13]	2.373[-13]	1.343[-13]	8.060[-14]	4.861[-14]	2.835[-14]	1.389[-14]	2.165[-15]	1.318[-16]	
2	2.253[-11]	1.021[-11]	5.009[-12]	2.657[-12]	1.490[-12]	8.602[-13]	5.025[-13]	2.820[-13]	1.364[-13]	2.137[-14]	1.287[-15]	
3	1.754[-10]	7.885[-11]	3.801[-11]	1.977[-11]	1.092[-11]	6.265[-12]	3.643[-12]	2.050[-12]	9.899[-13]	1.532[-13]	9.343[-15]	
4	1.081[-09]	4.750[-10]	2.272[-10]	1.158[-10]	6.262[-11]	3.542[-11]	2.049[-11]	1.155[-11]	5.585[-12]	8.693[-13]	5.276[-14]	
5	5.664[-09]	2.417[-09]	1.129[-09]	5.652[-10]	3.019[-10]	1.690[-10]	9.679[-11]	5.424[-11]	2.614[-11]	4.064[-12]	2.466[-13]	
6	2.639[-08]	1.084[-08]	4.907[-09]	2.413[-09]	1.263[-09]	6.981[-10]	3.968[-10]	2.209[-10]	1.060[-10]	1.645[-11]	9.972[-13]	
7	1.138[-07]	4.438[-08]	1.935[-08]	9.228[-09]	4.749[-09]	2.579[-09]	1.446[-09]	7.967[-10]	3.801[-10]	5.879[-11]	3.570[-12]	
8	4.726[-07]	1.712[-07]	7.094[-08]	3.259[-08]	1.631[-08]	8.710[-09]	4.807[-09]	2.623[-09]	1.244[-09]	1.921[-10]	1.165[-11]	
9	1.981[-06]	6.436[-07]	2.481[-07]	1.086[-07]	5.252[-08]	2.717[-08]	1.477[-08]	7.991[-09]	3.768[-09]	5.796[-10]	3.514[-11]	
10	8.935[-06]	2.458[-06]	8.532[-07]	3.487[-07]	1.605[-07]	8.061[-08]	4.271[-08]	2.268[-08]	1.059[-08]	1.624[-09]	9.849[-11]	
11	5.252[-05]	1.006[-05]	2.988[-06]	1.105[-06]	4.764[-07]	2.289[-07]	1.175[-07]	6.120[-08]	2.823[-08]	4.309[-09]	2.611[-10]	
12	2.893[-05]	5.348[-05]	1.112[-05]	3.564[-06]	1.399[-06]	6.324[-07]	3.118[-07]	1.582[-07]	7.188[-08]	1.092[-08]	6.614[-10]	
13	-6.655[-05]	3.013[-05]	5.368[-05]	1.205[-05]	4.163[-06]	1.724[-06]	8.072[-07]	3.944[-07]	1.758[-07]	2.636[-08]	1.596[-09]	
14	-1.229[-05]	-6.758[-05]	3.134[-05]	5.303[-05]	1.274[-05]	4.735[-06]	2.045[-06]	9.594[-07]	4.144[-07]	6.260[-08]	3.780[-09]	
15	-3.735[-06]	-1.348[-05]	-6.768[-05]	3.258[-05]	5.148[-05]	1.299[-05]	5.173[-06]	2.252[-06]	9.538[-07]	1.343[-07]	8.148[-09]	
16	-1.421[-06]	-4.416[-06]	-1.445[-05]	-6.679[-05]	3.388[-05]	4.910[-05]	1.249[-05]	5.264[-06]	2.016[-06]	3.326[-07]	1.983[-08]	
17	-6.284[-07]	-1.774[-06]	-5.100[-06]	-1.500[-05]	-6.493[-05]	3.533[-05]	4.633[-05]	1.065[-05]	4.651[-06]	4.141[-07]	2.603[-08]	
18	-3.065[-07]	-8.140[-07]	-2.139[-06]	-5.682[-06]	-1.478[-05]	-6.262[-05]	3.726[-05]	4.529[-05]	6.009[-06]	2.682[-06]	1.469[-07]	
19	-1.543[-07]	-3.941[-07]	-9.878[-07]	-2.409[-06]	-5.941[-06]	-1.307[-05]	-6.226[-05]	4.128[-05]	5.940[-05]	8.919[-07]	2.173[-08]	
20	-7.018[-08]	-1.759[-07]	-4.255[-07]	-1.015[-06]	-2.242[-06]	-5.478[-06]	-8.018[-06]	-7.943[-05]	6.100[-05]	2.123[-04]	8.351[-06]	
21	-1.173[-08]	-2.901[-08]	-7.063[-08]	-1.566[-07]	-4.024[-07]	-5.396[-07]	-3.480[-06]	-5.952[-07]	-2.618[-04]	3.091[-04]	1.410[-05]	
22	-1.129[-09]	-2.790[-09]	-6.769[-09]	-1.510[-08]	-3.782[-08]	-5.507[-08]	-2.889[-07]	-4.784[-09]	-1.409[-05]	-6.824[-05]	3.774[-04]	

Figure 1 shows the oscillator strengths for the rotational transitions between the levels of the same vibrational band (marked with \otimes in the plot) and between the levels of two adjacent vibrational bands ($v_f = v_i + 1$; marked with \oplus in the plot). It can be seen that, while the curves behave in an expected way for lower states, the higher states do not follow that trend. This is due to the purely nonadiabatic effect which arises from the electron localization on the deuteron in the top three vibrational states. This effect cannot be described within the Born-Oppenheimer approximation. Within this approximation, one would expect the value of $\langle \psi^{N=0} | x_1 | \psi^{N=1} \rangle$ to be twice the $\langle \psi^{N=0} | x_2 | \psi^{N=1} \rangle$ value. This is because the average position of the electron predicted by a calculation where the BO approximation is assumed is always in the middle of the bond. In non-BO calculations, such as the ones carried out in this work, there should be a small

deuteron in the top three vibrational states. This effect cannot be described within the Born-Oppenheimer approximation. Within this approximation, one would expect the value of $\langle \psi^{N=0} | x_1 | \psi^{N=1} \rangle$ to be twice the $\langle \psi^{N=0} | x_2 | \psi^{N=1} \rangle$ value. This is because the average position of the electron predicted by a calculation where the BO approximation is assumed is always in the middle of the bond. In non-BO calculations, such as the ones carried out in this work, there should be a small

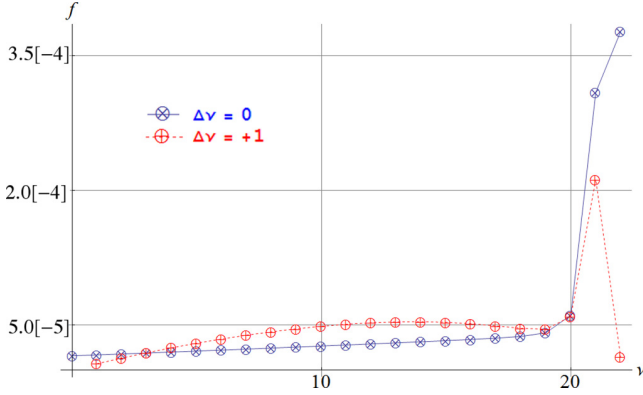


FIG. 1. (Color online) Oscillator strengths for $N(1 \rightarrow 0)$ transitions.

difference between the BO and non-BO results concerning the $\langle \psi^{N=0} | x_2 | \psi^{N=1} \rangle / \langle \psi^{N=0} | x_1 | \psi^{N=1} \rangle$ ratio for lower vibrational states. This is seen in Fig. 2 where this ratio is plotted. However, for the top three states, where the electron is much closer to the deuteron than to the proton, the BO and non-BO results are expected to diverge and this is also clearly seen in the plot.

The computed oscillator strengths can be used to calculate the transition probabilities per unit time as

$$W_{i \rightarrow f} = 2\alpha^3 \frac{2N_f + 1}{2N_f + 3} (E_i - E_f)^2 f_{i \rightarrow f}, \quad (8)$$

where α is a fine structure constant, and E_i and E_f are the energies of the initial and final states, respectively. Factor $(2N_f + 1)/(2N_f + 3)$ is introduced to reverse the transitions into the more intuitive $N + 1 \rightarrow N$ notation. The level lifetime is then calculated as

$$\tau_i = \left(\sum_{f(E_f < E_i)} W_{i \rightarrow f} \right)^{-1}. \quad (9)$$

The present calculations allow for determining the lifetimes of the rotationless levels, including the highest levels, with four significant figures. The results are shown in Table III. The results of the calculations performed by Peek *et al.* [12]

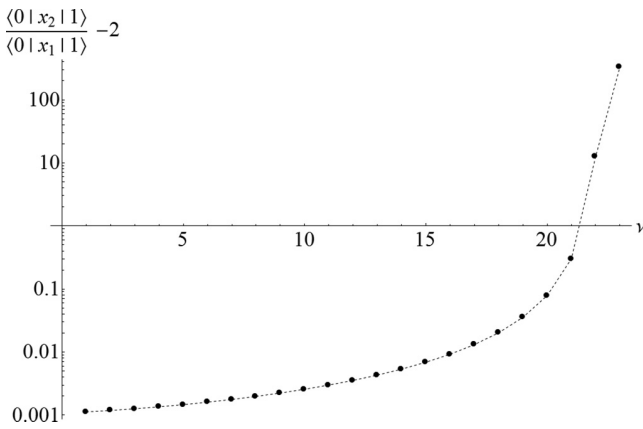


FIG. 2. Deviation from the simple BO prediction for the oscillator strength components.

TABLE III. Lifetimes of rotationless vibrational levels in ms.

v	Peek [12]	Amitay [13]	Tian [9]	Pilon [10]	Present study	Δ_{rel}
1	54.7	59	54.60856	54.60856	54.62	1.50[-4]
2	29.4	32	29.32100	29.32100	29.32	1.52[-4]
3	21.1	23	21.02754	21.02753	21.03	1.54[-4]
4	17.1	19	16.99992		17.00	1.56[-4]
5	14.7	16	14.69597		14.70	1.59[-4]
6	13.3	15				13.27
7	12.4	14				12.37
8	11.9	13				11.82
9	11.6	13				11.53
10	11.5	13				11.46
11	11.7					11.58
12	12.0					11.91
13	12.6					12.48
14	13.5					13.34
15	14.8					14.61
16	16.7					16.50
17	19.7					19.42
18	24.7					24.30
19	34.5					33.73
20	60.4					58.10
21	207.					236.8
22	2600.					2695.

and by Amitay *et al.* [13] within the BO approximation are shown for comparison. The non-BO results of Tian *et al.*, also shown in the table, were obtained by the authors using the oscillator strengths and the energies published in Ref. [9]. These values, as well as the non-BO results of Pilon *et al.* [10], are rounded off to seven significant figures in the table. Both Tian *et al.* and Pilon *et al.* results are limited to the lowest few vibrational states. All non-BO results compare well with the values obtained in the present study. The small deviations of the lifetimes obtained in the present study from those of Tian *et al.* are shown in the table as Δ_{rel} . A comparison of the present non-BO results and the BO results of Peek *et al.* [12] shows that the nonadiabatic effects are the largest for the top states. For example, for the $v = 21$ state, the BO lifetime differs from the non-BO lifetime by almost 15%.

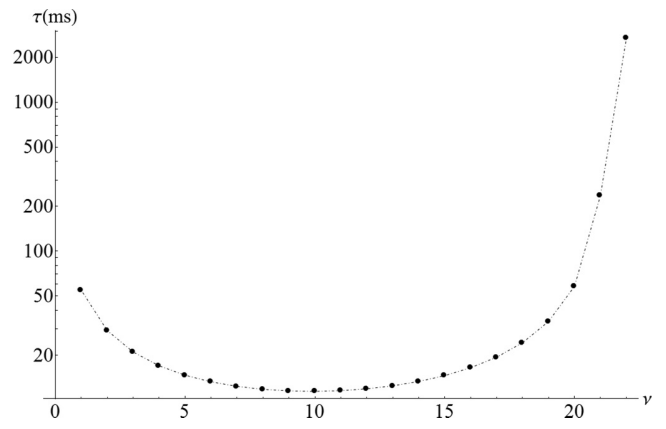


FIG. 3. Lifetimes of rotationless vibrational levels, ms.

Figure 3 visualizes the results obtained for the lifetimes. The lifetime of a particular state depends on the number of the states available for transitions originating from that state, on the corresponding transition energies, and on the corresponding oscillator strengths. As an increasingly higher excited state is considered, the number of terms in Eq. (9) increases, the transition energies in the most contributing terms become smaller, and the corresponding oscillator strengths also become smaller due to the increasing dissimilarity of the states' wave functions. These competing effects lead to the lifetimes being smaller for the intermediate states and higher for both the lower and higher states.

IV. CONCLUSIONS

The non-BO method for calculating bound states of diatomic molecules which are vibrationally excited, as well as rotationally excited to the $N = 1$ level, described in Refs. [11,18], was used in those works to determine the rovibrational energy spectrum of the HD⁺ ion. Along with the energies the corresponding wave functions were generated.

In this article the wave functions and the energies obtained in the previous HD⁺ calculations [11] are used to calculate the oscillator strengths for the transitions between all states described in the calculations. The lifetimes for the states are also calculated. It is shown that the charge asymmetry in HD⁺, which significantly increases in the top two $v = 21$ and $v = 22$ vibrational states, elongates their lifetime by up to 15%. These states are predicted to live 237 and 1695 ms, respectively. It should be mentioned that the present non-BO approach to calculate oscillator strengths and lifetimes can be easily expanded to diatomic molecules with a larger number of electrons. For example, work is currently in progress in our group on calculating these quantities for the HD molecule.

ACKNOWLEDGMENTS

We are grateful to the University of Arizona Research Computing Center for the use of their computer resources. This work has been supported in part by the National Science Foundation through the graduate research fellowship awarded to K.L.S. (Grant No. DGE1-1143953). We also thank Dr. Q. L. Tian and Dr. H. Olivares Pilon for answering questions about their studies.

-
- [1] R. E. Moss, *Mol. Phys.* **78**, 371 (1993).
 - [2] R. E. Moss, *J. Phys. B* **32**, L89 (1999).
 - [3] L. Hilico, N. Billy, B. Grémaud, and D. Delande, *Eur. Phys. J. D* **12**, 449 (2000).
 - [4] V. I. Frolov, *J. Phys. B* **35**, L331 (2002).
 - [5] Z. C. Yan and J. Y. Zhang, *J. Phys. B* **37**, 1055 (2004).
 - [6] V. I. Korobov, *Phys. Rev. A* **74**, 052506 (2006).
 - [7] J. P. Karr and L. Hilico, *J. Phys. B* **39**, 2095 (2006).
 - [8] Y. Hijikata, H. Nakashima, and H. Nakatsuji, *J. Chem. Phys.* **130**, 024102 (2009).
 - [9] Q. L. Tian, L. Y. Tang, Z. X. Zhong, Z. C. Yan, and T. Y. Shi, *J. Chem. Phys.* **137**, 024311 (2012).
 - [10] H. Olivares Pilón and D. Baye, *Phys. Rev. A* **88**, 032502 (2013).
 - [11] K. L. Sharkey, N. Kirnosov, and L. Adamowicz, *J. Chem. Phys.* **139**, 164119 (2013).
 - [12] J. M. Peek, A. R. Hashemi-Attar, and C. L. Beckel, *J. Chem. Phys.* **71**, 5382 (1979).
 - [13] Z. Amitay, D. Zajfman, and P. Forck, *Phys. Rev. A* **50**, 2304 (1994).
 - [14] S. Bubin, E. Bednarz, and L. Adamowicz, *J. Chem. Phys.* **122**, 041102 (2005).
 - [15] N. Kirnosov, K. L. Sharkey, and L. Adamowicz, *J. Chem. Phys.* **139**, 204105 (2013).
 - [16] A. Carrington, I. R. McNab, and C. A. Montgomerie, *Mol. Phys.* **64**, 679 (1988).
 - [17] A. Carrington, I. R. McNab, and C. A. Montgomerie, *Mol. Phys.* **64**, 983 (1988).
 - [18] K. L. Sharkey, N. Kirnosov, and L. Adamowicz, *Phys. Rev. A* **88**, 032513 (2013).

APPENDIX G

Charge asymmetry in the rovibrationally excited HD molecule

Charge asymmetry in the rovibrationally excited HD molecule

Nikita Kirnosov,¹ Keeper Sharkey,² and Ludwik Adamowicz^{1,2}

¹Department of Physics, University of Arizona, Tucson, Arizona 85721, USA

²Department of Chemistry and Biochemistry, University of Arizona, Tucson, Arizona 85721, USA

(Received 17 December 2013; accepted 25 February 2014; published online 13 March 2014)

The recently developed method for performing all-particle non-Born-Oppenheimer variational calculations on diatomic molecular systems excited to the first excited rotational state and simultaneously vibrationally excited is employed to study the charge asymmetry and the level lifetimes of the HD molecule. The method uses all-particle explicitly correlated Gaussian functions. The nonlinear parameters of the Gaussians are optimized with the aid of the analytical energy gradient determined with respect to these parameters. © 2014 AIP Publishing LLC. [<http://dx.doi.org/10.1063/1.4867912>]

I. INTRODUCTION

As it can be shown even with the simplest theoretical model, the average nucleus–electron distance differs in the hydrogen and deuterium atoms due to the larger mass of the nucleus in the latter. Even though this effect is subtle (on the order of $\times 10^{-4}$ bohr for H and D atoms¹), it also appears in the HD molecule, where the electron has a slightly larger reduced mass while being close to deuteron than while being close to the proton. This results in charge asymmetry in the HD molecule. The effect is purely nonadiabatic and can only be studied within an approach where the Born-Oppenheimer (BO) approximation is not assumed. The asymmetric electron behavior in HD results in appearance of a small dipole moment. We have studied the HD dipole moment in the ground state in one of our previous works² and the dipole-moment value obtained there agreed very well with the experimental value of $3.19(\pm 0.055) \times 10^{-4}$ a.u.³ Due to the non-zero dipole moment, pure rotational transitions in the HD molecule are visible in the experiment, though they are very weak. The charge asymmetry makes the HD molecule an interesting model for testing high-level quantum-mechanical methods. The calculations performed with such methods can be of interest to the astrophysics community, as HD is one of the most important molecular systems present in the interstellar space.

In our previous study, the HD charge asymmetry in the rotational ground state as a function of the vibrational quantum number was considered.¹ The non-BO calculations performed in that work showed that the asymmetry reaches maximum for the ninth ($v = 8$) vibrational excited state and then decreases for higher states to eventually approach zero at the dissociation. In the present study, we investigate the effect of rotation excitation on the HD charge asymmetry.

In the non-BO approach employed in present work, we use all-particle explicitly correlated Gaussian functions (ECGs).^{4,5} In these functions, the interparticle correlation effects are described through the dependence of the Gaussian exponents on the inter-particle distances. In addition, the Gaussians are multiplied by powers of the internuclear distance (for diatomics) or distances (for molecules with more

than two nuclei) to describe the inter-nuclear correlation. This correlation is much stronger than the inter-electron correlation because, as the nuclei are much heavier than the electrons, they avoid each other to much greater extent than the light electrons. This effect needs to be properly described in the wave function and the powers of the internuclear distance(s) facilitate this description.

The Hamiltonian (called the internal Hamiltonian) used in our non-BO calculations is obtained by rigorously separating out the operator representing the kinetic energy of the center-of-mass motion from the laboratory-frame non-relativistic Hamiltonian. The internal Hamiltonian represents the motion of pseudoparticles around the center of the internal coordinate system where the charge of the reference particle is located. We call the particles described by the internal Hamiltonian pseudoparticles because, while they have the same charges as the original particles, their masses are reduced masses (see Sec. II) not the original masses. One can call the system represented by the internal Hamiltonian a “generalized atom,” because it describes motion of charged particles (for a molecule some of these charges are equal to -1 , but some charges corresponding to pseudonuclei are positive) in the central potential created by the charge of the reference particle. As the internal Hamiltonian commutes with the square of the total angular momentum (\hat{N}^2) and its z component (\hat{N}_z), the manifold of the internal-Hamiltonian eigenfunctions can be divided into subsets, each corresponding to a different \hat{N}^2 quantum number, N . The eigenfunctions with $N = 0$ represent rotationless vibrational states. The eigenfunctions with $N = 1$ represent states where the rotational motion of the nuclei is excited to the first excited state. This again is only an approximation because angular excitations of the electrons can also contribute, although very little (as our previous calculations in Refs. 6 and 7 have shown), to the $N = 1$ wave functions. In view of the above, it is clear that direct variational single-step non-BO calculations of molecular bound ground and, particularly, excited state is not a simple matter.

In the first part of this work, we describe the method we used in the calculations (a more complete description of the method can be found in our recent reviews^{8,9}). The discussion

of the results obtained in the calculations is presented in the second part.

II. THE METHOD

As mentioned, the total non-relativistic laboratory-frame Hamiltonian of the system can be rigorously separated into an operator representing the motion of the center of mass and an operator representing the system's internal state. We perform this separation by making a transformation from the laboratory Cartesian coordinates, \mathbf{R}_i , $i = 1, \dots, N_{tot}$, where N_{tot} is the number of particles (nuclei+electrons) in the system, to an internal reference frame with origin at a selected reference particle (particle one): $\mathbf{r}_i = \mathbf{R}_{i+1} - \mathbf{R}_1$. This transformation to the internal coordinates together with the conjugate momentum transformation yields the following nonadiabatic Hamiltonian representing the internal state of the system (in atomic units):

$$\hat{H} = -\frac{1}{2} \left(\sum_{i=1}^n \frac{1}{\mu_i} \nabla_{\mathbf{r}_i}^2 + \sum_{i=1, j=1, i \neq j}^n \frac{1}{m_0} \nabla'_{\mathbf{r}_i} \nabla_{\mathbf{r}_j} \right) + \sum_{i=1}^n \frac{q_0 q_i}{r_i} + \sum_{j>i=1}^n \frac{q_i q_j}{r_{ij}}, \quad (1)$$

where m_0 is the mass of particle one (the reference particle; in the present calculations the deuteron), m_i , $i = 1, \dots, N_{tot} - 1$ are masses of particles 2, ..., N_{tot} , q_i , $i = 0, \dots, N_{tot} - 1$ are charges of particles 1, ..., N_{tot} , $\nabla_{\mathbf{r}_i}$ is the gradient with respect to the x , y , and z coordinates of \mathbf{r}_i , and $n = N_{tot} - 1$ ($n = 3$ in the HD calculations). In the calculations presented in this work, m_0 is the mass of the deuteron and m_1 is the mass of the proton ($m_d = 3670.4829652 m_e$ and $m_p = 1836.15267261 m_e$,¹⁰ where m_e is the electron mass), and m_2 and m_3 are the electron masses. The reduced masses, μ_i , are defined as: $\mu_i = m_0 m_i / (m_0 + m_i)$. The potential energy is the same as in the laboratory-frame Hamiltonian, but is now written using the internal coordinates, $r_{ij} = ||\mathbf{r}_j - \mathbf{r}_i|| = ||\mathbf{R}_{j+1} - \mathbf{R}_{i+1}||$ and $r_j = ||\mathbf{r}_j|| = ||\mathbf{R}_{j+1} - \mathbf{R}_1||$. The symbol prime ('') is used for vector/matrix transposition. More information on the nonadiabatic internal Hamiltonian and on the center-of-mass transformation can be found in Refs. 11 and 12.

The spatial part of the HD non-BO wave functions of the $N = 1$ vibrational states are expanded in terms of one-center, spherically symmetric ECGs multiplied by even powers (p_k) of the internuclear distance, r_1 , and by the x_1 coordinate of the \mathbf{r}_1 vector^{13–16}

$$\phi_k = x_1 r_1^{p_k} \exp[-\mathbf{r}'(A_k \otimes I_3)\mathbf{r}], \quad (2)$$

where $\mathbf{r} = \{\mathbf{r}'_1, \mathbf{r}'_2, \mathbf{r}'_3\}'$. The p_k powers in our calculations range from 0 to 250. The $r_1^{p_k}$ factors in functions (2) allow for describing the nucleus–nucleus correlations and for generating radial nodes in the wave function when the molecule becomes vibrationally excited. A_k in (2) is a symmetric matrix of exponential parameters. To make the Gaussians (2) square-integrable, A_k is represented in a Cholesky factorized form as $A_k = L_k L'_k$, where L_k is a lower triangular matrix. With this representation, A_k is automatically positive definite for any

real values of the L_k matrix elements. \otimes in (2) is the Kronecker product symbol. Before functions (2) are used in expanding the wave functions of HD they are symmetrized with respect to the permutation of the (pseudo)electron labels, as the considered states are electronic singlet states. Matrix elements of L_k and the p_k powers are the variational parameters which are optimized by the energy minimization. In this minimization, the analytical energy gradient determined with respect to the L_k matrix elements is employed. This greatly expedites the calculations and allows achieving high accuracy of the results. The capability for performing non-BO variational calculations for diatomic systems with basis functions (2) was recently developed.⁷

At present in basis functions (2) we only include the x_1 angular factor. However, in general, basis functions with factors x_i , where $i = 2, \dots, n$ should also appear as they may provide some contributions to the wave functions of the $N = 1$ states. However, as the ECGs with the x_i , $i = 2, \dots, n$, describe contributions where, instead of rotational excitation of the nuclei (which are described by ECGs with the x_1 factor) the i electron becomes excited to a higher angular-momentum state, these contributions are expected to be very small. This is because the electronic excitations are usually much higher in terms of energy than the rotational excitations. Also, it should be mentioned that ECGs (2), even though they do not explicitly include the x_i , $i = 2, \dots, n$, angular factors, they effectively include some contributions of the x_i , $i = 2, \dots, n$, ECGs because the x_1 ECGs and the x_i ECGs ($i = 2, \dots, n$) are not orthogonal if their A_k matrices have non-zero off-diagonal elements. However, it should be noted that this is certainly not the most effective way of including these contributions. A better way would be to include them explicitly in the basis set.

The main focus of the present calculations is to investigate how the HD charge asymmetry is affected by a rotational excitation. For such purpose, the basis functions (2) should suffice. They should also provide very good energies for the considered states. However, to converge the state energies to virtually exact values, the x_i , $i = 2, \dots, n$, ECGs are probably needed. Work is currently in progress in our laboratory to include such functions in the calculations of $N = 1$ states of diatomic molecules.

The aim of this work is to calculate the whole vibrational spectrum of the HD molecule in the first excited rotational state ($N = 1$). The calculations are performed with the variational method applied separately to each state. In the variational optimization, the total internal energy of the state expressed as the expectation value of the Hamiltonian (1) is minimized. The minimization is performed with respect to the linear expansion coefficients, $\{c_k\}$, by solving the generalized eigenvalue problem, and with respect to the Gaussian parameters, $\{p_k, L_k\}$,

$$E = \min \frac{c' H(\{p_k\}, \{L_k\}) c}{c' S(\{p_k\}, \{L_k\}) c}. \quad (3)$$

As mentioned the analytical energy gradient calculated with respect to the L_k matrix elements is used in the minimization. There are a number of minimization strategies one can consider using. The one, which we find effective and which allows for better control (and elimination) of linear

dependencies between ECGs that may arise in the minimization, involves optimization of L_k of one basis function at a time. In this optimization, each time the L_k parameters of the optimized function are changed, the generalized eigenvalue problem is resolved to assure that the total energy is an upper bound to the exact nonrelativistic energy of the state considered in the calculation.

There are 18 bound vibrational states of HD corresponding to $N = 1$. The ECG basis for each state is generated by taking the basis set of 10 000 ECGs for the corresponding $N = 0$ states and reoptimizing the L_k matrix elements of the Gaussians. No reoptimization of the p_k powers is performed. In the next step, 1000–3000 additional ECGs are added to the basis set of each state. More functions are used for higher states than for lower states. The addition of new functions is done stepwise by adding functions one-by-one in groups of 100. After each function is added to the basis set its L_k parameters and the p_k power is optimized. After the addition of each 100 functions the whole basis set is reoptimized by cycling over all ECGs and reoptimizing their L_k parameters with the gradient-based approach. At each optimization step the ECGs are checked for linear dependencies, and, if they appear, they are removed.

Next, after the generation of the basis sets for all considered $N = 1$ states is completed, the non-BO nonrelativistic wave functions are used to calculate the expectation values for the following interparticle distances and their squares: the deuteron–proton distance, $\langle r_{dp} \rangle = \langle r_1 \rangle$, the deuteron–electron distance, $\langle r_{de} \rangle = \langle r_2 \rangle$, the proton–electron distance, $\langle r_{pe} \rangle = \langle r_{12} \rangle$, the electron–electron distance, and $\langle r_{ee} \rangle = \langle r_{23} \rangle$. A comparison of the $\langle r_{de} \rangle$ and $\langle r_{pe} \rangle$ expectation values allows for determining the degree of the charge asymmetry in the different states of HD. The non-BO wave functions are also used to calculate the deuteron–proton correlation function (i.e., the one-particle relative density of the proton with respect to the deuteron associated with the coordinate \mathbf{r}_1). The correlation function is defined as¹⁷

$$g_i(\xi) = \langle \Psi_i(\mathbf{r}) | \delta(\mathbf{r}_1 - \xi) | \Psi_i(\mathbf{r}) \rangle = \int_{-\infty}^{\infty} |\Psi_i(\xi, \mathbf{r}_2, \mathbf{r}_3)|^2 d\mathbf{r}_2 d\mathbf{r}_3, \quad (4)$$

where $\delta(\mathbf{r}_1 - \xi)$ is the three-dimensional Dirac delta function. As in the non-BO calculations both electrons and nuclei are treated on equal footing, the only information on the molecular structure is obtained in the form of expectation values of the structural parameters. The nucleus-nucleus correlation functions also provide some information on the structure of the system in different states.

Another important quantity which is evaluated are the transition dipole moments corresponding to the $N \leftarrow N + 1$ deexcitations (ψ_i denotes the wave function of the initial $N + 1$ state and ψ_f is the wave function of the final N state, M is a total mass of the system)

$$\langle \psi_i | \hat{T} | \psi_f \rangle = \sum_{j=1}^n \left(\sum_{p=0}^n q_p \left(\delta_{pj} - \frac{m_j}{M} \right) \right) \langle \psi_i | x_j | \psi_f \rangle. \quad (5)$$

For the HD molecule, this general expression reduces to

$$\langle \psi_i | \hat{T}_{HD} | \psi_f \rangle = \sum_{j=1}^n (-1)^{\delta_{ij}} \langle \psi_i | x_j | \psi_f \rangle, \quad (6)$$

where $\langle \psi_i | x_j | \psi_f \rangle$ can be easily evaluated.¹⁸ While being an experimentally measurable quantity, the transition moment by itself does not provide much physical insight. Thus, in the next step we use it to calculate the dipole oscillator strength – a dimensionless quantity related to the probability of the transition – defined as

$$f_{i \rightarrow f} = \frac{8\pi}{3} (E_i - E_f) |\langle \psi_i | \sum_{j=1}^n r_j Y_{1m}(\hat{\mathbf{r}}_j) | \psi_f \rangle|^2. \quad (7)$$

Performing the manipulations described in Ref. 19 and integrating over the angular coordinates, we obtain

$$f_{i \rightarrow f} = \frac{2}{3(2N_f + 1)} (E_i - E_f) |\langle \psi_i | \hat{T} | \psi_f \rangle|^2. \quad (8)$$

In order to calculate the states lifetimes, we need to consider the transition probability per unit time

$$W_{i \rightarrow f} = 2\alpha^3 \frac{2N_f + 1}{2N_f + 3} (E_i - E_f)^2 f_{i \rightarrow f}, \quad (9)$$

where α is a fine structure constant and factor $(2N_f + 1)/(2N_f + 3)$ is introduced to reverse the transitions into the more intuitive $N + 1 \rightarrow N$ notation. The level lifetime is then calculated as

$$\tau_i = \left(\sum_{f(E_f < E_i)} W_{i \rightarrow f} \right)^{-1}. \quad (10)$$

The summation here is performed over all allowed final states which lie lower than the initial state.

III. THE RESULTS

The energy convergence pattern of all 18 $N = 1$ vibrational states of HD presented in Table I show that the energies of all states are converged better than 10^{-8} hartrees. For the two lowest states, this is accomplished with 11 000 ECGs, for the middle states with 12 000 ECGs, and for the top states with 13 000 ECGs.

In Table II, the dissociation energies with respect to the dissociation product, H + D, for each $N = 1$ rovibrational state are shown. In the table, we also show the energies corresponding to the pure $(N = 0, v) \rightarrow (N = 1, v)$ transitions, $E(\Delta v = 0)$, and the $(N = 0, v) \rightarrow (N = 1, v + 1)$ transitions, $E(\Delta v = 1)$. The transition energies obtained in this work can be compared with the nonrelativistic results of Pachucki and Komasa²⁰ obtained using the standard approach with the BO potential energy curve calculated first, correcting it with adiabatic and nonadiabatic effects, and determining the rovibrational transitions by solving the Schrödinger equation for the nuclear motion. In order to make the comparison, the nonrelativistic rovibrational energies taken from the supplementary material of Ref. 20 are used and the dissociation energies are recalculated with respect to the non-relativistic threshold of -0.99591655 hartree (as opposed to the relativistic value

TABLE I. Convergence of the total non-BO energy of the $N = 1$, $v = 0, 1, \dots, 17$ rovibrational states of the HD molecule as the ECG basis set is enlarged from 10 000 to 11 000 basis functions for the $v = 0$ and 1 states, to 12 000 basis functions for the $v = 2, \dots, 13$ states, and to 13 000 basis for the $v = 14, \dots, 17$ states. The energies are given in hartrees.

v /no. of ECGs	10 000	11 000	12 000	13 000
0	-1.16506533815	-1.16506533836		
1	-1.14853357535	-1.14853357577		
2	-1.13280993614	-1.13280993786	-1.13280993849	
3	-1.11787866107	-1.11787866160	-1.11787866212	
4	-1.10372859123	-1.10372859185	-1.10372859249	
5	-1.09035353975	-1.09035354152	-1.09035354249	
6	-1.07775280191	-1.07775280283	-1.07775280432	
7	-1.06593181392	-1.06593181531	-1.06593181648	
8	-1.05490307811	-1.05490308015	-1.05490308241	
9	-1.04468747784	-1.04468748014	-1.04468748245	
10	-1.03531586640	-1.03531586831	-1.03531587195	
11	-1.02683140816	-1.02683141173	-1.02683141456	
12	-1.01929260046	-1.01929260314	-1.01929260572	
13	-1.01277755048	-1.01277755425	-1.01277755899	
14	-1.00738992692	-1.00738993021	-1.00738993413	-1.00738993744
15	-1.00326738023	-1.00326738610	-1.00326739551	-1.00326740321
16	-1.00059345944	-1.00059346250	-1.00059346567	-1.00059347032
17	-0.99959350897	-0.99959353516	-0.99959355170	-0.99959356050

used in Ref. 20). The comparison yields the root mean square deviation between our and their results of 0.0052 cm^{-1} for the $\Delta v = 0$ transition energies and of 0.0059 cm^{-1} for the $\Delta v = 1$ transition energies.

In order to characterize the $N = 1$ wave functions obtained in the calculations, the (pseudo)particle density is calculated for each state. As the wave functions for the considered rovibrationally excited states show the highest variability in terms of the internuclear distance, because nodes

appear in terms of this distance in the wave functions with increasing vibrational excitation, the deuteron-proton density is the most interesting function to show. It is obtained by squaring the total wave function and integrating over the coordinates of the pseudoelectrons according to Eq. (4). As the rotationally excited $N = 1$ wave functions also have an angular node, this node should show up in the deuteron-proton density plot. It needs to be stressed that, while the total rotational quantum number N is a good quantum number in a molecular

TABLE II. The non-BO dissociation energy, E_{dis} , calculated relative to the energies of separated hydrogen and deuterium atoms, $E(\text{H+D}) = -0.99591655$ hartree, the ($\Delta N = 0, \Delta v = 1$) and ($\Delta N = 1, \Delta v = 1$) transition energies, the corresponding oscillator strengths, $f(\Delta v)$, and the lifetimes of the ($N = 0, v$) rotationless states, τ . All energies are in cm^{-1} and the lifetimes are in seconds. Notation $a[b]$ means $a \times 10^b$.

v	E_{dis}	$E(\Delta v = 0)$	$E(\Delta v = 1)$	$f(\Delta v = 0)$	$f(\Delta v = 1)$	τ
0	37 123.8681	89.2347		9.9364[-11]		
1	33 495.5655	85.3786	3717.5373	9.2549[-11]	1.5703[-11]	11 459
2	30 044.6260	81.5995	3536.3181	8.5983[-11]	2.6966[-11]	4873
3	26 767.5896	77.8787	3358.6359	7.9587[-11]	3.5011[-11]	2893
4	23 662.0083	74.1940	3183.4601	7.3298[-11]	4.0811[-11]	1994
5	20 726.5241	70.5218	3009.6782	6.7062[-11]	4.5062[-11]	1510
6	17 960.9817	66.8345	2836.0641	6.0806[-11]	4.8398[-11]	1216
7	15 366.5748	63.1019	2661.2414	5.4501[-11]	5.1143[-11]	1023
8	12 946.0475	59.2851	2483.6293	4.8111[-11]	5.3637[-11]	905.6
9	10 703.9824	55.3395	2301.3501	4.1621[-11]	5.6024[-11]	824.2
10	8 647.1517	51.2049	2112.1702	3.5058[-11]	5.7989[-11]	766.6
11	6 785.0285	46.8113	1913.3281	2.8466[-11]	5.9296[-11]	762.0
12	5 130.4512	42.0573	1701.3886	2.1954[-11]	5.9150[-11]	777.4
13	3 700.5637	36.8067	1471.9448	1.5692[-11]	5.6009[-11]	846.5
14	2 518.1173	30.8606	1219.2531	9.9609[-12]	4.8103[-11]	943.1
15	1 613.3258	23.9037	935.6521	5.1232[-12]	3.3993[-11]	1189
16	1 026.4653	15.3530	610.7641	1.6449[-12]	1.4869[-11]	2168
17	807.0105	3.2351	234.8078	4.1922[-14]	4.1474[-13]	20 834

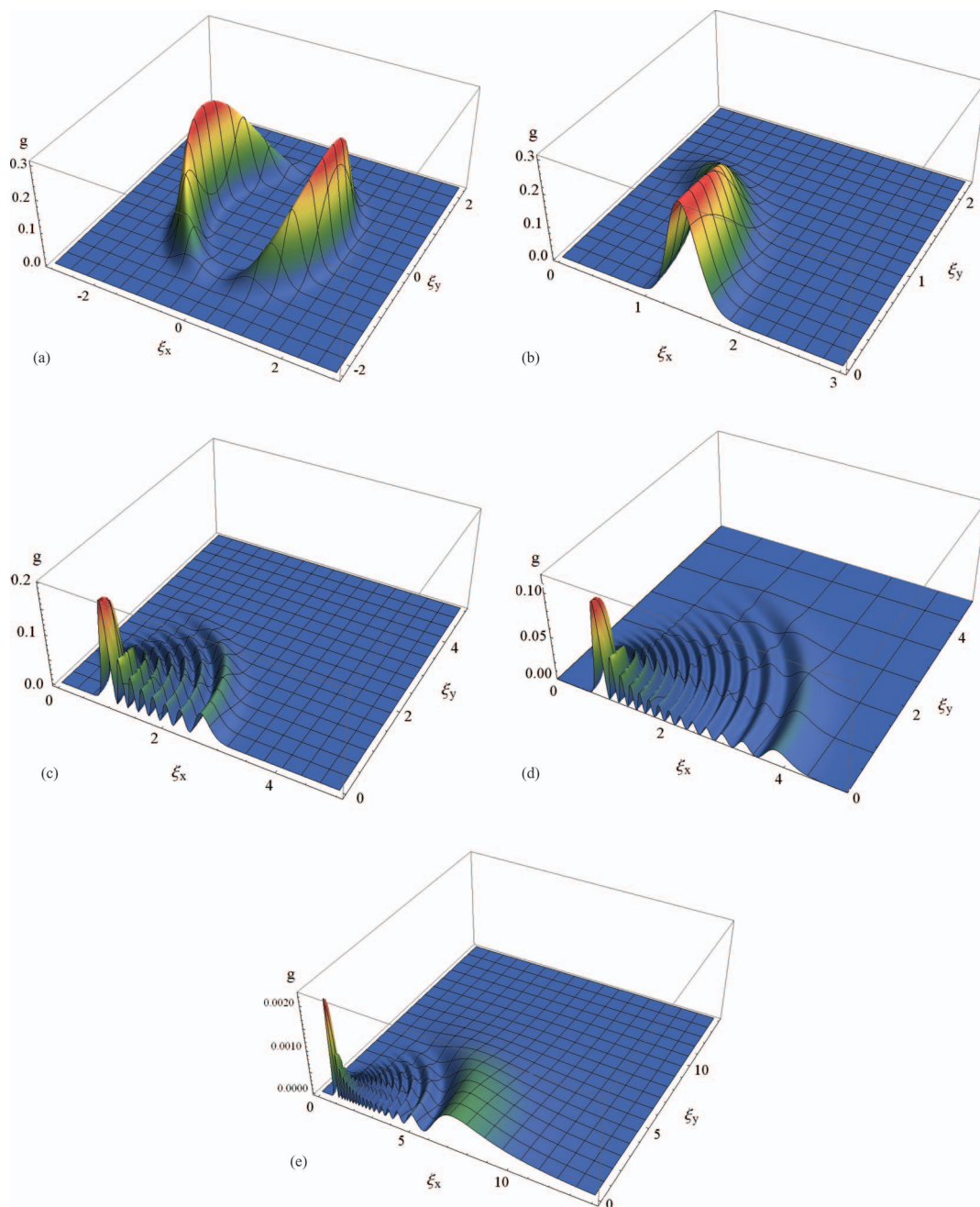


FIG. 1. Deuteron–proton correlation functions (CF), $g_i(\xi)$, for the $v = 0, 7, 13$, and $17 N = 1$ rovibrational states of the HD molecule. (a) is the $v = 0$ CF, shown as a two-dimensional function of the ξ_x and ξ_y coordinates with the ξ_z coordinate set to zero; (b) is the $v = 0$ CF, (c) is the $v = 7$ CF, (d) is the $v = 13$ CF, and (e) is the $v = 17$ CF. The last four CFs are also shown as two-dimensional functions for $\xi_x > 0$ and $\xi_y > 0$, and the ξ_z coordinate set to zero.

approach where the BO approximation is not assumed, the vibrational quantum number, v , is, strictly speaking, not. A particular non-BO state considered here, apart from the dominant adiabatic contribution, which is a product of the electronic ground-state wave function and the particular nuclear vibrational and rotational wave functions, also may contain some small contributions from products which involve electronic excited states and different vibrational states. The proton-deuteron density (also called the proton-deuteron correlation function) may show the coupling of these states, for example, it did for the highest excited $N=0$ and $N=1$ states of HD^+ .²¹ However, the effect is usually very small and hard to notice on the density plot.

The $N = 1$ proton-deuteron density function for HD are shown for some selected lowest, intermediate, and highest vibrational states in Figure 1. Let us examine plot (a) in the figure. It shows the deuteron-proton density for the lowest $N = 1$ vibrational state plotted for the xy plane with z coordinate set to zero. As the wave function is antisymmetric with respect to the reflection in the $x = 0$ plane, the density shown in the plot is zero along the y axis and has two maxima located along the x axis, one at positive x 's and one at negative x . These maxima show where the probability of finding the proton relative to the deuteron is the highest. As the density is symmetric with respect to $x \rightarrow -x$ and $y \rightarrow -y$ reflections, it is sufficient to only show the density in the positive

TABLE III. Some expectation values corresponding to the interparticle distances calculated for the $N = 1$, $v = 0, 1, \dots, 17$ rovibrational states of the HD molecule. $\langle r_{dp} \rangle$ is the deuteron–proton distance, $\langle r_{pe} \rangle$ is the proton–electron distance, $\langle r_{de} \rangle$ is the deuteron–electron distance, and $\langle r_{ee} \rangle$ is the electron–electron distance. All values are in a.u.

v	$\langle r_{dp} \rangle$	$\langle r_{pe} \rangle$	$\langle r_{de} \rangle$	$\langle r_{ee} \rangle$	$\langle r_{dp}^2 \rangle$	$\langle r_{pe}^2 \rangle$	$\langle r_{de}^2 \rangle$	$\langle r_{ee}^2 \rangle$
0	1.443860	1.572337	1.572047	2.198018	2.109055	3.134499	3.133389	5.787216
1	1.527156	1.616230	1.615935	2.253515	2.406117	3.323204	3.322056	6.089125
2	1.613422	1.661495	1.661195	2.311979	2.729372	3.524212	3.523025	6.414403
3	1.703172	1.708372	1.708069	2.374001	3.082389	3.739364	3.738139	6.767526
4	1.797055	1.757173	1.756866	2.440327	3.469731	3.971032	3.969769	7.154231
5	1.895914	1.808300	1.807990	2.511914	3.897351	4.222324	4.221025	7.581995
6	2.000849	1.862282	1.861969	2.589997	4.373131	4.497371	4.496038	8.060678
7	2.113345	1.919837	1.919522	2.676219	4.907835	4.801830	4.800467	8.603611
8	2.235428	1.981945	1.981629	2.772791	5.516468	5.143589	5.142201	9.229152
9	2.369941	2.049988	2.049673	2.882765	6.220626	5.533985	5.532580	9.963297
10	2.521025	2.125977	2.125665	3.010507	7.052629	5.989945	5.988531	10.84420
11	2.694934	2.212954	2.212645	3.162488	8.063051	6.537844	6.536434	11.93026
12	2.901631	2.315761	2.315460	3.348832	9.335955	7.221277	7.219887	13.31623
13	3.158197	2.442699	2.442408	3.586565	11.02294	8.118345	8.116996	15.16859
14	3.497136	2.609559	2.609282	3.907542	13.43158	9.386286	9.385005	17.81630
15	3.992217	2.852196	2.851937	4.383023	17.31976	11.40949	11.40831	22.04935
16	4.880354	3.286050	3.285815	5.240088	25.44194	15.57409	15.57305	30.67284
17	11.33121	6.467008	6.466802	11.53383	152.8215	79.40179	79.40095	158.7655

$(\xi_x > 0, \xi_y > 0)$ quadrant of the xy plane. This is shown in plot (b) for the lowest $N = 1$ vibrational state. Using the same “quadrant” convention, the densities for states $v = 7, 13$, and 17 are presented in plots (c)–(e) in the figure. These plots show the increasing number of density oscillations with the vibrational excitation. The presence of the r_1^m factors in the ECG basis functions is key to describe these oscillations.

In order to investigate charge asymmetry appearing in the HD molecule, we need to evaluate the expectation values of the interparticle distances for all vibrational states with single rotational excitation. These values, as well as expectation values of squares of interparticle distances are presented in Table III. Figure 2 shows the difference between the average proton–electron and deuteron–electron distances as a function of vibrational excitation. According to the plot, the $v = 8$ state has the highest charge asymmetry and the $v = 17$ has the lowest asymmetry. As the results suggest, even though the HD

permanent dipole moment is very small, in relative terms, it may change by as much as 50% as the molecule deexcites from $v = 17$ to $v = 8$.

Figure 3 shows the oscillator strengths computed for the $(N = 0, v = i) \rightarrow (N = 1, v = i)$ and $(N = 0, v = i) \rightarrow (N = 1, v = i - 1)$ transitions. Columns $f(\Delta\nu = 0)$ and $f(\Delta\nu = +1)$ of Table II contain numerical values of the plotted data. While the oscillator strength monotonically decreases for the $\Delta\nu = 0$ transitions, the $\Delta\nu = +1$ oscillator strength reaches a maximum for the $v = 11$ state and then decreases for the higher states. The oscillator strengths for the $\Delta\nu = +1$ transitions become greater than the oscillator strengths for the $\Delta\nu = 0$ transitions at $v = 8$, where the charge asymmetry is at maximum. The lifetimes of the HD $(N = 0, v = i)$, $i = 1, \dots, 17$, rotationless states calculated using the oscillator strengths of the $(N = 0, v = i) \rightarrow (N = 1, v = i - 1)$, $(N = 0, v = i) \rightarrow (N = 1, v = i - 2)$, ..., and $(N = 0, v = i) \rightarrow (N = 1,$

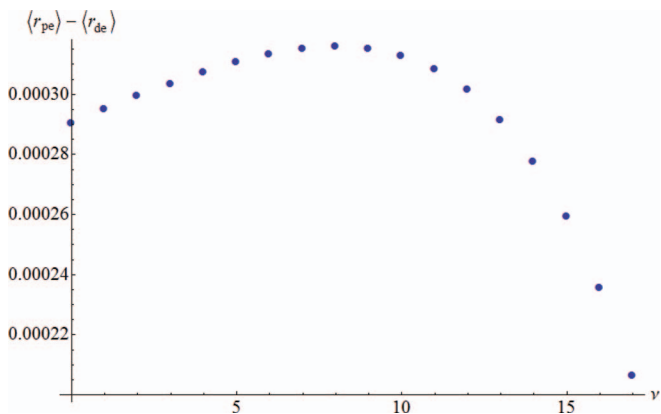


FIG. 2. The difference between the average proton–electron and deuteron–electron distances, $\langle r_{pe} \rangle - \langle r_{de} \rangle$.

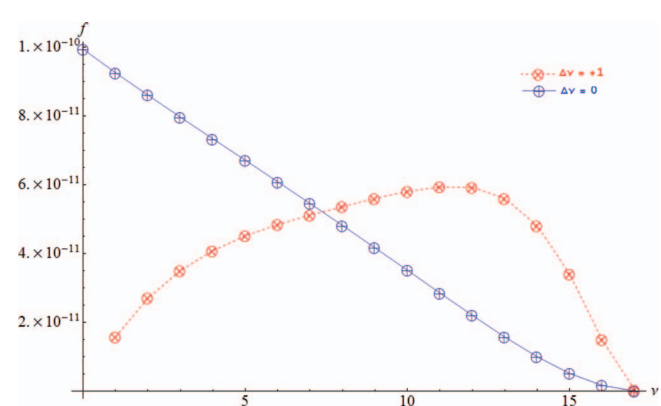


FIG. 3. Oscillator strengths for the pure rotational $N = 1 \rightarrow N = 0$ transitions.

TABLE IV. Dipole transition moments of $R(0)$ and $P(1)$ branches of $\nu(0 \rightarrow \nu')$ transitions. All values are in 10^{-4} D.

Ref. \ ν'	$R(0)$				$P(1)$		
	0	1	2	3	1	2	3
24		0.515(20)	0.19(2)	0.0795(35)	0.450(30)	0.17(2)	
25		0.504(12)			0.435(11)		
26	8.36	0.598	0.160	0.100			
27	8.306	0.560	0.192	0.082	0.485	0.176	0.076
28	8.463	0.552	0.200	0.0870	0.466	0.179	0.0742
29	8.560	0.5579	0.2022	0.0878	0.4708	0.1805	0.0749
Present	8.885	0.5472	0.1703	0.0696	0.4567	0.1481	0.0613

$\nu = 0$) transitions are shown in Figure 4. It is assumed that the lifetimes are primarily dependent on the $\Delta N = 1$ transitions. The values used in the plot can be found in Table II. Interestingly, the longest-living state is the ($N = 0, \nu = 17$) state. The highest longevity of this state is due to the oscillator strength for the ($N = 0, \nu = 17 \rightarrow N = 1, \nu = 16$) transition being considerably smaller than that for the corresponding transitions for the $\nu < 17$ states.

Due to the lack of experimental data concerning the state lifetimes for HD, as well as due to the lack of high-level calculations of these quantities, there is no direct way to verify our results. Such verification was possible in our previous study of HD^+ molecular ion,¹⁸ where the high-quality results of Tian²² and Pilon²³ were available. Nevertheless, a less direct approach can be still used to evaluate the quality of our predictions. Since the oscillator strength decreases almost by an order of magnitude as $\Delta\nu$ increases by one (the $\Delta\nu = 0$ and $\Delta\nu = 1$ cases are an exception), the lifetime of a particular state is almost fully defined by the transition-dipole moments of not more than the three lowest transitions in Eq. (5). Table IV shows a comparison of the transition dipole moments of the $\nu(0 \rightarrow \nu')$ transitions calculated in this work and the available experimental (Refs. 24 and 25) and theoretical BO (Refs. 26–29) results. As it can be seen, the present study yields results which are in a very good agreement with the experiment and with the most recent theoretical calculations. This indicates that the curve which shows the lifetime results presented in Figure 4 is accurate and reliable.

IV. SUMMARY

In this work, a non-BO approach is used to study rovibrational states of the HD molecule corresponding to single rotational excitation ($N = 1$ states). The complete $N = 1$ rovibrational spectrum is calculated. The dissociation energies and the transition energies are also determined for $N = 0$ and $N = 1$ states and compared with recent results obtained with a method based on the BO approximation. The comparison shows a very good agreement of the two sets of results and indicates that the ECG basis set used in the present calculations can reliably describe states with low and high oscillatory behavior. This oscillatory behavior of the HD rovibrational states considered in this work is demonstrated using plots of the proton-deuteron correlation functions.

In the present calculations, we also determined expectation values of the interparticle distances. These values are used to analyze the charge asymmetry in HD. The analysis shows that, as expected, the rotational excitation, elongates the average internuclear distance, but it has no significant effect on the charge asymmetry pattern of the $N = 1$ states as compared to the $N = 0$ states.

Since according to the selection rule the $N = 0$ rovibrational states can only deexcite to the $N = 1$ states with smaller vibrational quantum numbers, the present calculation provides sufficient data for evaluating the interstate transition moments and lifetimes of the $N = 0$ states. The obtained lifetimes plotted as a function of vibrational quantum number show a similar behavior as those obtained for the HD^+ ion in Ref. 18.

ACKNOWLEDGMENTS

We are grateful to the University of Arizona Research Computing Center for the use of their computer resources. This work has been supported in part by the National Science Foundation (NSF) through the graduate research fellowship awarded to Keeper L. Sharkey; Grant No. DGE1-1143953.

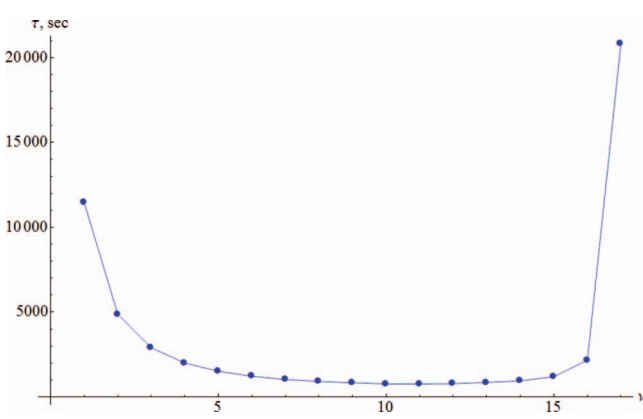


FIG. 4. Lifetimes of the rotationless states.

¹S. Bubin, F. Leonarski, M. Stanke, and L. Adamowicz, *J. Chem. Phys.* **130**, 124120 (2009).

²M. Cafiero and L. Adamowicz, *Phys. Rev. Lett.* **89**, 073001 (2002).

³Z. Lu, G. C. Tabisz, and L. Uliivi, *Phys. Rev. A* **47**, 1159 (1993).

⁴S. Bubin, M. Pavanello, W.-Ch. Tung, K. L. Sharkey, and L. Adamowicz, *Chem. Rev.* **113**, 36 (2013).

⁵J. Mitroy, S. Bubin, W. Horiuchi, Y. Suzuki, L. Adamowicz, W. Cencek, K. Szalewicz, J. Komasa, D. Blume, and K. Varga, *Rev. Mod. Phys.* **85**, 693 (2013).

- ⁶K. L. Sharkey, N. Kirnosov, and L. Adamowicz, *J. Chem. Phys.* **139**, 164119 (2013).
- ⁷K. L. Sharkey, N. Kirnosov, and L. Adamowicz, *Phys. Rev. A* **88**, 032513 (2013).
- ⁸M. Cafiero, S. Bubin, and L. Adamowicz, *Phys. Chem. Chem. Phys.* **5**, 1491 (2003).
- ⁹S. Bubin, M. Cafiero, and L. Adamowicz, *Adv. Chem. Phys.* **131**, 377 (2005).
- ¹⁰P. J. Mohr, B. N. Taylor, and D. B. Newell, *J. Phys. Chem. Ref. Data* **37**(3), 1187 (2008).
- ¹¹D. B. Kinghorn and R. D. Poshusta, *Phys. Rev. A* **47**, 3671 (1993).
- ¹²D. B. Kinghorn and R. D. Poshusta, *Int. J. Quantum Chem.* **62**, 223 (1997).
- ¹³D. B. Kinghorn and L. Adamowicz, *J. Chem. Phys.* **110**, 7166 (1999).
- ¹⁴D. B. Kinghorn and L. Adamowicz, *Phys. Rev. Lett.* **83**, 2541 (1999).
- ¹⁵S. Bubin and L. Adamowicz, *J. Chem. Phys.* **118**, 3079 (2003).
- ¹⁶M. Pavanello, S. Bubin, M. Molski, and L. Adamowicz, *J. Chem. Phys.* **123**, 104306 (2005).
- ¹⁷S. Bubin and L. Adamowicz, *Chem. Phys. Lett.* **403**, 185 (2005).
- ¹⁸N. Kirnosov, K. L. Sharkey, and L. Adamowicz, *Phys. Rev. A* **89**, 012513 (2014).
- ¹⁹Z. C. Yan, J. F. Babb, and A. Dalgarno, *Phys. Rev. A* **54**, 2824 (1996).
- ²⁰K. Pachucki and J. Komasa, *Phys. Chem. Chem. Phys.* **12**, 9188 (2010).
- ²¹N. Kirnosov, K. L. Sharkey, and L. Adamowicz, *J. Chem. Phys.* **139**, 204105 (2013).
- ²²Q. L. Tian, L. Y. Tang, Z. X. Zhong, Z. C. Yan, and T. Y. Shi, *J. Chem. Phys.* **137**, 024311 (2012).
- ²³H. O. Pilon and D. Baye, *Phys. Rev. A* **88**, 032502 (2013).
- ²⁴A. R. W. McKellar, *Can. J. Phys.* **51**, 389 (1973); *Astrophys. J.* **185**, L53 (1973); *Can. J. Phys.* **52**, 1144 (1974).
- ²⁵N. H. Rich, J. W. C. Johns, and A. R. W. McKellar, *J. Mol. Spectrosc.* **95**, 432 (1982).
- ²⁶L. Wolniewicz, *Can. J. Phys.* **53**, 1207 (1975); **54**, 672 (1976).
- ²⁷A. L. Ford and J. C. Browne, *Phys. Rev. A* **16**, 1992 (1977).
- ²⁸W. R. Thorson, J. H. Choi, and S. K. Knudson, *Phys. Rev. A* **131**, 22 (1985); **131**, 34 (1985).
- ²⁹K. Pachucki and J. Komasa, *Phys. Rev. A* **78**, 052503 (2008).

APPENDIX H

Charge asymmetry and rovibrational excitations of HD⁺

Charge asymmetry and rovibrational excitations of HD⁺

Keith Jones^a, Nikita Kirnosov^b, Keeper L. Sharkey^a, and Ludwik Adamowicz^{a,b}

^a*Department of Chemistry and Biochemistry, University of Arizona, Tucson, Arizona 85721, U.S.A.*

^b*Department of Physics, University of Arizona, Tucson, Arizona 85721, U.S.A.*

Average values of the interparticle distances for rovibrationally excited HD⁺ are calculated using a method where the Born-Oppenheimer (BO) approximation is not assumed. The difference between the proton-electron and deuteron-electron distances is used to describe the charge asymmetry in the system. All-particle one-center explicitly correlated Gaussian functions are used in the calculations of the HD⁺ rovibrational states. In this work the non-BO method is extended to calculate the rovibrational states corresponding to the total rotation quantum number of two ($N = 2$). The algorithms for calculating the Hamiltonian and overlap matrix elements, and the matrix elements of the analytical energy gradient determined with respect to the exponential parameters of the Gaussians are presented. The gradient is employed in the variational optimization of the parameters, which is key in obtaining very accurate rovibrational energies in the calculations. The algorithm for calculating the average interparticle distances is also shown. The charge asymmetry of HD⁺ near the dissociation limit occurs, as expected, with the electron preferentially being near the deuteron. The asymmetry for a particular vibrational level increases with rotational excitations. The rovibrational transition energies are also calculated and compared with available experimental data.

I. INTRODUCTION

The Born-Oppenheimer approximation allows for effective calculations of experimental observables as average values over the wave functions being products of electronic wave functions obtained by solving the electronic Schrödinger equation with fixed positions of the nuclei and nuclear rovibrational wave functions obtained by solving the Schrödinger equation describing the motion of the nuclei. The observables are usually obtained to acceptable degrees of accuracy in such calculations. However, there are certain cases where this approximation breaks down. For example, the property featured in this work, which is related to the fact that when HD⁺ dissociates, the electron preferentially accompanies the deuteron, cannot be described by a method where the Born-Oppenheimer (BO) approximation is assumed. It was observed by Ben-Itzhak *et al.*[1] that the H⁺ + D dissociation channel is 7% more likely to occur than the D⁺ + H channel. This phenomenon is nonadiabatic and is related to the fact that when the electron in HD⁺ approaches the deuteron, its energy is slightly lower than when it approaches the proton. This leads to the slight preference of the electron to be by the deuteron than by the proton. The preference, which gives rise to a non-zero dipole moment of HD⁺, increases with the vibrational excitation. In this work we study how the preference changes when the molecule becomes excited to the $N = 1$ and 2 rotational levels (where N is the total rotational quantum number).

In the approach used in the present work the BO approximation is not assumed and all particles forming the system (the proton, the deuteron, and the electron in the case of HD^+) are treated on equal footing. After rigorously separating out the center-of-mass motion from the total laboratory-frame nonrelativistic Hamiltonian, an internal Hamiltonian is obtained which is used in the present calculations (see the next section). As this Hamiltonian commutes with the operator representing the square of the total angular momentum, \hat{N}^2 , and the operator representing its z -axis projection, \hat{N}_z , the Hamiltonian matrix is block-diagonal if eigenfunctions of \hat{N}^2 and \hat{N}_z are used as the basis functions. This is the case in the present calculations. Thus, N and N_z are good quantum numbers for the problem. However, due to the coupling of the motion of the electrons with the motion of the nuclei, the vibrational quantum number is not, strictly speaking, a good quantum number. In this work it is used to number the consecutive states in the manifold corresponding to particular values of N and N_z . As it is described in the section, the basis functions used in our calculations correspond to $N_z = 0$.

In comparing the calculated rovibrational transition energies of HD^+ with the experimental spectroscopic data the results of the measurements performed in Ref. [2] are used. The comparison validates the ability of the computational method developed in this work to predict spectroscopic transitions with high accuracy. As many of these transitions have yet to be observed, the development of new computational methods that can aid the experimental work is a task worth pursuing. The present work makes a step in this direction.

II. HAMILTONIAN

In this work we are concerned with bound stationary internal states of a diatomic system. The problem is solved without invoking the Born-Oppenheimer approximation. We start with the total non-relativistic Hamiltonian written in terms of Cartesian laboratory-frame coordinate system. Next, the center-of-mass motion is rigorously separated out from this Hamiltonian. The separation of the laboratory-frame total Hamiltonian into the center-of-mass Hamiltonian and the internal Hamiltonian is accomplished by the coordinate transformation from the laboratory-frame coordinates to an internal frame coordinate system. The details of the transformation are described below.

First, let us start out by defining the problem we study. We take a molecule in a laboratory coordinate frame with the total number of nuclei (*nuc*) equal to N_{nuc} and the total number of electrons (*elec*) equal to N_{elec} . The total number of particles in the molecular system is then: $N_{tot} = N_{nuc} + N_{elec}$. The i -th particle in the system has mass M_i , charge Q_i , and its position in the laboratory Cartesian coordinate frame is described by the 3-component Cartesian vector \mathbf{R}_i . The laboratory-frame non-relativistic Hamiltonian for the system is:

$$\hat{H}_{\text{lab}} = - \sum_{i=1}^{N_{tot}} \frac{1}{2M_i} \nabla_{\mathbf{R}_i}^2 + \sum_{i=1, j>i}^{N_{tot}} \frac{Q_i Q_j}{R_{ij}}. \quad (1)$$

The gradient with respect to the position coordinates of the particle is $\nabla_{\mathbf{R}_i}$, and R_{ij} is the distance between the i and j particles determined by $R_{ij} = ||\mathbf{R}_j - \mathbf{R}_i||$. The double vertical bars stand for the absolute value of the Euclidean

norm.

The center-of-mass motion (or translational motion of the system as a whole) and the internal motion of the particles forming the system are separated in the laboratory-frame Hamiltonian, (1). The separation yields two Hamiltonians; one representing the kinetic energy of the motion of the center of mass described by the following vector in the laboratory coordinate frame:

$$\mathbf{r}_0 = \frac{M_1}{M_{\text{tot}}} \mathbf{R}_i + \frac{M_2}{M_{\text{tot}}} \mathbf{R}_2 + \dots + \frac{M_{N_{\text{tot}}}}{M_{\text{tot}}} \mathbf{R}_{N_{\text{tot}}}, \quad (2)$$

where $M_{\text{tot}} = \sum_{i=1}^{N_{\text{tot}}} M_i$ is the total mass of the system, and the second representing the internal motion of the particles. The second Hamiltonian, called internal, is expressed in terms of new internal coordinates described by the following vectors referring particles 2 through N_{tot} to particle 1 which is chosen to be the reference particle:

$$\begin{aligned} \mathbf{r}_1 &= -\mathbf{R}_1 + \mathbf{R}_2 \\ \mathbf{r}_2 &= -\mathbf{R}_1 + \mathbf{R}_3 \\ &\vdots \\ \mathbf{r}_{n_{\text{tot}}} &= -\mathbf{R}_1 + \mathbf{R}_{N_{\text{tot}}}. \end{aligned} \quad (3)$$

In general the internal coordinates are: $\mathbf{r}_i = \mathbf{R}_{i+1} - \mathbf{R}_1$ where $i = 1, \dots, n_{\text{tot}}$, and $n_{\text{tot}} = N_{\text{tot}} - 1$. With this the set of N_{tot} laboratory coordinate vectors, $\{\mathbf{R}_1, \dots, \mathbf{R}_{N_{\text{tot}}}\}$ is transformed to the coordinate set consisting of $\{\mathbf{r}_0, \mathbf{r}_1, \dots, \mathbf{r}_{n_{\text{tot}}}\}$. The reference particle is usually the heaviest particle in the system (i.e. one of the nuclei). There is a one-to-one correspondence between the laboratory coordinates and the coordinates of the new coordinate system consisting of the center-of-mass coordinates plus the internal coordinates. The distance between pseudoparticles i and j is the same as the distance between the original particles: $r_{ij} = \|\mathbf{r}_{ij}\| = \|\mathbf{r}_j - \mathbf{r}_i\| = \|\mathbf{R}_{j+1} - \mathbf{R}_{i+1}\|$.

In the new coordinate frame the internal coordinates, \mathbf{r}_i , are used to represent the motion of the n_{tot} pseudoparticles in the central field of the charge of the reference nucleus. The pseudoparticles described by the internal Hamiltonian have the same charges as the original real particles before the transformation, but their masses are now reduced masses. Physically, a pseudoparticle represents a pair consisting of an original particle and the reference particle. Denoting the mass of the reference nucleus as m_0 and its charge as q_0 , setting the pseudoparticle reduced masses be to $\mu_i = m_0 m_i / (m_0 + m_i)$ with $m_i = M_{i+1}$, and with the pseudoparticle charges equaling $q_i = Q_{i+1}$, the internal Hamiltonian is [7]:

$$\hat{H} = -\frac{1}{2} \left(\sum_{i=1}^{n_{\text{tot}}} \frac{1}{\mu_i} \nabla_{\mathbf{r}_i}^2 + \sum_{i \neq j}^{n_{\text{tot}}} \frac{1}{m_0} \nabla'_{\mathbf{r}_i} \nabla_{\mathbf{r}_j} \right) + \sum_{i=1}^{n_{\text{tot}}} \frac{q_0 q_i}{r_i} + \sum_{i=1, j>i}^{n_{\text{tot}}} \frac{q_i q_j}{r_{ij}}. \quad (4)$$

The motions of the pseudoparticles are coupled through the mass polarization term, $\sum_{i \neq j} (1/m_0) \nabla'_{\mathbf{r}_i} \nabla_{\mathbf{r}_j}$, and through the Coulombic interactions. The Coulombic interactions are dependent on the distances between the pseudoparticles and the reference particle located at the origin of the internal coordinate system, r_i , and on the relative distances

between pseudoparticles, r_{ij} . In the calculations performed in this work for the HD^+ ion we use the following masses: the mass of deuteron $M_d = 3670.4829652m_e$ and the mass of proton $M_p = 1836.15267245m_e$, where m_e is the electron mass ($m_e = 1$ in atomic mass units, *au*).

The molecular problem represented by the internal Hamiltonian (4) is “atom-like” because it describes the motion of particles in a spherically symmetric, isotropic potential. It is due to this feature that the Hamiltonian commutes with the square of the all-particle total angular-momentum operator, N^2 , which is a sum of the electronic, L , and nuclear, R , angular momenta (or, more precisely, the total angular momenta of the pseudoparticles), $N = L + R$. The commutation relation is $[\hat{H}, \hat{N}^2] = 0$ [9]. Therefore, by expanding the total internal wave function of the system in terms of basis functions which are eigenfunctions of the square of the total angular momentum operator, states corresponding to different eigenvalues of N^2 can be separated. While in previous works we have considered states with $N = 0$, i.e. so-called pure vibrational states [8], and states with $N = 1$ [5], in this work we consider states with $N = 2$, i.e. the second-rotationally-excited states.

III. THE BASIS FUNCTIONS

The main component of an ECG basis function for expanding the spatial part of an n_{tot} -pseudoparticle wave function for an “atomic molecule” is the following exponential function:

$$\phi_k(\mathbf{r}) \equiv \phi_k = \exp[-\mathbf{r}'(A_k \otimes I_3)\mathbf{r}], \quad (5)$$

where A_k is an $n_{tot} \times n_{tot}$ symmetric matrix, \otimes is the Kronecker product symbol, and I_3 is a 3×3 identity matrix. The basis functions used in bound-state calculations must be square integrable. This effectively imposes restrictions on the A_k matrix; it must be positive definite. Rather than limiting the elements of the A_k matrix, A_k is represented in a Cholesky factorized form as $A_k = L_k L'_k$, where L_k is a lower triangular matrix. With this representation, A_k is automatically positive definite for any values of the L_k matrix elements, positive or negative.

The ECG functions have a maximum when the distance between two particles is zero. This is ideal for particles with opposite charges; such as a proton and an electron. However, as two particles with like charges repel, the probability of them occupying the same point in space is very small; therefore having a maximum at the coalescence point is undesirable. The probability of two particles occupying the same point in space is much smaller for a pair of nuclei than for a pair of electrons [9, 10]. Therefore, the ECG functions (5) must be modified to describe the virtually zero probability of two nuclei closely approaching each other. Also, as a purpose of the molecular non-BO calculations is to describe the molecule in a vibrationally excited state, the system must be represented by a wavefunction with spatial nodes in terms of the coordinates describing the internuclear distances. Additional flexibility needs to be introduced in the ECGs to describe these features.

To achieve this additional flexibility, the ECG functions (5) are multiplied by non-negative even powers of the

internuclear distances. In diatomic non-BO calculations, this factor is $r_1^{m_k}$ where r_1 is the distance between the reference nucleus and the second nucleus (the deuteron-proton distance in the case of the HD^+ molecule):

$$\phi_k^{N=0} = r_1^{m_k} \phi_k, \quad (6)$$

such that $r_1 = (x_1^2 + y_1^2 + z_1^2)^{1/2} = (\mathbf{r}' \mathbf{J}_{11} \mathbf{r})^{1/2}$, where \mathbf{J}_{11} is a square diagonal $3n_{tot} \times 3n_{tot}$ matrix. Similar to the \mathbf{A}_k , the \mathbf{J}_{11} can be reduced to an $n_{tot} \times n_{tot}$ matrix J_{11} crossed with 3 dimensions I_3 : $\mathbf{J}_{11} = J_{11} \otimes I_3$. The only nonzero elements of J_{11} is the (1,1) element making the only nonzero elements of \mathbf{J}_{11} the (1,1), (2,2), and (3,3) elements. The m_k power in our calculations is an even integer variational parameter which is optimized (in the range from zero to 250). When m_k is equal to zero we have a usual ECG function (5).

The above functions are used for expanding the wave functions of states with rotational quantum number equal to zero ($N = 0$). For the second excited rotational states of a diatomic molecule corresponding to the rotational quantum number $N = 2$ and $N_z = 0$ (the quantum number associated with the projection of the total angular momentum on the z axis) functions (6) are multiplied by Cartesian angular factors and take the following form:

$$\phi_k^{N=2} = (x_1^2 + y_1^2 - 2z_1^2) \phi_k^{N=0}. \quad (7)$$

The coordinates in the Cartesian angular factor are the relative coordinates between the two nuclei. The states being described by basis functions (6) with angular factor (7) are rovibrational states of diatomic molecules corresponding to the second rotational excitation. Since the contribution from the angular excitations of the electrons to the total molecular angular momentum can be expected to be small, these basis functions are sufficient building blocks for our molecular wave functions of states studied in the present work.

Thus, in this work, the derivation of the Hamiltonian and overlap integrals and their computational implementation concerns the basis functions:

$$\phi_k^{N=2} = (x_1^2 + y_1^2 - 2z_1^2) r_1^{m_k} \exp[-\mathbf{r}' (A_k \otimes I_3) \mathbf{r}]. \quad (8)$$

This is the full form of the ECGs used in this work. The algorithms for calculating the overlap and Hamiltonian matrix elements with ECGs (8) are shown in the Appendix.

IV. THE TOTAL ENERGY AND THE ENERGY GRADIENT

The energy eigenvalues of the Hamiltonian (4) are obtained by using the standard Rayleigh-Ritz variational scheme:

$$\frac{\langle \Psi | \hat{H} | \Psi \rangle}{\langle \Psi | \Psi \rangle} \geq E_0. \quad (9)$$

The exact nonrelativistic energy of the system is E_0 . The total molecular wave function, Ψ , depends on the spatial coordinates, \mathbf{r} , of the particles and their spins, \mathbf{s} . The internal spatial coordinates \mathbf{r} is a $3n_{tot}$ -component vector

consisting of n_{tot} , 3-component \mathbf{r}_i vectors. Likewise, the spin coordinates (\mathbf{s}) are represented as a $3n_{tot}$ -component vector plus the three spin coordinates of the reference particle.

The internal Hamiltonian (4) is spin independent. The determination of the Hamiltonian and overlap matrix elements is first reduced by separating integration variables \mathbf{r} and \mathbf{s} , and integrating over the spin variables. Since the spin functions are normalized, each integration over the spin variables is equal to 1. This leaves behind only spatially dependent integrals, which can be calculated using the spatial wave function, $\Psi(\mathbf{r})$. This wave function is approximated by a linear combination of K basis functions, $\phi_k(\mathbf{r})$:

$$\Psi(\mathbf{r}) = \sum_{k=1}^K c_k \hat{Y} \phi_k(\mathbf{r}), \quad (10)$$

where c_k is the linear variational parameter, and \hat{Y} is a permutational symmetry projection operator specific to the considered state of the system. The specific form of $\phi_k(\mathbf{r})$ is described in detail in Section III. In the calculations of HD⁺ described in this work, there are no indistinguishable particles (all particles are different), and therefore $\hat{Y} = \hat{1}$.

To minimize the energy functional with respect to the parameters c_k the secular equation is used:

$$(\mathbf{H} - \varepsilon \mathbf{S})\mathbf{c} = 0, \quad (11)$$

where \mathbf{H} and \mathbf{S} are $K \times K$ hermitian matrices of the Hamiltonian and overlap integrals, with the elements $H_{kl} = \langle \phi_k | \hat{H} \hat{Y}^\dagger \hat{Y} | \phi_l \rangle$ and $S_{kl} = \langle \phi_k | \hat{Y}^\dagger \hat{Y} | \phi_l \rangle$, respectively. \mathbf{c} is a K -component vector of the linear expansion coefficients c_k . Solutions of the equation (11) give upper bounds, ε , to the exact ground and excited state energies of the system. There exist K solutions of (11).

The differential of (11) is:

$$d(\mathbf{H} - \varepsilon \mathbf{S})\mathbf{c} = (d\mathbf{H})\mathbf{c} - (d\varepsilon)\mathbf{S}\mathbf{c} - \varepsilon(d\mathbf{S})\mathbf{c} + (\mathbf{H} - \varepsilon \mathbf{S})d\mathbf{c}. \quad (12)$$

Multiplying (12) by \mathbf{c}^\dagger from the left and rearranging for $d\varepsilon$ we obtain:

$$d\varepsilon = \mathbf{c}^\dagger (d\mathbf{H} - \varepsilon d\mathbf{S})\mathbf{c}. \quad (13)$$

In the above equation it is assumed that the wave function is normalized, $\mathbf{c}^\dagger \mathbf{S} \mathbf{c} = 1$. The relation (13) is essentially the same as the well known Hellmann-Feynman theorem.

Now let us assume that α_t is some nonlinear parameter, on which the basis function ϕ_t depends. It is obvious that only the elements in the t -th row and t -th column of the matrices \mathbf{H} and \mathbf{S} depend on α_t . Thus, the derivative of an arbitrary element of \mathbf{H} (as well as \mathbf{S}) can be written as:

$$\frac{\partial H_{kl}}{\partial \alpha_t} = \frac{\partial H_{kl}}{\partial \alpha_t} (\delta_{kt} + \delta_{lt} - \delta_{kt}\delta_{lt}), \quad k, l, t = 1 \dots K. \quad (14)$$

From (13) and (14) it is easy to find that the derivative of the total energy, ε , with respect to the parameter α_t , is:

$$\begin{aligned}\frac{\partial \varepsilon}{\partial \alpha_t} &= \mathbf{c}_t^* \sum_{l=1}^K \mathbf{c}_l \left(\frac{\partial \mathbf{H}_{tl}}{\partial \alpha_t} - \varepsilon \frac{\partial \mathbf{S}_{tl}}{\partial \alpha_t} \right) + \mathbf{c}_t \sum_{l=1}^K \mathbf{c}_l^* \left(\frac{\partial \mathbf{H}_{lt}}{\partial \alpha_t} - \varepsilon \frac{\partial \mathbf{S}_{lt}}{\partial \alpha_t} \right) - \mathbf{c}_t \mathbf{c}_t^* \left(\frac{\partial \mathbf{H}_{tt}}{\partial \alpha_t} - \varepsilon \frac{\partial \mathbf{S}_{tt}}{\partial \alpha_t} \right) \\ &= 2\Re \left[\mathbf{c}_t^* \sum_{l=1}^K \mathbf{c}_l \left(\frac{\partial \mathbf{H}_{tl}}{\partial \alpha_t} - \varepsilon \frac{\partial \mathbf{S}_{tl}}{\partial \alpha_t} \right) \right] - \mathbf{c}_t \mathbf{c}_t^* \left(\frac{\partial \mathbf{H}_{tt}}{\partial \alpha_t} - \varepsilon \frac{\partial \mathbf{S}_{tt}}{\partial \alpha_t} \right).\end{aligned}\quad (15)$$

By calculating such a derivative for each α_t ($k = 1 \dots K$) we can get the entire energy-gradient vector. In practice, it is advantageous to evaluate the derivatives of ε with respect to the entire $\text{vech } L_k$ vector (this vector is obtained by taking the lower triangle of the L_k matrix and stacking its rows under each other; thus $\text{vech } L_k$ has the following elements: $(L_k)_{1,1}, (L_k)_{2,1}, (L_k)_{2,2}, \dots, (L_k)_{n,n}$ rather than doing this separately for individual parameters. This is because the calculation of the derivatives with respect to the elements of matrix L_k involves many identical operations and repeating them separately for each element is much less efficient than calculating all of them in a single step.

As it can be seen from (15), the calculation of the gradient of ε with respect to $\text{vech } L_k$ involves the following derivatives of the \mathbf{H} and \mathbf{S} matrix elements:

$$\frac{\partial \mathbf{H}_{kl}}{\partial (\text{vech } L_k)}, \quad \frac{\partial \mathbf{H}_{kl}}{\partial (\text{vech } L_l)}, \quad \frac{\partial \mathbf{S}_{kl}}{\partial (\text{vech } L_k)}, \quad \text{and} \quad \frac{\partial \mathbf{S}_{kl}}{\partial (\text{vech } L_l)}. \quad (16)$$

In the Appendix we derive expressions for the Hamiltonian (for this work $\mathbf{H}_{kl} \equiv \mathbf{H}_{kl}^{N=2} = \mathbf{T}_{kl}^{N=2} + \mathbf{V}_{kl}^{N=2}$) and overlap $\mathbf{S}_{kl}^{N=2}$ matrices and the above expressions for their derivatives. The derivatives of the normalized kinetic and potential matrix elements:

$$\frac{\partial \mathbf{T}_{kl}^{N=2}}{\partial (\text{vech } L_k)}, \quad \frac{\partial \mathbf{V}_{kl}^{N=2}}{\partial (\text{vech } L_k)}, \quad \frac{\partial \mathbf{S}_{kl}^{N=2}}{\partial (\text{vech } L_k)}, \quad \frac{\partial \mathbf{T}_{kl}^{N=2}}{\partial (\text{vech } L_l)}, \quad \frac{\partial \mathbf{V}_{kl}^{N=2}}{\partial (\text{vech } L_l)}, \quad \text{and} \quad \frac{\partial \mathbf{S}_{kl}^{N=2}}{\partial (\text{vech } L_l)}, \quad (17)$$

are derived separately and the corresponding algorithms are shown in the Appendix. The energy gradient is calculated and supplied to the energy-minimization procedure along with the energy value. The availability of the gradient greatly accelerates the optimization of the ECG exponential parameters.

V. RESULTS

In the present calculation we consider all bound rovibrational states of the HD^+ molecular ion corresponding to the second excited rotational state. The HD^+ system has been chosen due to the fact that in the highest bound vibrational states it possesses a significant charge-distribution asymmetry as a result of the electron becoming more stable when its density shifts towards the deuteron and away from the proton. This effect is purely non-adiabatic and, to describe it, one either needs to perform a direct non-BO calculation (as done in the present study) or use the perturbation theory. Also, extensive literature data exist on this system, allowing for a thorough method benchmarking. The benchmarking in this work involves performing non-BO calculations of the total energies of all $\nu = 0, \dots, 21$ bound vibrational states corresponding to the $N=2$ rotationally excited state. The total energies of the states are used

to determine the $(v,1) \rightarrow (v,2)$ transition energies and the dissociation energies. The wave functions obtained in the calculations are used calculate the expectation values of the proton-deuteron, proton-electron, and deuteron-electron distances. The values are used for describing the HD^+ charge asymmetry.

In the first step of the calculations we generated an ECG basis set for each of the twenty two considered states. For each $(v,2)$ state we started with the ECG basis set generated before for the $(v,0)$ state and, by multiplying all the basis functions by the $(x_1^2 + y_1^2 - 2z_1^2)$ angular factor, we produced the initial basis set for the $(v,2)$ state calculation. In the second, the exponential L_k parameters of all ECGs were variationally optimized using the gradient-based procedure; m_k powers in the preexponential factor, $r_1^{m_k}$, were kept the same. In the third step, a thousand ECGs were added to the basis set of each state with the m_k and L_k for each added function optimized. The optimization of L_k 's the gradient-based procedure was employed. The new functions were added to the basis set of each state one by one. The initial parameters of the added function have been obtained by randomly perturbing the parameters of one of the most contribution ECGs already included in the basis set. Afterwards, several cyclic optimizations were performed for each set to increase the accuracy of the calculated energy value. The results of each step are shown in the Table I. Since the wave functions for lower states have fewer nodes, a smaller number of ECGs is needed to accurately describe their wave functions. For higher states with more complicated nodal structures, more ECGs are needed to represent them with similar accuracy. It can be seen from the table that the addition of a thousand ECGs to each basis set leads to an energy decrease on the order of 1.0×10^{-9} hartrees, which indicates a reasonably tight convergence.

The most accurate total energy values were used to calculate dissociation energies (shown in Table II) and $(v,1) \rightarrow (v,2)$ transition energies (shown in Table III). In these tables we compare our results to the results obtained by Karr and Hiliko [6], Moss [15], and Balint-Kurti [14]. It can be seen that the deviations from [6] and [15] are the biggest for the ground vibrational state (0.0070 cm^{-1} in the dissociation and 0.0047 cm^{-1} in the transition energy) and the smallest for the highest state (0.0007 cm^{-1} and 0.0001 cm^{-1} , respectively). For the states in between the general trend is that the difference becomes smaller as the vibrational-state quantum number increases. In Table IV we compare the experimentally measured rovibrational transition energies to our calculated values. The difference between the two sets of results appears to be within the values of the radiative and relativistic corrections for the different vibrational levels.

As the main topic of the present study is the charge asymmetry in rovibrationally excited HD^+ , the non-BO wave functions obtained in the present calculations are use to calculate the expectation values of the interparticle distances. The algorithm used in the calculations are shown in the Appendix and results are presented in Table V. In the first three columns in the table the proton-deuteron, deuteron-electron, and proton-electron average distances are presented. The results show that the charge asymmetry in HD^+ increases with increasing vibrational. They also show that, as the dissociation limit is approached via vibrational excitation, the electron moves close to the deuteron (the average deuteron-electron distance decrease to 1.985 a.u.) and away from the proton (the average proton-electron

distance increases to 13.58 a.u. which is close to the average distance between the proton and the deuteron). This finding supports the experimental observation [1] of the preferred dissociation channel being $\text{HD}^+ \rightarrow \text{H}^+ + \text{D}$.

In Table V we also show the differences between the average interparticles distances obtained for the $N=2$ rovibrational states and the corresponding $N=0$ states, as well as the differences between the $N=1$ rovibrational states and the $N=0$ states. The results show that, as expected, the average proton-deuteron distance increases with the rotational excitation for each vibrational level due to the larger centrifuge force acting on the rotating molecule. For example, while difference between the average proton-deuteron distances between $\nu = 21$, $N=1$ state and $\nu = 21$, $N=0$ state is 0.3225 a.u., the corresponding difference for the $N=2$ state is 1.0725 a.u. The deuteron-electron and proton-electron average distances are also larger for the $N=2$ rovibrational states than for the corresponding $N=1$ states. In Fig. 1 we show by how much the difference between the average proton-electron and deuteron-electron distances change between the $N=2$ and $N=0$ states and between the $N=1$ and $N=0$ states. Only the results for the top vibrational states ($\nu = 18, 19, 20$, and 21) are presented in the plot. The plotted curves show that the charge asymmetry increases with the rotational excitation. Clearly the rotational excitation amplifies the asymmetry effect. This is intuitive behavior because an excitation of any kind, vibrational, or rotational, or both, will bring the system closer to the dissociation limit, where the charge asymmetry is at the highest point.

VI. SUMMARY AND FUTURE WORK

In conclusion, a new accurate method for direct variational non-BO calculations of rovibrational states of diatomic molecules in a Σ electronic state corresponding to the second rotationally excited state has been developed, implemented, and tested. It was assumed that the major contribution to the total energies of such states comes from the rotational excitation of the nuclei and the angular excitations of the electrons provide much smaller contributions. These latter contributions are only partially included in the present approach. This happens because the basis functions representing the angular excitations of the nuclei (Eq. 7) are not strictly orthogonal to basis functions one needs to add to the basis set to represent the angular excitations of the electrons. The results show that the contributions of the electronic angular excitations decrease for higher vibrational excitations to almost completely disappear for the pre-dissociation states. In those pre-dissociation states the electron becomes localized by the deuteron and its distance from the center of rotation (i.e. the center of mass) decreases significantly [16]. This charge asymmetry causes the moment of inertia of the electron to become much smaller than for lower states where the density of the electron is more evenly distributed between the two nuclei. The smaller is the moment of inertia of a particle, the smaller is the energy which can be accumulated in the rotational motion of the particle. This explains the behavior observed in the present calculations. As the charge asymmetry affects the molecular dipole moment, which in turn affects the intensities of the rotational excitations, the increase of the asymmetry with the rotational excitation should be an

experimentally detectable effect.

The work to follow will aim at the explicit inclusion of all-particle angular momentum excitations and of the coupling between them in the calculations. Also, in the future work the software developed here will be used to calculate rovibrational spectra of diatomic molecules with more than one electron.

Appendix - Matrix Element Derivations

First, we will describe the details of the overlap $S_{kl}^{N=2}$ matrix elements derivation (Section VI A) and the gradient of the formulas including all necessary transformations. Then we will show the derivations for the kinetic energy $T_{kl}^{N=2}$ matrix elements (Section VI B) and the potential energy $V_{kl}^{N=2}$ matrix elements (Section VI C) and display the gradient formulas.

A. Overlap Matrix Elements

The normalized overlap ($S_{kl}^{N=2}$) matrix elements for the $N = 2$ rotationally excited states of diatomic molecules is determined by the following expression:

$$S_{kl}^{N=2} = \frac{\langle \phi_k^{N=2} | \phi_l^{N=2} \rangle}{\sqrt{\langle \phi_k^{N=2} | \phi_k^{N=2} \rangle \langle \phi_l^{N=2} | \phi_l^{N=2} \rangle}}. \quad (18)$$

The numerator will be solved for first and that formula will be used to determine the denominator. The overlap integral between two $N = 2$ basis functions (8) is determined using the partial derivative of an ECG function. The prefactor $(x_1^2 + y_1^2 - 2z_1^2)^2$ is a quadratic function and is placed in the exponent using the partial differentiation:

$$-\frac{\partial}{\partial \omega} \exp[-\omega \mathbf{r}' \mathbf{W} \mathbf{r}] |_{\omega=0} = \mathbf{r}' \mathbf{W} \mathbf{r}, \quad (19)$$

where \mathbf{W} in general is a $3n_{tot} \times 3n_{tot}$ matrix constructed to satisfy any quadratic form. We apply this operation twice for the k and l basis function:

$$\begin{aligned} \langle \phi_k^{N=2} | \phi_l^{N=2} \rangle &= \langle \phi_k | (x_1^2 + y_1^2 - 2z_1^2)^2 r_1^{m_k+m_l} | \phi_l \rangle \\ &= \left. \frac{\partial}{\partial \omega_k} \frac{\partial}{\partial \omega_l} \langle \phi_k | r_1^\nu \exp[-\mathbf{r} (\omega_k \mathbf{W}_k^{N=2} + \omega_l \mathbf{W}_l^{N=2}) \mathbf{r}] | \phi_l \rangle \right|_{\omega_k=\omega_l=0}, \end{aligned} \quad (20)$$

where $\mathbf{W}_k^{N=2}$ and $\mathbf{W}_l^{N=2}$ have only nonzero elements being in the (1,1), (2,2), and (3,3) positions, of values 1, 1, and -2, respectively. In the work by Sharkey et al. [5] only one such derivative was taken. In that derivation a Dirac delta function was used to approximate the $r_1^{m_k+m_l}$ prefactor in the integration over all space. This was also used for the $N = 0$ derivation [11] however was not explained in detail. We would like to clarify the usage of the Delta function for the $N = 2$ case.

The $r_1^{m_k+m_l}$ prefactor obtained from the multiplication of two basis functions (8) depends on the distance between the central nucleus and the pseudonucleus. Therefore, the following general elemental integral is considered:

$$\langle \varphi_k^{\text{N}=2} | r_1^\nu | \varphi_l^{\text{N}=2} \rangle, \quad \nu > -3, , \quad (21)$$

where $\varphi_k^{\text{N}=2} = (x_1^2 + y_1^2 - 2z_1^2) \phi_k$. This integral allows for calculating the overlap matrix element by setting $\nu = (m_k + m_l)$. The criteria that $\nu > -3$ is related to the integration over the Gaussian variables and will be clarified in the derivation. To integrate (21) we first need to evaluate an auxiliary integral that involves the following three-dimensional Dirac delta function:

$$\begin{aligned} \delta(a_1 \mathbf{r}_1 + a_2 \mathbf{r}_2 + \dots + a_{n_{tot}} \mathbf{r}_{n_{tot}} - \boldsymbol{\xi}) &\equiv \delta((a \otimes I_3)' \mathbf{r} - \boldsymbol{\xi}) \\ &= \lim_{\beta \rightarrow \infty} \left(\frac{\beta}{\pi} \right)^{3/2} \exp \left[-\beta ((a \otimes I_3)' \mathbf{r} - \boldsymbol{\xi})^2 \right], \end{aligned} \quad (22)$$

where a is a real n_{tot} -component vector, $\boldsymbol{\xi}$ is a real three-dimensional parameter, and β is a parameter. When we set $a = e^1$, where e^1 is an n -component vector whose first component is 1 and all others are zeros, then (21) can be expressed as:

$$\langle \varphi_k^{\text{N}=2} | r_1^\nu | \varphi_l^{\text{N}=2} \rangle = \int_{-\infty}^{+\infty} |\boldsymbol{\xi}|^\nu \langle \varphi_k^{\text{N}=2} | \delta((a \otimes I_3)' \mathbf{r} - \boldsymbol{\xi}) | \varphi_l^{\text{N}=2} \rangle d\boldsymbol{\xi} \quad (23)$$

It should be noted that integrals involving Delta function (22) with different choices of vector a can be useful in evaluating matrix elements for other important quantities. For this reason, even though we are only concerned here with the evaluation of the overlap matrix elements, we will assume that the a vector has a general form when deriving integral (24). Now, we apply (22) to the above bra-ket:

$$\begin{aligned} \langle \varphi_k^{\text{N}=2} | \delta((a \otimes I_3)' \mathbf{r} - \boldsymbol{\xi}) | \varphi_l^{\text{N}=2} \rangle &= \lim_{\beta \rightarrow \infty} \left(\frac{\beta}{\pi} \right)^{3/2} \langle \varphi_k^{\text{N}=2} | \exp [-\beta \mathbf{r}' (aa' \otimes I_3) \mathbf{r} + 2\beta ((a \otimes I_3) \boldsymbol{\xi})' \mathbf{r} - \beta \boldsymbol{\xi}' \boldsymbol{\xi}] | \varphi_l^{\text{N}=2} \rangle \\ &= \frac{\partial}{\partial \omega_k} \frac{\partial}{\partial \omega_l} \lim_{\beta \rightarrow \infty} \left(\frac{\beta}{\pi} \right)^{3/2} \exp [-\beta \boldsymbol{\xi}' \boldsymbol{\xi}] \times \\ &\quad \langle \exp [-\mathbf{r} (\mathbf{G}_{kl} + \beta (aa' \otimes I_3)) \mathbf{r} + 2\beta ((a \otimes I_3) \boldsymbol{\xi})' \mathbf{r}] \rangle \Big|_{\omega_k=\omega_l=0}, \end{aligned} \quad (24)$$

where $\mathbf{G}_{kl} = \mathbf{A}_{kl} + \omega_k \mathbf{W}_l^{\text{N}=2} + \omega_l \mathbf{W}_k^{\text{N}=2}$. The following general p -dimensional Gaussian integral is the primary integral form used to evaluate the above:

$$\int_{-\infty}^{+\infty} \exp [-x' X x + y' x] d\mathbf{x} = \frac{\pi^{p/2}}{|X|^{1/2}} \exp \left[\frac{1}{4} y' X^{-1} y \right], \quad (25)$$

where x is a p -component vector of variables, A is a symmetric $p \times p$ positive definite matrix to ensure square integrability of the integrand, y is a p -component constant vector, and X^{-1} is the inverse of X . This is the primary integral that is used in the previous ECG work [3]. To relate the two equations to each other we set: $x \equiv \mathbf{r}$, $X \equiv \mathbf{G}_{kl} + \beta (aa' \otimes I_3)$, and $y \equiv 2\beta ((a \otimes I_3) \boldsymbol{\xi})$. Integrating over all space and taking the limit for β approaching infinity gives:

$$\langle \varphi_k^{\text{N}=2} | \delta((a \otimes I_3)' \mathbf{r} - \boldsymbol{\xi}) | \varphi_l^{\text{N}=2} \rangle = \frac{\partial}{\partial \omega_k} \frac{\partial}{\partial \omega_l} \pi^{(3n-1)/2} |\mathbf{G}_{kl}|^{-1/2} |\Lambda_{kl}|^{-1/2} \exp [-\boldsymbol{\xi}' \Lambda_{kl}^{-1} \boldsymbol{\xi}] \Big|_{\omega_k=\omega_l=0}. \quad (26)$$

Here $\Lambda_{kl} = (a \otimes I_3)' \mathbf{G}_{kl}^{-1} (a \otimes I_3)$. Taking the limit as β approaches infinity was shown before in [5] and is a rather complicated procedure, therefore we only show the final result. The next step is to take both derivatives. Applying the full derivative operator, the above becomes:

$$\begin{aligned} \langle \varphi_k^{N=2} | \delta((a \otimes I_3)' \mathbf{r} - \boldsymbol{\xi}) | \varphi_l^{N=2} \rangle &= \pi^{(3n-1)/2} |A_{kl}|^{-3/2} \lambda^{-3/2} \exp[-\lambda^{-1} \boldsymbol{\xi}' \boldsymbol{\xi}] \times \\ &\quad \left\{ \left(\frac{1}{2} \eta_k^{N=2} - \frac{1}{2} \lambda^{-1} \text{tr} [\mathbf{A}_{kl}^{-1} \mathbf{W}_k^{N=2} \mathbf{A}_{kl}^{-1} \mathbf{a} \mathbf{a}'] + \lambda^{-2} \boldsymbol{\xi}' \mathbf{a}' \mathbf{A}_{kl}^{-1} \mathbf{W}_k^{N=2} \mathbf{A}_{kl}^{-1} \mathbf{a} \boldsymbol{\xi} \right) \times \right. \\ &\quad \left(\frac{1}{2} \eta_l^{N=2} - \frac{1}{2} \lambda^{-1} \text{tr} [\mathbf{A}_{kl}^{-1} \mathbf{W}_l^{N=2} \mathbf{A}_{kl}^{-1} \mathbf{a} \mathbf{a}'] + \lambda^{-2} \boldsymbol{\xi}' \mathbf{a}' \mathbf{A}_{kl}^{-1} \mathbf{W}_l^{N=2} \mathbf{A}_{kl}^{-1} \mathbf{a} \boldsymbol{\xi} \right) \\ &+ \frac{1}{2} \eta_{k,l}^{N=2} + \frac{1}{2} \lambda^{-2} \text{tr} [\mathbf{A}_{kl}^{-1} \mathbf{W}_k^{N=2} \mathbf{A}_{kl}^{-1} \mathbf{a} \mathbf{a}' \mathbf{A}_{kl}^{-1} \mathbf{W}_l^{N=2} \mathbf{A}_{kl}^{-1} \mathbf{a} \mathbf{a}'] \\ &- \frac{1}{2} \lambda^{-1} (\text{tr} [\mathbf{A}_{kl}^{-1} \mathbf{W}_k^{N=2} \mathbf{A}_{kl}^{-1} \mathbf{W}_l^{N=2} \mathbf{A}_{kl}^{-1} \mathbf{a} \mathbf{a}'] + \text{tr} [\mathbf{A}_{kl}^{-1} \mathbf{W}_l^{N=2} \mathbf{A}_{kl}^{-1} \mathbf{W}_k^{N=2} \mathbf{A}_{kl}^{-1} \mathbf{a} \mathbf{a}']) \\ &+ \lambda^{-2} (\boldsymbol{\xi}' \mathbf{a}' \mathbf{A}_{kl}^{-1} \mathbf{W}_k^{N=2} \mathbf{A}_{kl}^{-1} \mathbf{W}_l^{N=2} \mathbf{A}_{kl}^{-1} \mathbf{a} \boldsymbol{\xi} + \boldsymbol{\xi}' \mathbf{a}' \mathbf{A}_{kl}^{-1} \mathbf{W}_l^{N=2} \mathbf{A}_{kl}^{-1} \mathbf{W}_k^{N=2} \mathbf{A}_{kl}^{-1} \mathbf{a} \boldsymbol{\xi}) \\ &- \lambda^{-3} (\boldsymbol{\xi}' \mathbf{a}' \mathbf{A}_{kl}^{-1} \mathbf{W}_k^{N=2} \mathbf{A}_{kl}^{-1} \mathbf{a} \mathbf{a}' \mathbf{A}_{kl}^{-1} \mathbf{W}_l^{N=2} \mathbf{A}_{kl}^{-1} \mathbf{a} \boldsymbol{\xi} \\ &\quad \left. + \boldsymbol{\xi}' \mathbf{a}' \mathbf{A}_{kl}^{-1} \mathbf{W}_l^{N=2} \mathbf{A}_{kl}^{-1} \mathbf{a} \mathbf{a}' \mathbf{A}_{kl}^{-1} \mathbf{W}_k^{N=2} \mathbf{A}_{kl}^{-1} \mathbf{a} \boldsymbol{\xi} \right), \end{aligned} \quad (27)$$

where the notation tr stands for the trace of a matrix. We also use η with sub- and superscripts to indicate the trace operation: $\eta_k^{N=2} = \text{tr} [\mathbf{A}_{kl}^{-1} \mathbf{W}_k^{N=2}]$, $\eta_l^{N=2} = \text{tr} [\mathbf{A}_{kl}^{-1} \mathbf{W}_l^{N=2}]$, and $\eta_{k,l}^{N=2} = \text{tr} [\mathbf{A}_{kl}^{-1} \mathbf{W}_k^{N=2} \mathbf{A}_{kl}^{-1} \mathbf{W}_l^{N=2}]$. For the specifics of the $N = 2$ case, $\eta_k^{N=2} = 0$, $\eta_l^{N=2} = 0$, and $\eta_{k,l}^{N=2} = 6\alpha$, where $\alpha = (A_{kl})_{(11)}^{-1}$. The scalar $\lambda = \text{tr} [A_{kl}^{-1} aa']$ such that $\mathbf{a}\mathbf{a}' = aa' \otimes I_3$ and $aa' = J_{11}$ where J_{11} is a $n \times n$ matrix with only one nonzero element in the $(1, 1)$ position with a value of 1.

The final step is to integrate over $\boldsymbol{\xi}$ from minus to plus infinity. To do this we use the following formulas:

$$\int_{-\infty}^{+\infty} |\boldsymbol{\xi}|^\nu \exp[-\lambda^{-1} \boldsymbol{\xi}^2] d\boldsymbol{\xi} = 2\pi\Gamma\left(\frac{3+\nu}{2}\right) \lambda^{(3+\nu)/2} ; \nu > -3, \quad (28)$$

$$\int_{-\infty}^{+\infty} |\boldsymbol{\xi}|^\nu (\boldsymbol{\xi}' \Omega^{(1)} \boldsymbol{\xi}) \exp[-\lambda^{-1} \boldsymbol{\xi}^2] d\boldsymbol{\xi} = \frac{2\pi}{3} \Gamma\left(\frac{5+\nu}{2}\right) \lambda^{(5+\nu)/2} \text{tr} [\Omega^{(1)}] ; \nu > -5, \quad (29)$$

$$\begin{aligned} &\int_{-\infty}^{+\infty} |\boldsymbol{\xi}|^\nu (\boldsymbol{\xi}' \Omega^{(2)} \boldsymbol{\xi}) (\boldsymbol{\xi}' \Omega^{(3)} \boldsymbol{\xi}) \exp[-\lambda^{-1} \boldsymbol{\xi}^2] d\boldsymbol{\xi} = \\ &\frac{2\pi}{3 \times 5} \Gamma\left(\frac{7+\nu}{2}\right) \lambda^{(7+\nu)/2} \left\{ 2 \text{tr} [\Omega^{(2)} \Omega^{(3)}] + \text{tr} [\Omega^{(2)}] \text{tr} [\Omega^{(3)}] \right\} ; \nu > -7, \end{aligned} \quad (30)$$

where $\Omega^{(1)}$, $\Omega^{(2)}$, and $\Omega^{(3)}$ are general representations for some 3×3 matrices. Using these and collecting like terms

to reduce the expression, we get the following overlap formula:

$$\begin{aligned}
\langle \phi_k^{N=2} | \phi_l^{N=2} \rangle = & \frac{2}{\sqrt{\pi}} \Gamma\left(\frac{3+\nu}{2}\right) \langle \phi_l | \phi_l \rangle \lambda^{\nu/2} \left\{ \frac{1}{4} \eta_k^{N=2} \eta_l^{N=2} + \frac{1}{2} \eta_{k,l}^{N=2} \right. \\
& - \lambda^{-1} \left(\frac{1}{4} \eta_k^{N=2} \text{tr} [\mathbf{A}_{kl}^{-1} \mathbf{W}_l^{N=2} \mathbf{A}_{kl}^{-1} \mathbf{aa}'] + \frac{1}{4} \eta_l^{N=2} \text{tr} [\mathbf{A}_{kl}^{-1} \mathbf{W}_k^{N=2} \mathbf{A}_{kl}^{-1} \mathbf{aa}'] \right. \\
& + \frac{1}{2} \text{tr} [\mathbf{A}_{kl}^{-1} \mathbf{W}_k^{N=2} \mathbf{A}_{kl}^{-1} \mathbf{W}_l^{N=2} \mathbf{A}_{kl}^{-1} \mathbf{aa}'] + \frac{1}{2} \text{tr} [\mathbf{A}_{kl}^{-1} \mathbf{W}_l^{N=2} \mathbf{A}_{kl}^{-1} \mathbf{W}_k^{N=2} \mathbf{A}_{kl}^{-1} \mathbf{aa}'] \Big) \\
& + \lambda^{-2} \left(\frac{1}{2} \text{tr} [\mathbf{A}_{kl}^{-1} \mathbf{W}_k^{N=2} \mathbf{A}_{kl}^{-1} \mathbf{aa}' \mathbf{A}_{kl}^{-1} \mathbf{W}_l^{N=2} \mathbf{A}_{kl}^{-1} \mathbf{aa}'] \right. \\
& + \frac{1}{4} \text{tr} [\mathbf{A}_{kl}^{-1} \mathbf{W}_k^{N=2} \mathbf{A}_{kl}^{-1} \mathbf{aa}'] \text{tr} [\mathbf{A}_{kl}^{-1} \mathbf{W}_l^{N=2} \mathbf{A}_{kl}^{-1} \mathbf{aa}'] \Big) \\
& + \left(\frac{3+\nu}{3} \right) \left[\lambda^{-1} \left(\frac{1}{4} \eta_k^{N=2} \text{tr} [\mathbf{A}_{kl}^{-1} \mathbf{W}_l^{N=2} \mathbf{A}_{kl}^{-1} \mathbf{aa}'] + \frac{1}{4} \eta_l^{N=2} \text{tr} [\mathbf{A}_{kl}^{-1} \mathbf{W}_k^{N=2} \mathbf{A}_{kl}^{-1} \mathbf{aa}'] \right. \right. \\
& + \frac{1}{2} \text{tr} [\mathbf{A}_{kl}^{-1} \mathbf{W}_k^{N=2} \mathbf{A}_{kl}^{-1} \mathbf{W}_l^{N=2} \mathbf{A}_{kl}^{-1} \mathbf{aa}'] + \frac{1}{2} \text{tr} [\mathbf{A}_{kl}^{-1} \mathbf{W}_l^{N=2} \mathbf{A}_{kl}^{-1} \mathbf{W}_k^{N=2} \mathbf{A}_{kl}^{-1} \mathbf{aa}'] \Big) \\
& - \lambda^{-2} (\text{tr} [\mathbf{A}_{kl}^{-1} \mathbf{W}_l^{N=2} \mathbf{A}_{kl}^{-1} \mathbf{aa}'] \text{tr} [\mathbf{A}_{kl}^{-1} \mathbf{W}_k^{N=2} \mathbf{A}_{kl}^{-1} \mathbf{aa}'] \\
& + 2 \text{tr} [\mathbf{A}_{kl}^{-1} \mathbf{W}_l^{N=2} \mathbf{A}_{kl}^{-1} \mathbf{aa}' \mathbf{A}_{kl}^{-1} \mathbf{W}_k^{N=2} \mathbf{A}_{kl}^{-1} \mathbf{aa}']) \\
& \left. \left. + \frac{1}{15} \left(\frac{3+\nu}{2} \right) \left(\frac{5+\nu}{2} \right) \lambda^{-2} (2 \text{tr} [\mathbf{A}_{kl}^{-1} \mathbf{W}_k^{N=2} \mathbf{A}_{kl}^{-1} \mathbf{aa}' \mathbf{A}_{kl}^{-1} \mathbf{W}_l^{N=2} \mathbf{A}_{kl}^{-1} \mathbf{aa}'] \right. \right. \right. \\
& \left. \left. \left. + \text{tr} [\mathbf{A}_{kl}^{-1} \mathbf{W}_k^{N=2} \mathbf{A}_{kl}^{-1} \mathbf{aa}'] \text{tr} [\mathbf{A}_{kl}^{-1} \mathbf{W}_l^{N=2} \mathbf{A}_{kl}^{-1} \mathbf{aa}'] \right) \right] \right). \tag{31}
\end{aligned}$$

The bra-ket in the above $\langle \phi_k | \phi_l \rangle = \pi^{3n/2} |A_{kl}|^{-3/2}$ which is the overlap between two ECG functions (5). Plugging in that $\mathbf{a} = \mathbf{e}^1$ and $\nu = m_k + m_l$, the terms in the above simplify such that $\lambda \rightarrow \alpha$ and the integral becomes:

$$\langle \phi_k^{N=2} | \phi_l^{N=2} \rangle = \frac{2}{\sqrt{\pi}} \Gamma\left(\frac{3+m_k+m_l}{2}\right) \langle \phi_k | \phi_l \rangle \alpha^{(m_k+m_l)/2} \left(\frac{15+\nu^2+8\nu}{5} \right) \alpha^2, \tag{32}$$

where we used the definitions of \mathbf{W}_k and \mathbf{W}_l . This formula can be reduced and rewritten as:

$$\langle \phi_k^{N=2} | \phi_l^{N=2} \rangle = \left(\frac{15+\nu^2+8\nu}{5} \right) \langle \phi_k^{N=0} | \phi_l^{N=0} \rangle \alpha^2, \tag{33}$$

where it was shown in [5] that the overlap integral for the $N = 0$ state for diatomics is:

$$\langle \phi_k^{N=0} | \phi_l^{N=0} \rangle = \langle \phi | r_1^{m_k+m_l} | \phi_l \rangle = \frac{2}{\sqrt{\pi}} \Gamma\left(\frac{3+m_k+m_l}{2}\right) \langle \phi_k | \phi_l \rangle \alpha^{(m_k+m_l)/2}. \tag{34}$$

To normalize the $N = 2$ overlap integral, the following two integrals are needed:

$$\langle \phi_k^{N=2} | \phi_k^{N=2} \rangle = \left(\frac{15+4m_k^2+16m_k}{5} \right) \langle \phi_k^{N=0} | \phi_k^{N=0} \rangle 2^{-2} (A_k^{-1})_{11}^2, \tag{35}$$

and

$$\langle \phi_l^{N=2} | \phi_l^{N=2} \rangle = \left(\frac{15+4m_l^2+16m_l}{5} \right) \langle \phi_l^{N=0} | \phi_l^{N=0} \rangle 2^{-2} (A_l^{-1})_{11}^2, \tag{36}$$

where in the above we need:

$$\langle \phi_k^{N=0} | \phi_k^{N=0} \rangle = \frac{2}{\sqrt{\pi}} \Gamma\left(\frac{3+2m_k}{2}\right) \langle \phi_k | \phi_k \rangle 2^{-m_k} (A_k^{-1})_{11}^{m_k} \tag{37}$$

and

$$\langle \phi_l^{N=0} | \phi_l^{N=0} \rangle = \frac{2}{\sqrt{\pi}} \Gamma\left(\frac{3+2m_l}{2}\right) \langle \phi_l | \phi_l \rangle 2^{-m_l} (A_l^{-1})_{11}^{m_l}. \quad (38)$$

Using all of these formulas, the final normalized formula for the overlap $N = 2$ integral is:

$$\begin{aligned} S_{kl}^{N=2} &= \frac{\langle \phi_k^{N=2} | \phi_l^{N=2} \rangle}{(\langle \phi_k^{N=2} | \phi_k^{N=2} \rangle \langle \phi_l^{N=2} | \phi_l^{N=2} \rangle)^{1/2}} \\ &= 2^2 \gamma_{N=2}(m_k, m_l) \gamma_1(m_k, m_l) S_{kl} \left[\left(\frac{\alpha}{(A_k^{-1})_{11}} \right)^{m_k+2} \left(\frac{\alpha}{(A_l^{-1})_{11}} \right)^{m_l+2} \right]^{1/2}, \end{aligned} \quad (39)$$

where $\gamma_1(m_k, m_l)$ and $\gamma_{N=2}$ are functions of m_k and m_l defined by:

$$\gamma_1(m_k, m_l) = \frac{2^{(m_k+m_l)/2} \Gamma\left(\frac{3+m_k+m_l}{2}\right)}{\left[\Gamma\left(m_k + \frac{3}{2}\right) \Gamma\left(m_l + \frac{3}{2}\right)\right]^{1/2}}. \quad (40)$$

and

$$\gamma_{N=2}(m_k, m_l) = \left(\frac{15 + \nu^2 + 8\nu}{(225 + 256 m_k m_l + 240(m_k + m_l) + 64(m_k^2 m_l + m_l^2 m_k) + 60(m_k^2 + m_l^2) + 16m_k^2 m_l^2)^{1/2}} \right). \quad (41)$$

The final normalized overlap formula $S_{kl}^{N=2}$ is dependent on the normalized overlap S_{kl} for two ECG basis functions (5):

$$S_{kl} = \frac{\langle \phi_k | \phi_l \rangle}{(\langle \phi_k | \phi_k \rangle \langle \phi_l | \phi_l \rangle)^{1/2}} = 2^{3n/2} \left(\frac{\|L_k\| \|L_l\|}{|A_{kl}|} \right)^{3/2}. \quad (42)$$

To determine the gradient for the $N = 2$ overlap matrix elements:

$$\frac{\partial S_{kl}^{N=2}}{\partial \text{vech } L_k} \text{ and } \frac{\partial S_{kl}^{N=2}}{\partial \text{vech } L_l}, \quad (43)$$

we start by showing the gradient for S_{kl} that was determined in [11]:

$$\frac{\partial S_{kl}}{\partial (\text{vech } L_k)'} = \frac{3}{2} S_{kl} \text{vech} \left[(L_k^{-1})' - 2A_{kl}^{-1} L_k \right]' \quad (44)$$

$$\frac{\partial S_{kl}}{\partial (\text{vech } L_l)'} = \frac{3}{2} S_{kl} \text{vech} \left[(P' L_l^{-1})' - 2P A_{kl}^{-1} P' L_l \right]' \quad (45)$$

To obtain this we used the following definition for the derivative of a matrix determinant:

$$d|X| = |X| \text{tr} [X^{-1} dX]. \quad (46)$$

In general X is some square matrix ($X \equiv A_{kl}$). Next, we apply $dA_{kl} = dA_k + dA_l$ where:

$$dA_k = dL_k L'_k + L_k dL'_k \quad (47)$$

and

$$dA_l = P' dL_l L'_l P + P' L_l dL'_l P. \quad (48)$$

Using the above, it is a short exercise to show:

$$\text{tr} [A_{kl}^{-1} \text{d} A_{kl}] = 2 (\text{tr} [L'_k A_{kl}^{-1} \text{d} L_k] + \text{tr} [PL'_l A_{kl}^{-1} P' \text{d} L_l]). \quad (49)$$

To write the derivative with respect to the ECG nonlinear parameters, $\text{vech } L_k$ and $\text{vech } L_l$, we apply the following general definition converting from the trace of a matrix to an equivalent vector operation:

$$(\text{vec } X)' \text{vec } Y = \text{tr} [X'Y], \quad (50)$$

and from there we can convert from a vector operation to a vech half operation:

$$(\text{vec } X)' \text{vec } L = (\text{vech } X)' \text{vech } L \quad (51)$$

because we are using a special lower triangle matrix $L \equiv L_k, L_l$ to construct the ECGs basis. We use these same transformations to determine the derivative of the additional terms present in $S_{kl}^{N=2}$. The gradient of the normalized overlap matrix element is:

$$\begin{aligned} \frac{\partial S_{kl}^{N=2}}{\partial (\text{vech } L_k)'} &= S_{kl}^{N=2} \left\{ \frac{3}{2} \text{vech} \left[(L_k^{-1})' - 2A_{kl}^{-1}L_k \right]' \right. \\ &\quad + (m_k + 2) (A_k^{-1})_{11}^{-1} \text{vech} [A_k^{-1}J_{11}A_k^{-1}L_k]' \\ &\quad \left. - (m_k + m_l + 4) \alpha^{-1} \text{vech} [A_{kl}^{-1}J_{11}A_{kl}^{-1}L_k]' \right\}, \end{aligned} \quad (52)$$

and

$$\begin{aligned} \frac{\partial S_{kl}^{N=2}}{\partial (\text{vech } L_l)'} &= S_{kl}^{N=2} \left\{ \frac{3}{2} \text{vech} \left[(P'L_l^{-1})' - 2PA_{kl}^{-1}P'L_l \right]' \right. \\ &\quad + (m_k + 2) (A_l^{-1})_{11}^{-1} \text{vech} [PA_l^{-1}J_{11}A_l^{-1}P'L_l]' \\ &\quad \left. - (m_k + m_l + 4) \alpha^{-1} \text{vech} [PA_{kl}^{-1}J_{11}A_{kl}^{-1}P'L_l]' \right\}. \end{aligned} \quad (53)$$

This concludes the derivation of the overlap matrix elements for the the $N = 2$ rotationally excited states of diatomic molecules. Next we present the derivations of the kinetic-energy matrix element followed by the derivation of the potential-energy matrix element.

B. Kinetic Energy Integral

The kinetic energy operator in (4) is written in the following quadratic form:

$$-\frac{1}{2} \left(\sum_{i=1}^n \frac{1}{\mu_i} \nabla_{\mathbf{r}_i}^2 + \sum_{i \neq j}^n \frac{1}{m_0} \nabla'_{\mathbf{r}_i} \nabla_{\mathbf{r}_j} \right) = -\nabla'_{\mathbf{r}} \mathbf{M} \nabla_{\mathbf{r}}. \quad (54)$$

In (54) the mass matrix is equal to: $\mathbf{M} = M \otimes I_3$, where in the M matrix the diagonal elements are set to $1/(2\mu_1)$, $1/(2\mu_2)$, ..., $1/(2\mu_{n_{tot}})$ while the off-diagonal elements are set to $1/(2m_0)$. Again, m_0 is the mass of the reference

nucleus and μ_1, \dots , and $\mu_{n_{tot}}$ are the reduced masses of the pseudoparticles with respect to the reference nucleus. The normalized kinetic energy matrix element is:

$$\mathsf{T}_{kl}^{N=2} = \frac{\langle \phi_k^{N=2} | -\nabla'_r \mathbf{M} \nabla_r | \phi_l^{N=2} \rangle}{\sqrt{\langle \phi_k^{N=2} | \phi_k^{N=2} \rangle \langle \phi_l^{N=2} | \phi_l^{N=2} \rangle}}. \quad (55)$$

To solve we apply integration by parts to obtain:

$$\langle \phi_k^{N=2} | -\nabla'_r \mathbf{M} \nabla_r | \phi_l^{N=2} \rangle = \langle \nabla_r \phi_k^{N=2} | \mathbf{M} | \nabla'_r \phi_l^{N=2} \rangle. \quad (56)$$

Now, we determine the derivative of the basis function (8):

$$\begin{aligned} \langle \nabla_r \phi_k^{N=2} | &= \langle 2(\mathbf{W}_k^{N=2} \mathbf{r}) (\mathbf{r}' \mathbf{J}_{11} \mathbf{r})^{m_k/2} \exp[-\mathbf{r}' \mathbf{A}_k \mathbf{r}] | \\ &+ \langle m_k (\mathbf{r}' \mathbf{W}_k^{N=2} \mathbf{r}) (\mathbf{r}' \mathbf{J}_{11} \mathbf{r})^{m_k/2-1} (\mathbf{J}_{11} \mathbf{r}) \exp[-\mathbf{r}' \mathbf{A}_k \mathbf{r}] | \\ &- \langle 2(\mathbf{A}_k \mathbf{r}) (\mathbf{r}' \mathbf{W}_k^{N=2} \mathbf{r}) (\mathbf{r}' \mathbf{J}_{11} \mathbf{r})^{m_k/2} \exp[-\mathbf{r}' \mathbf{A}_k \mathbf{r}] | \\ &= \langle 2(\mathbf{W}_k^{N=2} \mathbf{r}) \phi_k^{N=0} | + \langle \frac{m_k}{r_1^2} (\mathbf{J}_{11} \mathbf{r}) \phi_k^{N=2} | - \langle 2(\mathbf{A}_k \mathbf{r}) \phi_k^{N=2} |, \end{aligned} \quad (57)$$

and plug it back into the bra-ket above. By multiplying the above with the mass matrix and then by the corresponding ket containing the l -basis function, the following nine integrals are obtained:

$$\langle \nabla_r \phi_k^{N=2} | \mathbf{M} | \nabla'_r \phi_l^{N=2} \rangle = 4 \langle \phi_k^{N=0} | \mathbf{r}' \mathbf{W}_k^{N=2} \mathbf{M} \mathbf{W}_l^{N=2} \mathbf{r} | \phi_l^{N=0} \rangle \quad (58)$$

$$+ 2m_l \langle \phi_k^{N=0} | \frac{\mathbf{r}' \mathbf{W}_k^{N=2} \mathbf{M} \mathbf{J}_{11} \mathbf{r}}{r_1^2} | \phi_l^{N=2} \rangle \quad (59)$$

$$- 4 \langle \phi_k^{N=0} | \mathbf{r}' \mathbf{W}_k^{N=2} \mathbf{M} \mathbf{A}_l \mathbf{r} | \phi_l^{N=2} \rangle \quad (60)$$

$$+ 2m_k \langle \phi_k^{N=2} | \frac{\mathbf{r}' \mathbf{J}_{11} \mathbf{M} \mathbf{W}_l^{N=2} \mathbf{r}}{r_1^2} | \phi_l^{N=0} \rangle \quad (61)$$

$$+ m_k m_l \langle \phi_k^{N=2} | \frac{\mathbf{r}' \mathbf{J}_{11} \mathbf{M} \mathbf{J}_{11} \mathbf{r}}{r_1^4} | \phi_l^{N=2} \rangle \quad (62)$$

$$- 2m_k \langle \phi_k^{N=2} | \frac{\mathbf{r}' \mathbf{J}_{11} \mathbf{M} \mathbf{A}_l \mathbf{r}}{r_1^2} | \phi_l^{N=2} \rangle \quad (63)$$

$$- 4 \langle \phi_k^{N=2} | \mathbf{r}' \mathbf{A}_k \mathbf{M} \mathbf{W}_l^{N=2} \mathbf{r} | \phi_l^{N=0} \rangle \quad (64)$$

$$- 2m_l \langle \phi_k^{N=2} | \frac{\mathbf{r}' \mathbf{A}_k \mathbf{M} \mathbf{J}_{11} \mathbf{r}}{r_1^2} | \phi_l^{N=2} \rangle \quad (65)$$

$$+ 4 \langle \phi_k^{N=2} | \mathbf{r}' \mathbf{A}_k \mathbf{M} \mathbf{A}_l \mathbf{r} | \phi_l^{N=2} \rangle. \quad (66)$$

Each of the above nine integrals are evaluated separately. There are three general formulas that are used to solve them. First, there is only one integral (equation 58) of the following form:

$$\langle \phi_k^{N=0} | \mathbf{r}' \mathbf{Z} \mathbf{r} | \phi_l^{N=0} \rangle = \langle \phi_k | r_1^\nu (\mathbf{r}' \mathbf{Z} \mathbf{r}), |\phi_l \rangle \quad (67)$$

where \mathbf{Z} is some general symmetric positive-definite matrix. In the present case, $\mathbf{Z} \equiv \mathbf{W}_k^{N=2} \mathbf{M} \mathbf{W}_l^{N=2}$. This integral is similar to the $N = 1$ overlap derivation ([5], equations 49-54) and can be solved by first transforming the quadratic prefactor using partial differentiation as described in the overlap section. The first kinetic term (58) simplifies to the

following:

$$\begin{aligned}
4\langle \phi_k^{N=0} | \mathbf{r}' \mathbf{W}_k^{N=2} \mathbf{M} \mathbf{W}_l^{N=2} \mathbf{r} | \phi_l^{N=0} \rangle &= 4 \frac{2}{\sqrt{\pi}} \Gamma\left(\frac{3+\nu}{2}\right) \langle \phi_k | \phi_l \rangle \alpha^{\nu/2} M_{11} \alpha (3+\nu) \\
&= 4 M_{11} \alpha \langle \phi_k^{N=0} | \phi_l^{N=0} \rangle (3+\nu) \\
&= 4 M_{11} \alpha^{-1} \langle \phi_k^{N=2} | \phi_l^{N=2} \rangle \frac{5(3+\nu)}{(5+\nu)(3+\nu)} \\
&= \frac{20 M_{11} \alpha^{-1} \langle \phi_k^{N=2} | \phi_l^{N=2} \rangle}{5+\nu}
\end{aligned} \tag{68}$$

It is ideal to describe all integrals in terms of $\langle \phi_k^{N=2} | \phi_l^{N=2} \rangle$ to simplify the normalization process.

The second of the three integral types are of the following form:

$$\langle \phi_k^{N=0} | \mathbf{r}' \mathbf{Z} \mathbf{r} | \phi_l^{N=0} \rangle = \langle \phi_k | r_1^\nu (x_1^2 + y_1^2 - 2z_1^2) (\mathbf{r}' \mathbf{Z} \mathbf{r}) | \phi_l \rangle = \langle \phi_k | r_1^\nu (\mathbf{r}' \mathbf{W}_l^{N=2} \mathbf{r}) (\mathbf{r}' \mathbf{Z} \mathbf{r}) | \phi_l \rangle \tag{69}$$

and

$$\langle \phi_k^{N=2} | \mathbf{r}' \mathbf{Z} \mathbf{r} | \phi_l^{N=0} \rangle = \langle \phi_k | r_1^\nu (x_1^2 + y_1^2 - 2z_1^2) (\mathbf{r}' \mathbf{Z} \mathbf{r}) | \phi_l \rangle = \langle \phi_k | r_1^\nu (\mathbf{r}' \mathbf{W}_k^{N=2} \mathbf{r}) (\mathbf{r}' \mathbf{Z} \mathbf{r}) | \phi_l \rangle. \tag{70}$$

These can be solved by first transforming the entire integral into the following expression using the partial differentiation of an ECG function:

$$\frac{\partial}{\partial \omega_1} \frac{\partial}{\partial \omega_2} \langle \phi_k | r_1^\nu \exp [-\mathbf{r}' (\mathbf{A}_{kl} + \omega_1 \mathbf{Z} + \omega_2 \mathbf{W}_{k,l}^{N=2}) \mathbf{r}] | \phi_l \rangle \Big|_{\omega_1=\omega_2=0}, \tag{71}$$

which is very similar to the overlap for $N = 2$ described in Section VI A with different matrices substituted into the equation. For integrals (59), (60), (61), and (64), \mathbf{Z} is substituted by $\mathbf{W}_k^{N=2} \mathbf{M} \mathbf{J}_{11}$, $\mathbf{W}_k^{N=2} \mathbf{M} \mathbf{A}_l$, $\mathbf{J}_{11} \mathbf{M} \mathbf{W}_l^{N=2}$, and $\mathbf{A}_l \mathbf{M} \mathbf{W}_l^{N=2}$, respectively. For the the overlap, \mathbf{Z} is substituted by $\mathbf{W}_k^{N=2}$ (or $\mathbf{W}_l^{N=2}$ equivalently). This means that we can use equation (31) with appropriate substitutions.

For integral (59), r_1^ν becomes $r_1^{\nu-2}$ and $\mathbf{Z} = \mathbf{W}_k^{N=2} \mathbf{M} \mathbf{J}_{11}$. For this integral, it turns out that $\mathbf{W}_k^{N=2} \mathbf{M} \mathbf{J}_{11} = M_{11} \mathbf{W}_k^{N=2}$, which simplifies the problem. With this (59) becomes:

$$\begin{aligned}
M_{11} \langle \phi_k^{N=0} | \frac{\mathbf{r}' \mathbf{W}_k^{N=2} \mathbf{r}}{r_1^2} | \phi_l^{N=2} \rangle &= M_{11} \langle \phi_k^{N=0} | r_1^{\nu-2} (x_1^2 + y_1^2 - 2z_1^2) | \phi_l^{N=2} \rangle \\
&= M_{11} \langle \phi_k^{N=2} | r_1^{-2} (x_1^2 + y_1^2 - 2z_1^2) | \phi_l^{N=2} \rangle.
\end{aligned} \tag{72}$$

Using (31) with the proper substitutions, evaluating the traces in terms of α , and simplifying the problem leads to:

$$\frac{2 M_{11} \alpha^{-1} \langle \phi_k^{N=2} | \phi_l^{N=2} \rangle}{\nu + 5}. \tag{73}$$

(61) is equivalent to (59), and, in turn, equivalent to (73).

For integral (60), $\mathbf{Z} = \mathbf{W}_k^{N=2} \mathbf{M} \mathbf{A}_l$. Again, using (31) with proper substitutions and algebraic manipulation leads to a new parameter: $(M \mathbf{A}_l \mathbf{A}_{kl}^{-1})_{11} = \tau_4$. This parameter allows the expression to be simplified to the following:

$$\alpha^{-1} \tau_4 \langle \phi_k^{N=2} | \phi_l^{N=2} \rangle. \tag{74}$$

For integral (64), $\mathbf{Z} = \mathbf{A}_k \mathbf{M} \mathbf{W}_l^{N=2}$. After making the proper substitutions into (31), another parameter is obtained which is similar to τ_4 . It is $\tau_5 = (A_{kl}^{-1} A_k M)_{11}$. With this we have a comparable expression:

$$\alpha^{-1} \tau_5 \langle \phi_k^{N=2} | \phi_l^{N=2} \rangle. \quad (75)$$

Finally, the last integral type is of the form:

$$\langle \phi_k^{N=2} | \mathbf{r}' \mathbf{Z} \mathbf{r} | \phi_l^{N=2} \rangle = \langle \phi_k | (x_1^2 + y_1^2 - 2z_1^2)^2 (\mathbf{r}' \mathbf{Z} \mathbf{r}) r_1^\nu | \phi_l \rangle = \langle \phi_k | (\mathbf{r}' \mathbf{Z} \mathbf{r}) (\mathbf{r}' \mathbf{W}_k^{N=2} \mathbf{r}) (\mathbf{r}' \mathbf{W}_l^{N=2} \mathbf{r}) r_1^\nu | \phi_l \rangle. \quad (76)$$

It can be evaluated by transforming it into the following expression using the same technique as in the previous derivations:

$$\frac{\partial}{\partial \omega_1} \frac{\partial}{\partial \omega_2} \frac{\partial}{\partial \omega_3} \langle \phi_k | r_1^\nu \exp[-\mathbf{r}'(\mathbf{A}_{kl} + \omega_1 \mathbf{Z} + \omega_2 \mathbf{W}_k + \omega_3 \mathbf{W}_l) \mathbf{r}] | \phi_l \rangle \Big|_{\omega_1 = \omega_2 = \omega_3 = 0}. \quad (77)$$

Next we start from equation (31) and replace \mathbf{A}_{kl} with $\mathbf{A}_{kl} + \omega_1 \mathbf{A}_k \mathbf{M} \mathbf{A}_l$, and differentiate one more time. (77) can be transformed into an analytical expression (see ref [12], equations, 28, 74-82), which can be simplified further to various forms depending on the matrix, \mathbf{Z} .

For integral (62), $\mathbf{Z} = \mathbf{J}_{11}$:

$$\begin{aligned} \langle \phi_k^{N=2} | \frac{\mathbf{r}' \mathbf{J}_{11} \mathbf{M} \mathbf{J}_{11} \mathbf{r}}{r_1^4} | \phi_l^{N=2} \rangle &= M_{11} \langle \phi_k | r_1^{\nu-4} (x_1^2 + y_1^2 - 2z_1^2)^2 \mathbf{r}' \mathbf{J}_{11} \mathbf{r} | \phi_l \rangle \\ &= M_{11} \langle \phi_l | r_1^{\nu-4} (\mathbf{r}' \mathbf{W}_k^{N=2} \mathbf{r}) (\mathbf{r}' \mathbf{W}_l^{N=2} \mathbf{r}) (\mathbf{r}' \mathbf{J}_{11} \mathbf{r}) | \phi_l \rangle. \end{aligned} \quad (78)$$

After several simplifications and by evaluating the integral in terms of α , it can be shown that the integral is equivalent to:

$$\frac{2M_{11}\alpha^{-1} \langle \phi_k^{N=2} | \phi_l^{N=2} \rangle}{5+\nu}. \quad (79)$$

For integral (63), $\mathbf{Z} = \mathbf{J}_{11} \mathbf{M} \mathbf{A}_l$:

$$\begin{aligned} \langle \phi_k^{N=2} | \frac{\mathbf{r}' \mathbf{J}_{11} \mathbf{M} \mathbf{A}_l \mathbf{r}}{r_1^2} | \phi_l^{N=2} \rangle &= \langle \phi_k | r_1^{\nu-2} (x_1^2 + y_1^2 - 2z_1^2)^2 \mathbf{r}' \mathbf{J}_{11} \mathbf{M} \mathbf{A}_l \mathbf{r} | \phi_l \rangle = \\ &\langle \phi_k | r_1^{\nu-2} (\mathbf{r}' \mathbf{W}_k^{N=2} \mathbf{r}) (\mathbf{r}' \mathbf{W}_l^{N=2} \mathbf{r}) (\mathbf{r}' \mathbf{J}_{11} \mathbf{M} \mathbf{A}_l \mathbf{r}) | \phi_l \rangle, \end{aligned} \quad (80)$$

and with simplifications it becomes:

$$\alpha^{-1} \tau_4 \langle \phi_k^{N=2} | \phi_l^{N=2} \rangle. \quad (81)$$

For integral (65), $\mathbf{Z} = \mathbf{A}_k \mathbf{M} \mathbf{J}_{11}$:

$$\begin{aligned} \langle \phi_k^{N=2} | \frac{\mathbf{r}' \mathbf{A}_k \mathbf{M} \mathbf{J}_{11} \mathbf{r}}{r_1^2} | \phi_l^{N=2} \rangle &= \langle \phi_k | r_1^{\nu-2} (x_1^2 + y_1^2 - 2z_1^2)^2 \mathbf{r}' \mathbf{A}_k \mathbf{M} \mathbf{J}_{11} \mathbf{r} | \phi_l \rangle = \\ &\langle \phi_k | r_1^{\nu-2} (\mathbf{r}' \mathbf{W}_k^{N=2} \mathbf{r}) (\mathbf{r}' \mathbf{W}_l^{N=2} \mathbf{r}) (\mathbf{r}' \mathbf{A}_k \mathbf{M} \mathbf{J}_{11} \mathbf{r}) | \phi_l \rangle. \end{aligned} \quad (82)$$

With this, (65) can be simplified into the following:

$$\alpha^{-1} \tau_5 \langle \phi_k^{N=2} | \phi_l^{N=2} \rangle. \quad (83)$$

For integral (66), $\mathbf{Z} = \mathbf{A}_k \mathbf{M} \mathbf{A}_l$:

$$\begin{aligned}\langle \phi_k^{N=2} | \mathbf{r}' \mathbf{A}_k \mathbf{M} \mathbf{A}_l \mathbf{r} | \phi_l^{N=2} \rangle &= \langle \phi_k | r_1^\nu (x_1^2 + y_1^2 - 2z_1^2)^2 \mathbf{r}' \mathbf{A}_k \mathbf{M} \mathbf{A}_l \mathbf{r} | \phi_l \rangle \\ &= \langle \phi_k | r_1^\nu (\mathbf{r}' \mathbf{W}_k^{N=2} \mathbf{r}) (\mathbf{r}' \mathbf{W}_l \mathbf{r}) (\mathbf{r}' \mathbf{Z} \mathbf{r}) | \phi_l \rangle.\end{aligned}\quad (84)$$

For this final integral, two new quantities are defined: $\tau_1 = \text{tr}[A_{kl}^{-1} A_k M A_l]$, and $\tau_2 = (A_{kl}^{-1} A_k M A_l A_{kl}^{-1})_{11}$. Using the same approach as the last three integral the final formula is:

$$\frac{\langle \phi_k^{N=2} | \phi_l^{N=2} \rangle}{2\alpha} (3\alpha\tau_1 + \tau_2(4 + \nu)). \quad (85)$$

With all of this together the total kinetic energy can now be evaluated. Since all of the integrals have been solved and all of them contain $\langle \phi_k^{N=2} | \phi_l^{N=2} \rangle$, and the kinetic energy integral is a linear combination of the integrals, $\langle \phi_k^{N=2} | \phi_l^{N=2} \rangle$ can be factored out in the expression. With that the normalized kinetic-energy matrix element is:

$$T_{kl}^{N=2} = 2S_{kl}^{N=2} \alpha^{-1} \left[\frac{M_{11}}{\nu+5} (10 + 2\nu + m_k m_l) + \tau_4(-2 - m_k) + \tau_5(-2 - m_l) + 3\alpha\tau_1 + \tau_2(4 + \nu) \right]. \quad (86)$$

Four τ parameters named have been introduced above. Their formulas can be transformed and simplified such that there are only three unique τ parameters. These are the same three parameters as presented in [5]. This not only simplifies the formulas themselves, but helps with coding them in the computer program. Additionally, it can be shown that:

$$\tau_4(-2 - m_k) + \tau_5(-2 - m_l) = -\tau_3 - 2M_{11}, \quad (87)$$

where $\tau_3 = (A_{kl}^{-1} (m_l A_k + m_k A_l) M)_{11}$. The new kinetic energy formula becomes:

$$2S_{kl}^{N=2} \alpha^{-1} \left[\frac{M_{11}}{\nu+5} (10 + 2\nu + m_k m_l) - \tau_3 - 2M_{11} + 3\alpha\tau_1 + \tau_2(4 + \nu) \right] \quad (88)$$

To reiterate, $\tau_1 = \text{tr}[A_{kl}^{-1} A_k M A_l]$, $\tau_2 = (A_{kl}^{-1} A_k M A_l A_{kl}^{-1})_{11}$, and $\tau_3 = (A_{kl}^{-1} (m_l A_k + m_k A_l) M)_{11}$.

The gradient of the kinetic energy matrix element is:

$$\begin{aligned}\frac{\partial T_{kl}^{N=2}}{\partial (\text{vech } L_k)'} &= \frac{\partial S_{kl}^{N=2}}{\partial (\text{vech } L_k)'} \frac{T_{kl}^{N=2}}{S_{kl}^{N=2}} - \alpha^{-1} T_{kl}^{N=2} \frac{\partial \alpha}{\partial (\text{vech } L_k)'} \\ &+ \frac{2S_{kl}^{N=2}}{\alpha} \left\{ -\frac{\partial \tau_3}{\partial (\text{vech } L_k)'} + 3\tau_1 \frac{\partial \alpha}{\partial (\text{vech } L_k)'} + 3\alpha \frac{\partial \tau_1}{\partial (\text{vech } L_k)'} + \frac{\partial \tau_2}{\partial (\text{vech } L_k)'} (4 + \nu) \right\},\end{aligned}\quad (89)$$

and

$$\begin{aligned}\frac{\partial T_{kl}^{N=2}}{\partial (\text{vech } L_l)'} &= \frac{\partial S_{kl}^{N=2}}{\partial (\text{vech } L_l)'} \frac{T_{kl}^{N=2}}{S_{kl}^{N=2}} - \alpha^{-1} T_{kl}^{N=2} \frac{\partial \alpha}{\partial (\text{vech } L_l)'} \\ &+ \frac{2S_{kl}^{N=2}}{\alpha} \left\{ -\frac{\partial \tau_3}{\partial (\text{vech } L_l)'} + 3\tau_1 \frac{\partial \alpha}{\partial (\text{vech } L_l)'} + 3\alpha \frac{\partial \tau_1}{\partial (\text{vech } L_l)'} + \frac{\partial \tau_2}{\partial (\text{vech } L_l)'} (4 + \nu) \right\}.\end{aligned}\quad (90)$$

It should be noted that the gradient formulas for the τ parameters and their articulation in this paper are taken directly from [5]. For the τ_1 derivatives, we obtain:

$$\begin{aligned}\frac{\partial \tau_1}{\partial (\text{vech } L_k)'} &= -(\text{vech } A_{kl}^{-1} A_k M A_l A_{kl}^{-1} L_k)' - (\text{vech } A_{kl}^{-1} A_l M A_k A_{kl}^{-1} L_k)' \\ &\quad + (\text{vech } M A_l A_{kl}^{-1} L_k)' + (\text{vech } A_{kl}^{-1} A_l M L_k)',\end{aligned}\quad (91)$$

and

$$\begin{aligned} \frac{\partial \tau_1}{\partial (\text{vech } L_l)'} &= -(\text{vech } A_{kl}^{-1} A_k M A_l A_{kl}^{-1} L_l)' - (\text{vech } A_{kl}^{-1} A_l M A_k A_{kl}^{-1} L_l)' \\ &\quad + (\text{vech } A_{kl}^{-1} A_k M L_l)' + (\text{vech } M A_k A_{kl}^{-1} L_l)'. \end{aligned} \quad (92)$$

For τ_2 we have:

$$\begin{aligned} \frac{\partial \tau_2}{\partial (\text{vech } L_k)'} &= -(\text{vech } \mathbf{A}_{kl}^{-1} \mathbf{A}_k \mathbf{M} \mathbf{A}_l \mathbf{A}_{kl}^{-1} \mathbf{W}_{kl}^{N=1} \mathbf{A}_{kl}^{-1} \mathbf{L}_k)' \mathcal{T} - (\text{vech } \mathbf{A}_{kl}^{-1} \mathbf{W}_{kl}^{N=1} \mathbf{A}_{kl}^{-1} \mathbf{A}_l \mathbf{M} \mathbf{A}_k \mathbf{A}_{kl}^{-1} \mathbf{L}_k)' \mathcal{T} \\ &\quad - (\text{vech } \mathbf{A}_{kl}^{-1} \mathbf{A}_l \mathbf{M} \mathbf{A}_k \mathbf{A}_{kl}^{-1} \mathbf{W}_{kl}^{N=1} \mathbf{A}_{kl}^{-1} \mathbf{L}_k)' \mathcal{T} - (\text{vech } \mathbf{A}_{kl}^{-1} \mathbf{W}_{kl}^{N=1} \mathbf{A}_{kl}^{-1} \mathbf{A}_k \mathbf{M} \mathbf{A}_l \mathbf{A}_{kl}^{-1} \mathbf{L}_k)' \mathcal{T} \\ &\quad + (\text{vech } \mathbf{M} \mathbf{A}_l \mathbf{A}_{kl}^{-1} \mathbf{W}_{kl}^{N=1} \mathbf{A}_{kl}^{-1} \mathbf{L}_k)' \mathcal{T} + (\text{vech } \mathbf{A}_{kl}^{-1} \mathbf{W}_{kl}^{N=1} \mathbf{A}_{kl}^{-1} \mathbf{A}_l \mathbf{M} \mathbf{L}_k)' \mathcal{T}, \end{aligned} \quad (93)$$

and

$$\begin{aligned} \frac{\partial \tau_2}{\partial (\text{vech } L_l)'} &= -(\text{vech } \mathbf{A}_{kl}^{-1} \mathbf{A}_k \mathbf{M} \mathbf{A}_l \mathbf{A}_{kl}^{-1} \mathbf{W}_{kl}^{N=1} \mathbf{A}_{kl}^{-1} \mathbf{L}_l)' \mathcal{T} - (\text{vech } \mathbf{A}_{kl}^{-1} \mathbf{W}_{kl}^{N=1} \mathbf{A}_{kl}^{-1} \mathbf{A}_l \mathbf{M} \mathbf{A}_k \mathbf{A}_{kl}^{-1} \mathbf{L}_l)' \mathcal{T} \\ &\quad - (\text{vech } \mathbf{A}_{kl}^{-1} \mathbf{A}_l \mathbf{M} \mathbf{A}_k \mathbf{A}_{kl}^{-1} \mathbf{W}_{kl}^{N=1} \mathbf{A}_{kl}^{-1} \mathbf{L}_l)' \mathcal{T} - (\text{vech } \mathbf{A}_{kl}^{-1} \mathbf{W}_{kl}^{N=1} \mathbf{A}_{kl}^{-1} \mathbf{A}_k \mathbf{M} \mathbf{A}_l \mathbf{A}_{kl}^{-1} \mathbf{L}_l)' \mathcal{T} \\ &\quad + (\text{vech } \mathbf{A}_{kl}^{-1} \mathbf{W}_{kl}^{N=1} \mathbf{A}_{kl}^{-1} \mathbf{A}_k \mathbf{M} \mathbf{L}_l)' \mathcal{T} + (\text{vech } \mathbf{M} \mathbf{A}_k \mathbf{A}_{kl}^{-1} \mathbf{W}_{kl}^{N=1} \mathbf{A}_{kl}^{-1} \mathbf{L}_l)' \mathcal{T}. \end{aligned} \quad (94)$$

To transform the expression to the final form, a transformation matrix, \mathcal{T} , must be applied to the appropriate terms.

This transformation matrix has dimensions $\frac{3n(3n+1)}{2} \times \frac{n(n+1)}{2}$ and is defined as:

$$\mathcal{T} = \frac{d \text{vech } \mathbf{L}_k (\text{vech } L_k)}{d (\text{vech } L_k)'} \quad (95)$$

The notation $\text{vech } \mathbf{L}_k$ ($\text{vech } L_k$) indicates that the $3n(3n+1)/2$ -dimension vector $\text{vech } \mathbf{L}_k$ is a function of the $n(n+1)/2$ -dimension vector $\text{vech } L_k$. The derivative of $\text{vech } \mathbf{L}_k$ with respect to $\text{vech } L_k$ is defined as the $3n(3n+1)/2 \times n(n+1)/2$ matrix of partial derivatives whose ij -th element is the partial derivative of the i -th component of $\text{vech } \mathbf{L}_k$ (a column vector) with respect to the j -th element of $(\text{vech } L_k)'$ (a row vector). It should be noted that \mathcal{T} is a binary matrix and is independent of index k . (95) can be now rearranged to the following form:

$$d \text{vech } \mathbf{L}_k = \mathcal{T} \text{vech } L_k, \quad (96)$$

and to a similar form for $d \text{vech } \mathbf{L}_l$. The approach was first used in [13]. Next we substitute $(d \text{vech } \mathbf{L}_k)$ and $(d \text{vech } \mathbf{L}_l)$ with (96).

For τ_3 we have:

$$\begin{aligned} \frac{\partial \tau_3}{\partial (\text{vech } L_k)'} &= -(\text{vech } A_{kl}^{-1} (m_l A_k + m_k A_l) M J_{11} A_{kl}^{-1} L_k)' - (\text{vech } A_{kl}^{-1} J_{11} M (m_l A_k + m_k A_l) A_{kl}^{-1} L_k)' \\ &\quad + m_l (\text{vech } M J_{11} A_{kl}^{-1} L_k)' + m_l (\text{vech } A_{kl}^{-1} J_{11} M L_k)', \end{aligned} \quad (97)$$

and

$$\begin{aligned} \frac{\partial \tau_3}{\partial (\text{vech } L_l)'} &= -(\text{vech } A_{kl}^{-1} (m_l A_k + m_k A_l) M J_{11} A_{kl}^{-1} L_l)' - (\text{vech } A_{kl}^{-1} J_{11} M (m_l A_k + m_k A_l) A_{kl}^{-1} L_l)' \\ &\quad + m_k (\text{vech } M J_{11} A_{kl}^{-1} L_l)' + m_k (\text{vech } A_{kl}^{-1} J_{11} M L_l)'. \end{aligned} \quad (98)$$

C. Potential Energy Integral

To solve for the normalized potential energy matrix element, ($V_{kl}^{N=2}$), for the $N = 2$ rotationally excited states of a diatomic molecule, the element is defined as:

$$V_{kl}^{N=2} = \frac{\sum_{i=1, j>i}^{n_{tot}} q_i q_j \langle \phi_k^{N=2} | \frac{1}{r_{ij}} | \phi_l^{N=2} \rangle + \sum_{i=1}^{n_{tot}} q_0 q_i \langle \phi_k^{N=2} | \frac{1}{r_i} | \phi_l^{N=2} \rangle}{\sqrt{\langle \phi_k^{N=2} | \phi_k^{N=2} \rangle \langle \phi_l^{N=2} | \phi_l^{N=2} \rangle}}. \quad (99)$$

All bra-kets in the numerator can be solved for in a single derivation. To do this we take a similar approach as used in the evaluation of the overlap integral in the sense that we use the derivative of a Gaussian function defined in (19). However, instead of using the delta function (22) for $r_1^{m_k+m_l}$ we use the m^{th} -partial derivative:

$$(-1)^m \frac{\partial^m}{\partial u^m} \exp [-u \mathbf{r}' \mathbf{J}_{11} \mathbf{r}] \Big|_{u=0} = r_1^m, \quad (100)$$

where $m = (m_k + m_l)/2$. Recall that the sum of m_k and m_l is even in the present approach. To represent the $1/r_{ij}$ (or $1/r_i$) operator we use the following Gaussian integral transform:

$$\frac{2}{\sqrt{\pi}} \int_0^{+\infty} \exp [-t^2 \mathbf{r}' \mathbf{J}_{ij} \mathbf{r}] dt = \frac{1}{r_{ij}}. \quad (101)$$

With this the potential-energy matrix element is determined as the following integral:

$$\begin{aligned} \langle \phi_k^{N=2} | \frac{1}{r_{ij}} | \phi_l^{N=2} \rangle &= \langle (x_1^2 + y_1^2 - 2 z_1^2)^2 r_1^{(m_k+m_l)} \frac{1}{r_{ij}} \exp [-\mathbf{r}' \mathbf{A}_{kl} \mathbf{r}] \rangle \\ &= \frac{\partial}{\partial \omega_k} \frac{\partial}{\partial \omega_l} (-1)^m \frac{\partial^m}{\partial u^m} \frac{2}{\sqrt{\pi}} \times \\ &\quad \int_0^{+\infty} \langle \exp [-\mathbf{r}' (\mathbf{A}_{kl} + \omega_k \mathbf{W}_k^{N=2} + \omega_l \mathbf{W}_l^{N=2} + u \mathbf{J}_{11} + t^2 \mathbf{J}_{ij}) \mathbf{r}] \rangle dt \Big|_{\omega=u=0}, \end{aligned} \quad (102)$$

where $\mathbf{J}_{ij} = J_{ij} \otimes I_3$ and its structure is:

$$J_{ij} = \begin{cases} E_{ii} + E_{jj} - E_{ij} - E_{ji} & \text{for } i \neq j \\ E_{ii} & \text{for } i = j \end{cases} \quad (103)$$

(104)

E_{ij} has dimension $n \times n$ with 1's in the ij^{th} -position and zeros everywhere else. Next, we solve the bra-ket integrand. To do this we apply equation (25) and recover:

$$\begin{aligned} \langle \exp [-\mathbf{r}' (\mathbf{A}_{kl} + \omega_k \mathbf{W}_k^{N=2} + \omega_l \mathbf{W}_l^{N=2} + u \mathbf{J}_{11} + t^2 \mathbf{J}_{ij}) \mathbf{r}] \rangle &= \pi^{3n/2} |\mathbf{A}_{kl} + \omega_k \mathbf{W}_k^{N=2} + \omega_l \mathbf{W}_l^{N=2} + u \mathbf{J}_{11} + t^2 \mathbf{J}_{ij}|^{-1/2} \\ &= \pi^{3n/2} |A_{kl}|^{-3/2} |I_{3n} + \omega_k \mathbf{W}_k^{N=2} \mathbf{A}_{kl}^{-1} + \omega_l \mathbf{W}_l^{N=2} \mathbf{A}_{kl}^{-1} + u \mathbf{J}_{11} \mathbf{A}_{kl}^{-1} + t^2 \mathbf{J}_{ij} \mathbf{A}_{kl}^{-1}|^{-1/2} \end{aligned} \quad (105)$$

In the above we factor out the inverse of the determinant of the A_{kl} matrix using:

$$|X + Y| = |X| |I_p + Y X^{-1}|, \quad (106)$$

where X and Y are $p \times p$ square matrices.

Now we apply the derivative operation, $\frac{\partial}{\partial \omega_k} \frac{\partial}{\partial \omega_l}$, to the above and set ω_k and ω_l to zero:

$$\pi^{3n/2} |A_{kl}|^{-3/2} |I_n + u J_{11} A_{kl}^{-1} + t^2 J_{ij} A_{kl}^{-1}|^{-3/2} \left\{ \frac{1}{4} \eta_k^{N=2} \eta_l^{N=2} + \frac{1}{2} \eta_{k,l}^{N=2} \right\}, \quad (107)$$

where $\eta_k^{N=2} = \text{tr} [\mathbf{DW}_k^{N=2} \mathbf{A}_{kl}^{-1}] = 0$, $\eta_l^{N=2} = \text{tr} [\mathbf{DW}_l^{N=2} \mathbf{A}_{kl}^{-1}] = 0$, such that $\mathbf{D} = (I_{3n_{tot}} + u \mathbf{J}_{11} \mathbf{A}_{kl}^{-1} + t^2 \mathbf{J}_{ij} \mathbf{A}_{kl}^{-1})^{-1}$.

One can also show that:

$$\eta_{k,l}^{N=2} = \text{tr} [\mathbf{DW}_k^{N=2} \mathbf{A}_{kl}^{-1} \mathbf{DW}_l^{N=2} \mathbf{A}_{kl}^{-1}] = 6 \left(\frac{(\alpha + t^2 (\alpha\beta - \chi))}{(1 + u\alpha + t^2\beta + ut^2 (\alpha\beta - \chi))} \right)^2, \quad (108)$$

where

$$\beta = \text{tr} [A_{kl}^{-1} J_{ij}] = \begin{cases} (A_{kl}^{-1})_{(ii)} + (A_{kl}^{-1})_{(jj)} - (A_{kl}^{-1})_{(ij)} - (A_{kl}^{-1})_{(ji)} & \text{for } i \neq j, \\ (A_{kl}^{-1})_{(ii)} & \text{for } i = j, \end{cases} \quad (109)$$

(110)

and

$$\chi = \text{tr} [A_{kl}^{-1} J_{ij} A_{kl}^{-1} J_{11}] = \begin{cases} (A_{kl}^{-1})_{(1,i)} (A_{kl}^{-1})_{(i,1)} + (A_{kl}^{-1})_{(1,j)} (A_{kl}^{-1})_{(j,1)} \\ - (A_{kl}^{-1})_{(1,i)} (A_{kl}^{-1})_{(j,1)} - (A_{kl}^{-1})_{(1,j)} (A_{kl}^{-1})_{(i,1)} & \text{for } i \neq j, \\ (A_{kl}^{-1})_{(1,i)}^2 & \text{for } i = j. \end{cases} \quad (111)$$

(112)

Now, simplifying the determinant using:

$$|I_p + X| = 1 + \text{tr} [X], \quad (113)$$

and plugging in the quantities described above the bracket integrand is:

$$\begin{aligned} & \langle \exp [-\mathbf{r}' (\mathbf{A}_{kl} + \omega_k \mathbf{W}_k^{N=2} + \omega_l \mathbf{W}_l^{N=2} + u \mathbf{J}_{11} + t^2 \mathbf{J}_{ij}) \mathbf{r}] \rangle = \\ & = \frac{6}{2} \pi^{3n/2} |A_{kl}|^{-3/2} (1 + u\alpha + t^2\beta + ut^2 (\alpha\beta - \chi))^{-3/2} \frac{(\alpha + t^2 (\alpha\beta - \chi))^2}{(1 + u\alpha + t^2\beta + ut^2 (\alpha\beta - \chi))^2} = \\ & = \frac{6}{2} \pi^{3n/2} |A_{kl}|^{-3/2} \frac{(\alpha + t^2 (\alpha\beta - \chi))^2}{(1 + u\alpha + t^2\beta + ut^2 (\alpha\beta - \chi))^{7/2}}. \end{aligned} \quad (114)$$

Plugging this result back into initial integral and integrating over variable t results in:

$$\begin{aligned} \langle \phi_k^{N=2} | \frac{1}{r_{ij}} | \phi_l^{N=2} \rangle & = \frac{6}{2} \frac{2}{\sqrt{\pi}} \pi^{3n/2} |A_{kl}|^{-3/2} (-1)^m \frac{\partial^m}{\partial u^m} \int_0^{+\infty} \frac{\alpha^2 + 2t^2\alpha (\alpha\beta - \chi) + t^4 (\alpha\beta - \chi)^2}{(1 + u\alpha + t^2\beta + ut^2 (\alpha\beta - \chi))^{7/2}} dt \Big|_{u=0} \\ & = \alpha^2 \frac{6}{2} \frac{2}{\sqrt{\pi}} \pi^{3n/2} |A_{kl}|^{-3/2} (-1)^m \frac{\partial^m}{\partial u^m} \times \\ & \quad \left\{ \frac{8}{15} (\beta + u (\alpha\beta - \chi))^{-1/2} (1 + u\alpha)^{-3} + \frac{4 (\alpha\beta - \chi)/a}{15} (\beta + u (\alpha\beta - \chi))^{-3/2} (1 + u\alpha)^{-2} \right. \\ & \quad \left. + \frac{((\alpha\beta - \chi)/a)^2}{5} (\beta + u (\alpha\beta - \chi))^{-5/2} (1 + u\alpha)^{-1} \right\} \Big|_{u=0}. \end{aligned} \quad (115)$$

In the integration we use the following general integrals:

$$\int_0^{+\infty} 1/(s + rt^2)^{7/2} dt = \frac{8}{15} \left(\frac{r}{s} \right)^{-1/2} s^{-7/2} = \frac{8}{15} r^{-1/2} s^{-3}, \quad (116)$$

$$\int_0^{+\infty} t^2 / (s + rt^2)^{7/2} dt = \frac{2}{15} \left(\frac{r}{s}\right)^{-3/2} s^{-7/2} = \frac{2}{15} r^{-3/2} s^{-2}, \quad (117)$$

$$\int_0^{+\infty} t^4 / (s + rt^2)^{7/2} dt = \frac{1}{5} \left(\frac{r}{s}\right)^{-5/2} s^{-7/2} = \frac{1}{5} r^{-5/2} s^{-1}, \quad (118)$$

where $s \equiv 1 + u\alpha$ and $r \equiv \beta + u(\alpha\beta - \chi)$. Next the m^{th} -derivative with respect to u is determined using the well-known Leibniz equation:

$$\frac{d^m f_1(g_1(u)) f_2(g_2(u))}{du^m} = \sum_{q=0}^m \frac{\Gamma(m+1)}{\Gamma(q+1)\Gamma(-q+m+1)} \frac{d^q f_1(g_1(u))}{du^q} \frac{d^{m-q} f_2(g_2(u))}{du^{m-q}}. \quad (119)$$

To properly apply this formula we write some useful derivatives:

$$\frac{d^q r^{-1/2}}{du^q} = (-1)^q \frac{\Gamma(1/2+q)}{\Gamma(1/2)} \beta^{-1/2-q} (\alpha\beta - \chi)^q \quad (120)$$

$$\frac{d^q r^{-3/2}}{du^q} = (-1)^q \frac{\Gamma(3/2+q)}{\Gamma(3/2)} \beta^{-3/2-q} (\alpha\beta - \chi)^q \quad (121)$$

$$\frac{d^q r^{-5/2}}{du^q} = (-1)^q \frac{\Gamma(5/2+q)}{\Gamma(5/2)} \beta^{-5/2-q} (\alpha\beta - \chi)^q \quad (122)$$

$$\frac{d^{m-q} s^{-1}}{du^{m-q}} = (-1)^{m-q} \frac{\Gamma(-q+m+1)}{\Gamma(1)} \alpha^{m-q} \quad (123)$$

$$\frac{d^{m-q} s^{-2}}{du^{m-q}} = (-1)^{m-q} \frac{\Gamma(-q+m+2)}{\Gamma(2)} \alpha^{m-q} \quad (124)$$

$$\frac{d^{m-q} s^{-3}}{du^{m-q}} = (-1)^{m-q} \frac{\Gamma(-q+m+3)}{\Gamma(3)} \alpha^{m-q}. \quad (125)$$

$$\begin{aligned} \langle \phi_k^{N=2} | \frac{1}{r_{ij}} | \phi_l^{N=2} \rangle &= \alpha^2 \frac{6}{2} \frac{2}{\sqrt{\pi}} \pi^{3n/2} |A_{kl}|^{-3/2} \frac{4}{3 \times 5} \frac{\alpha^m}{\sqrt{\beta}} \Gamma(m+1) \left[m^2 + 4m + \frac{15}{4} - \left(m + \frac{5}{2}\right) \frac{\chi}{\alpha\beta} + \frac{3}{4} \left(\frac{\chi}{\alpha\beta}\right)^2 \right. \\ &+ \sum_{q=1}^m \gamma_3(q) \left(1 - \frac{\chi}{\alpha\beta}\right)^q \left[(-q+m+2)(-q+m+1) + 2(1/2+q)(-q+m+1) \left(1 - \frac{\chi}{\alpha\beta}\right) \right. \\ &\left. \left. + (1/2+q)(3/2+q) \left(1 - \frac{\chi}{\alpha\beta}\right)^2 \right] \right]. \end{aligned} \quad (126)$$

To write the above in terms of the normalized $N = 2$ overlap integral we apply:

$$\frac{5}{(15 + 16m + 4m^2)} \frac{1}{\Gamma(\frac{3+2m}{2})} \quad (127)$$

to the above and after some rearrangement and simplification we obtain the following final formula:

$$\begin{aligned} R_{kl}^{N=2} &= \frac{S_{kl}^{N=2}}{(3+2m)(5+2m)} \frac{\gamma_2(m)}{\sqrt{\beta}} \left\{ (3+2m)(5+2m) - 2(5+2m) \frac{\chi}{\alpha\beta} + 3 \left(\frac{\chi}{\alpha\beta}\right)^2 \right. \\ &+ 4 \sum_{q=1}^m \gamma_3(q) \left(1 - \frac{\chi}{\alpha\beta}\right)^q \left[(-q+m+2)(-q+m+1) + 2(1/2+q)(-q+m+1) \left(1 - \frac{\chi}{\alpha\beta}\right) \right. \\ &\left. \left. + (1/2+q)(3/2+q) \left(1 - \frac{\chi}{\alpha\beta}\right)^2 \right] \right\}. \end{aligned} \quad (128)$$

It is also important to mention that we used the following relation to effectively perform the simplification: $\Gamma(x) = (x - 1)!$, and $\Gamma(x + 1) = x!$. It should also be mentioned that $\mathbf{R}_{kl}^{N=2}$ needs to be multiplied by the appropriate charges to obtain $V_{kl}^{N=2}$.

The gradient formulas for the potential energy matrix elements are:

$$\begin{aligned} \frac{\partial R_{kl}^{N=2,ij}}{\partial (\text{vech } L_k)'} &= \frac{\partial S_{kl}^{N=2}}{\partial (\text{vech } L_k)'} \frac{R_{kl}^{N=2,ij}}{S_{kl}^{N=2}} - \frac{1}{2\beta} R_{kl}^{N=2} \frac{\partial \beta}{\partial (\text{vech } L_k)'} \\ &+ \frac{S_{kl}^{N=2}}{(3+2m)(5+2m)} \frac{\gamma_2(m)}{\sqrt{\beta}} \frac{\chi}{(\alpha\beta)^2} \left(\frac{\partial \alpha}{\partial (\text{vech } L_k)'} \beta + \frac{\partial \beta}{\partial (\text{vech } L_k)'} \alpha - \frac{\alpha\beta}{\chi} \frac{\partial \chi}{\partial (\text{vech } L_k)'} \right) \times \\ &\left\{ 2(5+2m) - 6 \left(\frac{\chi}{\alpha\beta} \right) + 4 \sum_{q=1}^m \gamma_3(q) \left(1 - \frac{\chi}{\alpha\beta} \right)^q \times \right. \\ &\left[q(-q+m+2)(-q+m+1) \left(1 - \frac{\chi}{\alpha\beta} \right)^{-1} + 2q(1/2+q)(-q+m+1) \right. \\ &\left. \left. + (q+1)(1/2+q)(3/2+q) \left(1 - \frac{\chi}{\alpha\beta} \right) \right] \right\} \end{aligned} \quad (129)$$

and

$$\begin{aligned} \frac{\partial R_{kl}^{N=2,ij}}{\partial (\text{vech } L_l)'} &= \frac{\partial S_{kl}^{N=2}}{\partial (\text{vech } L_l)'} \frac{R_{kl}^{N=2,ij}}{S_{kl}^{N=2}} - \frac{1}{2\beta} R_{kl}^{N=2} \frac{\partial \beta}{\partial (\text{vech } L_l)'} \\ &+ \frac{S_{kl}^{N=2}}{(3+2m)(5+2m)} \frac{\gamma_2(m)}{\sqrt{\beta}} \frac{\chi}{(\alpha\beta)^2} \left(\frac{\partial \alpha}{\partial (\text{vech } L_l)'} \beta + \frac{\partial \beta}{\partial (\text{vech } L_l)'} \alpha - \frac{\alpha\beta}{\chi} \frac{\partial \chi}{\partial (\text{vech } L_l)'} \right) \times \\ &\left\{ 2(5+2m) - 6 \left(\frac{\chi}{\alpha\beta} \right) + 4 \sum_{q=1}^m \gamma_3(q) \left(1 - \frac{\chi}{\alpha\beta} \right)^q \times \right. \\ &\left[q(-q+m+2)(-q+m+1) \left(1 - \frac{\chi}{\alpha\beta} \right)^{-1} + 2q(1/2+q)(-q+m+1) \right. \\ &\left. \left. + (q+1)(1/2+q)(3/2+q) \left(1 - \frac{\chi}{\alpha\beta} \right) \right] \right\}, \end{aligned} \quad (130)$$

where

$$\frac{\partial \alpha}{\partial (\text{vech } L_k)'} = \text{vech} [A_{kl}^{-1} J_{11} A_{kl}^{-1} L_k]', \quad (131)$$

$$\frac{\partial \alpha}{\partial (\text{vech } L_l)'} = \text{vech} [P A_{kl}^{-1} J_{11} A_{kl}^{-1} P' L_l]', \quad (132)$$

$$\frac{\partial \beta}{\partial (\text{vech } L_k)'} = \text{vech} [A_{kl}^{-1} J_{ij} A_{kl}^{-1} L_k]', \quad (133)$$

$$\frac{\partial \beta}{\partial (\text{vech } L_l)'} = \text{vech} [P A_{kl}^{-1} J_{ij} A_{kl}^{-1} P' L_l]', \quad (134)$$

$$\frac{\partial \chi}{\partial (\text{vech } L_k)'} = \text{vech} [A_{kl}^{-1} J_{ij} A_{kl}^{-1} J_{11} A_{kl}^{-1} L_k]' + \text{vech} [A_{kl}^{-1} J_{11} A_{kl}^{-1} J_{ij} A_{kl}^{-1} L_k]', \quad (135)$$

$$\frac{\partial \chi}{\partial (\text{vech } L_l)'} = \text{vech} [P A_{kl}^{-1} J_{ij} A_{kl}^{-1} J_{11} A_{kl}^{-1} P' L_l]' + \text{vech} [P A_{kl}^{-1} J_{11} A_{kl}^{-1} J_{ij} A_{kl}^{-1} P' L_l]'. \quad (136)$$

Again, we need to multiply $\frac{\partial \mathbf{R}_{kl}^{N=2}}{\partial \text{vech } L_k}$ and $\frac{\partial \mathbf{R}_{kl}^{N=2}}{\partial \text{vech } L_l}$ by the appropriate charges to obtain $\frac{\partial V_{kl}^{N=2}}{\partial \text{vech } L_k}$ and $\frac{\partial V_{kl}^{N=2}}{\partial \text{vech } L_l}$.

D. Interparticle Distance Matrix Elements

Exploiting equation (101), the fact that $r_{ij} = \frac{r_{ij}^2}{r_{ij}}$, and the fact that $r_{ij}^2 = \mathbf{r}' \mathbf{J}_{ij} \mathbf{r}$, where \mathbf{J}_{ij} is defined in equation (103), the following is obtained:

$$r_{ij} = \frac{2}{\sqrt{\pi}} \int_0^{+\infty} r_{ij}^2 \exp[-t^2 \mathbf{r}' \mathbf{J}_{ij} \mathbf{r}] dt = -\frac{\partial}{\partial \gamma} \frac{2}{\sqrt{\pi}} \int_0^{+\infty} \exp[-(t^2 + \gamma) \mathbf{r}' \mathbf{J}_{ij} \mathbf{r}] dt \Big|_{\gamma=0} \quad (137)$$

The expression for the matrix element of the r_{ij} interparticle distance is very similar to the potential-energy matrix element. The only difference is that it has the extra parameter γ in the exponent that the expression is differentiated with respect to. After the differentiation the parameter is set to zero. This extra parameter changes the operator from $\frac{1}{r_{ij}}$ to r_{ij} . The initial equation for the interparticle distance matrix element is therefore:

$$\langle \phi_k^{N=2} | r_{ij} | \phi_l^{N=2} \rangle = (-1)^{m+1} \frac{2}{\sqrt{\pi}} \frac{\partial}{\partial \gamma} \frac{\partial}{\partial \omega_k} \frac{\partial}{\partial \omega_l} \frac{\partial^m}{\partial u^m} \int_0^{+\infty} \langle \exp \left[-\mathbf{r}' \left(\mathbf{A}_{kl} + \omega_k \mathbf{W}_k + \omega_l \mathbf{W}_l + u \mathbf{J}_{11} + (t^2 + \gamma) \mathbf{J}_{ij} \right) \mathbf{r} \right] \rangle. \quad (138)$$

Up to the point where differentiation with respect to γ is carried out, the derivation is identical to the derivation of the potential energy matrix element, with the exception of the fact that the parameter γ is present throughout the derivation. Carrying out the derivation up to the point where the expression is differentiated with respect to γ , we have:

$$\begin{aligned} \langle \phi_k^{N=2} | r_{ij} | \phi_l^{N=2} \rangle = & -\frac{8\pi^{3n/2}}{5\sqrt{\beta}} \frac{|A_{kl}|^{-3/2}}{\sqrt{\pi}} \frac{\partial}{\partial \gamma} \left[\sum_{q=0}^m (\alpha\beta - \chi)^q (\alpha + \alpha\beta\gamma - \chi\gamma)^{m-q} \Gamma(m+1) \gamma_3(q) \right. \\ & \left[\left((\alpha\beta\gamma)^2 - 2\alpha\beta\chi\gamma^2 + (\alpha\chi)^2 + \alpha^2 + 2\alpha^2\beta\gamma - 2\alpha\chi\gamma \right) \beta^{-q} (2+m-q)(1+m-q)(1+\beta\gamma)^{-3-m+q} + \right. \\ & \left. \left(2\alpha^2\beta - 2\alpha\chi + 2\alpha^2\beta^2\gamma - 4\alpha\beta\chi\gamma + 2\chi^2\gamma \right) \beta^{-1-q} (q + \frac{1}{2})(1+m-q)(1+\beta\gamma)^{-2-m+q} + \right. \\ & \left. \left. \left((\alpha\beta)^2 - 2\alpha\beta\chi + \chi^2 \right) \beta^{-2-q} (q + \frac{3}{2})(q + \frac{1}{2})(1+\beta\gamma)^{-1-m+q} \right] \right] \end{aligned} \quad (139)$$

Taking the derivative of the above expression gives:

$$\begin{aligned} \langle \phi_k^{N=2} | r_{ij} | \phi_l^{N=2} \rangle = & -\frac{8\pi^{3n/2}}{5\sqrt{\pi}} |A_{kl}|^{-3/2} \alpha^{m+2} \frac{\Gamma(m+1)}{\sqrt{\beta}} \left[\sum_{q=0}^m \gamma_3(q) (\alpha\beta - \chi)^q \alpha^{-q} \left((m-q)\alpha^{-1}(\alpha\beta - \chi) \right. \right. \\ & \left. \left[\beta^{-q} (2+m-q)(1+m-q) + 2\beta^{-1-q} (q + \frac{1}{2})(1+m-q) \left(\beta - \frac{\chi}{\alpha} \right) + \beta^{-2-q} (q + \frac{3}{2})(q + \frac{1}{2}) \left(\beta - \frac{\chi}{\alpha} \right)^2 \right] + \right. \\ & \left. \left[\beta^{-q} (2+m-q)(1+m-q) \left(2\left(\beta - \frac{\chi}{\alpha} \right) + (-3-m+q)\beta \right) + 2\beta^{-1-q} (q + \frac{1}{2})(1+m-q) \right. \right. \\ & \left. \left. \left(\left(\beta - \frac{\chi}{\alpha} \right)^2 + (-2-m+q)\beta \left(\beta - \frac{\chi}{\alpha} \right) \right) + \beta^{-2-q} (q + \frac{3}{2})(q + \frac{1}{2})(-1-m+q)\beta \left(\beta - \frac{\chi}{\alpha} \right)^2 \right] \right] \end{aligned} \quad (140)$$

For the final expression, α^{-q} is incorporated into the preceding term, $(\alpha\beta - \chi)^q$. β^{-q} is factored out of the summation and incorporated into the same term. Additionally, the following equalities are used:

$$\frac{8\pi^{3n/2}}{5\sqrt{\pi}} |A_{kl}|^{-3/2} \alpha^{m+2} = \frac{4 \langle \phi_k^{N=2} | \phi_l^{N=2} \rangle}{\Gamma(\frac{3}{2} + m)(2m+3)(2m+5)} \quad (141)$$

and

$$\gamma_2(m) = \frac{\Gamma(m+1)}{\Gamma(m+\frac{3}{2})} \quad (142)$$

After normalization, the final expression for the interparticle distance matrix element is:

$$\begin{aligned} -\frac{4S_{kl}^{N=2}\gamma_2(m)}{\sqrt{\beta}(2m+3)(2m+5)} & \left[\sum_{q=0}^m \gamma_3(q) \left(1 - \frac{\chi}{\alpha\beta}\right)^q \left((m-q)\alpha^{-1}(\alpha\beta - \chi) \left[(2+m-q)(1+m-q) + \right. \right. \right. \\ & 2(q+\frac{1}{2})(1+m-q) \left(1 - \frac{\chi}{\alpha\beta}\right) + (q+\frac{3}{2})(q+\frac{1}{2}) \left(1 - \frac{\chi}{\alpha\beta}\right)^2 \left. \right] + \\ & \left[\beta(2+m-q)(1+m-q) \left(2 \left(1 - \frac{\chi}{\alpha\beta}\right) - 3 - m + q \right) \right. \\ & + 2\beta(q+\frac{1}{2})(1+m-q) \left(\left(1 - \frac{\chi}{\alpha\beta}\right)^2 + (-2-m+q) \left(1 - \frac{\chi}{\alpha\beta}\right) \right) \\ & \left. \left. \left. + \beta(q+\frac{3}{2})(q+\frac{1}{2})(-1-m+q) \left(1 - \frac{\chi}{\alpha\beta}\right)^2 \right] \right] \right] \end{aligned} \quad (143)$$

Acknowledgements

This material is based upon work supported by the National Science Foundation under grant number 1228509.

This work has also been supported in part by the National Science Foundation through the bridges to the doctorate fellowship (BD); grant number HRD-1249143 and through the graduate research fellowship program (GRFP) awarded to Keeper L. Sharkey; grant number DGE1-1143953. We are grateful to the University of Arizona Center of Computing and Information Technology for the use of their computer resources and the El Gato cluster, NSF grant number 1228509.

-
- [1] I. Ben-Itzhak, E. Wells, K. D. Carnes, V. Krishnamurthi, O. L. Weaver, B. D. Esry, Phys. Rev. Lett. **85**, 58 (2000).
 - [2] A. Carrington, I. R. McNab, and C. A. Montgomerie, J. Phys. B: At. Mol. Opt. Phys. **22**, 3551 (1989).
 - [3] S. Bubin, M. Pavanello, W. C. Tung, K. L. Sharkey, and L. Adamowicz, Chem. Rev. **113**, 36 (2013).
 - [4] J. Mitroy, S. Bubin, W. Horiuchi, Y. Suzuki, L. Adamowicz, W. Cencek, K. Szalewicz, J. Komasa, D. Blume, and K. Varga, Rev. Mod. Phys. **85**, 693 (2013).
 - [5] K. L. Sharkey, N. Kirnosov, and L. Adamowicz, J. Chem. Phys. **139**, 164119 (2013).
 - [6] J. Ph. Karr and L. Hilico, Journal of Physics B. **39**, 2095 (2006).
 - [7] D. B. Kinghorn and R. D. Poshusta, Int. J. Quantum Chem. **62**, 223 (1997).
 - [8] D. B. Kinghorn and L. Adamowicz, Phys. Rev. Lett. **83**, 2541 (1999).
 - [9] M. Cafiero and L. Adamowicz, Int. J. Quantum Chem. **107**, 2679 (2007).
 - [10] K. L. Sharkey and L. Adamowicz, J. Chem. Phys. **134**, 194114 (2011).
 - [11] D. B. Kinghorn and L. Adamowicz, J. Chem. Phys. **110**, 7166 (1999).
 - [12] K. L. Sharkey, N. Kirnosov, and L. Adamowicz, J. Chem. Phys. **138**, 104107 (2013).
 - [13] K. L. Sharkey, S. Bubin, and L. Adamowicz, Phys. Rev. A **83**, 012506 (2011).
 - [14] G. G. Balint-Kurti, R. E. Moss, I. A. Sadler, and M. Shapiro, Phys. Rev. A **41**, 4913 (1990).
 - [15] R. E. Moss, Mol. Phys. **78**, 371 (1993).
 - [16] N. Kirnosov, K. L. Sharkey, and L. Adamowicz, J. Chem. Phys. **139**, 204105 (2013).

TABLE I: Convergence of the total energy for the $(v,1)$ rovibrational states of HD^+ with the number of ECGs (# ECGs). Energy is given in hartrees.

v	# ECGs	Energy	v	no. ECGs	Energy
0	1000	-0.597 299 610 217	1	1000	-0.588 610 797 365
	2000	-0.597 299 611 105		2000	-0.588 610 797 941
2	2000	-0.580 359 164 718	3	2000	-0.572 531 780 588
	3000	-0.580 359 164 787		3000	-0.572 531 780 661
4	2000	-0.565 117 420 639	5	2000	-0.558 106 519 288
	3000	-0.565 117 420 998		3000	-0.558 106 520 143
6	3000	-0.551 491 145 286	7	3000	-0.545 264 987 807
	4000	-0.551 491 145 622		4000	-0.545 264 988 930
8	3000	-0.539 423 377 477	9	3000	-0.533 963 314 525
	4000	-0.539 423 379 396		4000	-0.533 963 314 945
10	3000	-0.528 883 519 289	11	3000	-0.524 184 528 797
	4000	-0.528 883 519 811		4000	-0.524 184 529 155
12	3000	-0.519 868 795 786	13	3000	-0.515 940 859 652
	4000	-0.519 868 796 738		4000	-0.515 940 860 542
14	4000	-0.512 407 502 496	15	4000	-0.509 278 015 092
	5000	-0.512 407 503 235		5000	-0.509 278 016 369
16	5000	-0.506 564 485 660	17	5000	-0.504 282 109 343
	6000	-0.506 564 496 790		6000	-0.504 282 114 277
18	5000	-0.502 449 457 544	19	6000	-0.501 088 749 185
	6000	-0.502 449 519 564		7000	-0.501 088 750 680
20	6000	-0.500 224 149 710	21	6000	-0.499 889 102 659
	7000	-0.500 224 150 080		7000	-0.499 889 105 498

TABLE II: Comparison of the dissociation energies obtained in this work for the ($v,2$) state of HD^+ with the literature values shown in the form [Ref.] - Present. All results are in cm^{-1}

ν	Present	[15]	[6]	[14]
0	21384.6854	0.0070	0.0069	0.0028
1	19477.7113	0.0069	0.0068	0.0028
2	17666.6872	0.0066	0.0066	0.0026
3	15948.7749	0.0065	0.0064	0.0026
4	14321.5111	0.0063	0.0062	
5	12782.7962	0.0062	0.0061	
6	11330.8893	0.0060	0.0059	
7	9964.4059	0.0059	0.0057	
8	8682.3208	0.0057	0.0056	
9	7483.9751	0.0055	0.0054	
10	6369.0890	0.0053	0.0053	
11	5337.7797	0.0051	0.0050	
12	4390.5859	0.0056	0.0055	
13	3528.5036	0.0048	0.0047	
14	2753.0213	0.0045	0.0045	0.0016
15	2066.1783	0.0049	0.0048	0.0021
16	1470.6296	0.0025	0.0024	-0.0002
17	969.7046	0.0041	0.0041	0.0016
18	567.4965	0.0041	0.0040	0.0018
19	268.8423	0.0035	0.0035	
20	79.0844	0.0018	0.0018	-0.0003
21	5.5506	0.0007	0.0008	

TABLE III: Pure rotational transition energies, the energy difference between the $(v,1)$ and $(v,2)$ states, Δ in cm^{-1} . $(v,1)$ energies taken from [5]. Difference between Δ obtained in this work and Δ taken from calculations performed by others in cm^{-1} shown in the form [Ref.] - Present.

ν	Δ	[15]	[6]	[14]
0	87.4620	-0.0047	-0.0046	-0.0019
1	83.4670	-0.0046	-0.0045	-0.0019
2	79.5932	-0.0045	-0.0043	-0.0018
3	75.8255	-0.0043	-0.0042	-0.0016
4	72.1491	-0.0042	-0.0041	
5	68.5493	-0.0041	-0.0040	
6	65.0112	-0.0039	-0.0038	
7	61.5199	-0.0039	-0.0037	
8	58.0594	-0.0036	-0.0036	
9	54.6138	-0.0036	-0.0035	
10	51.1649	-0.0034	-0.0034	
11	47.6938	-0.0033	-0.0033	
12	44.1786	-0.0031	-0.0031	
13	40.5951	-0.0030	-0.0030	
14	36.9144	-0.0027	-0.0027	-0.0008
15	33.1022	-0.0026	-0.0026	-0.0008
16	29.1135	-0.0004	-0.0003	0.0013
17	24.8989	-0.0015	-0.0015	-0.0003
18	20.3797	-0.0019	-0.0018	-0.0019
19	15.4485	-0.0016	-0.0016	
20	9.9136	-0.0011	-0.0011	0.0005
21	3.0013	-0.0001	-0.0002	

TABLE IV: Comparison to experiment. Rovibrational transition energies with and without relativistic and radiative corrections.

All values are in cm^{-1} . Experimental values taken from [2]. Corrections taken from [15].

$(\nu', N') - (\nu'', N'')$	Δ	Δ_{corr}	Exp- Δ	Exp- Δ_{corr}
(1,1)-(0,2)	1823.5071	1823.5282	0.026	0.005
(3,2)-(2,1)	1797.5054	1797.5267	0.017	-0.005
(3,1)-(2,2)	1642.0867	1642.1037	0.021	0.004
(18,2)-(16,1)	932.2466	932.2256	-0.023	-0.002
(18,1)-(16,2)	882.7534	882.7325	-0.022	-0.001
(17,2)-(14,1)	1820.2312	1820.2102	-0.022	-0.001
(17,1)-(15,2)	1071.5749	1071.5583	-0.014	0.003
(20,1)-(17,2)	880.7066	880.6649	-0.039	0.003
(20,2)-(17,1)	915.5191	915.4766	-0.043	-0.001
(21,2)-(17,1)	989.0529	988.9914	-0.061	0.001
(22,1)-(17,2)	969.5889	969.5246	-0.059	0.005

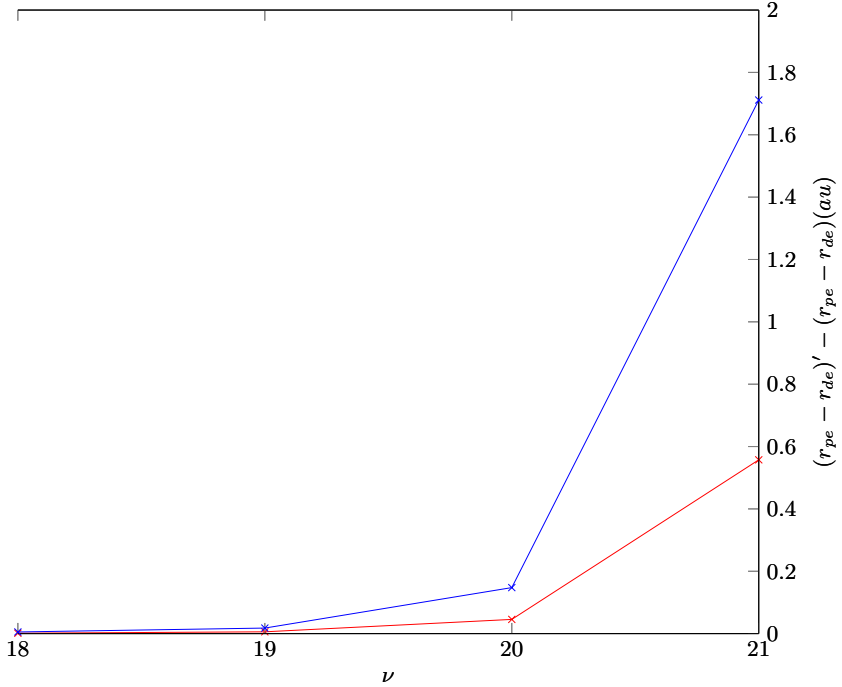
FIG. 1: The difference of $(r_{pe} - r_{de})$ values between the $(N=2)$ and $(N=0)$ states (in blue) and between the $(N=1)$ and $(N=0)$ states (in red) for HD^+ in au, indicating a higher degree of charge asymmetry at higher rotational states.

TABLE V: Average interparticle distances in atomic units, for all the bound vibrational states of HD^+ in the N=2 rotational level (first three columns). Differences between interparticle distances between the N=2 and N=0 rotational state (columns 4-6), and between the N=1 and N=0 rotational state (columns 7-9). Subscript notation is as follows: d corresponds to deuteron, p corresponds to proton, and e corresponds to electron.

v	$\langle r_{dp} \rangle$	$\langle r_{de} \rangle$	$\langle r_{pe} \rangle$	$\Delta_2 \langle r_{dp} \rangle$	$\Delta_2 \langle r_{de} \rangle$	$\Delta_2 \langle r_{pe} \rangle$	$\Delta_1 \langle r_{dp} \rangle$	$\Delta_1 \langle r_{de} \rangle$	$\Delta_1 \langle r_{pe} \rangle$
0	2.061	1.691	1.692	0.0058	0.0028	0.0035	0.0018	0.0008	0.0015
1	2.178	1.753	1.754	0.0074	0.0027	0.0035	0.0024	0.0007	0.0015
2	2.298	1.817	1.818	0.0060	0.0036	0.0035	0.0020	0.0016	0.0015
3	2.424	1.883	1.884	0.0070	0.0028	0.0029	0.0020	0.0008	0.0009
4	2.554	1.952	1.953	0.0071	0.0037	0.0029	0.0021	0.0017	0.0009
5	2.690	2.024	2.026	0.0070	-0.0005	0.0040	0.0020	0.0015	0.0010
6	2.833	2.100	2.101	0.0077	0.0049	0.0036	0.0027	0.0019	0.0016
7	2.984	2.179	2.181	0.0092	0.0043	0.0043	0.0032	0.0013	0.0013
8	3.144	2.264	2.266	0.0089	0.0054	0.0049	0.0029	0.0014	0.0019
9	3.315	2.353	2.357	0.0096	0.0051	0.0062	0.0036	0.0021	0.0022
10	3.500	2.450	2.454	0.0106	0.0045	0.0064	0.0036	0.0015	0.0024
11	3.701	2.555	2.560	0.0118	0.0061	0.0060	0.0038	0.0021	0.0020
12	3.922	2.670	2.677	0.0130	0.0058	0.0072	0.0040	0.0018	0.0022
13	4.169	2.798	2.807	0.0148	0.0072	0.0078	0.0048	0.0022	0.0028
14	4.449	2.943	2.955	0.0168	0.0090	0.0088	0.0058	0.0030	0.0028
15	4.775	3.109	3.127	0.0211	0.0102	0.0105	0.0071	0.0032	0.0035
16	5.163	3.305	3.333	0.0252	0.0127	0.0136	0.0082	0.0047	0.0046
17	5.644	3.543	3.590	0.0332	0.0164	0.0182	0.0112	0.0054	0.0062
18	6.274	3.842	3.936	0.0467	0.0210	0.0263	0.0157	0.0070	0.0083
19	7.173	4.226	4.467	0.0742	0.0281	0.0459	0.0242	0.0091	0.0149
20	8.708	4.575	5.670	0.1578	0.0061	0.1537	0.0508	0.0031	0.0487
21	14.02	1.985	13.58	1.0725	-0.3209	1.3905	0.3225	-0.1169	0.4405

APPENDIX I

Nuclear-nuclear correlation function from non-Born-Oppenheimer calculations of diatomic rovibrational states with total angular momentum equal to two ($N=2$).

Charge asymmetry in HD.

Nuclear-nuclear correlation function from non-Born-Oppenheimer calculations of diatomic rovibrational states with total angular momentum equal to two ($N=2$).

Charge asymmetry in HD.

Keith Jones^a, Martin Formanek^b, Rahik Mazumder^a, Nikita Kirnosov^b, Ludwik Adamowicz^{a,b}

^a*Department of Chemistry and Biochemistry, University of Arizona, Tucson, Arizona 85721, U.S.A.*

^b*Department of Physics, University of Arizona, Tucson, Arizona 85721, U.S.A.*

The HD molecule in rovibrational states where the total angular momentum quantum number is equal to two ($N = 2$) is characterized with quantum mechanical calculations without assuming the Born-Oppenheimer (BO) approximation. Explicitly correlated all-particle Gaussian functions are used in the calculations. The convergence of the total non-BO energies of the considered states with the basis set size is analyzed. The calculations of the averaged interparticle distances demonstrate the asymmetry of the electronic charge distribution. The algorithm to calculate the nuclear-nuclear correlation function for the $N = 2$ states is derived and implemented. Plots of this function for different rovibrational states provide a visual representation of the molecular structure.

I. INTRODUCTION

Calculating energies and wave functions of bound states of Coulombic systems like molecules has been accomplished with varying degrees of accuracy. Various approaches have been used. There are variational molecular calculations employing expansions of the wave functions in terms of functions dependent on all interparticle coordinates [1] and molecular calculations which use the adiabatic approximation [2], where the wave function is represented as a product of an electronic wave function and a nuclear wavefunction. The adiabatic approximation is satisfactory in most cases, but breaks down under certain conditions, for example, when energy spacings between electronic levels are comparable to the spacings between rovibrational levels [3]. In such cases a so called conical intersection or an avoided crossing, depending on the symmetry of the states, may appear. Conical intersections are common in reactions that occur through electronic excited states. Different methods have been applied to describe this phenomenon. These include the density functional methods whose application have achieved varying degrees of success [4].

In this study, explicitly all-particle correlated Gaussian functions (i.e. functions that explicitly depend on the distances between the particles forming the system) are employed to calculate the energies and the wave functions of rovibrational states of the HD molecule. The Born-Oppenheimer (BO) approximation is not assumed in the approach and all particles of the system are treated on equal footing. In very accurate non-BO calculations it is critical how the basis functions used in expanding the wave function of the system are designed. The design needs to correctly reproduce the known features of the wave function (i.e. the cusp conditions, the asymptotic behavior at large distances

away from the system) yet be practical and efficient when used in the calculations. The main feature the basis set is required to effectively describe is the interparticle correlation. In a system like HD where there are two particles with positive charges (the proton and the deuteron) and two particles with negative charges (the two electrons) there are three types of correlations, i.e. the correlation involving two positively charged particles (deuteron-proton), the correlation between a positively charged particle and a negatively charged particle (deuteron-electron and proton-electron), and the correlation between two negatively charged particles (electron-electron). Due to the particles having different masses, even the correlations between particles with alike charges are different. For example, the deuteron and proton avoid each other much more in their relative motion in the HD molecule than the two electrons. The probability of finding two electrons in a single point in space (as they have opposite spins this probability is not zero) is much higher than the probability of finding the deuteron and the proton in a single point (that probability is practically zero). The physical nature of the correlation effects needs to be correctly represented in designing the basis set. Also, the selected basis functions need to enable an efficient variational optimization of their intrinsic parameters. Usually such an optimization leads to much improved results. The optimization can be significantly accelerated if the analytical energy gradient determined with respect to the parameters is used and the algorithms for calculating the matrix elements of the Hamiltonian and the gradient are efficiently parallelized in the computer code.

As the HD molecule approaches dissociation via rovibrational excitation, the average interparticle distances increase. This is expected, however, this is only one aspect of the phenomenon, which in order to be fully described requires a detailed analysis of the molecular rovibrational excitations, i.e. their energies and the wave functions, up to the dissociation limit. The molecular structure takes a specific form during this process. The expectation values and the plots of the deuteron-proton correlation functions presented in this work allows for elucidation of this structure.

A direct calculation of rovibrationally excited states without assuming the BO approximation can only be done if the manifold of states are separated into subsets according to different values of a quantum number, which is a "good" quantum number for the system. Such a quantum number for non-BO calculations of a molecule is the total angular momentum quantum number, N , representing the overall angular symmetry of the considered subset of states of the system. N is not strictly speaking a rotational quantum number (although to a good approximation it is) because a state with a particular value of the N quantum number may have contributions to its wave function representing either pure rotational excitation of the nuclear motion, or pure angular excitation of the electrons, or a combination of the two. In addition, in a rovibrational excitation the vibrational motion of the molecule can be excited and this means that the non-BO wave function of the system needs to acquire nodes in terms of the coordinate representing the distance between the nuclei (for a diatomic molecule) or distances between the nuclei (for a polyatomic molecule). Of course, as the motion of the electrons is coupled with the motion of the nuclei, there has to be sufficient flexibility in the basis functions used in the non-BO calculation to describe this coupling. As discussed below, the vibrational oscillation of the wavefunction in terms of the internuclear distance (let us call it r) can be effectively described in the

wave function by multiplying the explicitly correlated Gaussian functions by powers of r [3]. In the r^{2m} prefactor used in the present calculations only even non-negative powers are used. They vary in the $0 < 2m < 250$ range. Although, the use of odd powers would help achieving better convergence in the calculations, our experience indicates that very accurate results can be achieved with only even powers if they and the non-linear exponential parameters of the Gaussians are thoroughly optimized.

When explicitly correlated all-particle Gaussians are used in the calculation, the BO approximation is not assumed. The analysis and interpretation of the wave function obtained in the calculation is not straightforward. A set of parameters that can be calculated to characterize the state of the system are average interparticle distances and their powers. Another way of the characterization is the calculation of interparticle correlation functions which show the relative probability density for a pair of particles. In particular, for rovibrational states corresponding to the same total rotational quantum number (N), the internuclear density function (also called nuclear-nuclear correlation function) is a function that reveals the differences between the states in the most transparent way. The inter-nuclear correlation function is expected to show the increasing oscillatory character of the density in terms of the internuclear distance as the level of the vibrational excitation gets higher. It should also show the angular nodes that appear in the nuclear-nuclear correlation function for any state corresponding to the N value different than zero, in particular, for the $N = 2$ states of HD calculated in the present work.

In this work, the derivation and computational implementation of the nuclear-nuclear correlation function for the $N = 2$ states for a diatomic molecule with an arbitrary number of electrons is described. The algorithm is used to plot the function for all bound rovibrational states with $N = 2$ for the HD molecule. In addition to the plots, the expectation values of the inter-particle distances are calculated and compared with the expectation values obtained before for the $N = 0$ and $N = 1$ states. The comparison allows for an analysis of how the rotational excitation affects the HD charge asymmetry. This asymmetry is a purely non-adiabatic effect that only non-BO calculations can reveal. In addition to the analysis of the rovibrational wave functions, the total non-BO energies of the considered rovibrational states along with the corresponding dissociation energies are presented. The latter energies are compared with the high-accuracy calculations of Komasa and Pachucki [5] performed using the conventional approach based on the BO approximation and involving perturbation-theory calculations of adiabatic and non-adiabatic effects. These effects are automatically included to infinite order in the results of our non-BO variational calculations.

II. BACKGROUND

A. Coordinate Transformation

For an N -particle system with the mass, charge, and position vector in the laboratory coordinate system of particle i denoted as M_i , Q_i , and \mathbf{R}_i , respectively, the general, laboratory-frame non-relativistic Hamiltonian is as follows:

$$\hat{H}_{LAB} = - \sum_{i=1}^N \frac{\nabla_{\mathbf{R}_i}^2}{2M_i} + \sum_{i=1, j>i}^N \frac{Q_i Q_j}{|\mathbf{R}_j - \mathbf{R}_i|} \quad (1)$$

In \hat{H}_{LAB} the center-of-mass motion can be rigorously separated from the internal motion of the system through a coordinate transformation to a new coordinate system where the first three coordinates, \mathbf{r}_0 , correspond to the center-of-mass of the system in the laboratory frame and the remaining $3N-3$ coordinates, \mathbf{r}_i , correspond to the relative coordinates of $N-1$ particles with respect to the reference particle. The reference particle is usually chosen to be the heaviest particle and for HD it is the deuteron. The transformation of the coordinate system and consequently, the Hamiltonian, as shown below, leads to a Hamiltonian called the internal Hamiltonian that describes a simpler system with $n = N-1$ pseudoparticles, rather than N particles. The convenience of the specific form of the internal Hamiltonian is discussed next. The transformation of the laboratory-frame coordinates to the new coordinates can be described as follows:

$$\mathbf{r}_0 = \sum_{i=1}^N \frac{M_i \mathbf{R}_i}{\tilde{M}}, \quad \mathbf{r}_i = \mathbf{R}_{i+1} - \mathbf{R}_1, \quad (2)$$

where $\tilde{M} = \sum_{j=1}^N M_j$. The coordinate transformation matrix is:

$$T = \begin{pmatrix} \frac{M_1 \mathbf{R}_1}{\tilde{M}} & \frac{M_2 \mathbf{R}_2}{\tilde{M}} & \frac{M_3 \mathbf{R}_3}{\tilde{M}} & \dots & \frac{M_N \mathbf{R}_N}{\tilde{M}} \\ -1 & 1 & 0 & \dots & 0 \\ -1 & 0 & 1 & \dots & \vdots \\ \vdots & \vdots & \ddots & \ddots & 0 \\ -1 & 0 & \dots & 0 & 1 \end{pmatrix} \otimes I_3, \quad \mathbf{r}' = \begin{pmatrix} \mathbf{r}_0 \\ \mathbf{r}_1 \\ \mathbf{r}_2 \\ \vdots \\ \mathbf{r}_n \end{pmatrix}, \quad \mathbf{R} = \begin{pmatrix} \mathbf{R}_1 \\ \mathbf{R}_2 \\ \mathbf{R}_3 \\ \vdots \\ \mathbf{R}_N \end{pmatrix}$$

Where $T\mathbf{R} = \mathbf{r}'$ and I_3 is the 3 by 3 square identity matrix. The coordinate transformation separates the Hamiltonian (1) into the internal Hamiltonian, which is isotropic (or spherically symmetric) and depends only upon the $3N-3$ internal coordinates, $\mathbf{r}_1, \mathbf{r}_2, \dots, \mathbf{r}_n$, and the center-of-mass Hamiltonian, which depends upon the center-of-mass laboratory-frame coordinates, \mathbf{r}_0 . This separation simplifies the problem. With that in mind, the following $3N-3$

dimensional vector of the internal coordinates is introduced:

$$\mathbf{r} = \begin{pmatrix} \mathbf{r}_1 \\ \mathbf{r}_2 \\ \vdots \\ \mathbf{r}_n \end{pmatrix} = \begin{pmatrix} X_2 - X_1 \\ Y_2 - Y_1 \\ Z_2 - Z_1 \\ X_3 - X_1 \\ \vdots \\ Z_N - Z_1 \end{pmatrix} = \begin{pmatrix} x_1 \\ y_1 \\ z_1 \\ x_2 \\ \vdots \\ z_n \end{pmatrix}$$

The internal Hamiltonian is as follows:

$$\hat{H} = -\frac{1}{2} \left[\sum_{i=1}^n \frac{\nabla_{r_i}^2}{\mu_i} + \sum_{i \neq j}^n \frac{\nabla'_{r_i} \nabla_{r_j}}{\widetilde{M}} \right] + \sum_{i=1}^n \frac{q_0 q_i}{r_i} + \sum_{i=1, j>i}^n \frac{q_i q_j}{|r_j - r_i|}, \quad (3)$$

where q_i is the charge on pseudoparticle i (q_i is equal to Q_{i+1} and q_0 equal to Q_1 is the charge of the reference particle; $q_0 = +1$ for HD), and $\mu_i = m_0 m_i / (m_0 + m_i)$ is the reduced mass of pseudoparticle i with respect to the reference particle. The pseudoparticle motion is coupled through the mass polarization term (the second summation in the above expression for the internal Hamiltonian (3)) and through the Coulombic interaction terms (the last two terms in (3)).

B. The Basis Set

The Hamiltonian is atom-like due to the fact that it is spherically symmetric with respect to the reference particle. Eigenfunctions of this Hamiltonian are also Eigenfunctions of the total angular momentum squared and its projection upon a particular axis. With this in mind, the wavefunction for a diatomic molecule with total angular momentum equal to two and for an arbitrary vibrational level can be described by a linear combination of the following basis functions:

$$\phi_k^{N=2} = (x_1^2 + y_1^2 - 2z_1^2) r_1^{m_k} \exp \left[-\mathbf{r}' (A_k \otimes I_3) \mathbf{r} \right]. \quad (4)$$

The first premultiplier is the non-normalized spherical harmonic Y_2^0 as a function of the relative Cartesian coordinates, x_1 , y_1 , and z_1 , describing in HD the position of the proton relative to the position of the deuteron. The use of only x_1^2 , y_1^2 , and z_1^2 in the angular factor and not the general x_i^2 , y_i^2 , and z_i^2 terms or even the more general $x_i x_j$, $y_i y_j$, and $z_i z_j$ terms is somewhat an approximation that assumes that the majority of the angular excitation of the molecule comes from the nuclei. However, as can be shown, Gaussians (4) with the $(x_1^2 + y_1^2 - 2z_1^2)$ angular prefactor are not orthogonal to the Gaussians with the $(x_i^2 + y_i^2 - 2z_i^2)$ (with $i \neq 1$) and $(x_i x_j + y_i y_j - 2z_i z_j)$ (with $i \neq j$) prefactors when the A_k matrix has non-zero off-diagonal matrix elements. Thus some contribution from the Gaussians with the more general angular factors are accounted for when only Gaussians with the $(x_1^2 + y_1^2 - 2z_1^2)$ factor are used in the calculation. The second term, $r_1^{m_k}$, in (4) is a (even) power of the internuclear distance which contains one integer parameter, m_k .

This parameter is variationally optimized in the calculation (along with other non-linear parameters). The presence of the $r_1^{m_k}$ factors in the basis functions allows, as mentioned in the introduction, for describing the vibrational nodes in the wave function. It also allows for describing the nuclear-nuclear cusp and the decreasing probability of the two nuclei being found close to each other as their relative distance becomes shorter.

A_k in (4) is an n by n , positive definite matrix. This is ensured by representing it the Cholesky decomposition form as: $A_k = L_k L'_k$ with L_k being a lower triangular matrix. A_k in this form is always positive definite for any (real) values of the L_k matrix elements. This feature is important in the optimization of the Gaussian non-linear parameters, which in the present calculations are the L_k matrix elements and not the A_k matrix elements. Using the L_k matrix elements as the variables allows for an unconstrained variational optimization. The optimization would not be unconstrained if the A_k matrix elements were used as variables, as their values are constrained due to the positive-definite requirement which is imposed on the A_k matrix.

Taking the Kronecker product, $(A_k \otimes I_3)$, in (4) generates the $3n$ by $3n$ matrix, \mathbf{A}_k . This general notation is important when discussing the derivations in the appendix. Thus, in general, bold, capital, Roman letters represent $3n$ by $3n$ matrices and capital, Roman letters represent n by n matrices. Many $3n$ by $3n$ matrices used in this work (\mathbf{Z}) are of the form $\mathbf{Z} = Z \otimes I_3$.

C. Building the Basis

The basis set for each rovibrational state considered in this work is generated independently from other states. As shown in other work [6][7], an efficient way of building the basis is by incrementally enlarging it one function at a time. Each step of the enlargement process involves selecting a new basis function by taking a subset of the most contributing functions already included in the basis set and randomly perturbing their L_k non-linear parameters. Then it is determined which function among the perturbed functions in the subset lowers the energy the most. That function, after checking if it is linearly independent from the functions already included in the basis set, is variationally optimized. In the optimization both m_k power and the L_k matrix elements are varied. After the function is optimized the function is again checked for linear dependency and if none is found the function is included in the basis set. If linear dependency occurs a new function is selected and optimized. After a set of several functions are added this way to the basis set the whole set is reoptimized by again using a one-function-at-a-time approach. The procedure continues until a basis size is reached where there are diminishing returns with respect to enlarging the basis and lowering the energy. The analytical gradient of the energy with respect to the L_k matrix elements is used in the optimization. The derivation and the implementation of the gradient for a diatomic basis set corresponding to the second rotationally excited state (i.e. $N = 2$ state) was described in [8].

The code used in this work is written in FORTRAN and runs in parallel using Intel's message passing interface

(MPI). The vibrational quantum number is not strictly speaking, a quantum number. The code includes the calculation of the nuclear-nuclear correlation function derived in this work. When the basis set is diagonalized, there are K eigenvalues and K corresponding eigenfunctions, where K is the basis size. Starting from the lowest energy eigenvalue and stepping up by going to the next higher eigenvalue is equivalent to vibrational excitation. This is why, in general, the higher vibrational states require larger basis-set sizes to achieve a similar level of the energy convergence as achieved for the lower states. As the vibrational level increases, the number of radial nodes (i.e. nodes in terms of the r_1 coordinate, where r_1 is the length of the \mathbf{r}_1 vector) in the wave function also increases.

D. HD

The calculations performed in this work target all 17 bound rovibrational states corresponding to the second rotationally excited state of the HD molecule. The 18th state, which was bound in the rotationless and first rotationally excited states was found to be unbound in the second rotationally excited state. The wave functions and the corresponding energies are determined and used in the analysis. The matrix elements for the nuclear-nuclear correlation function are derived, implemented, and used to determine the correlation functions corresponding to the proton density with respect to the deuteron for all considered states. For a basis with functions ϕ_k given in the form specified in (4) the correlation function matrix element is as follows:

$$\langle \phi_k^{N=2} | \delta(r_1 - \xi) | \phi_l^{N=2} \rangle \quad (5)$$

Where \mathbf{r}_1 is the internuclear vector and ξ is a vector of the coordinates of a point for which the matrix element is determined. An analytical expression for the matrix element is derived in section VI. The correlation function is determined for a cross section along a selected plane and visualized in a 3D plot. The correlation function plots allow for the analysis of the HD molecular structure in an unorthodox manner, as the structure is a result of calculations which are performed without assuming the BO approximation.

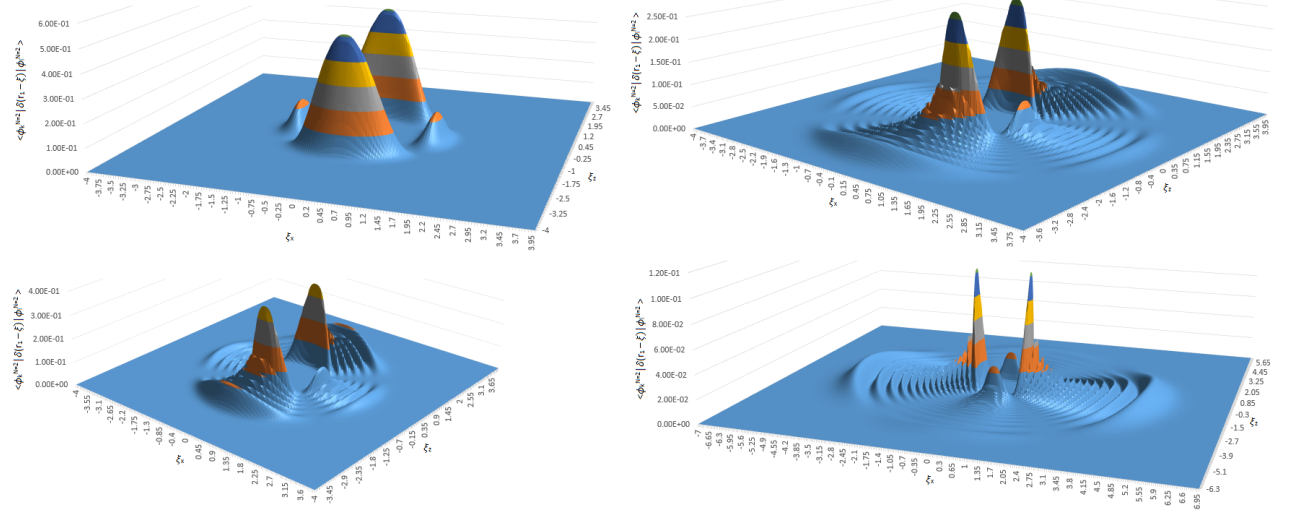
III. RESULTS

The energy convergence with the number of basis functions for the considered 17 bound rovibrational states of HD is shown in Table II. The fact that increasing the basis set by 1000 functions in the final basis enlargement only changes the energy in the 7th - 9th decimal place indicates a reasonably tight convergence.

Fig. 1 shows the plots of the nuclear-nuclear correlation function for selected rovibrational states of HD with respect to the cross section along the xz plane. Because of the spherical harmonic prefactor, $(x_1^2 + y_1^2 - 2z_1^2)$, there are angular nodes where $x_1 = \sqrt{2}z_1$ and $x_1 = -\sqrt{2}z_1$. The spherical vibrational nodes appear due to vibrational excitations.

Attempts to calculate the $(\nu, N) = (17, 2)$ state failed, as it is unbound. Enlarging the basis for this state from 10,000

FIG. 1: Nuclear-nuclear correlation functions for HD in the $(\nu, 2)$ rovibrational state, with the upper left, bottom left, upper right, and bottom right corresponding to the $\nu=0, 5, 10$, and 15 states, respectively.



to 11,000 to 12,000 functions shows the average proton-deuteron distance increasing from 23.161 au to 31.759 au to 41.999 au respectively. As the size of the basis increases, the rate at which the proton-deuteron distance increases also increases, indicating that the state is unbound.

Rovibrational excitation of HD causes the average interparticle distances to increase. This effect has the most dramatic manifestation close to the dissociation limit. In Table I the proton-deuteron and electron-electron distances are shown for all considered rovibrational states. In the table we also show the charge asymmetry measured as the difference between the average values of the proton-electron and deuteron-electron distances. The charge asymmetry first increases with the level of the vibrational excitation and then goes down as the molecule approaches the dissociation limit. This is because HD dissociates into a hydrogen atom and a deuterium. It was shown in Ref. [9] that the charge asymmetry in HD in the $N = 0$ rovibrational states reaches a maximum around the ninth vibrational state, beyond which it declines.

Dissociation energies for all vibrational states of the second rotationally excited state of HD are shown in table III with comparisons to [5].

TABLE I: Average proton-deuteron distances, electron-electron distances, and charge asymmetries for states near the dissociation limit (all values in a.u.)

$(\nu, J) \rightarrow$	(16,2)	(16,1)	(17,1)	(16,0)	(17,0)
r_{pd}	4.949568	4.880354	11.33121	4.847562	8.990613
r_{ee}	5.306791	5.240088	11.53383	5.208489	9.227924
$r_{pe} - r_{de}$	0.000234	0.000235	0.000206	0.000236	0.000208

TABLE II: Convergence of the total Energy for the $(\nu, 2)$ rovibrational states of HD with the number of ECGs. Energy is given in hartrees. K = Number of ECGs.

ν	K=10000	K=11000	K=12000
0	-1.164 254 969 218	-1.164 254 970 981	-1.164 254 971 380
1	-1.147 758 262 559	-1.147 758 266 394	-1.147 758 267 183
2	-1.132 068 978 530	-1.132 068 983 718	-1.132 068 985 031
3	-1.117 171 538 245	-1.117 171 541 870	-1.117 171 543 053
4	-1.103 054 978 501	-1.103 054 980 106	-1.103 054 981 400
5	-1.089 713 322 928	-1.089 713 329 376	-1.089 713 332 224
6	-1.077 146 121 120	-1.077 146 127 708	-1.077 146 131 137
7	-1.065 359 091 137	-1.065 359 102 024	-1.065 359 104 568
8	-1.054 365 088 369	-1.054 365 100 887	-1.054 365 105 646
9	-1.044 185 396 051	-1.044 185 424 167	-1.044 185 428 822
10	-1.034 851 437 109	-1.034 851 457 321	-1.034 851 462 492
11	-1.026 407 028 986	-1.026 407 045 527	-1.026 407 050 191
12	-1.018 911 573 698	-1.018 911 596 695	-1.018 911 601 751
13	-1.012 444 451 458	-1.012 444 477 272	-1.012 444 484 336
14	-1.007 111 175 631	-1.007 111 199 627	-1.007 111 205 255
15	-1.003 052 344 980	-1.003 052 387 508	-1.003 052 402 442
16	-1.000 457 209 732	-1.000 457 231 759	-1.000 457 238 123

IV. CONCLUSION

A basis set of explicitly correlated Gaussian functions has been built for all-particle non-BO calculations of each of the 17 bound rovibrational states of the HD molecule with total angular momentum quantum number equal to two. As expected, rovibrational excitation increases the average interparticle distances. Near the dissociation limit, the differences between interparticle distances for different rotational states in the same vibrational state is significant. Also near the dissociation limit, the rotation excitation for a particular vibrational state decreases the charge asymmetry due to the fact that HD, when rotationally excited, closer approaches the dissociation into a hydrogen atom and a deuterium where the asymmetry is very small. In general, the charge asymmetry for the rovibrational states corresponding all three lowest rotational levels first increases with the vibrational excitation and then starting around the ninth vibrational state decreases. The maximum asymmetry is at the ninth vibrational state [9].

The nuclear-nuclear correlation function provides a unique description of the molecular structure that is obtained

TABLE III: Dissociation energies (second column) and the difference between dissociation energies in [5] and the present study, $\Delta=[5]\text{-present}$. All values given in cm^{-1} .

ν	E_{diss}	Δ
0	36139.4206717	0.0244
1	32518.8125992	0.0242
2	29075.4131824	0.0246
3	25805.802596	0.0240
4	22707.575431	0.0238
5	19779.4218962	0.0245
6	17021.2400701	0.0248
7	14434.286759	0.0244
8	12021.3828984	0.0262
9	9787.20207986	0.0263
10	7738.63326049	0.0277
11	5885.29898354	0.0281
12	4240.23820016	0.0281
13	2820.86998939	0.0280
14	1650.35052911	0.0270
15	759.54627802	0.0310
16	189.973545688	0.0217

from all-particle non-BO calculations. Molecular wave functions contain extra information when calculated outside of the confines of the Born-Oppenheimer approximation. This information for a small molecule like HD provides a unique way of probing the molecular structure of the system through an entirely different lens.

V. ACKNOWLEDGEMENTS

We are grateful to the University of Arizona Center of Computing and Information Technology for the use of their computer resources and the El Gato cluster, NSF grant number 1228509.

VI. APPENDIX - CORRELATION FUNCTION DERIVATION

The matrix elements of the nuclear-nuclear correlation function for diatomic molecules with total angular momentum equal to two ($N=2$) are derived using the Gaussian representation of the 3D Dirac delta function.

$$\langle \phi_k^{N=2} | \delta(r_1 - \xi) | \phi_l^{N=2} \rangle = \lim_{\beta \rightarrow \infty} \left(\frac{\beta}{\pi} \right)^{3/2} \left\langle (x_1^2 + y_1^2 - 2z_1^2)^2 r_1^{m_k+m_l} \exp \left[-\mathbf{r}' (\mathbf{A}_{kl} + \beta \mathbf{J}_{11}) \mathbf{r} + 2\beta \xi' (a'_1 \otimes I_3) \mathbf{r} - \beta \xi' \xi \right] \right\rangle \quad (6)$$

Exploiting the following:

$$(x_1^2 + y_1^2 - 2z_1^2) = -\frac{\partial}{\partial \omega_k} \exp[-\omega_k \mathbf{r}' \mathbf{W}_k \mathbf{r}] \Big|_{\omega_k=0} \quad (7)$$

and

$$r_1^{m_k+m_l} = (-1)^m \frac{\partial^m}{\partial u^m} \exp[-u \mathbf{r}' \mathbf{J}_{11} \mathbf{r}] \Big|_{u=0} \quad (8)$$

Where $m = \frac{m_k+m_l}{2}$, \mathbf{W}_k is a $3n$ by $3n$ matrix with 1 in the (1,1) and (2,2) positions and -2 in the (3,3) position and zeros elsewhere and \mathbf{J}_{11} is a $3n$ by $3n$ matrix with ones in the (1,1), (2,2), and (3,3) positions and zeros elsewhere. The nuclear-nuclear correlation function matrix elements can then be expressed as the following:

$$\begin{aligned} \langle \phi_k^{N=2} | \delta(r_1 - \xi) | \phi_l^{N=2} \rangle &= (-1)^m \frac{\partial^m}{\partial u^m} \frac{\partial}{\partial \omega_l} \frac{\partial}{\partial \omega_k} \lim_{\beta \rightarrow \infty} \left(\frac{\beta}{\pi} \right)^{3/2} \left\langle \exp \left[-\mathbf{r}' (\mathbf{A}_{kl} + (\beta + u) \mathbf{J}_{11} + \omega_k \mathbf{W}_k + \omega_l \mathbf{W}_l) \mathbf{r} \right. \right. \\ &\quad \left. \left. + 2\beta \xi' (a'_1 \otimes I_3) \mathbf{r} - \beta \xi' \xi \right] \right\rangle \Big|_{\omega_k=\omega_l=u=0} \end{aligned} \quad (9)$$

Using equations (42)-(53) in ref. [10] and 2nd and 3rd order expansions for equation (48), taking the limit as β approaches ∞ results in:

$$\begin{aligned} \langle \phi_k^{N=2} | \delta(r_1 - \xi) | \phi_l^{N=2} \rangle &= (-1)^m \frac{\partial^m}{\partial u^m} \frac{\partial}{\partial \omega_l} \frac{\partial}{\partial \omega_k} \pi^{3(n-1)/2} |\mathbf{G}_{kl}|^{-1/2} |\Lambda_{kl}|^{-1/2} \exp[-\xi' \Lambda_{kl}^{-1} \xi] \Big|_{\omega_k=\omega_l=u=0} \\ &= (-1)^m \frac{\partial^m}{\partial u^m} \frac{\partial}{\partial \omega_l} \frac{\partial}{\partial \omega_k} \mathbf{Y}_{kl}^{N=2} \Big|_{\omega_k=\omega_l=u=0}. \end{aligned} \quad (10)$$

Where, in this case,

$$\mathbf{G}_{kl} = \mathbf{A}_{kl} + u \mathbf{J}_{11} + \omega_k \mathbf{W}_k + \omega_l \mathbf{W}_l \quad (11)$$

and

$$\Lambda_{kl} = (a'_1 \otimes I_3) \mathbf{G}_{kl}^{-1} (a_1 \otimes I_3). \quad (12)$$

We will first take the two derivatives with respect to ω_k and ω_l of the portion of the total expression that depends on ω_k and ω_l . This will be referred to as the intermediate expression. The intermediate expression is equivalent to:

$$\begin{aligned} \frac{\partial}{\partial \omega_l} \frac{\partial}{\partial \omega_k} |\mathbf{G}_{kl}|^{-1/2} |\Lambda_{kl}|^{-1/2} \exp[-\xi' \Lambda_{kl}^{-1} \xi] \Big|_{\omega_k=\omega_l=0} &= \frac{\partial}{\partial \omega_l} \left[\frac{\partial}{\partial \omega_k} (|\mathbf{G}_{kl}|^{-1/2}) |\Lambda_{kl}|^{-1/2} \exp[-\xi' \Lambda_{kl}^{-1} \xi] + \right. \\ &\quad \left. |\mathbf{G}_{kl}|^{-1/2} \frac{\partial}{\partial \omega_k} (|\Lambda_{kl}|^{-1/2}) \exp[-\xi' \Lambda_{kl}^{-1} \xi] + |\mathbf{G}_{kl}|^{-1/2} |\Lambda_{kl}|^{-1/2} \frac{\partial}{\partial \omega_k} (\exp[-\xi' \Lambda_{kl}^{-1} \xi]) \right] \Big|_{\omega_k=\omega_l=0}. \end{aligned} \quad (13)$$

Expanding further:

$$\begin{aligned} \left. \frac{\partial}{\partial \omega_l} \frac{\partial}{\partial \omega_k} |\mathbf{G}_{kl}|^{-1/2} |\Lambda_{kl}|^{-1/2} \exp[-\xi' \Lambda_{kl}^{-1} \xi] \right|_{\omega_k=\omega_l=0} &= \left[\frac{\partial^2}{\partial \omega_l \partial \omega_k} \left(|\mathbf{G}_{kl}|^{-1/2} \right) |\Lambda_{kl}|^{-1/2} \exp[-\xi' \Lambda_{kl}^{-1} \xi] + \right. \\ &\quad \frac{\partial}{\partial \omega_k} \left(|\mathbf{G}_{kl}|^{-1/2} \right) \frac{\partial}{\partial \omega_l} \left(|\Lambda_{kl}|^{-1/2} \right) \exp[-\xi' \Lambda_{kl}^{-1} \xi] + \frac{\partial}{\partial \omega_k} \left(|\mathbf{G}_{kl}|^{-1/2} \right) |\Lambda_{kl}|^{-1/2} \frac{\partial}{\partial \omega_l} \left(\exp[-\xi' \Lambda_{kl}^{-1} \xi] \right) + \\ &\quad \frac{\partial}{\partial \omega_l} \left(|\mathbf{G}_{kl}|^{-1/2} \right) \frac{\partial}{\partial \omega_k} \left(|\Lambda_{kl}|^{-1/2} \right) \exp[-\xi' \Lambda_{kl}^{-1} \xi] + |\mathbf{G}_{kl}|^{-1/2} \frac{\partial^2}{\partial \omega_l \partial \omega_k} \left(|\Lambda_{kl}|^{-1/2} \right) \exp[-\xi' \Lambda_{kl}^{-1} \xi] + \\ &\quad |\mathbf{G}_{kl}|^{-1/2} \frac{\partial}{\partial \omega_k} \left(|\Lambda_{kl}|^{-1/2} \right) \frac{\partial}{\partial \omega_l} \left(\exp[-\xi' \Lambda_{kl}^{-1} \xi] \right) + \frac{\partial}{\partial \omega_l} \left(|\mathbf{G}_{kl}|^{-1/2} \right) |\Lambda_{kl}|^{-1/2} \frac{\partial}{\partial \omega_k} \left(\exp[-\xi' \Lambda_{kl}^{-1} \xi] \right) + \\ &\quad \left. |\mathbf{G}_{kl}|^{-1/2} \frac{\partial}{\partial \omega_l} \left(|\Lambda_{kl}|^{-1/2} \right) \frac{\partial}{\partial \omega_k} \left(\exp[-\xi' \Lambda_{kl}^{-1} \xi] \right) + |\mathbf{G}_{kl}|^{-1/2} |\Lambda_{kl}|^{-1/2} \frac{\partial^2}{\partial \omega_l \partial \omega_k} \left(\exp[-\xi' \Lambda_{kl}^{-1} \xi] \right) \right] \Big|_{\omega_k=\omega_l=0}. \end{aligned} \quad (14)$$

There are nine terms. The second, third, fourth, and seventh terms are all zero because (using the chain rule):

$$\begin{aligned} \left. \frac{\partial}{\partial \omega_k} |\mathbf{G}_{kl}|^{-1/2} \right|_{\omega_k=0} &= -\frac{1}{2} |\mathbf{G}_{kl}|^{-3/2} \frac{\partial}{\partial \omega_k} |\mathbf{G}_{kl}| \Big|_{\omega_k=0} = -\frac{1}{2} |\mathbf{G}_{kl}|^{-3/2} |\mathbf{G}_{kl}| \text{tr} \left[\mathbf{G}_{kl}^{-1} \frac{\partial}{\partial \omega_k} (\mathbf{G}_{kl}) \right] \Big|_{\omega_k=0} = \\ &\quad -\frac{1}{2} |\mathbf{A}_{kl} + u \mathbf{J}_{11}|^{-1/2} \text{tr} [(\mathbf{A}_{kl} + u \mathbf{J}_{11})^{-1} \mathbf{W}_k] = 0. \end{aligned} \quad (15)$$

This is because

$$\text{tr} [(\mathbf{A}_{kl} + u \mathbf{J}_{11})^{-1} \mathbf{W}_k] = 0. \quad (16)$$

The sixth and eighth terms are also equal to zero because:

$$\begin{aligned} \left. \frac{\partial}{\partial \omega_k} |\Lambda_{kl}|^{-1/2} \right|_{\omega_k=0} &= -\frac{1}{2} |\Lambda_{kl}|^{-3/2} \frac{\partial}{\partial \omega_k} |\Lambda_{kl}| \Big|_{\omega_k=0} = -\frac{1}{2} |\Lambda_{kl}|^{-3/2} |\Lambda_{kl}| \text{tr} \left[\Lambda_{kl}^{-1} \frac{\partial}{\partial \omega_k} (\Lambda_{kl}) \right] \Big|_{\omega_k=0} = \\ &\quad -\frac{1}{2} |\Lambda_{kl}|^{-1/2} \text{tr} \left[((a'_1 \otimes I_3)(\mathbf{A}_{kl} + u \mathbf{J}_{11})^{-1}(a_1 \otimes I_3))^{-1} (a'_1 \otimes I_3)(\mathbf{A}_{kl} + u \mathbf{J}_{11})^{-2} \mathbf{W}_k (a_1 \otimes I_3) \right] = 0. \end{aligned} \quad (17)$$

Because, again, the trace equals zero. The first, fifth, and ninth terms remain, leaving behind the following:

$$\begin{aligned} \left. \frac{\partial}{\partial \omega_l} \frac{\partial}{\partial \omega_k} |\mathbf{G}_{kl}|^{-1/2} |\Lambda_{kl}|^{-1/2} \exp[-\xi' \Lambda_{kl}^{-1} \xi] \right|_{\omega_k=\omega_l=0} &= \left[\frac{\partial^2}{\partial \omega_l \partial \omega_k} \left(|\mathbf{G}_{kl}|^{-1/2} \right) |\Lambda_{kl}|^{-1/2} \exp[-\xi' \Lambda_{kl}^{-1} \xi] + \right. \\ &\quad \left. |\mathbf{G}_{kl}|^{-1/2} \frac{\partial^2}{\partial \omega_l \partial \omega_k} \left(|\Lambda_{kl}|^{-1/2} \right) \exp[-\xi' \Lambda_{kl}^{-1} \xi] + |\mathbf{G}_{kl}|^{-1/2} |\Lambda_{kl}|^{-1/2} \frac{\partial^2}{\partial \omega_l \partial \omega_k} \left(\exp[-\xi' \Lambda_{kl}^{-1} \xi] \right) \right] \Big|_{\omega_k=\omega_l=0} \end{aligned} \quad (18)$$

$\tilde{\mathbf{Y}}_{kl}^{N=2} = \frac{\mathbf{Y}_{kl}^{N=2}}{\pi^{3(n-1)/2}}$. The third term in this expression is equivalent to:

$$\begin{aligned} &\left[|\mathbf{G}_{kl}|^{-1/2} |\Lambda_{kl}|^{-1/2} \frac{\partial^2}{\partial \omega_l \partial \omega_k} \left(\exp[-\xi' \Lambda_{kl}^{-1} \xi] \right) \right] \Big|_{\omega_k=\omega_l=0} = \\ &\left[\frac{\tilde{\mathbf{Y}}_{kl}^{N=2}}{\exp[-\xi' \Lambda_{kl}^{-1} \xi]} \right] \Big|_{\omega_k=\omega_l=0} \cdot \frac{\partial}{\partial \omega_l} \left(\exp[-\xi' \Lambda_{kl}^{-1} \xi] \Big|_{\omega_k=0} \cdot \frac{\partial}{\partial \omega_k} [-\xi' \Lambda_{kl}^{-1} \xi] \Big|_{\omega_k=0} \right) \Big|_{\omega_l=0} = \\ &\left[\frac{\tilde{\mathbf{Y}}_{kl}^{N=2}}{\exp[-\xi' \Lambda_{kl}^{-1} \xi]} \right] \Big|_{\omega_k=\omega_l=0} \cdot \frac{\partial}{\partial \omega_l} \left(\exp[-\xi' \Lambda_{kl}^{-1} \xi] \Big|_{\omega_k=0} \cdot \left[\xi' \Lambda_{kl}^{-1} \left(\frac{\partial}{\partial \omega_k} \Lambda_{kl} \right) \Lambda_{kl}^{-1} \xi \right] \Big|_{\omega_k=0} \right) \Big|_{\omega_l=0} = \\ &\left[\frac{\tilde{\mathbf{Y}}_{kl}^{N=2}}{\exp[-\xi' \Lambda_{kl}^{-1} \xi]} \right] \Big|_{\omega_k=\omega_l=0} \cdot \frac{\partial}{\partial \omega_l} \left(\exp[-\xi' \Lambda_{kl}^{-1} \xi] \Big|_{\omega_k=0} \cdot \left[-\xi' \Lambda_{kl}^{-1} (a'_1 \otimes I_3) \mathbf{G}_{kl}^{-1} \mathbf{W}_k \mathbf{G}_{kl}^{-1} (a_1 \otimes I_3) \Lambda_{kl}^{-1} \xi \right] \Big|_{\omega_k=0} \right) \Big|_{\omega_l=0} = \\ &\left[\frac{\tilde{\mathbf{Y}}_{kl}^{N=2}}{\exp[-\xi' \Lambda_{kl}^{-1} \xi]} \right] \Big|_{\omega_k=\omega_l=0} \cdot \frac{\partial}{\partial \omega_l} \left(\exp[-\xi' \Lambda_{kl}^{-1} \xi] \Big|_{\omega_k=0} \left[-\xi_x^2 - \xi_y^2 + 2\xi_z^2 \right] \right) \Big|_{\omega_l=0} = \\ &\tilde{\mathbf{Y}}_{kl}^{N=2} \left[-\xi_x^2 - \xi_y^2 + 2\xi_z^2 \right]^2 \Big|_{\omega_k=\omega_l=0} \end{aligned} \quad (19)$$

The first term in the expression is equivalent to:

$$\left[\frac{\partial^2}{\partial \omega_l \partial \omega_k} \left(|\mathbf{G}_{kl}|^{-1/2} \right) |\boldsymbol{\Lambda}_{kl}|^{-1/2} \exp[-\xi' \boldsymbol{\Lambda}_{kl}^{-1} \xi] \right]_{\omega_k=\omega_l=0} = \frac{\tilde{\mathbf{Y}}_{kl}^{N=2}}{|\mathbf{G}_{kl}|^{-1/2}} \cdot 3|\mathbf{A}_{kl} + u\mathbf{J}_{11}|^{-1/2} \tilde{\alpha}^2 = 3\tilde{\alpha}^2 \tilde{\mathbf{Y}}_{kl}^{N=2}. \quad (20)$$

Where $\tilde{\alpha}$ is equal to the (1,1) element of the $(A_{kl} + uJ_{11})^{-1}$ matrix and also equivalent to $\text{tr}[(A_{kl} + uJ_{11})^{-1} J_{11}]$. The second term in the expression is equivalent to:

$$|\mathbf{G}_{kl}|^{-1/2} \frac{\partial^2}{\partial \omega_l \partial \omega_k} \left(|\boldsymbol{\Lambda}_{kl}|^{-1/2} \right) \exp[-\xi' \boldsymbol{\Lambda}_{kl}^{-1} \xi] = -3\tilde{\alpha}^2 \tilde{\mathbf{Y}}_{kl}^{N=2}. \quad (21)$$

The simplified intermediate expression for the correlation function is now:

$$\tilde{\mathbf{Y}}_{kl}^{N=2} \left[-3\alpha^2 + 3\tilde{\alpha}^2 + \left(-\xi_x^2 - \xi_y^2 + 2\xi^2 \right)^2 \right] = \tilde{\mathbf{Y}}_{kl}^{N=2} \left(-\xi_x^2 - \xi_y^2 + 2\xi^2 \right)^2. \quad (22)$$

The following is what remains of the correlation function derivation:

$$\langle \phi_k^{N=2} | \delta(r_1 - \xi) | \phi_l^{N=2} \rangle = (-1)^m \frac{\partial^m}{\partial u^m} \pi^{3(n-1)/2} |\mathbf{G}_{kl}|^{-1/2} |\boldsymbol{\Lambda}_{kl}|^{-1/2} \exp[-\xi' \boldsymbol{\Lambda}_{kl}^{-1} \xi] \left(-\xi_x^2 - \xi_y^2 + 2\xi^2 \right)^2 \quad (23)$$

Before differentiating the expression, we will take advantage of some transformation properties that are now accessible. Now that the dependences on the \mathbf{W}_k and \mathbf{W}_l matrices have been removed via the initial differentiations, all of the remaining $3n$ by $3n$ matrices, \mathbf{Z} are of the form where it is true that $\mathbf{Z} = \mathbf{Z} \otimes I_3$, where Z is an n by n matrix and I_3 is the 3 by 3 identity matrix. Because of this, the following can be shown:

$$|\mathbf{G}_{kl}^{-1/2}| \Big|_{\omega_k=\omega_l=0} = |G_{kl}|^{-3/2} = |A_{kl} + uJ_{11}|^{-3/2}, \quad (24)$$

$$|\boldsymbol{\Lambda}_{kl}|^{-1/2} \Big|_{\omega_k=\omega_l=0} = \text{tr}[(A_{kl} + uJ_{11})^{-1} J_{11}]^{-3/2}, \quad (25)$$

$$\exp[-\xi' \boldsymbol{\Lambda}_{kl}^{-1} \xi] \Big|_{\omega_k=\omega_l=0} = \exp \left[\frac{-\xi^2}{\text{tr}[(A_{kl} + uJ_{11})^{-1} J_{11}]} \right]. \quad (26)$$

We will now take the first derivative with respect to u of the portion of the entire expression with u dependence to lay the groundwork for the complete derivation.

$$\begin{aligned} \frac{\partial}{\partial u} \left(|A_{kl} + uJ_{11}|^{-3/2} \text{tr}[(A_{kl} + uJ_{11})^{-1} J_{11}]^{-3/2} \exp \left[\frac{-\xi^2}{\text{tr}[(A_{kl} + uJ_{11})^{-1} J_{11}]} \right] \right) &= \\ \frac{\partial}{\partial u} \left(|A_{kl} + uJ_{11}|^{-3/2} \right) \text{tr}[(A_{kl} + uJ_{11})^{-1} J_{11}]^{-3/2} \exp \left[\frac{-\xi^2}{\text{tr}[(A_{kl} + uJ_{11})^{-1} J_{11}]} \right] &+ \\ |A_{kl} + uJ_{11}|^{-3/2} \frac{\partial}{\partial u} \left(\text{tr}[(A_{kl} + uJ_{11})^{-1} J_{11}]^{-3/2} \right) \exp \left[\frac{-\xi^2}{\text{tr}[(A_{kl} + uJ_{11})^{-1} J_{11}]} \right] &+ \\ |A_{kl} + uJ_{11}|^{-3/2} \text{tr}[(A_{kl} + uJ_{11})^{-1} J_{11}]^{-3/2} \frac{\partial}{\partial u} \exp \left[\frac{-\xi^2}{\text{tr}[(A_{kl} + uJ_{11})^{-1} J_{11}]} \right]. & \end{aligned} \quad (27)$$

These three terms will be evaluated independently and combined afterwards. The first term is equivalent to:

$$\begin{aligned} -\frac{3}{2}|A_{kl} + uJ_{11}|^{-5/2}|A_{kl} + uJ_{11}|tr[(A_{kl} + uJ_{11})^{-1}J_{11}]tr[(A_{kl} + uJ_{11})^{-1}J_{11}]^{-3/2}exp\left[\frac{-\xi^2}{tr[(A_{kl} + uJ_{11})^{-1}J_{11}]} \right] = \\ -\frac{3}{2}|A_{kl} + uJ_{11}|^{-3/2}tr[(A_{kl} + uJ_{11})^{-1}J_{11}]^{-1/2}exp\left[\frac{-\xi^2}{tr[(A_{kl} + uJ_{11})^{-1}J_{11}]} \right]. \end{aligned} \quad (28)$$

The second term is equivalent to:

$$\begin{aligned} \frac{3}{2}|A_{kl} + uJ_{11}|^{-3/2}tr[(A_{kl} + uJ_{11})^{-1}J_{11}]^{-5/2}tr[(A_{kl} + uJ_{11})^{-1}J_{11}(A_{kl} + uJ_{11})^{-1}J_{11}]exp\left[\frac{-\xi^2}{tr[(A_{kl} + uJ_{11})^{-1}J_{11}]} \right] = \\ \frac{3}{2}|A_{kl} + uJ_{11}|^{-3/2}tr[(A_{kl} + uJ_{11})^{-1}J_{11}]^{-1/2}exp\left[\frac{-\xi^2}{tr[(A_{kl} + uJ_{11})^{-1}J_{11}]} \right]. \end{aligned} \quad (29)$$

This is true because $\text{tr}[(ZJ_{11})^2] = \text{tr}[ZJ_{11}]^2 = (Z_{11})^2$. The first two terms in the summation cancel. The third term is equivalent to:

$$\begin{aligned} |A_{kl} + uJ_{11}|^{-3/2}tr[(A_{kl} + uJ_{11})^{-1}J_{11}]^{-3/2}\frac{-\xi^2}{tr[(A_{kl} + uJ_{11})^{-1}J_{11}]^{-2}}tr[((A_{kl} + uJ_{11})^{-1}J_{11})^2]exp\left[\frac{-\xi^2}{tr[(A_{kl} + uJ_{11})^{-1}J_{11}]} \right] = \\ -\xi^2|A_{kl} + uJ_{11}|^{-3/2}tr[(A_{kl} + uJ_{11})^{-1}J_{11}]^{-3/2}exp\left[\frac{-\xi^2}{tr[(A_{kl} + uJ_{11})^{-1}J_{11}]} \right] \end{aligned} \quad (30)$$

Due to the fact that the first two terms cancel and the third term just results in a constant multiplicative factor, the n^{th} derivative with respect to u of the portion of the entire expression with u dependence is equal to:

$$(-1)^n(\xi^2)^n|A_{kl} + uJ_{11}|^{-3/2}tr[(A_{kl} + uJ_{11})^{-1}J_{11}]^{-3/2}exp\left[\frac{-\xi^2}{tr[(A_{kl} + uJ_{11})^{-1}J_{11}]} \right]. \quad (31)$$

After setting u equal to zero and reintroducing the constants, the nuclear-nuclear correlation function is equivalent to:

$$\begin{aligned} \langle \phi_k^{N=2} | \delta(r_1 - \xi) | \phi_l^{N=2} \rangle = \pi^{3(n-1)/2}(\xi^2)^m |A_{kl}|^{-3/2}tr[A_{kl}^{-1}J_{11}]^{-3/2}exp\left[\frac{-\xi^2}{tr[A_{kl}^{-1}J_{11}]} \right] \left(-\xi_x^2 - \xi_y^2 + 2\xi_x^2 \right)^2 = \\ \pi^{3(n-1)/2}(\xi^2)^m |A_{kl}|^{-3/2} \alpha^{-3/2} exp\left[\frac{-\xi^2}{\alpha} \right] \left(-\xi_x^2 - \xi_y^2 + 2\xi_x^2 \right)^2. \end{aligned} \quad (32)$$

Where α is the (1,1) element of the A_{kl}^{-1} matrix. Writing the function in terms of the overlap matrix element leads to:

$$\langle \phi_k^{N=2} | \delta(r_1 - \xi) | \phi_l^{N=2} \rangle = \frac{\langle \phi_k^{N=2} | \phi_l^{N=2} \rangle}{2\pi\alpha^{7/2}\Gamma(m + \frac{3}{2})} \left(\frac{5}{15 + 16m + 4m^2} \right) \left(\frac{\xi^2}{\alpha} \right)^m \left(-\xi_x^2 - \xi_y^2 + 2\xi_x^2 \right)^2 exp\left[\frac{-\xi^2}{\alpha} \right], \quad (33)$$

where:

$$\langle \phi_k^{N=2} | \phi_l^{N=2} \rangle = \frac{2}{\sqrt{\pi}} \Gamma\left(\frac{3}{2} + m\right) \langle \phi_k | \phi_l \rangle \alpha^m \left(\frac{15 + 16m + 4m^2}{5} \right) \alpha^2, \quad (34)$$

and:

$$\langle \phi_k | \phi_l \rangle = \pi^{3n/2} |A_{kl}|^{-3/2}. \quad (35)$$

Previous correlation function derivations in the $N = 1$ and $N = 0$ basis sets can be found in Ref. [11] and [12].

-
- [1] Frolov, A. M., Smith Jr., V. H. J. Phys. B. **28**, L449 (1995).
 - [2] W. Kolos, L. Wolniewicz, J. Chem. Phys. **49**, 404 (1968).
 - [3] J. Mitroy, S. Bubin, W. Horiuchi, Y. Suzuki, L. Adamowicz, W. Cencek, K. Szalewicz, J. Komasa, D. Blume, K. Varga, Rev. Mod. Phys. **85**, 693 (2013).
 - [4] M. Huix-Rotllant, A. Nikiforov, W. Thiel, M. Filatov, Top. Curr. Chem. **368**, 445 (2016).
 - [5] K. Pachucki, J. Komasa, Phys. Chem. Chem. Phys. **12**, 9188 (2010).
 - [6] N. Kirnosov, K. L. Sharkey, L. Adamowicz, J. Phys. B. **48**, 195101 (2015).
 - [7] K. L. Sharkey, N. Kirnosov, L. Adamowicz Phys. Rev. A. **88**, 032513 (2013).
 - [8] K. A. Jones, N. Kirnosov, K. L. Sharkey, L. Adamowicz, (Submitted).
 - [9] S. Bubin, F. Leonarski, M. Stanke, L. Adamowicz J. Chem. Phys. **130**, 124120 (2009).
 - [10] K. L. Sharkey, M. Pavanello, S. Bubin, L. Adamowicz, Phys. Rev. A. **80**, 062510 (2009).
 - [11] S. Bubin, L. Adamowicz, Chem. Phys. Lett. **403**, 185 (2005).
 - [12] N. Kirnosov, K. L. Sharkey, L. Adamowicz, J. Chem. Phys. **139**, 204105 (2013).

APPENDIX J

Paraortho isomerization of H_2^+ . Non-BornOppenheimer direct variational calculations with explicitly correlated all-particle Gaussian functions



Para-ortho isomerization of H_2^+ . Non-Born–Oppenheimer direct variational calculations with explicitly correlated all-particle Gaussian functions

Nikita Kirnosov^a, Keeper L. Sharkey^b, Ludwik Adamowicz^{b,a,*}

^a Department of Physics, University of Arizona, Tucson, AZ 85721, USA

^b Department of Chemistry and Biochemistry, University of Arizona, Tucson, AZ 85721, USA



ARTICLE INFO

Article history:

Received 24 November 2014
In final form 31 December 2014
Available online 10 January 2015

ABSTRACT

Direct variational calculations are performed for all bound rovibrational states of the H_2^+ ion corresponding to the ground and first excited rotational levels (the $N=0$ and $N=1$ states). The Born–Oppenheimer (BO) approximation is not assumed in the calculations and all-particle explicitly correlated Gaussian basis functions are used for the wave-function expansion. The exponential parameters of the Gaussians are optimized with the aid of analytically calculated energy gradient determined with respect to these parameters. The non-BO energies are used to determine the ortho–para nuclear-spin isomerization energies and the non-BO wave functions are used to determine the expectation values of the interparticle distances.

© 2015 Elsevier B.V. All rights reserved.

1. Introduction

For over two decades we have been involved in the development of methods for direct non-relativistic variational calculations of bound states of molecular systems with an arbitrary numbers of nuclei and electrons without assuming the Born–Oppenheimer (BO) approximation [1,2]. We use the term ‘direct’ to describe an approach where energies and wave functions of the system are obtained by solving the Schrödinger equation with the Hamiltonian which provides an exact and complete representation of the system’s internal state and does not involve separation of the equation into an electronic equation and an equation describing the motion of the nuclei. In the first phase of the development of the molecular non-BO methods we presented an approach for calculating pure (rotationless) vibrational states of diatomic molecules with σ electrons [3,4]. Recently we presented a non-BO method for calculating bound rovibrational states of diatomics, where the rotational motion is excited to the first excited level and the vibrational excitation spans all possible vibrational quantum numbers (i.e. the $N=1, v=1, 2, \dots$ states) [5]. So far this method has been used to study the $N=1, v=1, 2, \dots$ states of HD^+ and HD [6,7].

The approach used in our non-BO calculations employs a Hamiltonian, called the internal Hamiltonian, which is obtained by rigorously separating out the operator representing the kinetic energy of the center-of-mass motion from the laboratory-frame nonrelativistic Hamiltonian of the system. The wave function in the approach is expanded in terms of explicitly correlated all-particle Gaussian basis functions (ECGs). In these functions the Gaussian exponents explicitly depend on all inter-particle distances and the preexponential factors depend on the distances between the nuclei and include angular functions which describe the total angular-momentum of the state. The key to achieving high accuracy in the non-BO calculations is a thorough variational optimization of the non-linear exponential parameters of the Gaussians. This optimization in our approach involves the use the analytical energy gradient determined with respect to these parameters by direct differentiation of the energy expression. The use of the gradient allows for extending the ECG basis sets to large sizes exceeding in many cases 10 000 functions.

It should be stressed that our non-BO approach is not limited to any particular number of electrons in the molecule. Only limitations of the computational resources restrict the size of the molecule which can be calculated. Also the method involves no separation of the Schrödinger equation of the molecule into the electronic equation solved for different configurations of the stationary nuclei and the equation describing the motion of the nuclei where the interaction potential is the energy hyper-surface (the energy curve in the case of a diatomic molecule) obtained in

* Corresponding author at: Department of Chemistry and Biochemistry, University of Arizona, Tucson, AZ 85721, USA.

E-mail address: ludwik@u.arizona.edu (L. Adamowicz).

the electronic calculations. Such a scheme is used in the conventional approach. In that approach the adiabatic and nonadiabatic coupling of the electronic and nuclear motions is included through corrections calculated using the perturbation-theory approach and added to the potential energy surface. In the non-BO approach the coupling is explicitly and directly included in the internal Hamiltonian, which is used in the calculation.

The aim of this work is to calculate the complete $N=0$ and $N=1$ rovibrational spectrum of the H_2^+ ion and demonstrate how a systematic increase of the size of the ECG basis set allows us to achieve high and uniform accuracy level for all the considered states. The non-BO calculations produce total energies and the corresponding non-BO wave function. The energies are used to calculate the para-ortho isomerization energies of H_2^+ corresponding to all bound vibrational levels. The wave functions are used to calculate the averaged proton-proton and proton-electron interparticle distances, and the inter-proton correlation functions. These functions provide an illustration of the relative distribution of the protons in different rovibrational states of the H_2^+ ion. To the best of our knowledge, this is the first time the H_2^+ correlations functions are directly calculated using the non-BO wave functions.

2. Method

We start with the total laboratory-frame nonrelativistic Hamiltonian describing a system of particles with masses M_i and charges Q_i . Without invoking any approximations this Hamiltonian can be separated into an operator representing the motion of the center of mass and an operator representing the internal energy of the system. The separation can be performed by making a transformation from the laboratory Cartesian coordinates, \mathbf{R}_i , $i=1, \dots, n+1$, where $n+1$ is the number of particles (nuclei + electrons) in the system, to the internal reference frame with the origin at a selected particle called the reference particle (number one particle): $\mathbf{r}_i = \mathbf{R}_{i+1} - \mathbf{R}_1$. The new coordinate system comprises the three laboratory coordinates of the center of mass and the $3n$ \mathbf{r}_i coordinates. The transformation of the laboratory-frame Hamiltonian to the new coordinate system yields the operator of the kinetic energy of the center-of-mass motion, which only depends on the three coordinates of the center of mass, and the following Hamiltonian representing the internal energy of the system, which only depends on the $3n$ \mathbf{r}_i , $i=1, \dots, n$ coordinates and does not depend on the coordinates of the center of mass:

$$\hat{H} = -\frac{1}{2} \left(\sum_{i=1}^n \frac{1}{\mu_i} \nabla_{\mathbf{r}_i}^2 + \sum_{i=1, j=1, i \neq j}^n \frac{1}{m_0} \nabla'_{\mathbf{r}_i} \nabla_{\mathbf{r}_j} \right) + \sum_{i=1}^n \frac{q_0 q_i}{r_i} + \sum_{j>i=1}^n \frac{q_i q_j}{r_{ij}}, \quad (1)$$

where M_1 is the mass of particle one (the reference particle), and $\nabla_{\mathbf{r}_i}$ is the gradient with respect to the x , y , and z coordinates of \mathbf{r}_i . The charges and masses are mapped from the original particles as: $\{Q_1, \dots, Q_{n+1}\} \rightarrow \{q_0, \dots, q_n\}$, and $\{M_1, \dots, M_{n+1}\} \rightarrow \{m_0, \dots, m_n\}$. In the present calculations M_1 and M_2 are the proton masses ($M_p = 1836.15267245 m_e$, where m_e is the electron mass [8]), and M_3 is the mass of an electron. The reduced masses, μ_i , are defined by $\mu_i = m_0 m_i / (m_0 + m_i)$. The potential energy is the same as in the laboratory-frame Hamiltonian, but is now written using the internal coordinates, $r_{ij} = ||\mathbf{r}_j - \mathbf{r}_i|| = ||\mathbf{R}_{j+1} - \mathbf{R}_{i+1}||$ and $r_j = ||\mathbf{r}_j|| = ||\mathbf{R}_{j+1} - \mathbf{R}_1||$. For vector/matrix transposition the symbol prime ('') is used. More information on the nonadiabatic Hamiltonian and the center of mass transformation can be found in Refs. [3,4].

As the internal Hamiltonian is fully symmetric (isotropic or atom-like) with respect to all rotations around the center of the internal coordinate system, its eigenfunctions transform as irreducible representations of the fully symmetric group of rotations. Thus, these functions are atom-like functions, which, besides being eigenfunctions of the Hamiltonian, are also eigenfunctions of the square of the total orbital angular momentum operator of the system and the operator representing its projection on a selected axis. Using basis functions that are eigenfunctions of these operators makes the Hamiltonian matrix block-diagonal. This allows us to separate the calculations of states corresponding to different total orbital angular momentum quantum numbers, N . In the present work we examine H_2^+ states corresponding to $N=0$ and $N=1$. The $N=0$ states are called rotationless states. These states correspond to the ground and excited pure 'vibrational' states of the system. We put 'vibrational' in quotes because, if the BO approximation is not assumed in the calculation, the electronic and vibrational degrees of freedom mix and the wave function for a particular 'vibrational' state may contain contributions from products of different electronic wave functions and different vibrational wave functions. Same is true for the $N=1$ states. Due to the coupling of the vibrational and electronic motions the vibrational quantum number is not, strictly speaking, a good quantum number. It should be, perhaps more correctly, regarded as an 'approximate vibrational quantum number' which numbers the consecutive states in the manifold corresponding to the particular total orbital angular momentum quantum number.

Two types of ECG basis sets are employed in the present calculations. The first used to expand wave functions of the rotationless ($N=0$) states of H_2^+ has the following form [3,4]:

$$\phi_k(\mathbf{r}) = r_1^{m_k} \exp[-\mathbf{r}'(L_k L'_k \otimes I_3)\mathbf{r}], \quad (2)$$

where \mathbf{r} is a vector of the internal coordinates, $\mathbf{r} = \{\mathbf{r}'_1, \dots, \mathbf{r}'_n\}$, L_k is an $n \times n$ rank n lower triangular matrix of nonlinear variational parameters, and I_3 is the 3×3 identity matrix. The Kronecker product, \otimes , with the identity ensures rotational invariance of the basis functions, thus they are angular momentum eigenfunctions corresponding to $N=0$. The Cholesky-factored form, $L_k L'_k$, of the nonlinear exponential parameters ensures the square integrability of the Gaussian for any real values of the L_k matrix elements. As these matrix elements are the parameters which are variationally optimized in the calculation, the optimization can be performed without any constraints between the parameters. The preexponential factor in (2), $r_1^{m_k}$, where r_1 is the internuclear, is needed to describe the very strong internuclear correlation, i.e., the effect of the nuclei staying apart from each other at a considerable distance. The $r_1^{m_k}$ factors also enable us to generate radial nodes in the wave function as the system becomes excited to higher vibrational states. The m_k power of r_1 is a non-negative even number which is an additional variational parameter subject to optimization (in the calculations performed so far for diatomic systems m_k has ranged from 0 to 250).

In systems with one electron and two identical fermionic nuclei (like H_2^+) the total (internal) wave function is a product of the nucleus-electron spatial function, the spin function for the electron, and the spin function for the nuclei. In the ground state of H_2^+ the spatial function is symmetric with respect to the permutation of the nuclear labels and the nuclear spin function is antisymmetric. This is H_2^+ in the (nuclear) low-spin state called para- H_2^+ . The permutational symmetry of the electrons and the nuclei is implemented in the basis functions (2) by projecting each basis function using symmetry-projection operator \mathcal{P} :

$$\psi_k(\mathbf{r}) = \mathcal{P}\phi_k(\mathbf{r}) = \sum_P \chi_P r_1^{m_k} \exp[-\mathbf{r}'(\tau'_P L_k L'_k \tau_P \otimes I_3)\mathbf{r}], \quad (3)$$

where the sum runs over all permutations of the labels of identical particles and where τ_P are permutational matrices transforming the internal coordinates. As P symmetrizes ϕ_k with respect to the permutation of the proton labels, it is convenient to refer to the laboratory coordinates to perform the symmetry operations and then express the results in the internal coordinates. If we wanted to construct τ_P corresponding to permuting the proton labels, for example, we would need to recall that $\mathbf{r}_1 = \mathbf{R}_2 - \mathbf{R}_1$ and permuting 1 and 2 gives $\mathbf{R}_1 - \mathbf{R}_2$ which is equal to $-\mathbf{r}_1$. Similarly the permutation of $\mathbf{r}_2 = \mathbf{R}_3 - \mathbf{R}_1$ gives $\mathbf{R}_3 - \mathbf{R}_2 = \mathbf{R}_3 - \mathbf{R}_1 - \mathbf{R}_2 + \mathbf{R}_1 = \mathbf{r}_2 - \mathbf{r}_1$. Thus \sum_P in (3) comprises two permutation matrices τ_P which in the internal coordinates have the following form:

$$\begin{pmatrix} 1 & 0 \\ 0 & 1 \end{pmatrix}, \quad \begin{pmatrix} -1 & 0 \\ -1 & 1 \end{pmatrix}. \quad (4)$$

The coefficients χ_P are obtained from the matrix elements of the irreducible representation of the considered state, and for para H_2^+ they are both equal to one. Note that the $r_1^{m_k}$ factor is always symmetric with respect to permuting the protons. The states with the wave functions constructed this way are $N=0$ states, i.e. the rotational ground states.

In the other form of H_2^+ , called ortho, the nuclear spin wave function is symmetric with respect to permuting the labels of the protons (high spin state) and the spatial function is antisymmetric. The antisymmetric spatial function corresponds to the first excited rotational state with $N=1$. The ECG basis functions which can describe such a state are obtained by multiplying the $N=0$ ECGs (2) by an angular factor in the form of the z coordinate of the \mathbf{r}_1 vector, z_1 (note that $z_1 = Z_2 - Z_1$ is antisymmetric with respect to the proton permutation):

$$\phi_k(\mathbf{r}) = z_1 r_1^{m_k} \exp[-\mathbf{r}'(L_k L'_k \otimes I_3)\mathbf{r}], \quad (5)$$

and symmetrizing the exponential part of the function as it is done in (3) with permutation matrices (4).

It should be noted that, in general, $N=1$ basis functions can also be obtained by replacing the z_1 multiplier in (5) by z_2 . Such functions represent promoting the electron to π excited states, but deexciting the rotational motion of the nuclei to the ground rotational state. However, these kinds of states are significantly higher in energy than the rotational excitations of the nuclei and they are likely to provide only a small contribution to the energy. Also, as Gaussians (5) are not orthogonal to the Gaussians which z_1 replaced by z_2 , i.e. Gaussians: $z_2 r_1^{m_k} \exp[-\mathbf{r}'(L_k L'_k \otimes I_3)\mathbf{r}]$, they effectively include contributions from the latter functions. Therefore, if the contribution of the $z_2 r_1^{m_k} \exp[-\mathbf{r}'(L_k L'_k \otimes I_3)\mathbf{r}]$, $i=2, \dots, n$, basis function is small, as it is expected to be for the $N=1$ state of H_2^+ , this contribution should be approximately accounted for by only including the $z_1 r_1^{m_k} \exp[-\mathbf{r}'(L_k L'_k \otimes I_3)\mathbf{r}]$ Gaussians in the basis set.

The spatial wave function for each state, $\Psi(\mathbf{r})$, is approximated by a linear combination of K properly symmetrized basis functions, $\psi_k(\mathbf{r})$. The linear variational parameter obtained by solving the secular equation. The optimization of the nonlinear parameters of the Gaussians (i.e. the L_k matrix elements and the m_k powers of r_1) is carried out by the minimization of the total non-BO internal energy of the system. This minimization employs the analytical energy gradient determined with respect to the L_k matrix elements. The formula for the gradient was presented in [9].

3. Results

The calculations are performed for each state separately using basis functions (2) for the $N=0$ states and basis functions (5) for the $N=1$ states. The goal of the calculations is not to push the accuracy of the results to limits of the available computational resources, but rather to generate a basis set for each state with

a minimal number of functions that gives the energy accuracy of about 3×10^{-9} hartree. Such an accuracy is sufficient to determine the dissociation energy with the accuracy of about 0.001 cm^{-1} . Thus for different states the number of ECGs is, in general, different and increases with the vibrational excitation. The results of the calculation allow for determining the dissociation energies corresponding to the considered states and the para-ortho isomerization energy for each vibrational level of H_2^+ . One of the results of the calculations are the non-BO wave functions for the considered rovibrational states. These functions can be provided upon request to interested readers. They are also used in this work to calculate expectation values of the interparticle distances (i.e., the proton-proton and proton-electron distances) and to calculate the proton-proton correlation functions.

The para-ortho isomerization was recently studied using the approach employed in the present calculations for H_2^+ [10]. The results agreed with the experimental results with the accuracy of the experimental data. The approach was also recently used to calculate energies and lifetimes of rovibrational states of the HD^+ ion [9]. In those two works a procedure was developed to generate ECG basis sets for calculating $N=0$ and $N=1$ states. The procedure is employed in the present calculations.

In the first step of the calculations the $N=0$ states are considered. We start with the ($N=0, v=0$) state and we generate a small (20-30 ECGs) basis set for it using a standard Gaussian orbital basis set with some randomly chosen values for the m_k parameters. This basis set is optimized with the gradient-based method and then enlarged in increments of 20 functions. The starting guess for a new ECG is generated by randomly perturbing the L_k parameters of some most contributing ECGs already included in the basis set and choosing the one which gives the largest lowering of the total energy. After checking if the new ECG is linearly independent with the ECGs already included in the basis set, its m_k power is optimized followed with the optimization of its L_k parameters. After the optimization is finished the ECG is again checked for linear dependency and if none is found it is included in the basis set. After each 20 ECGs are added this way to the basis set, the whole set is reoptimized by cycling over all basis functions one by one and reoptimizing their L_k parameters. The cyclic optimization is repeated several times. This process is terminated when the energy obtained with K basis functions is only by about 1.0×10^9 hartree lower than the energy obtained with (K-100) basis functions. In this way the 400-ECG and 500-ECG results for the ($N=0, \neq=0$) shown in Table 1 are generated. In generating a basis set for the next ($N=0, v=1$) state the 400-ECG basis set of the ($N=0, v=0$) state is used as the initial guess and the L_k of ECGs are reoptimized using the cyclic optimization. Next, the size of the basis set is increased by 100 using the above-described approach. If this increase causes the energy to only change by about 1.0×10^9 hartree the optimization stops. If not additional 100 ECGs are added to the basis set. In this way the energies for all ($N=0, v=0, \dots, 19$) states shown in Table 1 are generated. For the top $v=19$ state the basis set has to be increased to 1700 to reach the target accuracy.

The initial guesses for the basis sets for ($N=1, v=0, \dots, 19$) states are generated from the basis sets of the $N=0$ states by adding the z_1 factor to each ECG. For example, such a set for the ($N=1, v=0$) state is generated from the 400-ECG basis set of the ($N=0, v=0$) state. Then, after reoptimization of the L_k parameters of the ECGs in the initial set, 100 ECGs are added to the set with the procedure used for the basis set enlargement for the $N=0$ states. Again, if addition of the new 100 ECGs lowers the energy of the the $N=1$ state by only about 1.0×10^9 hartree the growing of the basis set stops. In this way the results for the ($N=1, v=0, \dots, 19$) states shown in Table 1 are generated.

The total $N=0$ and $N=1$ energies from Table 1 are used to calculate the corresponding dissociation energies and the energy

Table 1
The convergence of the total nonrelativistic non-BO energies of the $N=0$ and $N=1$, $v=0, \dots, 19$ rovibrational states of H_2^+ with the number of basis functions. All values are given in a.u. (hartrees).

	v	No. ECGs	Energy		v	No. ECGs	Energy		v	No. ECGs	Energy		v	No. ECGs	Energy
$N=0$	0	400	-0.59713906290	1	500	-0.58715567889	2	500	-0.57775190369	3	500	-0.56890849601	4	600	-0.56890849753
		500	-0.59713906299		600	-0.58715567902		600	-0.57775190407		600	-0.56890849753		700	-0.56868369552
$N=1$	0	400	-0.59687372753	1	500	-0.58690430984	2	500	-0.577751402288	3	500	-0.56868369689	4	600	-0.56868369689
		500	-0.59687372764		600	-0.58690430997		600	-0.577751402315		600	-0.56868369689		700	-0.56885738413
$N=0$	4	600	-0.56060921837	5	700	-0.55284074771	6	700	-0.54559264508	7	800	-0.53885738151	8	900	-0.53885738151
		700	-0.56060921981		800	-0.55284074870		800	-0.54559264804		900	-0.53885738151		1000	-0.53868221358
$N=1$	4	600	-0.56039715903	5	800	-0.55264116021	6	800	-0.54540533114	7	1000	-0.53868221291	8	1100	-0.53868221358
		700	-0.56039716022		900	-0.55264116074		900	-0.54540533238		1100	-0.53868221358		1200	-0.51700035938
$N=0$	8	1000	-0.53263037643	9	1000	-0.52691011999	10	1000	-0.52169836327	11	1100	-0.51700036138	12	1200	-0.51700036138
		1100	-0.53263037755		1100	-0.52691012142		1100	-0.52169836528		1200	-0.51700036138		1300	-0.51687416262
$N=1$	8	1100	-0.53246730009	9	1100	-0.52675917290	10	1100	-0.52155967388	11	1200	-0.51687416262	12	1300	-0.51687416262
		1200	-0.53246730075		1200	-0.52675917384		1200	-0.52155967520		1300	-0.51687416262		1400	-0.50359508060
$N=0$	12	1200	-0.51282519809	13	1200	-0.50918624171	14	1200	-0.50610167207	15	1300	-0.50359507812	16	1400	-0.50359507812
		1300	-0.51282519968		1300	-0.50918624366		1300	-0.50610167448		1400	-0.50359507812		1500	-0.50352426904
$N=1$	12	1300	-0.51271185535	13	1300	-0.50908627218	14	1300	-0.50601579200	15	1400	-0.50352426904	16	1500	-0.50352427021
		1400	-0.51271185634		1400	-0.50908627352		1400	-0.50601579419		1500	-0.50352427021		1600	-0.49983742855
$N=0$	16	1400	-0.50169576822	17	1400	-0.50043703353	18	1400	-0.49983742764	19	1600	-0.49973122997	20	1700	-0.49973123011
		1500	-0.50169576967		1500	-0.50043703582		1500	-0.49983742855		1700	-0.49973123011		1800	-0.49972884568
$N=1$	16	1500	-0.50164138415	17	1500	-0.50040097552	18	1500	-0.49982178676	19	1600	-0.49972884568	20	1700	-0.49972884583
		1600	-0.50164138521		1600	-0.50040097679		1600	-0.49982178765		1700	-0.49972884583		1800	-0.49972884583
	H		-0.49972783971												

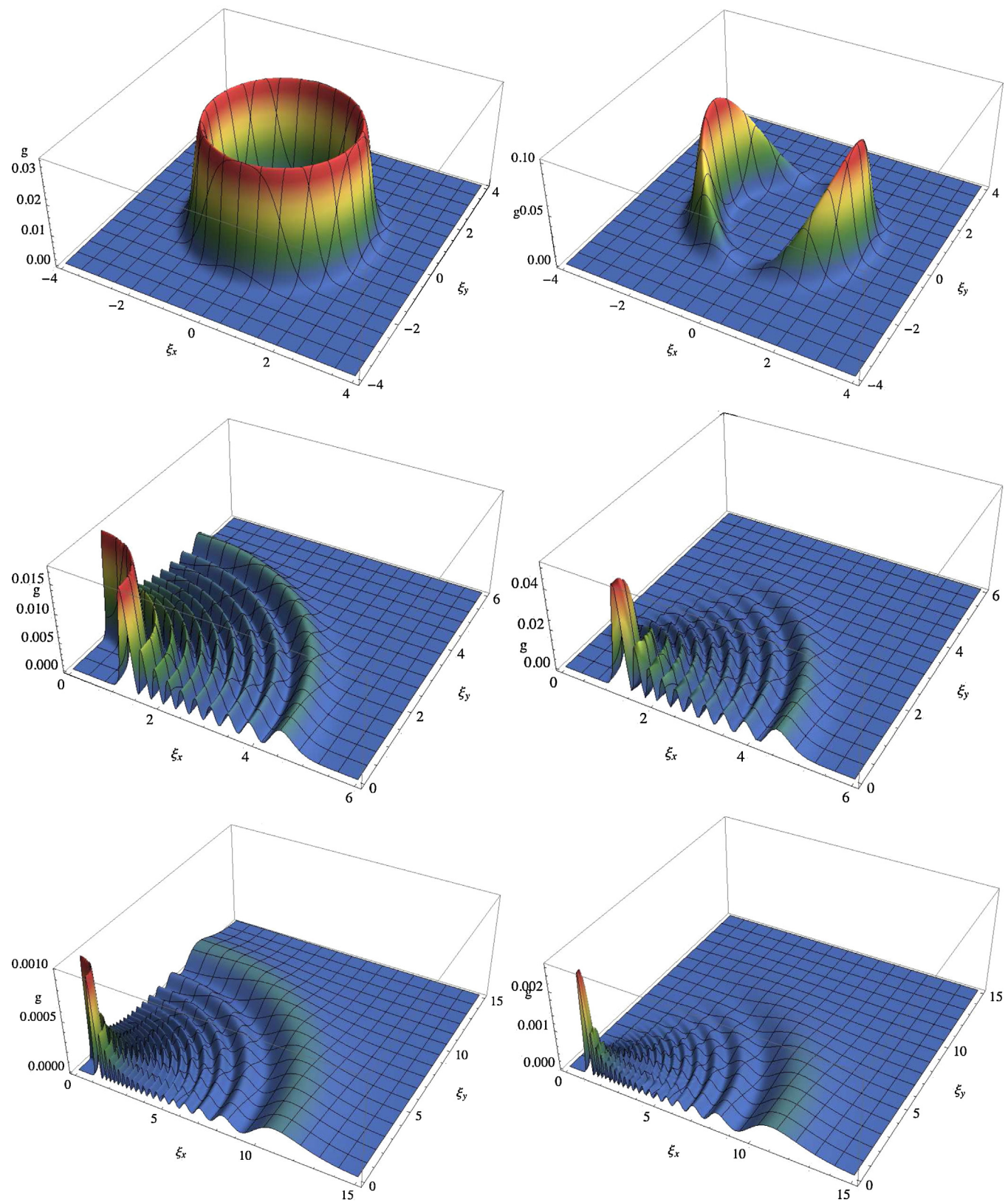


Figure 1. Comparison of the nuclear correlation functions for the $\nu=0, 9, \text{and} 18, N=0$ states (on the left) and the $\nu=0, 9, \text{and} 19, N=1$ states (on the right) of H_2^+ . Correlation functions for $\nu=0$ are plotted for $(-\xi_{\max} < \xi_x < \xi_{\max}, -\xi_{\max} < \xi_y < \xi_{\max})$, and those for $\nu=10$ and 19 are plotted in the range $(0 < \xi_x < \xi_{\max}, 0 < \xi_y < \xi_{\max})$ to better show the oscillatory behavior.

Table 2

Dissociation energies for the ($v, 0$) and ($v, 1$) states of H_2^+ ($E_{\text{diss}}^{N=0} = E(v, 0) - E_{\text{H}}$ and $E_{\text{diss}}^{N=1} = E(v, 1) - E_{\text{H}}$) and the para-ortho isomerization energies ($\Delta = E(v, 1) - E(v, 0)$). The isomerization energies are compared with the results of Wolniewicz and Poll [11] and Karr and Hilico [12]. All values are in cm^{-1} .

v	$E_{\text{diss}}^{N=0}$	$E_{\text{diss}}^{N=1}$	Δ	Δ [11]	Δ [12]
0	21 379.292	21 321.058	58.234	58.234	58.232
1	19 188.193	19 133.024	55.169	55.169	55.167
2	17 124.303	17 072.094	52.209	52.208	52.207
3	15 183.399	15 134.061	49.338	49.338	49.336
4	13 361.918	13 315.377	46.542	46.541	46.539
5	11 656.936	11 613.132	43.804	43.804	43.802
6	10 066.162	10 025.051	41.111	41.110	41.109
7	8 587.942	8 549.497	38.445	38.445	38.444
8	7 221.272	7 185.481	35.791	35.791	35.789
9	5 965.821	5 932.692	33.129	33.129	33.127
10	4 821.973	4 791.534	30.439	30.438	30.437
11	3 790.880	3 763.183	27.697	27.696	27.696
12	2 874.538	2 849.662	24.876	24.874	24.874
13	2 075.880	2 053.939	21.941	21.940	21.940
14	1 398.895	1 380.046	18.849	18.847	18.847
15	848.761	833.220	15.541	15.540	15.540
16	431.911	419.975	11.936	11.935	11.935
17	155.651	147.737	7.914	7.913	7.913
18	24.052	20.619	3.433	3.433	3.433
19	0.744	0.221	0.523		0.523

Table 3

Expectation values of the proton–proton ($\langle r_{pp} \rangle$), and proton–electron ($\langle r_{pe} \rangle$) distances calculated for the ($v, N=0$) and ($v, N=1$) states of H_2^+ . All values are in a.u.

v	$\langle r_{pp}(v, N=0) \rangle$	$\langle r_{pp}(v, N=1) \rangle$	$\langle r_{pe}(v, N=0) \rangle$	$\langle r_{pe}(v, N=1) \rangle$
0	2.0639	2.0666	1.6930	1.6944
1	2.1991	2.2019	1.7648	1.7662
2	2.3398	2.3427	1.8394	1.8409
3	2.4866	2.4897	1.9172	1.9189
4	2.6408	2.6440	1.9989	2.0006
5	2.8035	2.8070	2.0850	2.0869
6	2.9764	2.9801	2.1764	2.1784
7	3.1616	3.1656	2.2742	2.2763
8	3.3618	3.3662	2.3797	2.3820
9	3.5808	3.5857	2.4948	2.4974
10	3.8235	3.8291	2.6222	2.6251
11	4.0972	4.1036	2.7654	2.7687
12	4.4123	4.4199	2.9297	2.9336
13	4.7851	4.7944	3.1234	3.1282
14	5.2428	5.2547	3.3600	3.3662
15	5.8344	5.8510	3.6643	3.6728
16	6.6640	6.6899	4.0881	4.1013
17	8.0145	8.0660	4.7727	4.7987
18	11.1748	11.3827	6.3604	6.4645
19	25.2429	30.4520	13.3887	15.991

difference between $N=0$ and $N=1$ states for each v vibrational state, which is the spin isomerization energy between the para and ortho H_2^+ for that v . Both isomerization and dissociation energies are shown in Table 2. In the table we also show the para-ortho isomerization energies obtained from the results of Wolniewicz and Poll [11]. Even though those results include the relativistic and radiative corrections they only differ from our results by less than 0.002 cm^{-1} . One can notice that the ($N=0, v=19$) and ($N=1, v=19$) states, which according to our calculations are only bound by 0.744 and 0.221 cm^{-1} , respectively, were not found in the calculations of Wolniewicz and Poll. This result is confirmed by the comparison with the results of Karr and Hilico [12], which are in excellent agreement with our calculations.

Finally in Table 3 we show expectation values of the proton–proton (r_{pp}) and proton–electron (r_{pe}), distances calculated using the non-BO $N=0$ and $N=1$ wave functions expanded in terms of the largest basis set generated for these states in the calculations. Comparing the ($N=0, v=0$) results to those reported by Frolov [13] and rovibrationally averaged distances obtained by Alexander

and Coldwell [14,15] we conclude that our distances are accurate to the number of significant figures used. The values show expected increasing trends with the increasing excitation level. The results can be useful in benchmarking calculations performed with conventional BO-approximation-based method. It is interesting to examine the expectation values obtained for the highest bound ($N=0, v=19$) and ($N=1, v=19$) states. The average r_{pp} distance already large for the former state (of 25.2429 a.u.) increases further upon rotational excitation (to 30.4520 a.u.). Increases of r_{pp} upon rotation excitations also happen for lower states, but they are not as significant as for the top states.

Another property which can be calculated using a non-BO wave function is the interparticle correlation function [6,16]. For example, the inter-nuclear correlation function is calculated as:

$$g(\xi) = \langle \Psi(\mathbf{r}) | \delta(\mathbf{r}_1 - \xi) | \Psi(\mathbf{r}) \rangle, \quad (6)$$

where $\delta(\mathbf{r}_1 - \xi)$ is a 3D Dirac delta function and ξ is the vector of the coordinates of the point at which the nuclear correlation function is calculated. The plotting of the correlation function is done by first calculating this function on a grid of points and then plotting the results. $g(\xi)$ is plotted for some selected $N=0$ and $N=1$ rovibrational states and the results are shown in Figure 1. The plots show the angular behavior of the densities being spherically symmetric for the $N=0$ states and radially symmetric for the $N=1$ states. Also, the plots demonstrate how the vibrational nodal (oscillatory) structure of the inter-nuclear correlation function changes with increasing vibrational excitation level. The $r_1^{m_k}$ factor in the $N=0$ and $N=1$ basis functions allows to represent these oscillations of the wave functions.

4. Summary

A direct variational non-BO calculation is performed for all bound $N=0$ and $N=1$ states of the H_2^+ ion using large sets of explicitly correlated Gaussian functions. Each state is calculated separately and for each state the ECG basis set is extensively optimized in terms of the Gaussian non-linear parameters using a energy-minimization method which employs the analytical energy gradient determined with respect to these parameters. The aim of this work is to generate the most compact ECG basis sets for the considered states, but still obtain energies accurate to about 3×10^{-9} hartrees. The non-BO wave functions are used to calculate expectation values of the proton–proton and proton–electron interparticle distances and the internuclear correlation functions.

Future work will involve including ECGs with z_1 replaced by z_i in the $N=1$ basis set in the non-BO calculations of the H_2^+ rovibrational states. This will allow to account for the angular-momentum coupling between the nuclear and electronic rotational excitations. Also, work is in progress in the development of algorithms for calculating $N=2$ and $N=3$ states of diatomic molecules.

Acknowledgements

This work has been supported in part by the National Science Foundation through the graduate research fellowship program (GRFP) awarded to Keeper L. Sharkey; grant number DGE1-1143953. We are grateful to the University of Arizona Center of Computing and Information Technology for the use of their computer resources.

References

- [1] S. Bubin, M. Pavanello, W.-Ch. Tung, K.L. Sharkey, L. Adamowicz, Chem. Rev. 113 (2013) 36.
- [2] J. Mitroy, et al., Rev. Mod. Phys. 85 (2013) 693.
- [3] D.B. Kinghorn, L. Adamowicz, Phys. Rev. Lett. 83 (1999) 2541.

- [4] D.B. Kinghorn, L. Adamowicz, *J. Chem. Phys.* 110 (1999) 7166.
- [5] K.L. Sharkey, N. Kirnosov, L. Adamowicz, *J. Chem. Phys.* 139 (2013) 164119.
- [6] N. Kirnosov, K.L. Sharkey, L. Adamowicz, *J. Chem. Phys.* 139 (2013) 204105.
- [7] N. Kirnosov, K.L. Sharkey, L. Adamowicz, *J. Chem. Phys.* 140 (2014) 104115.
- [8] See CODATA 2002 recommended values and NIST Physical Reference Data at <http://physics.nist.gov/>
- [9] K.L. Sharkey, N. Kirnosov, L. Adamowicz, *J. Chem. Phys.* 139 (2013) 164119.
- [10] K.L. Sharkey, N. Kirnosov, L. Adamowicz, *Phys. Rev. A* 88 (2013) 032513.
- [11] L. Wolniewicz, J.D. Poll, *Mol. Phys.* 59 (1986) 953.
- [12] J.Ph. Karr, L. Hilico, *J. Phys. B: At. Mol. Opt. Phys.* 39 (2006) 2095.
- [13] A.M. Frolov, *Phys. Rev. A* 59 (1999) 4270.
- [14] S.A. Alexander, R.L. Coldwell, *Chem. Phys. Lett.* 413 (2005) 253.
- [15] S.A. Alexander, R.L. Coldwell, *Int. J. Quantum Chem.* 112 (2012) 3703.
- [16] S. Bubin, L. Adamowicz, *Chem. Phys. Lett.* 403 (2005) 185.

APPENDIX K

Non-Born-Oppenheimer method for direct variational calculations of diatomic first excited rotational states using explicitly correlated all-particle Gaussian functions

Non-Born-Oppenheimer method for direct variational calculations of diatomic first excited rotational states using explicitly correlated all-particle Gaussian functions

Keeper L. Sharkey,¹ Nikita Kirnosov,² and Ludwik Adamowicz^{1,2,*}

¹Department of Chemistry and Biochemistry, University of Arizona, Tucson, Arizona 85721, USA

²Department of Physics, University of Arizona, Tucson, Arizona 85721, USA

(Received 28 May 2013; published 20 September 2013)

We report the development of a direct variational method for calculating the first rotational excited state of diatomic molecules with σ electrons where the Born-Oppenheimer approximation is not assumed. The method employs all-particle explicitly correlated Gaussian basis functions. The exponential parameters of the Gaussians are optimized with the aid of an analytically calculated energy gradient determined with respect to these parameters. The method is tested in calculations of the ortho-para spin isomerization of the hydrogen molecule in its all-bound vibrational states.

DOI: 10.1103/PhysRevA.88.032513

PACS number(s): 31.15.xt, 33.20.Sn, 03.65.-w, 33.15.-e

I. INTRODUCTION

More than a decade ago a method for calculating pure (rotationless) vibrational states of diatomic molecules with σ electrons was introduced [1,2]. The method did not assume the Born-Oppenheimer (BO) approximation and utilized explicitly correlated all-particle Gaussian basis functions for expanding the total wave function of the system. Since then several applications of the method have been shown [3–5] ranging from systems with two electrons such as HeH^+ and all isotopologues of H_2 to a six-electron system, the BH molecule.

In this paper we report the development of a method for extending the very accurate non-BO calculations with explicitly correlated Gaussians (ECGs) to states where the diatomic molecule is excited to the first rotational state and also vibrationally excited to an arbitrary level. The development includes the derivation and implementation of the Hamiltonian matrix elements and the matrix elements of the energy gradient determined with respect to the exponential parameters of the Gaussians. The availability of the analytically calculated gradient is key in carrying out the variational optimization of the Gaussian parameters by the minimization of the total energy.

The method is not limited to any particular number of electrons in the molecule. Only practical limits related to the computational resources restrict the size of the molecules which can be calculated. Also the method is direct and does not involve separation of the Schrödinger equation of the molecule into the electronic equation solved for different configurations of the stationary nuclei and the equation describing the motion of the nuclei, from which the rovibrational levels are obtained. Furthermore, not assuming the BO approximation means that the adiabatic and nonadiabatic coupling of the electronic motion and nuclear motions (vibrational and rotational) in the present approach is included to infinite order and a single Schrödinger equation is solved for each rovibrational state of the system. Furthermore, as the method is strictly variational, upper bounds to the exact nonrelativistic energies are obtained and, if a sufficiently complete basis set is used in the calculation, the results are exact within the nonrelativistic

limit. Thus, there is no need for using a combination of the variational and perturbational techniques to describe the adiabatic and nonadiabatic energy corrections, as is done in methods based in the first order on the BO approximation.

In this work we test the method in calculations of the $N = 1$ states of the H_2 molecule, as this model system has been studied with very high accuracy by other methods. The quantities we determine are the ortho-para spin isomerization energies for all H_2 bound vibrational states. The increase of the average internuclear distance with the vibrational excitation and weakening of the intermolecular bonding affects the rotational motion of the molecule. These effects are directly and precisely described in the present approach without any approximations concerning the separability of the motions of the electrons and the nuclei.

II. NON-BORN-OPPENHEIMER APPROACH

In the fully nonadiabatic approach considered in this work all particles forming the molecule are treated equally with rigorous accounting for their given masses M_i and the electrostatic interactions between their charges Q_i . Without invoking any approximations, the total laboratory-frame Hamiltonian of the system can be separated into an operator representing the motion of the center of mass and an operator representing the internal energy. We perform this separation by making a transformation from the laboratory Cartesian coordinates, \mathbf{R}_i , $i = 1, \dots, N$, where N is the number of particles (nuclei + electrons) in the system, to an internal reference frame with origin at a selected reference particle (particle 1): $\mathbf{r}_i = \mathbf{R}_{i+1} - \mathbf{R}_1$. This transformation to the internal coordinates together with the conjugate momentum transformation yields the following nonadiabatic Hamiltonian representing the internal energy of the system:

$$\hat{H} = -\frac{1}{2} \left(\sum_{i=1}^n \frac{1}{\mu_i} \nabla_{\mathbf{r}_i}^2 + \sum_{j \neq i}^n \frac{1}{m_0} \nabla'_{\mathbf{r}_i} \nabla_{\mathbf{r}_j} \right) + \sum_{i=1}^n \frac{q_0 q_i}{r_i} + \sum_{j > i=1}^n \frac{q_i q_j}{r_{ij}}, \quad (1)$$

*Corresponding author: ludwik@u.arizona.edu

where M_1 is the mass of particle 1 (the reference particle), and $\nabla_{\mathbf{r}_i}$ is the gradient with respect to the x , y , and z coordinates of \mathbf{r}_i . The charges and masses are mapped from the original particles as $\{Q_1, \dots, Q_N\} \rightarrow \{q_0, \dots, q_n\}$, and $\{M_1, \dots, M_N\} \rightarrow \{m_0, \dots, m_n\}$, where $n = N - 1$. In the calculations on para-ortho hydrogen presented in this work M_1 and M_2 are the proton masses ($M_p = 1836.152\,672\,61m_e$, where m_e is the electron mass), and M_3 and M_4 are electron masses. The reduced masses are μ_i defined by $\mu_i = m_0 m_i / (m_0 + m_i)$. The potential energy is the same as in the laboratory-frame Hamiltonian, but is now written using the internal distance coordinates $r_{ij} = \|\mathbf{r}_j - \mathbf{r}_i\| = \|\mathbf{R}_{j+1} - \mathbf{R}_{i+1}\|$ and $r_j = \|\mathbf{r}_j\| = \|\mathbf{R}_{j+1} - \mathbf{R}_1\|$. For vector-matrix transposition the prime is used. More general information on the nonadiabatic Hamiltonian and the center-of-mass transformation can be found in Refs. [1,2].

III. EXPLICITLY CORRELATED GAUSSIAN BASIS FUNCTIONS

The basis set of explicitly correlated Gaussian functions used in the calculations of the rotationless states of diatomic molecules [1,2] has the following form:

$$\phi_k(\mathbf{r}) = r_1^{m_k} \exp[-\mathbf{r}'(L_k L'_k \otimes I_3)\mathbf{r}], \quad (2)$$

where \mathbf{r} is a vector of the internal coordinates, $\mathbf{r} = \{\mathbf{r}'_1, \dots, \mathbf{r}'_n\}'$, L_k is an $n \times n$ rank- n lower triangular matrix of nonlinear variational parameters, and I_3 is the 3×3 identity matrix. The Kronecker product \otimes with the identity ensures rotational invariance of the basis functions; thus they are angular momentum eigenfunctions with $N = 0$. By writing the exponential parameters of the Gaussians in the Cholesky factored form, $L_k L'_k$ ensures the square integrability of the Gaussians. The preexponential factor in (2), $r_1^{m_k}$, where r_1 is the distance between the two nuclei, is necessary to describe the very strong internuclear correlation (i.e., the effect of the nuclei staying apart from each other at a considerable distance in the molecule) and the radial nodes of the wave functions of vibrationally excited vibrational states. The m_k power of r_1 is a non-negative even number which is an additional variational parameter subject to optimization (in the application calculations performed so far m_k has ranged from 0 to 250).

The permutational symmetry is implemented in the basis functions (2) by projecting each basis function using a symmetry-projection operator \mathcal{P} :

$$\psi_k = \mathcal{P}\phi_k = \sum_P \chi_P r_1^{m_k} \exp[-\mathbf{r}'(\tau'_P L_k L'_k \tau_P \otimes I_3)\mathbf{r}], \quad (3)$$

where the sum runs over all permutations of the labels of identical particles and where τ_P are permutational matrices transforming the internal coordinates. For the lowest-energy state of the hydrogen molecules (para-hydrogen), the total spatial wave function is symmetric with respect to permuting the proton labels and with respect to permuting the electron labels. Thus, there are four permutations P in the sum on the right-hand side of (3) and the τ_P matrices in the internal

coordinates have the following form:

$$\begin{aligned} \begin{pmatrix} 1 & 0 & 0 \\ 0 & 1 & 0 \\ 0 & 0 & 1 \end{pmatrix}, \quad & \begin{pmatrix} -1 & 0 & 0 \\ -1 & 1 & 0 \\ -1 & 0 & 1 \end{pmatrix}, \\ \begin{pmatrix} 1 & 0 & 0 \\ 0 & 0 & 1 \\ 0 & 1 & 0 \end{pmatrix}, \quad & \begin{pmatrix} -1 & 0 & 0 \\ -1 & 0 & 1 \\ -1 & 1 & 0 \end{pmatrix}. \end{aligned} \quad (4)$$

The coefficients χ_P are obtained from the matrix elements of the irreducible representation of the considered state, and for the ground state of H_2 they are all 1's.

To describe the $N = 1$ rotationally excited molecule considered in this work, the Gaussian basis functions (2) are multiplied by an angular factor in the form of the z_1 coordinate:

$$\phi_k(\mathbf{r}) = z_1 r_1^{m_k} \exp[-\mathbf{r}'(L_k L'_k \otimes I_3)\mathbf{r}]. \quad (5)$$

In general, $N = 1$ basis functions can also be obtained by replacing the z_1 multiplier by z_i , $i = 2, \dots, n$, multipliers, but, as such functions represent promotion of the electrons to π excited states, but deexciting the rotational motion of the nuclei to the ground rotational state. However, such states are much higher in energy than the rotational excitations of the nuclei and they do not need to be explicitly included in the basis set used in the present calculations. Also, one should realize that the Gaussians used in the present calculations, even though they do not explicitly include z_i , $i = 2, \dots, n$, preexponential multipliers, they effectively include contributions of the $z_i \exp[-\mathbf{r}'(L_k L'_k \otimes I_3)\mathbf{r}]$, $i = 2, \dots, n$, functions, because the functions $z_1 \exp[-\mathbf{r}'(L_k L'_k \otimes I_3)\mathbf{r}]$ and the functions $z_i \exp[-\mathbf{r}'(L_k L'_k \otimes I_3)\mathbf{r}]$, $i = 2, \dots, n$, have nonzero overlap if the $L_k L'_k$ matrix product has nonzero off-diagonal elements. Therefore, if the contributions of the $z_i \exp[-\mathbf{r}'(L_k L'_k \otimes I_3)\mathbf{r}]$, $i = 2, \dots, n$, basis functions are small, as they are expected to be for the vibrational states of the H_2 molecule excited to the first excited rotational state, these contributions should be well described by including only $z_1 \exp[-\mathbf{r}'(L_k L'_k \otimes I_3)\mathbf{r}]$ Gaussians in the basis set. If the contributions are larger (this happens, for example, in muonic molecules), one needs to explicitly include $z_i \exp[-\mathbf{r}'(L_k L'_k \otimes I_3)\mathbf{r}]$, $i = 2, \dots, n$, Gaussians in the calculation.

In the $N = 1$ states the spatial wave functions need to be antisymmetric with respect to permuting the proton labels, as these states describe ortho-hydrogen with parallel nuclear spins. As the $z_1 = Z_2 - Z_1$ factor is antisymmetric with respect to this permutation, the remaining part of the basis function (5) has to be symmetric to make the whole basis function antisymmetric. Thus, in the calculation of the $N = 1$ states the same projection operator \mathcal{P} is applied to the $r_1^{m_k} \exp[-\mathbf{r}'(L_k L'_k \otimes I_3)\mathbf{r}]$ part of (5) as used for the $N = 0$ basis functions (2).

Since the total internal molecular wave function Ψ is dependent on the spatial coordinates \mathbf{r} and the spin coordinates \mathbf{m} of the particles: $\Psi = \Psi(\mathbf{r}, \mathbf{m})$, and because the internal Hamiltonian (1) is spin independent, the calculation of the Hamiltonian and overlap matrix elements can be carried out by first integrating over spin variables, which leaves behind only spatially dependent integrals. The spatial wave function for each state, $\Psi(\mathbf{r})$, is approximated by a linear combination

of K properly symmetrized basis functions $\psi_k(\mathbf{r})$:

$$\Psi(\mathbf{r}) = \sum_{k=1}^K c_k \psi_k(\mathbf{r}), \quad (6)$$

where c_k is the linear variational parameter.

IV. VARIATIONAL METHOD AND ENERGY MINIMIZATION

To obtain the energy eigenvalues of Hamiltonian (1) the Rayleigh-Ritz variational scheme based on the minimization of the Rayleigh quotient,

$$\varepsilon(a, c) = \min_{(a, c)} \frac{\mathbf{c}' \mathbf{H}(a) \mathbf{c}}{\mathbf{c}' \mathbf{S}(a) \mathbf{c}} \quad (7)$$

is used, where $\mathbf{H}(a)$ and $\mathbf{S}(a)$ are the Hamiltonian and overlap $K \times K$ matrices, respectively. $\mathbf{H}(a)$ and $\mathbf{S}(a)$ are functions of the nonlinear parameters contained in the basis-set exponent matrices L_k . We write a for the set of these parameters and \mathbf{c} for the vector of the linear expansion coefficients of the wave function in terms of basis functions. The expressions for the overlap and Hamiltonian matrix elements with basis functions (5) will be presented elsewhere [6].

A very important aspect of the variational calculations with ECGs is that achieving high accuracy is possible only when the nonlinear exponential parameters of the Gaussians are extensively optimized based on the minimization of the energy. This process usually takes large amounts of computer time. To accelerate the basis-set optimization it is beneficial to derive and implement the analytic gradient of the energy, (7), with respect to the nonlinear parameters of the Gaussians. This was done in this work for the energy calculated using basis functions (5).

To determine the gradient, we start with the differential of the secular equation $(\mathbf{H} - \varepsilon \mathbf{S})\mathbf{c} = 0$:

$$d(\mathbf{H} - \varepsilon \mathbf{S})\mathbf{c} = (d \mathbf{H})\mathbf{c} - (\varepsilon d \mathbf{S})\mathbf{c} - \varepsilon(d \mathbf{S})\mathbf{c} + (\mathbf{H} - \varepsilon \mathbf{S})d \mathbf{c}. \quad (8)$$

Multiplying this equation by \mathbf{c}' from the left we obtain

$$d \varepsilon = \mathbf{c}'(d \mathbf{H} - \varepsilon d \mathbf{S})\mathbf{c}. \quad (9)$$

To get (9) we utilize the secular equation and assume that the wave function is normalized, i.e., $\mathbf{c}' \mathbf{S} \mathbf{c} = 1$. The expression for $d \varepsilon$ involves $d \mathbf{H}$ and $d \mathbf{S}$ which depend on the first derivatives of the Hamiltonian and overlap integrals with respect to the Gaussian nonlinear parameters. The formulas for these derivatives will be provided elsewhere [6]. The relation in (9) constitutes the well-known Hellmann-Feynman theorem.

V. NUMERICAL ILLUSTRATION

In our previous paper [4], very accurate non-BO calculations for the $v = 0, \dots, 14, N = 0$ states (rotationless states) of the H_2 molecule were described. The calculations were performed for each state separately using the basis set (2) containing 10 000 explicitly correlated Gaussian functions. The gradient-based method was used in the optimization of the exponential parameters of the Gaussians. Prior to the present calculation on ortho- H_2 ($N = 1$ states), we performed some test non-BO calculations of $N = 0$ and $N = 1, v = 0, \dots, 22$ rovibrational states of the HD^+ ion [6]. The point we tested was how to generate good basis sets for the $N = 1$ states given very well-converged and complete ECG basis sets for the $N = 0$ states. The tests showed that one can obtain very accurate results if for a particular $N = 1$ state one takes the basis set of the corresponding $N = 0$ state with the same v , multiplies it by z_1 , and reoptimizes only the exponential parameters of the Gaussians (i.e., the elements of the L_k matrices) without changing the m_k powers in the preexponential $r_1^{m_k}$ factor. This is the approach employed in the present calculations. The reoptimization has been carried out using the gradient-based method.

The results of the calculations are presented in Table I. The total $N = 0$ and $N = 1$ energies for all-bound vibrational states ($v = 0, \dots, 14$; note that, strictly speaking, the vibrational quantum number is not a “good” quantum number

TABLE I. Total energies (in hartrees) of the $(v, 0)$ and $(v, 1)$ states of H_2 obtained in the present calculations and the $(v, 1) - (v, 0)$ energy difference [$\Delta = E(v, 1) - E(v, 0)$; in cm^{-1}], which is the ortho-para spin isomerization energy. Δ is compared with the results of the experiment of Dabrowski [7] and, for the $v = 0$ state also with the results of the experiment of Salumbides *et al.* [8] (Expt. – Δ). We also compare the experiments with the Δ calculated by Komasa *et al.* [9] (Expt. – [9]). Estimated accuracy of the calculated total energies is shown in parentheses.

v	$E(v, 0)$ [5]	$E(v, 1)$	Δ	Expt. – Δ	Expt. – [9]
0	-1.164 025 030 84(100)	-1.163 485 139 52(100)	118.4924	0.01	0.01
				-0.0056	0.0016
1	-1.145 065 372 10(100)	-1.144 552 418 73(100)	112.5803	0.03	0.04
2	-1.127 177 935 74(100)	-1.126 691 329 65(200)	106.7977	0.08	0.09
3	-1.110 340 478 97(100)	-1.109 879 819 21(200)	101.1031	0.05	0.05
4	-1.094 539 172 82(100)	-1.094 104 267 67(200)	95.4506	0.05	0.06
5	-1.079 769 446 51(100)	-1.079 360 346 27(200)	89.7871	0.00	0.01
6	-1.066 037 235 56(100)	-1.065 654 272 60(200)	84.0507	-0.01	0.00
7	-1.053 360 761 46(100)	-1.053 004 616 18(200)	78.1649	0.06	0.07
8	-1.041 773 036 77(100)	-1.041 444 827 94(200)	72.0335	-0.01	-0.01
9	-1.031 325 382 01(200)	-1.031 026 800 71(200)	65.5310	0.02	0.03
10	-1.022 092 394 52(200)	-1.021 825 908 77(200)	58.4869	-0.03	-0.02
11	-1.014 179 060 63(200)	-1.013 948 238 40(200)	50.6596	0.01	0.02
12	-1.007 731 114 94(200)	-1.007 541 192 25(200)	41.6832	0.05	0.05
13	-1.002 950 400 07(200)	-1.002 809 397 10(200)	30.9466	0.00	0.01
14	-1.000 115 946 89(200)	-1.000 037 714 46(200)	17.1700	-0.03	-0.03

when the BO approximation is not assumed and the vibrational degrees of freedom are allowed to couple with the degrees of freedom of the electrons) are shown in the table. These energies are used to calculate the energy difference between $N = 0$ and $N = 1$ states for each v , which is the spin isomerization energy between the ortho- and para-hydrogen for that v . The transition energies are compared with the experimental values of Dabrowski [7] by showing in the table the differences between the two sets of results. As one can see, these differences oscillate around the (claimed) accuracy of the experimental data. In the table we also show the differences between the experimental transition energies and the energies obtained by Komasa *et al.* [9] using the conventional approach, where, at the zeroth order, the BO approximation is assumed and a potential energy curve (PEC) is generated. Subsequently this PEC is corrected for adiabatic and nonadiabatic effects and used to calculate the rovibrational energy levels by solving the Schrödinger equation for the nuclear motion. Interestingly, the two sets of differences are very similar; when the deviation between the experimental result and our calculated result is larger, it is also larger between the experimental and the Komasa *et al.* result (and nearly the same). This agreement brings additional credence to our approach.

VI. CONCLUSION

A direct variational method for calculating rovibrational states of diatomic molecules corresponding to the total rotational quantum number equal to 1 ($N = 1$) has been developed and implemented. The method employs explicitly correlated all-particle Gaussian functions for expanding the wave function of the system. The nonlinear parameters of the Gaussians are variationally optimized with an approach employing an analytical energy gradient determined with respect to these parameters. The method is tested in calculations of the ortho-para spin isomerization energies of the hydrogen molecule in its all-bound vibrational states. The results agree with the experimental data and with a previous calculation obtained with the conventional approach based in the zeroth order on the BO approximation.

ACKNOWLEDGMENTS

K.L.S. was supported in part by the National Science Foundation through the graduate research fellowship program (GRFP), Grant No. DGE1-1143953. We are grateful to the University of Arizona Center of Computing and Information Technology for the use of their computer resources.

-
- [1] D. B. Kinghorn and L. Adamowicz, *Phys. Rev. Lett.* **83**, 2541 (1999).
 - [2] D. B. Kinghorn and L. Adamowicz, *J. Chem. Phys.* **110**, 7166 (1999).
 - [3] S. Bubin, M. Stanke, and L. Adamowicz, *Chem. Phys. Lett.* **500**, 229 (2010).
 - [4] S. Bubin, F. Leonarski, M. Stanke, and L. Adamowicz, *Chem. Phys. Lett.* **477**, 12 (2009).
 - [5] S. Bubin, M. Stanke, and L. Adamowicz, *J. Chem. Phys.* **131**, 044128 (2009).
 - [6] K. L. Sharkey, N. Kirnosov, and L. Adamowicz (unpublished).
 - [7] I. Dabrowski, *Can. J. Phys.* **62**, 1639 (1984).
 - [8] E. J. Salumbides, G. D. Dickenson, T. I. Ivanov, and W. Ubachs, *Phys. Rev. Lett.* **107**, 043005 (2011).
 - [9] J. Komasa, K. Piszczałowski, G. Lach, M. Przybytek, B. Jeziorski, and K. Pachucki, *J. Chem. Theor. Comput.* **7**, 3105 (2011).

APPENDIX L

Direct non-Born-Oppenheimer variational calculations of all bound vibrational states corresponding to the first rotational excitation of D₂ performed with explicitly correlated all-particle Gaussian functions

Direct non-Born-Oppenheimer variational calculations of all bound vibrational states corresponding to the first rotational excitation of D₂ performed with explicitly correlated all-particle Gaussian functions

Keeper L. Sharkey,¹ Nikita Kirnosov,² and Ludwik Adamowicz^{1,2,a)}

¹Department of Chemistry and Biochemistry, University of Arizona, Tucson, Arizona 85721, USA

²Department of Physics, University of Arizona, Tucson, Arizona 85721, USA

(Received 24 October 2014; accepted 20 April 2015; published online 5 May 2015)

Direct variational calculations where the Born-Oppenheimer approximation is not assumed are done for all rovibrational states of the D₂ molecule corresponding to first excited rotational level (the $N = 1$ states). All-particle explicitly correlated Gaussian basis functions are used in the calculations. The exponential parameters of the Gaussians are optimized with the aid of analytically calculated energy gradient determined with respect to these parameters. The results allow to determine the *ortho-para* spin isomerization energies as a function of the vibrational quantum number. © 2015 AIP Publishing LLC. [<http://dx.doi.org/10.1063/1.4919417>]

I. INTRODUCTION

The interest in high-accuracy calculations of the rovibrational spectra of small molecular systems has been present in the quantum chemistry research from its very early stages. In recent years, examples of such calculations include calculations performed with artificial-channels method of Balint-Kurti *et al.*¹ and Moss,² the Lagrange-mesh method of Pilon and Baye,³ and various other methods specifically designed to study three-particle systems^{4–6} where the Born-Oppenheimer (BO) approximation was not assumed, as well as methods based on the BO potential energy curve (PEC) (surface) augmented with adiabatic, non-adiabatic, relativistic, and radiative corrections.^{7,8}

Direct variational calculations of bound states of molecular systems with an arbitrary number of nuclei and an arbitrary number of electrons without assuming the BO approximations have also been a focus of our works for over two decades.^{9,10} More than decade ago, we introduced a non-BO method for calculating pure (rotationless) vibrational states of diatomic molecules in Σ states.¹¹ Recently, we implemented a non-BO method for calculating bound rovibrational states of diatomics where the rotational motion is excited to the first excited level and the vibrational excitation span all possible vibrational quantum numbers ($N = 1, v = 1, 2, \dots$).¹² The method has been applied to study charge asymmetry in the ($N = 1, v = 1, 2, \dots$) states of the HD⁺ ion and in the HD molecule.^{13,14}

The approach we use in the non-BO molecular calculations employs explicitly correlated all-particle Gaussian basis functions (ECGs) for expanding the wave function of the system. In the variational optimization of the non-linear exponential parameters of these functions, we have used the analytical energy gradient determined with respect to these parameters by direct differentiation of the energy expression. The use of the gradient is key in obtaining very accurate results in the

calculations. Also, the use of the gradient allows for extending the basis set of ECGs in the calculations to the size exceeding 10 000 functions. In this work, we apply the $N = 1$ method to study the *ortho-para* isomerization of the D₂ molecule. The isomerization energy is determined as a function of the vibrational quantum number.

It is important to stress that the approach we use is not limited to any particular number of electrons in the molecule. Only practical limits related to the computational resources restrict the size of the molecules which can be calculated. Also, the method is direct and does not involve separation of the Schrödinger equation of the molecule into the electronic equation solved for different configurations of the stationary nuclei and the equation describing the motion of the nuclei, from which the rovibrational levels are obtained, as it is done in the conventional approach. Furthermore, not assuming the BO approximation means that the adiabatic and nonadiabatic coupling of the electronic motion and the nuclear motion (vibrational and rotational) is directly included in the calculations and does not need to be accounted for using the perturbation theory as it is done in the conventional approach.

The quantities we determine in this work are the *ortho-para* spin isomerization energies for all D₂ bound vibrational states. The increase of the average internuclear distance with the vibrational excitation and weakening of the inter-molecular bonding affects the rotational motion of the molecule. The present approach describes these effects directly and precisely without any approximations concerning the separability of the motions of the electrons and the nuclei.

II. METHOD

Not assuming the BO approximation means treating all particles forming the system on equal footing with rigorous accounting for their given masses, M_i , and the electrostatic interactions between their charges, Q_i . Without invoking any approximations, the total laboratory-frame Hamiltonian of the

^{a)}Author to whom correspondence should be addressed. Electronic mail: ludwik@u.arizona.edu

system can be separated into an operator representing the motion of the center of mass and an operator representing the internal energy of the system. This separation can be performed by making a transformation from the laboratory Cartesian coordinates, \mathbf{R}_i , $i = 1, \dots, n + 1$, where $n + 1$ is the number of particles (nuclei + electrons) in the system, to the internal reference frame with the origin at a selected reference particle (particle one): $\mathbf{r}_i = \mathbf{R}_{i+1} - \mathbf{R}_1$. The transformation to the internal coordinates together with the conjugate momentum transformation yields the following nonadiabatic Hamiltonian representing the internal energy of the system:

$$\hat{H} = -\frac{1}{2} \left(\sum_{i=1}^n \frac{1}{\mu_i} \nabla_{\mathbf{r}_i}^2 + \sum_{i=1, j=1, i \neq j}^n \frac{1}{m_0} \nabla'_{\mathbf{r}_i} \nabla_{\mathbf{r}_j} \right) + \sum_{i=1}^n \frac{q_i q_i}{r_i} + \sum_{j>i=1}^n \frac{q_i q_j}{r_{ij}}, \quad (1)$$

where M_1 is the mass of particle one (the reference particle) and $\nabla_{\mathbf{r}_i}$ is the gradient with respect to the x , y , and z coordinates of \mathbf{r}_i . The charges and masses are mapped from the original particles as $\{Q_1, \dots, Q_{n+1}\} \rightarrow \{q_0, \dots, q_n\}$ and $\{M_1, \dots, M_{n+1}\} \rightarrow \{m_0, \dots, m_n\}$. In the calculations on the *para-ortho* dideuterium (D_2) presented in this work M_1 and M_2 are the deuteron masses ($M_d = 3670.482\,965\,4m_e$, where m_e is the electron mass¹⁵) and M_3 and M_4 are electron masses. The reduced masses, μ_i , are defined by $\mu_i = m_0 m_i / (m_0 + m_i)$. The potential energy is the same as in the laboratory-frame Hamiltonian but is now written using the internal distance coordinates, $r_{ij} = \|\mathbf{r}_j - \mathbf{r}_i\| = \|\mathbf{R}_{j+1} - \mathbf{R}_{i+1}\|$ and $r_j = \|\mathbf{r}_j\| = \|\mathbf{R}_{j+1} - \mathbf{R}_1\|$. For vector/matrix transposition, the symbol prime ('') is used. More information on the nonadiabatic Hamiltonian and the center of mass transformation can be found in Ref. 11.

The basis set of explicitly correlated Gaussian functions used in the calculations of the rotationless ($N = 0$) states of diatomic molecules¹¹ have the following form:

$$\phi_k(\mathbf{r}) = r_1^{m_k} \exp[-\mathbf{r}'(L_k L'_k \otimes I_3)\mathbf{r}], \quad (2)$$

where \mathbf{r} is a vector of the internal coordinates, $\mathbf{r} = \{\mathbf{r}'_1, \dots, \mathbf{r}'_n\}'$, L_k is an $n \times n$ rank n lower triangular matrix of nonlinear variational parameters, and I_3 is the 3×3 identity matrix. The Kronecker product, \otimes , with the identity ensures rotational invariance of the basis functions, thus they are eigenfunctions of the square of the total angular momentum operator with $N = 0$. By writing the exponential parameters of the Gaussians in the Cholesky factored form, $L_k L'_k$ ensures the square integrability of the Gaussians. The pre-exponential factor in (2), $r_1^{m_k}$, where r_1 is the internuclear distance, is needed to describe the very strong internuclear correlation, i.e., the effect of the nuclei staying apart from each other at a considerable distance in the molecule, and the radial nodes which appear in the wave function when the system is vibrationally excited. The m_k power of r_1 is a non-negative even number which is an additional variational parameter subject to optimization (in the application calculations performed so far, m_k has ranged from 0 to 250).

In systems with two electrons and two identical bosonic-nuclei (like D_2 ; $S_{(D)} = 1$), the total (internal) wave function is a product of the spatial function, the spin function for the elec-

trons, and the spin function for the nuclei. In the ground state of D_2 , the spin and spatial functions are symmetric with respect to the permutation of the nuclear labels. A symmetric spatial wave function can be constructed using basis function (2). The spatial functions has to be also symmetric with respect to the permutation of the electron labels, as the ground electronic state of D_2 is ${}^1\Sigma_g^+$. This is dideuterium in the (nuclear) high-spin state called *ortho*- D_2 . The permutational symmetry of the electrons and the nuclei is implemented in basis functions (2) by projecting each basis function using a symmetry-projection operator \mathcal{P} ,

$$\psi_k = \mathcal{P} \phi_k = \sum_P \chi_P r_1^{m_k} \exp[-\mathbf{r}'(\tau'_P L_k L'_k \tau_P \otimes I_3)\mathbf{r}], \quad (3)$$

where the sum runs over all permutations of the labels of identical particles and where τ_P are permutational matrices transforming the internal coordinates. There are four permutations in the sum over P on the right hand side of (3) and the corresponding τ_P matrices in the internal coordinates have the following form:

$$\begin{pmatrix} 1 & 0 & 0 \\ 0 & 1 & 0 \\ 0 & 0 & 1 \end{pmatrix}, \begin{pmatrix} -1 & 0 & 0 \\ -1 & 1 & 0 \\ -1 & 0 & 1 \end{pmatrix}, \begin{pmatrix} 1 & 0 & 0 \\ 0 & 0 & 1 \\ 0 & 1 & 0 \end{pmatrix}, \begin{pmatrix} -1 & 0 & 0 \\ -1 & 0 & 1 \\ -1 & 1 & 0 \end{pmatrix}. \quad (4)$$

The coefficients χ_P are obtained from the matrix elements of the irreducible representation of the considered state, and for the ground state of D_2 , they are all ones. Note that the $r_1^{m_k}$ factor is always symmetric with respect to permuting the deuterons. The states with the wave functions constructed this way are $N = 0$ states, i.e., the rotational ground states.

In the other form of dideuterium called *para* deuterium, the nuclear spin wave function (low spin state) and the spatial wave function are both antisymmetric with respect to permuting the labels of the nuclei. The spatial wave function is still symmetric with respect to the permutation of the electrons and the electronic spin function is antisymmetric with respect to this permutation. The spatial wave function antisymmetric with respect to the permutation of the nuclear labels of *para* dideuterium corresponds to the first excited rotational state with $N = 1$. The ECG basis functions which can describe such a state are obtained by multiplying $N = 0$ ECGs (2) by an angular factor in the form of the z coordinate of the \mathbf{r}_1 vector, z_1 ,

$$\phi_k(\mathbf{r}) = z_1 r_1^{m_k} \exp[-\mathbf{r}'(L_k L'_k \otimes I_3)\mathbf{r}]. \quad (5)$$

These functions are eigenfunctions of the square of the total angular momentum operator with $N = 1$ and eigenfunctions of the operator representing the z -axis projection of the total angular momentum. In general, $N = 1$ basis functions can also be obtained by replacing the z_1 multiplier by any of the z_i , $i = 2, \dots, n$ multipliers. Such functions represent promoting the electrons to π excited states, but de-exciting the rotational motion of the nuclei to the ground rotational state. However, these kinds of states are significantly higher in energy than the rotational excitations of the nuclei (particularly for heavier nuclei as deuterons) and they are likely to provide only a small contribution to the energy. It is

however difficult to predict how small. Also, as Gaussians (5) are not orthogonal to the Gaussians which explicitly include the z_i , $i = 2, \dots, n$ pre-exponential multipliers, i.e., Gaussians: $z_i r_1^{m_k} \exp[-\mathbf{r}'(L_k L'_k \otimes I_3)\mathbf{r}]$, $i = 2, \dots, n$, they effectively include a contribution from these latter functions. Therefore, if the contributions of the $z_i r_1^{m_k} \exp[-\mathbf{r}'(L_k L'_k \otimes I_3)\mathbf{r}]$, $i = 2, \dots, n$, basis functions are small, as they expect to be for the vibrational states of the D₂ molecule excited to the first excited rotational level, these contributions should be to some degree accounted for by only including the $z_1 r_1^{m_k} \exp[-\mathbf{r}'(L_k L'_k \otimes I_3)\mathbf{r}]$ Gaussians in the basis set. Work is currently in progress in our lab on the implementation of the $z_i r_1^{m_k} \exp[-\mathbf{r}'(L_k L'_k \otimes I_3)\mathbf{r}]$, $i = 2, \dots, n$, Gaussians. This implementation will allow us to determine the magnitude of these contributions for different vibrational excitations and for different H₂ isotopologues. It will also allow us to test the importance of the coupling between nuclear and electronic angular excitations in the $N = 1$ states.

The $z_1 = Z_2 - Z_1$ factor in (5) is antisymmetric with respect to the permutation of the nuclei. Thus, if the remaining part of the basis function is made symmetric with respect to this permutation, the whole basis function will be antisymmetric. The symmetric character of the exponential part of (5) is invoked by operating on this part with the same projection operator, \mathcal{P} , as applied to the $r_1^{m_k} \exp[-\mathbf{r}'(L_k L'_k \otimes I_3)\mathbf{r}]$ part of (5) as used for $N = 0$ basis functions (2). Thus, in the calculations of states of the *ortho* dideuterium in the present work, ECGs (2) are used and in the calculations of states of *para* dideuterium, ECGs (5) are used.

The situation would be somewhat different if the z_1 angular factor is replaced with the general z_i factors in ECGs (5). Making such functions antisymmetric with respect to the permutation of the nuclear labels (1 and 2) leads to the following transformation of the angular factor: $z_i = Z_{i+1} - Z_1 \rightarrow (Z_{i+1} - Z_2) = (Z_{(i+1)} - Z_1) - (Z_2 - Z_1) = z_i - z_1$. Thus, after the 1-2 permutation, two ECGs are generated, the first one with the z_i factor and the second one with the z_1 factor. As both ECGs belong to generalized (5) basis set with the general z_i factors, the nuclear permutational symmetry can be easily implemented.

Since the total internal molecular wave function, Ψ , is dependent on the spatial coordinates, \mathbf{r} , and the spin coordinates of the particles, and because internal Hamiltonian (1) is spin independent, the calculation of the Hamiltonian and overlap matrix elements can be carried out by first integrating over spin variables, which leaves behind only spatially dependent integrals. The spatial wave function for each state, $\Psi(\mathbf{r})$, is approximated by a linear combination of K properly symmetrized basis functions, $\psi_k(\mathbf{r})$,

$$\Psi(\mathbf{r}) = \sum_{k=1}^K c_k \psi_k(\mathbf{r}), \quad (6)$$

where c_k is the linear variational parameter.

To solve the Schrödinger equation with the internal Hamiltonian (1), the Rayleigh-Ritz variational scheme is used. It involves the minimization of the Rayleigh quotient,

$$\epsilon(a, c) = \min_{(a, c)} \frac{\mathbf{c}' \mathbf{H}(a) \mathbf{c}}{\mathbf{c}' \mathbf{S}(a) \mathbf{c}}, \quad (7)$$

where $\mathbf{H}(a)$ and $\mathbf{S}(a)$ are the Hamiltonian and overlap $K \times K$ matrices, respectively. $\mathbf{H}(a)$ and $\mathbf{S}(a)$ are functions of the nonlinear parameters contained in the basis functions, i.e., the L_k matrix elements and m_k powers of r_1 . We write a for the set of these parameters and \mathbf{c} for the vector of the linear expansion coefficients of the wave function in terms of basis functions. The expressions for the overlap and Hamiltonian matrix elements with basis functions (5) were presented in the recent paper.¹⁶ Also, as mentioned, the variational energy minimization performed in this work involves the use of the energy gradient determined with respect to the L_k matrix elements. The gradient is determined by starting with the differential form of the secular equation, $(\mathbf{H} - \epsilon \mathbf{S})\mathbf{c} = 0$,

$$d(\mathbf{H} - \epsilon \mathbf{S})\mathbf{c} = (d\mathbf{H})\mathbf{c} - (d\epsilon)\mathbf{S}\mathbf{c} - \epsilon(d\mathbf{S})\mathbf{c} + (\mathbf{H} - \epsilon \mathbf{S})d\mathbf{c}. \quad (8)$$

Multiplying this equation by \mathbf{c}' from the left, we obtain

$$d\epsilon = \mathbf{c}'(d\mathbf{H} - \epsilon d\mathbf{S})\mathbf{c}. \quad (9)$$

To get (9), it is assumed that the secular equation is satisfied for \mathbf{c} and the wave function is normalized, i.e., $\mathbf{c}'\mathbf{S}\mathbf{c} = 1$. $d\mathbf{H}$ and $d\mathbf{S}$ in the expression for $d\epsilon$ are the first derivatives of the Hamiltonian and overlap matrix elements with respect to the Gaussian nonlinear parameters. The formulas for these derivatives were presented in Refs. 12 and 16.

In the previous paper,¹⁷ we reported very accurate direct non-BO calculations for the $v = 0, \dots, 21$, $N = 0$ states (i.e., pure vibrational states) of the D₂ molecule (*ortho* D₂). The calculations were performed for each state separately using basis set (2) of 10 000 ECGs. The exponential parameters of the Gaussians were optimized with the gradient-based method.

The *para*-*ortho* isomerization was recently studied using the approach employed in the present calculations for H₂.¹⁸ The results agreed with the experimental results with the accuracy of the experimental data. The approach for non-BO calculations of $N = 0$ and $N = 1$ states was also recently used to calculate energies and lifetimes of rovibrational states of the HD⁺ ion.¹⁶ The point tested in those calculations was how to generate good basis sets for the $N = 1$ states given very well converged and complete ECG basis sets for the $N = 0$ states. The procedure that has emerged from the testing as effective and leading to very accurate results involves taking the ECG basis sets generated for the $N = 0$ states and after addition of the z_1 factor using them as the initial starting basis sets in the calculations of the $N = 1$ states. To increase the accuracy of the calculations, the L_k matrix elements for all ECGs in each basis set are first reoptimized (without changing the m_k powers in the pre-exponential $r_1^{m_k}$ factors). The reoptimization involves taking one function at a time and reoptimizing its non-linear parameters with gradient-based method. This step is performed for all ECGs in the basis set and repeated by cycling several times over the whole set. Next, additional 1000 ECGs are added to each basis set (2000 ECGs are added to the basis set of the highest $v = 21$). The addition process involves addition of one ECG at a time and the optimization of its non-linear parameters (including the m_k power). The initial guess for a new added function is generated by randomly perturbing parameters of some most contributing ECGs already included in the basis and choosing the best one from this subset. After

TABLE I. The convergence of the total nonrelativistic non-BO energies of the $N = 1, v = 1, \dots, 21$ rovibrational states of D_2 with the number of basis functions. The $N = 0, v = 1, \dots, 21$ rovibrational states taken from Ref. 17 are also shown. All values are given in a.u. (hartrees).

	No.		No.		No.		No.					
	v	ECGs		v	ECGs		v	ECGs		v	ECGs	
$N = 0$	0	10 000	-1.167 168 809 21	1	10 000	-1.153 528 895 91	2	10 000	-1.140 431 695 37	3	10 000	-1.127 867 676 22
$N = 1$	0	10 000	-1.166 896 424 06	1	10 000	-1.153 266 124 64	2	10 000	-1.140 178 370 16	3	10 000	-1.127 623 661 28
		11 000	-1.166 896 424 10		11 000	-1.153 266 124 80		11 000	-1.140 178 370 53		11 000	-1.127 623 661 81
$N = 0$	4	10 000	-1.115 829 305 19	5	10 000	-1.104 311 147 12	6	10 000	-1.093 310 001 43	7	10 000	-1.082 825 088 02
$N = 1$	4	10 000	-1.115 594 498 55	5	10 000	-1.104 085 483 07	6	10 000	-1.093 093 453 90	7	10 000	-1.082 617 675 30
		11 000	-1.115 594 499 30		11 000	-1.104 085 483 97		11 000	-1.093 093 455 08		11 000	-1.082 617 676 60
$N = 0$	8	10 000	-1.072 858 285 95	9	10 000	-1.063 414 434 81	10	10 000	-1.054 501 734 16	11	10 000	-1.046 132 242 97
$N = 1$	8	10 000	-1.072 660 075 01	9	10 000	-1.063 225 551 00	10	10 000	-1.054 322 367 89	11	10 000	-1.045 962 664 51
		11 000	-1.072 660 076 41		11 000	-1.063 225 552 63		11 000	-1.054 322 371 09		11 000	-1.045 962 667 33
$N = 0$	12	10 000	-1.038 322 491 81	13	10 000	-1.031 094 267 83	14	10 000	-1.024 475 850 67	15	10 000	-1.018 502 907 07
$N = 1$	12	10 000	-1.038 163 065 09	13	10 000	-1.030 945 469 33	14	10 000	-1.024 338 313 20	15	10 000	-1.018 377 436 46
		11 000	-1.038 163 070 03		11 000	-1.030 945 492 32		11 000	-1.024 338 317 98		11 000	-1.018 377 449 86
$N = 0$	16	10 000	-1.013 220 707 84	17	10 000	-1.008 686 112 56	18	10 000	-1.004 970 759 27	19	10 000	-1.002 164 981 42
$N = 1$	16	10 000	-1.013 108 360 77	17	10 000	-1.008 588 277 23	18	10 000	-1.004 889 024 86	19	10 000	-1.002 102 535 09
		11 000	-1.013 108 370 25		11 000	-1.008 588 286 28		11 000	-1.004 889 278 06		11 000	-1.002 102 550 99
											12 000	-1.002 102 558 28
$N = 0$	20	10 000	-1.000 381 789 95	21	10 000	-0.999 735 148 48	D + D		-0.999 727 630 49			
$N = 1$	20	10 000	-1.000 342 422 89	21	10 000	^a						
		11 000	-1.000 342 434 60		11 000	-0.999 727 754 04						
		12 000	-1.000 342 446 00		12 000	-0.999 727 845 47						

^aReoptimization of the 10 000 ECG basis set did not give an energy lower than the dissociation limit. To get an energy below this limit the basis set had to be increased to 10 700 functions.

addition of each 100 ECGs, the cyclic optimization of all basis functions already included in the basis set is performed.

III. RESULTS

In this work, the focus of the calculations is the $v = 0, \dots, 21, N = 1$ of D_2 (*para* D_2). The results of the calculation allow for determining the dissociation energies corresponding to the considered states and the *ortho-para* isomerization energy for each vibrational level.

The energies of the $N = 1, v = 0, \dots, 21$ states obtained in the calculations with 10 000 and 11 000 ECGs (also with 12 000 ECGs for the $v = 21$ state) are presented in Table I. The energies obtained in the previous calculations¹⁷ are also shown. The use of the vibrational quantum number v is approximate, as this is not, strictly speaking, a “good” quantum number in nonrelativistic non-BO calculations because the vibrational motion of the nuclei couples with the electronic motion. Only the quantum number N associated with the square of the total angular momentum is a good quantum number.

The total $N = 0$ and $N = 1$ energies from Table I are used to calculate the energy difference between $N = 0$ and $N = 1$ states for each v , which is the spin isomerization energy between the *ortho* and *para* deuterium for that v . The total energies for the $N = 1$ are also used to calculate the dissociation energies. Both the isomerization and dissociation energies are shown in Table II. The dissociation energies are compared with the energies obtained from the results of Komasa *et al.*²⁰ by only including the BO contributions and the adiabatic and non-adiabatic corrections (taken from the supplementary materials

included in the paper by Komasa *et al.*²⁰). As one notices, our result deviate somewhat from the results of Komasa *et al.* and the difference increases with the vibrational excitation till the excitation reaches the $v = 18$ state after which the difference decreases. The difference is equal to 0.0017 cm^{-1} for the ground vibrational state and increases to 0.0195 cm^{-1} for the $v = 18$ state. Clearly, the approach used by Komasa *et al.*, which employs the Born-Oppenheimer potential energy curves augmented with the adiabatic and non-adiabatic corrections obtained from finite-order perturbation-theory calculations, is very different from our direct non-BO variational approach, where the corrections are included to infinite order. So, this can be a reason for the two sets of the dissociation energies to differ. The second reason is related to the convergence of each set of the results with the number of basis functions used in the calculations. In the case of the calculations of Komasa *et al.*, those are the basis functions used in calculating the PEC and in the present case are the ECG basis functions used in expanding the non-BO wave functions of the considered states. The third reason is neglecting in our calculations for the $N = 1$ states basis functions representing angular excitations of the electrons. This last reason is likely to be the main source of the discrepancy between the two sets of results.

In Table II, we also show the difference between the isomerization energies obtained in this work and the energies derived from the experimental data.¹⁹ Except for the highest $v = 21$ state, the present results and the experimental results agree within the estimated accuracy of the experiment. For the $v = 21$ state, the calculated result of 1.6028 cm^{-1} is lower by 0.37 cm^{-1} than the experimental value of 1.97 cm^{-1} . In the last column in Table II, we show the difference between the

TABLE II. Comparison of the dissociation energies for the ($v, 1$) states of D₂ obtained in the present calculations ($E_{diss}^{present} = E(v, 1) - 2 E_D$) and the dissociation energies determined using the result from Ref. 20 that include the BO energies and the adiabatic and non-adiabatic corrections (in parenthesis, the difference between the two sets of results is shown). The *ortho-para* isomerization energies ($\Delta = E(v, 1) - E(v, 0)$), the differences between the experimental isomerization energies¹⁹ and the present results ($\Delta_{exp} - \Delta$), and the corresponding differences between the experimental energies and the energies derived from the calculated results of Komasa *et al.*²⁰ are also shown. The results of Komasa *et al.*²⁰ were obtained using the conventional approach involving solving the nuclear rovibrational problem with the potential obtained from the electronic calculations. All values are in cm⁻¹.

v	$E_{diss}^{present}$	E_{diss}^{20}	Δ	$\Delta_{exp} - \Delta$	$\Delta_{exp} - \Delta^{20}$
0	36 689.3094	36 689.3111 (0.0017)	59.7816	0.01 -0.000 32(95) ^a -0.001 12(95) ^b	0.01 -0.001 30(95) ^a -0.000 68(95) ^b
1	33 697.8044	33 697.8063 (0.0019)	57.6716	0.01	0.01
2	30 825.3744	30 825.3763 (0.0019)	55.5984	-0.05	-0.05
3	28 069.9343	28 069.9365 (0.0022)	53.5550	-0.02	-0.02
4	25 429.8383	25 429.8407 (0.0024)	51.5339	-0.02	-0.02
5	22 903.9014	22 903.9039 (0.0025)	49.5273	-0.01	-0.01
6	20 491.4299	20 491.4327 (0.0028)	47.5264	-0.06	-0.05
7	18 192.2623	18 192.2653 (0.0030)	45.5215	-0.01	-0.01
8	16 006.8217	16 006.8247 (0.0030)	43.5020	-0.01	-0.01
9	13 936.1831	13 936.1867 (0.0036)	41.4548	0.08	0.08
10	11 982.1606	11 982.1649 (0.0043)	39.3656	-0.01	0.00
11	10 147.4177	10 147.4225 (0.0048)	37.2176	-0.02	-0.02
12	8 435.6039	8 435.6095 (0.0056)	34.9890	-0.01	-0.01
13	6 851.5287	6 851.5421 (0.0134)	32.6524	-0.03	-0.03
14	5 401.4216	5 401.4302 (0.0086)	30.1849	0.02	0.02
15	4 093.1622	4 093.1726 (0.0104)	27.5347	0.03	0.02
16	2 936.7329	2 936.7430 (0.0101)	24.6552	-0.03	-0.03
17	1 944.6892	1 944.7001 (0.0109)	21.4704	-0.03	-0.03
18	1 132.8507	1 132.8702 (0.0195)	17.8831	-0.02	-0.02
19	521.2364	521.2459 (0.0095)	13.7003	-0.01	-0.01
20	134.9364	134.9426 (0.0062)	8.6350	0.00	-0.01
21 ^c	0.0472	0.0542 (0.0070)	1.6028	0.37	0.35

^aThis difference is calculated with respect to the experimental result of Liu *et al.*²¹ The calculated *ortho-para* isomerization energy of Komasa *et al.* only includes the BO contributions and the contributions from the adiabatic and non-adiabatic corrections.

^bAlso determined with respect to the experimental result of Liu *et al.*,²¹ but the calculated values (both ours and Komasa's *et al.*) include the contributions from the relativistic and QED corrections taken from Komasa *et al.*²⁰

^cIn the calculation of the dissociation energy and the *ortho-para* isomerization energy for the $v = 21$ state using the results from Ref. 20, it is assumed that the BO energy for that state is equal to twice the energy of the D atom, as this state is unbound at the BO level.

experimental isomerization energies and the energies derived from the calculated energies of Komasa *et al.*²⁰ In their calculations they used the conventional approach, where at the zeroth order, the BO approximation was assumed and the PEC was generated. Next, the PEC was corrected for the adiabatic and non-adiabatic effects, as well as relativistic and QED effects, and used to calculate the rovibrational energy levels by solving the Schrödinger equation for the nuclear motion. Even though Komasa *et al.* calculated the vibrational energies with the inclusion of the adiabatic, nonadiabatic, relativistic, and QED corrections, in the present comparison, we use their energies which only include the adiabatic and nonadiabatic corrections (taken from supplementary materials from their paper), as these effects are the only two of the above-mentioned four corrections accounted for in the present calculations. The two sets of differences shown in the last two columns of Table II are almost identical indicating that the present direct non-BO approach and the conventional approach yield, as they should, very similar results. Interestingly, the BO calculations of Komasa *et al.* did not produce an energy for the top $N = 1$, $v = 21$ state, which the present calculations estimate to be

0.0472 cm⁻¹ below the dissociation limit. Only after the addition of the adiabatic corrections, this state became bound in their calculations. The two sets of results shown in the last two columns of Table II differ by less than 0.003 cm⁻¹ (except the next to the last level where the difference is 0.004 cm⁻¹). The difference of 0.003 cm⁻¹ is similar to the estimated uncertainty of the present calculations.

The more accurate recent experimental results of Liu *et al.*²¹ for the $N = 0$ and $N = 1$, $v = 0$ states of D₂ allow for making a more detail comparison of the *ortho-para* isomerization energy for that vibrational state. The comparison is shown in Table II. The estimated uncertainty of the experimental value is 0.000 95 cm⁻¹. While our energy differs from the experimental value by -0.000 32 cm⁻¹, the difference for the Komasa *et al.* result (without the relativistic and QED corrections) is -0.001 30 cm⁻¹. Including the relativistic and QED corrections taken from the calculations of Komasa *et al.* in both results raises the difference for our result to -0.001 12 cm⁻¹, but reduces the difference for the their result to -0.000 68 cm⁻¹. All differences are close to the uncertainty of the experiment.

TABLE III. Expectation values of the deuteron-deuteron, deuteron-electron, electron-electron distances, and expectation values of the squares of these distances calculated for the $(v, 1)$ states of D_2 . All values are in a.u.

v	$\langle r_{dd} \rangle$	$\langle r_{de} \rangle$	$\langle r_{ee} \rangle$	$\langle r_{dd}^2 \rangle$	$\langle r_{de}^2 \rangle$	$\langle r_{ee}^2 \rangle$
0	1.4356	1.5678	2.1926	2.0808	3.1155	5.7580
1	1.5032	1.6034	2.2375	2.3196	3.2678	6.0012
2	1.5727	1.6400	2.2842	2.5752	3.4280	6.2593
3	1.6444	1.6775	2.3332	2.8494	3.5970	6.5343
4	1.7185	1.7161	2.3847	3.1445	3.7759	6.8292
5	1.7954	1.7561	2.4391	3.4630	3.9661	7.1472
6	1.8757	1.7976	2.4971	3.8083	4.1694	7.4926
7	1.9598	1.8410	2.5592	4.1845	4.3879	7.8703
8	2.0486	1.8865	2.6262	4.5969	4.6243	8.2870
9	2.1429	1.9347	2.6993	5.0524	4.8824	8.7513
10	2.2440	1.9860	2.7797	5.5602	5.1670	9.2743
11	2.3535	2.0415	2.8691	6.1327	5.4844	9.8710
12	2.4737	2.1020	2.9700	6.7871	5.8439	10.5616
13	2.6076	2.1691	3.0855	7.5481	6.2583	11.3750
14	2.7596	2.2449	3.2202	8.4524	6.7466	12.3528
15	2.9364	2.3328	3.3808	9.5570	7.3384	13.5588
16	3.1486	2.4377	3.5776	10.9562	8.0821	15.0959
17	3.4140	2.5685	3.8284	12.8192	9.0643	17.1452
18	3.7668	2.7416	4.1660	15.4887	10.4592	20.0660
19	4.2845	2.9948	4.6651	19.8126	12.6946	24.7294
20	5.2223	3.4527	5.5699	28.9375	17.3502	34.3168
21	12.9601	7.2753	13.1397	199.0823	102.5360	205.0505

Finally in Table III, we show expectation values of the deuteron-deuteron (r_{dd}), deuteron-electron (r_{de}), and electron-electron (r_{ee}) distances and their squares calculated using the non-BO $N = 1$ wave functions expanded in terms of 11 000 ECGs. The results show expected increasing trends. The results can be used to benchmark calculations performed with conventional BO-approximation-based method. Of particular interest is the expectation values of the last bound vibrational state ($N = 1, v = 21$). As indicated in Table I, this state is still not bound when the number of ECGs used is 10 000. Only after increasing the basis size to 10 700 basis functions, its energy dropped below the energy of two separate deuterium atoms. As mentioned, its bonding energy obtained with 12 000 ECGs is only 0.0472 cm^{-1} . This is consistent with expectation values of the interparticle distances calculated for this state. The average r_{dd} and r_{ee} distances are about 2.5 longer than the results obtained for the next highest state.

IV. SUMMARY

Direct variational non-BO calculations are performed for all bound $N = 1$ states of the D_2 molecule using large sets of explicitly correlated Gaussian functions. Each state is calculated separately and for each state, the ECG basis set is extensively optimized in terms of the Gaussian non-linear parameters using a energy-minimization method which employs the analytical energy gradient determined with respect to these parameters. The calculated energies of the $N = 1, v = 0, \dots, 21$ states and the energies of the $N = 0, v = 0, \dots, 21$ states calculated before are used to determine the *ortho-para* isomerization energy for each vibrational state. These isomerization energies show, as expected, a decreasing trend with

increasing value of v . The results agree with the previous calculations performed with the conventional approach based in the zeroth-order on the BO approximation.

Future work will involve including ECGs with z_1 replaced by z_i in the $N = 1$ basis set. This will allow for determining the degree of the angular-momentum coupling between the nuclear and electronic rotational excitations. Also, work is in progress on the development of algorithms for calculating $N = 2$ and $N = 3$ rovibrationally excited states of diatomic systems.

ACKNOWLEDGMENTS

This work has been supported in part by the National Science Foundation through the graduate research fellowship program (GRFP) awarded to Keeper L. Sharkey, Grant No. DGE1-1143953. We are grateful to the University of Arizona Center of Computing and Information Technology for the use of their computer resources.

- ¹G. G. Balint-Kurti, R. E. Moss, I. A. Sadler, and M. Shapiro, *Phys. Rev. A* **41**, 4913 (1990).
- ²R. E. Moss, *Mol. Phys.* **78**, 371 (1993).
- ³H. O. Pilon and D. Baye, *Phys. Rev. A* **88**, 032502 (2013).
- ⁴J.-P. Karr and L. Hilico, *J. Phys. B: At., Mol. Opt. Phys.* **39**, 2095 (2006).
- ⁵Q. L. Tian, L. Y. Tang, Z. X. Zhong, Z. C. Yan, and T. Y. Shi, *J. Chem. Phys.* **137**, 024311 (2012).
- ⁶V. I. Korobov, *Phys. Rev. A* **74**, 052506 (2006).
- ⁷L. Wolniewicz, *J. Chem. Phys.* **78**, 6173 (1983).
- ⁸L. Wolniewicz and T. Orlikowski, *Mol. Phys.* **74**, 103 (1991).
- ⁹S. Bubin, M. Pavanello, W.-C. Tung, K. L. Sharkey, and L. Adamowicz, *Chem. Rev.* **113**, 36 (2013).
- ¹⁰J. Mitroy, S. Bubin, W. Horiuchi, Y. Suzuki, L. Adamowicz, W. Cencek, K. Szalewicz, J. Komasa, D. Blume, and K. Varga, *Rev. Mod. Phys.* **85**, 693 (2013).
- ¹¹D. B. Kinghorn and L. Adamowicz, *Phys. Rev. Lett.* **83**, 2541 (1999).

¹²K. L. Sharkey, N. Kirnosov, and L. Adamowicz, *J. Chem. Phys.* **139**, 164119 (2013).

¹³N. Kirnosov, K. L. Sharkey, and L. Adamowicz, “Charge asymmetry in rovibrationally excited HD⁺ determined using explicitly correlated all-particle Gaussian functions,” *J. Chem. Phys.* **139**, 204105 (2013).

¹⁴N. Kirnosov, K. L. Sharkey, and L. Adamowicz, “Charge asymmetry in the rovibrationally excited HD molecule,” *J. Chem. Phys.* **140**, 104115 (2014).

¹⁵See CODATA 2002 recommended values and NIST Physical Reference Data at <http://physics.nist.gov/>.

¹⁶K. L. Sharkey, N. Kirnosov, and L. Adamowicz, *Phys. Rev. A* **88**, 032513 (2013).

¹⁷S. Bubin, M. Stanke, and L. Adamowicz, *J. Chem. Phys.* **135**, 074110 (2011).

¹⁸K. L. Sharkey, N. Kirnosov, and L. Adamowicz, *Phys. Rev. A* **88**, 032513 (2013).

¹⁹H. Bredohl and G. Herzberg, *Can. J. Phys.* **51**, 867 (1973).

²⁰J. Komasa, K. Piszczałowski, G. Lach, M. Przybytek, B. Jeziorski, and K. Pachucki, *J. Chem. Theory Comput.* **7**, 3105 (2011).

²¹J. Liu, D. Sprecher, C. Junge, W. Ubachs, and F. Merkt, *J. Chem. Phys.* **132**, 154301 (2010).

APPENDIX M

Orthopara nuclear-spin isomerization energies for all bound vibrational states of
ditritium (T_2) from non-BornOppenheimer variational calculations performed with
explicitly correlated all-particle Gaussian functions



Ortho–para nuclear-spin isomerization energies for all bound vibrational states of ditritium (T_2) from non-Born–Oppenheimer variational calculations performed with explicitly correlated all-particle Gaussian functions



Nikita Kirnosov^a, Keeper L. Sharkey^b, Ludwik Adamowicz^{b,a,*}

^a Department of Physics, University of Arizona, Tucson, AZ 85721, USA

^b Department of Chemistry and Biochemistry, University of Arizona, Tucson, AZ 85721, USA

ARTICLE INFO

Article history:

Received 3 August 2015

In final form 8 October 2015

ABSTRACT

Direct variational calculations, where the Born–Oppenheimer (BO) approximation is not assumed, are performed for all 26 bound rovibrational states corresponding to the lowest rotational excitation (i.e. the $N=1$ states) of the tritium molecule (T_2). The non-BO energies are used to determine the ortho–para isomerization energies. All-particle explicitly correlated Gaussian basis functions are employed in the calculations and over 11 000 Gaussians independently generated for each state are used. The exponential parameters of the Gaussians are optimized with the aid of analytically calculated energy gradient determined with respect to these parameters. The non-BO wave functions are used to calculate expectation values of the inter-particle distances and the triton–triton correlation functions.

© 2015 Elsevier B.V. All rights reserved.

1. Introduction

As triton has a spin of one half, the tritium molecule, like the hydrogen molecule, can appear in isomeric forms corresponding to the parallel (ortho) and antiparallel (para) orientations of the nuclear spins. The para tritium has the total nuclear spin of zero (singlet state) and it is the lower energy species of the two isomers. The ortho tritium has the total nuclear spin of one (triplet state), and in the room temperature, similarly to hydrogen, should constitute 75% of the tritium gas because of its three-fold degeneracy in opposite to the para tritium whose singlet nuclear state is not degenerate. The isotopologues of hydrogen involving tritium have been of interest for more than three decades mainly because of their importance in fusion research. There have been surprisingly few experimental studies of the rovibrational spectrum of T_2 . Souers and coworkers measured the infrared spectra of the tritium isotopologues of hydrogen in both liquid and solid states [1,2]. Also, the Raman spectrum of T_2 was recorded by Edwards et al. [3].

The interest in high-accuracy calculations of the rovibrational spectra of small molecular systems has been present in the

quantum chemistry research from the very beginning. In recent years such calculations have involved the artificial-channels method of Balint-Kurti et al. [4] and Moss [5], the Lagrange-mesh method of Pilon and Baye [6], and various other methods specifically designed to study three-particle systems [7–9]. In some of these methods the Born–Oppenheimer (BO) approximation was not assumed from the start. Other methods assumed the BO approximation and employed the electronic BO potential energy surface augmented with adiabatic, non-adiabatic, relativistic, and radiative corrections as the potential in the Schrödinger equation representing the motion of the nuclei, which is solved to determine the rovibrational energies [10,11].

Direct variational calculations of bound states of atomic and molecular systems with an arbitrary number of nuclei and an arbitrary number of electrons without assuming the Born–Oppenheimer (BO) approximations have also been a focus of our works for over two decades [12–14]. Recently we have developed a method to perform non-BO calculations for rotationally excited diatomic molecules with an arbitrary number of σ electrons [15]. The method was applied to study charge asymmetry in all bound vibrational levels of the HD^+ ion and the HD molecule [16,17]. In the present study the method is used to determine the ortho–para isomerization energies for all bound vibrational states of T_2 . The isomerization energies are calculated using the total non-BO energies of the vibrational states obtained for the ground and

* Corresponding author at: Department of Chemistry and Biochemistry, University of Arizona, Tucson, AZ 85721, USA.

E-mail address: ludwik@u.arizona.edu (L. Adamowicz).

first-excited rotational states of the system. The total energies of the states are also used to calculate the energies of the corresponding rovibrational transitions. These transitions are compared with the experimental Q-branch lines in the Raman spectrum of T_2 recorded by Edwards et al. [3]. A comparison is also made with the results of the calculations performed by Hunt et al. [18] where the adiabatic approximation was used to determine the energies of the rovibrational levels.

In our non-BO calculations we employ explicitly correlated all-particle Gaussian functions (ECGs) for expanding the wave function of the system. The non-linear parameters of the Gaussians are extensively optimized using the variational method. In the variational energy minimization we employ the analytical energy gradient determined with respect to these parameters. The use of the gradient is key in obtaining very accurate results in the calculations. Also, the use of the gradient allows for extending the basis set of ECGs in the calculations to sizes exceeding 10 000 functions.

2. Method

Not assuming the BO approximation means treating all particles forming the system on equal footing with rigorous accounting for their given masses, M_i and the electrostatic interactions between their charges, Q_i . Without invoking any approximations, the total non-relativistic laboratory-frame Hamiltonian of the system can be separated into an operator representing the motion of the center of mass and an operator representing the internal energy of the system. This separation in our approach is performed by a coordinate transformation from the laboratory Cartesian coordinate system, to an internal Cartesian coordinate system. The center of the internal coordinate frame is placed at a selected reference particle. The transformation to the internal coordinates together with the conjugate momentum transformation yields the Hamiltonian representing the internal energy of the system (called the internal Hamiltonian) that is used in the present calculations. The Hamiltonian explicitly depends on the masses of the nuclei. The triton mass in the present calculations is: $M_t = 5496.92158m_e$, where m_e is the electron mass [19]. More information on the nonadiabatic Hamiltonian and the center-of-mass transformation can be found in Ref. [12].

As internal Hamiltonian is isotropic (spherically symmetric; atom-like), its eigenfunctions transform according to the irreducible representations of the SO(3) rotation group. These eigenfunctions separate into subsets of states corresponding to different values of the total rotational quantum number, N . For the ground and first-excited rotational states they are $N=0$ and $N=1$, respectively. Within each subset of states corresponding to a particular N , the states represent different ‘vibrational’ excitations. We put the term vibrational in quotes, because, strictly speaking, the vibrational quantum number (ν) is not a good quantum number due to the coupling between the electronic and vibrational motions in the calculations where the BO approximation is not assumed. Thus, ν should be regarded as a number that enumerates the consecutive states in a particular manifold corresponding to a certain value of the total rotational quantum number N .

The ECG basis set used in the calculations of the rotationless $N=0$ states of T_2 was introduced in Ref. [12] and has the following form:

$$\phi_k(\mathbf{r}) = r_1^{m_k} \exp[-\mathbf{r}'(L_k L'_k \otimes I_3)\mathbf{r}], \quad (1)$$

where \mathbf{r} is a vector of the internal coordinates of the particles 2 to N forming the system with respect to the reference particle 1 (in the present calculations one of the two triton nuclei). L_k in (1) is an $n \times n$ rank n lower triangular matrix of nonlinear variational parameters, I_3 is the 3×3 identity matrix, and \otimes denotes the Kronecker product.

r_1 is the distance between particle 2 (the other triton nucleus) and particle 1 and m_k is an even non-negative integer, which in the present calculations varies in the 0–250 range.

In systems with two electrons and two identical fermionic nuclei (like T_2 ; the spin of triton is: $S_t = \frac{1}{2}$) the wave function representing the internal state of the system is a product of a spatial function representing the nuclei and the electrons, a spin function for the electrons, and a spin function for the nuclei. In the ground state of T_2 both electronic and nuclear spin functions are antisymmetric with respect to the permutation of the respective particles because they represent singlet states. The spatial function is symmetric with respect to the permutation of the nuclei and also symmetric with respect to the permutation of the electrons. A symmetric spatial wave function can be constructed using basis function (1). This is ditritium in the (nuclear) low-spin state called para- T_2 . The permutational symmetry of the electrons and the nuclei is implemented in basis functions (1) by projecting each basis function using the symmetry-projection operator \mathcal{P} :

$$\psi_k = \mathcal{P}\phi_k = \sum_P \chi_P r_1^{m_k} \exp[-\mathbf{r}'(\tau_p L_k L'_k \tau_p \otimes I_3)\mathbf{r}], \quad (2)$$

where the sum runs over all permutations of the labels of identical particles and where τ_p are permutational matrices transforming the internal coordinates. There are four permutations in the sum over P on the right hand side of (2) and the corresponding τ_p matrices in the internal coordinates have the following form:

$$\begin{pmatrix} 1 & 0 & 0 \\ 0 & 1 & 0 \\ 0 & 0 & 1 \end{pmatrix}, \quad \begin{pmatrix} -1 & 0 & 0 \\ -1 & 1 & 0 \\ -1 & 0 & 1 \end{pmatrix}, \quad \begin{pmatrix} 1 & 0 & 0 \\ 0 & 0 & 1 \\ 0 & 1 & 0 \end{pmatrix}, \quad \begin{pmatrix} -1 & 0 & 0 \\ -1 & 0 & 1 \\ -1 & 1 & 0 \end{pmatrix}. \quad (3)$$

The coefficients χ_P are obtained from the matrix elements of the irreducible representation of the considered state, and for the ground state of T_2 they are all ones. Note that the $r_1^{m_k}$ factor is symmetric with respect to permuting the tritons. The states with the wave functions constructed this way are $N=0$ states, i.e. the rotational ground states.

In the other form of ditritium, the ortho ditritium, the nuclear spin wave function (high-spin state) is symmetric with respect to the permutation of the tritons and the spatial wave function is symmetric. The spatial wave function is still symmetric with respect to the permutation of the electrons and the electronic spin function is antisymmetric. The antisymmetric nuclear component of the spatial wave function of ortho ditritium represents the first excited rotational state with $N=1$, as the permutation of the nuclei is equivalent to rotating the molecule by 180° around its rotational axis. The ECG basis functions which can describe such a state are obtained by multiplying the $N=0$ ECGs (1) by the z coordinate of the \mathbf{r}_1 vector, z_1 [20]:

$$\phi_k(\mathbf{r}) = z_1 r_1^{m_k} \exp[-\mathbf{r}'(L_k L'_k \otimes I_3)\mathbf{r}]. \quad (4)$$

These functions are $N=1$ eigenfunctions of the square of the total angular momentum operator and also eigenfunctions of the operator representing the z -axis projection of the total angular momentum.

In ortho ditritium the spatial wave function is antisymmetric with respect to the permutation of the tritons. In Gaussians (4), the asymmetry automatically happens because the $z_1 = Z_2 - Z_1$ factor (Z_1 and Z_2 are the z coordinates of the nuclei in the laboratory coordinate frame) is antisymmetric with respect to the permutation of the tritons. Thus, if the remaining part of the basis function, i.e. the $r_1^{m_k} \exp[-\mathbf{r}'(L_k L'_k \otimes I_3)\mathbf{r}]$, is made symmetric with respect to this permutation, the whole basis function is antisymmetric. This symmetrization is achieved by operating on this part of the Gaussian with the same projection operator, \mathcal{P} , as applied to Gaussians (1) used for expanding the $N=0$ wave functions. Thus,

in the calculations of states of the para and ortho ditritium basis functions (1) and (4), respectively, are used.

The approach used in the present T_2 calculations is the same as used before in the H_2 [21] and D_2 [22] calculations. In the optimization of the linear expansions coefficients of the wave function in terms of ECGs and the ECG non-linear parameters Gaussian basis functions the Rayleigh-Ritz variational scheme is employed. As mentioned, the variational energy minimization is performed with the aid of the energy gradient determined with respect to the L_k matrix elements. The gradient is obtained analytically by the direct differentiation of the non-BO energy of the particular state with respect to the matrix elements. The algorithms for calculating the overlap and Hamiltonian matrix elements and the matrix elements of the energy gradient for ECGs (1) and (4) were presented in Refs. [12,20], respectively. In Refs. [21,22] we also described how the ECG basis set is grown for each state and how the total non-BO energy is typically converging with the number of basis functions.

In the previous paper on T_2 [23] we reported very accurate direct non-BO calculations for the $v = 0, \dots, 26$, $N=0$ states (i.e. pure vibrational states). Up to 16 000 of the $N=0$ ECGs were used in the basis set for each state in the calculations. The results of that work are used in the present calculations of the ortho–para isomerization energies.

The ortho–para isomerization energies of H_2 calculated with the approach employed in the present work [21] agreed with the experimental results with the accuracy of the experimental data. A similar accuracy level one can expect to be achieved in the present calculations.

3. Results

In this work the focus of the calculations are the 26 bound $N=1$, $v = 0, \dots, 25$ rovibrational levels of T_2 (ortho ditritium). At the $N=0$ level there are 27 bound states, but the top $v = 26$ one is only marginally bound [23]. An attempt to converge the $N=1$, $v = 26$ state below the dissociation threshold made in this work failed. The present $N=1$ calculations has yielded energies and the corresponding wave functions. The energies allow for determining the dissociation energy and the ortho–para isomerization energy for each vibrational level. The wave functions are used to calculate the expectation values of the inter-particle distances and the triton–triton correlation function (see below).

The total energies of the $N=1$, $v = 0, \dots, 25$ states obtained in the calculations are presented in Table 1. For each states three energy values are shown. The first is the energy obtained for the $N=0$ state with K ECGs (note that K increases with the increase of the level of the vibrational excitation from $K = 11\,000$ for the $v = 0$ state to $K = 16\,000$ for the $v = 26$ state). The second is the energy obtained for the corresponding $N=1$ state with the number of ECGs equal to $K - 1000$ (this is the number of functions in the $N=0$ basis set used to generate the starting set in the $N=1$ calculation). The third in the energy of the $N=1$ state obtained after addition of 1000 ECGs to the $(K - 1000)$ basis set (after this addition the number of functions in the basis set becomes equal to K , which is the same number of functions as in the $N=0$ basis set).

A comparison of the energies obtained for each $N=1$ rovibrational state with $K - 1000$ and K basis functions allows for assessing the energy convergence. That convergence varies from state to state and, as one can see, is much better for the lower states than for top ones. So, while for the $v = 0$ state ten digits in the energy are practically converged, only eight digits are converged for the $v = 25$ state.

The total energies of the $N=1$ states from Table 1 are used to calculate the corresponding dissociation energies shown in Table 2. These energies are compared with the results of Hunt et al. [18] obtained within the adiabatic approximation. In Table 2 we also

show the ortho–para isomerization energies obtained by subtracting the $N=0$ energy from the $N=1$ energy for each vibrational state. The energies of the $N=0$ rovibrational states are taken from our previous work [23]. The present isomerization energies are compared in Table 2 with the adiabatic results of Hunt et al. [18] for the six lowest states they considered in their calculations. As one can see, while our dissociation energies differ from the results of Hunt et al. by about $1\text{--}2\text{ cm}^{-1}$, the isomerization energies are essentially identical.

There exists in the literature a set of Raman experimental transition energies [3] the present results can be compared to. The comparison is show in Table 3 and also includes a comparison with the results of Hunt et al. [18] obtained using the adiabatic approximation. As one can see, including adiabatic and non-adiabatic effects to infinite order, as it is done in the present non-BO calculations, reduces the discrepancies between the adiabatic results of Hunt et al. and the experimental results for the $(v = 0, N=0) \rightarrow (v = 1, N=0)$ and $(v = 0, N=1) \rightarrow (v = 1, N=1)$ transitions by approximately a factor of two. The remaining discrepancy is likely due to the relativistic and QED effects which are not included in the present calculations because the algorithms for calculating these effects with the non-BO wave functions have not been implemented yet (apart from the relativistic effects implemented for $N=0$ states of diatomic systems [24,25]).

Finally, in Table 4 we show expectation values of the triton–triton (r_{tt}), triton–electron (r_{te}), and electron–electron (r_{ee}) distances calculated using the non-BO $N=0$ and $N=1$ wave functions expanded in terms of K ECGs. The results show the expected trends. All distances for both $N=0$ and $N=1$ groups of states increase with the vibrational excitation. Also, an increase occurs, as expected, in moving from the $N=0$ state to the $N=1$ state for each particular vibrational quantum number. This increase, which is due to the centrifuge force, is the smallest for the $v = 1$ state (0.0004 a.u.) and the largest for the $v = 25$ state (0.0160 a.u.). Apparently, the centrifuge force is too strong to allow the $(v = 26, N=1)$ state to be bound. The results shown in Table 4 can be used to benchmark calculations performed using the conventional approach bases in the lowest order on the BO approximation.

The complexity of the non-BO wave functions of the $N=1$ states of T_2 can be, perhaps, best represented by plotting the triton–triton correlation functions for various rovibrational states. The T–T correlation function is the one-particle relative density of the two tritons associated with the internal coordinate \mathbf{r}_1 . The correlation function is defined as [26]:

$$g_i(\xi) = \langle \Psi_i(\mathbf{r}) | \delta(\mathbf{r}_1 - \xi) | \Psi_i(\mathbf{r}) \rangle = \int_{-\infty}^{\infty} |\Psi_i(\xi, \mathbf{r}_2, \mathbf{r}_3)|^2 d\mathbf{r}_2 d\mathbf{r}_3, \quad (5)$$

where $\delta(\mathbf{r}_1 - \xi)$ is the 3-dimensional Dirac delta function. In Figure 1 the correlation functions calculated for the $v = 0, 12$, and 25 rovibrational states with $N=1$ rotational quantum number are shown and compared with the correlation functions calculated for the corresponding $N=0$ states. The oscillatory character of the density provide a clear justification for including the $r_1^{m_k}$ factors in basis functions (4). These factors allow for representing the radial (vibrational) oscillation in the wave function associated with the vibrational excitation level of the state the wave function represents. The correlation functions plotted in Figure 1 also show the angular behavior of the T–T relative density associated with the rotational $N=0 \rightarrow N=1$ excitation.

4. Summary

All bound vibrational states corresponding to the $N=1$ rotational excitation of the T_2 molecule have been studies with direct variational non-BO calculations using large sets of explicitly

Table 1

The convergence of the total nonrelativistic non-BO energies of the $N = 1, v = 0, \dots, 25$ rovibrational states of T_2 with the number of basis functions. The energies of the $N=0, v = 0, \dots, 26$ rovibrational states taken from Ref. [23] are also shown. All values are given in a.u. (hartrees).

v	No. ECGs	Energy	v	No. ECGs	Energy	v	No. ECGs	Energy	v	No. ECGs	Energy	
$N=0$	0	11 000	-1.168 535 675 71	1	12 000	-1.157 306 577 87	2	12 000	-1.146 441 883 89	3	12 000	-1.135 936 002 23
$N=1$	0	10 000	-1.168 353 133 91	1	11 000	-1.157 129 301 92	2	11 000	-1.146 269 794 93	3	11 000	-1.135 769 033 18
		11 000	-1.168 353 133 98		12 000	-1.157 129 302 16		12 000	-1.146 269 795 55		12 000	-1.135 769 034 05
$N=0$	4	12 000	-1.125 784 216 46	5	12 000	-1.115 982 714 88	6	12 000	-1.106 528 629 62	7	12 000	-1.097 420 089 95
$N=1$	4	11 000	-1.125 622 311 98	5	11 000	-1.115 825 832 16	6	11 000	-1.106 376 737 60	7	11 000	-1.097 273 176 58
		12 000	-1.125 622 313 15		12 000	-1.115 825 833 62		12 000	-1.106 376 740 96		12 000	-1.097 273 178 78
$N=0$	8	12 000	-1.088 656 283 24	9	12 000	-1.080 237 540 97	10	13 000	-1.072 165 433 95	11	13 000	-1.064 442 896 27
$N=1$	8	11 000	-1.088 514 347 15	9	11 000	-1.080 100 599 78	10	12 000	-1.072 033 523 45	11	12 000	-1.064 316 073 59
		12 000	-1.088 514 350 00		12 000	-1.080 100 603 21		13 000	-1.072 033 527 97		13 000	-1.064 316 079 57
$N=0$	12	14 000	-1.057 074 373 28	13	15 000	-1.050 065 987 64	14	15 000	-1.043 425 812 66	15	15 000	-1.037 164 004 89
$N=1$	12	13 000	-1.056 952 722 68	13	14 000	-1.049 949 610 08	14	14 000	-1.043 314 858 44	15	14 000	-1.037 058 691 53
		15 000	-1.056 952 729 39		15 000	-1.049 949 620 16		15 000	-1.043 314 869 46		15 000	-1.037 058 703 42
$N=0$	16	15 000	-1.031 293 408 60	17	15 000	-1.025 829 523 61	18	15 000	-1.020 791 412 19	19	15 000	-1.016 202 103 84
$N=1$	16	14 000	-1.031 193 876 42	17	14 000	-1.025 736 099 00	18	14 000	-1.020 704 424 05	19	14 000	-1.016 121 978 41
		15 000	-1.031 193 890 94		15 000	-1.025 736 107 76		15 000	-1.020 704 442 21		15 000	-1.016 121 997 98
$N=0$	20	15 000	-1.012 089 379 99	21	15 000	-1.008 486 791 66	22	15 000	-1.005 434 807 53	23	15 000	-1.002 982 415 44
$N=1$	20	14 000	-1.012 016 640 80	21	14 000	-1.008 422 115 41	22	14 000	-1.005 379 039 56	23	14 000	-1.002 936 675 72
		15 000	-1.012 016 670 98		15 000	-1.008 422 146 74		15 000	-1.005 379 058 48		15 000	-1.002 936 696 63
$N=0$	24	16 000	-1.001 188 692 49	25	16 000	-1.000 122 488 00	26	16 000	-0.999 818 403 64	T+T		-0.999 818 113 08
$N=1$	24	15 000	-1.001 154 527 86	25	15 000	-1.000 102 296 95						
		16 000	-1.001 154 544 35		16 000	-1.000 102 308 02						

Table 2

Comparison of the dissociation energies for the ($v, 1$) states of T_2 obtained in the present calculations (E_{diss} (present) = $E(v, 1) - 2E_D$) and the dissociation energies calculated by Hunt et al. [18] using the adiabatic approximation (in parenthesis the difference between the two sets of results are shown). The para–ortho isomerization energies ($\Delta = E(v, 1) - E(v, 0)$) obtained in the present calculations are compared with the isomerization energies calculated using the results of Hunt et al. All values are in cm^{-1} .

v	E_{diss} (present)	E_{diss} [18]	Δ (present)	Δ [18]
0	36989.1616	36988.311 (0.851)	40.0633	40.064
1	34525.8152	34524.766 (1.049)	38.9075	38.908
2	32142.4290	32141.205 (1.224)	37.7690	37.769
3	29837.7783	29836.377 (1.401)	36.6453	36.646
4	27610.8304	27609.271 (1.559)	35.5337	35.534
5	25460.7517	25459.040 (1.712)	34.4315	34.432
6	23386.9156		33.3357	
7	21388.9146		32.2433	
8	19466.5739		31.1507	
9	17619.9699		30.0544	
10	15849.4516		28.9500	
11	14155.6674		27.8330	
12	12539.5989		26.6977	
13	11002.5940		25.5397	
14	9546.4346		24.3492	
15	8173.3648		23.1198	
16	6886.1873		21.8416	
17	5688.3423		20.5024	
18	4584.0194		19.0877	
19	3578.2891		17.5812	
20	2677.2740		15.9578	
21	1888.3671		14.1879	
22	1220.4865		12.2355	
23	684.4500		10.0341	
24	293.3127		7.4947	
25	62.3736		4.4290	

Table 3

Comparison of the experimental Raman ($v = 0, N = 0 \rightarrow v = 1, N = 0$) and ($v = 0, N = 1 \rightarrow v = 1, N = 1$) transition energies of T_2 [3] with the present results and the results of Hunt et al. [18]. All values are in a.u.

Transition	Experiment Raman [3]	Present work	Hunt et al. [18]
$(v = 0, N = 0) \rightarrow (v = 1, N = 0)$	2464.320	2464.5021	2464.701
$(v = 0, N = 1) \rightarrow (v = 1, N = 1)$	2463.155	2463.3464	2463.545

correlated all-particle Gaussian functions. Each state has been calculated separately by generating a basis set of ECGs specifically for that state. The ECGs in the basis set have been extensively optimized in terms of the Gaussian non-linear parameters using a

energy-minimization method. The optimization of the exponential Gaussian parameters has been aided by the analytical energy gradient determined with respect to these parameters. The sizes of the basis sets used in the calculations range from 11 000 for

Table 4

Expectation values of the triton–triton, triton–electron, and electron–electron distances calculated for the ($v, 0$) and ($v, 1$) states of T_2 . All values are in a.u.

v	$\langle r_{tt} \rangle, N=0$	$\langle r_{te} \rangle, N=1$	$\langle r_{te} \rangle, N=0$	$\langle r_{te} \rangle, N=1$	$\langle r_{ee} \rangle, N=0$	$\langle r_{ee} \rangle, N=1$
0	1.4284	1.4291	1.5639	1.5643	2.1877	2.1882
1	1.4833	1.4840	1.5929	1.5933	2.2241	2.2246
2	1.5395	1.5402	1.6225	1.6229	2.2617	2.2622
3	1.5970	1.5978	1.6526	1.6530	2.3007	2.3012
4	1.6560	1.6568	1.6835	1.6839	2.3412	2.3417
5	1.7167	1.7175	1.7152	1.7156	2.3834	2.3840
6	1.7793	1.7802	1.7477	1.7481	2.4276	2.4282
7	1.8440	1.8449	1.7812	1.7817	2.4741	2.4747
8	1.9112	1.9121	1.8159	1.8164	2.5231	2.5238
9	1.9811	1.9821	1.8519	1.8524	2.5751	2.5758
10	2.0543	2.0553	1.8894	1.8899	2.6306	2.6313
11	2.1312	2.1323	1.9286	1.9292	2.6901	2.6909
12	2.2125	2.2137	1.9700	1.9706	2.7544	2.7553
13	2.2991	2.3003	2.0139	2.0145	2.8244	2.8254
14	2.3920	2.3933	2.0608	2.0615	2.9012	2.9022
15	2.4926	2.4940	2.1114	2.1121	2.9862	2.9874
16	2.6027	2.6043	2.1666	2.1674	3.0813	3.0827
17	2.7247	2.7265	2.2275	2.2284	3.1891	3.1906
18	2.8621	2.8642	2.2959	2.2969	3.3129	3.3147
19	3.0198	3.0222	2.3740	2.3752	3.4576	3.4598
20	3.2050	3.2078	2.4655	2.4669	3.6306	3.6333
21	3.4293	3.4329	2.5759	2.5777	3.8430	3.8464
22	3.7127	3.7175	2.7150	2.7174	4.1141	4.1187
23	4.0937	4.1007	2.9015	2.9050	4.4810	4.4878
24	4.6633	4.6754	3.1798	3.1857	5.0308	5.0425
25	5.7479	5.7807	3.7095	3.7255	6.0766	6.1082
26	20.6605		11.1115		20.7849	

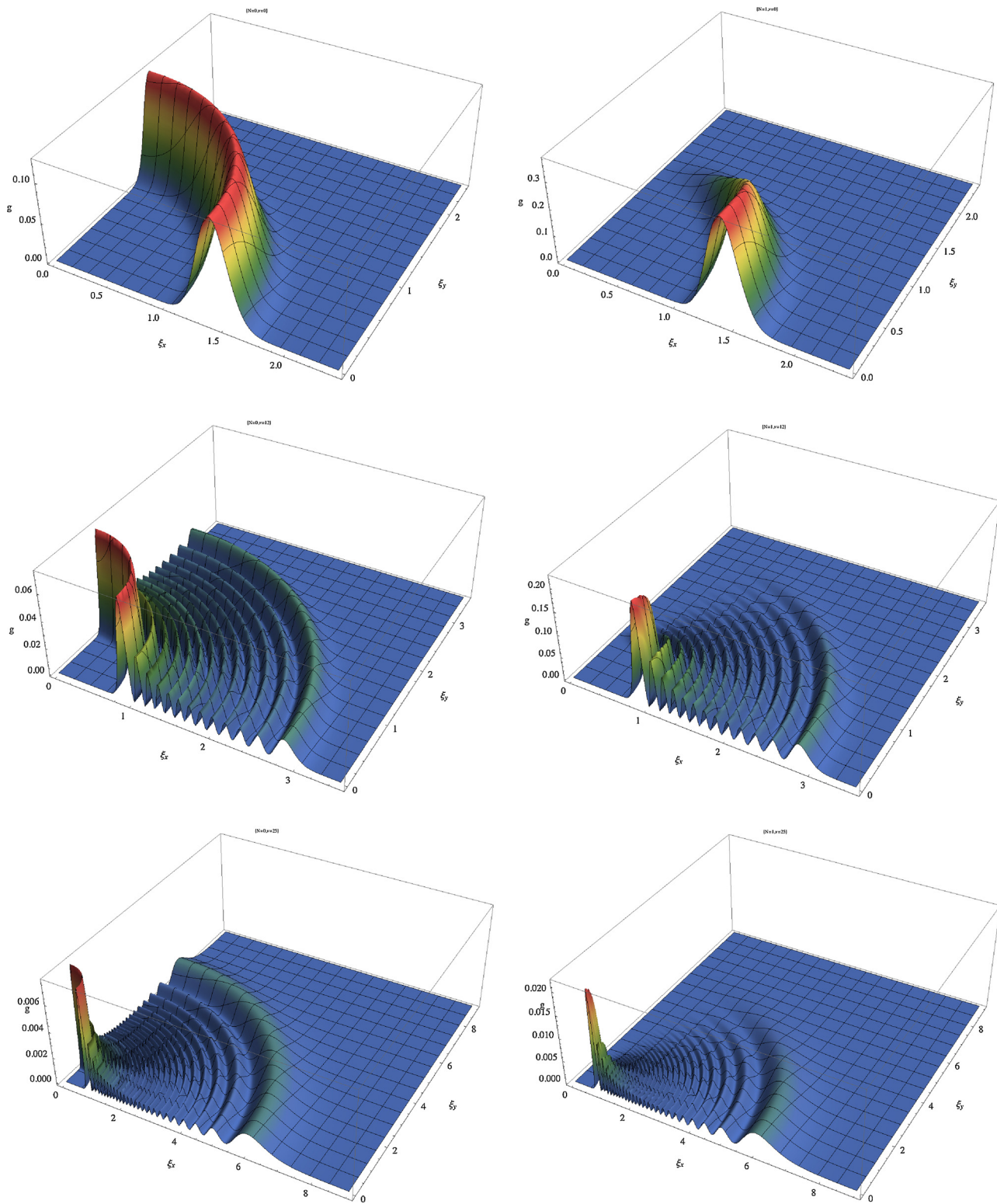


Figure 1. Correlation functions for rovibrational states corresponding to the $v = 1, 12$, and 25 vibrational quantum numbers and the $N = 0$ (on the left) and $N = 1$ (on the right) rotational quantum numbers. One quarter of the cross section along the xy plane for each correlation function is shown. To obtain the whole cross section, the presented density has to be reflected in the xz and xy planes. For the $N = 0$ states this reflection produces a spherically symmetric function. For the $N = 1$ states the reflection generates a function which is zero along the y axis, but non-zero along the x axis.

the lowest state to 16 000 for the two highest states. 26 bound $N = 1$ states have been obtained in the calculations. The calculated energies of the $N = 1$ states and the corresponding energies of the $N = 0$ states obtained in the earlier calculations [23] have been used to determine the ortho–para isomerization energy for each

vibrational state. The isomerization energies show, as expected, a decreasing trend with increasing vibrational excitation. The results agree with the previous calculations performed for the lowest six vibrational states with the conventional approach based in the zeroth-order on the BO approximation [18]. Future work

will involve implementation of the algorithm for calculating the leading relativistic corrections for the $N=1$ rovibrational states of diatomic systems. Development of algorithms to calculate diatomic rovibrational states with N greater than one will also be carried out.

Acknowledgements

This work has been supported in part by the National Science Foundation through the graduate research fellowship program (GRFP) awarded to Keeper L. Sharkey; grant number DGE1-1143953. It has been also supported in part by the National Science Foundation with grant number IIA-1444127. We are grateful to the University of Arizona Center of Computing and Information Technology for the use of their computer resources. This work has been also supported in part by the National Science Foundation with grant #IIA-1444127.

References

- [1] P.C. Souers, D. Fearon, R. Garza, E.M. Kelly, P.E. Roberts, R.H. Sanborn, R.T. Tsugava, J.L. Hunt, J.D. Poll, *J. Chem. Phys.* **70** (1979) 1581.
- [2] P.C. Souers, J. Fuentes, E.M. Fearon, P.E. Roberts, R.T. Tsugava, J.L. Hunt, J.D. Poll, *J. Chem. Phys.* **72** (1980) 1679.
- [3] H.G.M. Edwards, D.A. Long, H.R. Mansour, *J. Chem. Soc., Faraday Trans. 2* **74** (1978) 1203.
- [4] G.G. Balint-Kurti, R.E. Moss, I.A. Sadler, M. Shapiro, *Phys. Rev. A* **41** (1990) 4913.
- [5] R.E. Moss, *Mol. Phys.* **78** (1993) 371.
- [6] H.O. Pilon, D. Baye, *Phys. Rev. A* **88** (2013) 032502.
- [7] J.-Ph. Karr, L. Hilico, *J. Phys. B: At. Mol. Opt. Phys.* **39** (2006) 2095.
- [8] Q.L. Tian, L.Y. Tang, Z.X. Zhong, Z.C. Yan, T.Y. Shi, *J. Chem. Phys.* **137** (2012) 024311.
- [9] V.I. Korobov, *Phys. Rev. A* **74** (2006) 052506.
- [10] L. Wolniewicz, *J. Chem. Phys.* **78** (1983) 6173.
- [11] L. Wolniewicz, T. Orlikowski, *Mol. Phys.* **74** (1991) 103.
- [12] D.B. Kinghorn, L. Adamowicz, *Phys. Rev. Lett.* **83** (1999) 2541.
- [13] S. Bubin, M. Pavanello, W.-Ch. Tung, K.L. Sharkey, L. Adamowicz, *Chem. Rev.* **113** (2013) 36.
- [14] J. Mitroy, S. Bubin, W. Horiuchi, Y. Suzuki, L. Adamowicz, W. Cencek, K. Szalewicz, J. Komasa, D. Blume, K. Varga, *Rev. Mod. Phys.* **85** (2013) 693.
- [15] K.L. Sharkey, N. Kirnosov, L. Adamowicz, *J. Chem. Phys.* **139** (2013) 164119.
- [16] N. Kirnosov, K.L. Sharkey, L. Adamowicz, *J. Chem. Phys.* **139** (2013) 204105.
- [17] N. Kirnosov, K.L. Sharkey, L. Adamowicz, *J. Chem. Phys.* **140** (2014) 104115.
- [18] J.L. Hunt, J.D. Poll, L. Wolniewicz, *Can. J. Phys.* **62** (1984) 1719.
- [19] See CODATA 2002 recommended values and NIST Physical Reference Data at <http://physics.nist.gov/>.
- [20] K.L. Sharkey, N. Kirnosov, L. Adamowicz, *J. Chem. Phys.* **139** (2013) 164119.
- [21] K.L. Sharkey, N. Kirnosov, L. Adamowicz, *Phys. Rev. A* **88** (2013) 032513.
- [22] K.L. Sharkey, N. Kirnosov, L. Adamowicz, *J. Chem. Phys.* **142** (2015) 174307.
- [23] M. Stanke, L. Adamowicz, *J. Chem. Phys.* **141** (2014) 154302.
- [24] D. Kędziera, M. Stanke, S. Bubin, M. Barysz, L. Adamowicz, *J. Chem. Phys.* **125** (2006) 014318.
- [25] M. Stanke, D. Kędziera, S. Bubin, M. Molski, L. Adamowicz, *J. Chem. Phys.* **128** (2008) 114313.
- [26] S. Bubin, L. Adamowicz, *Chem. Phys. Lett.* **403** (2005) 185;
N. Kirnosov, K.L. Sharkey, L. Adamowicz, *J. Chem. Phys.* **139** (2013) 204105.

APPENDIX N

Non-BornOppenheimer variational method for calculation of rotationally excited
binuclear systems

Non-Born–Oppenheimer variational method for calculation of rotationally excited binuclear systems

Nikita Kirnosov¹, Keeper L Sharkey² and Ludwik Adamowicz^{1,2}

¹ Department of Physics, University of Arizona, Tucson, Arizona 85721, USA

² Department of Chemistry and Biochemistry, University of Arizona, Tucson, Arizona 85721, USA

E-mail: kirnosov@email.arizona.edu

Received 26 February 2015, revised 11 June 2015

Accepted for publication 17 July 2015

Published 26 August 2015



Abstract

An algorithm for direct non-Born–Oppenheimer quantum mechanical variational calculations of bound states of binuclear systems with Coulombic interactions corresponding to the total angular momentum quantum number equal to one ($N = 1$) is derived and implemented. Contributions corresponding to each of the particles being angularly excited are taken into account. All-particle explicitly correlated Gaussian basis functions with Cartesian angular factors are used in the approach. The method is tested in the calculations of various three-particle systems including heteronuclear electronic (HD^+) and muonic (e.g. $p\mu$) ions.

Keywords: rovibrational states, non-Born–Oppenheimer method, explicitly correlated Gaussian functions

(Some figures may appear in colour only in the online journal)

1. Introduction

In our recent work [1] we developed an algorithm employing explicitly correlated Gaussian (ECG) functions for the calculation of bound rovibrational states of diatomic molecules with an arbitrary number of σ electrons corresponding to the first excited rotational ($N = 1$) state. The approach used the variational method and did not assume the Born–Oppenheimer (BO) approximation. The procedure was applied to generate the $N = 1$ rovibrational spectra of HD^+ [1], H_2 [2], and HD [3]. For the HD^+ [4] and HD [3] molecules the effect of the rotational excitation on the asymmetry of the charge distribution in the molecule was investigated. The lifetimes of all rotationless levels of HD^+ [5] and HD [3] were also calculated. The agreement between the total energies obtained in those calculations for the $N = 1$ states and the most accurate calculations found in the literature was on the order of 10^{-8} hartree in most cases. This was sufficient to match the experimental accuracy for the transition energies, but demonstrated that some inaccuracy was present in the calculations of the $N = 1$ states. This inaccuracy was significantly higher than the inaccuracy in the ECG calculations

of the $N = 0$ states performed before [6–8]. The attempt was also made to apply the procedure to simple three particle muonic molecules, but, even though again for $N = 0$ states the agreement with the previous calculations was very good, for the $N = 1$ there results were off from the previously reported values by as much as 10^{-4} in muonic atomic units.

As the inaccuracy of the $N = 1$ calculations increased with the increase of the mass of the lightest particle in the system, we attributed it to the deficiency of the ECG basis set used to represent the wave functions of the $N = 1$ rovibrational states in [1]. In this work we remedy this deficiency. The proper handling of the angular excitations of all particles involved in the system, as well as the coupling of these excitations, not only allows us to obtain much more accurate energies of the rovibrational states, but, more importantly, opens a possibility of performing accurate calculations of a number of expectation values. For example, our recent study of the lifetimes of rotationless levels [3, 5] involved the evaluation of the $\langle \psi^{N=0} | x_i | \psi^{N=1} \rangle$ expectation values. These matrix elements are usually sensitive to the inclusion in the basis set used in the calculation of functions representing angular excitations of the lighter particles that form the

system. To your knowledge, the new approach developed in the present work outperforms other methods in terms of delivering high accuracy and flexibility.

For an $n + 1$ particle system the Hamiltonian, \hat{H}_{nonrel} , used in the present approach is obtained by separating out the operator representing the centre-of-mass kinetic energy from the laboratory-frame nonrelativistic Hamiltonian, \hat{H}_{nonrel} (called the internal Hamiltonian) in the following form:

$$\begin{aligned}\hat{H}_{\text{nonrel}} = & -\frac{1}{2} \left(\sum_{i=1}^n \frac{1}{\mu_i} \nabla_{\mathbf{r}_i}^2 + \sum_{i=1}^n \sum_{j \neq i}^n \frac{1}{m_0} \nabla_{\mathbf{r}_i} \cdot \nabla_{\mathbf{r}_j} \right) \\ & + \sum_{i=1}^n \frac{q_i q_i}{r_i} + \sum_{i < j}^n \frac{q_i q_j}{r_{ij}}.\end{aligned}\quad (1)$$

In (1), q_i , $i = 0, \dots, n$ are the charges of the particles and \mathbf{r}_i , $i = 1, \dots, n$, are the position vectors of the $(i + 1)$ th particle with respect to a chosen reference particle, which is numbered as 0. Usually the reference particle in our calculations is the heaviest particle in the system. The separation of the laboratory-frame Hamiltonian into the Hamiltonian representing the kinetic energy of the centre-of-mass motion and the internal Hamiltonian is exact (rigorous). In \hat{H}_{nonrel} r_i are the lengths of the \mathbf{r}_i vectors, $r_{ij} = |\mathbf{r}_j - \mathbf{r}_i|$, m_0 is the mass of the reference particle, and $\mu_i = m_0 m_i / (m_0 + m_i)$ is the reduced mass of particle i . Hamiltonian (1) is rotationally invariant and represents n ‘pseudoparticles’ with charges equal to the charges of the original particles, but with masses being replaced by the reduced masses, moving in the central potential of the charge of the reference particle. Each pseudoparticle represents a pair of particles, one of which being a moving particle (i.e. not the reference particle) and the other being the reference particle.

Due to the invariant character of (1) its eigenfunctions transform according to the irreducible representations of the group of 3D rotations (SO(3)). In particular, the ground state or any rotationless state of a system with positive (natural) parity is represented by a spherically symmetric wave function. Excited states have angular symmetries consistent with the SO(3) group of rotations. The coupling of the motions of the pseudoparticles in (1) is due to the Coulomb interactions and due to the mass-polarization terms, $-\frac{1}{2} \sum_{i=1}^n \sum_{j \neq i}^n \frac{1}{m_0} \nabla_{\mathbf{r}_i} \cdot \nabla_{\mathbf{r}_j}$.

If the BO approximation is not assumed, the square of the total angular momentum operator commutes with the Hamiltonian and the total angular momentum quantum number, N , is a good quantum number. For molecules with electrons the all-particle total angular-momentum operator, \hat{N} , which is a sum of the operators representing the electronic, \hat{L} , and nuclear, \hat{R} , angular momenta. In [1] an assumption was made that, as the electrons are much lighter than the nuclei, in the calculations of $N = 1$ states the contributions from electronic angular excitations should be much smaller than the contributions where the nuclei are rotationally excited and they can be neglected. We argued that, due to lack of the orthogonality between basis functions with the angular factors corresponding to the rotational excitations of the nuclei and basis functions with the angular factors representing the

angular excitations of the electrons, the latter approximately describe the former. With that assumption the explicitly correlated all-particle Gaussian (ECG) functions used in our diatomic non-BO $N = 1$ calculations had the following form (we assume that particles 0 and 1 are nuclei; thus r_1 , which is the length of the \mathbf{r}_1 vector, is the internuclear distance and x_1 is the x coordinate of \mathbf{r}_1):

$$\varphi_k^{N=1} = x_1 r_1^{m_k} \exp[-\mathbf{r}'(A_k \otimes I_3)\mathbf{r}], \quad (2)$$

where \mathbf{r} is a vector of the length $3n$ whose first three coordinates are the coordinates of the \mathbf{r}_1 vector, next three are the coordinates of the \mathbf{r}_2 , etc. Only non-negative even powers, m_k , of the internuclear distance are used. In (2) A_k , which is a symmetric $n \times n$ matrix, has to be positive-definite in order for the function to be square integrable. This is achieved by representing A_k in a Cholesky-factored form as: $A_k \equiv L_k L_k'$, where L_k is a lower triangular real matrix. No restrictions need to be placed on the L_k matrix elements and they can be varied in the $(-\infty, +\infty)$ range. The elements of the L_k matrices are the nonlinear parameters which are variationally optimized for each basis function in our calculations. The optimization process involves minimization of the total non-BO energy and employs the analytical gradient of the energy functional determined with respect to the L_k matrix elements. The use of the gradient significantly accelerates the optimization. Additionally, the m_k powers of the internuclear distance, r_1 , are also optimized. This is done only once after the function is first included in the basis set.

Even though we have been able to obtain quite accurate results for the $N = 1$ states of some simple diatomic systems using basis functions (2), the question of the completeness of this set of functions has remained unanswered. The lack of completeness may result from only including in the basis set ECGs with the x_1 angular prefactor and not include ECGs with x_i , $i = 2, \dots, n$ prefactors. For a molecule ECGs with such prefactors would describe the coupling between rotational excitations of the nuclei with excitations where the electrons and not the nuclei are excited to higher angular-momentum states. The modified ECGs, which can describe this coupling have the form:

$$\varphi_k^{(i)} = x_i r_1^{m_k} \exp[-\mathbf{r}'(A_k \otimes I_3)\mathbf{r}], \quad (3)$$

where index i ranges from 1 to the total number of pseudoparticles in the system, n . Basis set (3) includes basis set (2).

This work has the following structure. First we derive the Hamiltonian and overlap matrix elements with ECGs (3) and the element of the energy gradient vector comprising the first derivatives of the energy with respect to the L_k matrix elements. Next we briefly describe the computational implementation of the algorithm. In the last section we show an application of the approach to calculate some lowest $N = 0$ and $N = 1$ bound states of heteronuclear isotopologues of H_2^+ , and systems derived from HD^+ with the electron replaced by a muon.

2. Formula derivation

In order to derive analytical expressions for the Hamiltonian and overlap matrix elements we follow the approach explained in more detail in [1]. We also adapt the notation used in that work. Thus, similarly as before, we use derivatives with respect to parameters to write the overlap between two basis functions (3), k th and l th, as:

$$\begin{aligned} \langle \varphi_k^{(i)} | \varphi_l^{(j)} \rangle &= \langle \phi_k | x_i x_j r_1^{m_k+m_l} | \phi_l \rangle \\ &= \frac{\partial}{\partial \nu_k} \frac{\partial}{\partial \nu_l} \langle \phi_k | r_1^{m_k+m_l} \\ &\quad \times \exp [\mathbf{r} (\nu_k \mathbf{v}_k + \nu_l \mathbf{v}_l)'] | \phi_l \rangle \Big|_{\nu_k=\nu_l=0} \\ &= -\frac{\partial}{\partial \omega_{kl}} \langle \phi_k | r_1^{m_k+m_l} \\ &\quad \times \exp [-\mathbf{r}' (\omega_{kl} \mathbf{W}^{(ij)}) \mathbf{r}] | \phi_l \rangle \Big|_{\omega_{kl}=0}, \end{aligned} \quad (4)$$

where $\phi_k = \exp[-\mathbf{r}'(A_k \otimes I_3)\mathbf{r}]$, \mathbf{v}_k and \mathbf{v}_l are $3n$ -element vectors such that $\mathbf{v}_k \mathbf{r} = x_i$ and $\mathbf{v}_l \mathbf{r} = x_j$; $\mathbf{W}^{(ij)}$ is a $3n \times 3n$ matrix such that $\mathbf{r}' \mathbf{W}^{(ij)} \mathbf{r} = x_i x_j$. The way to construct these vectors and the matrix was described in [9].

Using this approach and implementing the short hand notation, $\alpha_{ij} = (A_{kl}^{-1})_{ij}$, the normalized overlap has the following form:

$$\begin{aligned} S_{kl}^{(ij)} &= \frac{\langle \varphi_k^{(i)} | \varphi_l^{(j)} \rangle}{\sqrt{\langle \varphi_k^{(i)} | \varphi_k^{(i)} \rangle \langle \varphi_l^{(j)} | \varphi_l^{(j)} \rangle}} \\ &= 2 f_{kl} \gamma_1(m_k, m_l) \left(\frac{\alpha_{11}}{\left(A_k^{-1} \right)_{11}} \right)^{\frac{m_k}{2}} \left(\frac{\alpha_{11}}{\left(A_l^{-1} \right)_{11}} \right)^{\frac{m_l}{2}} \\ &\quad \times \left(\alpha_{ij} + \frac{m_k + m_l}{3} \cdot \frac{\alpha_{1i} \alpha_{1j}}{\alpha_{11}} \right) / \\ &\quad \left(\left(A_k^{-1} \right)_{ii} + \frac{2m_k}{3} \cdot \frac{\left(A_k^{-1} \right)_{1i}^2}{\left(A_k^{-1} \right)_{11}} \right)^{-\frac{1}{2}} \right) \\ &\quad \times \left(\left(A_l^{-1} \right)_{jj} + \frac{2m_l}{3} \cdot \frac{\left(A_l^{-1} \right)_{1j}^2}{\left(A_l^{-1} \right)_{11}} \right)^{-\frac{1}{2}}, \end{aligned} \quad (5)$$

where

$$\begin{aligned} f_{kl} &= \frac{1}{2^{3n/2}} \left(\frac{|A_{kl}|}{\| L_k \| \| L_k \|} \right)^{-3/2}, \\ \gamma_1(m_k, m_l) &= \frac{2^{\frac{m_k+m_l}{2}} \Gamma \left(\frac{3+m_k+m_l}{2} \right)}{\sqrt{\Gamma \left(\frac{3+2m_k}{2} \right) \Gamma \left(\frac{3+2m_l}{2} \right)}}. \end{aligned}$$

The final expression used to compute the potential energy integral takes the following form:

$$V_{kl}^{(ij)} = \sum_{p,g>p}^n q_p q_g R_{kl}^{(ij,pg)} + \sum_{p=1}^n q_0 q_p R_{kl}^{(ij,pp)}, \quad (6)$$

where

$$\begin{aligned} R_{kl}^{(ij,pg)} &= \frac{S_{kl}^{(ij)}}{\beta^{3/2} (3\alpha_{11}\alpha_{ij} - m\eta)} \frac{\Gamma(m+1)}{\Gamma(m+3/2)} \\ &\quad \times \left\{ \alpha_{11} (3\alpha_{ij}\beta - \theta) + 2m\beta\eta \right. \\ &\quad + \frac{1}{\sqrt{\pi}} \sum_{k=1}^m \frac{\Gamma(k+1/2)}{\Gamma(k+1)} \left(1 - \frac{\chi}{\alpha_{11}\beta} \right)^k \\ &\quad \times \left. \left(\alpha_{11} ((3+2k)\alpha_{ij}\beta - (1+2k)\theta) + 2(m-k)\beta\eta \right) \right\}. \end{aligned} \quad (7)$$

and

$$\begin{aligned} \beta &= \begin{cases} \alpha_{pg} & \text{if } p = g \\ \alpha_{pp} + \alpha_{gg} - 2\alpha_{pg} & \text{otherwise} \end{cases}, \\ \eta &= \alpha_{1i}\alpha_{1j}, \\ \chi &= \begin{cases} \alpha_{pg}^2 & \text{if } p = g \\ (\alpha_{1p} - \alpha_{1g})^2 & \text{otherwise} \end{cases}, \\ \theta &= \begin{cases} \alpha_{ig}\alpha_{jp} & \text{if } p = g \\ (\alpha_{ip} - \alpha_{ig})(\alpha_{jp} - \alpha_{ig}) & \text{otherwise} \end{cases}. \end{aligned} \quad (8)$$

The kinetic energy operator can be written in the following quadratic form:

$$-\frac{1}{2} \left(\sum_{i=1}^n \frac{1}{\mu_i} \nabla_{\mathbf{r}_i}^2 + \sum_{i \neq j}^n \frac{1}{m_0} \nabla'_{\mathbf{r}_i} \nabla_{\mathbf{r}_j} \right) = -\nabla'_{\mathbf{r}} \mathbf{M} \nabla_{\mathbf{r}}, \quad (9)$$

where the mass matrix, \mathbf{M} , is $\mathbf{M} = M \otimes I_3$ with the diagonal elements set to $1/(2\mu_1), 1/(2\mu_2), \dots, 1/(2\mu_n)$ and with the off-diagonal elements set to $1/(2m_0)$. m_0 is the mass of the reference nucleus and μ_1, \dots and μ_n are the reduced masses of the pseudoparticles.

The matrix element for (9) are evaluated as:

$$\begin{aligned} T_{kl}^{(ij)} &= 2 S_{kl}^{(ij)} \left(\alpha_{ij} + \frac{2m\alpha_{1i}\alpha_{1j}}{3\alpha_{11}} \right)^{-1} \\ &\quad \times \left\{ M_{ij} + \frac{m_l M_{1i} \alpha_{1j} + m_k M_{1j} \alpha_{1i}}{3\alpha_{11}} \right. \\ &\quad - \left((A_{kl}^{-1} A_l M)_{ji} + (A_{kl}^{-1} A_k M)_{ij} \right. \\ &\quad + \frac{2m}{3\alpha_{11}} \left(\alpha_{1j} (A_{kl}^{-1} A_l M)_{1i} + \alpha_{1i} (A_{kl}^{-1} A_k M)_{1j} \right) \\ &\quad \left. \left. + \frac{m_k + m_l}{2m+1} \frac{M_{11}}{\alpha_{11}} \left(\alpha_{ij} + \frac{2m-2}{3\alpha_{11}} \alpha_{1i} \alpha_{1j} \right) \right) \right\} \end{aligned}$$

$$\begin{aligned}
& - \frac{1}{3\alpha_{11}} \left((3\alpha_{ij} + 2(m-1)\alpha_{lj}) \left(m_k (A_{kl}^{-1} A_l M)_{11} \right. \right. \\
& + m_l (A_{kl}^{-1} A_k M)_{11} \left. \right) + \alpha_{lj} \left(m_k (A_{kl}^{-1} A_l M)_{il} \right. \\
& + m_l (A_{kl}^{-1} A_k M)_{il} \left. \right) + \alpha_{li} \left(m_k (A_{kl}^{-1} A_l M)_{jl} \right. \\
& \left. \left. + m_l (A_{kl}^{-1} A_k M)_{jl} \right) \right) \\
& + \frac{4m(m-1)}{3} \frac{\alpha_{li}\alpha_{lj}}{\alpha_{11}^2} \left(A_{kl}^{-1} A_k M A_l A_{kl}^{-1} \right)_{11} \\
& + \frac{2m}{3\alpha_{11}} \left(\alpha_{lj} \left((A_{kl}^{-1} A_k M A_l A_{kl}^{-1})_{11} \right. \right. \\
& + (A_{kl}^{-1} A_l M A_k A_{kl}^{-1})_{il} \left. \right) \\
& + \alpha_{li} \left((A_{kl}^{-1} A_k M A_l A_{kl}^{-1})_{lj} \right. \\
& \left. \left. + (A_{kl}^{-1} A_l M A_k A_{kl}^{-1})_{jl} \right) \right) \\
& + 3\alpha_{ij} \left(A_{kl}^{-1} A_k M A_l A_{kl}^{-1} \right)_{11} + 3\alpha_{li}\alpha_{lj}\tau \\
& + 3\alpha_{ij}\tau \left((A_{kl}^{-1} A_k M A_l A_{kl}^{-1})_{ij} \right. \\
& \left. + (A_{kl}^{-1} A_l M A_k A_{kl}^{-1})_{ji} \right), \tag{10}
\end{aligned}$$

where $\tau = \text{tr} [A_{kl}^{-1} A_k M A_l]$.

The details of the derivation can be found in appendix together with the description of the method used to calculate the analytical energy gradient determined with respect to nonlinear parameters L_k and L_l . It has to be noted that providing the energy gradient to the variational energy-minimization procedure significantly speeds up the calculation and enables to achieve high accuracy of the energy and the wave function.

3. Numerical illustration

The above-described algorithm is implemented in a parallel Fortran90 code. Even though the main purpose of developing the above algorithms is to use them in the calculations of ordinary (electronic) diatomic molecules, systems where the electron is replaced by a heavier particle, the muon, are considered first to test the method. Muonic systems are highly non-adiabatic and in the $N = 1$ states the coupling between configurations, where the nuclei are rotationally excited, with configurations, where rotational excitation involves the muon, is much larger than in molecules that involve electrons. Thus, one can expect that basis functions (2) with $i \neq 1$ are going to have much larger contributions than in the case of a molecule composed of electrons. Therefore testing and validation of the derived algorithms on muonic molecules is likely to be more revealing of any possible error. Also, the existence of very accurate results obtained for the $N = 0$ and $N = 1$ states of the muonic molecules used here for the testing [10] provides excellent grounds for a comparison. Thus, this section has two parts. The first deals with the application and testing of

the method in the calculations of some simple muonic systems and the second describes the application of the method in the calculations of the simplest electronic heteronuclear system, the HD^+ ion.

In order to compare our results to the literature, we use the CODATA 2006 values of the proton, deuteron, and triton masses expressed in terms of the electron mass:

$$m_\mu = 206.768\,282\,3m_e, \quad m_p = 1836.152\,672\,47m_e,$$

$$m_d = 3670.482\,965\,4m_e, \quad m_t = 5496.921\,526\,9m_e;$$

for muonic systems we also report the results obtained with the CODATA 2010 masses:

$$m_\mu = 206.768\,284\,3m_e, \quad m_p = 1836.152\,672\,45m_e,$$

$$m_d = 3670.482\,965\,2m_e, \quad m_t = 5496.921\,526\,7m_e.$$

3.1. Muonic systems

The three-particle muonic systems chosen for the testing are: deuteron–proton–muon ($d\mu\mu$), triton–proton–muon ($t\mu\mu$), and triton–deuteron–muon ($td\mu$). Since the muon is much heavier than the electron, the muonic density in these systems shifts considerably closer towards the heavier nucleus in comparison to the corresponding systems involving an electron. This makes the approach based on the BO approximation completely inadequate to study muonic molecules. Also, as mentioned, the contribution of the angular momentum of the muon in the muonic systems to the total all-particle angular momentum can be expected to be significant, more significant than the corresponding contribution of the electrons in the electronic molecules.

The ground $N = 0$ states of the three tested systems are calculated using the algorithm described in [6]. The method employs the $\phi_k^{N=0} = r_1^{m_k} \exp[-\mathbf{r}'(A_k \otimes I_3)\mathbf{r}]$ ECG basis functions which, as demonstrated before [7], for ordinary diatomic molecules produce very accurate results. Table 1 shows the comparison between the energies obtained for the ground vibrational rotationless ($N = 0$) states of $d\mu\mu$, $t\mu\mu$, and $td\mu$ ions, as well as for the first vibrational rotationless state of $td\mu$ obtained with 4000 ECG functions. The results are compared with the energies obtained by Frolov [10].

Table 2 shows the energies of the three muonic systems in the first rotationally excited state ($N = 1$) obtained using 4000 basis functions (3) employing the algorithm discussed in [1] and the algorithm presented in the present work. Since the first method yields the discrepancies on the order of 10^{-4} m. a.u., we will only discuss the second, much more accurate method. The variational optimization of the nonlinear parameters of the Gaussians is performed using the analytical-gradient-based procedure. Powers m_k in the preexponential factors, r_k^m , are optimized stochastically in the range from 0 to 250. Also the i index in the x_i prefactor ($i = 1$ or 2 in the present calculations) is optimized. The optimization of powers m_k and index i is completely unbiased.

From the results shown in the tables one can see that our present results show very good agreement with the very accurate calculations of Frolov. For the ground states of the

Table 1. $N = 0$ energies of $d\mu$, $t\mu$, and $td\mu$ expressed in muonic atomic units (m.a.u.) Energies obtained with [6] method are presented in the form of E_K , were K is a basis size. E_F are the energies obtained by Frolov [10] (only twelve significant figures are shown). Notation * denotes the first excited state.

	$d\mu$	$t\mu$	$td\mu$	$td\mu^*$
E_{1000}	-0.512 711 791 255	-0.519 880 084 674	-0.538 594 970 644	-0.488 065 322 286
E_{2000}	-0.512 711 792 261	-0.519 880 085 656	-0.538 594 971 639	-0.488 065 353 954
E_{3000}	-0.512 711 792 470	-0.519 880 085 694	-0.538 594 971 688	-0.488 065 354 202
E_{4000}	-0.512 711 792 477	-0.519 880 085 698	-0.538 594 971 703	-0.488 065 354 168
E_F	-0.512 711 792 482	-0.519 880 085 704	-0.538 594 971 709	-0.488 065 354 216
$E_{4000}-E_F$	-4.99[-12]	-5.82[-12]	-6.38[-12]	-4.81[-11]
CODATA 2010	-0.512 711 790 089	-0.519 880 084 097	-0.538 594 970 521	-0.488 065 352 973

Table 2. $N = 1$ energies of $d\mu$, $t\mu$, and $td\mu$ expressed in muonic atomic units (m.a.u.). $E_{2000}^{(1)}$ are energies obtained with 2000 ECGs with the method described in [1]. $E_K^{(i)}$ are energies obtained with the basis set of size K ; E_F are energies obtained by [10] (only twelve significant figures are shown).

	$d\mu$	$t\mu$	$td\mu$	$td\mu^*$
$E_{2000}^{(1)}$	-0.490 472 092 275	-0.499 290 669 563	-0.523 121 437 589	-0.481 962 411 413
$E_{1000}^{(i)}$	-0.490 664 162 274	-0.499 492 022 813	-0.523 191 450 721	-0.481 991 524 546
$E_{2000}^{(i)}$	-0.490 664 164 411	-0.499 492 024 751	-0.523 191 451 941	-0.481 991 526 580
$E_{3000}^{(i)}$	-0.490 664 164 591	-0.499 492 024 976	-0.523 191 451 991	-0.481 991 526 995
$E_{4000}^{(i)}$	-0.490 664 164 602	-0.499 492 024 990	-0.523 191 451 999	-0.481 991 527 042
% of $\varphi^{(2)}$	28.58	28.27	25.92	24.46
E_F	-0.490 664 164 604	-0.499 492 0249 90	-0.523 191 452 004	-0.481 991 527 055
$E_{4000}^{(i)}-E_F$	-1.51[-12]	-5.97[-13]	-4.88[-12]	-1.30[-11]
CODATA 2010	-0.490 664 161 706	-0.499 492 023 032	-0.523 191 450 474	-0.481 991 526 283

muonic systems the accuracy on the order of 10^{-12} a.u. or better is achieved, and for the vibrationally excited state of $td\mu$ the difference grows up to several 10^{-11} a.u. Such behavior is expected since the wave functions of the higher vibrational states have a more complex nodal structure and thus require larger number of basis functions to be described. Nevertheless, at this point we can conclude that the proposed method for calculating the $N = 1$ rotational excitation employing the ECG functions is efficient.

In table 2 we also show for each system the percentage of the basis functions with angular prefactor x_2 in the basis set. These are the functions describing the angular excitation of the muon. The numbers are relatively consistent for all considered systems and range approximately between 25% and 28%. The remaining basis functions have the x_1 prefactor. It is interesting to note that for the system where the first excited ‘vibrational’ state with $N = 1$ exists, i.e. $td\mu$, the number of ECGs with the x_2 prefactor is somewhat smaller than for the ground vibrational $N = 1$ state. This seems to indicate that with the vibrational excitation the muon contribution to the total angular momentum decreases.

3.2. HD^+

Now, as the algorithm is proven to be correct and efficient, we apply it to a more chemically relevant system, the HD^+

molecular ion, and determine the contribution of the angular excitation of the electron to its bound $N = 1$ rovibrational states designated as $(\nu, N = 1)$. The contribution is being determined by comparing the total non-BO energies of the states obtained using Gaussians (2) taken from our previous work [1] and using Gaussians (3) obtained in this work. The accuracy of the present results obtained for the $N = 1$, $\nu = 0, \dots, 22$ states of HD^+ is determined by comparing the energies of the $(\nu, N = 0 \rightarrow 1)$ transition frequencies with the literature values obtained with various theoretical and experimental methods.

Let us denote by $K + 1000$ the size of the largest basis set of Gaussians (2) generated for a particular state in our previous work [1]. In the process of growing the basis set to the size of $K + 1000$ for that state we also generated a basis set containing K functions of $\varphi_k^{(1)}$ type. In the present calculations we take this K basis set and augment it with additional functions allowing these new functions in the variational optimization to be either $\varphi_k^{(1)}$ or $\varphi_k^{(i)}$ functions. In the process of adding new Gaussians to the basis set, functions are added one at a time. The initial nonlinear parameters of a new Gaussian are obtained by randomly perturbing the parameters of one of the most contributing basis functions already included in the basis set. Next, the i index (this index in the present calculations can be either 1 or 2) and the p_k power of the Gaussian is optimized. This is followed by the

Table 3. Energy convergence for $N = 1$ rovibrational states of HD^+ . ν is the vibrational quantum number, K is the initial basis size, other four lines represent the energy obtained with a number of basis functions in the subscript. Energy values are in hartrees.

ν	0	1	2	3	4
K	1000	1000	2000	2000	2000
E_K	-0.597 698 117 270	-0.588 991 101 048	-0.580 721 817 887	-0.572 877 266 933	-0.565 446 156 398
E_{K+10}	-0.597 698 127 975	-0.588 991 111 313	-0.580 721 827 617	-0.572 877 275 535	-0.565 446 164 609
E_{K+500}	-0.597 698 128 074	-0.588 991 111 833	-0.580 721 828 085	-0.572 877 276 896	-0.565 446 166 105
E_{K+1000}	-0.597 698 128 157	-0.588 991 111 891	-0.580 721 828 098	-0.572 877 276 952	-0.565 446 166 143
ν	5	6	7	8	9
K	2000	3000	3000	3000	3000
E_K	-0.558 418 853 179	-0.551 787 358 384	-0.545 545 294 252	-0.539 687 917 327	-0.534 212 153 253
E_{K+10}	-0.558 418 861 196	-0.551 787 365 231	-0.545 545 301 459	-0.539 687 923 683	-0.534 212 157 760
E_{K+500}	-0.558 418 862 906	-0.551 787 367 601	-0.545 545 303 174	-0.539 687 926 107	-0.534 212 161 582
E_{K+1000}	-0.558 418 863 010	-0.551 787 367 661	-0.545 545 303 218	-0.539 687 926 437	-0.534 212 161 742
ν	10	11	12	13	14
K	3000	3000	3000	3000	4000
E_K	-0.529 116 643 823	-0.524 401 837 382	-0.520 070 088 900	-0.516 125 824 708	-0.512 575 697 349
E_{K+10}	-0.529 116 648 788	-0.524 401 841 604	-0.520 070 093 634	-0.516 125 828 801	-0.512 575 700 831
E_{K+500}	-0.529 116 652 013	-0.524 401 845 301	-0.520 070 097 370	-0.516 125 832 245	-0.512 575 704 067
E_{K+1000}	-0.529 116 652 126	-0.524 401 845 428	-0.520 070 097 632	-0.516 125 832 377	-0.512 575 704 189
ν	15	16	17	18	19
K	4000	5000	5000	5000	6000
E_K	-0.509 428 840 269	-0.506 697 146 745	-0.504 395 560 512	-0.502 542 374 245	-0.501 159 138 174
E_{K+10}	-0.509 428 843 651	-0.506 697 149 108	-0.504 395 563 332	-0.502 542 377 619	-0.501 159 140 158
E_{K+500}	-0.509 428 847 023	-0.506 697 153 282	-0.504 395 566 965	-0.502 542 381 685	-0.501 159 144 151
E_{K+1000}	-0.509 428 847 467	-0.506 697 153 483	-0.504 395 567 424	-0.502 542 382 117	-0.501 159 144 677
E_{K+2000}	-0.509 428 847 836	-0.506 697 153 549	-0.504 395 568 117	-0.502 542 383 121	-0.501 159 145 991
ν	20	21	22		
K	6000	6000	6000		
E_K	-0.500 269 319 648	-0.499 902 780 157	-0.499 864 341 698		
E_{K+10}	-0.500 269 321 257	-0.499 902 780 768	-0.499 864 341 829		
E_{K+500}	-0.500 269 322 485	-0.499 902 781 287	-0.499 864 342 132		
E_{K+1000}	-0.500 269 322 550	-0.499 902 781 600	-0.499 864 342 146		

optimization of the L_k matrix elements of the Gaussian performed with the gradient-aided method. After checking if the Gaussian generated this way is not linearly dependent with any Gaussian already included in the basis set, the new optimized Gaussian is included in the set. If a linear dependency is found, the Gaussian is discarded, and a new Gaussian is generated and optimized. After an addition of each new 100 Gaussians, the whole basis set is reoptimized with the gradient-based method (again reoptimizing one Gaussian at a time). In this way basis sets with the sizes $K + 10$, $K + 500$, and $K + 1000$ are generated.

The reason for starting the augmentation of the basis set of each state from the basis set of the size K and not $K + 1000$ is the realization that the results obtained in [1] were already practically converged for all states with the number of Gaussians equal to K . The addition of 1000 Gaussians and generating the basis set with $K + 1000$ functions changed the energy less than 10^{-9} hartree.

The results showing the energy changes for each state with the addition of 10, 500, and 1000 $\varphi_k^{(i)}$ functions are presented in table 3. It is interesting that the addition of just

10 $\varphi_k^{(i)}$ functions already leads to a significant energy lowering. By further addition of basis functions, the $K + 500$ and $K + 1000$ basis sets are generated. Comparing the energies obtained with the $K + 500$ and $K + 1000$ basis sets for each state shows that the energy changes less than 5×10^{-10} hartree between these two basis-set sizes. Upon a close examination of the obtained convergence, another thousand functions was added to both $N = 0$ and $N = 1$ basis sets for states $\nu = 15, \dots, 19$. Thus the results shown in the table should be considered as converged for all practical purposes.

The dissociation energies for the $(\nu, \nu = 1, \dots, 22; N = 1)$ rovibrational states obtained with the maximum number of $\varphi_k^{(i)}$ basis functions generated for each state in the present study, $E^{(i)}$, are shown in table 4. They are compared with the dissociation energies, $E^{(1)}$, obtained before [1] using $K + 1000$ $\varphi_k^{(1)}$ functions (see $\Delta^{(1-i)}$ which is the difference between $E^{(1)}$ and $E^{(i)}$). In the table we also show the percentage of the $\varphi_k^{(2)}$ functions in the basis set for each state, as well as the differences between the present dissociation energies for the $N = 1$ states and the results of Karr and Hilico [11] (see $\Delta_{N=1}$). The corresponding differences for the $N = 0$

Table 4. The effect of the addition of $\varphi_k^{(i)}$ functions to the basis set on the $N = 1$ rovibrational energies of HD^+ . Here ν is the vibrational state number, $E^{(1)}$ —dissociation energy obtained in [1] with only $\varphi_k^{(1)}$ basis functions, $E^{(i)}$ —dissociation energy obtained in the present study, %—percentage of $\varphi_k^{(2)}$ functions in the basis set, $\Delta^{(1-i)} = E^{(1)} - E^{(i)}$, $\Delta_{N=1}$ is a difference between $E^{(i)}$ and the energy obtained for $N = 1$ in [11], $\Delta_{N=0}$ is a difference between the energy reported in [6] and the result obtained for $N = 0$ in [11]. All values are in cm^{-1} and reported to the maximum number of significant figures given by the least accurate calculation.

ν	$E^{(1)}$	$E^{(i)}$	%	$\Delta^{(1-i)}$	$\Delta_{N=1}$	$\Delta_{N=0}$
0	21472.147 407	21472.149 761	7.00	0.002 354	-0.000 008	-0.000 011
1	19561.178 272	19561.180 576	7.00	0.002 304	0.000 009	-0.000 033
2	17746.280 336	17746.282 564	7.07	0.002 227	-0.000 005	-0.000 004
3	16024.600 431	16024.602 593	7.67	0.002 162	-0.000 031	-0.000 029
4	14393.660 190	14393.662 287	8.13	0.002 097	-0.000 030	-0.000 027
5	12851.345 495	12851.347 523	7.53	0.002 028	-0.000 055	-0.000 052
6	11395.900 525	11395.902 525	7.80	0.002 000	-0.000 054	-0.000 073
7	10025.925 790	10025.927 733	8.77	0.001 943	-0.000 042	-0.000 065
8	8740.380 198	8740.382 123	7.38	0.001 925	-0.000 133	-0.000 218
9	7538.588 892	7538.590 685	7.97	0.001 793	-0.000 079	-0.000 099
10	6420.253 872	6420.255 591	8.73	0.001 718	-0.000 175	-0.000 180
11	5385.473 473	5385.475 129	8.93	0.001 655	-0.000 113	-0.000 116
12	4434.764 561	4434.766 378	7.60	0.001 817	-0.000 602	-0.000 865
13	3569.098 721	3569.100 215	9.02	0.001 494	-0.000 230	-0.000 239
14	2789.935 720	2789.937 139	8.22	0.001 419	-0.000 289	-0.000 219
15	2099.280 533	2099.281 921	5.58	0.001 469	-0.000 715	-0.000 727
16	1499.743 107	1499.744 390	5.77	0.001 305	-0.000 746	-0.000 271
17	994.603 455	994.604 638	6.29	0.001 335	-0.001 228	-0.001 180
18	587.876 170	587.877 476	6.61	0.001 527	-0.000 696	-0.000 872
19	284.290 742	284.291 949	5.20	0.001 507	-0.000 420	-0.000 407
20	88.997 980	88.998 566	7.50	0.000 586	-0.000 126	-0.000 165
21	8.551 893	8.552 126	5.03	0.000 288	-0.000028	-0.00047
22	0.115 616	0.115 641	4.80	0.000 025	0.0000	0.0000
rms				0.001 715	0.000 412	0.000 424

states obtained by subtracting the results of Kinghorn and Adamowicz [6] from the results of Karr and Hilico [11] are also shown in the table (see $\Delta_{N=0}$).

The comparison of the dissociation energies calculated with the $\varphi_k^{(2)}$ basis functions included in the basis set with those computed using only the $\varphi_k^{(1)}$ functions shows that the explicit inclusion of angular excitations of the electron leads to a noticeable energy improvement for all states. In figure 1 the relative differences between the two energies, $(E^{(i)} - E^{(1)})/E^{(i)}$, for all 23 bound vibrational states are plotted as a function of the vibrational quantum number. The plot shows that the improvement slowly decreases as the vibrational quantum number increases from 0 to 19 and then rapidly decreases for the three highest states. This behavior can be easily explained when the charge asymmetry in the vibrationally excited HD^+ molecular ion is considered. In the non-BO calculations performed before [4] we showed that in lower vibrational states of HD^+ the electron is on average slightly closer to the deuteron than to the proton, but in the highest states the bond in HD^+ becomes more ionic and the electron significantly shifts towards the deuteron. This behavior is shown in figure 1 where the difference between the proton-electron and deuteron-electron average distances is plotted as a function of the vibrational quantum number for the (ν , $N=1$) states. As the electron moves closer to the deuteron it also moves closer to the centre of mass of the

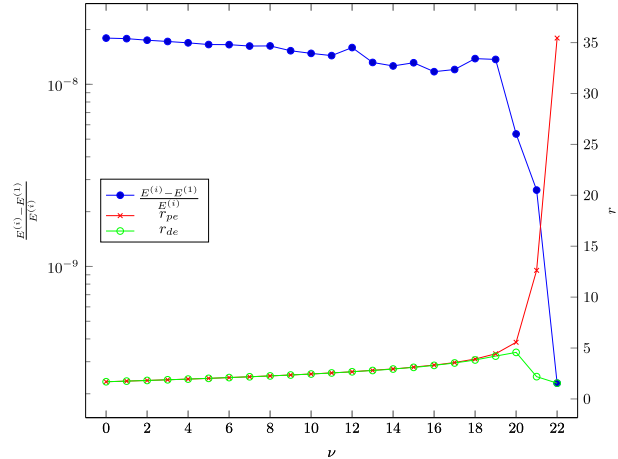


Figure 1. Relative contribution of the electronic excitation to the total energies of the $N = 1$ rovibrational states of HD^+ correlated with the charge asymmetry. $E^{(i)}$ and $E^{(1)}$ have the same meaning as in table 4, r_{pe} and r_{de} are the proton-electron and deuteron-electron distances in a.u. calculated in [4].

system (i.e., the centre of rotation for the molecule). This makes the moment of inertia of the rotating electron smaller and results in less energy being accumulated in its rotation. This, in turn, makes the energy lowering resulting from including basis functions ($\varphi_k^{(i)}$) to decrease for top vibrational

states. A smaller contribution from the angular excitation of the electron to the total rotational excitation means that the results obtained with only basis functions $\varphi_k^{(1)}$ in [1] for the highest vibrational excitations are more accurate than the results obtained for the lower states.

Another property which can be calculated using the results of the present calculations are the rotational transition energies. These energies are obtained by subtracting the dissociation energies of the ($\nu, N = 1$) states from the dissociation energies of the ($\nu, N = 0$) states. The results are shown in table 5. The present transition energies are compared in the table with the transition energies obtained using other highly accurate theoretical methods, such as the artificial-channels method of Blaust-Kurti *et al* [12] and Moss [13], the Lagrange-mesh method of Pilon and Baye [14], the method based on the BO potential energy curve augmented with adiabatic, non-adiabatic, and relativistic corrections [15], and non-BO methods utilizing various three-particle basis functions [11, 16, 17]. The transition energies obtained in [1] using the $\varphi_k^{(1)}$ basis functions are also shown for comparison. The experimental values for the (21,0)→(21,1) and (22,0)→(22,1) transitions shown in table 5 are taken from [18], the experimental value for the (17,0)→(17,1) transition is determined using the (17,0)→(22,0) and (17,1)→(22,1) transitions taken from [19], and the (22,0)→(22,1) transition is taken from [18].

As one can see the agreement of the present results with the most recent results of Karr and Hilico [11], Tian *et al* [16], Korobov [17], and Pilon and Baye [14] and with the relatively old results of Moss [13] is very good. The root-mean-square (rms) deviations of our results from the results of Moss [13] and Karr and Hilico [11], where the full set of the transitions were evaluated, are under 0.0003 cm⁻¹. The rms deviations from the highly accurate results of Tian *et al* [16], Korobov [17], and Pilon and Baye [14] for the lowest few states are on the order of 10⁻⁶ cm⁻¹.

4. Conclusion

A method for describing a rotational excitation of a diatomic molecule without assuming the BO approximation is developed and implemented. The approach can be applied to diatomic molecules with an arbitrary number of σ electrons. The method treats all particles forming the system, i.e. the nuclei and the electrons, on equal footing. Thus, the wave function representing a rotational excitation is a superposition of terms describing a rotational excitation of the nuclei (the dominant contribution) and an angular excitation of the electron. The results of the present calculations show that, only if both contributions are included in the calculation, high accuracy of the results can be reached. That conclusion is important for our future work targeting the extension of the method to arbitrary N values.

The property, which is evaluated and compared with the results of other high-accuracy calculation, is the dissociation energy. This energy is determined for all 23 bound rovibrational states of HD⁺ corresponding to the lowest rotationally

excited state of the system (i.e., the $N = 1$ states). The rms deviation between the dissociation energies obtained using the present method and the best literature results of Karr and Hilico [11] obtained with a method specifically designed to handle three-particle systems is only 0.000 412 cm⁻¹. The deviation is smaller than the rms deviation of 0.000 424 m⁻¹ for the rotation-less states calculated using an approach similar to the one used here. Interestingly, when one assumes that the contribution of the angular excitation of the electron to the rovibrational excitations of the molecule is negligible and the corresponding terms are not included in the wavefunction expansion, the rms energy deviation for the $N = 1$ rovibrational states increases to 0.001 715 m⁻¹.

It is also demonstrated that the method is applicable to systems containing particles with any masses and charges without any additional modifications. We should also note that many of the calculations of the muonic ions have been performed using methods restricted to three-particle systems and significant complications have arisen when attempts were made to use these methods to systems with the number of particles increased even by one ([20]). Most of these previous calculations have been based on the work of Delves and Kalotas [21]. These include the very high accuracy calculations of Frolov and co-workers ([10, 22–24]). Other approaches such as, for example, the hyperspherical approach [25], the Hylleraas method ([26]), and the methods employing sturmian basis sets (e.g., [27]), are also limited to few-body problems by design. However, as mentioned, the present method can be applied to calculate binuclear systems with an arbitrary numbers of particles. Thus, rotationally excited states of larger systems can be considered. At this point the only limitation that constrains the applicability of the method are the computer resources.

Another interesting discussion point is the effect of the well-known improper cusp and long-range behavior of the Gaussian functions. The possibility to achieve the energy accuracy on the order of 10⁻¹² a.u. achieved for some systems in present study suggests that the accuracy of the present calculations is probably more limited by the numerical precision used in the calculations (the double precision) rather than by the cusp deficiencies. Though, the improper cusp behavior is likely also a contributing factor. It would be interesting to test this point by increasing the accuracy of the calculations by, for example, using the Bailey arbitrary-precision computation package [28, 29].

It has to be noted that, while the accuracy of several of 10⁻¹² a.u. can, in principle, be reached, such calculations require extensive basis sets and significant computational resources. For that reason most of the calculations performed in this work are stopped when the accuracy on the order of 10⁻¹⁰ a.u. is achieved. While such accuracy is not competitive with the most accurate calculations of the three-body systems, the major advantage of the present method is that it is applicable to systems with more than three particles. In that context, it would be interesting to see how much the inclusion of the electronic angular excitations affects other properties such as, for example, the interparticle distances, the oscillator strengths, etc. It would also be interesting to apply the present

Table 5. Energies of the ($\nu, N = 0 \rightarrow 1$) transitions, Δ , of HD $^+$ compared to those calculated in [1, 11–17] and measured in [18, 19]. All values are in cm $^{-1}$ and reported to the maximum number of significant figures given by the least accurate calculation.

ν	Δ	[13]	[12]	[15]	[1]	[11]	[16]	[17]	[14]	[18, 19]
0	43.859 898	0.000 002	−0.0014		0.002 402	−0.000 003	−0.000 003	−0.000 003	−0.000 003	
1	41.857 657	−0.000 057	−0.0013		0.002 343	−0.000 042	−0.000 011	−0.000 011	−0.000 010	
2	39.916 312	0.000 088	−0.0014		0.002 188	0.000 001	0.000 001	0.000 001	0.000 000	
3	38.028 253	0.000 047	−0.0012		0.002 147	0.000 002	0.000 002	0.000 002	0.000 015	
4	36.186 058	0.000 042	−0.0012		0.002 142	0.000 003	0.000 003	0.000 003		
5	34.382 364	0.000 036	−0.0012		0.002 036	0.000 002	0.000 002			
6	32.609 752	0.000 048	−0.0012		0.002 048	−0.000 019				
7	30.860 718	0.000 082	−0.0013		0.001 982	−0.000 023				
8	29.127 381	0.000 119	−0.0012		0.001 919	−0.000 085				
9	27.401 707	−0.000 007	−0.0012		0.001 793	−0.000 021				
10	25.674 717	−0.000 017	−0.0012		0.001 683	−0.000 005				
11	23.936 828	−0.000 028	−0.0013		0.001 672	−0.000 003				
12	22.177 078	0.000 322	−0.0015		0.001 822	−0.000 263				
13	20.384 035	0.000 065	−0.0012		0.001 465	−0.000 009				
14	18.542 768	−0.000 068	−0.0009		0.001 432	0.000 070				
15	16.636 071	0.000 129	−0.0012		0.001 429	−0.000 159				
16	14.643 321	0.000 179	−0.0011		0.001 279	−0.000 210				
17	12.537 067	0.000 433	−0.0017		0.001 333	−0.000 455		−0.001		
18	10.280 950	0.000 950	−0.0016		0.001 550	−0.000 887				
19	7.823 680	0.000 820	−0.0015		0.0015 20	−0.000 846				
20	5.076 647	0.000 053	−0.0006	−0.0004	0.000553	−0.000 039				
21	1.663 065	0.000 135	−0.0014	0.0011	0.000 335	−0.00019		0.000		
22	0.315 202	−0.000 002		0.0002	−0.000 002	−0.0001		0.000		
rms		0.000 294	0.0013	0.0007	0.001 721	0.000 288	0.000 005	0.000 005	0.000 009	0.001

method to study rovibrational excitations of diatomics with more electrons such as H_2 , LiH^+ , LiH , etc.

Another class of systems which can be considered using the method involves the systems of interest for muon-catalyzed fusion, e.g. systems where an electron is attached to the muonic systems considered in the present study. Calculations of such systems are forthcoming.

It should be noted that, while the current study is limited to only systems with Coulombic interactions, the convenient analytical properties of Gaussian functions allow for relatively simple extension of the method to study systems with more general forms of interactions. Bound states of clusters of ultracold atoms are one of such possible applications.

Acknowledgments

This material is based upon work supported by the National Science Foundation under Grant No. 1228509. This work has been supported in part by the National Science Foundation through the graduate research fellowship program (GRFP) awarded to Keeper L Sharkey (Grant No. DGE1-1143953). We are grateful to the University of Arizona Center of Computing and Information Technology for the use of their computer resources.

Appendix

Matrix element and gradient derivations are shown in a step-by-step fashion in this section.

A.1. Overlap

It was shown in [1] that

$$\begin{aligned} & -\frac{\partial}{\partial \omega_{kl}} \langle \phi_k | r_1^{m_k+m_l} \exp[-\mathbf{r}'(\omega_{kl} \mathbf{W}^{(ij)}) \mathbf{r}] | \phi_l \rangle \Big|_{\omega_{kl}=0} \\ &= \frac{1}{\sqrt{\pi}} \Gamma\left(\frac{3+m_k+m_l}{2}\right) \langle \phi_k | \phi_l \rangle \operatorname{tr}\left[A_{kl}^{-1} J_{11}\right]^{\frac{m_k+m_l}{2}} \\ & \quad \times \left(\operatorname{tr}\left[\mathbf{A}_{kl}^{-1} \mathbf{W}^{(ij)}\right] + \frac{m_k+m_l}{3} \right. \\ & \quad \left. \cdot \frac{\operatorname{tr}\left[\mathbf{A}_{kl}^{-1} \mathbf{W}^{(ij)} \mathbf{A}_{kl}^{-1} \mathbf{J}_{11}\right]}{\operatorname{tr}\left[\mathbf{A}_{kl}^{-1} J_{11}\right]} \right), \end{aligned} \quad (11)$$

where

$$\langle \phi_k | \phi_l \rangle = \pi^{3n/2} |A_{kl}|^{-3/2} \quad (12)$$

and $\mathbf{J}_{11} = J_{11} \otimes I_3$, where J_{11} is a particular case of the matrix defined as:

$$J_{ij} = \begin{cases} E_{ii}, & \text{if } i=j \\ E_{ii} + E_{jj} - E_{ij} - E_{ji}, & \text{otherwise} \end{cases} \quad (13)$$

where E_{ij} is a matrix with 1 in the (i, j) position and 0's elsewhere. Evaluating traces, we obtain:

$$\begin{aligned} \operatorname{tr}\left[A_{kl}^{-1} J_{11}\right] &= \left(A_{kl}^{-1}\right)_{11}, \\ \operatorname{tr}\left[\mathbf{A}_{kl}^{-1} \mathbf{W}^{(ij)}\right] &= \left(A_{kl}^{-1}\right)_{ij}, \\ \operatorname{tr}\left[\mathbf{A}_{kl}^{-1} \mathbf{W}^{(ij)} \mathbf{A}_{kl}^{-1} \mathbf{J}_{11}\right] &= \left(A_{kl}^{-1}\right)_{ii} \left(A_{kl}^{-1}\right)_{jj}. \end{aligned}$$

Plugging these into equation (11) and implementing the short hand notation, $\alpha_{ij} = (A_{kl}^{-1})_{ij}$, we can write:

$$\begin{aligned} \langle \varphi_k^{(i)} | \varphi_l^{(j)} \rangle &= \frac{1}{\sqrt{\pi}} \Gamma\left(\frac{3+m_k+m_l}{2}\right) \\ & \times \langle \phi_k | \phi_l \rangle \alpha_{11}^{\frac{m_k+m_l}{2}} \left(\alpha_{ij} + \frac{m_k+m_l}{3} \cdot \frac{\alpha_{1i}\alpha_{1j}}{\alpha_{11}} \right). \end{aligned} \quad (14)$$

In order to normalize the expression above, two integrals are needed:

$$\begin{aligned} \langle \varphi_k^{(i)} | \varphi_k^{(i)} \rangle &= \frac{\pi^{\frac{3n-1}{2}}}{2^{\frac{3n-2-2m_k}{2}}} \frac{\Gamma\left(\frac{3+2m_k}{2}\right)}{\|L_k\|} \left(A_k^{-1}\right)_{11}^{m_k} \\ & \times \left(\left(A_k^{-1}\right)_{ii} + \frac{2m_k}{3} \cdot \frac{\left(A_k^{-1}\right)_{1i}^2}{\left(A_k^{-1}\right)_{11}} \right) \end{aligned} \quad (15)$$

and

$$\begin{aligned} \langle \varphi_l^{(j)} | \varphi_l^{(j)} \rangle &= \frac{\pi^{\frac{3n-1}{2}}}{2^{\frac{3n-2-2m_l}{2}}} \frac{\Gamma\left(\frac{3+2m_l}{2}\right)}{\|L_l\|} \left(A_l^{-1}\right)_{11}^{m_l} \\ & \times \left(\left(A_l^{-1}\right)_{jj} + \frac{2m_l}{3} \cdot \frac{\left(A_l^{-1}\right)_{1j}^2}{\left(A_l^{-1}\right)_{11}} \right). \end{aligned} \quad (16)$$

Thus, the normalized overlap has the following form:

$$\begin{aligned} S_{kl}^{(ij)} &= \frac{\langle \varphi_k^{(i)} | \varphi_l^{(j)} \rangle}{\sqrt{\langle \varphi_k^{(i)} | \varphi_k^{(i)} \rangle \langle \varphi_l^{(j)} | \varphi_l^{(j)} \rangle}} \\ &= 2f_{kl} \gamma_1(m_k, m_l) \left(\frac{\alpha_{11}}{\left(A_k^{-1}\right)_{11}} \right)^{\frac{m_k}{2}} \left(\frac{\alpha_{11}}{\left(A_l^{-1}\right)_{11}} \right)^{\frac{m_l}{2}} \\ & \times \left(\alpha_{ij} + \frac{m_k+m_l}{3} \cdot \frac{\alpha_{1i}\alpha_{1j}}{\alpha_{11}} \right) / \\ & \left(\left(\left(A_k^{-1}\right)_{ii} + \frac{2m_k}{3} \cdot \frac{\left(A_k^{-1}\right)_{1i}^2}{\left(A_k^{-1}\right)_{11}} \right)^{-\frac{1}{2}} \right. \\ & \quad \left. \times \left(\left(A_l^{-1}\right)_{jj} + \frac{2m_l}{3} \cdot \frac{\left(A_l^{-1}\right)_{1j}^2}{\left(A_l^{-1}\right)_{11}} \right)^{-\frac{1}{2}} \right), \end{aligned} \quad (17)$$

where

$$f_{kl} = \frac{1}{2^{3n/2}} \left(\frac{|A_{kl}|}{\|L_k\| \|L_l\|} \right)^{-3/2},$$

$$\gamma_1(m_k, m_l) = \frac{2^{\frac{m_k+m_l}{2}} \Gamma\left(\frac{3+m_k+m_l}{2}\right)}{\sqrt{\Gamma\left(\frac{3+2m_k}{2}\right) \Gamma\left(\frac{3+2m_l}{2}\right)}}.$$

Before we evaluate the derivative of the overlap integral with respect to the Gaussian exponential parameters, let us define two derivative operators:

$$\partial_k \equiv \frac{\partial}{\partial(\text{vech } L_k)'}, \quad \partial_l \equiv \frac{\partial}{\partial(\text{vech } L_l)'}$$

Using these operators we evaluate the following derivatives:

$$\partial_k \alpha_{ij}^x = -x \alpha_{ij}^{x-1} \cdot \text{vech}[A_{kl}^{-1}(E_{ij} + E_{ji}) A_{kl}^{-1} L_k] \quad (18)$$

$$\partial_k (A_k^{-1})_{ij}^x = -x (A_k^{-1})_{ij}^{x-1} \cdot \text{vech}[A_k^{-1}(E_{ij} + E_{ji})(L_k^{-1})'] \quad (19)$$

$$\partial_k |A_{kl}|^x = 2x |A_{kl}|^x \cdot \text{vech}[A_{kl}^{-1} L_k] \quad (20)$$

$$\partial_k \|L_k\|^x = x \|L_k\|^x \cdot \text{vech}[(L_k^{-1})'] \quad (21)$$

Now we write the gradient of the overlap integral with respect to the exponential parameters of the k function as:

$$\begin{aligned} \partial_k S_{kl}^{(ij)} &= S_{kl}^{(ij)} \left\{ \frac{3}{2} \text{vech}[(L_k^{-1})' - 2A_{kl}^{-1} L_k] \right. \\ &\quad + \frac{m_k + m_l}{2\alpha_{11}} \partial_k \alpha_{11} - \frac{m_k}{2(A_k^{-1})_{11}} \partial_k (A_k^{-1})_{11} \\ &\quad + \left(\alpha_{ij} + \frac{m_k + m_l}{3} \frac{\alpha_{1i} \alpha_{1j}}{\alpha_{11}} \right)^{-1} \\ &\quad \times \left(\partial_k \alpha_{ij} + \frac{m_k + m_l}{3} \frac{\alpha_{1i}}{\alpha_{11}} \left(\frac{\alpha_{1j}}{\alpha_{1i}} \partial_k \alpha_{1i} \right. \right. \\ &\quad \left. \left. + \partial_k \alpha_{1j} - \frac{\alpha_{1j}}{\alpha_{11}} \partial_k \alpha_{11} \right) \right) \\ &\quad - \frac{1}{2} \left((A_k^{-1})_{ii} + \frac{2m_k}{3} \frac{(A_k^{-1})_{1i}^2}{(A_k^{-1})_{11}} \right)^{-1} \\ &\quad \times \left(\partial_k (A_k^{-1})_{ii} + \frac{2m_k}{3} \frac{(A_k^{-1})_{1i}}{(A_k^{-1})_{11}} \left(2\partial_k (A_k^{-1})_{1i} \right. \right. \\ &\quad \left. \left. - \frac{(A_k^{-1})_{1i}}{(A_k^{-1})_{11}} \partial_k (A_k^{-1})_{11} \right) \right) \left. \right\}. \end{aligned} \quad (22)$$

Similarly, we can calculate the derivatives with respect to the exponential parameters of the l function:

$$\begin{aligned} \partial_l \alpha_{ij}^x &= -x \alpha_{ij}^{x-1} \\ &\quad \cdot \text{vech}[PA_{kl}^{-1}(E_{ij} + E_{ji}) A_{kl}^{-1} P' L_l] \end{aligned} \quad (23)$$

$$\begin{aligned} \partial_l (A_l^{-1})_{ij}^x &= -x (A_l^{-1})_{ij}^{x-1} \\ &\quad \cdot \text{vech}[PA_l^{-1}(E_{ij} + E_{ji}) A_l^{-1} P' L_l] \end{aligned} \quad (24)$$

$$\partial_l |A_{kl}|^x = 2x |A_{kl}|^x \cdot \text{vech}[PA_{kl}^{-1} P' L_l] \quad (25)$$

$$\partial_l \|L_l\|^x = x \|L_l\|^x \cdot \text{vech}[PA_l^{-1} P' L_l] \quad (26)$$

and

$$\begin{aligned} \partial_l S_{kl}^{(ij)} &= S_{kl}^{(ij)} \left\{ \frac{3}{2} \text{vech}[PA_l^{-1} P' L_l - 2PA_{kl}^{-1} P' L_l] \right. \\ &\quad + \frac{m_k + m_l}{2\alpha_{11}} \partial_l \alpha_{11} - \frac{m_l}{2(A_l^{-1})_{11}} \partial_l (A_l^{-1})_{11} \\ &\quad + \left(\alpha_{ij} + \frac{m_k + m_l}{3} \frac{\alpha_{1i} \alpha_{1j}}{\alpha_{11}} \right)^{-1} \\ &\quad \times \left(\partial_l \alpha_{ij} + \frac{m_k + m_l}{3} \frac{\alpha_{1i}}{\alpha_{11}} \left(\frac{\alpha_{1j}}{\alpha_{1i}} \partial_l \alpha_{1i} \right. \right. \\ &\quad \left. \left. + \partial_l \alpha_{1j} - \frac{\alpha_{1j}}{\alpha_{11}} \partial_l \alpha_{11} \right) \right) \\ &\quad - \frac{1}{2} \left((A_l^{-1})_{jj} + \frac{2m_l}{3} \frac{(A_l^{-1})_{1j}^2}{(A_l^{-1})_{11}} \right)^{-1} \\ &\quad \times \left(\partial_l (A_l^{-1})_{jj} + \frac{2m_l}{3} \frac{(A_l^{-1})_{1j}}{(A_l^{-1})_{11}} \left(2\partial_l (A_l^{-1})_{1j} \right. \right. \\ &\quad \left. \left. - \frac{(A_l^{-1})_{1j}}{(A_l^{-1})_{11}} \partial_l (A_l^{-1})_{11} \right) \right) \left. \right\}. \end{aligned} \quad (27)$$

A.2. Potential Energy

In order to evaluate the potential energy integral we calculate the expectation value of the $1/r_{pg}$ operator. To represent this operator we use the following integral transform:

$$\frac{1}{r_{pg}} = \frac{2}{\sqrt{\pi}} \int_0^\infty \exp[-u^2 r_{pg}^2] d u. \quad (28)$$

Now, using the partial differentiation with respect to two parameter, u and ω we get:

$$\begin{aligned} \langle \phi_k^{(i)} | \frac{1}{r_{pg}} | \phi_l^{(j)} \rangle &= \langle x_i x_j r_1^{(m_k+m_l)} \frac{1}{r_{pg}} \\ &\times \exp[-\mathbf{r}' \mathbf{A}_{kl} \mathbf{r}] \rangle \\ &= -\frac{\partial}{\partial \omega} (-1)^m \frac{\partial^m}{\partial u^m} \frac{2}{\sqrt{\pi}} \int_0^{+\infty} \\ &\times \langle \exp[-\mathbf{r}' (\mathbf{A}_{kl} + \omega \mathbf{W}^{(ij)} \\ &+ u \mathbf{J}_{11} + t^2 \mathbf{J}_{pg}) \mathbf{r}] \rangle d t \Big|_{\omega=u=0}, \quad (29) \end{aligned}$$

where $m_k + m_l = 2m$, $m = 0, 1, 2, \dots$. Integrating over the spatial coordinates gives:

$$\begin{aligned} &\langle \exp[-\mathbf{r}' (\mathbf{A}_{kl} + \omega \mathbf{W}^{(ij)} + u \mathbf{J}_{11} + t^2 \mathbf{J}_{pg}) \mathbf{r}] \rangle \\ &= \pi^{3n/2} |\mathbf{A}_{kl} + \omega \mathbf{W}^{(ij)} + u \mathbf{J}_{11} + t^2 \mathbf{J}_{pg}|^{-1/2} \\ &= \pi^{\frac{3n}{2}} |A_{kl}|^{-\frac{3n}{2}} |I_{3n} + \omega \mathbf{W}^{(ij)} \mathbf{A}_{kl}^{-1} \\ &\quad + u \mathbf{J}_{11} \mathbf{A}_{kl}^{-1} + t^2 \mathbf{J}_{pg} \mathbf{A}_{kl}^{-1}|^{-\frac{1}{2}}. \quad (30) \end{aligned}$$

Applying the derivative with respect to ω gives:

$$\begin{aligned} &- \frac{\partial}{\partial \omega} \langle \exp[-\mathbf{r}' (\mathbf{A}_{kl} + \omega \mathbf{W}^{(ij)} + u \mathbf{J}_{11} + t^2 \mathbf{J}_{pg}) \mathbf{r}] \rangle \\ &= \frac{\pi^{\frac{3n}{2}}}{2} |A_{kl}|^{-\frac{3n}{2}} \frac{\alpha_{ij} + u(\alpha_{11}\alpha_{ij} - \eta) + t^2(\beta\alpha_{ij} - \theta)}{\left(1 + u\alpha_{11} + t^2(\beta + u(\alpha_{11}\beta - \chi))\right)^{\frac{s}{2}}}, \quad (31) \end{aligned}$$

where

$$\begin{aligned} \beta &= \begin{cases} \alpha_{pg} & \text{if } p = g \\ \alpha_{pp} + \alpha_{gg} - 2\alpha_{pg} & \text{otherwise,} \end{cases} \\ \eta &= \alpha_{1i}\alpha_{1j}, \\ \chi &= \begin{cases} \alpha_{pg}^2 & \text{if } p = g \\ (\alpha_{1p} - \alpha_{1g})^2 & \text{otherwise,} \end{cases} \\ \theta &= \begin{cases} \alpha_{ig}\alpha_{jp} & \text{if } p = g \\ (\alpha_{ip} - \alpha_{ig})(\alpha_{jp} - \alpha_{jg}) & \text{otherwise.} \end{cases} \quad (32) \end{aligned}$$

Next the integration over parameter t is performed and the operator $(-1)^{m+1} \partial^m / \partial u^m$ is applied. With that the expectation value (29) becomes:

$$\begin{aligned} \langle \phi_k^{(i)} | \frac{1}{r_{pg}} | \phi_l^{(j)} \rangle &= \frac{\pi^{\frac{3n-1}{2}}}{3 |A_{kl}|^{\frac{3n}{2}}} \left\{ \Gamma(m+1) \alpha_{11}^{m-1} \beta^{-\frac{3}{2}} \right. \\ &\times (3\alpha_{11}\alpha_{ij}\beta - \alpha_{11}\theta + 2m\beta\eta) \\ &+ \frac{1}{\sqrt{\pi}} \sum_{k=1}^m \frac{\Gamma(m+1)\Gamma(k+1/2)}{\Gamma(k+1)} \\ &\times \alpha_{11}^{m-k-1} \beta^{-k-3/2} (\alpha_{11}\beta - \chi)^k \\ &\times (\alpha_{11}((3+2k)\alpha_{ij}\beta \\ &\left. - (1+2k)\theta) + 2(m-k)\beta\eta \right\}. \quad (33) \end{aligned}$$

Normalization and simplification yields the final expression used to compute the potential energy integral:

$$V_{kl}^{(ij)} = \sum_{p,g>p}^n q_p q_g R_{kl}^{(ij,pg)} + \sum_{p=1}^n q_0 q_p R_{kl}^{(ij,pp)}, \quad (34)$$

where

$$\begin{aligned} R_{kl}^{(ij,pg)} &= \frac{S_{kl}^{(ij)}}{\beta^{3/2}(3\alpha_{11}\alpha_{ij} - m\eta)} \\ &\times \frac{\Gamma(m+1)}{\Gamma(m+3/2)} \{ \alpha_{11}(3\alpha_{ij}\beta - \theta) + 2m\beta\eta \\ &+ \frac{1}{\sqrt{\pi}} \sum_{k=1}^m \frac{\Gamma(k+1/2)}{\Gamma(k+1)} \left(1 - \frac{\chi}{\alpha_{11}\beta}\right)^k \\ &\times (\alpha_{11}((3+2k)\alpha_{ij}\beta - (1+2k)\theta) \\ &+ 2(m-k)\beta\eta) \}. \quad (35) \end{aligned}$$

Since the expressions for $\partial_k S_{kl}^{ij}$, $\partial_l S_{kl}^{ij}$, $\partial_k \alpha^{ij}$, and $\partial_l \alpha^{ij}$ are known, one can easily compute the gradient of (34) treating operators ∂_k and ∂_l as ordinary partial differentiation operators.

A.3. Kinetic Energy

The kinetic energy operator can be written in the following quadratic form:

$$-\frac{1}{2} \left(\sum_{i=1}^n \frac{1}{\mu_i} \nabla_{\mathbf{r}_i}^2 + \sum_{i \neq j} \frac{1}{m_0} \nabla_{\mathbf{r}_i} \nabla_{\mathbf{r}_j} \right) = -\nabla'_{\mathbf{r}} \mathbf{M} \nabla_{\mathbf{r}}, \quad (36)$$

where the mass matrix, \mathbf{M} , is $\mathbf{M} = M \otimes I_3$ with the diagonal elements set to $1/(2\mu_1)$, $1/(2\mu_2)$, ..., $1/(2\mu_n)$ and with the off-diagonal elements set to $1/(2m_0)$. m_0 is the mass of the reference nucleus and μ_1 , ..., and μ_n are the reduced masses of the pseudoparticles.

The kinetic-energy matrix element is:

$$\langle \phi_k^{(i)} | -\nabla'_{\mathbf{r}} \mathbf{M} \nabla_{\mathbf{r}} | \phi_l^{(j)} \rangle = \langle \nabla_{\mathbf{r}} \phi_k^{(i)} | \mathbf{M} | \nabla'_{\mathbf{r}} \phi_l^{(j)} \rangle. \quad (37)$$

First, we determine the derivative of the basis function (3):

$$\begin{aligned} \langle \nabla'_{\mathbf{r}} \phi_k^{(i)} | &= \langle \mathbf{v}_k (\mathbf{r}' \mathbf{J}_{11} \mathbf{r})^{m_k/2} \exp[-\mathbf{r}' \mathbf{A}_k \mathbf{r}] | \\ &+ \langle m_k (\mathbf{v}_k' \mathbf{r}) (\mathbf{r}' \mathbf{J}_{11} \mathbf{r})^{m_k/2-1} (\mathbf{J}_{11} \mathbf{r}) \exp[-\mathbf{r}' \mathbf{A}_k \mathbf{r}] | \\ &- \langle 2(\mathbf{A}_k \mathbf{r}) (\mathbf{v}_k^{N=1'} \mathbf{r}) (\mathbf{r}' \mathbf{J}_{11} \mathbf{r})^{m_k/2} \exp[-\mathbf{r}' \mathbf{A}_k \mathbf{r}] | \\ &= \langle \mathbf{v}_k \phi_k^{N=0} | + \left\langle \frac{m_k}{r_1^2} (\mathbf{J}_{11} \mathbf{r}) \phi_k^{(i)} \right\rangle - \langle 2(\mathbf{A}_k \mathbf{r}) \phi_k^{(i)} |, \quad (38) \end{aligned}$$

where $\phi_k^{N=0} = r_1^{m_k} \exp[-\mathbf{r}' (A_k \otimes I_3) \mathbf{r}]$. Multiplying the above by the mass matrix and then by the corresponding ket containing the l function, the following nine integrals are obtained:

$$\langle \nabla_{\mathbf{r}} \varphi_k^{(i)} | \mathbf{M} | \nabla'_{\mathbf{r}} \varphi_l^{(j)} \rangle = \langle \phi_k^{N=0} | \mathbf{v}_k' \mathbf{M} \mathbf{v}_l | \phi_l^{N=0} \rangle \quad (39)$$

$$+ m_l \langle \phi_k^{N=0} | \frac{\mathbf{v}_k' \mathbf{M} \mathbf{J}_{11} \mathbf{r}}{r_1^2} | \varphi_l^{(j)} \rangle \quad (40)$$

$$- 2 \langle \phi_k^{N=0} | \mathbf{v}_k' \mathbf{M} \mathbf{A}_l \mathbf{r} | \varphi_l^{(j)} \rangle \quad (41)$$

$$+m_k \langle \varphi_k^{(i)} | \frac{\mathbf{r}' \mathbf{J}_{11} \mathbf{M} \mathbf{v}_l}{r_l^2} | \phi_l^{N=0} \rangle \quad (42)$$

$$+m_k m_l \langle \varphi_k^{(i)} | \frac{\mathbf{r}' \mathbf{J}_{11} \mathbf{M} \mathbf{J}_{11} \mathbf{r}}{r_l^4} | \varphi_l^{(j)} \rangle \quad (43)$$

$$-2 m_k \langle \varphi_k^{(i)} | \frac{\mathbf{r}' \mathbf{J}_{11} \mathbf{M} \mathbf{A}_l \mathbf{r}}{r_l^2} | \varphi_l^{(j)} \rangle \quad (44)$$

$$-2 \langle \varphi_k^{(i)} | \mathbf{r}' \mathbf{A}_k \mathbf{M} \mathbf{v}_l | \phi_l^{N=0} \rangle \quad (45)$$

$$-2 m_l \langle \varphi_k^{(i)} | \frac{\mathbf{r}' \mathbf{A}_k \mathbf{M} \mathbf{J}_{11} \mathbf{r}}{r_l^2} | \varphi_l^{(j)} \rangle \quad (46)$$

$$+4 \langle \varphi_k^{(i)} | \mathbf{r}' \mathbf{A}_k \mathbf{M} \mathbf{A}_l \mathbf{r} | \varphi_l^{(j)} \rangle. \quad (47)$$

Each of the above nine integrals is evaluated separately using the formulas obtained in [1]:

$$\langle \phi_k^{N=0} | \mathbf{v}'_k \mathbf{M} \mathbf{v}_l | \phi_l^{N=0} \rangle = M_{ij} \frac{2}{\sqrt{\pi}} \Gamma\left(\frac{3+m_k+m_l}{2}\right) \langle \phi_k | \phi_l \rangle \alpha_{11}^{\frac{m_k+m_l}{2}}, \quad (48)$$

$$\begin{aligned} \langle \phi_k^{N=0} | \frac{\mathbf{v}'_k \mathbf{M} \mathbf{J}_{11} \mathbf{r}}{r_l^2} | \varphi_l^{(j)} \rangle &= M_{1i} \frac{1}{\sqrt{\pi}} \Gamma\left(\frac{1+m_k+m_l}{2}\right) \\ &\times \langle \phi_k | \phi_l \rangle \operatorname{tr}\left[A_{kl}^{-1} J_{11}\right]^{\frac{m_k+m_l-2}{2}} \\ &\times \left(\operatorname{tr}\left[\mathbf{A}_{kl}^{-1} \mathbf{W}^{(ij)}\right]\right. \\ &+ \frac{m_k+m_l-2}{3} \\ &\left.\cdot \frac{\operatorname{tr}\left[\mathbf{A}_{kl}^{-1} \mathbf{W}^{(ij)} \mathbf{A}_{kl}^{-1} \mathbf{J}_{11}\right]}{\operatorname{tr}\left[A_{kl}^{-1} J_{11}\right]}\right), \end{aligned} \quad (49)$$

$$\begin{aligned} \langle \phi_k^N = 0 | \mathbf{v}'_k \mathbf{M} \mathbf{A}_l \mathbf{r} | \varphi_l^{(j)} \rangle &= \frac{2}{\sqrt{\pi}} \Gamma\left(\frac{3+m_k+m_l}{2}\right) \\ &\times \langle \phi_k | \phi_l \rangle \operatorname{tr}\left[A_{kl}^{-1} J_{11}\right]^{\frac{m_k+m_l}{2}} \\ &\times \left(\frac{1}{2} \operatorname{tr}\left[\mathbf{A}_{kl}^{-1} \mathbf{W}^{(ij)} \mathbf{M} \mathbf{A}_l\right]\right. \\ &+ \frac{m_k+m_l}{3} \\ &\left.\cdot \frac{\operatorname{tr}\left[\mathbf{A}_{kl}^{-1} \mathbf{W}^{(ij)} \mathbf{M} \mathbf{A}_l \mathbf{A}_{kl}^{-1} \mathbf{J}_{11}\right]}{\operatorname{tr}\left[A_{kl}^{-1} J_{11}\right]}\right), \end{aligned} \quad (50)$$

$$\begin{aligned} \langle \varphi_k^{(i)} | \frac{\mathbf{r}' \mathbf{J}_{11} \mathbf{M} \mathbf{J}_{11} \mathbf{r}}{r_l^4} | \varphi_l^{(j)} \rangle &= M_{11} \frac{1}{\sqrt{\pi}} \Gamma\left(\frac{1+m_k+m_l}{2}\right) \\ &\times \langle \phi_k | \phi_l \rangle \operatorname{tr}\left[A_{kl}^{-1} J_{11}\right]^{\frac{m_k+m_l-2}{2}} \\ &\times \left(\operatorname{tr}\left[\mathbf{A}_{kl}^{-1} \mathbf{W}^{(ij)}\right]\right. \\ &+ \frac{m_k+m_l-2}{3} \\ &\left.\cdot \frac{\operatorname{tr}\left[\mathbf{A}_{kl}^{-1} \mathbf{W}^{(ij)} \mathbf{A}_{kl}^{-1} \mathbf{J}_{11}\right]}{\operatorname{tr}\left[A_{kl}^{-1} J_{11}\right]}\right), \end{aligned} \quad (51)$$

$$\langle \phi_k^{N=1} | \frac{\mathbf{r}' (m_l \mathbf{A}_k + m_k \mathbf{A}_l) \mathbf{M} \mathbf{J}_{11} \mathbf{r}}{r_l^2} | \phi_l^{N=1} \rangle \quad (42)$$

$$= \frac{2}{\sqrt{\pi}} \Gamma\left(\frac{1+m_k+m_l}{2}\right) \langle \phi_k | \phi_l \rangle \alpha_{11}^{(m_k+m_l-2)/2} \quad (43)$$

$$\times \left\{ \frac{3}{4} \operatorname{tr}\left[\mathbf{A}_{kl}^{-1} \mathbf{W}^{(ij)}\right] \operatorname{tr}\left[A_{kl}^{-1} (m_l \mathbf{A}_k + m_k \mathbf{A}_l) \mathbf{M} \mathbf{J}_{11}\right] \right. \quad (44)$$

$$+ \frac{1}{2} \operatorname{tr}\left[\mathbf{A}_{kl}^{-1} \mathbf{W}^{(ij)} \mathbf{A}_{kl}^{-1} (m_l \mathbf{A}_k + m_k \mathbf{A}_l) \mathbf{M} \mathbf{J}_{11}\right] \quad (45)$$

$$\cdot \left(\frac{m_k+m_l-2}{3} \right) \alpha_{11}^{-1} \left(\frac{3}{4} \operatorname{tr}\left[\mathbf{A}_{kl}^{-1} \mathbf{W}^{(ij)}\right] \right) \quad (46)$$

$$\times \operatorname{tr}\left[A_{kl}^{-1} (m_l \mathbf{A}_k + m_k \mathbf{A}_l) \mathbf{M} \mathbf{J}_{11} \mathbf{A}_{kl}^{-1} \mathbf{J}_{11}\right] \quad (47)$$

$$+ \frac{3}{4} \operatorname{tr}\left[A_{kl}^{-1} (m_l \mathbf{A}_k + m_k \mathbf{A}_l) \mathbf{M} \mathbf{J}_{11}\right] \operatorname{tr}\left[\mathbf{A}_{kl}^{-1} \mathbf{W}^{(ij)} \mathbf{A}_{kl}^{-1} \mathbf{J}_{11}\right] \quad (48)$$

$$+ \frac{1}{2} \operatorname{tr}\left[\mathbf{A}_{kl}^{-1} \mathbf{W}^{(ij)} \mathbf{A}_{kl}^{-1} (m_l \mathbf{A}_k + m_k \mathbf{A}_l) \mathbf{M} \mathbf{J}_{11} \mathbf{A}_{kl}^{-1} \mathbf{J}_{11}\right] \quad (49)$$

$$\cdot \left(\frac{3+m_k^2+m_l^2+2m_km_l-4(m_k+m_l)}{15} \right) \quad (50)$$

$$\times \left(\frac{1}{2} \operatorname{tr}\left[\mathbf{A}_{kl}^{-1} \mathbf{W}^{(ij)} \mathbf{A}_{kl}^{-1} \mathbf{J}_{11} \mathbf{A}_{kl}^{-1} (m_l \mathbf{A}_k + m_k \mathbf{A}_l) \mathbf{M} \mathbf{J}_{11} \mathbf{A}_{kl}^{-1} \mathbf{J}_{11}\right] \right. \quad (51)$$

$$+ \frac{1}{4} \operatorname{tr}\left[\mathbf{A}_{kl}^{-1} \mathbf{W}^{(ij)} \mathbf{A}_{kl}^{-1} \mathbf{J}_{11}\right] \quad (52)$$

$$\times \operatorname{tr}\left[A_{kl}^{-1} (m_l \mathbf{A}_k + m_k \mathbf{A}_l) \mathbf{M} \mathbf{J}_{11} \mathbf{A}_{kl}^{-1} \mathbf{J}_{11}\right] \Big\}, \quad (52)$$

$$\langle \varphi_k^{(i)} | \mathbf{r}' \mathbf{A}_k \mathbf{M} \mathbf{A}_l \mathbf{r} | \varphi_l^{(j)} \rangle$$

$$= \frac{2}{\sqrt{\pi}} \Gamma\left(\frac{3+m_k+m_l}{2}\right) \langle \phi_k | \phi_l \rangle \alpha_{11}^{(m_k+m_l)/2} \quad (53)$$

$$\times \left\{ \frac{3}{4} \operatorname{tr}\left[\mathbf{A}_{kl}^{-1} \mathbf{W}^{(ij)}\right] \operatorname{tr}\left[A_{kl}^{-1} D\right] \right. \quad (54)$$

$$+ \frac{1}{2} \operatorname{tr}\left[\mathbf{A}_{kl}^{-1} \mathbf{W}^{(ij)} \mathbf{A}_{kl}^{-1} \mathbf{D}\right] \left(\frac{m_k+m_l}{3} \right) \quad (55)$$

$$\alpha_{11}^{-1} \left(\frac{3}{4} \operatorname{tr}\left[\mathbf{A}_{kl}^{-1} \mathbf{W}^{(ij)}\right] \operatorname{tr}\left[A_{kl}^{-1} D\right] \right) \quad (56)$$

$$+ \frac{3}{4} \operatorname{tr}\left[A_{kl}^{-1} D\right] \operatorname{tr}\left[\mathbf{A}_{kl}^{-1} \mathbf{W}^{(ij)} \mathbf{A}_{kl}^{-1} \mathbf{J}_{11}\right] \quad (57)$$

$$+ \frac{1}{2} \operatorname{tr}\left[\mathbf{A}_{kl}^{-1} \mathbf{W}^{(ij)} \mathbf{A}_{kl}^{-1} \mathbf{D} \mathbf{A}_{kl}^{-1} \mathbf{J}_{11}\right] \quad (58)$$

$$+ \frac{1}{2} \operatorname{tr}\left[\mathbf{A}_{kl}^{-1} \mathbf{D} \mathbf{A}_{kl}^{-1} \mathbf{W}^{(ij)} \mathbf{A}_{kl}^{-1} \mathbf{J}_{11}\right] \quad (59)$$

$$\cdot \left(\frac{3+m_k^2+m_l^2+2m_km_l}{15} \right) \quad (60)$$

$$\times \left(\frac{1}{2} \operatorname{tr}\left[\mathbf{A}_{kl}^{-1} \mathbf{W}^{(ij)} \mathbf{A}_{kl}^{-1} \mathbf{J}_{11} \mathbf{A}_{kl}^{-1} \mathbf{D} \mathbf{A}_{kl}^{-1} \mathbf{J}_{11}\right] \right. \quad (61)$$

$$+ \frac{1}{4} \operatorname{tr}\left[\mathbf{A}_{kl}^{-1} \mathbf{W}^{(ij)} \mathbf{A}_{kl}^{-1} \mathbf{J}_{11}\right] \operatorname{tr}\left[A_{kl}^{-1} \mathbf{D}\right] \Big\}, \quad (62)$$

where $\mathbf{D} = D \otimes I_3 = \frac{1}{2}(A_k M A_l + A_l M A_k) \otimes I_3$. It is also easy to see that integrals (42) and (45) have the same form as

integrals (40) and (41), respectively, and thus produce analogous analytical expressions.

In order to simplify expressions (52) and (53) the following traces need to be evaluated:

$$\text{tr} \left[\mathbf{A}_{kl}^{-1} \mathbf{W}^{(ij)} \mathbf{A}_{kl}^{-1} \mathbf{Q} \right] = \text{tr} \left[\mathbf{A}_{kl}^{-1} \mathbf{Q} \mathbf{A}_{kl}^{-1} \mathbf{W}^{(ij)} \right] = \left(\mathbf{A}_{kl}^{-1} \mathbf{Q} \mathbf{A}_{kl}^{-1} \right)_{ij} \quad (54)$$

$$\text{tr} \left[\mathbf{A}_{kl}^{-1} \mathbf{Q} \mathbf{A}_{kl}^{-1} \mathbf{J}_{11} \right] = 3 \left(\mathbf{A}_{kl}^{-1} \mathbf{Q} \mathbf{A}_{kl}^{-1} \right)_{11} \quad (55)$$

$$\text{tr} \left[\mathbf{A}_{kl}^{-1} \mathbf{W}^{(ij)} \mathbf{A}_{kl}^{-1} \mathbf{Q} \mathbf{A}_{kl}^{-1} \mathbf{J}_{11} \right] = \left(\mathbf{A}_{kl}^{-1} \mathbf{Q} \mathbf{A}_{kl}^{-1} \right)_{1j} \left(\mathbf{A}_{kl}^{-1} \right)_{1i} \quad (56)$$

$$\text{tr} \left[\mathbf{A}_{kl}^{-1} \mathbf{Q} \mathbf{A}_{kl}^{-1} \mathbf{W}^{(ij)} \mathbf{A}_{kl}^{-1} \mathbf{J}_{11} \right] = \left(\mathbf{A}_{kl}^{-1} \right)_{1j} \left(\mathbf{A}_{kl}^{-1} \mathbf{Q} \mathbf{A}_{kl}^{-1} \right)_{1i} \quad (57)$$

$$\begin{aligned} & \text{tr} \left[\mathbf{A}_{kl}^{-1} \mathbf{Q} \mathbf{A}_{kl}^{-1} \mathbf{J}_{11} \mathbf{A}_{kl}^{-1} \mathbf{W}^{(ij)} \mathbf{A}_{kl}^{-1} \mathbf{J}_{11} \right] \\ &= \text{tr} \left[\mathbf{A}_{kl}^{-1} \mathbf{W}^{(ij)} \mathbf{A}_{kl}^{-1} \mathbf{J}_{11} \mathbf{A}_{kl}^{-1} \mathbf{Q} \mathbf{A}_{kl}^{-1} \mathbf{J}_{11} \right] \\ &= \left(\mathbf{A}_{kl}^{-1} \right)_{1i} \left(\mathbf{A}_{kl}^{-1} \right)_{1j} \left(\mathbf{A}_{kl}^{-1} \mathbf{Q} \mathbf{A}_{kl}^{-1} \right)_{11}, \end{aligned} \quad (58)$$

where \mathbf{Q} is $(m_l \mathbf{A}_k + m_k \mathbf{A}_l) \mathbf{M} \mathbf{J}_{11}$ for (52) and $\frac{1}{2} (\mathbf{A}_k \mathbf{M} \mathbf{A}_l + \mathbf{A}_l \mathbf{M} \mathbf{A}_k)$ for (53).

Using (48)–(53) to evaluate (39)–(47) and using (54)–(58) to simplify the resulting expression, after normalization we obtain:

$$\begin{aligned} T_{kl}^{(ij)} = & 2S_{kl}^{(ij)} \left(\alpha_{ij} + \frac{2m\alpha_{1i}\alpha_{1j}}{3\alpha_{11}} \right)^{-1} \\ & \times \left\{ M_{ij} + \frac{m_l M_{1i} \alpha_{1j} + m_k M_{1j} \alpha_{1i}}{3\alpha_{11}} \right. \\ & - \left(\left(\mathbf{A}_{kl}^{-1} \mathbf{A}_l \mathbf{M} \right)_{ji} + \left(\mathbf{A}_{kl}^{-1} \mathbf{A}_k \mathbf{M} \right)_{ij} \right. \\ & + \frac{2m}{3\alpha_{11}} \left(\alpha_{1j} \left(\mathbf{A}_{kl}^{-1} \mathbf{A}_l \mathbf{M} \right)_{1i} + \alpha_{1i} \left(\mathbf{A}_{kl}^{-1} \mathbf{A}_k \mathbf{M} \right)_{1j} \right) \\ & + \frac{m_k + m_l}{2m + 1} \frac{M_{11}}{\alpha_{11}} \left(\alpha_{ij} + \frac{2m - 2}{3\alpha_{11}} \alpha_{1i} \alpha_{1j} \right) \\ & - \frac{1}{3\alpha_{11}} \left((3\alpha_{ij} + 2(m-1)\alpha_{1j}) \left(m_k \left(\mathbf{A}_{kl}^{-1} \mathbf{A}_l \mathbf{M} \right)_{11} \right. \right. \\ & + m_l \left(\mathbf{A}_{kl}^{-1} \mathbf{A}_k \mathbf{M} \right)_{11} \left. \right) + \alpha_{1j} \left(m_k \left(\mathbf{A}_{kl}^{-1} \mathbf{A}_l \mathbf{M} \right)_{1i} \right. \\ & + m_l \left(\mathbf{A}_{kl}^{-1} \mathbf{A}_k \mathbf{M} \right)_{1i} \left. \right) + \alpha_{1i} \left(m_k \left(\mathbf{A}_{kl}^{-1} \mathbf{A}_l \mathbf{M} \right)_{1j} \right. \\ & \left. \left. + m_l \left(\mathbf{A}_{kl}^{-1} \mathbf{A}_k \mathbf{M} \right)_{1j} \right) \right) \\ & + \frac{4m(m-1)}{3} \frac{\alpha_{1i}\alpha_{1j}}{\alpha_{11}^2} \left(\mathbf{A}_{kl}^{-1} \mathbf{A}_k \mathbf{M} \mathbf{A}_l \mathbf{A}_{kl}^{-1} \right)_{11} \\ & + \frac{2m}{3\alpha_{11}} \left(\alpha_{1j} \left(\left(\mathbf{A}_{kl}^{-1} \mathbf{A}_k \mathbf{M} \mathbf{A}_l \mathbf{A}_{kl}^{-1} \right)_{1i} \right. \right. \\ & + \left(\mathbf{A}_{kl}^{-1} \mathbf{A}_l \mathbf{M} \mathbf{A}_k \mathbf{A}_{kl}^{-1} \right)_{1i} \left. \right) + \alpha_{1i} \left(\left(\mathbf{A}_{kl}^{-1} \mathbf{A}_k \mathbf{M} \mathbf{A}_l \mathbf{A}_{kl}^{-1} \right)_{1j} \right. \\ & + \left(\mathbf{A}_{kl}^{-1} \mathbf{A}_l \mathbf{M} \mathbf{A}_k \mathbf{A}_{kl}^{-1} \right)_{1j} \left. \right) \\ & + 3\alpha_{ij} \left(\mathbf{A}_{kl}^{-1} \mathbf{A}_k \mathbf{M} \mathbf{A}_l \mathbf{A}_{kl}^{-1} \right)_{11} + 3\alpha_{1i}\alpha_{1j}\tau \left. \right) \\ & + 3\alpha_{ij}\tau \left(\left(\mathbf{A}_{kl}^{-1} \mathbf{A}_k \mathbf{M} \mathbf{A}_l \mathbf{A}_{kl}^{-1} \right)_{1j} + \left(\mathbf{A}_{kl}^{-1} \mathbf{A}_l \mathbf{M} \mathbf{A}_k \mathbf{A}_{kl}^{-1} \right)_{1i} \right) \Big\}, \end{aligned} \quad (59)$$

where $\tau = \text{tr} [\mathbf{A}_{kl}^{-1} \mathbf{A}_k \mathbf{M} \mathbf{A}_l]$.

In order to evaluate the kinetic energy gradient, we need to evaluate the following elementary derivatives first:

$$\begin{aligned} \partial_k \tau = & - \text{vech} \left[\mathbf{A}_{kl}^{-1} (\mathbf{A}_l \mathbf{M} \mathbf{A}_k + \mathbf{A}_k \mathbf{M} \mathbf{A}_l) \mathbf{A}_{kl}^{-1} \mathbf{L}_k \right] \\ & + \text{vech} \left[(\mathbf{A}_{kl}^{-1} \mathbf{A}_l \mathbf{M} + \mathbf{M} \mathbf{A}_l \mathbf{A}_{kl}^{-1}) \mathbf{L}_k \right] \end{aligned} \quad (60)$$

$$\begin{aligned} \partial_k (\mathbf{A}_{kl}^{-1} \mathbf{A}_k \mathbf{M})_{ij} = & - \text{vech} \left[\mathbf{A}_{kl}^{-1} (\mathbf{E}_{ji} \mathbf{M} \mathbf{A}_k + \mathbf{A}_k \mathbf{M} \mathbf{E}_{ij}) \mathbf{A}_{kl}^{-1} \mathbf{L}_k \right] \\ & + \text{vech} \left[(\mathbf{A}_{kl}^{-1} \mathbf{E}_{ji} \mathbf{M} + \mathbf{M} \mathbf{E}_{ij} \mathbf{A}_l \mathbf{A}_{kl}^{-1}) \mathbf{L}_k \right] \end{aligned} \quad (61)$$

$$\begin{aligned} \partial_k (\mathbf{A}_{kl}^{-1} \mathbf{A}_l \mathbf{M})_{ji} = & - \text{vech} \left[\mathbf{A}_{kl}^{-1} (\mathbf{E}_{ij} \mathbf{M} \mathbf{A}_l + \mathbf{A}_l \mathbf{M} \mathbf{E}_{ji}) \mathbf{A}_{kl}^{-1} \mathbf{L}_k \right] \\ & + \text{vech} \left[(\mathbf{A}_{kl}^{-1} \mathbf{E}_{ij} \mathbf{M} + \mathbf{M} \mathbf{E}_{ji} \mathbf{A}_k \mathbf{A}_{kl}^{-1}) \mathbf{L}_k \right] \end{aligned} \quad (62)$$

$$\begin{aligned} \partial_k (\mathbf{A}_{kl}^{-1} \mathbf{A}_k \mathbf{M} \mathbf{A}_l \mathbf{A}_{kl}^{-1})_{ij} = & - \text{vech} \left[\mathbf{A}_{kl}^{-1} (\mathbf{E}_{ji} \mathbf{A}_{kl}^{-1} \mathbf{A}_l \mathbf{M} + \mathbf{A}_k \mathbf{M} \mathbf{A}_l \mathbf{A}_{kl}^{-1} \mathbf{E}_{ij}) \mathbf{A}_{kl}^{-1} \mathbf{L}_k \right] \\ & + \text{vech} \left[(\mathbf{A}_{kl}^{-1} \mathbf{E}_{ji} \mathbf{A}_{kl}^{-1} \mathbf{A}_l \mathbf{M} + \mathbf{M} \mathbf{A}_l \mathbf{A}_{kl}^{-1} \mathbf{E}_{ij} \mathbf{A}_{kl}^{-1}) \mathbf{L}_k \right] \\ & - \text{vech} \left[\mathbf{A}_{kl}^{-1} (\mathbf{A}_l \mathbf{M} \mathbf{A}_k \mathbf{A}_{kl}^{-1} \mathbf{E}_{ji} + \mathbf{E}_{ij} \mathbf{A}_{kl}^{-1} \mathbf{A}_k \mathbf{M} \mathbf{A}_l) \mathbf{A}_{kl}^{-1} \mathbf{L}_k \right] \end{aligned} \quad (63)$$

$$\begin{aligned} \partial_l \tau = & - \text{vech} \left[\mathbf{P} \mathbf{A}_{kl}^{-1} (\mathbf{A}_l \mathbf{M} \mathbf{A}_k + \mathbf{A}_k \mathbf{M} \mathbf{A}_l) \mathbf{A}_{kl}^{-1} \mathbf{P}' \mathbf{L}_l \right] \\ & + \text{vech} \left[\mathbf{P} (\mathbf{A}_{kl}^{-1} \mathbf{A}_k \mathbf{M} + \mathbf{M} \mathbf{A}_l \mathbf{A}_{kl}^{-1}) \mathbf{P}' \mathbf{L}_l \right] \end{aligned} \quad (64)$$

$$\begin{aligned} & \times \partial_l (\mathbf{A}_{kl}^{-1} \mathbf{A}_k \mathbf{M})_{ij} \\ = & - \text{vech} \left[\mathbf{P} \mathbf{A}_{kl}^{-1} (\mathbf{A}_k \mathbf{M} \mathbf{E}_{ij} + \mathbf{E}_{ji} \mathbf{A}_k \mathbf{A}_l) \mathbf{A}_{kl}^{-1} \mathbf{P}' \mathbf{L}_l \right] \end{aligned} \quad (65)$$

$$\begin{aligned} & \times \partial_l (\mathbf{A}_{kl}^{-1} \mathbf{A}_l \mathbf{M})_{ji} \\ = & - \text{vech} \left[\mathbf{P} \mathbf{A}_{kl}^{-1} (\mathbf{A}_l \mathbf{M} \mathbf{E}_{ji} + \mathbf{E}_{ij} \mathbf{A}_l \mathbf{A}_k) \mathbf{A}_{kl}^{-1} \mathbf{P}' \mathbf{L}_l \right] \\ & + \text{vech} \left[\mathbf{P} (\mathbf{A}_{kl}^{-1} \mathbf{E}_{ij} \mathbf{M} + \mathbf{M} \mathbf{E}_{ji} \mathbf{A}_{kl}^{-1}) \mathbf{P}' \mathbf{L}_l \right] \end{aligned} \quad (66)$$

$$\begin{aligned} & \times \partial_l (\mathbf{A}_{kl}^{-1} \mathbf{A}_k \mathbf{M} \mathbf{A}_l \mathbf{A}_{kl}^{-1})_{ij} \\ = & - \text{vech} \left[\mathbf{P} \mathbf{A}_{kl}^{-1} (\mathbf{E}_{ji} \mathbf{A}_{kl}^{-1} \mathbf{A}_l \mathbf{M} \mathbf{A}_k + \mathbf{A}_k \mathbf{M} \mathbf{A}_l \mathbf{A}_{kl}^{-1} \mathbf{E}_{ij}) \mathbf{A}_{kl}^{-1} \mathbf{P}' \mathbf{L}_l \right] \\ & + \text{vech} \left[\mathbf{P} (\mathbf{A}_{kl}^{-1} \mathbf{E}_{ji} \mathbf{A}_{kl}^{-1} \mathbf{A}_k \mathbf{M} + \mathbf{M} \mathbf{A}_k \mathbf{A}_{kl}^{-1} \mathbf{E}_{ij} \mathbf{A}_{kl}^{-1}) \mathbf{P}' \mathbf{L}_l \right] \\ & - \text{vech} \left[\mathbf{P} \mathbf{A}_{kl}^{-1} (\mathbf{A}_l \mathbf{M} \mathbf{A}_k \mathbf{A}_{kl}^{-1} \mathbf{E}_{ji} + \mathbf{E}_{ij} \mathbf{A}_{kl}^{-1} \mathbf{A}_k \mathbf{M} \mathbf{A}_l) \right. \\ & \left. \times \mathbf{A}_{kl}^{-1} \mathbf{P}' \mathbf{L}_l \right]. \end{aligned} \quad (67)$$

Using these elementary derivatives the evaluation of the kinetic energy gradient becomes trivial and can be completed.

References

- [1] Sharkey K L, Kirnosov N and Adamowicz L 2013 *J. Chem. Phys.* **139** 164119
- [2] Sharkey K L, Kirnosov N and Adamowicz L 2013 *Phys. Rev. A* **88** 032513
- [3] Kirnosov N, Sharkey K L and Adamowicz L 2014 *J. Chem. Phys.* **140** 104115

- [4] Kirnosov N, Sharkey K L and Adamowicz L 2013 *J. Chem. Phys.* **139** 204105
- [5] Kirnosov N, Sharkey K L and Adamowicz L 2014 *Phys. Rev. A* **89** 012513
- [6] Kinghorn D B and Adamowicz L 1999 *J. Chem. Phys.* **110** 7166
- [7] Kinghorn D B and Adamowicz L 1999 *Phys. Rev. Lett.* **83** 2541
- [8] Bubin S, Leonarski F, Stanke M and Adamowicz L 2009 *J. Chem. Phys.* **130** 124120
- [9] Sharkey K L, Kirnosov N and Adamowicz L 2013 *J. Chem. Phys.* **138** 104107
- [10] Frolov A M 2012 *Eur. Phys. J. D* **22** 212
- [11] Karr J and Hilico L 2006 *J. Phys. B: At. Mol. Opt. Phys.* **39** 2095
- [12] Balint-Kurti G G, Moss R E, Sadler I A and Shapiro M 1990 *Phys. Rev. A* **41** 4913
- [13] Moss R E 1993 *Mol. Phys.* **78** 371
- [14] Pilon H O and Baye D 2013 *Phys. Rev. A* **88** 032502
- [15] Wolniewicz L and Orlikowski T 1991 *Mol. Phys.* **74** 103
- [16] Tian Q L, Tang L Y, Zhong Z X, Yan Z C and Shi T Y 2012 *J. Chem. Phys.* **137** 024311
- [17] Korobov V I 2006 *Phys. Rev. A* **74** 052506
- [18] Carrington A, McNab I R, Montgomerie C A and Brown J M 1989 *Mol. Phys.* **66** 1279
- [19] Carrington A, McNab I R and Montgomerie C A 1988 *Mol. Phys.* **65** 751
- [20] Harris F E 2004 *Adv. Quantum Chem.* **47** 129
- [21] Delves L M and Kalotas T 1968 *Aust. J. Phys.* **21** 1
- [22] Frolov A M and Wardlaw D M 2011 *Eur. Phys. J. D* **63** 339
- [23] Frolov A M 2001 *J. Phys. B* **34** 3813
- [24] Frolov A M 2001 *Phys. Rev. E* **64** 036704
- [25] Eskandari M R and Mahdavi M 2003 *Phys. Rev. A* **68** 032511
- [26] Drake G W F, Cassar M M and Nistor R A 2002 *Phys. Rev. A* **65** 054501
- [27] Kilic S, Karr J-Ph and Hilico L 2004 *Phys. Rev. A* **70** 042506
- [28] Bailey D H 1995 *ACM Trans. Math. Soft.* **21** 379
- [29] Bailey D H 2000 *Comput. Sci. Eng.* **2** 24

APPENDIX O

A comparison of two types of explicitly correlated Gaussian functions for non-Born-Oppenheimer molecular calculations using a model potential

A comparison of two types of explicitly correlated Gaussian functions for non-Born-Oppenheimer molecular calculations using a model potential

Martin Formanek,^{1,2} Keeper L. Sharkey,³ Nikita Kirnosov,^{1,3} and Ludwik Adamowicz^{1,3}

¹Department of Physics, University of Arizona, Tucson, Arizona 85721, USA

²Institute of Theoretical Physics, Charles University, V Holešovickach 2, 180 00, Prague, Czech Republic

³Department of Chemistry and Biochemistry, University of Arizona, Tucson, Arizona 85721, USA

(Received 20 July 2014; accepted 30 September 2014; published online 15 October 2014)

A new functional form of the explicitly correlated Gaussian-type functions (later called Gaussians or ECGs) for performing non-Born-Oppenheimer (BO) calculations of molecular systems with an arbitrary number of nuclei is presented. In these functions, the exponential part explicitly depends on all interparticle distances and the preexponential part depends only on the distances between the nuclei. The new Gaussians are called sin/cos-Gaussians and their preexponential part is a product of sin and/or cos factors. The effectiveness of the new Gaussians in describing non-BO pure vibrational states is investigated by comparing them with r^m -Gaussians containing preexponential multipliers in the form of non-negative powers of internuclear distances (the internuclear distance in the diatomic case). The testing is performed for a diatomic system with the nuclei interacting through a Morse potential. It shows that the new sin/cos-Gaussian basis set is capable of providing equally accurate results as obtained with the r^m -Gaussians. However, especially for lower vibrational states, more sin/cos-Gaussians are needed to reach a similar accuracy level as obtained with the r^m -Gaussians. Implementation of the sin/cos-Gaussians in non-BO calculations of diatomic and, in particular, of triatomic systems, which will follow, will provide further assessment of the efficiency of the new functions. © 2014 AIP Publishing LLC. [<http://dx.doi.org/10.1063/1.4897634>]

I. INTRODUCTION

Accurate quantum-mechanical calculations of molecular systems without assuming the Born-Oppenheimer (BO) approximation require the use of unconventional basis sets, because the motion of all particles in the system, nuclei and electrons, has to be simultaneously described in the wave function. To achieve high accuracy in the calculation the basis functions have to be explicitly dependent on the interparticle (i.e., electron-electron, electron-nucleus, and nucleus-nucleus) distances. In our atomic and molecular non-BO calculations, the explicitly correlated Gaussians (ECGs) have been such functions.^{1,2} The nature of the electron-electron correlation is different than the nature of the nucleus-nucleus correlation. Even though both correlations result from the Coulombic repulsion of the particles with charges being either both negative or both positive, the significantly different masses of the two types of particles make them behave differently when they approach each other. For the much lighter electrons, their wave functions more significantly overlap than the wave functions of the much heavier nuclei. In effect, the nuclei avoid each other to much greater extent than the electrons. As we have demonstrated with the non-BO calculations of bound states of some small diatomic molecules,² the nucleus-nucleus correlation requires addition to the exponentially correlated all-particle Gaussians preexponential multipliers which are powers of the internuclear distance. These powers, which also include the zero power, allow for separating the nuclei from each other in the wave function and also allow for describing nodes in the wave function which appear when the molecule is excited to higher vibrational states. The

preexponential correlation multipliers are not needed for the electrons, as the electron correlation can be quite adequately described through the dependency of the Gaussian exponent on the inter-electron distances. For molecules with three nuclei, the Gaussians have to be multiplied by powers of all three internuclear distances. With that the highly correlated motion of the nuclei and the oscillation of the wave function corresponding to vibrational excitations can be effectively described.

The third type of correlation in the non-BO calculation is the nucleus-electron correlation. The electrons, particularly the core electrons, follow the moving nuclei due to the attractive interaction. This effect needs to be described in the non-BO wave function and thus by the basis functions used in the wave-function expansion. As the exponential parts of the Gaussians have maxima at the zero electron-nuclei distances, these functions can very effectively describe the correlated coupled motions of the nuclei and the electrons. Thus, also in this case no preexponential correlation multipliers are needed.

Quantum mechanical molecular calculations without assuming the BO approximations regarding the separability of the motion of electrons (presumed fast) and the nuclear motion (presumed slow) are rare. Low interest in such calculations is due to the fact that most problems in chemistry can be adequately described within the BO framework. The non-adiabatic effects, which are accounted for in non-BO calculations, rarely come into play at the level of accuracy relevant to chemistry, and, if they do, in most cases they can be treated using a local approach developed to describe conical intersections of the potential energy surfaces of two interacting electronic states. However, if the results of quantum-

mechanical calculations are to be used to predict results of high-resolution gas-phase spectroscopy, the BO approximation has to be revoked. For example, in our recent studies of the HD⁺ molecule³ it was shown that in rovibrational states located near the dissociation limit, the electron density is shifted almost entirely to the deuteron. This charge asymmetry can only be described with a method where the BO approximation is not assumed.

Another aspect of basis set selection is related to the spatial symmetry of the non-BO wave function. The basis functions have to reflect the symmetry of the non-BO Hamiltonian used in the calculation. This Hamiltonian is obtained by separating out the center-of-mass motion from the full non-relativistic laboratory-frame Hamiltonian of the system. In our approach, the procedure starts with the laboratory-frame Hamiltonian expressed in terms of laboratory Cartesian coordinates. In this Hamiltonian, all particles involved in the system are treated on equal footing. If the total number of particles (i.e., the electrons and the nuclei) is set to be $n + 1$ and their masses, charges, and laboratory-frame position vectors are denoted as M_i , Q_i , and \mathbf{R}_i , respectively, where $i = 1, \dots, n + 1$, the laboratory-frame nonrelativistic Hamiltonian, \hat{H}_{lab} , that includes the kinetic energy operators of all particles and the Coulombic interactions within each pair of particles is

$$\hat{H}_{lab} = -\sum_{i=1}^{n+1} \frac{1}{2M_i} \nabla_i^2 + \sum_{i=1}^{n+1} \sum_{j>i}^{n+1} \frac{Q_i Q_j}{R_{ij}}, \quad (1)$$

where $R_{ij} = |\mathbf{R}_j - \mathbf{R}_i|$ are the interparticle distances.

The separation of the center-of-mass motion from \hat{H}_{lab} is accomplished by a transformation to a new Cartesian coordinate system, whose first three coordinates are the coordinates of the center of mass in the laboratory coordinate system, and the remaining $3n$ coordinates are coordinates describing the internal motion of the system. The internal coordinate system is generated by placing a selected particle (usually the heaviest one) at the origin of the system and calling it particle 1, and by referring all other particles to this reference particle using Cartesian position vectors \mathbf{r}_i defined as $\mathbf{r}_i = \mathbf{R}_{i+1} - \mathbf{R}_1$, $i = 1, \dots, n$. After the coordinate transformation \hat{H}_{lab} rigorously separates into the kinetic energy operator of the center-of-mass motion and a Hamiltonian, \hat{H} , dependent on the \mathbf{r}_i coordinates which represents in internal motion of the system. The internal Hamiltonian has the following form:

$$\hat{H} = -\frac{1}{2} \left(\sum_i^n \frac{1}{\mu_i} \nabla_i^2 + \sum_{i \neq j}^n \frac{1}{M_1} \nabla'_i \nabla'_j \right) + \sum_{i=1}^n \frac{q_0 q_i}{r_i} + \sum_{i \neq j}^n \frac{q_i q_j}{r_{ij}}. \quad (2)$$

This Hamiltonian describes a system of n particles (pseudoparticles) with charges $q_i = Q_{i+1}$ and masses $\mu_i = M_1 M_{i+1} / (M_1 + M_{i+1})$ moving in the central field of the charge of the reference particle. The second term in parentheses in (2) is the mass polarization term that arises from the transformation of the laboratory frame coordinate system to the internal coordinate system. This term along with the terms describing the Coulombic interactions between the particles couples the internal motions of the pseudoparticles. In the potential energy term, r_i and r_{ij} are defined as $r_i = |\mathbf{R}_i|$ and $r_{ij} = |\mathbf{R}_j - \mathbf{R}_i|$. Due to its spherical symmetry, the internal Hamiltonian, (2), resembles an atomic Hamiltonian. However, while in an atom, the particles moving in the central potential of the (positive) charge of the nucleus are all electrons, the pseudoparticles described by Hamiltonian (2) may have both positive and negative charges. Also, the masses of the pseudoparticles may be significantly different from the masses of the electrons in the atomic Hamiltonian. The spherical symmetry (isotropy) of the internal Hamiltonian dictates that its eigenfunctions form an irreducible representation of a fully symmetric group of 3D rotations. The basis functions have to reflect this symmetry.

By taking all the above-described necessary features of the basis functions into the consideration, the following all-particle ECGs have been chosen as the basis functions in our non-BO calculations of rotationless states of diatomic systems:²

$$\phi_k = r_1^{2m_k} \exp[-\mathbf{r}'(\mathbf{A}_k \otimes \mathbf{I}_3)\mathbf{r}], \quad (3)$$

where r_1 is the internuclear distance, \mathbf{A}_k is a positive-definite symmetric matrix of exponential coefficients, \mathbf{r} is a $3n \times 1$ vector of the internal Cartesian coordinates, \mathbf{r}_i , of the n pseudoparticles ($\mathbf{r}' = (\mathbf{r}'_1, \mathbf{r}'_2, \dots, \mathbf{r}'_n)$), and \mathbf{I}_3 is the 3×3 identity matrix. The preexponential multiplier in (3) is the internuclear distance, r_1 , raised to a non-negative even power $2m_k$. This power varies from 0 to 250 in our non-BO diatomic calculations.

As ϕ_k is a rotationally invariant function of the internal coordinates, they have the right symmetry to be used for expanding rotationless eigenfunctions of Hamiltonian (2). The presence of $r_1^{2m_k}$ in (3) makes the ϕ_k functions well suited for describing the nucleus-nucleus correlation. As each ϕ_k has a maximum on a sphere centered at the origin with a radius dependent on the values of m_k and the exponential parameters, \mathbf{A}_k , the shape of the wave function, which for the lowest state has a maximum around the equilibrium internuclear distance of the system ($r_1 \approx r_e$), can be properly described. For vibrationally excited states, the corresponding wave functions oscillate in term of the r_1 coordinate and these oscillations can also be effectively described using superpositions of the ϕ_k functions.

In our approach, the basis functions are optimized using the variational method. The optimization is performed for the elements of the \mathbf{A}_k matrices and for the m_k powers r_1 . In several papers, we have demonstrated that ECGs (3) form very effective basis sets for non-BO calculations for the ground and excited pure “vibrational” states of diatomic molecules with σ electrons. We put the term “vibrational” in quotes because, in the non-BO approach, the vibrational and electronic degrees of freedom couple and cannot be rigorously separated. Hence, the vibrational quantum number is not, strictly speaking, a good quantum number. Thus, the “vibrational states” obtained in our calculations are states corresponding to a particular value of the total rotational quantum number, N , which is a good quantum number. So far our diatomic non-BO calculations have been limited to states with $N = 0$ and 1.^{2,4}

The diatomic basis functions (3) can be easily extended to triatomic systems. Such an extension can be achieved

by including in the Gaussian premultiplier powers of all internuclear distances. With that the basis functions are

$$\phi_k = r_1^{2m_k} r_2^{2n_k} r_{12}^{2p_k} \exp[-\mathbf{r}'(\mathbf{A}_k \otimes \mathbf{I}_3)\mathbf{r}], \quad (4)$$

where r_1 is the distance between the reference nucleus and nucleus 2, r_2 is the distance between the reference nucleus and nucleus 3, and r_{12} is the distance between nuclei 2 and 3. In (4), \mathbf{A}_k is again a symmetric positive-definite matrix of exponential coefficients. Functions (4) should be good basis functions for expanding wave functions of rotationless (i.e., pure vibrational) states of triatomic systems with σ electrons, for example, H_3^+ , H_3 , or LiH_2 . They should be able to effectively describe the three types of correlations, i.e., the electron-electron, nucleus-nucleus, and nucleus-electron correlations in the non-BO calculation.

As demonstrated in our non-BO calculations of rovibrational states of diatomic systems, the powers of the internuclear distance, r_1 , in basis functions (3) have to range from 0 to at least 250 to accurately describe the nucleus-nucleus correlation and the nodes in the non-BO wave functions of excited vibrational states. As the excitation level increases larger powers of r_1 are needed in the preexponential multipliers. Similar trend is expected to occur in the basis functions of triatomic systems (4) and here also the m_k , n_k , and p_k powers need to range from 0 to at least 250. We have derived algorithms for calculating Hamiltonian and overlap matrix elements with Gaussians (4) and we had made an attempt to implement them in a computer program.⁵ However, the test calculations showed that the algorithms are not numerically stable because they involve oscillating series with finite number of elements whose values are large but have opposite signs. We have not been able to overcome this problem yet and thus this line of the development is presently on hold. In mean time, we have been searching for other alternative types of basis functions for use in triatomic non-BO calculations.

One type of functions which can potentially be as effective in expanding non-BO triatomic wave functions as functions (4) are all-particle Gaussians multiplied by sin and cos functions dependent on squares of the internuclear distances

$$\phi_k = f_1(a_1^k r_1^2) f_2(a_2^k r_2^2) f_{12}(a_{12}^k r_{12}^2) \exp[-\mathbf{r}'(\mathbf{A}_k \otimes \mathbf{I}_3)\mathbf{r}], \quad (5)$$

where $f_1(a_1^k r_1^2)$ is either $\sin(a_1^k r_1^2)$ or $\cos(a_1^k r_1^2)$ and f_2 and f_{12} having analogical forms. In the diatomic case, basis function (4) has the following form:

$$\phi_k = f_1(a_1^k r_1^2) \exp[-\mathbf{r}'(\mathbf{A}_k \otimes \mathbf{I}_3)\mathbf{r}], \quad (6)$$

where the f_1 functions is again either a sin or a cos function. The sin and cos preexponential multipliers of the Gaussians can be expressed using the Euler relations

$$\sin(a_1^k r_1^2) = \frac{e^{ia_1^k r_1^2} - e^{-ia_1^k r_1^2}}{2i} \quad \text{and} \quad \cos(a_1^k r_1^2) = \frac{e^{ia_1^k r_1^2} + e^{-ia_1^k r_1^2}}{2}, \quad (7)$$

where $i = \sqrt{-1}$.

We now express r_1^2 as the following quadratic form: $r_1^2 = \mathbf{r}'(\mathbf{J}_1 \otimes \mathbf{I}_3)\mathbf{r}$, where \mathbf{J}_1 is an $n \times n$ matrix whose elements are all zero except for the (1, 1) element which is equal to one. With that the complex exponents can be incorporated into the Gaussian exponent leading to the following form of (6) for $\cos(a_1^k r_1^2)$ being the premultiplier:

$$\begin{aligned} \phi_k = & \frac{1}{2} \{ \exp[-\mathbf{r}'((\mathbf{A}_k + i\mathbf{B}_k) \otimes \mathbf{I}_3)\mathbf{r}] \\ & + \exp[-\mathbf{r}'((\mathbf{A}_k - i\mathbf{B}_k) \otimes \mathbf{I}_3)\mathbf{r}] \}, \end{aligned} \quad (8)$$

where \mathbf{B}_k is an $n \times n$ matrix whose elements are all zero except for the (1, 1) element which is equal to a_1^k . Analogically, for $\sin(a_1^k r_1^2)$ being the premultiplier in (6) we have

$$\begin{aligned} \phi_k = & \frac{1}{2i} \{ \exp[-\mathbf{r}'((\mathbf{A}_k + i\mathbf{B}_k) \otimes \mathbf{I}_3)\mathbf{r}] \\ & - \exp[-\mathbf{r}'((\mathbf{A}_k - i\mathbf{B}_k) \otimes \mathbf{I}_3)\mathbf{r}] \}. \end{aligned} \quad (9)$$

In ECGs (5) to be used as basis functions in the calculation of triatomic pure vibrational states each of the f_1 , f_2 , and f_{12} premultipliers in (5) has to be either a sin or a cos function. This results in eight different combinations, i.e., sin sin sin, sin sin cos, etc. Again each of these combinations can be expressed using the Euler representation of the sin/cos functions. With that and with r_{12}^2 expressed as a quadratic form as: $r_{12}^2 = \mathbf{r}'(\mathbf{J}_{12} \otimes \mathbf{I}_3)\mathbf{r}$, where \mathbf{J}_{12} is an $n \times n$ matrix whose elements are all zero except for $J_{12}(1, 1) = 1$, $J_{12}(2, 2) = 1$, $J_{12}(1, 2) = -1$, and $J_{12}(2, 1) = -1$, Gaussian (5) with, for example, a (cos cos cos) premultiplier can be expressed in a similar way as (8), i.e.,

$$\phi_k = \frac{1}{8} \sum_{l=1}^8 \exp[-\mathbf{r}'((\mathbf{A}_k + i\mathbf{B}_k^l) \otimes \mathbf{I}_3)\mathbf{r}] \quad (10)$$

with the matrix elements of the \mathbf{B}_k^l matrices being all zero except for

$$\begin{array}{llll} B_k^1(1, 1) = a_1^k + a_{12}^k, & B_k^1(2, 2) = a_2^k + a_{12}^k, & B_k^1(1, 2) = -a_{12}^k, & B_k^1(2, 1) = -a_{12}^k, \\ B_k^2(1, 1) = -a_1^k + a_{12}^k, & B_k^2(2, 2) = a_2^k + a_{12}^k, & B_k^2(1, 2) = -a_{12}^k, & B_k^2(2, 1) = -a_{12}^k, \\ B_k^3(1, 1) = a_1^k + a_{12}^k, & B_k^3(2, 2) = -a_2^k + a_{12}^k, & B_k^3(1, 2) = -a_{12}^k, & B_k^3(2, 1) = -a_{12}^k, \\ B_k^4(1, 1) = -a_1^k + a_{12}^k, & B_k^4(2, 2) = -a_2^k + a_{12}^k, & B_k^4(1, 2) = -a_{12}^k, & B_k^4(2, 1) = -a_{12}^k, \\ B_k^5(1, 1) = a_1^k - a_{12}^k, & B_k^5(2, 2) = a_2^k - a_{12}^k, & B_k^5(1, 2) = a_{12}^k, & B_k^5(2, 1) = a_{12}^k, \\ B_k^6(1, 1) = -a_1^k - a_{12}^k, & B_k^6(2, 2) = a_2^k - a_{12}^k, & B_k^6(1, 2) = a_{12}^k, & B_k^6(2, 1) = a_{12}^k, \\ B_k^7(1, 1) = a_1^k - a_{12}^k, & B_k^7(2, 2) = -a_2^k - a_{12}^k, & B_k^7(1, 2) = a_{12}^k, & B_k^7(2, 1) = a_{12}^k, \\ B_k^8(1, 1) = -a_1^k - a_{12}^k, & B_k^8(2, 2) = -a_2^k - a_{12}^k, & B_k^8(1, 2) = a_{12}^k, & B_k^8(2, 1) = a_{12}^k. \end{array}$$

In an analogical way, basis functions with the $(\sin \sin \sin)$, $(\sin \sin \cos)$, $(\sin \cos \sin)$, etc., premultipliers can be represented.

The calculation of the overlap and Hamiltonian matrix elements with basis functions (5) with f_1 , f_2 , and f_{12} being either sin or cos functions reduces to calculating integrals over functions $\exp[-\mathbf{r}'((\mathbf{A}_k + i\mathbf{B}_k)\otimes\mathbf{I}_3)\mathbf{r}]$. The algorithms for such calculation were presented in our previous work.⁶ In that work, we also derived algorithms for calculating the analytical energy gradient determined with respect to the \mathbf{A}_k and \mathbf{B}_k matrix elements. The gradient is used to the variational minimization of the energy and in the optimization of the \mathbf{A}_k and \mathbf{B}_k matrix elements.

The question we aim to answer in this work concerns the efficiency of the ECGs with sin and cos premultipliers in non-BO calculations of pure vibrational states of a molecular system. In our previous work, where the efficiency of Gaussians (3) was examined,⁷ tests were performed for two diatomic models. To simplify these models, the calculations were not done with the complete non-BO Hamiltonian (2), but with the Hamiltonian where the electrons were removed and replaced with a potential energy curve (PEC). In the first model, the PEC was a Morse potential and in the second model it was a H₂ PEC. In both models, the PECs were fitted with superpositions of origin-centered Gaussian functions, $r^m \exp(-ar^2)$ (the function becomes origin-centered in 3D space), which were also used for expanding the wave functions representing the pure vibrational states. The origin centering of these functions was important because in generalizing these types of functions to the case of calculating non-BO rotationless states of the internal Hamiltonian (2), spherically symmetric basis functions need to be formed. As function $r^m \exp(-ar^2)$ with r replaced by r_1 (i.e., with the internuclear distance) is spherically symmetric in the three-dimensional internal coordinate system, { \mathbf{r}_i }, and this symmetry is not changed when $\exp(-ar^2)$ is replaced with $\exp[-\mathbf{r}'(\mathbf{A}_k\otimes\mathbf{I}_3)\mathbf{r}]$, the model used in the testing correctly represented the problem, which was studied.

The test calculations showed that the origin-centered $r^m \exp(-ar^2)$ basis functions provide an excellent representation for the diatomic rotationless vibrational wave functions. This conclusion led to the development of a diatomic non-BO approach where ECGs (3) were used and where the system was represented by the complete internal nonrelativistic Hamiltonian (2).⁸ A number of non-BO calculations performed for pure vibrational states of some small diatomic systems – the largest one being the BH molecule – has demonstrated the high efficiency of Gaussians (3) in describing bound rotationless states of these systems.² The aim of this work is to test basis functions which we hope will allow for extending the non-BO approach to triatomic systems and beyond. These functions are ECGs with sin and cos premultipliers later called sin/cos-Gaussians.

The testing, which is described in Sec. II is done for a diatomic model system with the PEC represented by a Morse potential. The wave functions in the calculations are represented as superpositions of $\sin(br^2)\exp(-ar^2)$ and $\cos(br^2)\exp(-ar^2)$ basis functions. These functions are also origin-centered (in 3D space) as functions $r^m \exp(-ar^2)$.

They also have spherical symmetry as required in expanding the wave functions of pure vibrational states. The a and b parameters of the basis functions are optimized by the variational minimization of the total energy of the system. The results of the calculations are compared with the exact solutions of the Morse diatomic problem and with the results obtained with r^m -Gaussians containing as preexponential factors non-negative powers of the internuclear distance.

II. DETAILS OF THE CALCULATION

Expanding the wave function in terms of basis functions $\{\phi_i\}_{i=1}^N$

$$|\psi\rangle = \sum_{i=1}^N c_i |\phi_i\rangle \quad (11)$$

and using the variational method to determine the energy and the expansion coefficients, c_i , results in the standard secular equation

$$\sum_{j=1}^N H_{ij} c_j = E \sum_{j=1}^N S_{ij} c_j, \quad (12)$$

where H_{ij} and S_{ij} are the Hamiltonian and overlap matrix elements, $H_{ij} = \langle \phi_i | \hat{H} | \phi_j \rangle$ and $S_{ij} = \langle \phi_i | \phi_j \rangle$, respectively. Equation (12) has, in general, N solutions, i.e., N vectors $\{c_i^k\}_{k=1}^N$ and energies E^k . According to the Hylleraas-Undheim-McDonald theorem, the n th lowest eigenvalue of the equation is an upper bound to the exact nonrelativistic energy of the n th excited state of the system. This property facilitates a method for determining the nonlinear parameters of the basis set, i.e., powers m and exponents a for the r^m -Gaussians and exponents a and b for the sin/cos-Gaussians, that involves energy minimization with respect to these parameters. In this work, the minimization is carried out with the simplex Amoeba method.⁹

The calculations involve determining the Hamiltonian and overlap matrix elements in the sin/cos-Gaussian and r^m -Gaussian basis sets. Analytical formulas for the elements of overlap and kinetic-energy matrices in these two basis sets can be found in Appendixes A and B, respectively. The potential-energy matrix elements are discussed in Secs. II A and II B. Section II C deals with issue of how to avoid linear dependencies between the basis functions in their variational optimization. In Sec. II D, we describe the approach used to grow the basis set to the size that gives the energy value of the considered state accurate to a certain assumed threshold.

A. Parametrization of the potential

For the testing purposes, the same Morse potential as in Ref. 7 is used. The potential mimics the real potential for the H₂ molecule but, unlike the real potential, it has analytically solvable energy eigenvalues which can be used for comparison with the results obtained using the basis-set approach. The form of the Morse potential is

$$V_{\text{Morse}}(r) = D_e (1 - e^{-a(r-r_e)})^2 - \varepsilon_{\text{H}_2}, \quad (13)$$

where the depth of the well is $D_e = 0.17449 E_h$, the width of the potential is $a = 1.4556 a_0^{-1}$, the equilibrium distance is $r_e = 1.4011 a_0$, and $\varepsilon_{H_2} = 1.17449 E_h$. The exact analytical solution of the Schrödinger equation for the Morse potential is

$$E_n = \frac{a}{\mu} \sqrt{2\mu D_e} \left(n + \frac{1}{2} \right) - \frac{a^2}{2\mu} \left(n + \frac{1}{2} \right)^2 - \varepsilon_{H_2}, \quad (14)$$

where $n = 0$ is the ground state. The reduced mass in the testing is taken as $\mu = 918.076341$ a.u. Also note that the Morse potential can only support a limited number of bound states, n_{\max} , given by the condition

$$n_{\max} \leq \frac{\sqrt{2\mu D_e}}{a} - 1. \quad (15)$$

n_{\max} for the Morse potential used in the present calculations is equal to 11.

B. Numerical integration of the potential matrix elements

The optimization procedure requires evaluation of the potential-energy matrix elements for the given basis functions in each iteration step. For the r^m -Gaussians, the matrix elements are calculated using the approach described in Ref. 7. In that approach, the Morse potential is expressed as a linear combination of the basis functions with powers m and the exponents optimized using the least-square method and the Minpack package.¹⁰ With such an expansion of the Morse potential the potential-energy matrix elements are simple and can be evaluated analytically. The same holds true for the sin/cos-Gaussians, but the corresponding formulas are more complicated. Each consists of eight terms which, for large exponents, may have very similar values but opposite signs. Thus, in the evaluation of the matrix elements some loss of precision may occur. In the best fit of the Morse potential with sin/cos-Gaussian functions generated in this work some large exponents can be found. Functions with such exponents are needed to describe the behavior of the potential near zero. Even though we believe it is possible to represent the Morse potential without using such high-exponent functions, we have not attempted to find such a representation because it is outside the aim of the present work. Instead, numerical integration is used in the present calculations to evaluate the potential-energy matrix elements. The numerical integration is performed on a grid spanning from 0 to 30 a.u. using the Romberg integration method of the 13th order. The approach ensures that the matrix elements are calculated with the accuracy of about 13–14 digits as determined by a comparison with the exact results obtained from Mathematica.

C. Linear dependencies

It is undesirable to include linearly dependent functions in the basis set, as they may lead to numerical instabilities and loss of the precision in the calculation. In order to prevent the optimization of the basis set to converge to linearly dependent functions, we use the penalty approach described in work of

Tung.¹¹ In this approach, a positive-valued penalty term,

$$\mathcal{P} = \sum_{ij} \beta (|S_{ij}|^2 - t^2), \quad \forall i, j : |S_{ij}| > t, \quad (16)$$

is added to the total variational energy of the optimized state whenever two or more basis functions have the normalized overlap, S_{ij} , higher than the chosen threshold, t . β in (16) is a scaling factor. The penalty term depends on the overlap integrals between the basis functions and increases as these overlaps become closer to one. In the present calculations, the penalty threshold is set to 0.98. This effectively ensures that during the optimization no two basis functions overlap more than 0.98. As a higher overlap than that would lead to an increase of the value of the variational energy functional, which includes the penalty term, basis functions never become linearly dependent.

D. Adding new functions to the existing basis

In order to successfully run an optimization of the basis set, it is necessary to devise a method for increasing the size of the set and still maintaining the already achieved precision of the energy. For the r^m -Gaussians, the integer index m_i for every newly added basis function is optimized by performing calculations for the power ranging from 0 to 50 and selecting the power leading to the lowest energy. The initial value of the exponent, a_i , for a new added basis function is selected randomly within the range between 0 and 9 and the whole process is repeated a couple of times for each choice of m_i .

The sin/cos-Gaussian basis set is grown by gradually adding sin/cos-Gaussians one by one. In the present calculations, we arbitrarily set the number of sin-Gaussians to be equal to the number of cos-Gaussians. However, as these two numbers do not need to be equal, in the future calculation their ratio will be determined variationally. After a new basis function is added to the basis set its a_i and b_i parameters are optimized. The optimization also includes reoptimization of the other Gaussians already included in the basis set.

III. RESULTS

The aim of this study is to compare the effectiveness of the sin/cos and r^m -Gaussian basis sets in determining the bound states of a diatomic system represented by the assumed Morse potential. For the purpose of the test, the target difference (precision) of the energies obtained in the calculations and the exact energies (14) is set to be at least $10^{-7} E_h$. It turned out that both basis sets can provide results with such precision. In Tables I and II, we show the numbers of basis functions of the two types which are necessary for each state to obtain an energy within the target precision. The results are also depicted in Figure 1. An analysis of the plots and of the data in the tables shows that more sin/cos-Gaussians than r^m -Gaussians are needed to achieve the target precision of $10^{-7} E_h$. However, the ratio of the numbers of r^m and sin/cos-Gaussians decreases with the excitation level, as can be seen from Figure 2. This is an expected behavior. As the excitation level increases, the number of nodes in the wave function and its oscillatory character also increase. The sin/cos-Gaussians

TABLE I. Best energies obtained with the r^m -Gaussians. The enlarging of the basis set is stopped when the difference between the energy obtained in the calculation and the exact energy drops below $10^{-7} E_h$.

r^m -Gaussian basis set				
State n	Exact energy (E_h)	Best energy (E_h)	No. of funct.	Difference (E_h)
0	-1.160588789	-1.160588753	3	3.65×10^{-8}
1	-1.134517246	-1.134517185	3	6.06×10^{-8}
2	-1.110753541	-1.110753513	4	2.77×10^{-8}
3	-1.089297674	-1.089297660	5	1.41×10^{-8}
4	-1.070149644	-1.070149628	7	1.61×10^{-8}
5	-1.053309453	-1.053309377	7	7.58×10^{-8}
6	-1.038777099	-1.038777038	10	6.15×10^{-8}
7	-1.026552583	-1.026552506	10	7.73×10^{-8}
8	-1.016635905	-1.016635832	11	7.31×10^{-8}
9	-1.009027065	-1.009026991	13	7.45×10^{-8}
10	-1.003726063	-1.003726041	14	2.22×10^{-8}
11	-1.000732899	-1.000732808	16	9.14×10^{-8}

are oscillating functions and they should be increasingly better suited to represent the wave functions for higher vibrational states than the r^m -Gaussians, each of which has only one maximum.

The complete set of data obtained from the optimization of the basis functions for each bound state is presented in Figure 3. It shows how the difference between the calculated energy and the exact energy decreases as more sin/cos-Gaussians are added to the basis set.

IV. SUMMARY

In this work, we introduce a new form of explicitly correlated Gaussian functions for non-BO calculations of bound states of molecular systems with an arbitrary number of nuclei. It is an alternative to the Gaussians with the preexponential multipliers in the form of non-negative powers of the internuclear distances (r^m -Gaussians). In the new-type Gaussians, the preexponential parameters are products of sin and cos functions dependent on squares of the internuclear distances (sin/cos-Gaussians). The new basis functions are tested

TABLE II. Best energies obtained with sin/cos-Gaussians. The enlarging of the basis set is stopped when the difference between the energy obtained in the calculation and the exact energy drops below $10^{-7} E_h$.

sin/cos-Gaussian basis set				
State n	Exact energy (E_h)	Best energy (E_h)	No. of funct.	Difference (E_h)
0	-1.160588789	-1.160588691	8	9.82×10^{-8}
1	-1.134517246	-1.134517168	11	7.83×10^{-8}
2	-1.110753541	-1.110753462	12	7.91×10^{-8}
3	-1.089297674	-1.089297591	14	8.30×10^{-8}
4	-1.070149644	-1.070149605	16	3.92×10^{-8}
5	-1.053309453	-1.053309374	15	7.84×10^{-8}
6	-1.038777099	-1.038777002	18	9.68×10^{-8}
7	-1.026552583	-1.026552534	22	4.94×10^{-8}
8	-1.016635905	-1.016635841	22	6.47×10^{-8}
9	-1.009027065	-1.009026992	23	7.34×10^{-8}
10	-1.003726063	-1.003725972	24	9.11×10^{-8}
11	-1.000732899	-1.000732832	28	6.68×10^{-8}

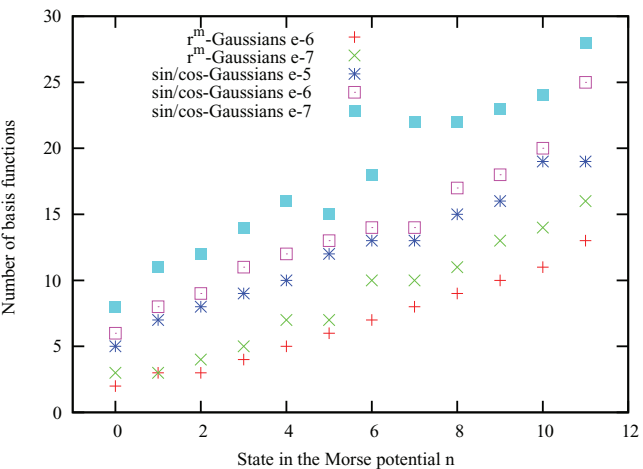


FIG. 1. Comparison of the number of basis functions necessary to reach the given precession level of the energy in the calculations performed with sin/cos and r^m -Gaussians.

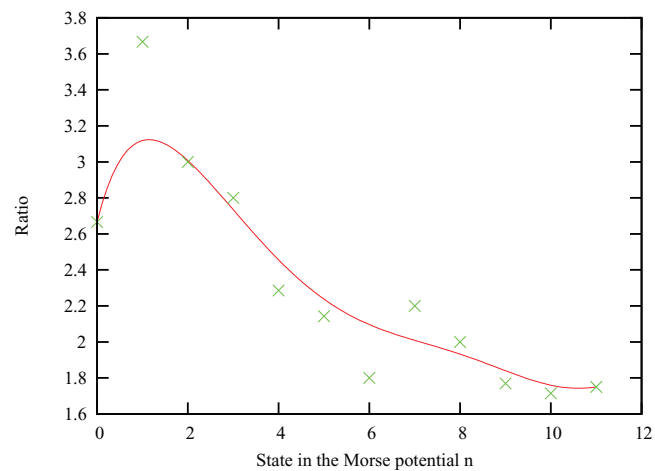


FIG. 2. Ratio of numbers of sin/cos and r^m -Gaussians needed to reach the precision of the energy better than $10^{-7} E_h$. The solid line represents a smooth bezier fit done in gnuplot.

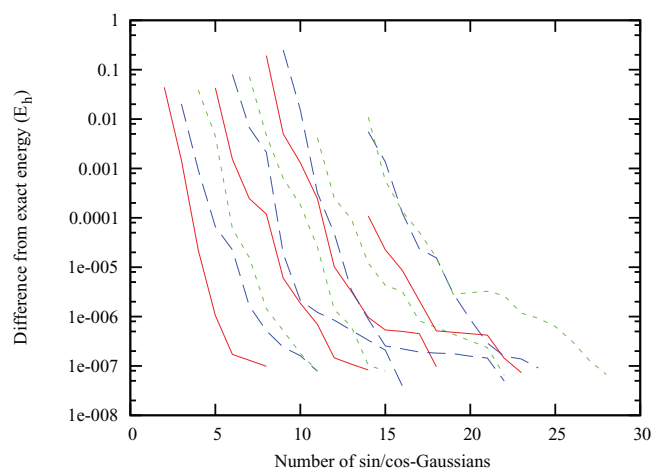


FIG. 3. The convergence of the energy of individual states with the number of sin/cos-Gaussians. The curve corresponding to the ground state is on far left. The excitation level increases moving to the right.

in the calculations of bound pure vibrational states of a diatomic system with the interaction of the nuclei represented by a Morse potential. The test shows that, even though it takes more sin/cos-Gaussians than r^m -Gaussians to achieve similar precision of the energy, the former functions can effectively describe the vibrational states. Future work will involve implementation and testing of the sin/cos-Gaussians in all-particle non-BO calculations of the pure vibrational states of diatomic systems. Subsequently, some small triatomics (e.g., H_3^+) will also be studied.

ACKNOWLEDGMENTS

We would like to express our gratitude to Dr. Donald Kinghorn for providing his computer code for the calculation of a diatomic system interacting with a Morse potential using r^m -Gaussians and helping us with our own implementation. An allocation of computer time from the UA Research Computing High Performance Computing (HPC) and High Throughput Computing (HTC) at the University of Arizona is gratefully acknowledged. Martin Formanek is thankful for the support from the Fulbright Student Program allowing his stay in the United States. Keeper L. Sharkey is a National Science Foundation (NSF) Graduate Research Fellow (Grant No. DGE1-1143953) and would also like to extend a thank you.

APPENDIX A: MATRIX ELEMENTS IN THE r^m -GAUSSIAN BASIS SET

To evaluate the elements of the overlap and kinetic-energy matrices, the following integral is needed to be

calculated:

$$\int_0^\infty r^m e^{-ar^2} dr = \frac{1}{2} a^{-\frac{m+1}{2}} \Gamma\left(\frac{m+1}{2}\right), \quad (\text{A1})$$

where Γ being Euler's gamma function. Let us start with the overlap integral between the $\phi_i(r) = r^{m_i} e^{-a_i r^2}$ and $\phi_j(r) = r^{m_j} e^{-a_j r^2}$ Gaussians

$$S_{ij} = \langle \phi_i | \phi_j \rangle = \int_0^\infty 4\pi r^2 r^{m_i} e^{-a_i r^2} r^{m_j} e^{-a_j r^2} dr, \quad (\text{A2})$$

where $m = m_i + m_j + 2$ and $a = a_i + a_j$. Straightforward use of Eq. (A1) gives us

$$S_{ij} = 2\pi(a_i + a_j)^{-(m_i + m_j)/2 - 3/2} \Gamma\left(\frac{m_i + m_j}{2} + \frac{3}{2}\right). \quad (\text{A3})$$

Analogically for an element of the kinetic-energy matrix, we have

$$T_{ij} = \langle \phi_i | \hat{T} | \phi_j \rangle = -\frac{1}{2\mu} \langle \phi_i | \nabla^2 | \phi_j \rangle \quad (\text{A4})$$

and with using integration by parts we obtain a following integral:

$$T_{ij} = \frac{1}{2\mu} \int_0^\infty 4\pi r^2 \frac{d}{dr} \phi_i(r) \frac{d}{dr} \phi_j(r) dr. \quad (\text{A5})$$

The derivative with respect to r of $r^{m_i} e^{-a_i r^2}$ as seen above is

$$\frac{d}{dr} r^{m_i} e^{-a_i r^2} = (m_i r^{m_i-1} - 2a_i r^{m_i+1}) e^{-a_i r^2}. \quad (\text{A6})$$

Inserting this expression into the equation for kinetic energy (A5) and multiplying the brackets gives us three terms of the type (A1).

$$T_{ij} = \frac{2\pi}{\mu} \left(+ m_i m_j \int_0^\infty r^{m_i+m_j} e^{-(a_i+a_j)r^2} dr, \quad m = m_i + m_j, \quad a = a_i + a_j, \right. \\ \left. - 2(m_i a_j + m_j a_i) \int_0^\infty r^{m_i+m_j+2} e^{-(a_i+a_j)r^2} dr, \quad m = m_i + m_j + 2, \quad a = a_i + a_j, \right. \\ \left. + 4a_i a_j \int_0^\infty r^{m_i+m_j+4} e^{-(a_i+a_j)r^2} dr \right), \quad m = m_i + m_j + 4, \quad a = a_i + a_j.$$

Finally, using the well known identity $\Gamma(x) = (x-1)\Gamma(x-1)$ allows us to express all terms using a single gamma function as

$$T_{ij} = \frac{\pi}{\mu} (a_i + a_j)^{-(m_i + m_j)/2 - 1/2} \Gamma\left(\frac{m_i + m_j}{2} + \frac{1}{2}\right) \\ \times \left[m_i m_j - 2(m_i a_j + m_j a_i)(a_i + a_j)^{-1} \left(\frac{m_i + m_j}{2} + \frac{1}{2}\right) \right. \\ \left. + 4a_i a_j (a_i + a_j)^{-2} \left(\frac{m_i + m_j}{2} + \frac{3}{2}\right) \left(\frac{m_i + m_j}{2} + \frac{1}{2}\right) \right].$$

APPENDIX B: MATRIX ELEMENTS IN THE SIN/COS-GAUSSIAN BASIS SET

This time the overlap integral reads

$$S_{ij} = \langle \phi_i | \phi_j \rangle \\ = \int_0^\infty 4\pi r^2 \sin/\cos(b_i r^2) e^{-a_i r^2} \sin/\cos(b_j r^2) e^{-a_j r^2} dr. \quad (\text{B1})$$

Now by inserting the Euler representation of the sin and cos functions we get four integrations of the type

$$\int_0^\infty r^2 e^{-(a+bi)r^2} dr = \frac{\sqrt{\pi}}{4(a+bi)^{3/2}}, \quad (\text{B2})$$

where $a = a_i + a_j$ for all four terms and $b = \pm b_i \pm b_j$. The sign and the factor of i in front of each term depends on if the basis function is of a sin or cos character. For example, the overlap integral between functions $\phi_1(r) = \sin(b_1 r^2) e^{-a_1 r^2}$ and $\phi_2(r) = \cos(b_2 r^2) e^{-a_2 r^2}$ is

$$S_{12} = i \frac{\pi^{3/2}}{4} \left[\frac{1}{(a_1 + a_2 + i(b_1 - b_2))^{3/2}} + \frac{1}{(a_1 + a_2 + i(b_1 + b_2))^{3/2}} - \frac{1}{(a_1 + a_2 - i(b_1 + b_2))^{3/2}} - \frac{1}{(a_1 + a_2 - i(b_1 - b_2))^{3/2}} \right].$$

Note that, even though all terms in the integral above are complex functions, the result of integration has to be a real number because the initial functions are real functions. This means that the complex part has to cancel out.

For the kinetic-energy matrix elements, we start again with the formula (A5). The derivatives of the basis elements in this case are

$$\begin{aligned} \frac{d}{dr} \sin/\cos(b_i r^2) e^{-a_i r^2} \\ = 2r(b_i \cos - \sin(b_i r^2) - a_i \sin/\cos(b_i r^2)) e^{-a_i r^2}. \end{aligned} \quad (\text{B3})$$

It does not matter if one takes a derivative of a trigonometric function or an exponential function, in both cases an additional factor of r appears. This gives a combined r^4 factor in the main integration and all terms are of the type

$$\int_0^\infty r^4 e^{-(a+bi)r^2} dr = \frac{3\sqrt{\pi}}{8(a+bi)^{5/2}}. \quad (\text{B4})$$

Since we have two derivatives consisting of two terms and Euler's representation gives us two terms for each sin/cos function, we get $4^2 = 16$ terms in total for every matrix element. Once again in each case $a = a_i + a_j$ and $b = \pm b_i \pm b_j$ with every possible sign combination for the parameter products: $b_i b_j, b_i a_j, a_i b_j, a_i a_j$ in front. The sign and the factor of i for each term of type (B4) has to be carefully worked out by an explicit calculation. Using, for example, the same ϕ_1 and ϕ_2

functions as above we get the following kinetic-energy matrix element:

$$\begin{aligned} T_{12} = \frac{3\pi^{3/2}}{4\mu} & [+ib_1 b_2 (I - II + III - IV) \\ & - b_1 a_2 (I + II + III + IV) \\ & - a_1 b_2 (I - II - III + IV) \\ & - ia_1 a_2 (I + II - III - IV)], \end{aligned}$$

where abbreviations I, II, III, and IV stand for terms of type (B4) with different b 's

$$\begin{aligned} I &= \frac{1}{(a_1 + a_2 - i(b_1 + b_2))^{5/2}}, \\ II &= \frac{1}{(a_1 + a_2 - i(b_1 - b_2))^{5/2}}, \\ III &= \frac{1}{(a_1 + a_2 + i(b_1 - b_2))^{5/2}}, \\ IV &= \frac{1}{(a_1 + a_2 + i(b_1 + b_2))^{5/2}}. \end{aligned}$$

Other needed terms can be calculated analogically.

¹J. Mitroy, S. Bubin, W. Horiuchi, Y. Suzuki, L. Adamowicz, W. Cencek, K. Szalewicz, J. Komasa, D. Blume, and K. Varga, *Rev. Mod. Phys.* **85**, 693 (2013).

²S. Bubin, M. Pavanello, W.-C. Tung, K. L. Sharkey, and L. Adamowicz, *Chem. Rev.* **113**, 36 (2013).

³N. Kirnosov, K. L. Sharkey, and L. Adamowicz, *J. Chem. Phys.* **139**, 204105 (2013).

⁴K. L. Sharkey, N. Kirnosov, and L. Adamowicz, *J. Chem. Phys.* **139**, 164119 (2013).

⁵E. Bednarz, S. Bubin, and L. Adamowicz, *Mol. Phys.* **103**, 1169 (2005).

⁶S. Bubin and L. Adamowicz, *J. Chem. Phys.* **124**, 224317 (2006).

⁷D. B. Kinghorn and L. Adamowicz, *J. Chem. Phys.* **106**, 8760 (1997).

⁸D. B. Kinghorn and L. Adamowicz, *Phys. Rev. Lett.* **83**, 2541 (1999).

⁹W. H. Press, S. A. Teukolsky, W. T. Vetterling, and B. P. Flannery, *Numerical Recipes* (Cambridge University Press, New York, 2007).

¹⁰J. More, D. Sorenson, B. Garbow, and K. Hillstrom, *The MINPACK Project, in Sources and Development of Mathematical Software*, edited by W. Cowell (Prentice-Hall, 1984).

¹¹W.-C. Tung, M. Pavanello, and L. Adamowicz, *J. Chem. Phys.* **133**, 124106 (2010).